

Project Number: 101072443

3rd NETWORK TRAINING SCHOOL

Deliverable 4.4

Dissemination level: PU - Public

Prepared by:

Javier López Lara, FIHAC Principal Investigator in SEDIMARE



This project has received funding from the European Union's (EU) Horizon Europe Framework Programme (HORIZON) under Grant Agreement No. 101072443 as a MSCA Doctoral Network (HORIZON-MSCA-2021-DN-01).

Document Information

Project Title	Sediment Transport and Morphodynamics in Marine and Coastal Waters with Engineering Solutions
Project Acronym	SEDIMARE
Grant Agreement No.	101072443
Call	MSCA Doctoral Networks 2021 (HORIZON-MSCA-2021-DN-01)
Start Date of Project	01-02-2023
Duration of Project	48 months
Deliverable	D4.4: 3rd NETWORK TRAINING SCHOOL
No. of pages including cover	452

Disclaimer: The content of this document does not represent the opinion of the European Union, and the European Union is not responsible for any use that might be made of such content.

Version	Publication Date	Author(s)	Change
1.0	17.03.2025	Javier López Lara	Initial version

Date and Signature of Author(s):

Table of Contents

	Page
1. Program	5
2. Presentations	7

1. Program

The SEDIMARE “3rd Training School” was organized by Fundación Instituto de Hidráulica Ambiental de Cantabria (FIHAC)¹, in Santander (Spain), on 11-13 March 2025. Local organizers were Prof. Javier López Lara and Silvia Fernández Rodicio (EU Projects Department). The event was attended in person by all DCs, with the exception of DC Van Thi To Nguyen, who was conducting her experiments in Aberdeen during that time.

The SEDIMARE meeting consisted of:

- **PROJECT REVIEW & SCIENTIFIC EXCHANGE MEETING**
 - PhD progress presentations
 - Supervisory Board meeting
- **TRAINING SCHOOL**
 - This training school will consist of seminars with topics related to “effective monitoring techniques”, “building adaptive capacity for resilient coast” and “coastal zone management - examples and best practices”

Day 1 – Tuesday 11 March

Morning

8:45 Walk-in

9:00-9:30 Welcome by **PI Javier López Lara (IHCantabria)**

9:30-10:30 KEYNOTE 1 – “*Shoreline Evolution Modeling*” by **Camilo Jaramillo (IHCantabria)**

10:30 *Coffee Break*

11:00-13:05 DCs presentations (15 min presentation + 10 min discussion)

11:00-11:25 **DC Buckle Subbiah Elavazhagan**

11:25-11:50 **DC Jowi Miranda**

11:50-12:15 **DC Nasim Soori**

12:15-12:40 **DC Nishchay Tiwari**

12:40-13:05 **DC Muhammed Said Parlak**

13:05 *Lunch*

Afternoon

14:00-15:00 Presentation of “*COMMONCOAST: A common coast to cherish – capping climate change*” by **Jara Martínez (IHCantabria)**

15:00-15:15 Presentation of SEDIMARE LinkedIn page by **DC Jowi Miranda**

15:15-16:15 Supervisory Board meeting

Evening

20:00 Project social dinner – **Restaurante ABRA Sardinero (Plaza Brisas, 1, Santander)**

¹ Also known as “IHCantabria”.

Day 2 – Wednesday 12 March

Morning

8:45 Walk-in

9:00-10:00 KEYNOTE 2 – “*Sediment transport in vegetated ecosystems*” by **María Maza (IHCantabria)**

10:00 *Coffee Break*

10:30-12:00 DCs presentations (15 min presentation + 10 min discussion)

10:30-10:55 **DC Van Thi To Nguyen** (online)

10:55-11:20 **DC Siyuan Wang**

11:20-11:45 **DC Eloah Rosas**

12:00-13:00 Interactive session with FIHAC PhD students by **Andrea Costales, Lucas de Freitas and Arnau García (IHCantabria)**

13:00 *Lunch*

Afternoon

14:00-14:45 Presentation of IHCantabria and visit to its facilities by **Javier López Lara (IHCantabria)**

14:45-15:55 Practical issues regarding the field trip on Day 3 by **Silvia Fernández (IHCantabria)**

15:55-16:30 DCs presentations (15 min presentation + 10 min discussion)

15:55-15:20 **DC Saeed Osouli**

15:20-15:45 **DC Ioannis Gerasimos Tsipas**

15:45-16:05 **DC Quan Nguyen**

16:05-16:30 **DC Evangelos Petridis**

16:30 End of the SEDIMARE 3rd Training School

Day 3 – Thursday 13 March

Morning

11:30-14:15 Field trip by **Camilo Jaramillo (IHCantabria)** – El Puntal, Somo and Loredó (Cantabria)

Meeting point: *Palacete del Embarcadero (Calle Muelle de Calderón, 0, Santander)*

2. Presentations

The theme of the 3rd Network Training School was “Advanced Integrated Coastal Zone Monitoring and Management”.

The keynote presentations by invited speakers, as well as the presentations of all the DCs, are shown in the next pages.

“Shoreline Evolution Modeling”

(Invited Speaker Camilo Jaramillo, IHCantabria)

SHORELINE EVOLUTION MODELING

CAMILO JARAMILLO CARDONA



Coastal Management and Engineering Group

March, 2025



1

Introduction



2

PhD thesis



3

Applications



4

IH-SET



5

GESEM



SEDIMARE





Sediment Transport and Morphodynamics in Marine and Coastal Waters with Engineering Solutions



Coastal Management and Engineering Group

March, 2025

MOTIVATION

- **Many coastal inhabitants** → More than 66% of the global population lives within 100 km of coastlines (Biausque *et al.*, 2016). 
- **Sandy beaches are facing erosion and accretion**
 - Mentaschi *et al.* (2018) made a global shoreline variability analysis. They found that the overall surface of eroded land is about twice the surface of gained land.
 - Luijendijk *et al.*, (2018) estimated that 24% of the world's sandy beaches are eroding at rates exceeding 0.5 m/yr
- **From climate change**
 - Sea level rise → Church *et al.* (2013). 
 - Increase in storm intensity and frequency → Reguero *et al.* (2019) found an increase in global wave power as a consequence of oceanic warming. 

Cartagena de Indias, Colombia








Santander, Spain



Somo, Spain

MOTIVATION

- **Many coastal inhabitants** → More than 66% of the global population lives within 100 km of coastlines (Biausque *et al.*, 2016). 
- **Sandy beaches are facing erosion and accretion**
 - Mentaschi *et al.* (2018) made a global shoreline variability analysis. They found that the overall surface of eroded land is about twice the surface of gained land. 
 - Luijendijk *et al.*, (2018) estimated that 24% of the world's sandy beaches are eroding at rates exceeding 0.5 m/yr 
- **From climate change**
 - Sea level rise → Church *et al.* (2013). 
 - Increase in storm intensity and frequency → Reguero *et al.* (2019) found an increase in global wave power as a consequence of oceanic warming. 

Cartagena de Indias, Colombia



Santander, Spain



Australia (2025)

1

2

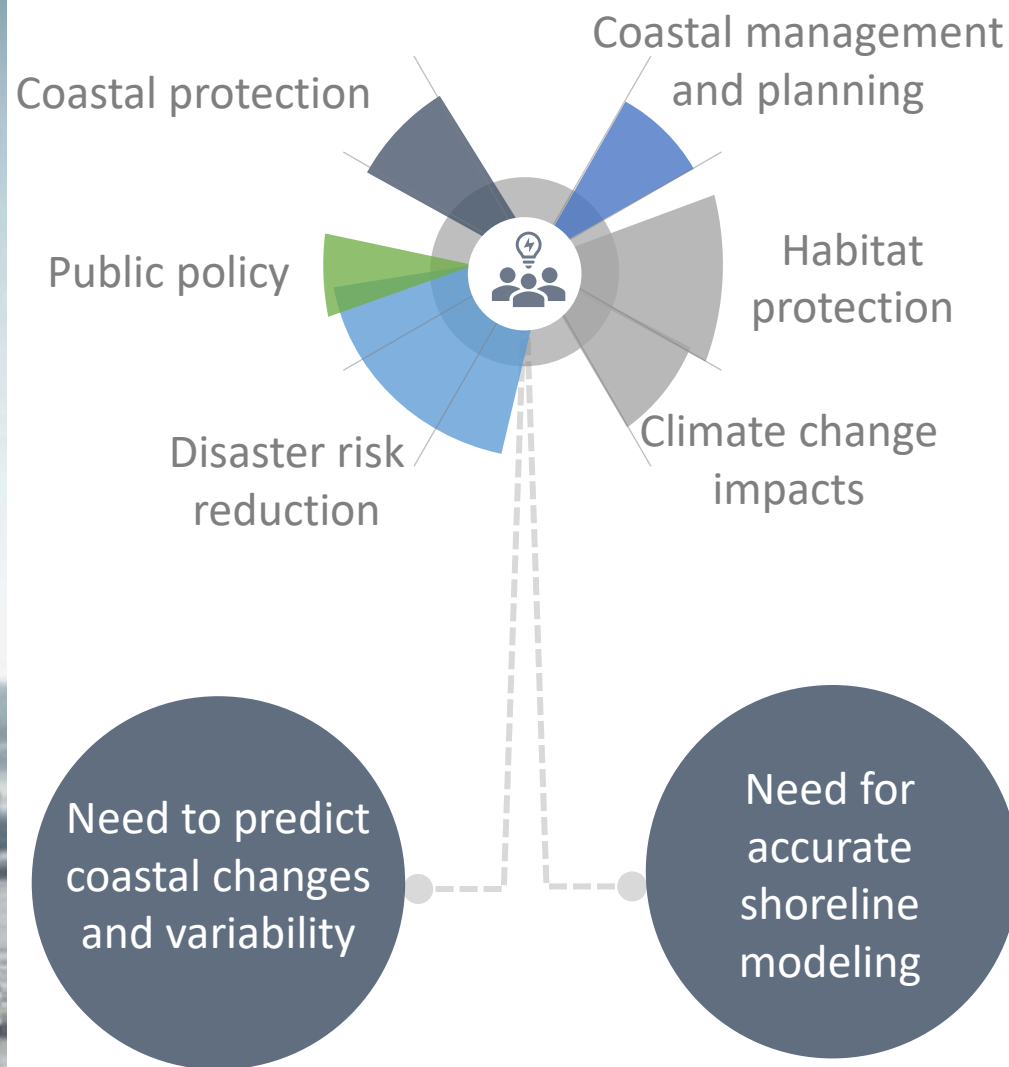
3

4

5



Introduction



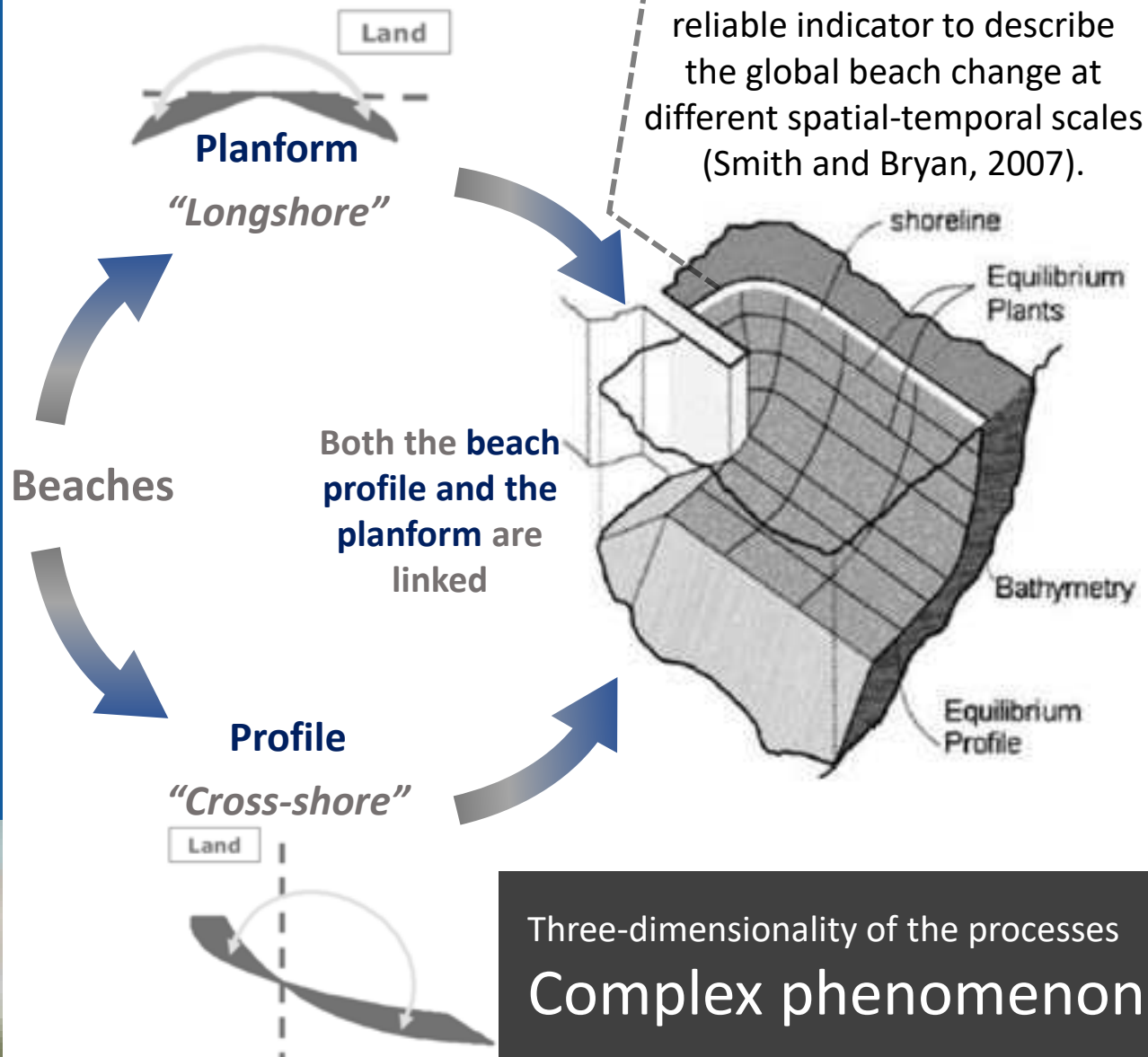
1

2

3

4

5



Introduction

Knowing the **shoreline evolution**

Estimate erosion trends

Regulate coastal development

Design protection works

...

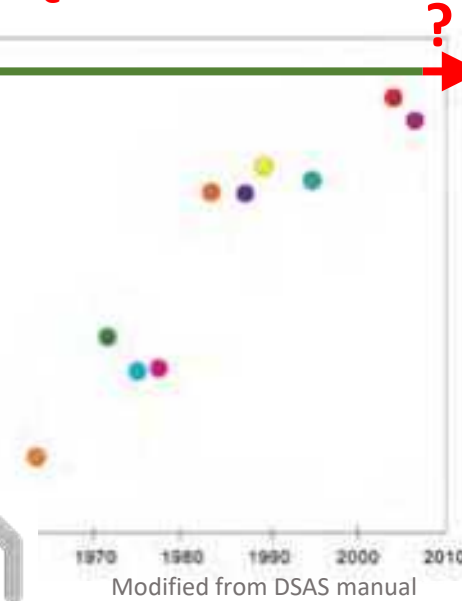
We need to know:

1. ¿Where the shoreline has been?

2. ¿Where it will be?



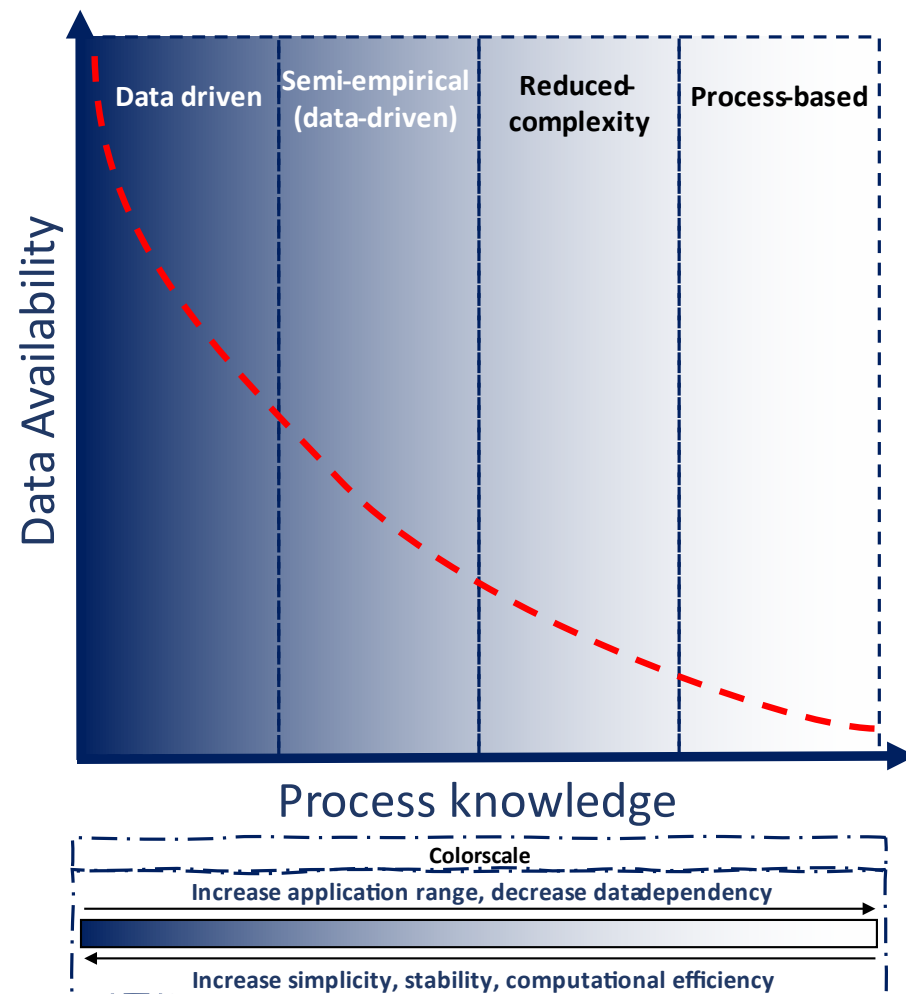
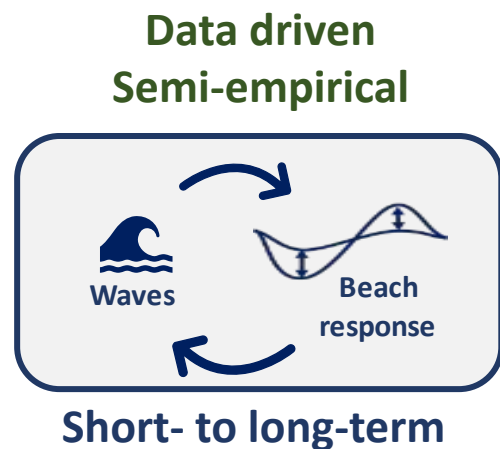
DATA



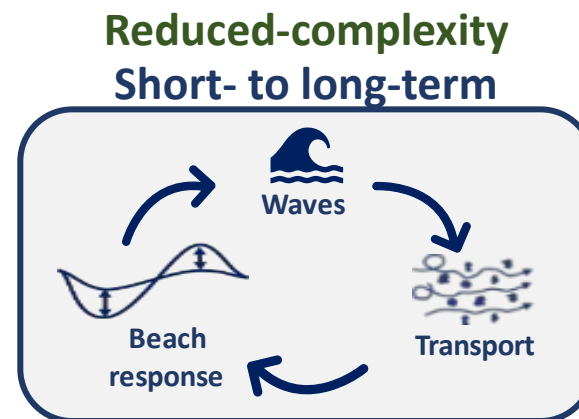
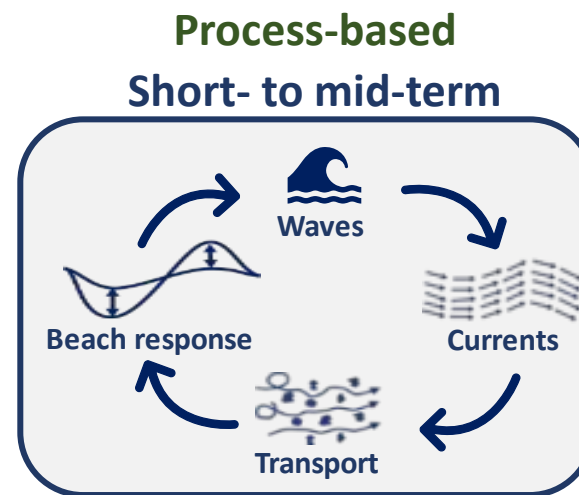
Modified from DSAS manual



Shoreline modeling



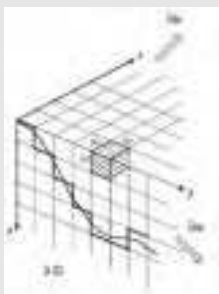
Modified from Hunt et al. 2023



→ The shoreline variability has been estimated through multiple evolution models

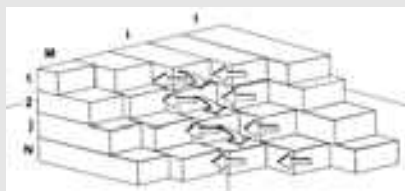
3D models

de Vriend et al. 1993;
Nicholson et al. 1997;
Lesser et al. 2004; ...



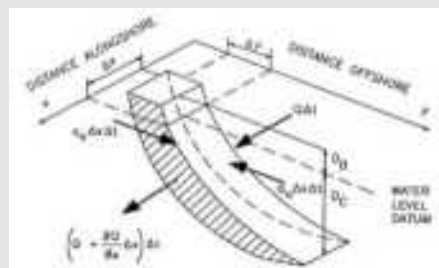
Multiline shoreline models

Bakker, 1970;
Perlin and Dean, 1979;
1983; Hanson and
Larson, 2000; ...



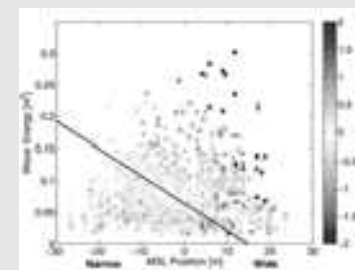
One-line shoreline models

Pelnard-Considere, 1956;
Hanson and Kraus, 1991;
Dabees and Kamphuis,
1998; ...



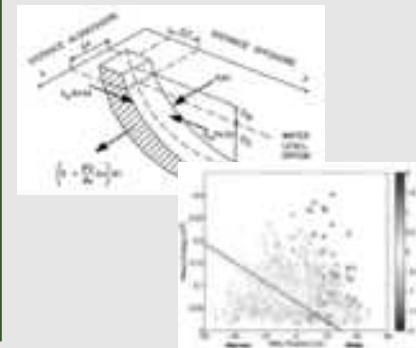
Equilibrium shoreline evolution models

Miller and Dean, 2004;
Yates et al., 2009;
Davidson et al., 2013;
Castelle et al., 2014;
Jara et al., 2015; ...



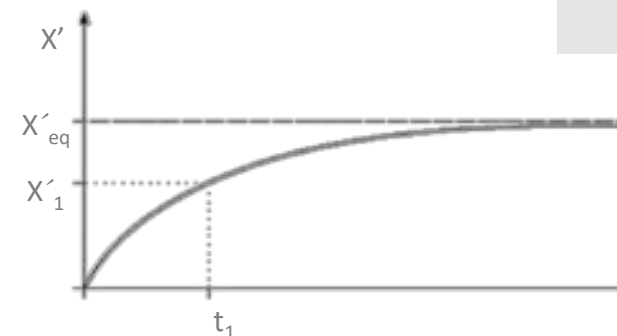
Combined models

Vitousek et al., 2017;
Robinet et al., 2018;
Antolínez et al. 2019; ...



$$\frac{dX'(t)}{dt} = K' \cdot \Delta X'$$

● $f(\text{wave conditions/ beach morphology})$
 ● Disequilibrium between current conditions and a theoretical equilibrium
 $\Delta X' = X' - X'_{eq}$



1

2

3

4

5



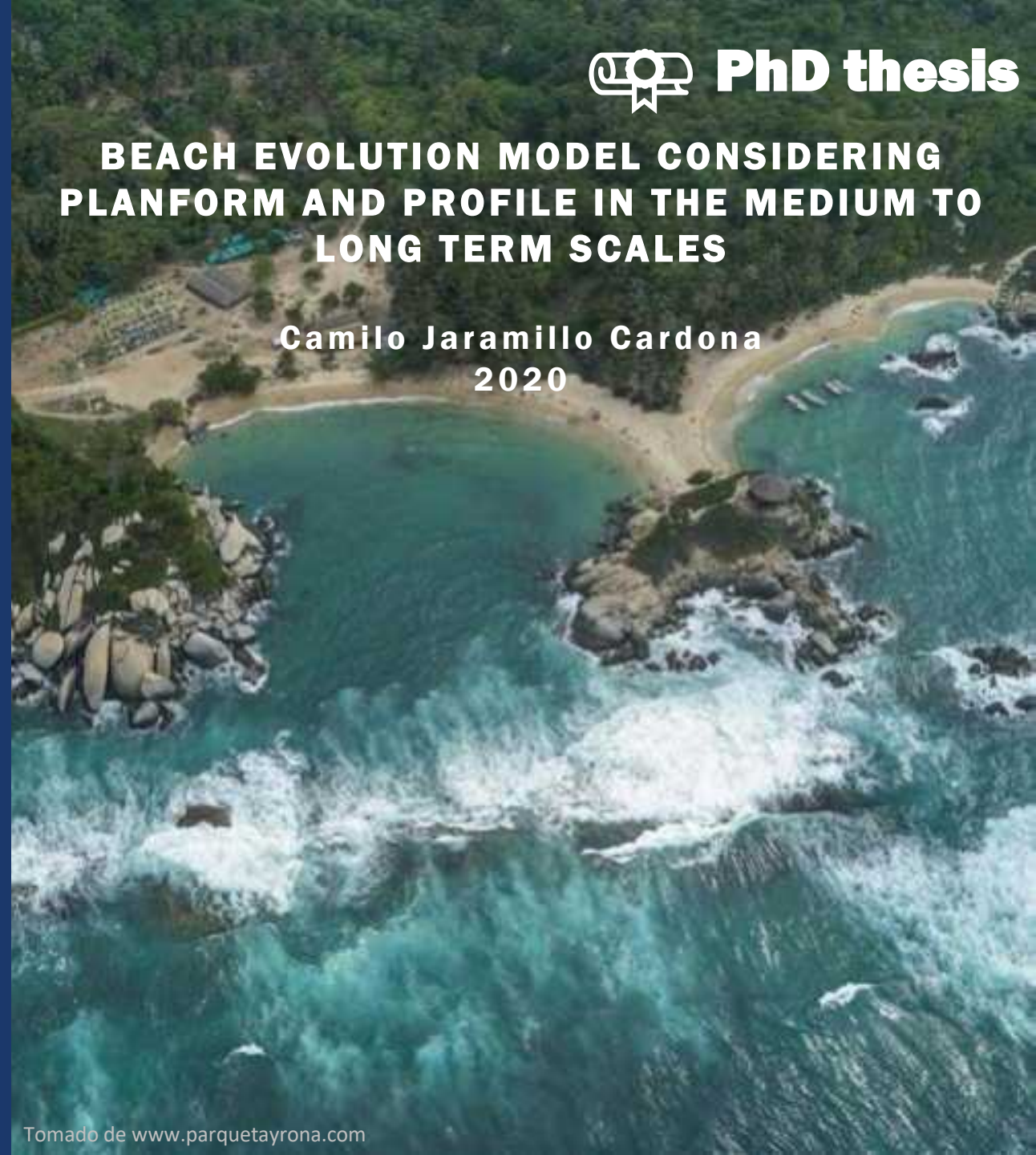
Embayed
beaches



PhD thesis

BEACH EVOLUTION MODEL CONSIDERING PLANFORM AND PROFILE IN THE MEDIUM TO LONG TERM SCALES

Camilo Jaramillo Cardona
2020



1

2

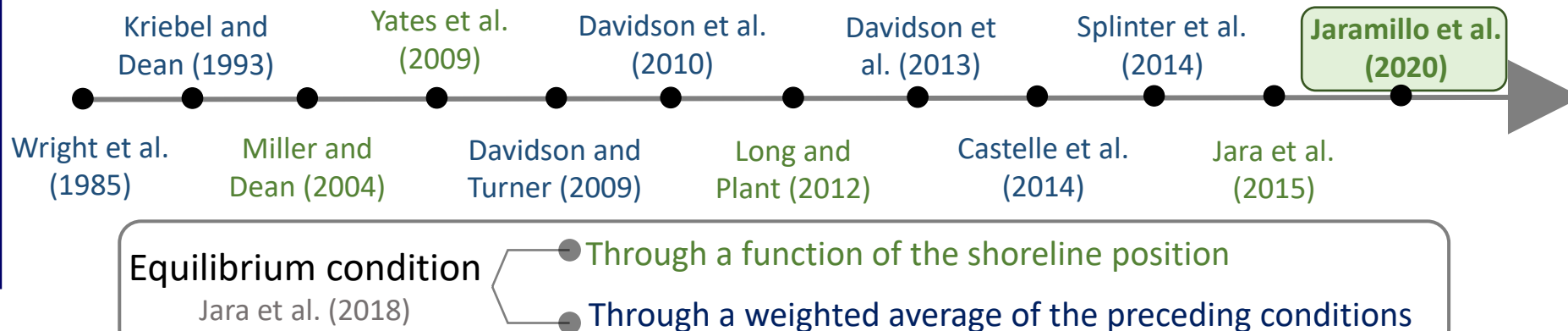
3

4

5



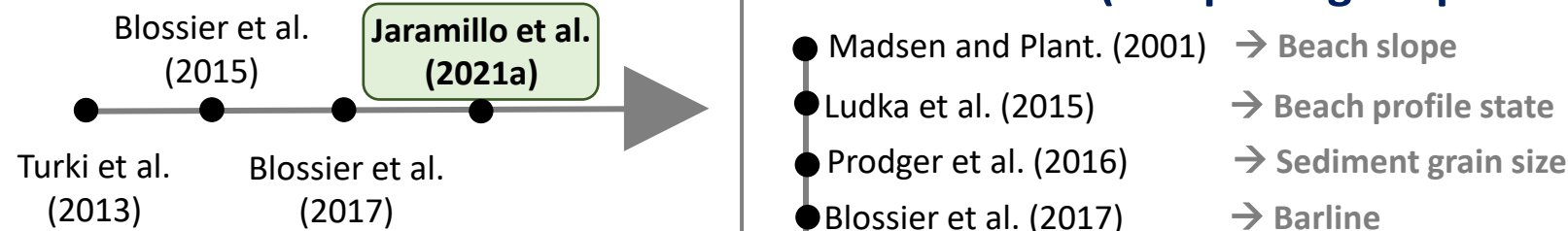
Equilibrium-based shoreline evolution models



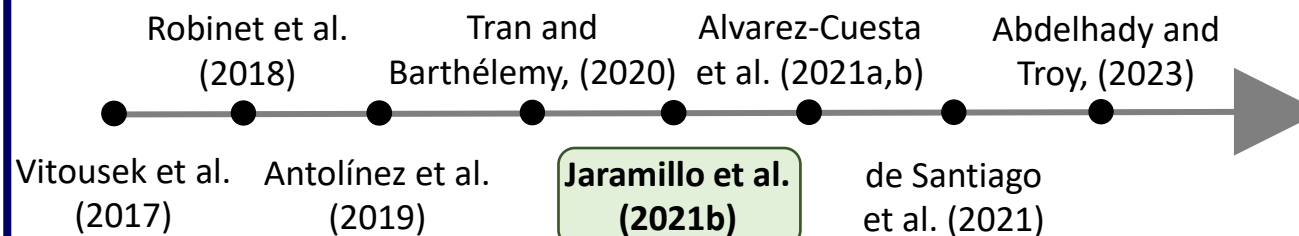
Cross-shore migration

Beach rotation

Other models (morphological parameters)



Combined or hybrid models



Cross-shore + longshore

1

2

3

4

5

Study sites

**Nova Icaria Beach, Spain**

Microtidal
Length: 400m
 \overline{D}_{50} : 0.43mm

**Campo Poseidón beach profile, Spain**

Mesotidal
 \overline{D}_{50} : 0.3mm

**Tairua Beach, New Zealand**

Microtidal
Length: 1200m
 \overline{D}_{50} : 0.45mm

**Narrabeen Beach, Australia**

Microtidal
Length: 3600m
 \overline{D}_{50} : 0.30mm



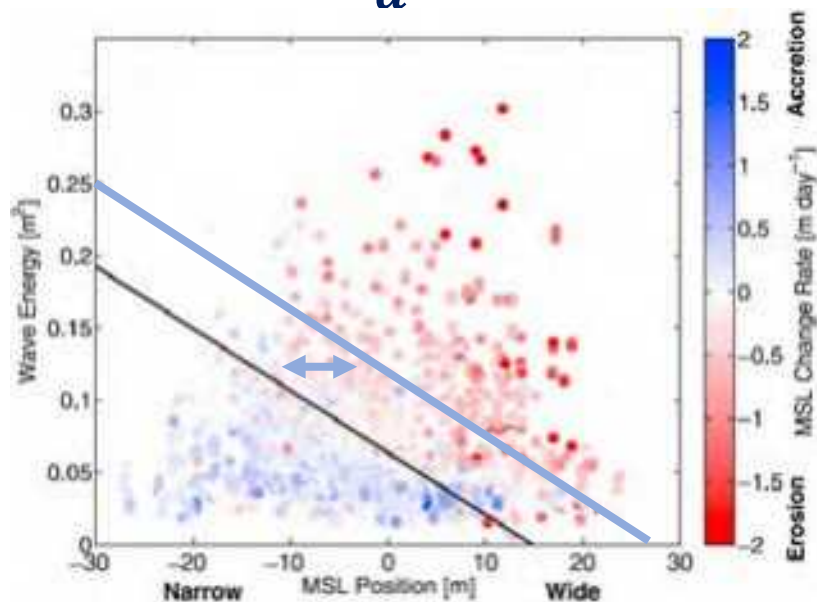
Equilibrium cross-shore shoreline evolution model

Yates et al. (2009) / Jaramillo et al. (2020)a

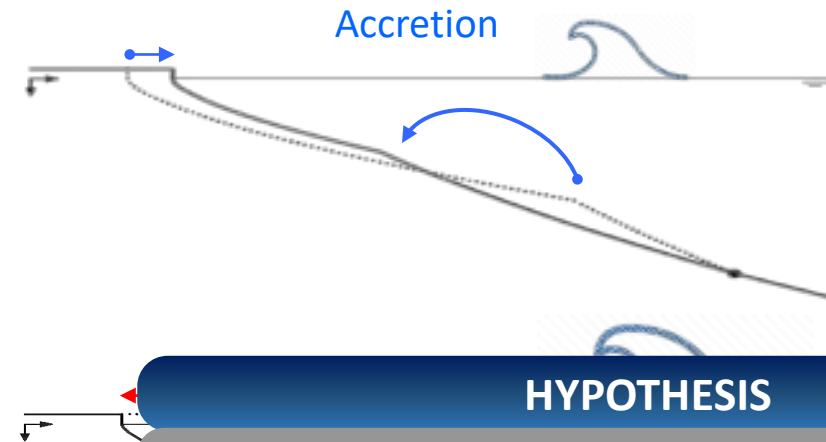
“YA09 model”

$$\frac{\partial S(t)}{\partial t} = C^{\pm} \cdot E^{1/2} (E - E_{eq})$$

$$S_{eq} = \frac{E - b}{a} + v_{lt} * t$$

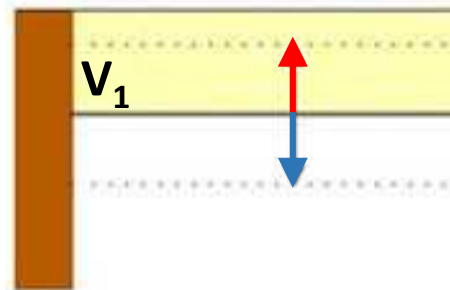


Model parameters (a , b , C^{\pm} and v_{lt})



HYPOTHESIS

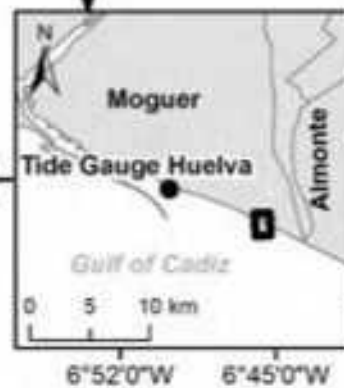
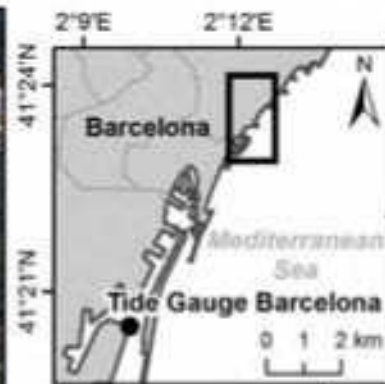
- The **shoreline variability** responds mainly to the magnitude of the **incident energy**.
- The model is applicable to beaches that are subject to **net sediment gain or loss**.
- The **parameters** $C^{+/-}$ remain constant during the simulation.
- The model **does not include** an additional term for **tidal range**. However, as recommended by Castle et al. (2014), in meso- / macrotidal environments it is preferable to evaluate a high contour of the beach profile, to avoid rising bar and berm dynamics.



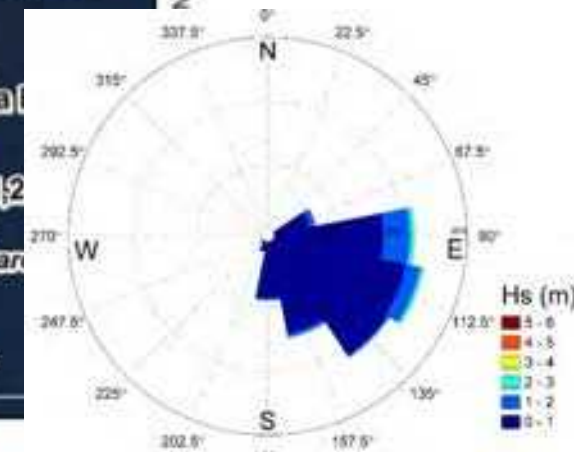
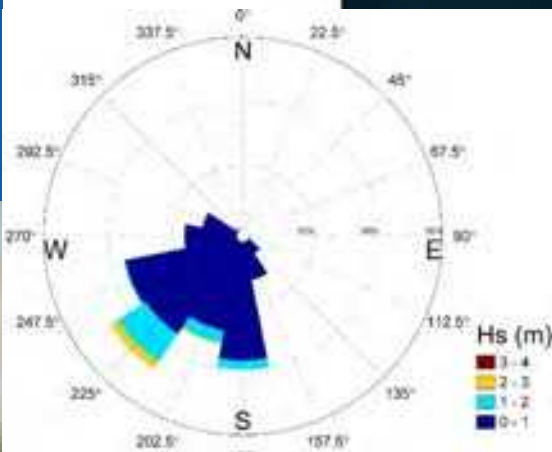
LOCATION OF SELECTED STUDY SITES



Campo Poseidón beach profile



Nova Icaria Beach



Equilibrium cross-shore shoreline evolution model

Campo Poseidón beach profile, Spain

Mesotidal

\overline{D}_{50} : 0.43mm

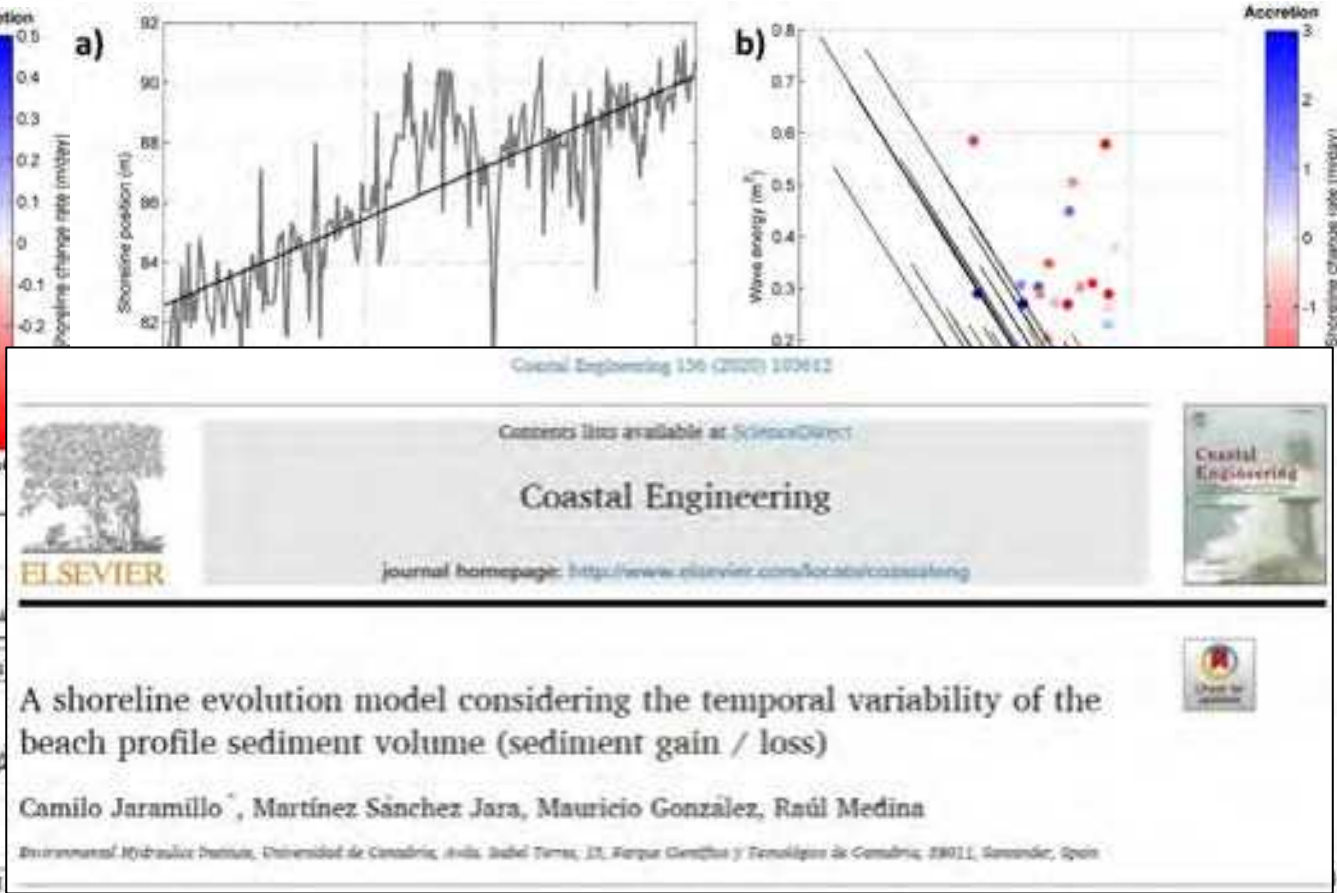
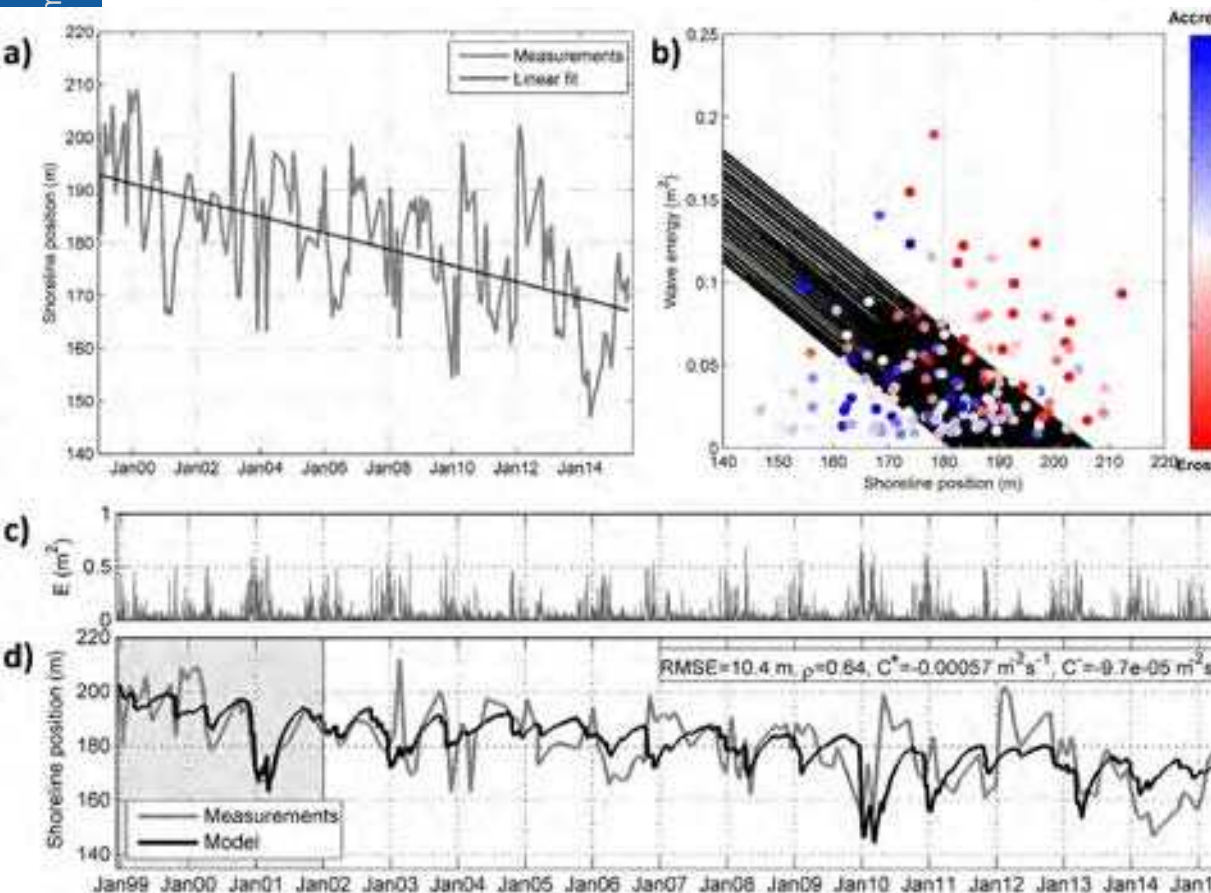


Nova Icaria Beach, Spain

Microtidal

Length: 400m

\overline{D}_{50} : 0.43mm



An equilibrium-based shoreline rotation model

$$\frac{d\alpha_s(t)}{dt} = L^\pm P \Delta\alpha_s(\theta)$$

$$\Delta\alpha_s(\theta) = \alpha_s - \alpha_{seq}$$

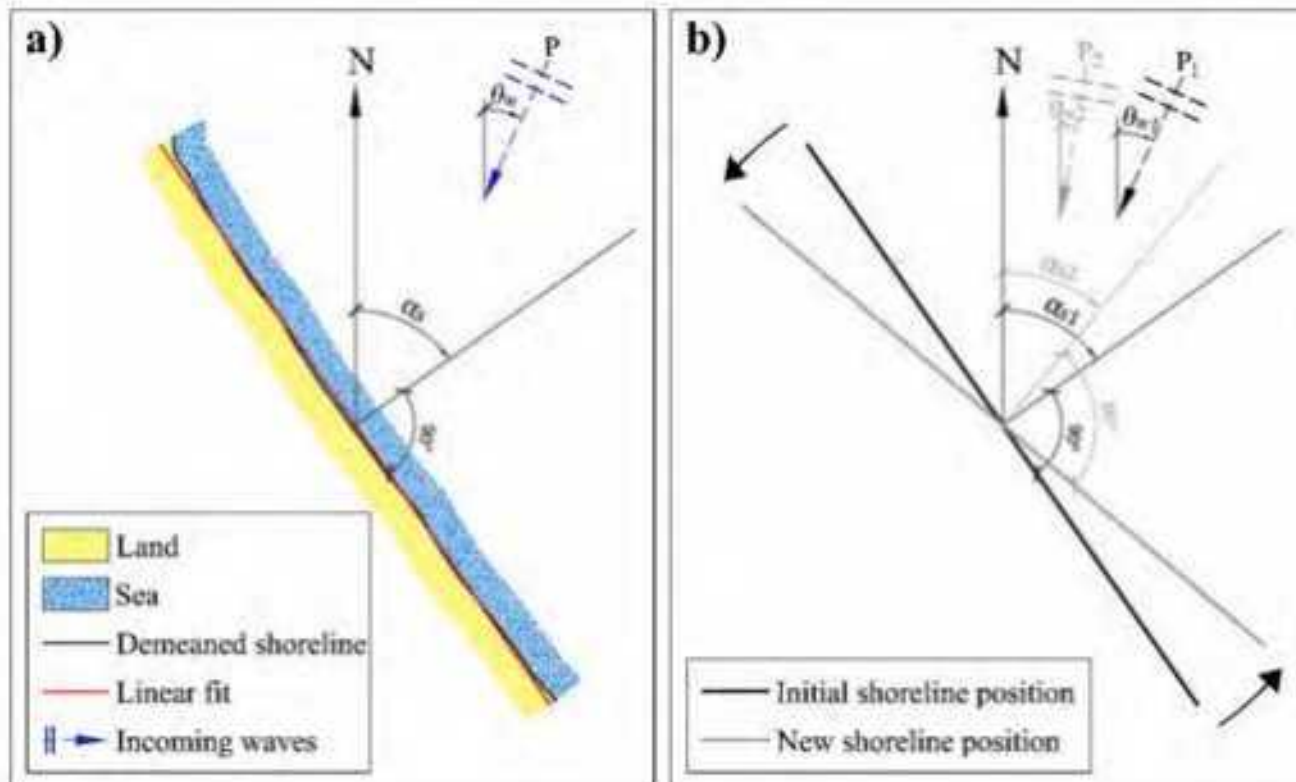
$\alpha_s(t)$: shoreline orientation (°) at the time “t”

P: incident wave power (m^2s) $\rightarrow P = Hs^2 \cdot Tp$

L^\pm : proportionality constants ($m^{-2}s^{-2}$) $\rightarrow L^+$

$\Delta\alpha_s(\theta)$: shoreline orientation disequilibrium

$$\alpha_s(t) = (\alpha_{s0} - \alpha_{seq}) e^{-L^\pm P t} + \alpha_{seq}$$

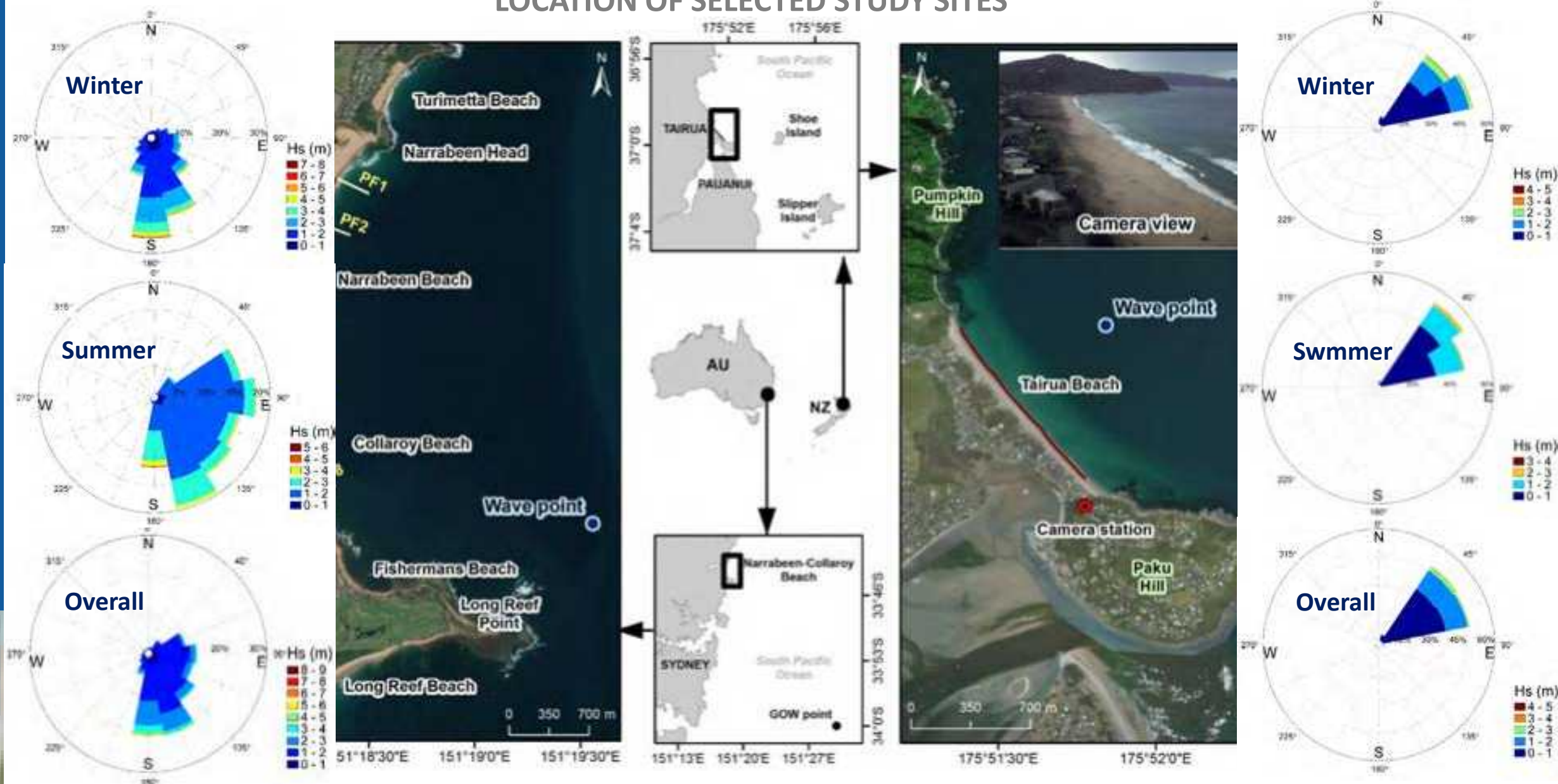


HYPOTHESIS

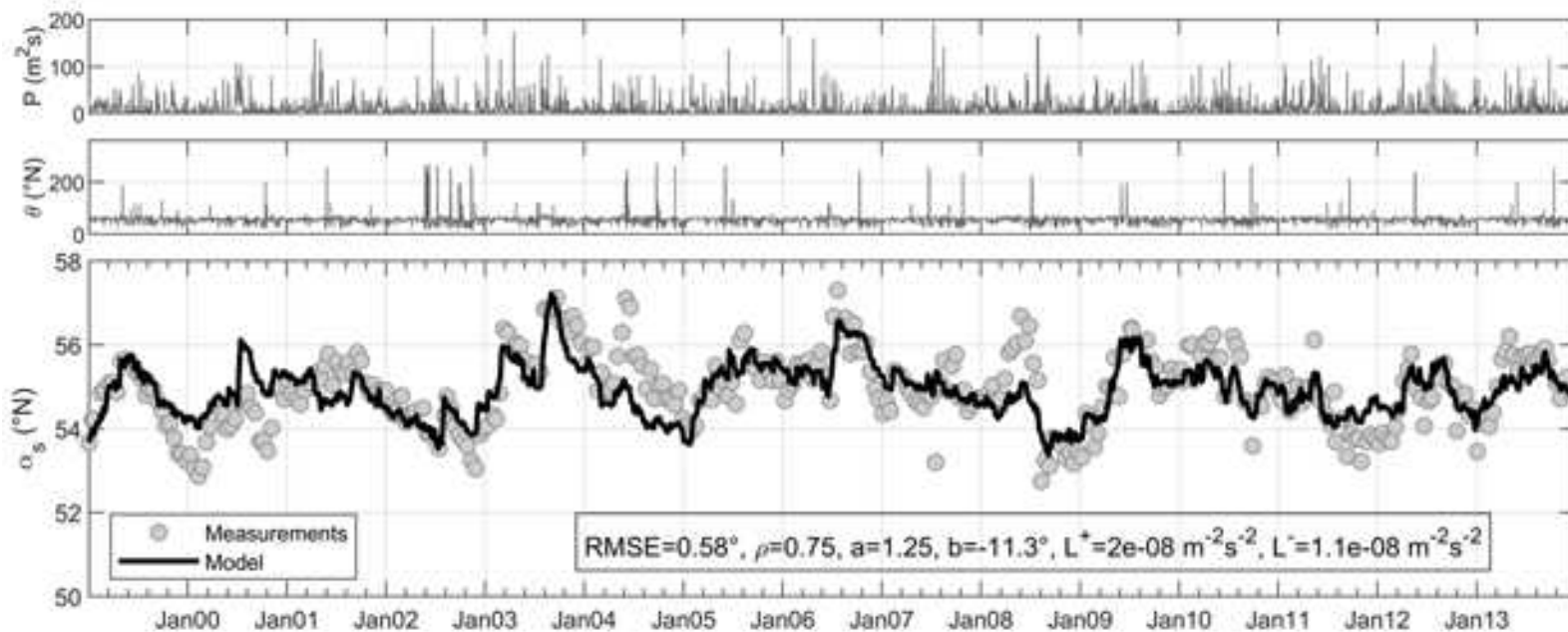
- The **beach rotation** is assumed to be **isolated from other beach movements**.
- The beach rotation mainly depends on the **energy and the directionality** of the incident waves.
- A **single wave point** is assumed as model forcing.
- The model does **not** account for **short-scale processes** (e.g. cusps, rips, etc.).
- The model does **not** explicitly include any additional parameter related to the **tidal range**.

Relationship ($\langle \theta \rangle - \alpha_s$):
**“Equilibrium Wave Direction
 Function, EWDF”**

LOCATION OF SELECTED STUDY SITES



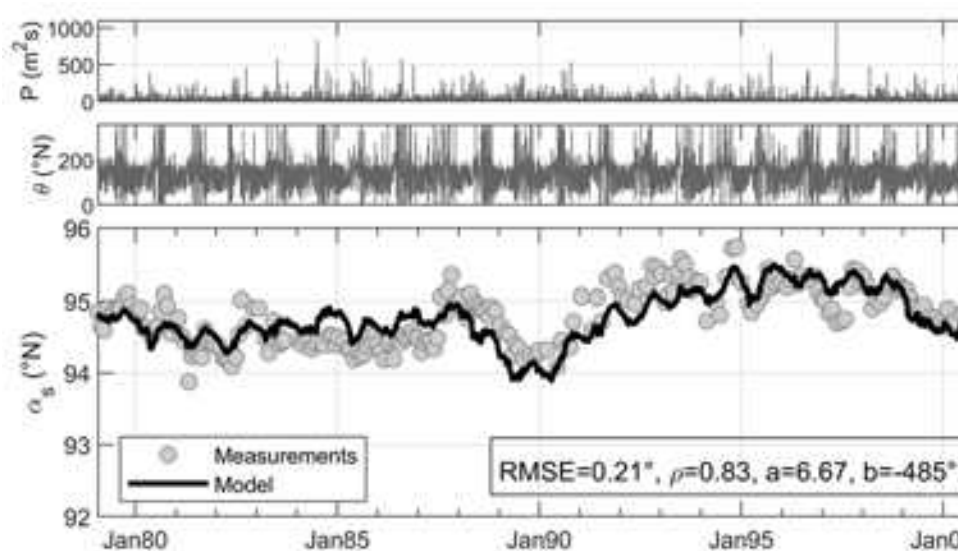
An equilibrium-based shoreline rotation model



Tairua Beach
~ 15 years



Tairua Beach, NZ
Microtidal
Length: 1200m
 \overline{D}_{50} : 0.45mm



Coastal Engineering 143 (2021) 103789

Contents lists available at ScienceDirect

Coastal Engineering

journal homepage: <http://www.elsevier.com/locate/coasteng>

An equilibrium-based shoreline rotation model

Camilo Jaramillo ^{a,*}, Mauricio González ^a, Raúl Medina ^a, Imen Turki ^b

^a Environmental Hydraulics Institute, Universidad de Cantabria - Avda. Siles 15, 39, Parque Científico y Tecnológico de Cantabria, 39011, Santander, Spain

^b UMR CNRS 6143 Continuum and Coastal Morphodynamics (3C2M), University of Rouen, 76821, Mont-Saint-Etienne Cedex, France

1

2

3

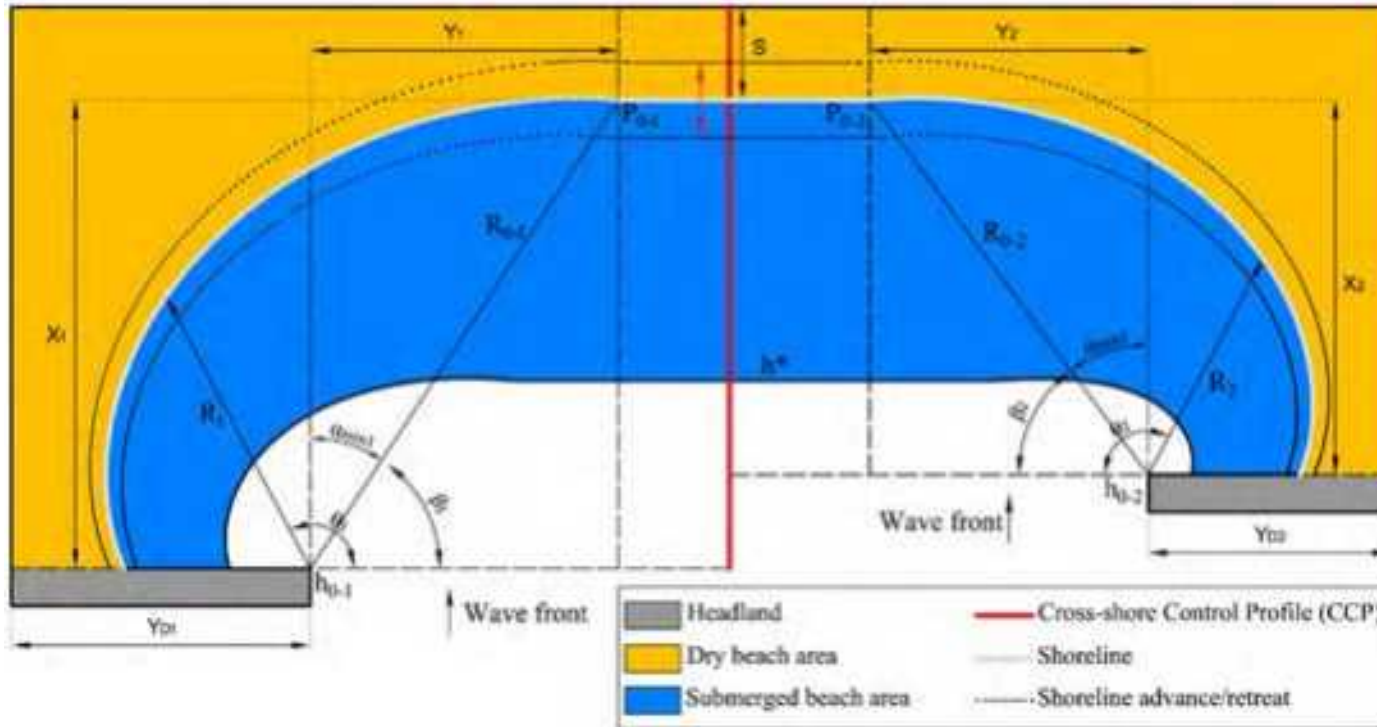
4

5

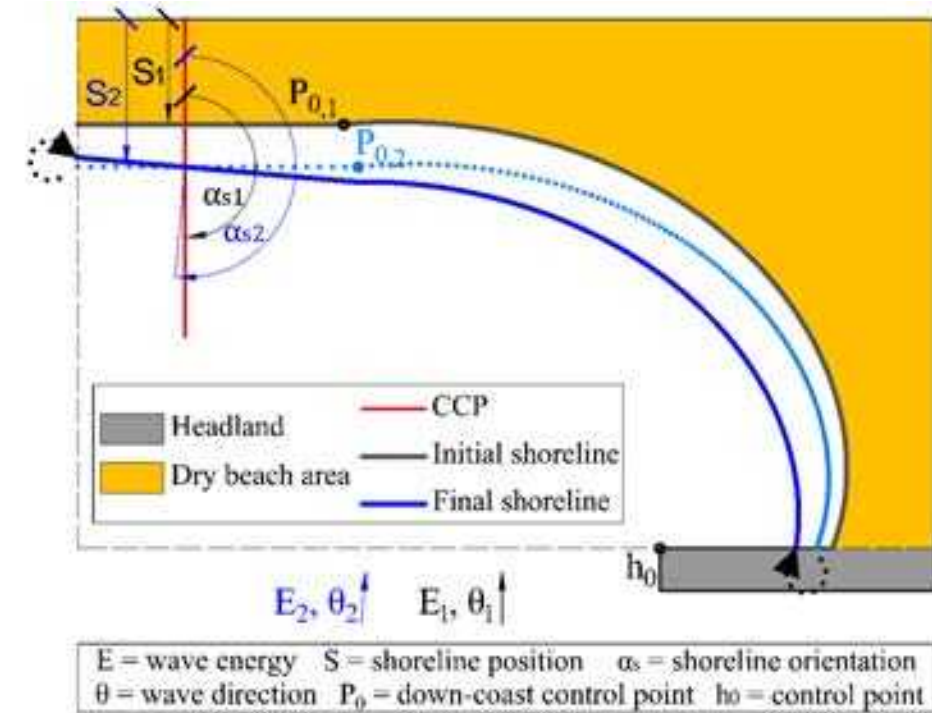


MODEL Of Shoreline Evolution (IH-MOOSE) **INTEGRATION**

Yates et al. (2009) / Jaramillo et al. (2020) + Hsu and Evans (1989)



+ Jaramillo et al. (2021a)



HYPOTHESIS

- The **beach profile** and **beach planform** tend to have an **equilibrium shape**
- The **beach profile** and **beach planform** are **linked**

APPLICABILITY

- Embayed beaches** with parabolic shape

LIMITATIONS

- It is not considered **beach breathing**
- Others**

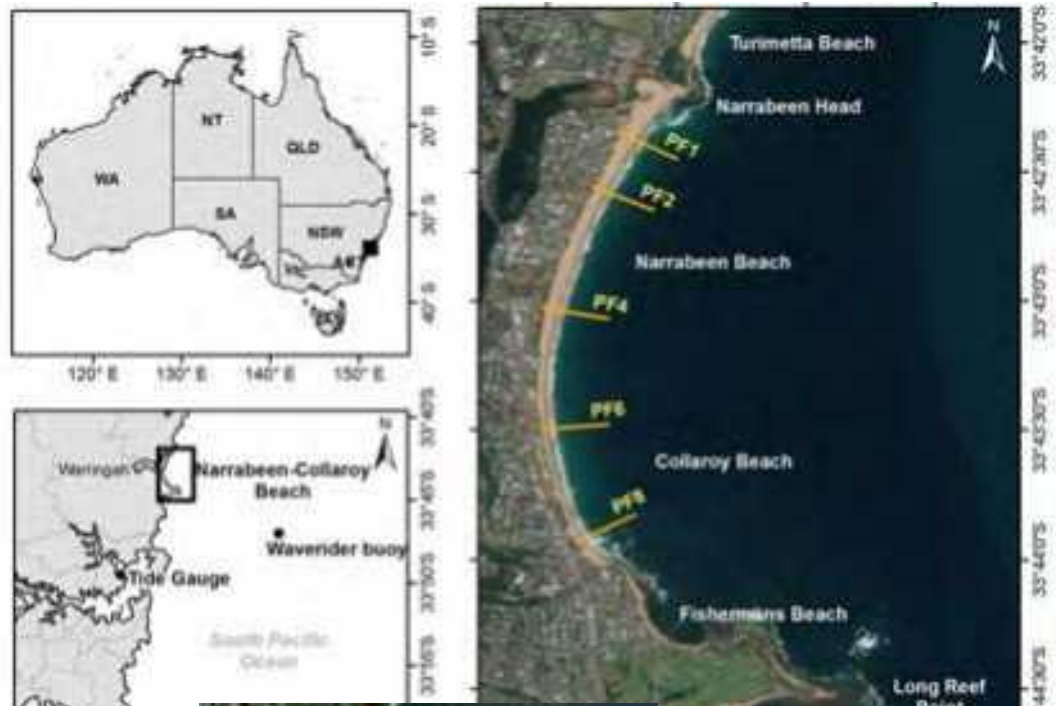
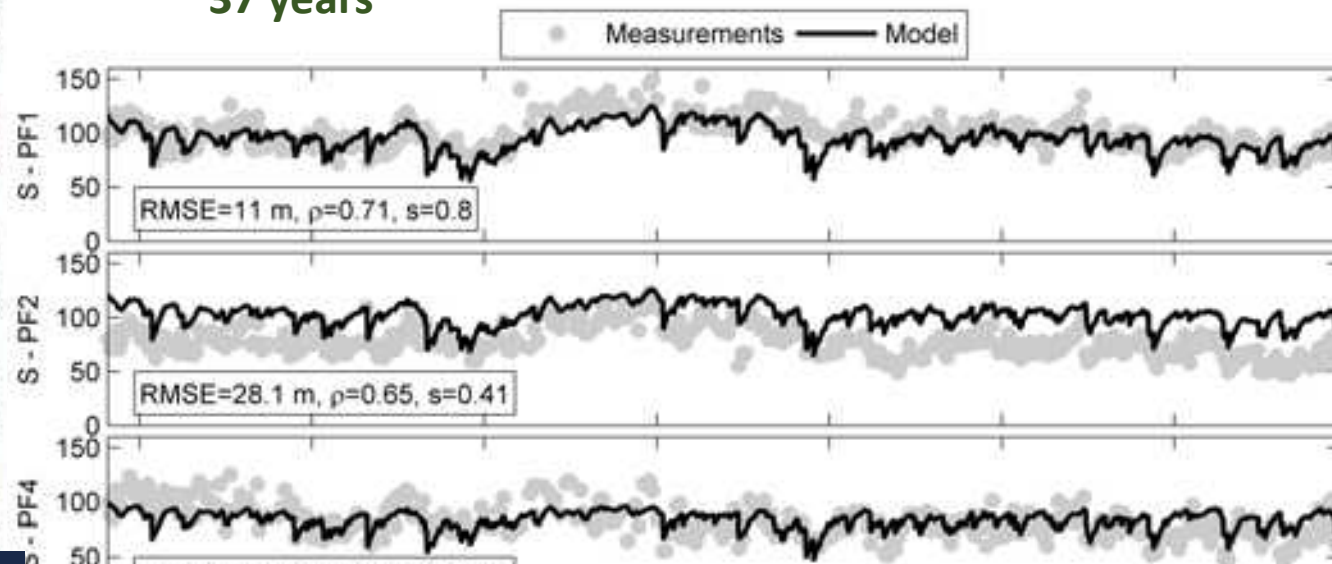
1

2

3

4

5


Narrabeen Beach
37 years

2016

Coastal Engineering 169 (2021) 103963

Contents lists available at [ScienceDirect](https://www.sciencedirect.com)

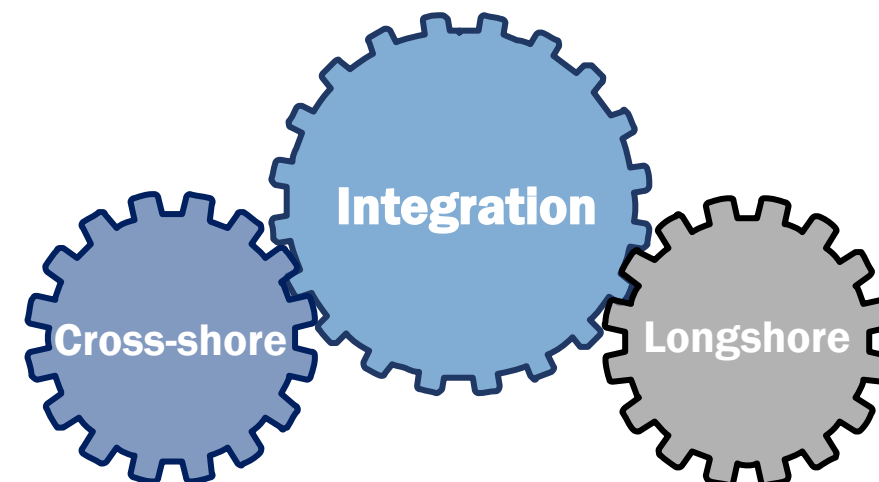
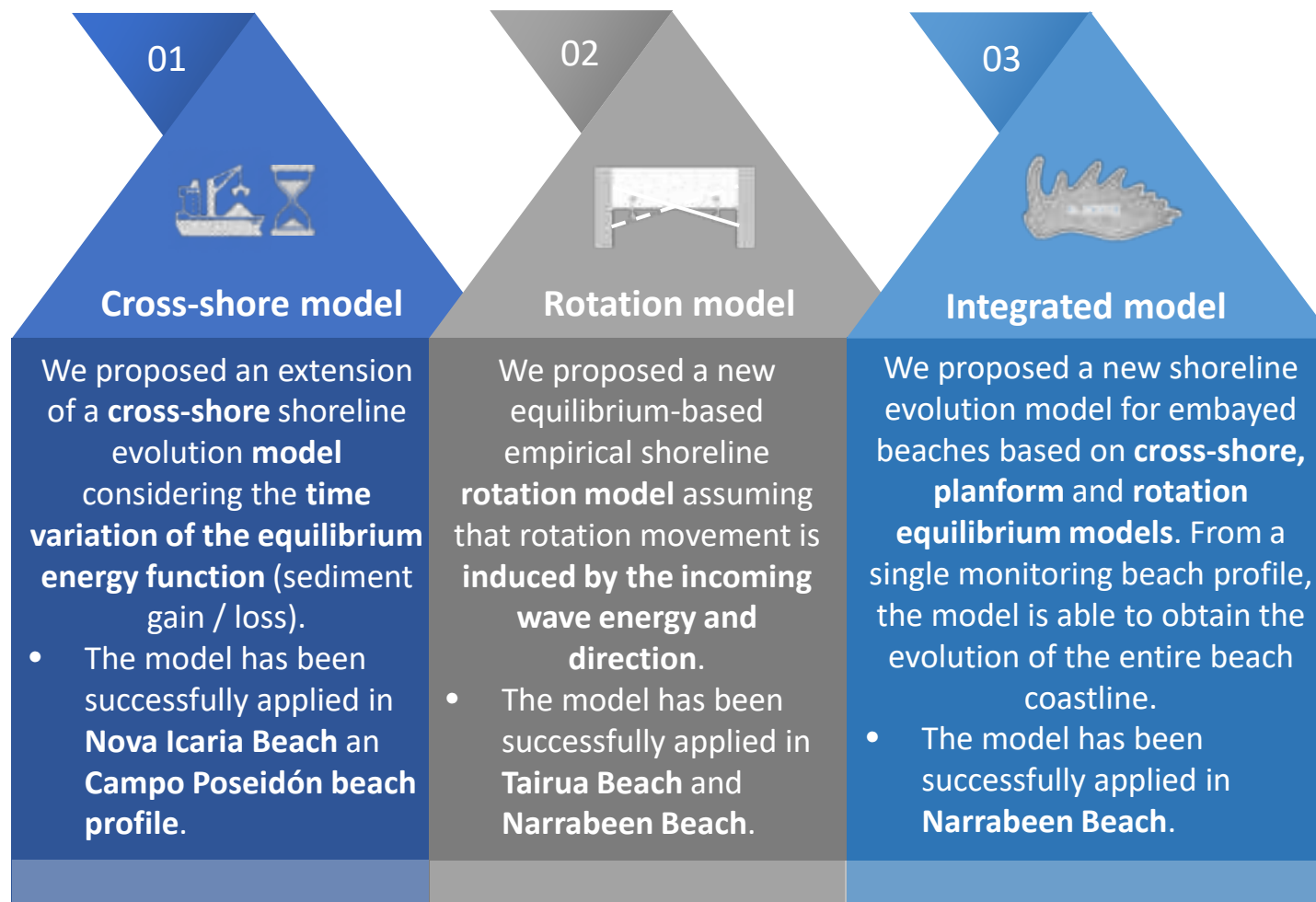
Coastal Engineering

journal homepage: www.elsevier.com/locate/coastaleng

A shoreline evolution model for embayed beaches based on cross-shore, planform and rotation equilibrium models

Camilo Jaramillo^{*}, Martínez Sánchez Jara, Mauricio González, Raúl Medina

Environmental Hydrology Institute, Universidad de Cantabria – Avda. Isabel Torres, 15, Parque Científico y Tecnológico de Cantabria, 39011, Santander, Spain



1

2

3

4

5

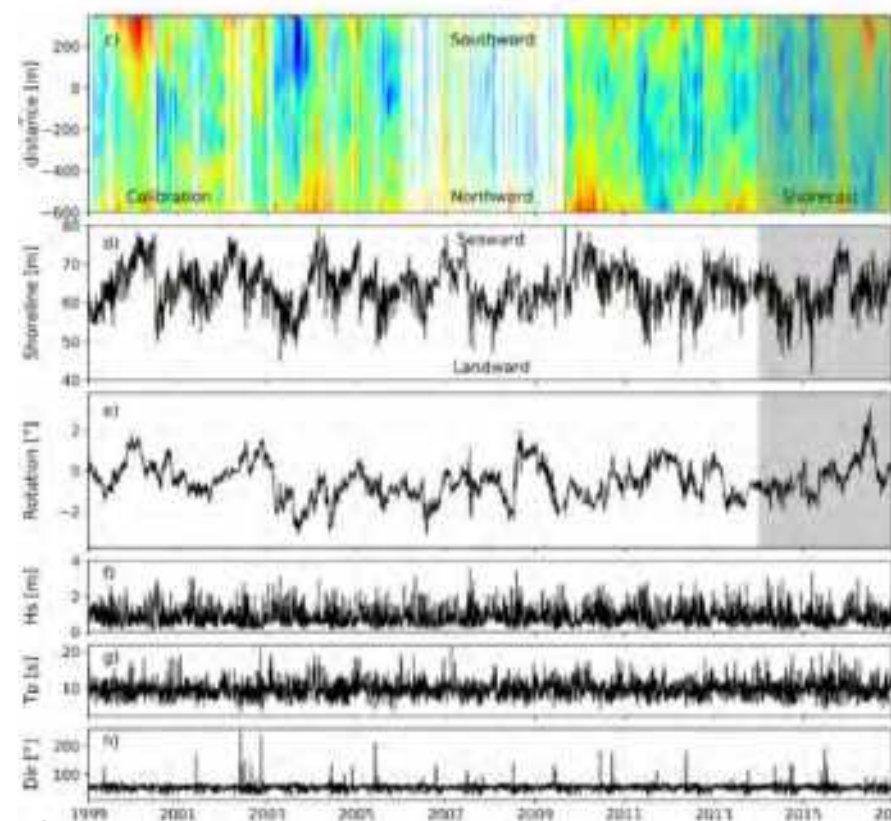
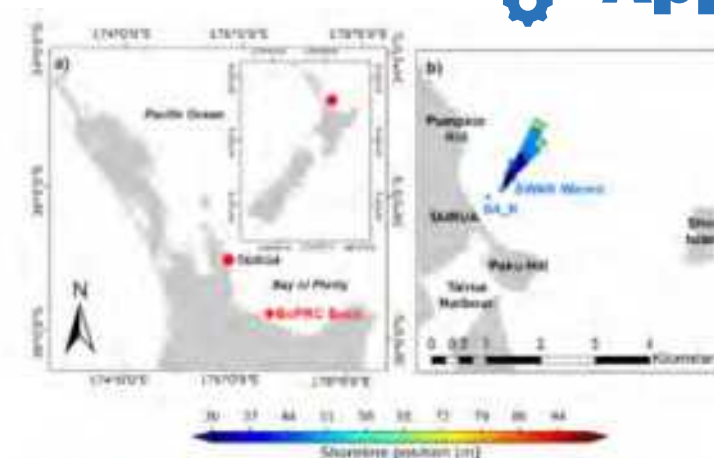
Shoreshop 1 (2018)

SCIENTIFIC
REPORTS
nature research

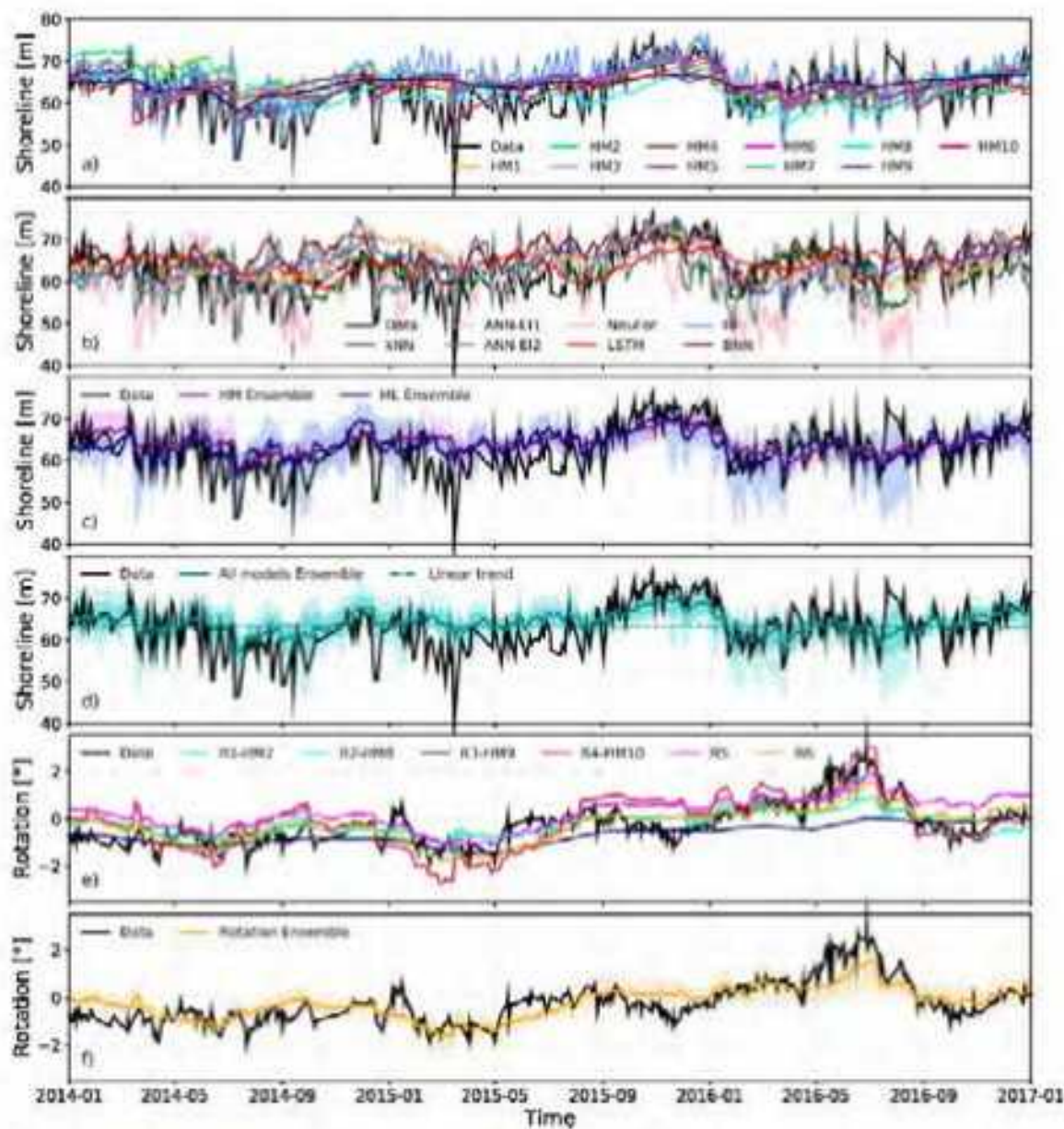
OPEN

Blind testing of shoreline evolution models

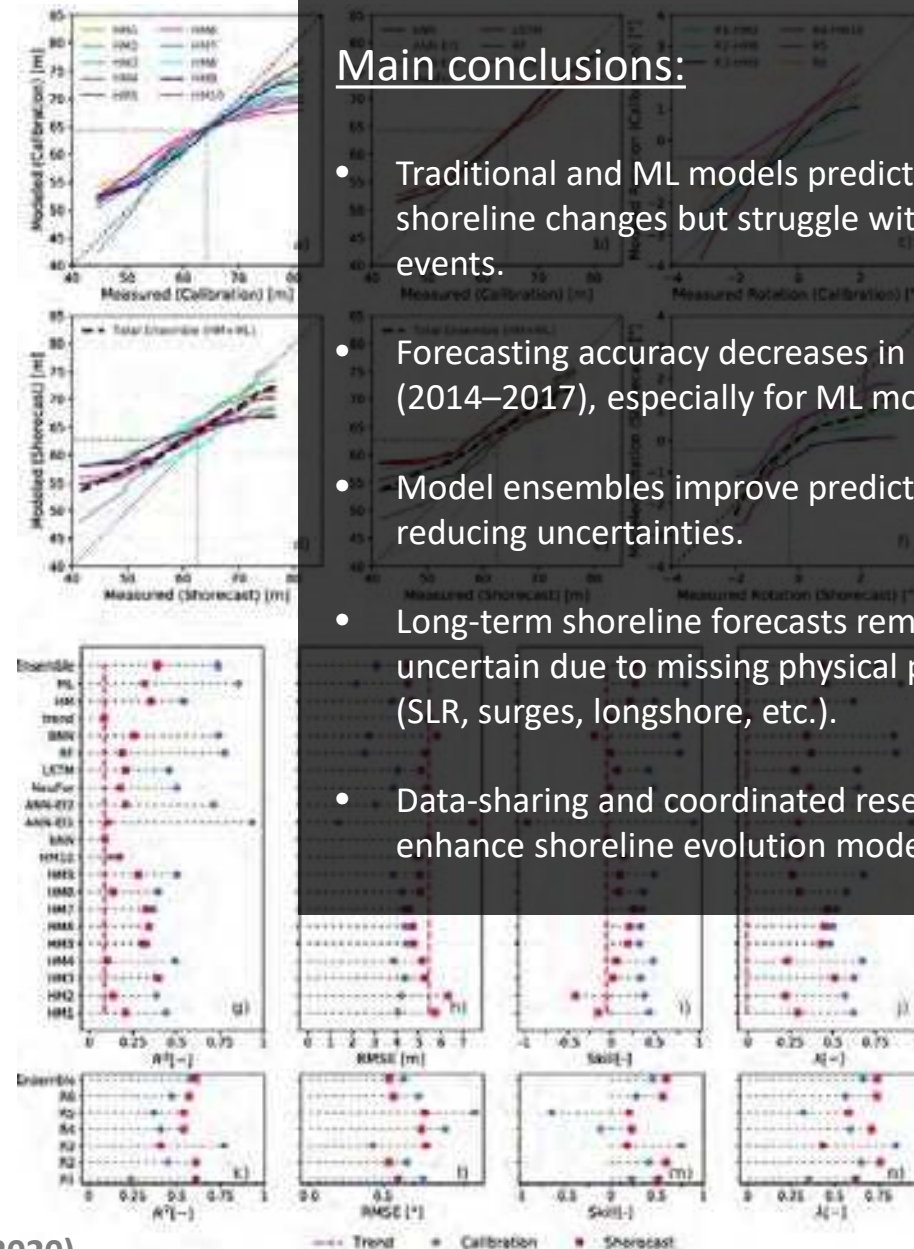
Jennifer Montañó^{1*}, Giovanni Coco¹, Jose A. A. Antolínez², Tomas Beuzen³, Karin R. Bryan⁴, Laura Cagigal^{1,2}, Bruno Castelle⁵, Mark A. Davidson⁶, Evan B. Goldstein⁷, Raimundo Ibaceta¹, Déborah Idier⁸, Bonnie C. Ludka⁹, Sina Masoud-Ansari¹, Fernando J. Méndez², A. Brad Murray¹⁰, Nathaniel G. Plant¹¹, Katherine M. Ratliff¹⁰, Arthur Robinet^{1,8}, Ana Rueda², Nadia Sénéchal⁵, Joshua A. Simmons³, Kristen D. Splinter¹, Scott Stephens¹², Ian Townsend¹³, Sean Vitousek^{14,15} & Kilian Vos³



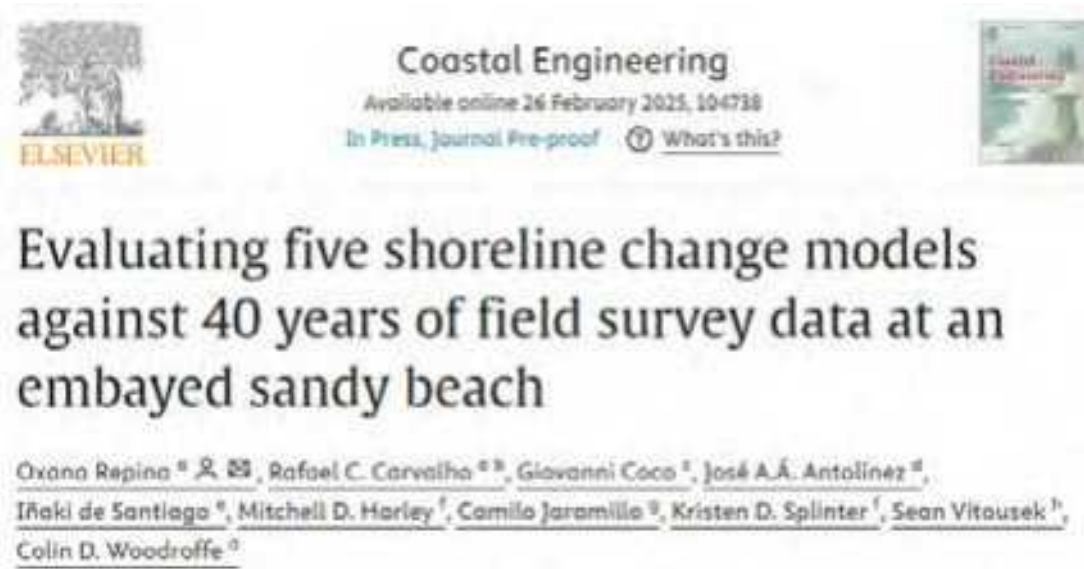
Montañó et al. (2020)



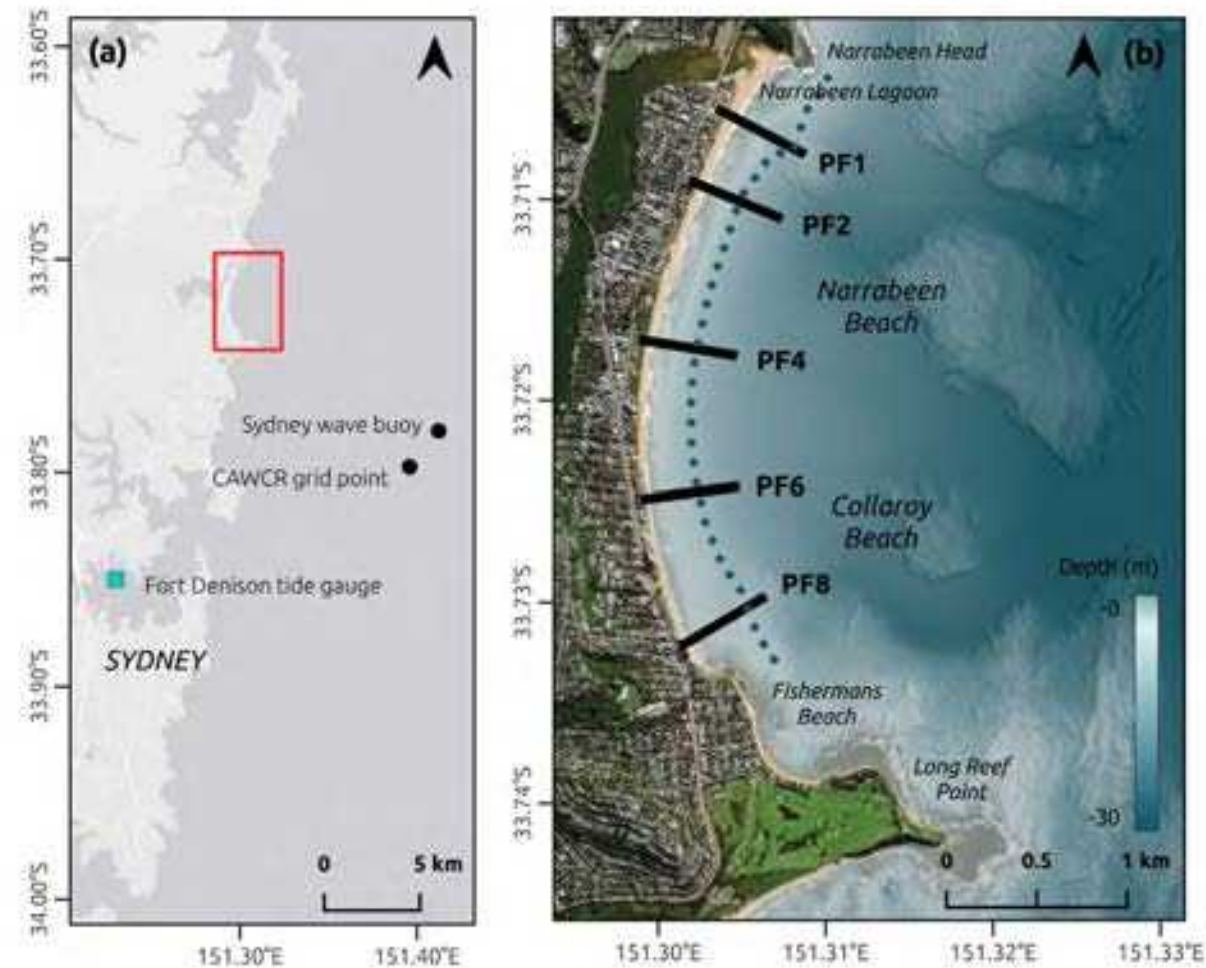
Montaño et al. (2020)

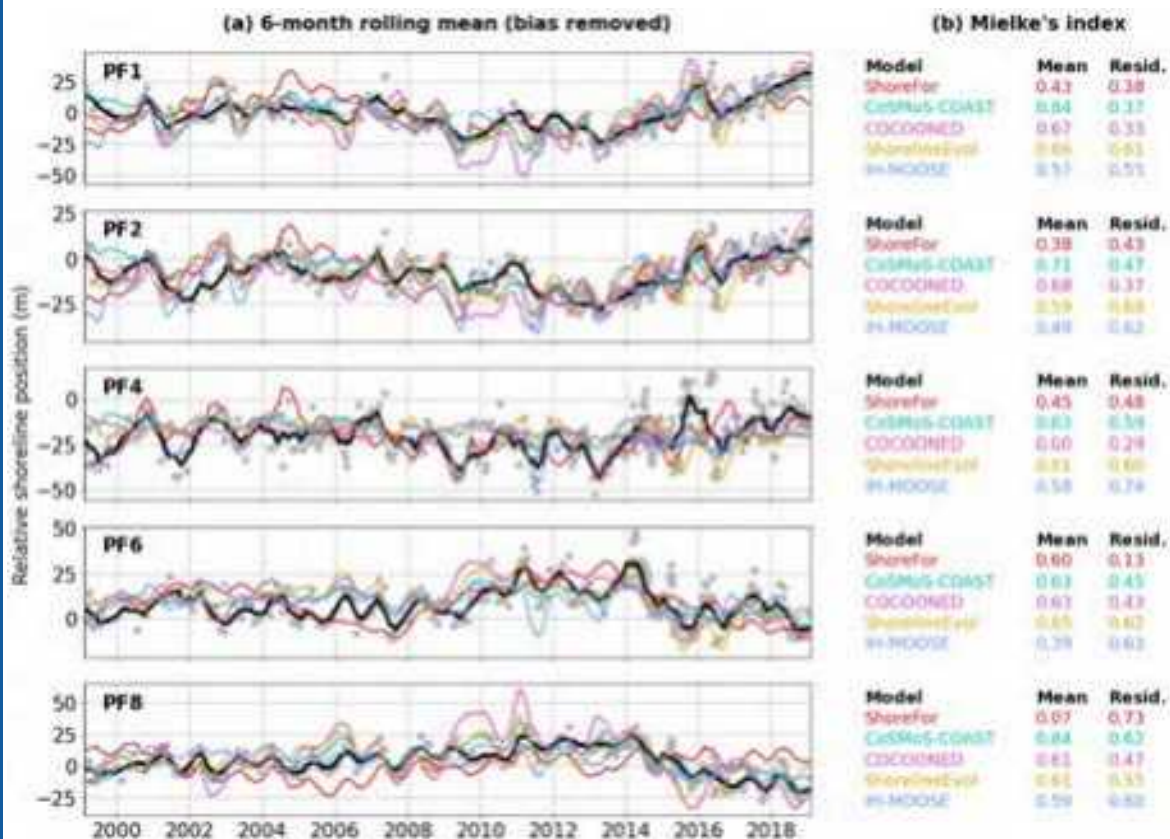


- ## Main conclusions:
- Traditional and ML models predict seasonal shoreline changes but struggle with extreme events.
 - Forecasting accuracy decreases in unseen data (2014–2017), especially for ML models.
 - Model ensembles improve predictions by reducing uncertainties.
 - Long-term shoreline forecasts remain highly uncertain due to missing physical processes (SLR, surges, longshore, etc.).
 - Data-sharing and coordinated research enhance shoreline evolution modeling.



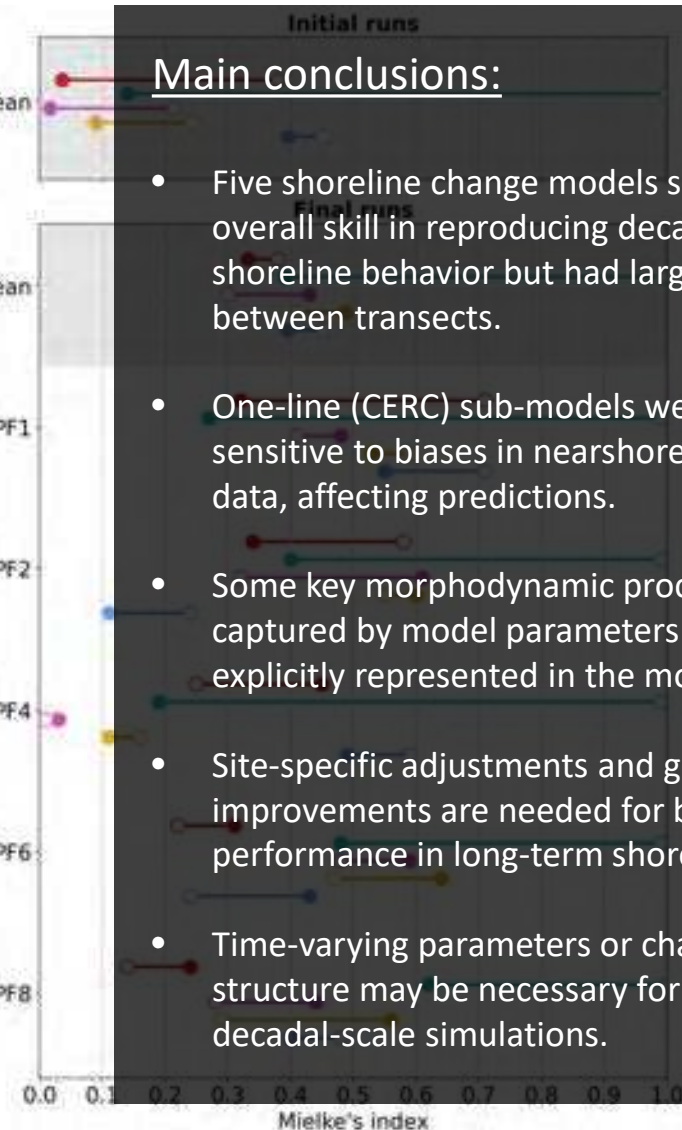
- **ShoreFor** - (Davidson et al., 2013; Splinter et al., 2014)
- **CoSMoS-COAST** - (Vitousek et al., 2017, 2023)
- **COCOONED** - (Antolínez et al., 2019)
- **ShorelineEvol** - (de Santiago et al., 2021)
- **IH-MOOSE** - (Jaramillo et al., 2021)





Main conclusions:

- Five shoreline change models showed similar overall skill in reproducing decadal-scale shoreline behavior but had large variability between transects.
- One-line (CERC) sub-models were highly sensitive to biases in nearshore wave direction data, affecting predictions.
- Some key morphodynamic processes were captured by model parameters rather than explicitly represented in the models.
- Site-specific adjustments and general improvements are needed for better model performance in long-term shoreline evolution.
- Time-varying parameters or changes in model structure may be necessary for reliable decadal-scale simulations.



1

2

3

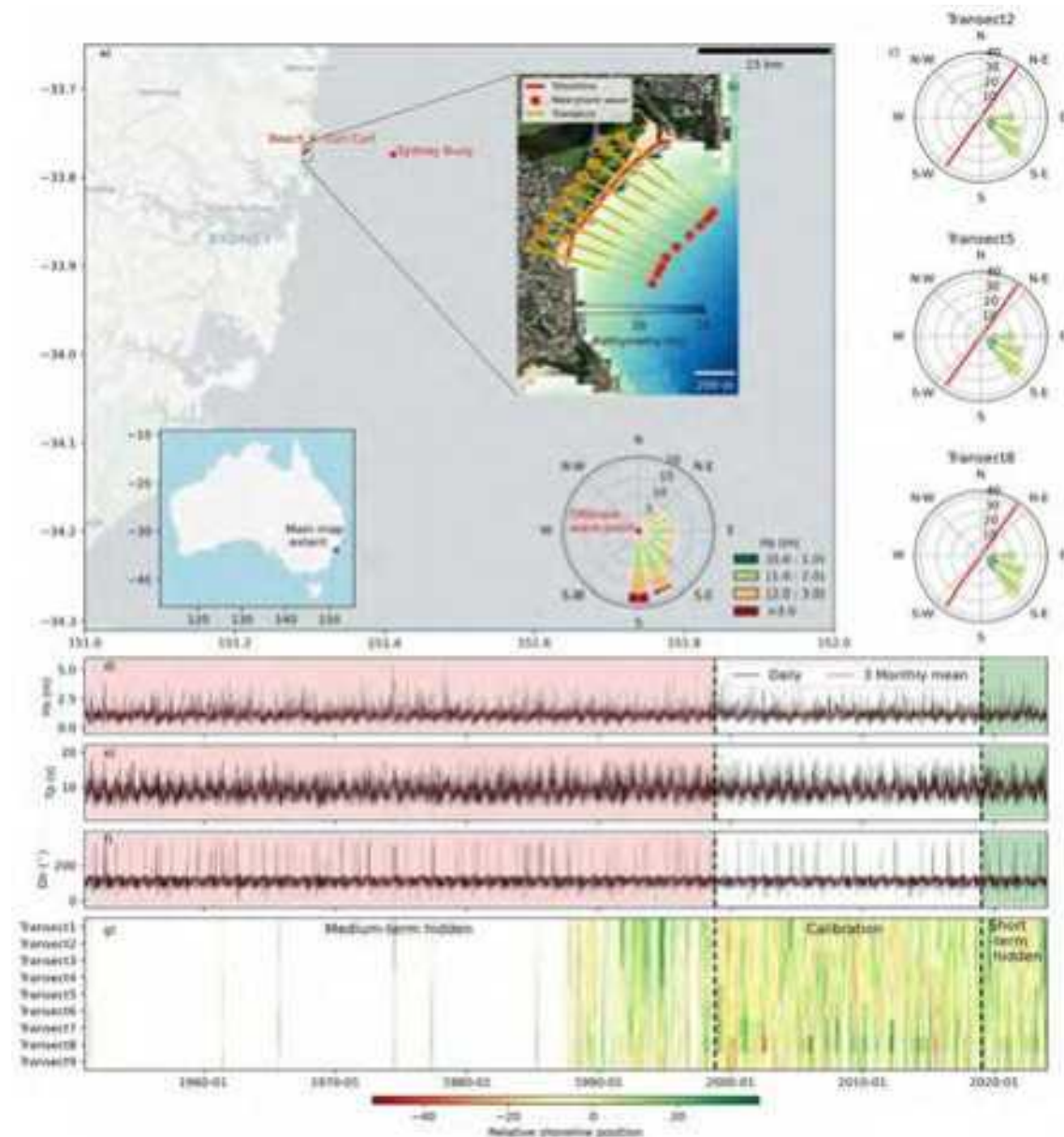
4

5

Shoreshop 2 (2024)

Benchmarking shoreline prediction models over multi-decadal timescales

Yongjing Mao^{1*}, Kristen D. Splinter¹, Giovanni Coco², Sean Vitousek³, Jose A. A. Antolinez⁴, Georgios Azorakos⁵, Masayuki Banno⁶, Clément Bouvier⁷, Karin Bryan², Laura Cagigal⁸, Kit Calcraft¹, Bruno Castelle⁵, Xinyu Chen⁹, Maurizio D'Anna^{2,10}, Lucas de Freitas Pereira¹¹, Iñaki de Santiago¹², Aditya N. Deshmukh¹, Bixuan Dong¹, Ahmed Elghandour¹³, Amirmahdi Gohari², Eduardo Gomez-de la Peña², Mitchell D. Harley¹, Michael Ibrahim¹⁴, Déborah Idier¹⁵, Camilo Jaramillo Cardona¹¹, Changbin Lim¹¹, Ivana Mingo⁵, Julian O'Grady¹⁶, Daniel Pais^{17, 18}, Oxana Repina¹⁹, Arthur Robinet⁷, Dano Roelvink^{4, 13, 20}, Joshua Simmons²¹, Erdinc Sogut²², and Katie Wilson¹



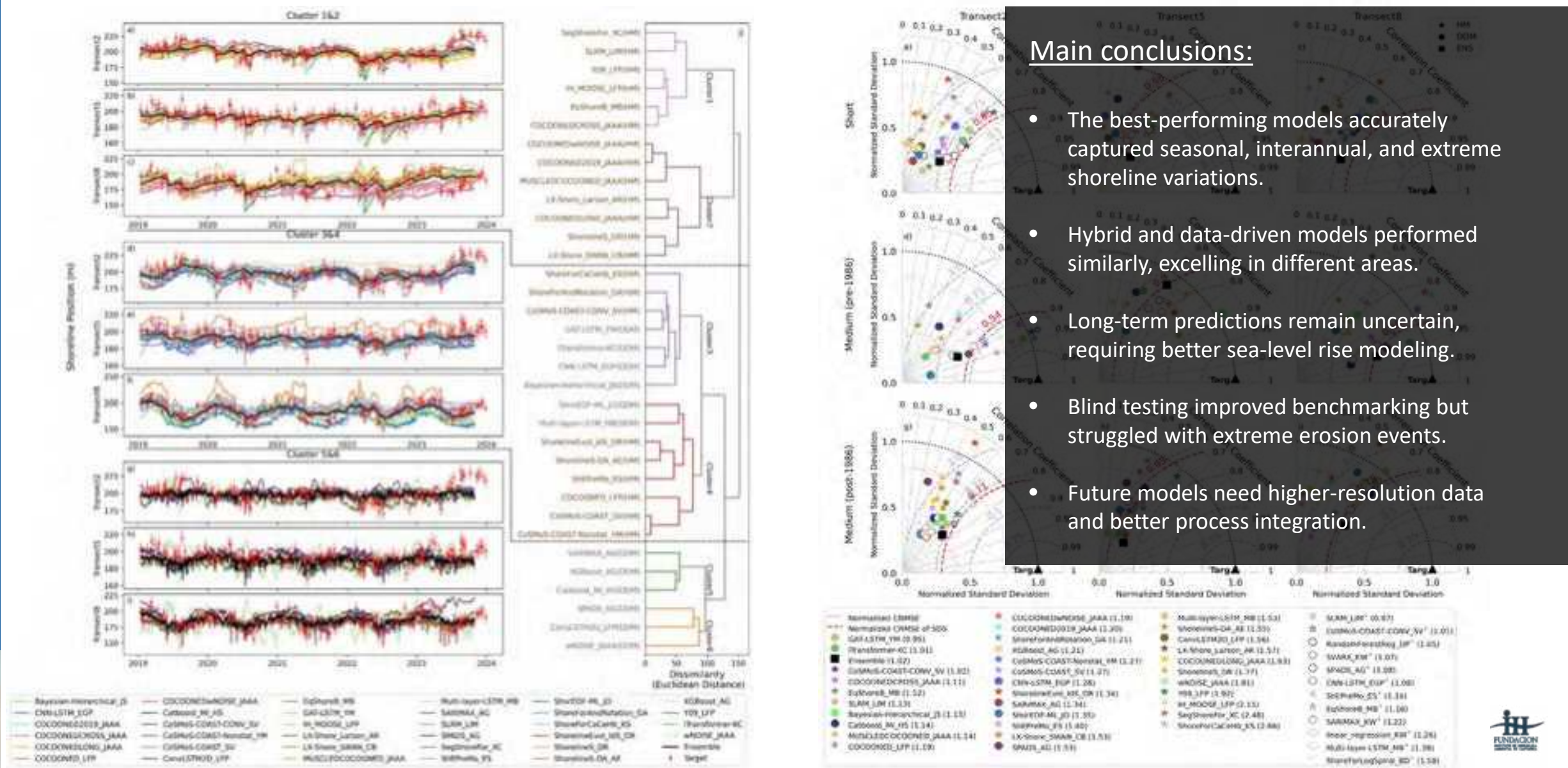
1

2

3

4

5



1

2

3

4

5



GOBIERNO
de
CANTABRIA



50 UC
Universidad de Cantabria



CSIC
CONSEJO SUPERIOR DE INVESTIGACIONES CIENTÍFICAS



INSTITUTO
ESPAÑOL DE
OCEANOGRAFÍA



IHSET

Shoreline Evolution Tools



Financiado por
la Unión Europea
NextGenerationEU



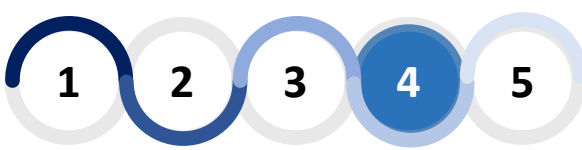
Plan de
Recuperación,
Transformación
y Resiliencia



GOBIERNO
de
CANTABRIA

40 años de autonomía





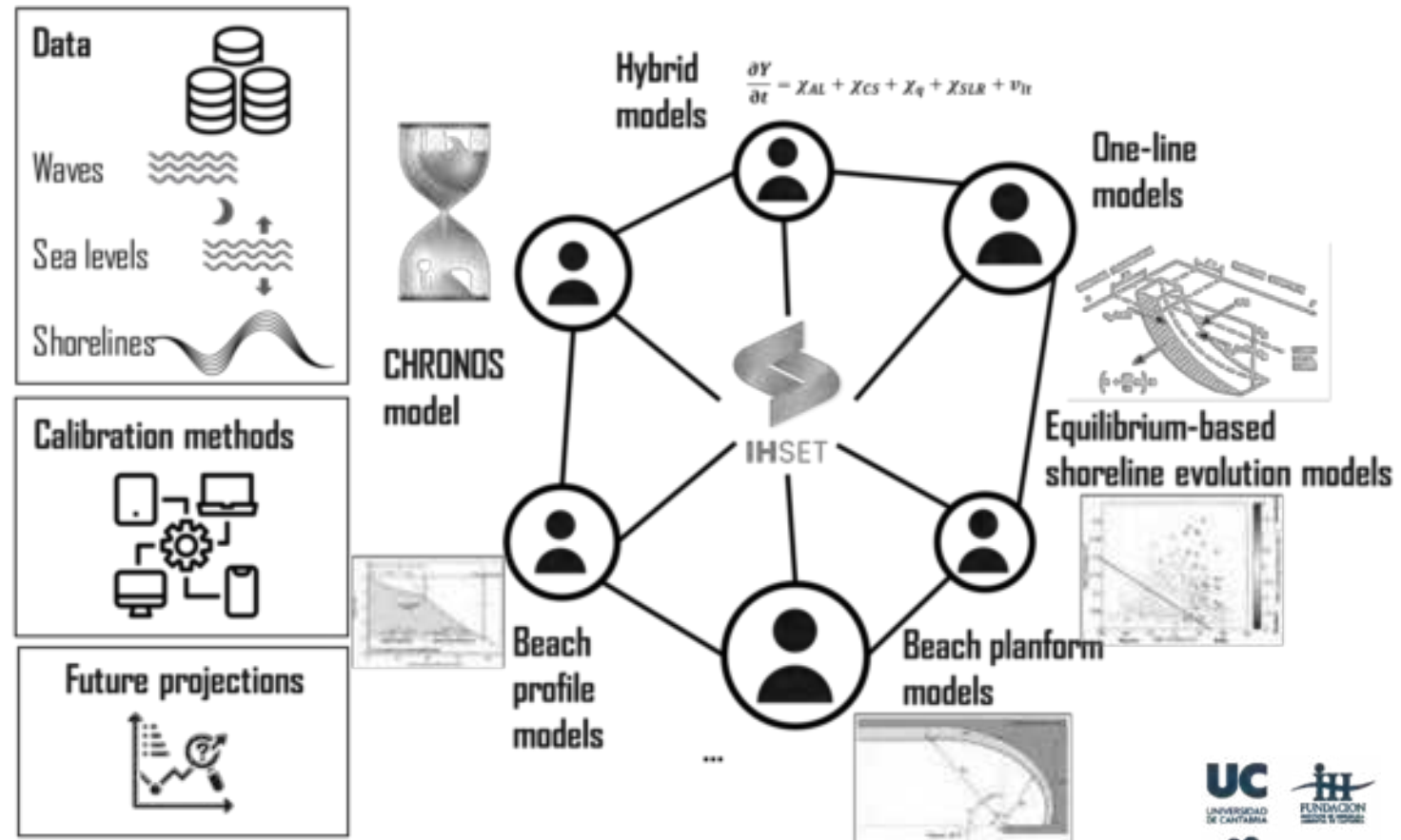
Objective:

Develop the **Shoreline Evolution Tools system, IH-SET**—a versatile tool designed to enable engineers and coastal managers to conduct morphodynamic studies at varying spatial and temporal scales. This system can be applied within the context of project development or the assessment of a beach as a distinct physiographic unit.

Motivation

The Coastal Group at IHCantabria has spent years researching new proposals for morphodynamic models. Two primary needs have emerged that require attention:

- 1) The creation of a unified system for shoreline morphodynamic models, enabling users to select and implement the most suitable methodology quickly based on the project's scope and goals.
- 2) Increased research efforts to develop a shoreline evolution model that integrates cross-shore and longshore processes while ensuring sediment conservation.



Contents - IH-SET





Ana M. Bernabeu Tello



Marine Geology 197 (2003) 95–116

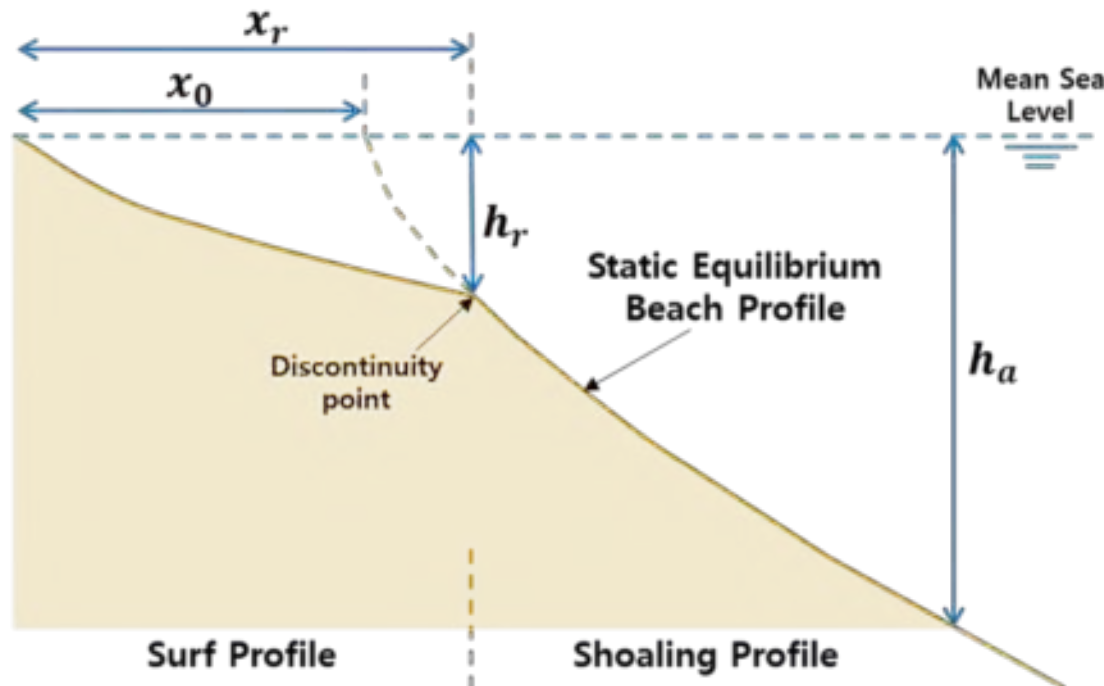
A morphological model of the beach profile integrating wave and tidal influences

A.M. Bernabeu^{a,*}, R. Medina^b, C. Vidal^b

^a Departamento de Geociencias Marítimas y O.T., Universidad de Vigo, 36200 Vigo, Spain

^b Ocean and Coastal Research Group, Departamento de Ciencias y Técnicas del Agua y del M. A., Universidad de Cantabria, 39005 Santander, Spain

Received 26 February 2002; accepted 6 March 2003



Surf profile :

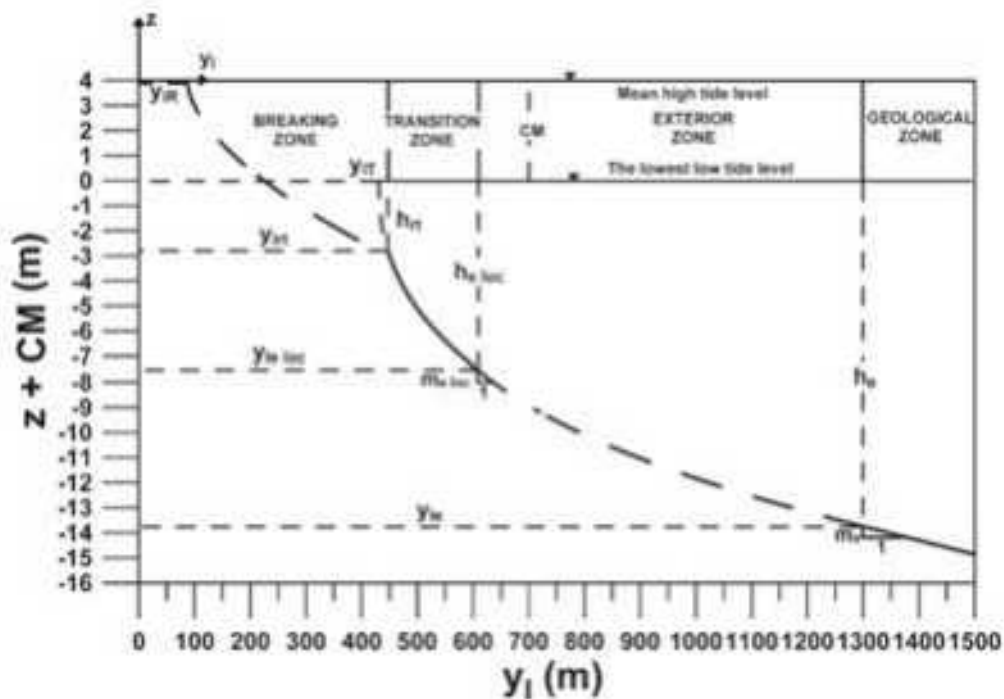
$$x = \left(\frac{h}{A}\right)^{3/2} + \frac{B}{A^{3/2}}h^3 \quad 0 \leq x \leq x_r$$

Shoaling profile :

$$X = x - x_0 = \left(\frac{h}{C}\right)^{3/2} + \frac{D}{C^{3/2}}h^3 \quad x_r \leq x \leq x_a$$



**Maria Soledad Requejo
Landeira**



Coastal Engineering 55 (2008) 1004–1008



Contents lists available at ScienceDirect

Coastal Engineering

journal homepage: www.elsevier.com/locate/coasteng



Development of a medium–long term beach evolution model

S. Requejo ^a, R. Medina, M. González

^a Ocean and Coastal Research Group, Environmental Hydraulics Institute IH Cantabria, IITEX Consorcio, Cádiz y Puerto, Avda. de los Capitanes s/n, 39005 Santander, Spain

1

2

3

4

5



**Mauricio González
Rodríguez**



**Raúl Medina
Santamaría**

González and Medina (2001) proposed the methodology for estimating the location of the down-coast limit distance R_o from the control point as a function of $\alpha_{\min}(=90^\circ-\beta)$



Coastal Engineering 43 (2001) 209–225



**Coastal
Engineering**

An International Journal for Coastal,
Harbour and Offshore Engineers

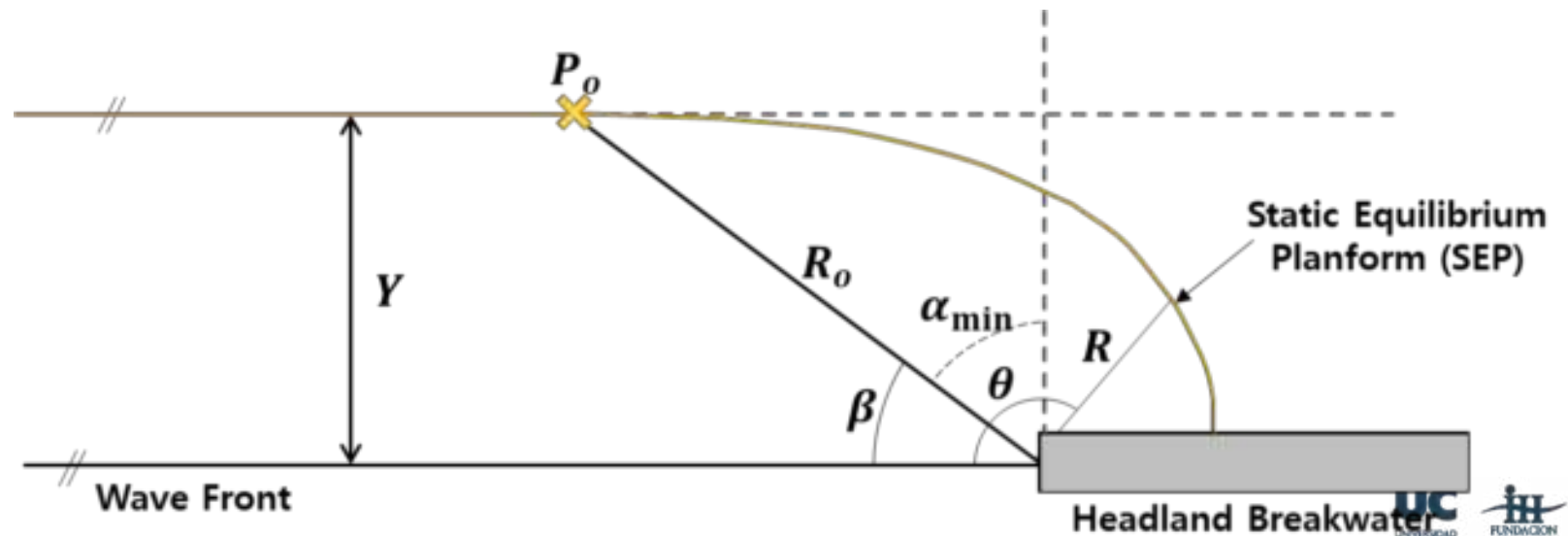
www.elsevier.com/locate/coastaleng

On the application of static equilibrium bay formulations to natural and man-made beaches

Mauricio González*, Raul Medina

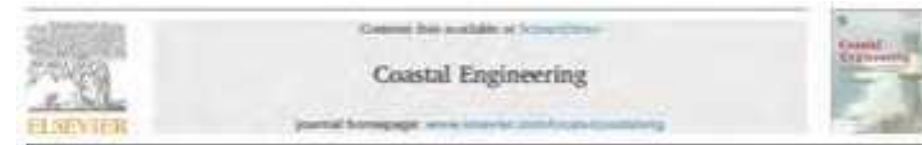
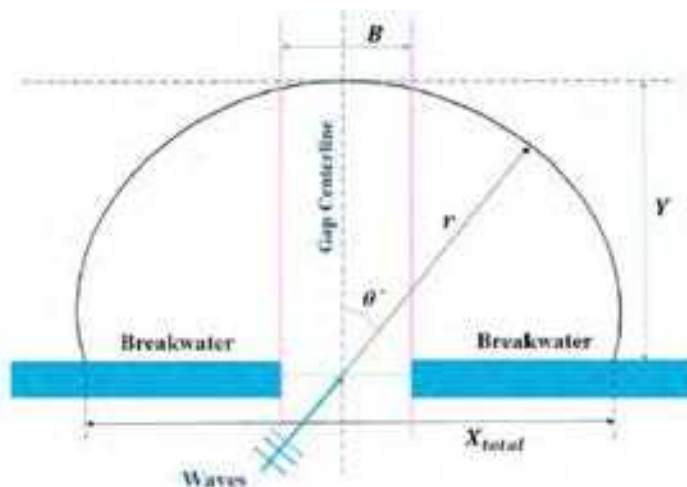
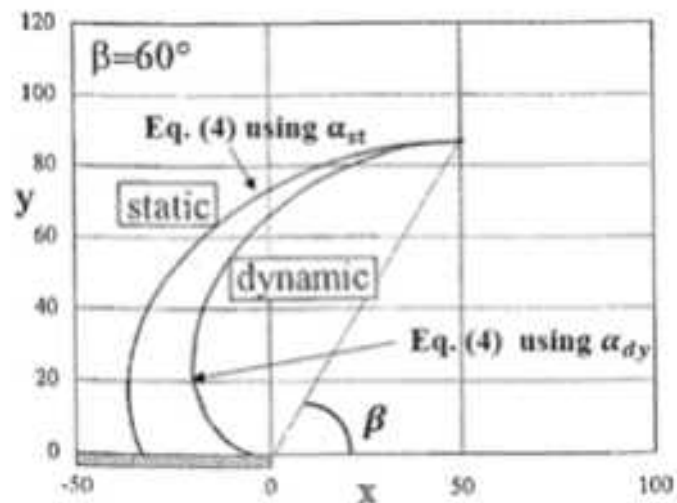
Ocean and Coastal Research Group, Departamento Ciencias y Técnicas del Agua y del Medio Ambiente, Universidad de Cantabria, E.T.S. Ingenieros de Caminos, C. y P., Avda. de los Castros, s/n. 39005 Santander, Spain

Received 9 August 2000; received in revised form 2 April 2001; accepted 1 May 2001





Ahmed Ibrahim Abdelmagid Elshinnaway

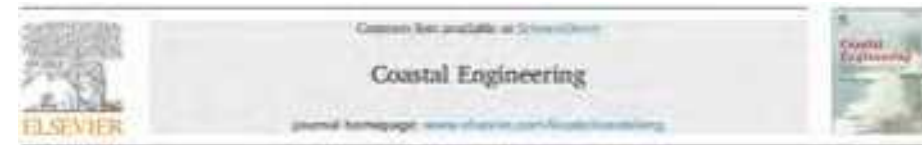


Dynamic equilibrium planform of embayed beaches: Part 1. A new model and its verification

Ahmed I. Elshinnaway^{a,b,*}, Raúl Medina^b, Mauricio González^b

^a Environmental Hydrology Institute – ICH, Universidad de Cantabria, Avda. Siles 15, 39011 Santander, Cantabria, Spain

^b Angewandte und Hydrologische Ingenieurwissenschaften, Faculty of Engineering, Tübingen University, 72076 Tübingen, Germany



Dynamic equilibrium planform of embayed beaches: Part 2. Design procedure and engineering applications

Ahmed I. Elshinnaway^{a,b,*}, Raúl Medina^b, Mauricio González^b

^a Environmental Hydrology Institute – ICH, Universidad de Cantabria, Avda. Siles 15, 39011 Santander, Cantabria, Spain

^b Angewandte und Hydrologische Ingenieurwissenschaften, Faculty of Engineering, Tübingen University, 72076 Tübingen, Germany



Equilibrium planform of pocket beaches behind breakwater gaps: On the shape of the equilibrium shoreline.

Ahmed I. Elshinnaway^{a,b,*}, Raúl Medina^b, Mauricio González^b

^a Angewandte und Hydrologische Ingenieurwissenschaften, Faculty of Engineering, Tübingen University, 72076 Tübingen, Germany

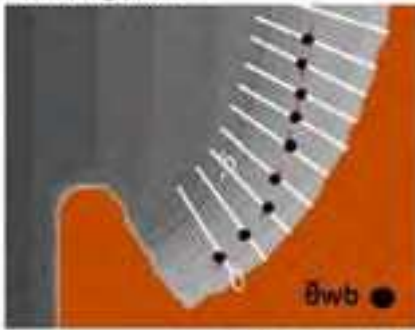
^b ICH Cantabria – Instituto de Hidráulica Ambiental de la Universidad de Cantabria, Avda. Siles 15, 39011 Santander, Spain



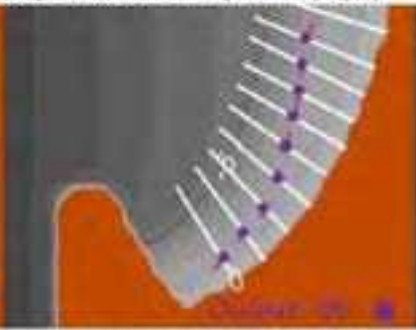
**June Gainza
Thalamas**



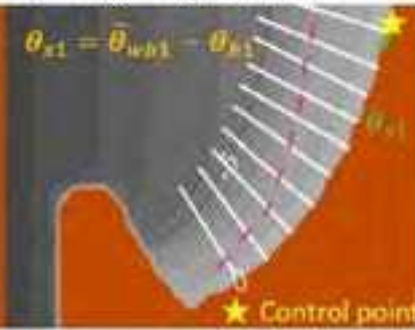
a) Wave characteristics at the breaking point



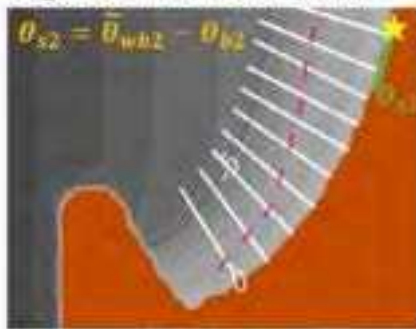
b) Equilibrium planform equation at each profile (eq.9)



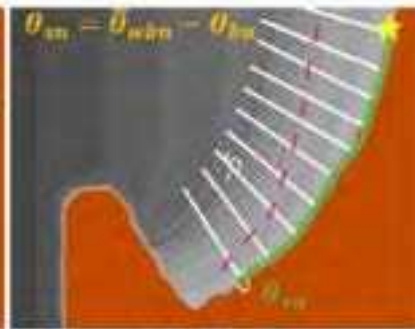
c) Shoreline angle (eq.15):
 $\theta_s = \bar{\theta}_{wb} - \theta_b$ per profile



d) Concatenation of the shoreline angle obtained at each profile



e) Final planform



Profile 1

Profile n

Gainza et al. (2018) proposed a process-based shape equation that is able to overcome the limitations that current models present and estimate the static equilibrium shoreline of complex bathymetry beaches. The equation is based on the hypothesis that a pocket beach gets its static equilibrium planform when the mean surf-zone longshore velocity averaged over a period of time is null in every point along the beach.

1

2

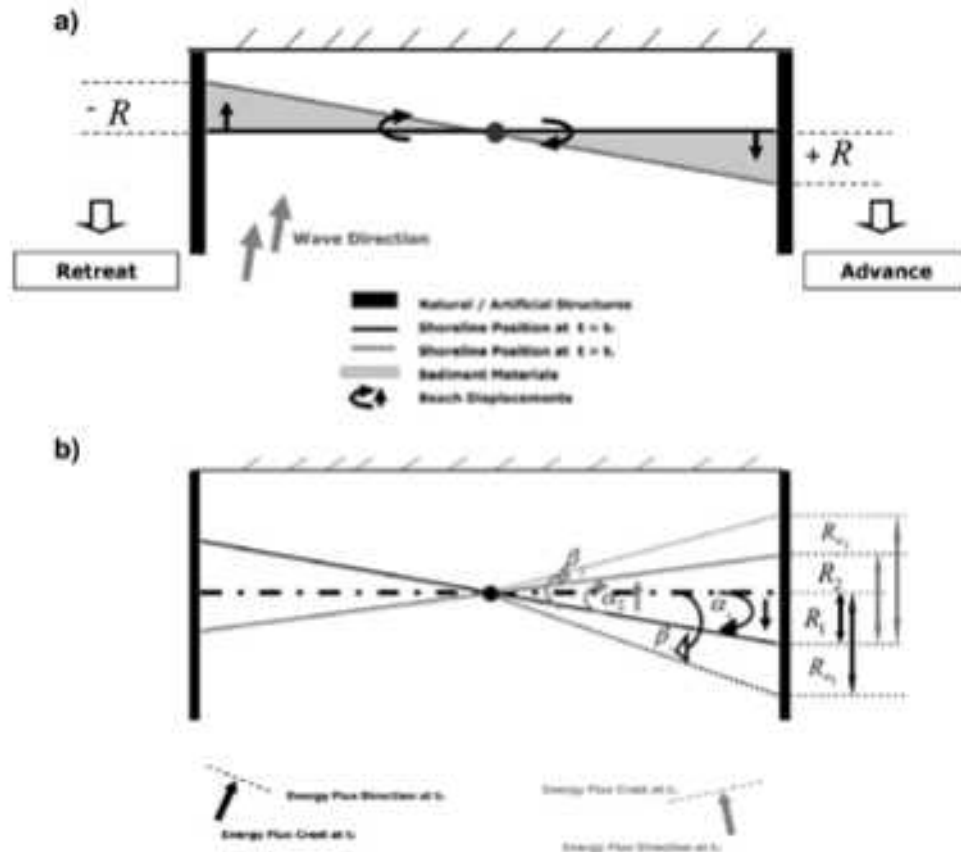
3

4

5



Imen Turki



An equilibrium model to predict shoreline rotation of pocket beaches

I. Turki ^{a,b,*}, R. Medina ^a, G. Coco ^a, M. Gonzalez ^a

^a Environmental Hydraulics Institute IH Cantabria, University of Cantabria, s/n, 39011 Santander, Spain

^b UMR CNRS 6143, Continental and Coastal Morphodynamics "MOC", University of Rouen, 76821 Mont-Saint-Aignan Cedex, France

Turki et al. (2013) proposed a shoreline evolution model for predicting the shoreline rotation considering that the shoreline response rate can be expressed as proportional to the difference between the instantaneous position and the equilibrium rotation.

$$\frac{dR(t)}{dt} = \omega \cdot (R_{\infty} - R(t))$$

1

2

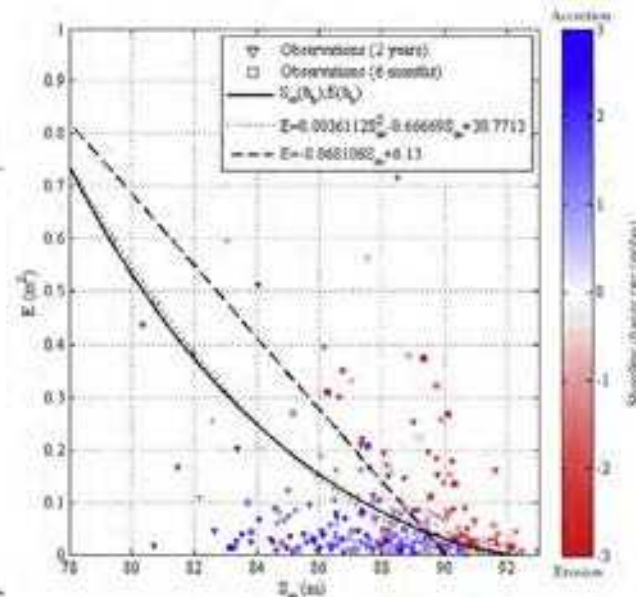
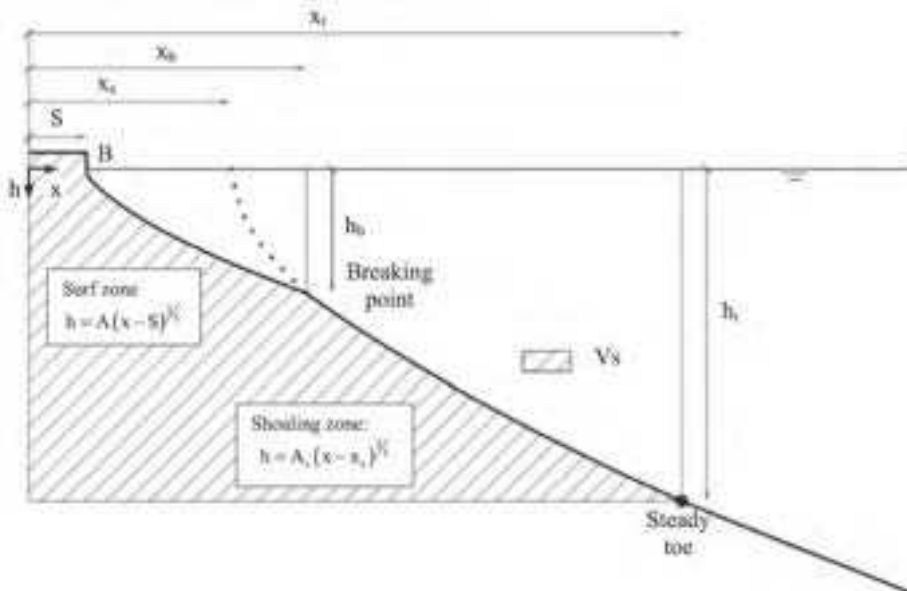
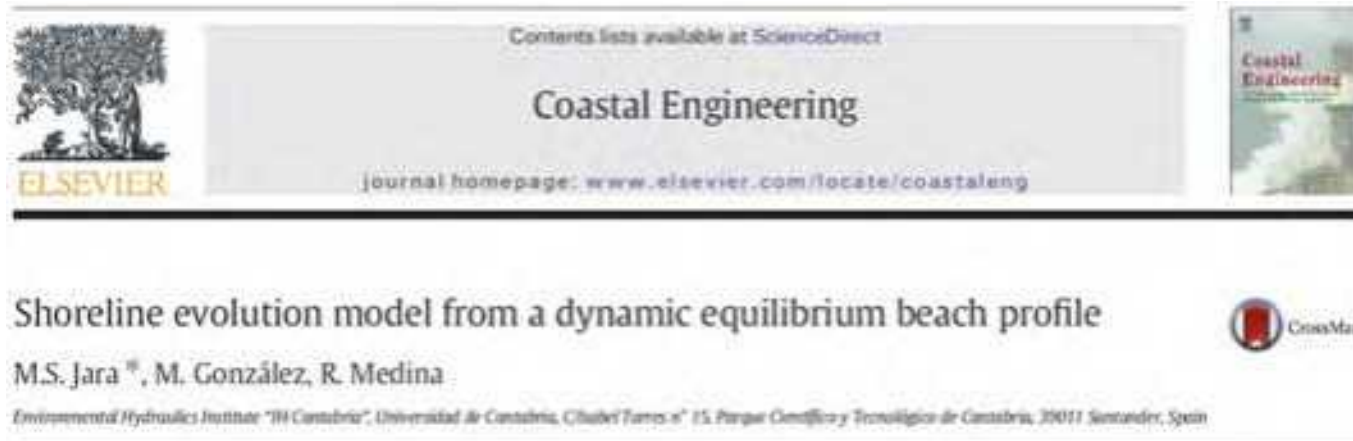
3

4

5



**Jara Martínez
Sánchez**



$$\frac{dS(t)}{dt} = C^{\pm} \cdot (E - E_{\infty}(S))$$

1

2

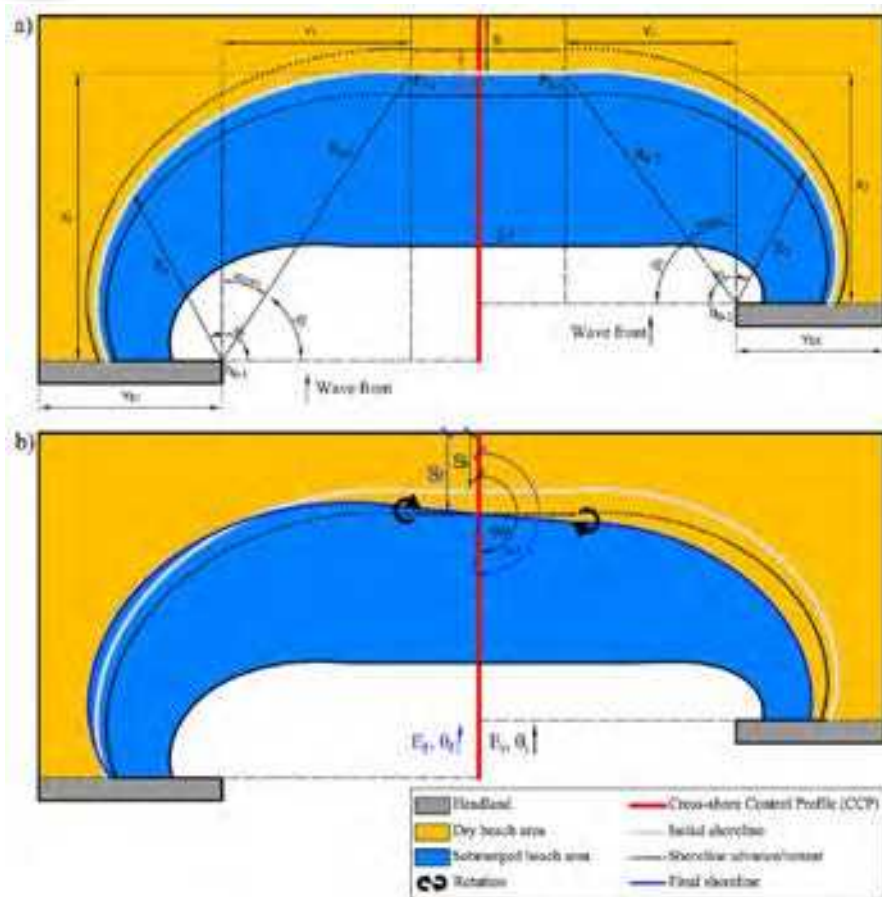
3

4

5



**Camilo Jaramillo
Cardona**



A shoreline evolution model considering the temporal variability of the beach profile sediment volume (sediment gain / loss)

Camilo Jaramillo^a, Martínez Sánchez-Jara, Mauricio González, Raúl Medina

^a Environmental Hydraulics Institute, Universidad de Cantabria, Avda. Siles 13, 39015 Santander, Spain



An equilibrium-based shoreline rotation model

Camilo Jaramillo^{a,*}, Mauricio González^a, Raúl Medina^a, İsmail Turki^b

^a Environmental Hydraulics Institute, Universidad de Cantabria – Avda. Siles 13, 39015 Santander, Spain
^b IMR CNRS 4440 Continental and Coastal Morphodynamics, M2C, University of Brest, 29231, Morlaix-Argentan Cedex, France



A shoreline evolution model for embayed beaches based on cross-shore, planform and rotation equilibrium models

Camilo Jaramillo^a, Martínez Sánchez-Jara, Mauricio González, Raúl Medina

^a Environmental Hydraulics Institute, Universidad de Cantabria – Avda. Siles 13, 39015 Santander, Spain

1

2

3

4

5



Erica Pellón de Pablo

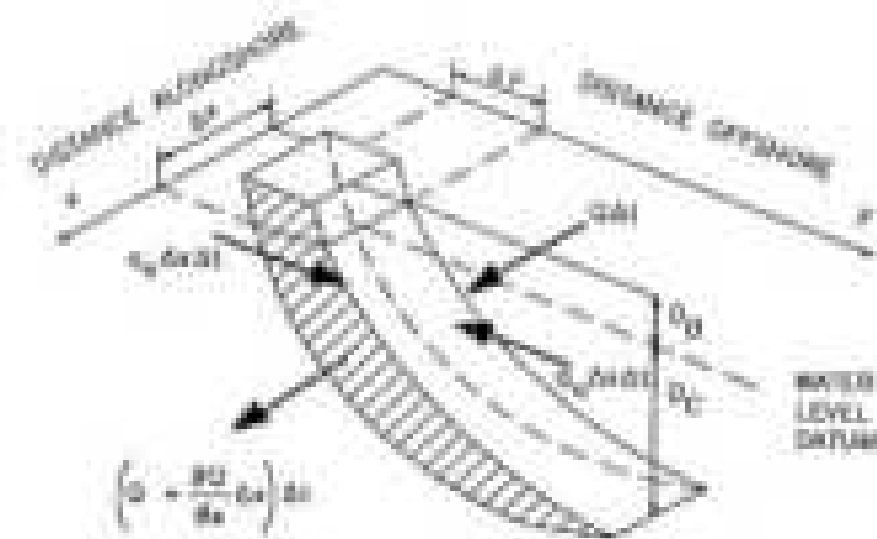
XV Jornadas Españolas de Ingeniería de Costas y Puertos
Torremolinos, Málaga 8 y 9 de mayo de 2019

CHRONOS: Modelo de evolución costera en el medio y largo plazo

Pellón, E.^a; Jara, M.S.^a; González-Ondina, J.^b; González, M.^a; Medina, R.^a y Garnier, R.

^aInstituto de Hidráulica Ambiental (IHCantabria), Universidad de Cantabria, Santander, España ^bPlymouth Ocean Forecasting Center

Email: pellone@unican.es



CHRONOS MODEL

1

2

3

4

5

Research under development within the project:



Lucas de Freitas Pereira

Modeling shoreline evolution on medium- to long-term scales integrating longshore and cross-shore processes

PhD: 12/2022 - 2026



Mayowa Abdusalam

Forecasting the shoreline rotation variability at different beaches around the world

MSc: 01/2024 – 08/2024



Estefanía Giraldo

Validación de modelos de evolución de costa en playas del litoral valenciano

MSc: 04/2024 – 09/2024

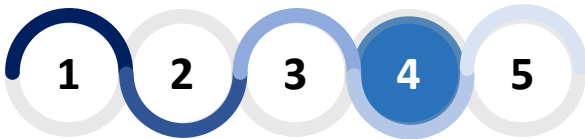


Carlos Muñoz Toaboaba

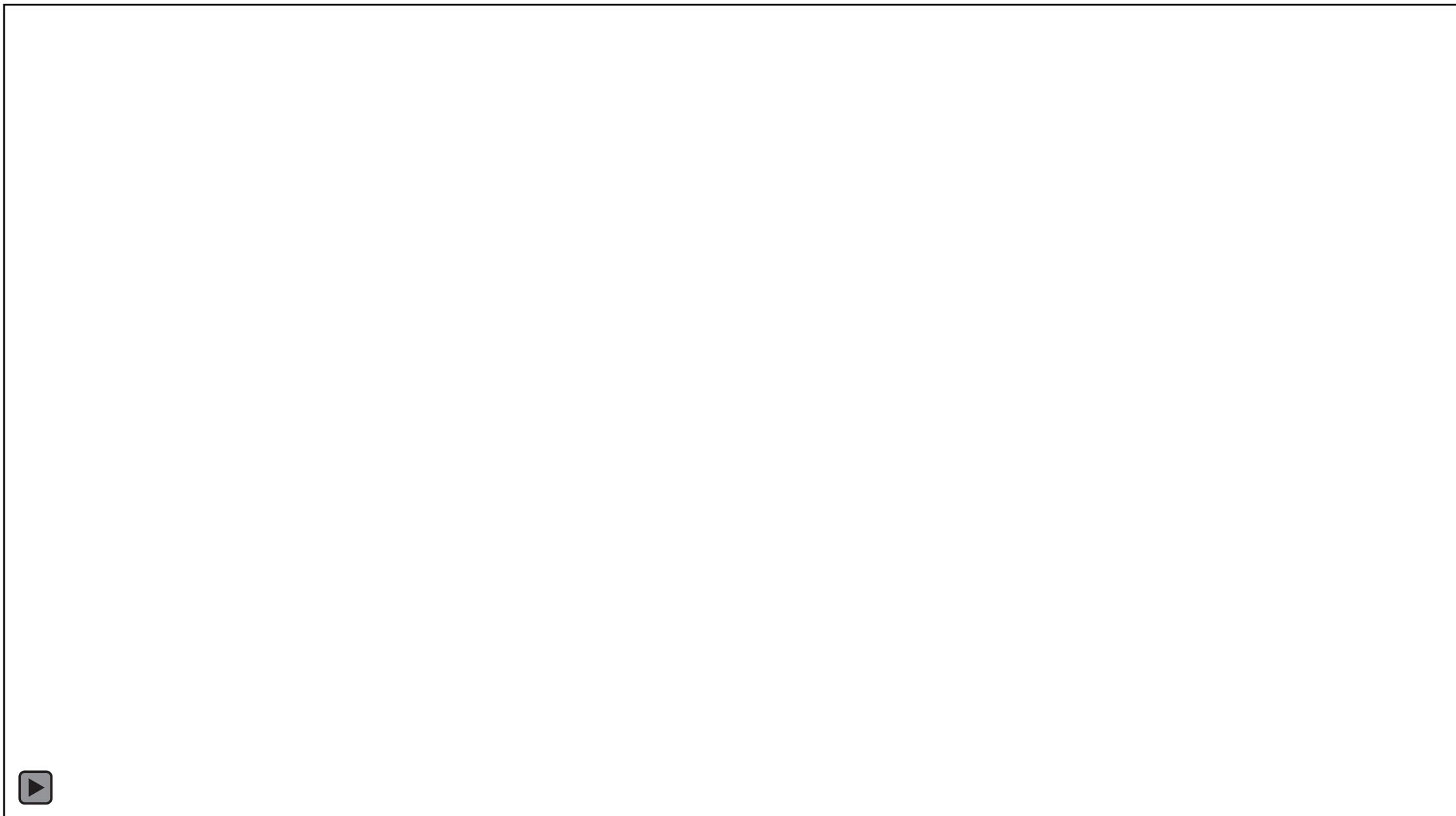
Modelo de evolución de línea de costa IH-MOOSE considerando distintos enfoques de transporte de sedimentos

MSc: 04/2024 – 09/2024





Research under development within the project:



Research under development within the project:



CoastSnap
community beach monitoring

Help record our changing coastline

How to get involved:

- 1 Take photo in adjacent phone cradle
- 2 Submit photo here:

Regular visitor? Become a CoastSnap Volunteer!
Download the free CoastSnap App (available on any App store) and take regular snaps at this site!

#CoastSnapPenneshaw
Scan the QR code to contribute your snap

UNSW Water Research Laboratory

UNSW

KANGAROO ISLAND TOURISM AUTHORITY

CoastSnap is a global citizen science project to capture changing coastlines. For more info, visit: www.coastsnap.com



CoastSnap
community beach monitoring

#CoastSnapCaves

How to get involved:

1. Take photo in cradle above
2. Submit photo here:

Regular visitor? Become a CoastSnap Volunteer!
Download the free CoastSnap App and help measure our changing coastline.

www.coastsnap.com



CoastSnap
community beach monitoring

Our dynamic coastline

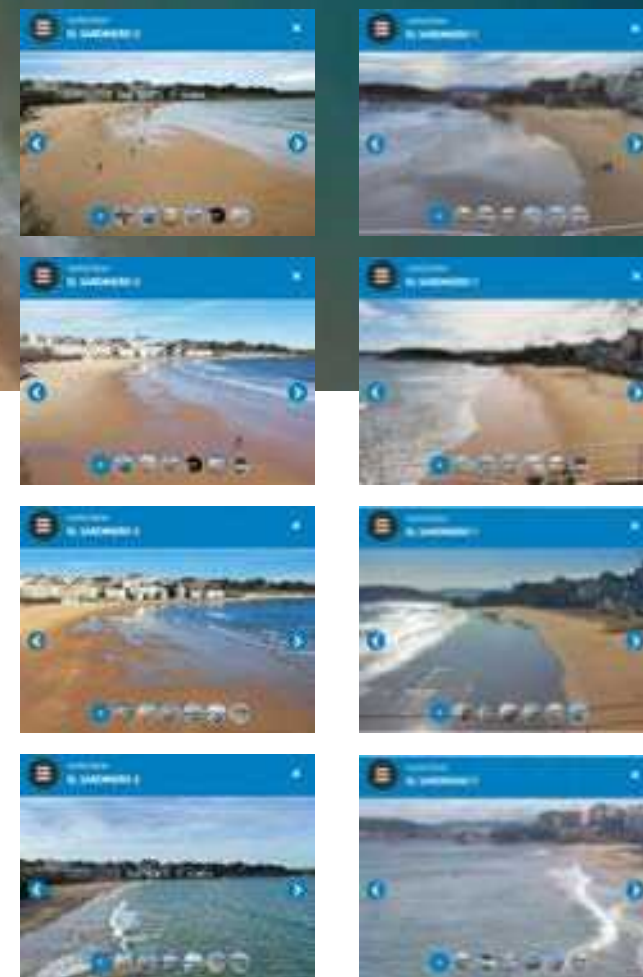
Our coastlines are always changing. Powerful storms, waves and offshore, which typically retreats during calmer conditions. Your snaps help us to understand and manage coastal environments for future generations.

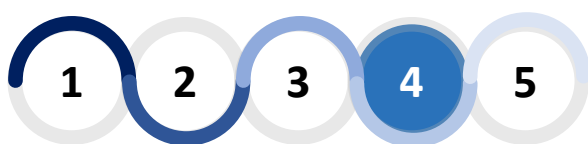
CoastSnap is a community beach monitoring technology that uses smartphones to monitor coastal change.

UNSW



Research under development within the project:



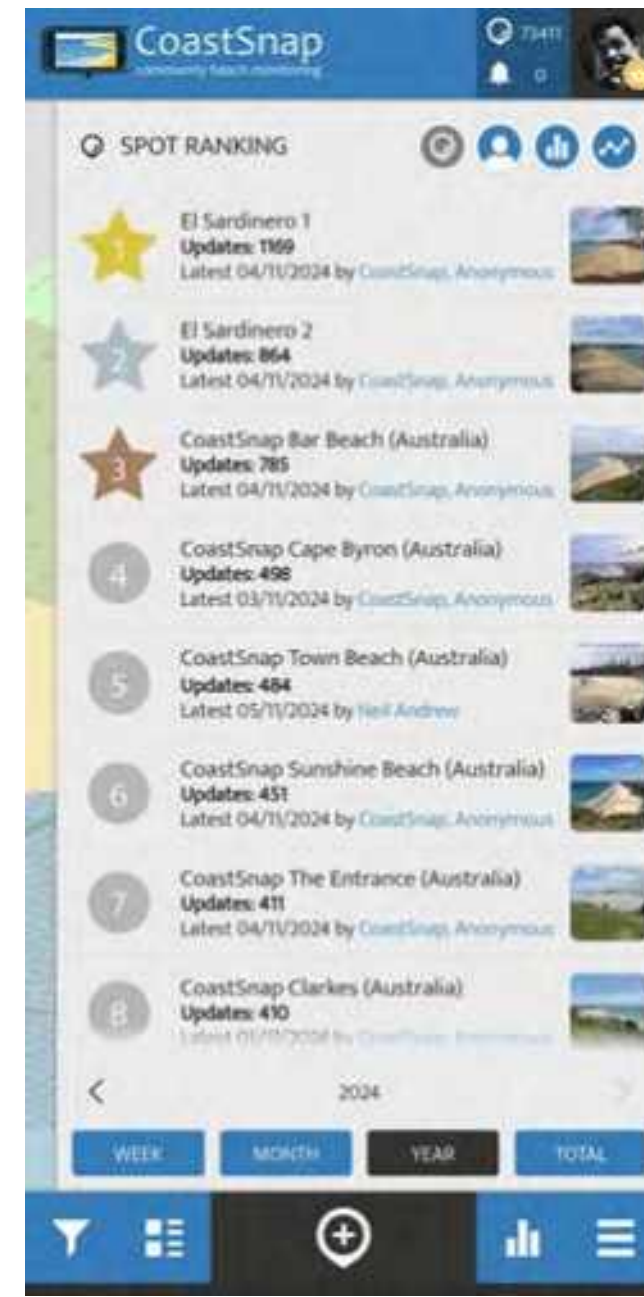


Research under development within the project:



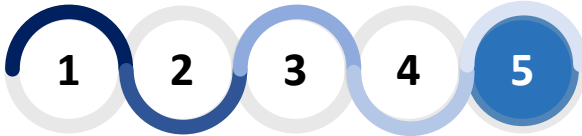
CoastSnap
community beach monitoring

Nov 2024



Global Equilibrium Shoreline Evolution Models (GESEM) network to predict medium to long-term beach change





Who? What?



17 October 2022

Initial call to join the GESEM network



The GESEM (Global Equilibrium Shoreline Evolution Models) network

Who?

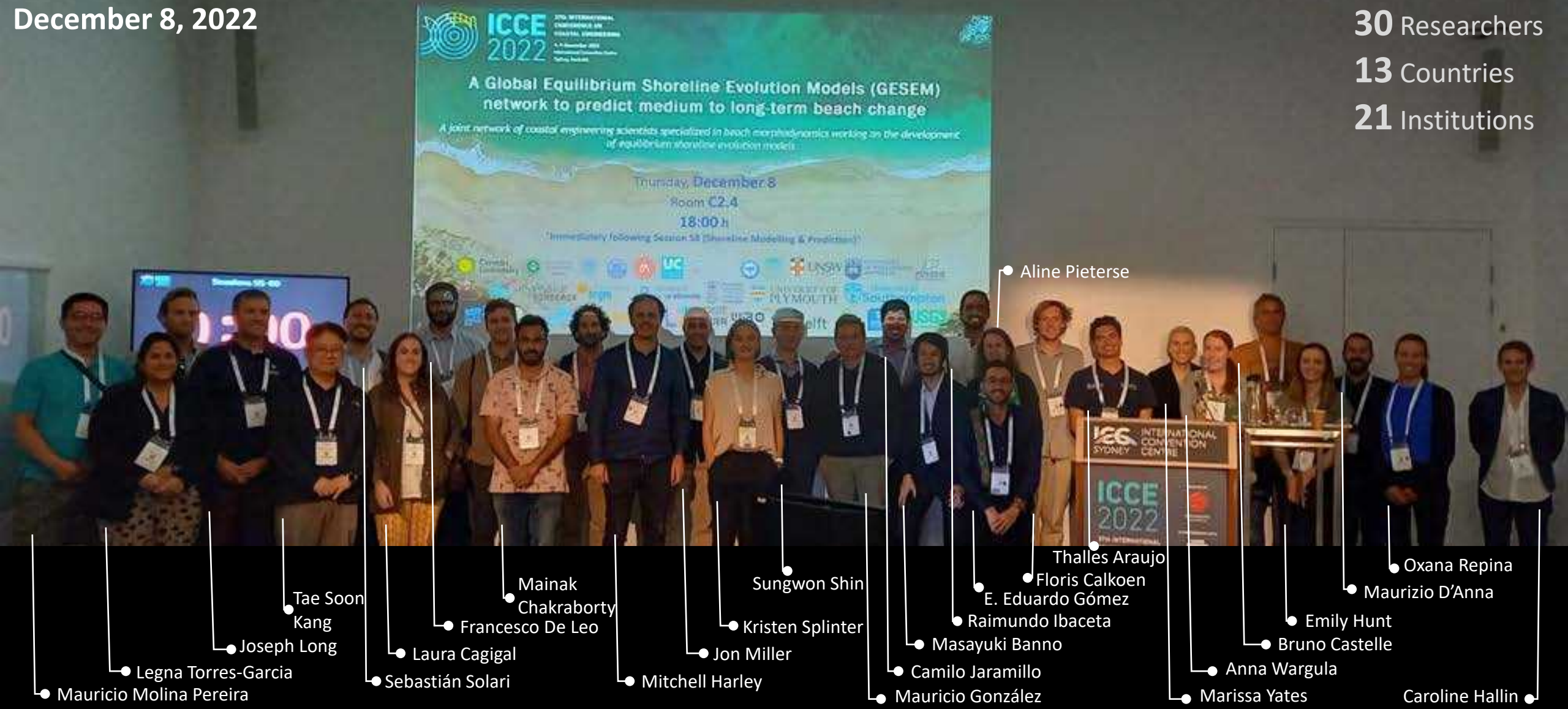
Brings together coastal engineers and scientists with expertise in beach morphodynamics to research shoreline evolution models

What?

- **GESEM** aims at improving the predictability of shoreline evolution models and will focus on investigating key physical processes governing beach evolution across a range of spatial and temporal scales.
- **GESEM** will employ diverse datasets, as well as numerical, statistical, and machine-learning approaches to address the challenge of predicting past and future shoreline evolution.

December 8, 2022

30 Researchers
13 Countries
21 Institutions



Aline Pieterse

Thalles Araujo

Floris Calkoen

E. Eduardo Gómez

Raimundo Ibaceta

Masayuki Banno

Camilo Jaramillo

Mauricio González

Sungwon Shin

Kristen Splinter

Jon Miller

Mitchell Harley

Mainak Chakraborty

Francesco De Leo

Laura Cagigal

Sebastián Solari

Tae Soon Kang

Joseph Long

Legna Torres-Garcia

Mauricio Molina Pereira

Oxana Repina

Maurizio D'Anna

Emily Hunt

Bruno Castelle

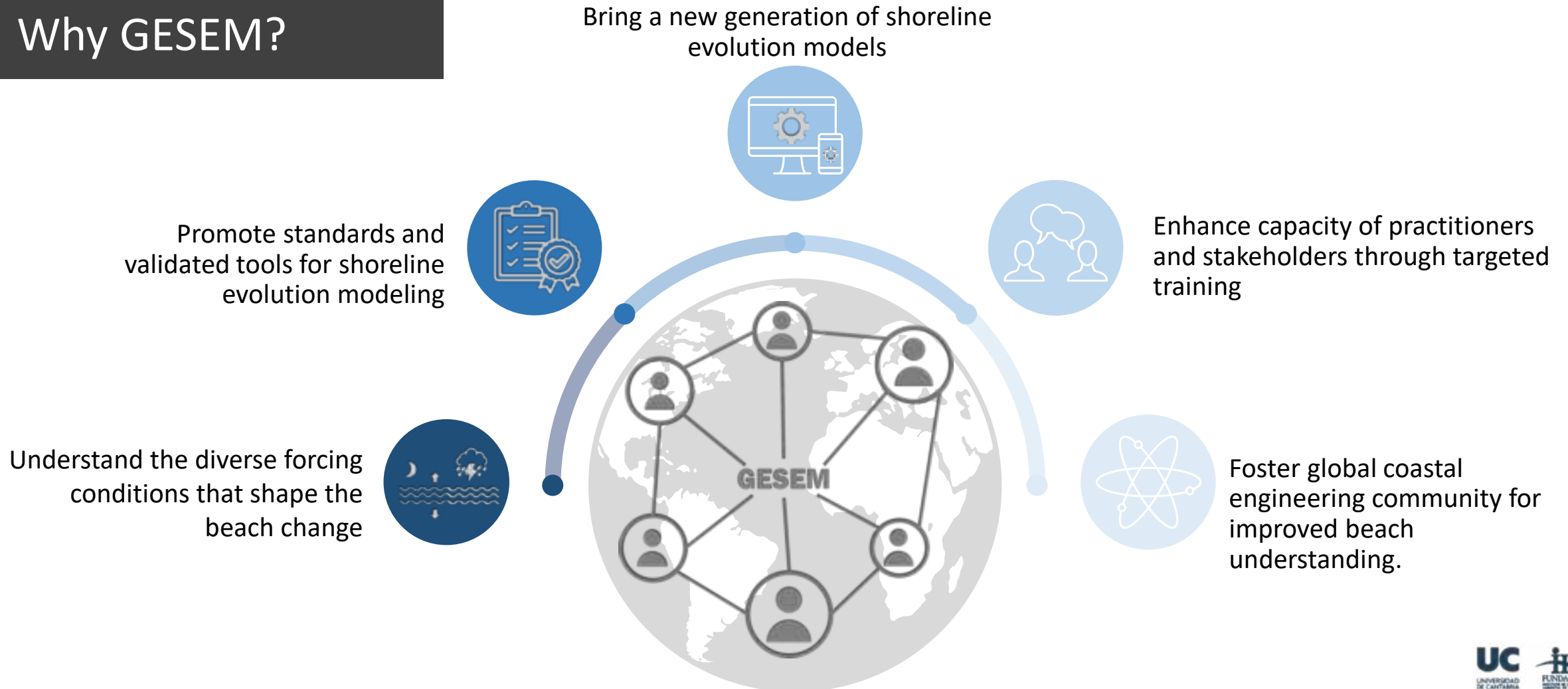
Anna Wargula

Marissa Yates

Caroline Hallin

GESEM - towards integrating, standardizing, and harmonizing work on shoreline evolution modeling

Why GESEM?



GESEM objectives

Integrate cross-shore and longshore processes, preserving the sediment budget and considering climate change impacts

Mutualize efforts testing and improving the ability of models to predict shoreline changes

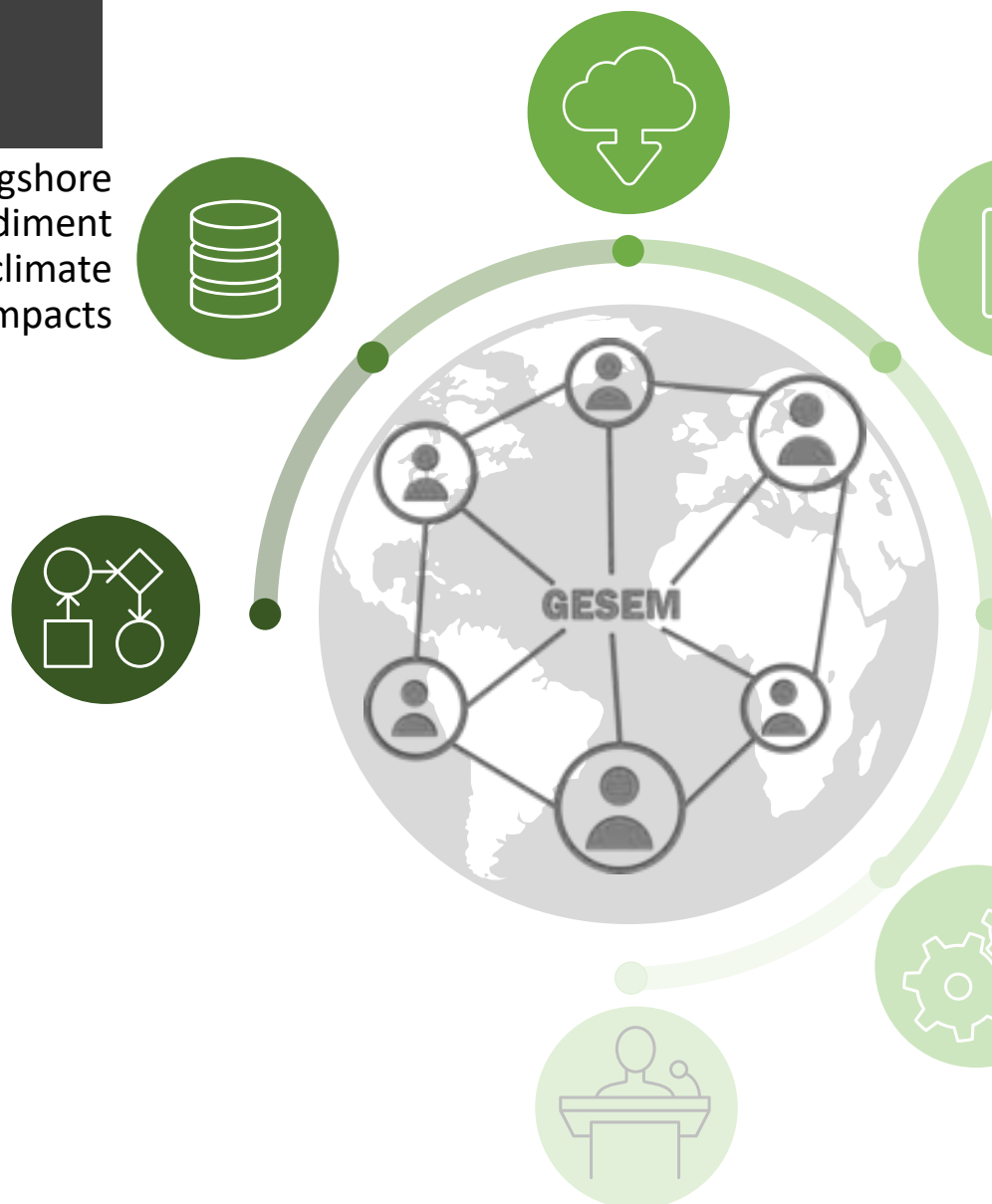
Develop robust methods and models

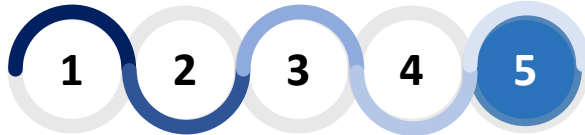
Share standardized, open-source tools, guidelines, and practices

Predict future shoreline evolution integrating different spatial scales from local to regional scales

Provide effective tools of coastal evolution, useful for different applications (e.g., beach nourishment, coastal adaptation plans) accessible to engineers and stakeholders

Disseminate results





GESEM CORE GROUP



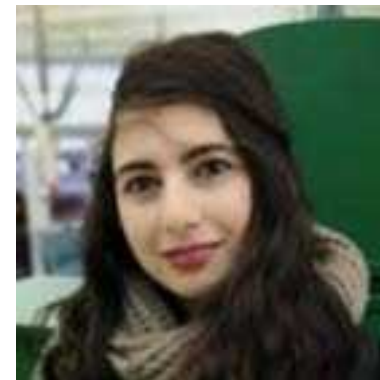
Camilo Jaramillo Cardona
IHCantabria



Lucas de Freitas Pereira
IHCantabria



Marissa Yates
Ecole des Ponts / Saint-Venant
Hydraulics Laboratory



Imen Turki
University of Rouen



Nicolas Le Dantec
Université de Bretagne
Occidentale



José A. Álvarez Antolínez
Delft University of
Technology



Mauricio González Rodríguez
IHCantabria



Raúl Medina Santamaría
IHCantabria



Giovanni Coco
University of Auckland



Sean Vitousek
Pacific Coastal and Marine
Science Center, USGS

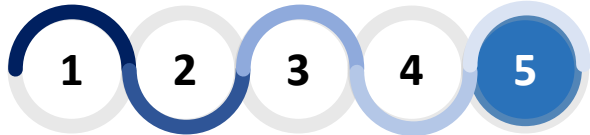


Kristen Splinter
University of New South
Wales, UNSW



Mitchell Dean Harley
University of New South
Wales, UNSW





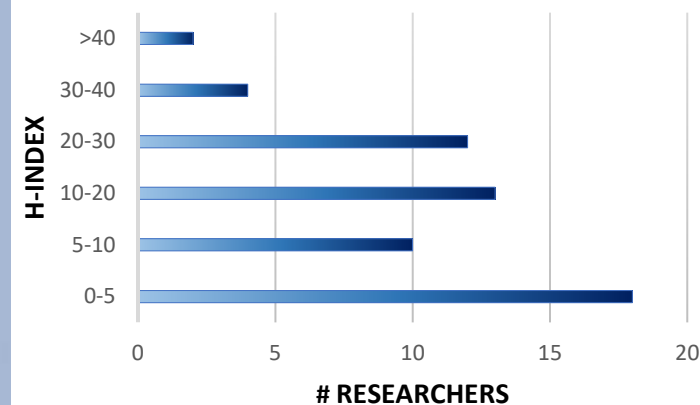
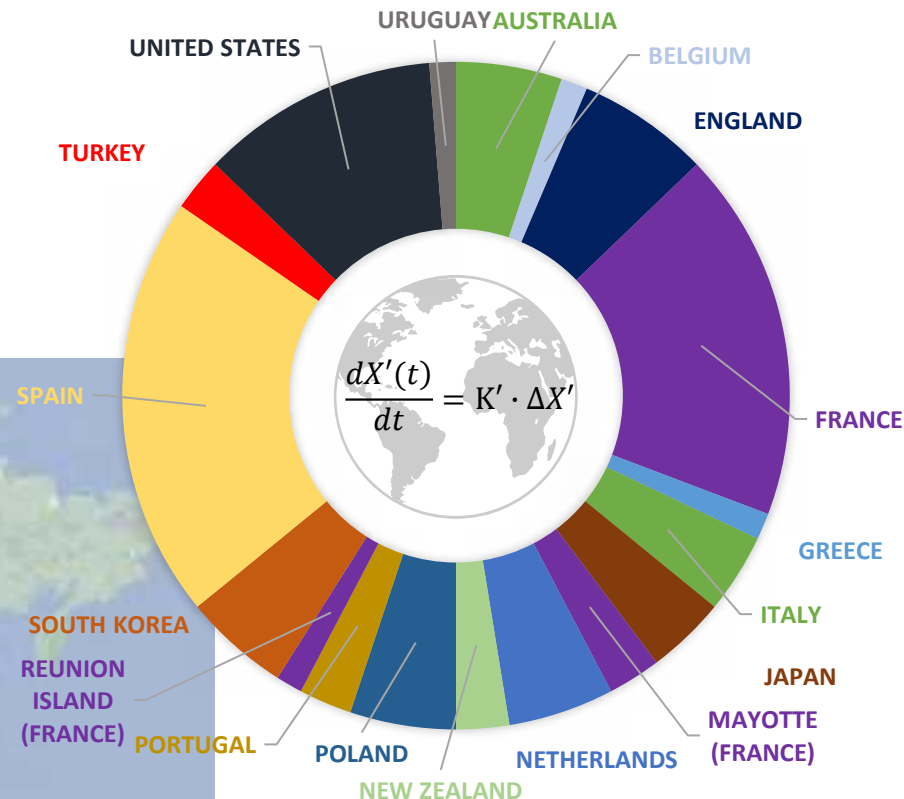
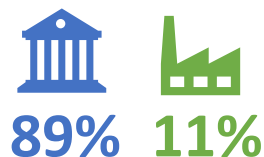
GESEM status



80 Researchers

16 Countries

56 Institutions



Activities



Journal of
*Marine Science
and Engineering*

Special issue: **Assessment of Multi-scale Coastal Evolution in a Changing Climate: from Observation to Modelling**

A special issue of Journal of Marine Science and Engineering (ISSN 2077-1312). This special issue belongs to the section "Coastal Engineering".

Deadline for manuscript submissions: 31 December 2024

Special Issue Editors:

Dr. E. Imen Turki

Dr. Marissa Yates

Dr. Camilo Jaramillo Cardona

Dr. Nicolas Le Dantec



Special session: **'Shoreline Evolution Modeling'**

Session Details:

Conveners: Camilo Jaramillo Cardona, E. Imen Turki, Jose A. Á. Antolínez, Marissa Yates, Nicolas Le Dantec

Abstract Submission Dates: From 01/03/2024 to 30/06/2024

10th Coastal Dynamics Conference Dates: 7th – 11th April 2025

Location: Aveiro, Portugal

- **18 oral presentations (divided into 3 sessions)**
- **7 posters**



“COMMONCOAST: A common coast to cherish – capping climate change”

(Invited Speaker Jara Martínez, IHCantabria)

“COMMONCOAST: A common coast to cherish – capping climate change in MALTA”

Let's close the risk information gap!

Dr. Jara Martínez
11th March 2025



DRR and CCA

[Thought Leadership Course - Synergizing Disaster Risk Reduction and Climate Change Adaptation | UNSSC | United Nations System Staff College](#)



The screenshot shows the United Nations System Staff College website. The header includes the college's name and navigation links: Courses, Tailor-made Learning, Campuses, Latest, In Focus, and About. A search bar and a 'Log in' button are also present. The main banner features the course title 'Thought Leadership Course - Synergizing Disaster Risk Reduction and Climate Change Adaptation' with the dates '01 JAN 2025 - 31 DEC 2025'. It includes tags for 'CLIMATE CHANGE' and 'SUSTAINABLE DEVELOPMENT AND THE SDGs', and a 'Sign up' button. To the right of the text is a photograph of two people in traditional Maasai attire; one person is filling a metal water container from a wooden stand, while another stands nearby. Below the banner, a row of icons provides key details: LANGUAGE (English), DURATION (2 hours), ENROLL BY (31 Dec 2025), PRICE (Free), LOCATION (ONLINE), TARGET (Everyone), CONTACT US (by email), and FAQ (Read more).

This project is funded by the European Union via the Technical Support Instrument and implemented by EUCC in collaboration with its experts, in cooperation with the European Commission



DRR and CCA in Coastal Areas

- International works since 2007: Oman, Qatar, Egypt, Tunisia, Gabon, Belize, Bahamas, Peru, Uruguay...



DRR and CCA in Coastal Areas

- International works since 2007: Oman, Qatar, Egypt, Tunisia, Gabon, Belize, Bahamas, Peru, Uruguay...
- Request from European countries since 2019: 4 regional and 2 national strategies – Spain and Malta



The Maltese Islands



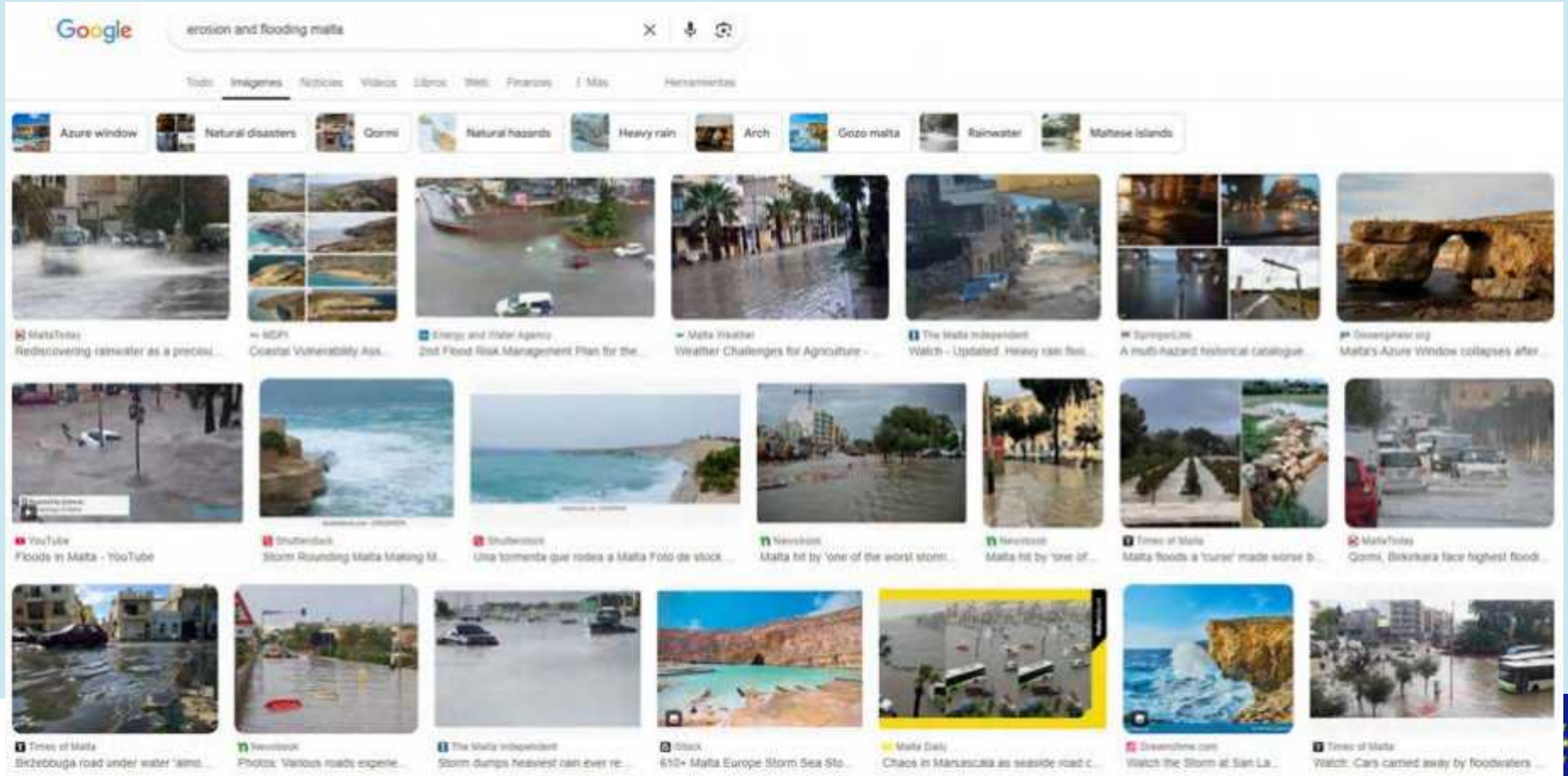
The world's 10th-smallest country
and the 9th most densely populated



This project is funded by the European Union via the
Technical Support Instrument and implemented by EUCC in collaboration with its experts,
in cooperation with the European Commission



Coastal erosion and flooding hazards in Malta



“COMMONCOAST: A common coast to cherish – capping climate change in MALTA”

From Coastal-COVER (2022-2023)

- *Coastal-Climate Overall Vulnerability and Exposure Risk*

to Climate-MATCH (2024-2025)

- *Mainstreaming of Climate Adaptation for Horizontal Coordination*

PUBLIC CLEANLINESS

Project 1. Coastal-COVER (2022-2023)

YEAR 1 - Diagnosis

YEAR 2 - Development of the strategy

Governance
Analysis

Physical Assessment &
Integrative coastal erosion
and flooding risk assessment

Baseline
data &
information

Perception of
risks, key
issues &
hotspots

EU practical
experiences
in coastal
protection &
beach
management
plans

Proposals of suitable coastal
protection measures

Methodology for the selection
of the courses of action

Design &
development of
the National
Coastal
Protection
Strategy

Strategy
for coastal
protection
and
adaptation
to climate
change
in the
Maltese
Islands

Plan

CONSULTATION

Stakeholder Engagement & Communication

CONSULTATION

Factsheets

Project 2. Climate-MATCH (2024-2025)

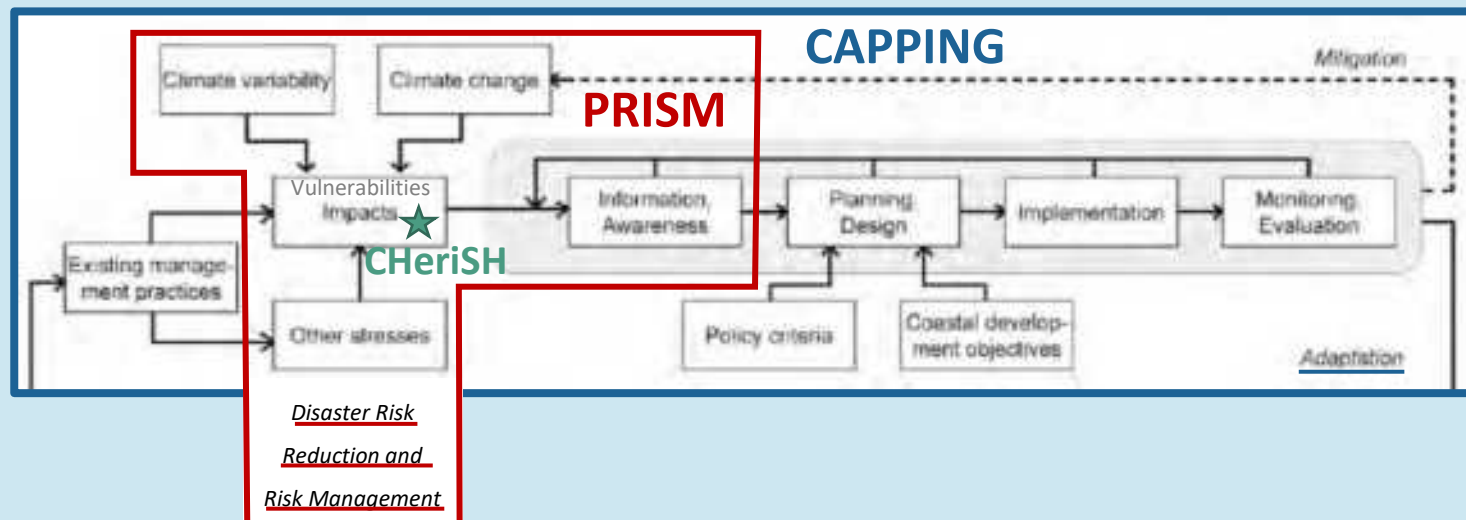


Risk information > Risk management
through a model for multi-layered
data integration into a central hub for
interinstitutional data sharing



PRISM

~ Preparation towards Risk Interdisciplinary
Surveillance and Management in Coastal areas ~



CAPPING


~Climate Adaptation in Policy and
Planning with integrated governance and
knowledge~



CHERISH

~Coastal Heritage and Safeguards against
Hazards~

Contents

- 
1. Background Analysis
 - Data gathering process and baseline data
 - Coastal Hydro-morphodynamics
 2. Coastal Risk Assessment
 3. Integrative Risk Assessment
 4. Risk Information Hub



1. Background Analysis

- **Baseline information**

 Pre-existing segmentation of the coastal area

  Physical geography

  Marine climate

Sea wind

Waves

Astronomical tide

Storm surge

Climate change projections

 Hydrology

 Geology

 Geomorphology

   Erosion evidence

 Protected natural areas

  Land cover

 Uses of coastal areas

Urban areas and buildings

Tourism sector

Cultural, ethnographic and heritage

Critical infrastructures

 Permanent population



1. Background Analysis

- **Data gathering process**

- ✓ 16 Local Data Contributors



Participants were provided with a data collection form, which divided categorised expected inputs into four broad categories

- Public Works Department
- Malta Tourism Authority
- Continental Shelf Department
- Ministry for Gozo
- Superintendence of Cultural Heritage
- Transport Malta
- Planning Authority
- Ministry for the Environment, Energy and Enterprise
- National Statistics Office
- ADI Associates
- Ministry for the National Heritage, the Arts and Local Government
- Project Green
- University of Malta
- Infrastructure Malta
- National Statistics Office
- Environment and Resources Agency
- **Participants in Consultation**



1. Background Analysis

- **Data gathering process**

- ✓ 16 Local Data Contributors
- ✓ Challenges

Local data gathering was fruitful but posed many challenges including

- ❑ Data errors or outdated software suites
- ❑ Identical data sets from different entities, sometimes with differing parameters
- ❑ Lack of standardization
- ❑ Paperwork delays (information management, NDAs)
- ❑ Unclear or missing metadata
- ❑ Uncertain ownership of data



1. Background Analysis

- **Data gathering process**

- ✓ 16 Local Data Contributors
- ✓ Challenges
- ✓ Compilation of data

- ❑ The data gathering process took **six months** to complete (excluding quality control)
- ❑ Uncertainties arose during technical appraisal and necessitated **further inquiry** concerning certain data sets
- ❑ Datasets were inspected and **quality control** flags were assigned

Entity	Data Type Index	Data Name	Format
PA (SintegraM)	BN, APE	Base Map (coastal buffer)	GIS (vector)
PA (SintegraM)	BN, APE	Base Map (portal link)	GIS service
PA (SintegraM)	BN	DTM (Mosaic)	GIS (raster)
PA (SintegraM)	BN	DSM (Mosaic & Tiles)	GIS (raster)
PA (SintegraM)	BN6	Orthophotos (Mosaic)	GIS (raster image)
PA (SintegraM)	BN6	Orthophotos (Portal link) (BN_PA_SintegraM_Portal_Links.txt)	GIS service (WMS)
PA	BN	PA MapServer (BN_PA_SintegraM_Portal_Links.txt)	Weblinks (html) / WebGIS
PA (MSD)	APER.2	msd.data.gov.mt (APER.2_PA_MSD.txt)	Weblinks (html) / WebGIS
PA	BN2	Bathymetric data from (ERDF156 Project)	GIS (raster image)
PA	BN4	1998, 2004, 2008, 2016 & 2018 Orthophotos	GIS (File Geodatabase Raster)
PA	BN4	2018 Orthophoto	GIS (raster image)
PA	BN1, BN5	Urban and Rural Coastal Regions	GIS (vector)
PA (ERDF156)	BN2	DTM (Mosaic)	GIS (raster)
CSD	BN8	Malta Water Line	GIS (vector)
CSD	NPE2	Geological Map Of Malta	GIS (vector)
CSD	NPE8	EMODnet Coastal Migration	GIS (vector)
PARKS	NPE3	Water Catchments	GIS (vector)
PARKS	NPE3	Stream Network Malta	GIS (vector)
PARKS	NPE3	Stream Network Guze	GIS (vector)
PARKS	NPE3	Flow Observation Names	GIS (vector)



1. Background Analysis

- **Data gathering process**

- ✓ 16 Local Data Contributors
- ✓ Challenges
- ✓ Compilation of data
- ✓ Local knowledge gaps

Examples of missing/incomplete local knowledge

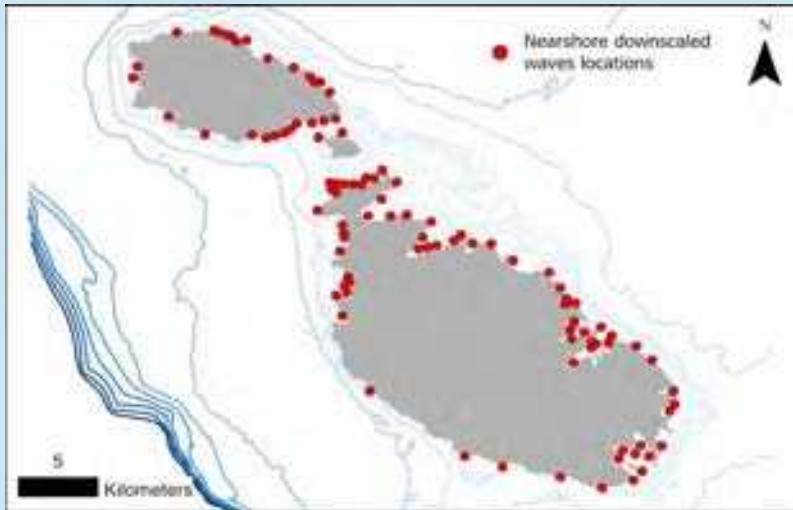
- ☐ **Caves:** No formal dataset denoting all cave systems in Malta.
- ☐ **Coastline:** No agreed upon local definition for what constitutes coastline/shoreline. As such, there is no national physical shoreline.
- ☐ **Coastal heritage:** Available heritage data sets often only demark location of coastal heritage sites and lack other details.
- ☐ **2018 DTM:** Recent digital terrain model (2018) has insufficient vertical resolution to be used for wave modelling. The interface between land and sea was done using 2012 data.
- ☐ **Coastal structures:** Structural typology and design parameters of the built-up waterfront to characterise their sensitivity under wave loads.



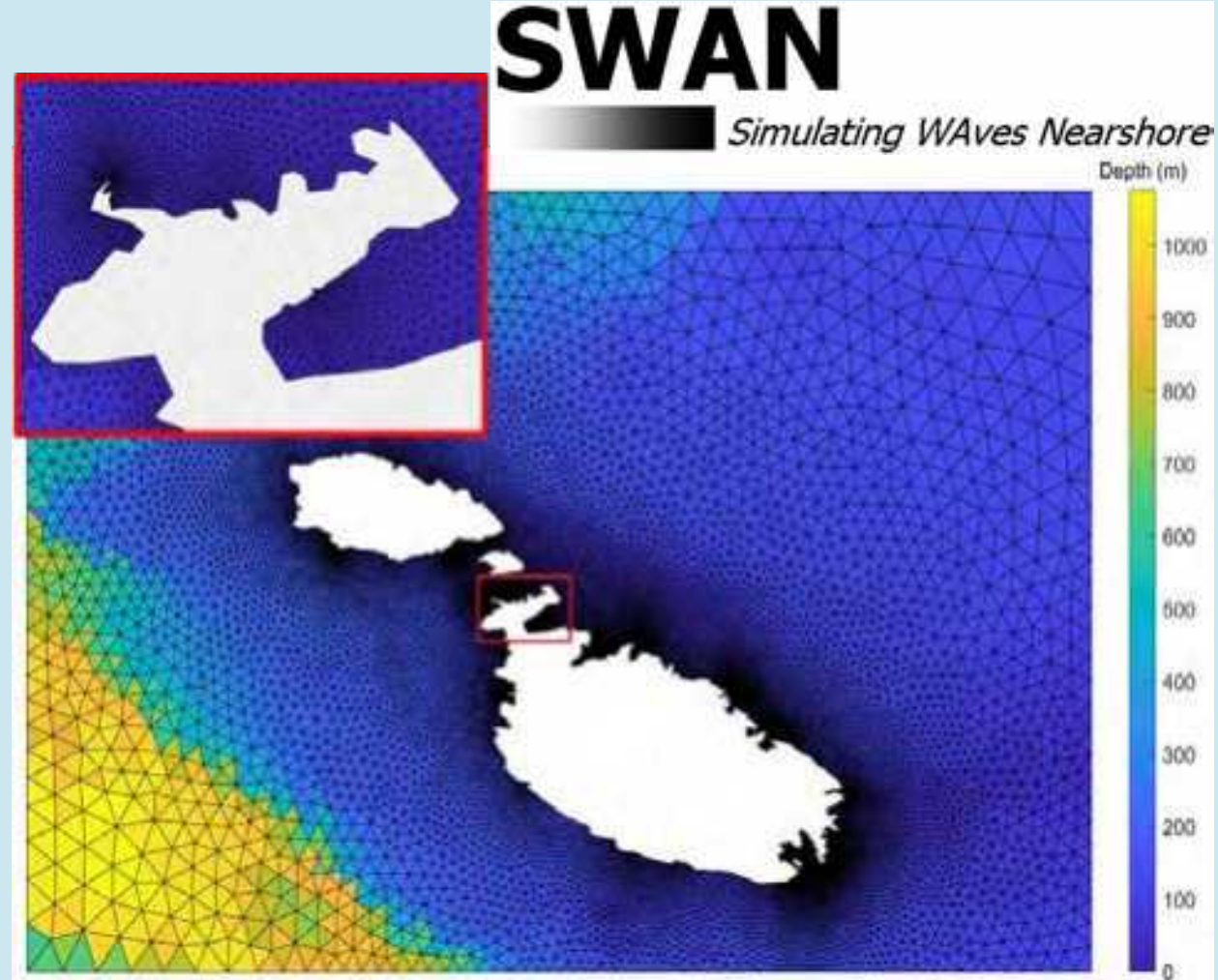
1. Background Analysis

- Coastal hydro-morphodynamics

- ✓ Nearshore wave regime

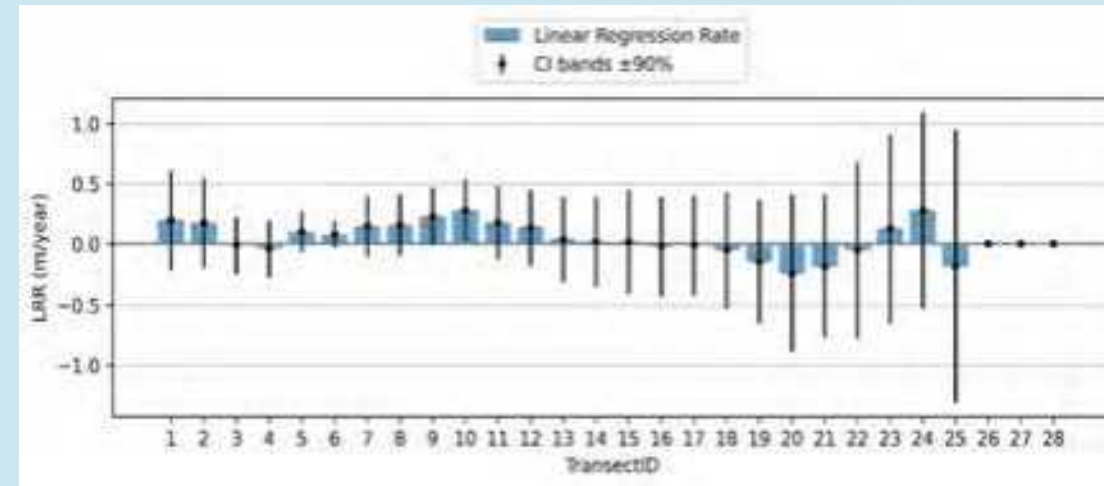
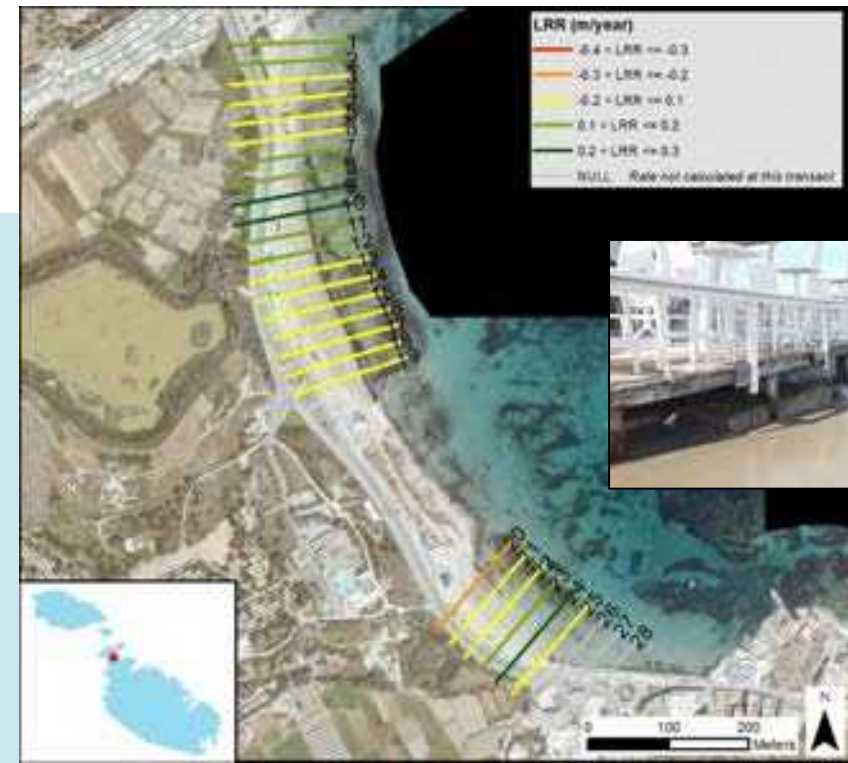


- ☐ Total water level (tide+surge+run-up)
- ☐ Wave overtopping discharge
- ☐ Wave force



1. Background Analysis

- **Coastal hydro-morphodynamics**
 - ✓ Nearshore wave regime
 - ✓ Morphological changes in 14 beaches
 - ❑ Not significant observed change rates (past 20 years) in most beaches
 - ❑ Erosion in Armier Bay and Ġnejna Bay
 - ❑ Accretion in St. George's Bay – Saint Julian's (replenishment since 2004)



Contents

1. Background Analysis
 - Data gathering process and
 - Coastal Hydro-morphodynamics
- ➔ 2. Coastal Risk Assessment
 - Framework and scope
 - Interpretation of results
3. Integrative Risk Assessment
4. Risk Information Hub



2. Coastal Risk Assessment

$$\text{HAZARD} \times \text{VULNERABILITY} = \text{RISK}$$

- ✓ Beach erosion
- ✓ Rocky coast erosion
- ✓ Coastal flooding
- ✓ Population
- ✓ Tourism sector
- ✓ Cultural, ethnographic and heritage
- ✓ Critical infrastructures
- ✓ Other buildings
- ✓ Vehicles
- ✓ Coastal structures
- ✓ (built-up waterfront)



H, V & R Level
None (0)
Very low (>0 and ≤1)
Low (>1 and ≤2)
Medium (>2 and ≤3)
High (>3 and ≤4)
Very high (>4 and ≤5)



2. Coastal Risk Assessment

HAZARD

x

VULNERABILITY

=

RISK

- ✓ **Beach erosion**, potential for the loss of dry beach area

- ☐ Observed erosion trend
- ☐ Wave power
- ☐ Sediment grain size
- ☐ Sediment confinement
- ☐ Dry beach area
- ☐ Beach backshore
- ☐ Runoff



2. Coastal Risk Assessment

$$\text{HAZARD} \times \text{VULNERABILITY} = \text{RISK}$$

- ✓ **Beach erosion**, potential for the loss of dry beach area
- ✓ **Rocky coast erosion**, rockfalls, landslides and rock mass collapses

*Different values in the frontshore and backshore

- ☐ Wave power*
- ☐ Weathering (wind, runoff)
- ☐ Geology*
- ☐ Fault, subsidence, caves, arcs
- ☐ Erosion evidences
- ☐ Geometry*
- ☐ Bare soil
- ☐ Coastal* typologies



2. Coastal Risk Assessment

HAZARD

x

VULNERABILITY

=

RISK

- ✓ **Beach erosion**, potential for the loss of dry beach area
- ✓ **Rocky coast erosion**, rockfalls, landslides and rock mass collapses

1. Shore platform.



2. Sloping coast.



3. Scree.



4. Cliff with exposed toe.



5. Plunging cliff.



6. Backshore cliff (landward of a beach).



☐ Coastal typologies



2. Coastal Risk Assessment

HAZARD

x

VULNERABILITY

=

RISK

- ✓ **Beach erosion**, potential for the loss of dry beach area
- ✓ **Rocky coast erosion**, rockfalls, landslides and rock mass collapses
- ✓ **Coastal flooding**, addressing the total water level rise during storms resulting in a quasi-steady inundation, the **wave overtopping** in terms of the sea water discharge, and the **wave force**, which refers to the hydrodynamic loads of sea waves



Xlendi (Gozo) 2019
Flood height



Xemxija 2019
Drag force



St Julians 2016(Sliema)
Wave loads



2. Coastal Risk Assessment

HAZARD

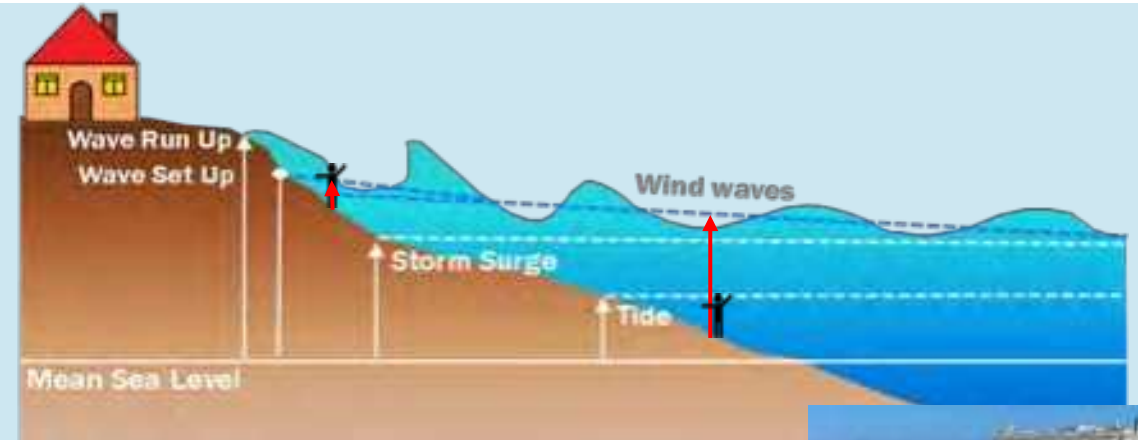
x

VULNERABILITY

=

RISK

- ✓ **Beach erosion**, potential for the loss of dry beach area
- ✓ **Rocky coast erosion**, rockfalls, landslides and rock mass collapses
- ✓ **Coastal flooding**, addressing the total water level rise during storms resulting in a quasi-steady inundation, the **wave overtopping** in terms of the sea water discharge, and the **wave force**, which refers to the hydrodynamic loads of sea waves



- ☐ Total Water Level – Flood height
- ☐ Frequency of overtopping events exceeding the safety values for pedestrians and vehicles
- ☐ Wave power at the front-shore. Water excursion at the back-shore



2. Coastal Risk Assessment

- **Horizon and scenario**

- ✓ **Current situation (2022)**

Hazard indexes H_{BE} H_{RE} H_{TWL} H_{WO} H_{WF}

- ✓ **Future horizon year: 2050 + SSP5-8.5
(0.25 m sea level rise)**

- ☐ H_{BE} : Reduction of the dry beach area (1 of 7 indicators)
- ☐ H_{RE} : Waves reaching backshore cliffs more often (1 of 11 indicators and only in backshore cliffs)
- ☐ H_{TWL} : Increased flood height
- ☐ H_{WO} : Reduced freeboard, thus increased water discharge
- ☐ H_{WF} : Waves reaching backshore structures more often



2. Coastal Risk Assessment

- Target impacts

$$\text{HAZARD} \times \text{VULNERABILITY} = \text{RISK}$$

Impacts		Coastal hazard				
		Beach erosion	Rocky coast erosion	Coastal flooding		
				Quasi-steady	Wave overtopping	Wave force
Receptors at risk	Population	Indirect	Direct	Indirect	Direct	
	Tourism sector	Indirect	Direct	Direct		
	Cultural, ethnographic and heritage		Direct	Direct		
	Critical infrastructures		Direct	Direct		
	Other buildings		Direct	Direct		
	Vehicles				Direct	
	Coastal structures (built-up waterfront)					Direct



2. Coastal Risk Assessment

- **Geographical scope**

- ✓ **61 Coastal Units**

- ✓ **417 Coastal Stretches**

- ☐ Indirect impacts of beach erosion: walking distance from the beaches, topography, roads, urban fabric
 - ☐ Special locations: Comino and Cominotto, Fort Ricasoli, main ports
 - ☐ Coastal typology
 - ☐ Locality boundaries
 - ☐ Flood prone area
 - ☐ Erosion evidences



2. Coastal Risk Assessment



- Beach erosion impacts



✓ V_{BE-POP} , indirect impacts to the population (use and enjoyment of coastal areas)

✓ V_{BE-TS} , indirect impacts to the tourism sector (tourism economic activity)

☐ Exposed population: The highest exposure in Malta and lowest in Cominotto

☐ Social value of the beach: Managed by the MTA; services, equipment and facilities; type of sediment

☐ Natural value of the beach: Protected Beaches managed by the ERA

☐ Accommodation stock in the Coastal Unit: N° of beds

☐ Tourism infrastructures and services in the Coastal Unit: N° of tourism facilities



2. Coastal Risk Assessment

- Rocky coast erosion impacts



✓ V_{RE-POP} , direct impacts to the population (injuries or death)

✓ V_{BE-TS} , V_{BE-CEH} , V_{BE-CI} , V_{BE-OB} , direct impacts to coastal assets (damages)

- ☐ Exposed population: Probability to find an attraction (beaches, swimming, diving, climbing, mooring zones, view points, paths, CEH assets) in any given standard section (100 m long) of the Coastal Stretch
- ☐ Exposed assets: Probability to find some coastal asset in any given standard section (100 m long)



2. Coastal Risk Assessment

- Coastal flooding impacts



- ✓ V_{CF-POP} , indirect impacts to the population due to the quasi-steady coastal flooding (disruption of the use of the public space)
- ✓ V_{CF-TS} , V_{CF-CEH} , V_{CF-CI} , V_{CF-OB} , direct impacts to coastal assets (damages)
- ✓ V_{WO} , direct impacts to the population (safety)
- ✓ V_{WF-Str} , direct impacts to coastal structures (damages)

- ☐ Exposed population: N° of inhabitants of the Coastal Unit
- ☐ Re...
inc...
acc...
pe...
- ☐ Exp...
- ☐ Exp...
the...
inc...
- ☐ Exposed vehicles: parking or roads along the crest
- ☐ Exposure: Length of structures in the Coastal Stretch



2. Coastal Risk Assessment

- Coastal flooding impacts

HAZARD

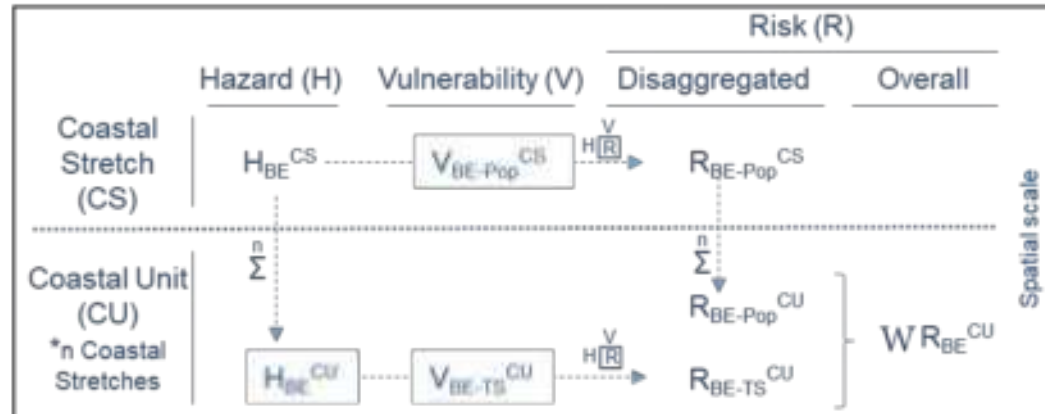
x

VULNERABILITY

=

RISK

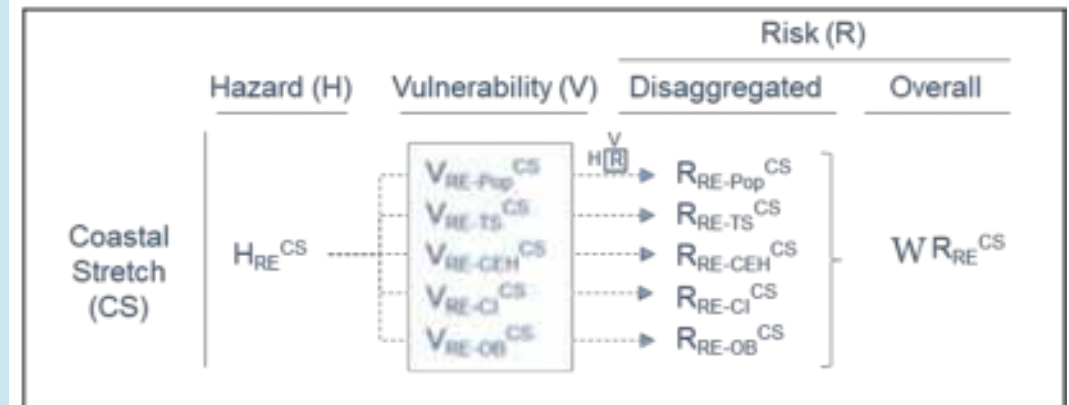
Beach Erosion (BE)



Operations	
$\frac{V}{H[R]}$	Hazard x Vulnerability=Risk
\sum^n	Spatial aggregation
W	Weighted averaging

Receptors at risk	
Pop	Population
TS	Tourism sector

Rocky Coast Erosion (RE)



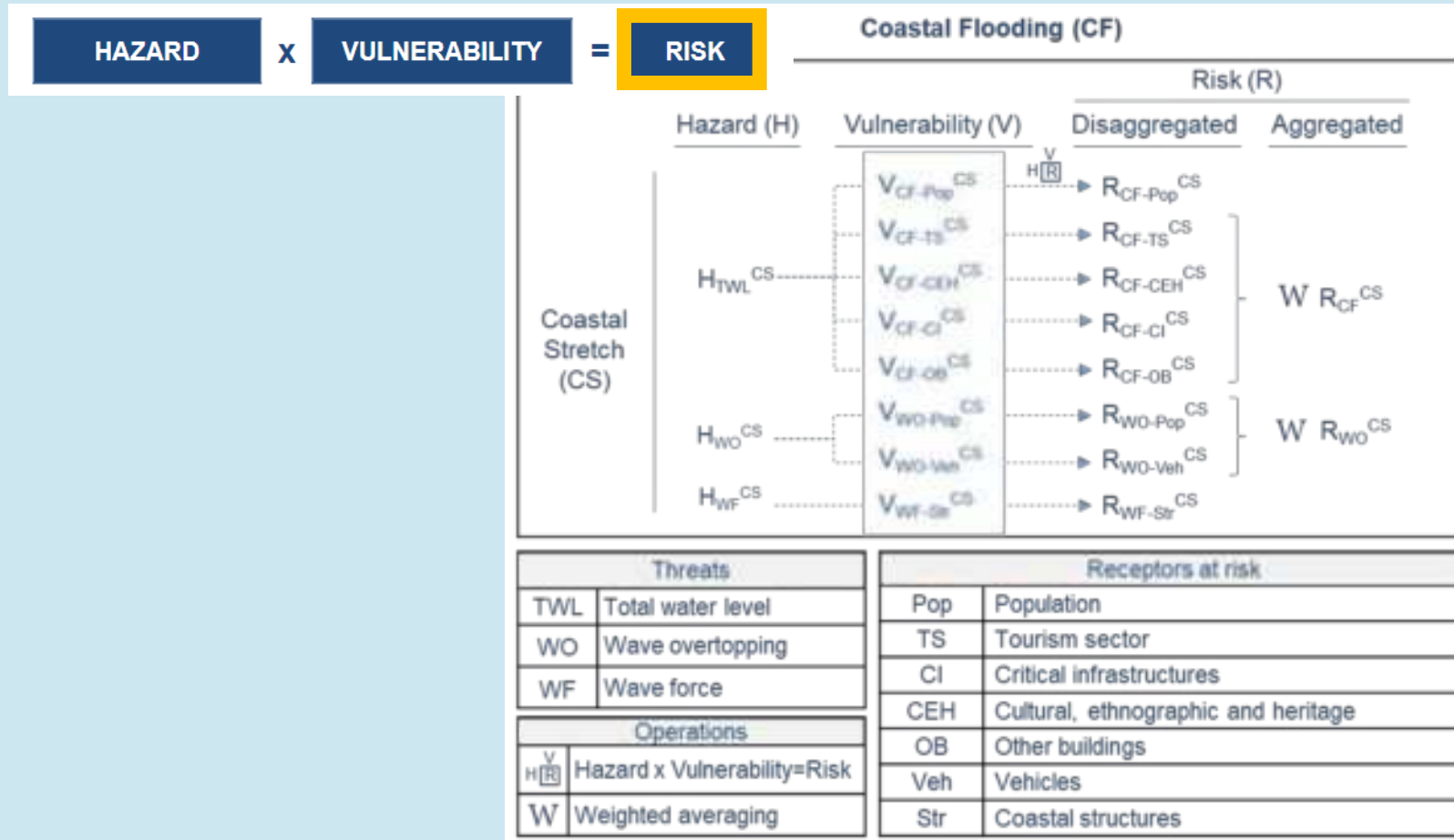
Operations	
$\frac{V}{H[R]}$	Hazard x Vulnerability=Risk
W	Weighted averaging

Receptors at risk	
Pop	Population
TS	Tourism sector
CEH	Cultural, ethnographic and heritage
CI	Critical infrastructures
OB	Other buildings



2. Coastal Risk Assessment

- Coastal flooding impacts



H, V & R Level
None (0)
Very low (>0 and ≤1)
Low (>1 and ≤2)
Medium (>2 and ≤3)
High (>3 and ≤4)
Very high (>4 and ≤5)



Contents

1. Background Analysis
 - Data gathering process and
 - Coastal Hydro-morphodynamics
2. Coastal Risk Assessment
 - Framework and scope
 - Interpretation of results
- ➔ 3. Integrative Risk Assessment
 - Perceptions of risks
 - Key issues and hotspots
4. Risk Information Hub

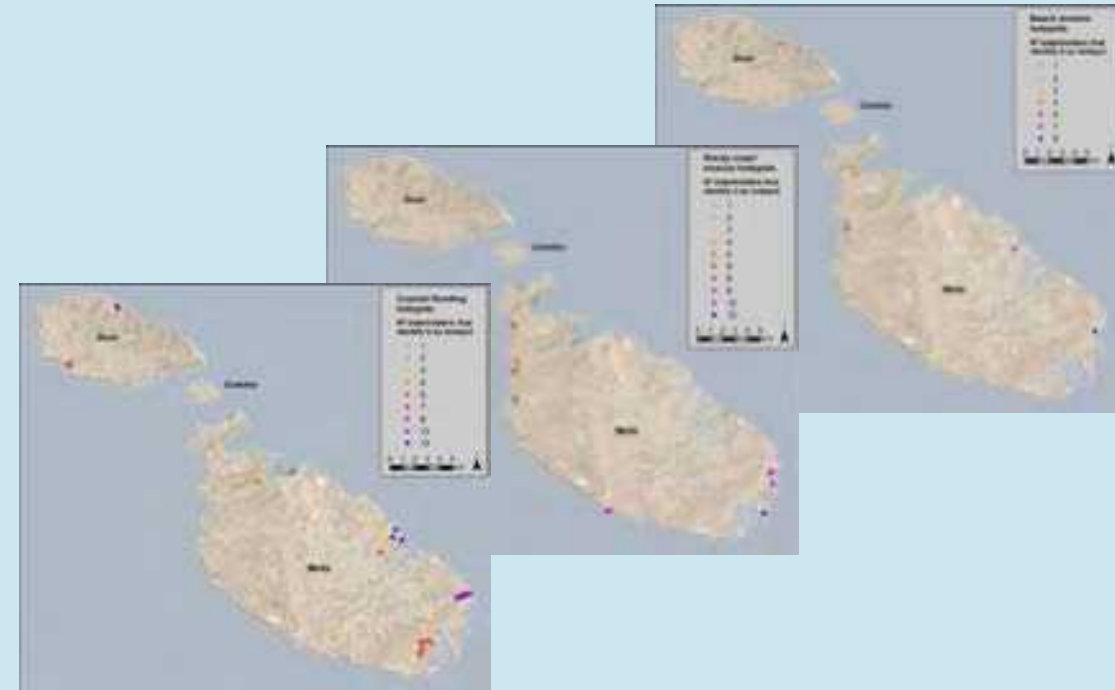


3. Integrative Risk Assessment

- **Perceptions of risk**
 - **2nd Consultation** -
 - ✓ **Classes of severity and extension of perceived hazards o impacts**
 - ✓ **Identification of perceived hotspots**
 - ✓ **Relative value of receptors at risk**

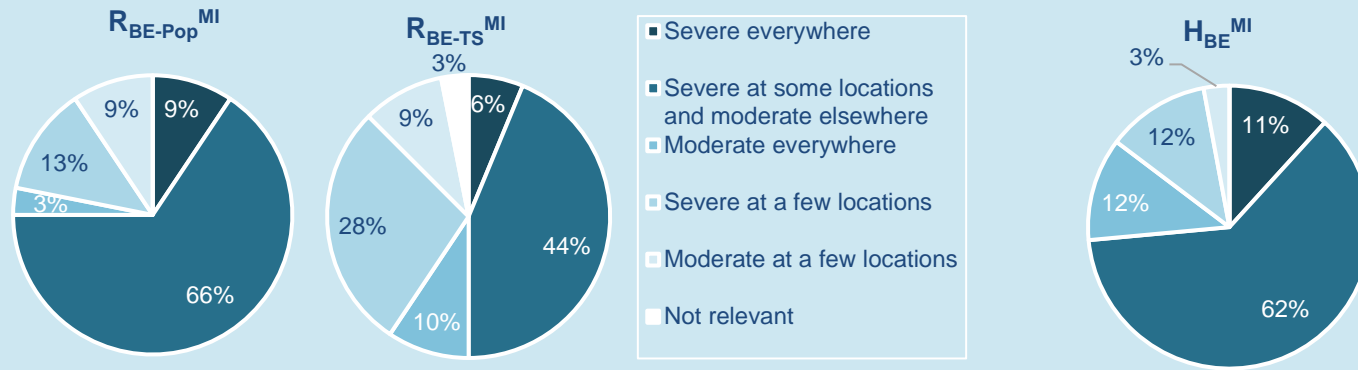
Perception levels
Not relevant
Moderate at a few locations
Critical / Severe at very few locations
Moderate everywhere
Critical / Severe at some locations and moderate elsewhere
Critical / Severe everywhere

Weights (%)		Coastal hazard				
		Beach erosion	Rocky coast erosion	Coastal flooding		
				Quasi-steady	Wave overtopping	Wave force
Receptors at risk	Population	60	35	-	60	
	Tourism sector	40	15	20		
	Cultural, ethnographic and heritage		20	30		
	Critical infrastructures		20	30		
	Other buildings		10	20		
	Vehicles				40	
	Coastal structures (built-up waterfront)					-

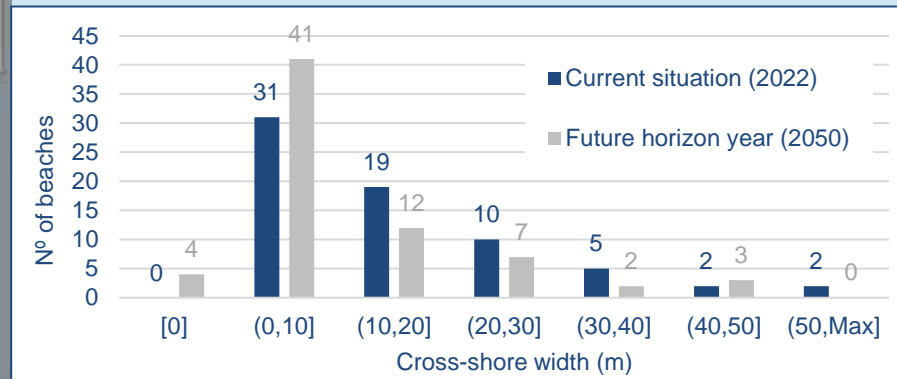
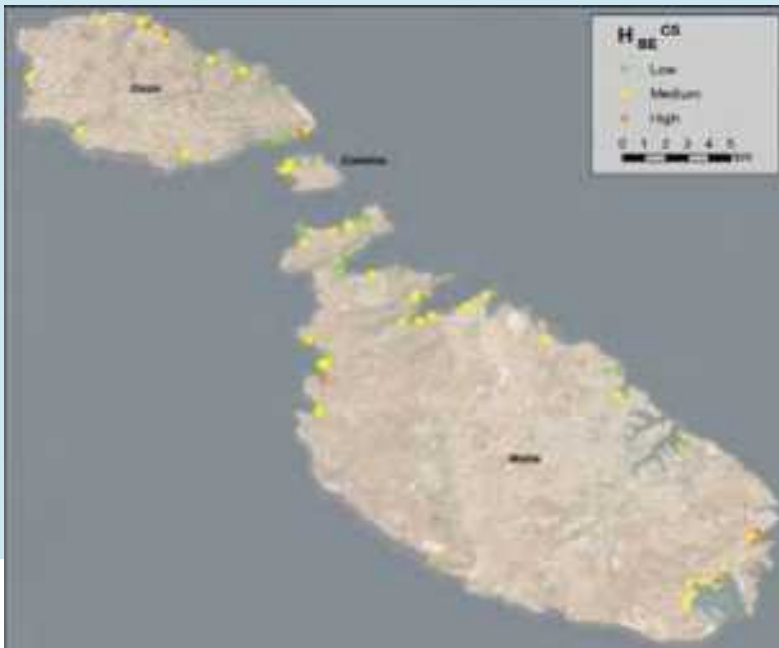


3. Integrative Risk Assessment

- Beach erosion key issues

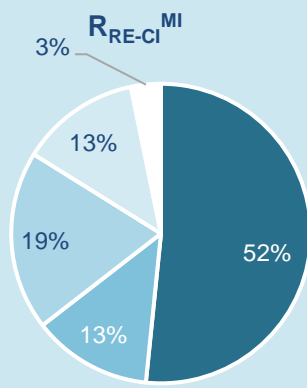
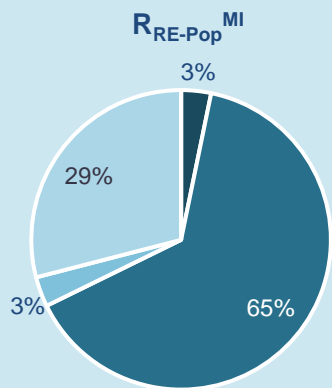
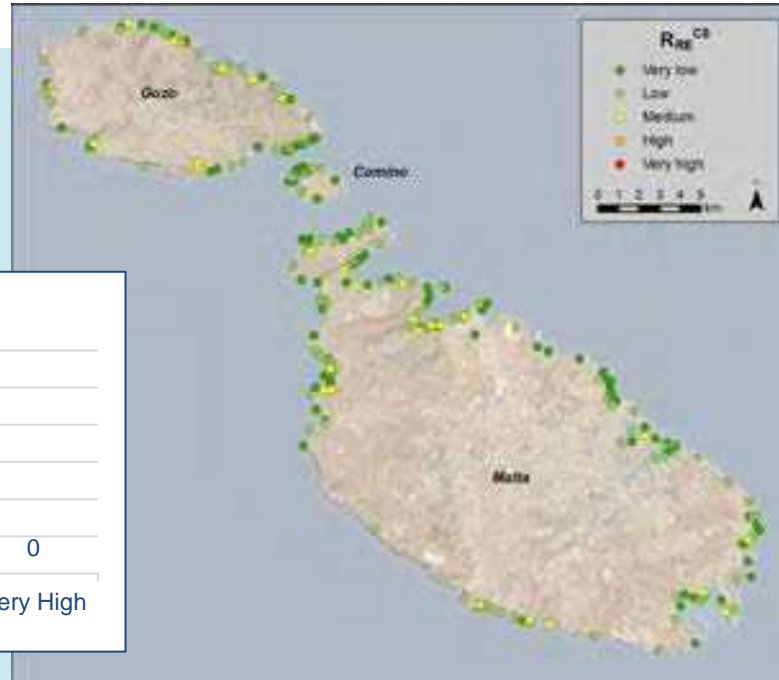
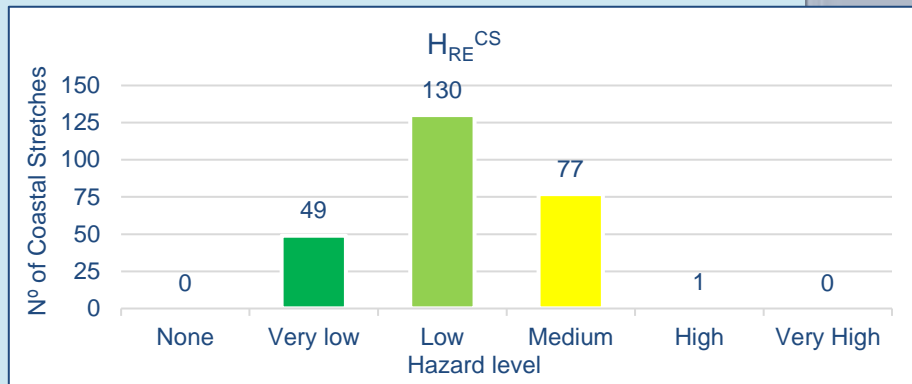


- ❑ The impacts of beach erosion on the socioeconomic environment, with focus on the population but also on the tourism sector.
- ❑ The beach erosion in terms of the reduction of the dry beach area due to the loss of beach sediments.
- ❑ The effects of climate change on beach erosion, which exacerbates the reduction of the dry beach area in the long term.

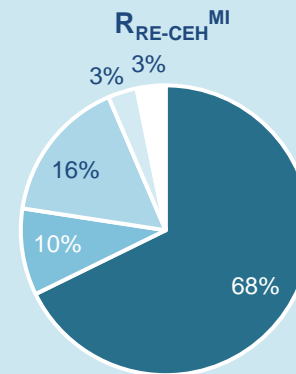


3. Integrative Risk Assessment

Rocky coast erosion Key issues



- Severe everywhere
- Severe at some locations and moderate elsewhere
- Moderate everywhere
- Severe at a few locations
- Moderate at a few locations
- Not relevant

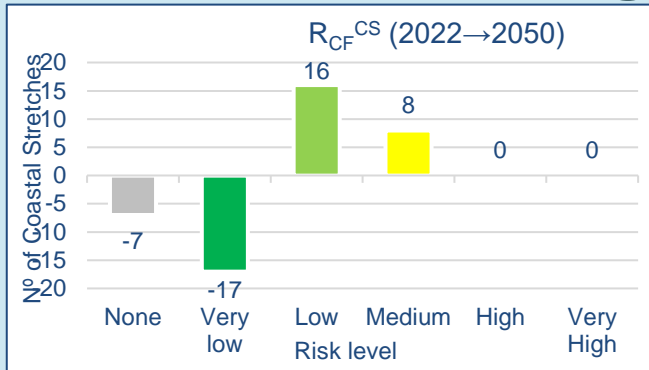


- The **prediction of rocky coast erosion events** is still a challenge not resolved.
- The **impacts of rocky coast erosion on the population and coastal assets**, in terms of injuries / death or damages.
- The **public safety**, with focus on the population but also on the critical infrastructures.
- The **damages to irreplaceable cultural, ethnographic and heritage assets**, which are critical losses for the Maltese society but also at a global scale.

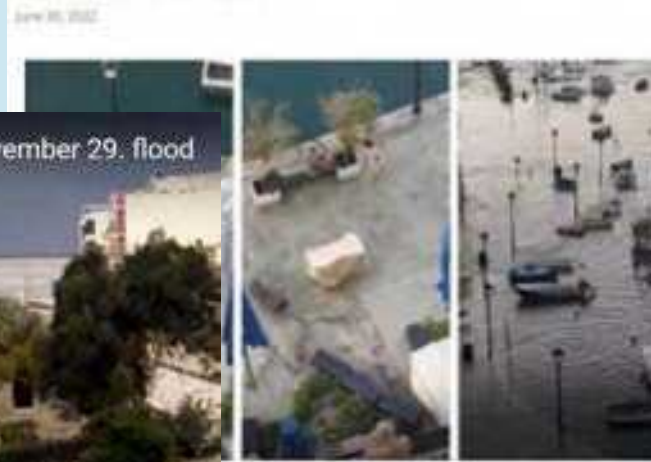


3. Integrative Risk Assessment

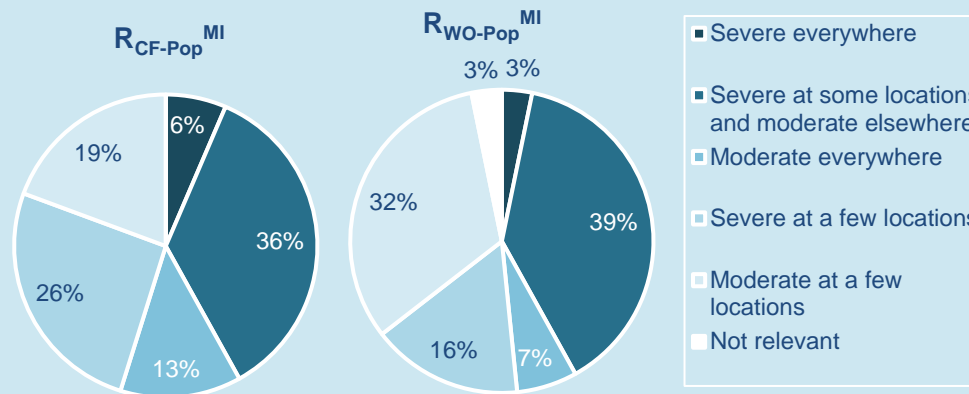
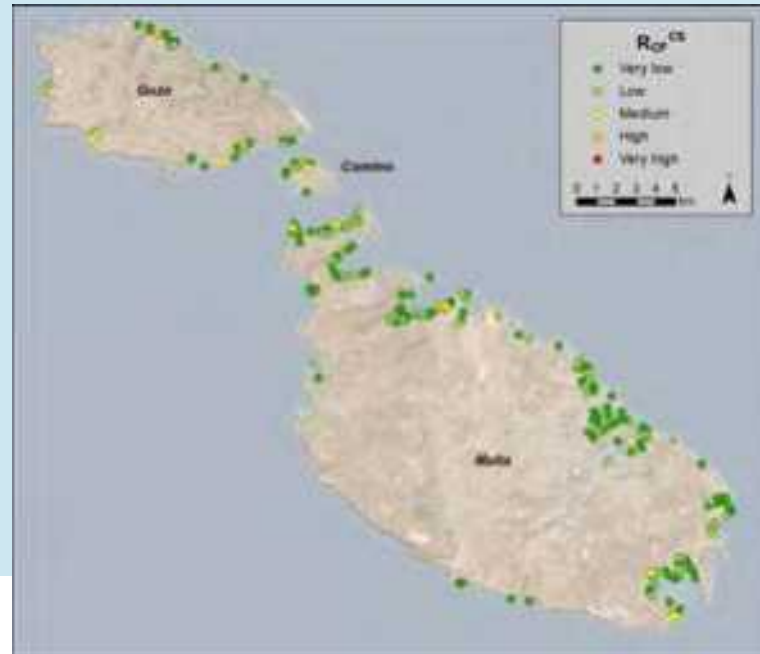
Coastal flooding key issues



VIDEO: Marsascala and St Julians hit by phenomenon known as seiche waves



- ☐ The knowledge gap with regards to relevant physical processes such as local rainfall or the *milghuba* seiche waves.
- ☐ The indirect and direct impacts of coastal flooding on the population.
- ☐ The direct impacts of coastal flooding on coastal assets.
- ☐ The knowledge gap with regards to the sensitivity of coastal structures to wave force.



3. Integrative Risk Assessment

- Selection and prioritisation of hotspots

- ✓ Relevant hazard and risk results
- ✓ Perceived hotspots
- ✓ Relevant baseline information

Beach erosion	Rocky shore erosion	Coastal flooding
Fajtata		Sliema
Balluta	St Peters Pool	Marsaskala
Ghajn Tuffieha	Munxa	Marsalforn
Ghadira	Ghar Lapsi	Msida
Golden Bay	-	Xlendi



Contents

1. Background Analysis ← Geodatabase

- Data gathering process and
- Coastal Hydro-morphodynamics

2. Coastal Risk Assessment

- Framework and scope
- Interpretation of results

3. Integrative Risk Assessment

- Perceptions of risks
- Key issues and hotspots

→ 4. Risk Information Hub

- C-COVER
- PRISM

C-COVER
Integrative Coastal
Geodatabase
(2.5 Gb)



This project is funded by the European Union via the Technical Support Instrument and implemented by EUCC in collaboration with its experts, in cooperation with the European Commission



4. Risk Information Hub

Beach erosion hazard index,
potential for the loss of dry
beach area in one Coastal Unit



Hazard classes
None (0)
Very low (>0 and ≤1)
Low (>1 and ≤2)
Medium (>2 and ≤3)
High (>3 and ≤4)
Very high (>4 and ≤5)

Combination of
beach erosion indicators
(expressed in classes)

- ☐ Sediment grain size
- ☐ Wave power
- ☐ Observed erosion trend
- ☐ Sediment confinement
- ☐ Dry beach area
- ☐ Beach backshore
- ☐ Runoff

Input variables



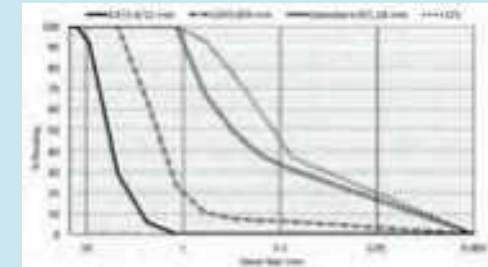
D50 (mm)



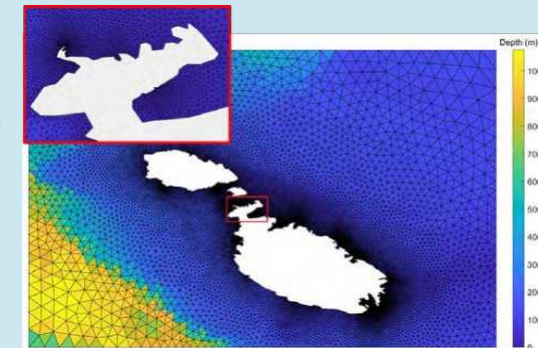
Difference between the
50% and 95% percentile
of the wave power

Raw data

Sand samples
granulometry



Time series of wave
parameters from
the waves onshore




4. Risk Information Hub

Project 1. Coastal-COVER (2022-2023)



Project 2. Climate-MATCH (2024-2025)

PRISM outputs

- Inception report: methods and results 
- **Content:** Risk Assessment Technical Guidelines (Output 1)
- **Technology:** Risk Information Hub Blueprint (Output 2)
- **Governance:** Information Management Framework (Output 3)
- **Skills:** Capacity Building Program (Output 4)





1. Background Assessment:

- Data needs across different entities
- Local, national and international sources of information (EO, citizen science, previous/ongoing projects)
- Data gaps and overlaps
- Key issues and challenges for a cooperative approach

2. Outline of PRISM outputs:

- Clear definition of specific objectives
- Rough outline of final deliverables

Working methods:

- National PRISM Consultation
 1. Online
 2. Workshop
 3. Interviews
- Synergies between components and other on-going projects



4. Risk Information Hub

July-August 2024



- 35 questions in 4 blocks
- 34 public agencies, 11 NGOs/associations, 9 University departments/faculties: 98 persons invited.
- 37 participated, from 26 different entities

24th October 2024



- ✓ Refinement of answers from online survey
- ✓ New questions that require previous explanation

slido

November 2024



- Assessment of current capabilities:
- Technology
 - Skills
 - Governance



4. Risk Information Hub



Conceptual framework for Hazard, Exposure, Vulnerability and Risk Assessment

- in C-COVER: coastal erosion and flooding hazards and socioeconomic impacts
- in PRISM: additional coastal hazards and environmental / intangible impacts

Critical factors for success: Shared understanding of the proposed risk assessment approach (across 3 project components and Risk Information Hub users)

Scope:

- ✓ Development of methods
(Risk Assessment Technical Guidelines)
- x Calculations and mapping



4. Risk Information Hub



Relevant coastal hazards (examples for impact chain development)

- **Marine hazards (forcing hazards)** : sea waves overtopping, sea waves forces, **storm surge (TWL)**, meteo-tsunamis (*milghuba*), sea level rise
- **Marine hazards (non-forcing)**: **water temperature**, water acidity, saline intrusion
- **Geo-hazards**: earthquake, **tsunami**, **beaches erosion**, landfall, **rockfalls**, ground movement, subsidence, marine sedimentation shifts, volcanoes
- **Atmospheric hazards**: meteorological, climatological, air quality
- **Biological hazards**: **invasive species**, vegetation cover, aquatic bloom, loss of habitat
- **Human stressors**: trampling, **anchoring**, water pollution, storm water discharge, construction



4. Risk Information Hub



Cross-sectoral at-risk receptors

- **Health, safety and wellbeing:** local population, visitors, vehicles, vulnerable groups
- **Infrastructure and transport:** Water supply, sewage. Roads, vehicles, energy, telecommunications, industrial harbours, public service infrastructures (hospitals, schools, police stations, fire stations), maritime transport
- **Urban areas and economic activities:** Coastal structures (built-up waterfront), other buildings, urban fabric, industrial and commercial areas, parks and recreation, accommodation stock, tourism services and infrastructure, fishery capacities, livestock activities
- **Natural heritage:** Beaches, sand dunes, coastal wetlands (saltmarshes), coastal reefs, Posidonia meadows, coastal cliffs, natural streams and aquifers, aquatic and terrestrial biodiversity, caves, coastal garrigue. Intangible impacts
- **Historical, cultural and ethnographic heritage:** Paths and tracks, buildings and assets, climbing zones, viewpoints, cultural landscapes, diving sites, bathing waters, recreational activities, archaeological sites. Intangible impacts
- **Public services:** Local councils, ecosystem monitoring. Intangible impact



4. Risk Information Hub



The **Risk Information Hub Blueprint** will include the conceptual development of methods and tools for:

1. Data acquisition (local and global sources)
2. Data integration (processing and analysis)
3. Data update (and continuous upgrade)
4. Information management: specific task

And a roadmap for the implementation of recommended developments including technical specifications

Objectives

- Data centralization and standardization
- Data sharing to promote science-based decision-making



4. Risk Information Hub



Development of the **Information Management Framework**

1. Roles and responsibilities:

- Maintenance of the Risk Information Hub
- Data acquisition, integration, update

2. Data access:

- Ownership of data
- Utilization

Critical factors for success:

- **Engagement** with all relevant stakeholders from early stages
- **Agreement** on working methods and project specific objectives



4. Risk Information Hub



Design of a **Capacity Building Program** for the uptake of the Risk Conceptual Framework:

- Identification of potential trainees and needs
- Assessment of current capabilities
- Description of training and capacity building activities:
 - Contents
 - Methods and Timeline
 - Quality control and certification
 - Cost estimates
- Alumni action plan

Critical factors for success.

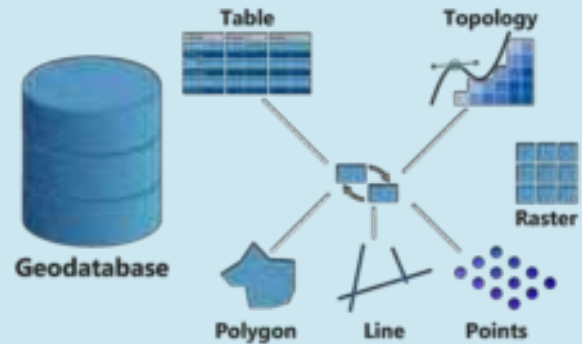
- Robust commitment by **participant institutions** (after project finalisation)



CONCLUSIONS

Impacts		Coastal hazard				
		Beach erosion	Rocky coast erosion	Coastal flooding		
				Quasi-steady	Wave overtopping	Wave force
Receptors at risk	Population	Indirect	Direct	Indirect	Direct	
	Tourism sector	Indirect	Direct	Direct		
	Cultural, ethnographic and heritage		Direct	Direct		
	Critical infrastructures		Direct	Direct		
	Other buildings		Direct	Direct		
	Vehicles				Direct	
	Coastal structures (built-up waterfront)					Direct

GeoData stored in a GeoDataBase





A Coastal Protection Strategy for Malta - European Commission

Elisa Ferreira

Commissioner for Cohesion and Regional
European Commission

Stefan Zrinzo Azzopardi

Minister for Public Works and Planning, Malta



THANK YOU FOR YOUR ATTENTION

Dr. Jara Martínez
jara.martinez@unican.es



“Sediment transport in vegetated ecosystems”

(María Maza, IHCantabria)

Sediment transport in vegetated ecosystems



Maria Maza

Instituto de Hidráulica Ambiental de la Universidad de Cantabria (IHCantabria)

mazame@unican.es



• **Motivation**



• **HyWedges**



• **SHACC**



• **Conclusions**

- The World Economic Forum's (WEF) Global Risks 2023 report identifies the **failure of climate-change adaptation** as one of the main global risks in 10 years.
- **Adaptation** to climate change is a key priority for our society. An example is the Agenda 2030 of AIVP (International Association of Cities and Ports)



Motivation

10 years

- 1 Failure to mitigate climate change
- 2 Failure of climate-change adaptation
- 3 Natural disasters and extreme weather events
- 4 Biodiversity loss and ecosystem collapse
- 5 Large-scale involuntary migration
- 6 Natural resource crises
- 7 Erosion of social cohesion and societal polarization
- 8 Widespread cybercrime and cyber insecurity
- 9 Geoeconomic confrontation
- 10 Large-scale environmental damage incidents

- In the last fifty years, human action has transformed ecosystems more rapidly and extensively than in any other period. This has resulted in a considerable, and largely irreversible, **biodiversity loss**. This loss has consequences for human well-being (Millennium Assessment Report).
- The **climate crisis and the biodiversity crisis are intimately linked**; while ecosystems play an important role in climate regulation and can help sequester and store carbon, their loss has contributed significantly to climate change.



Motivation

- Adaptation to climate change requires **multifunctional solutions**: solutions that maximize benefits for both society and the natural system.
- During the United Nations Climate Change Conference COP25 and COP26 there was a common view that **Nature-based Solutions** (NBS) are an invaluable part of the solution



Motivation

- Coastal areas are experiencing an increasing risk and **NbS based on coastal ecosystems** are specially important to for disaster risk reduction in these areas.
- These solutions provide with several ecosystem services, among them we find the **coastal protection service**.



International Guidelines on Natural and Nature-Based Features for Flood Risk Management, 2021



Climate change
mitigation and
adaptation



Disaster risk
reduction



Economic
and social
development



Human health



Food security



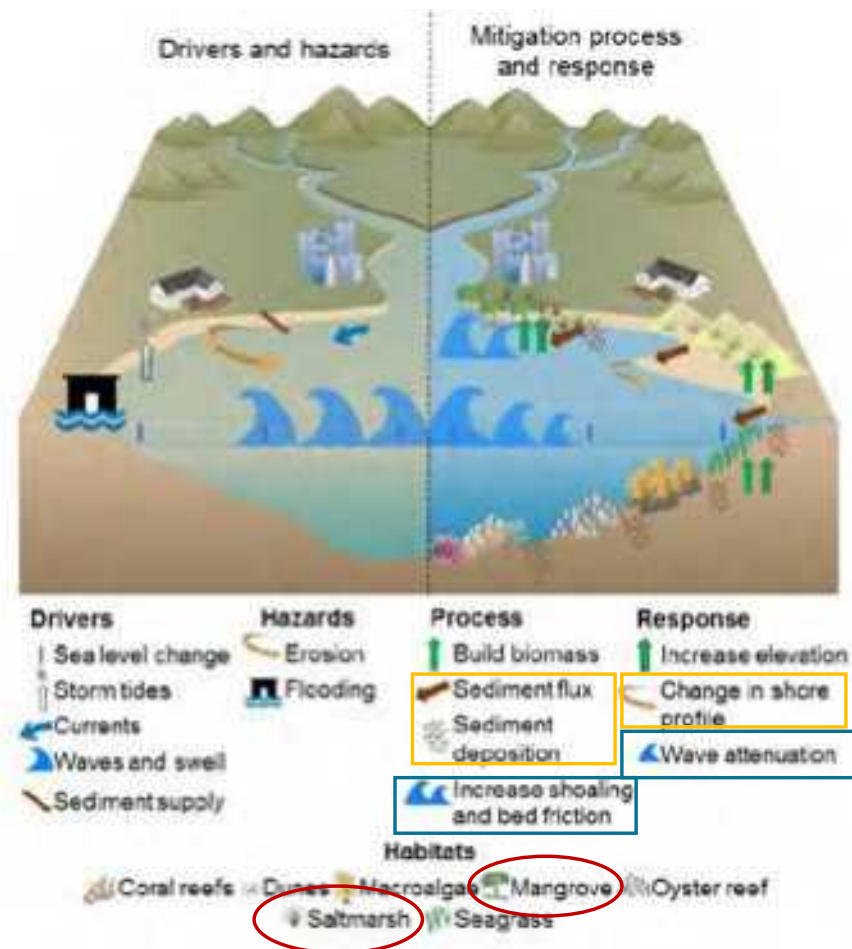
Water security



Environmental
degradation and
biodiversity loss



Motivation



Morris et al. (2018)

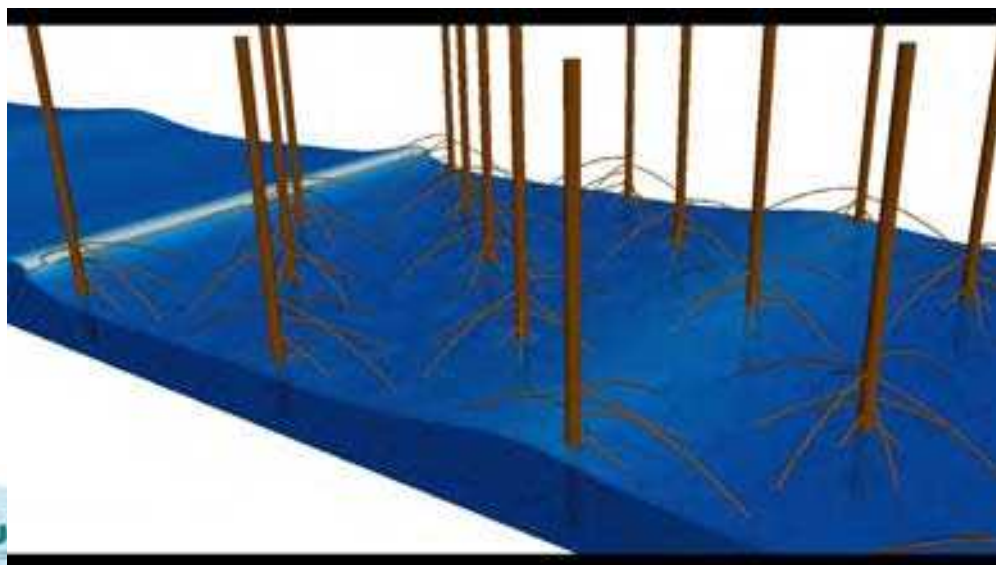


Mangroves

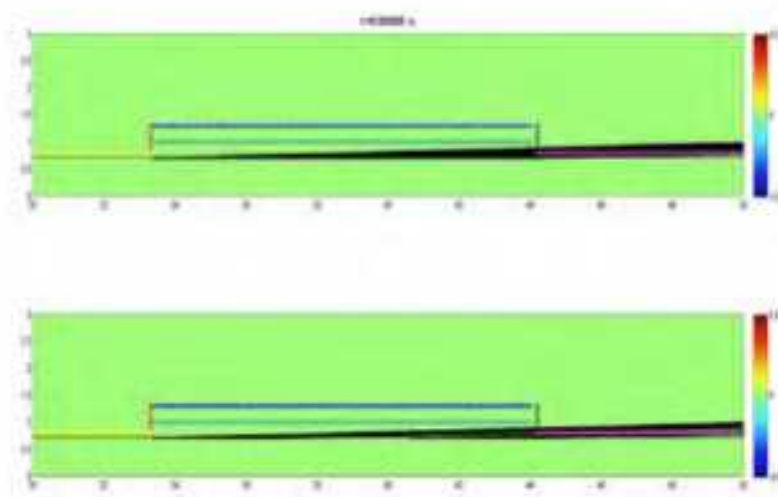
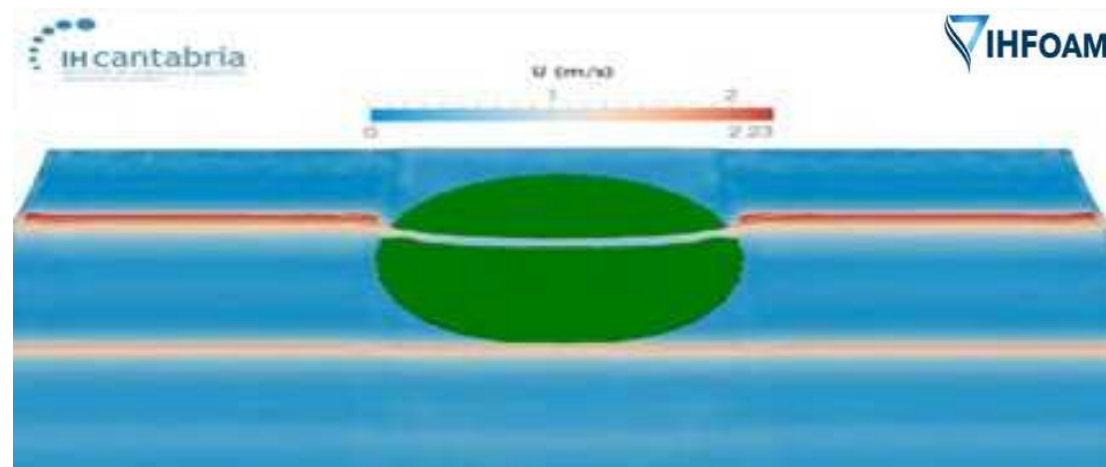
Saltmarshes



- Coastal protection service:
 - Flow energy attenuation
 - Erosion reduction



Motivation



- It is still necessary to know in depth and characterize the **sediment transport** in these ecosystems.
- **HyWEges** (hydrodynamics at coastal wetland edges) and **SHACC** (Hybrid Solutions for Coastal Adaptation to Climate Change Climate Change) projects aimed to evaluate sediment transport patterns in vegetation fields.



European
Commission





• **Motivation**



• **HyWedges**



• **SHACC**

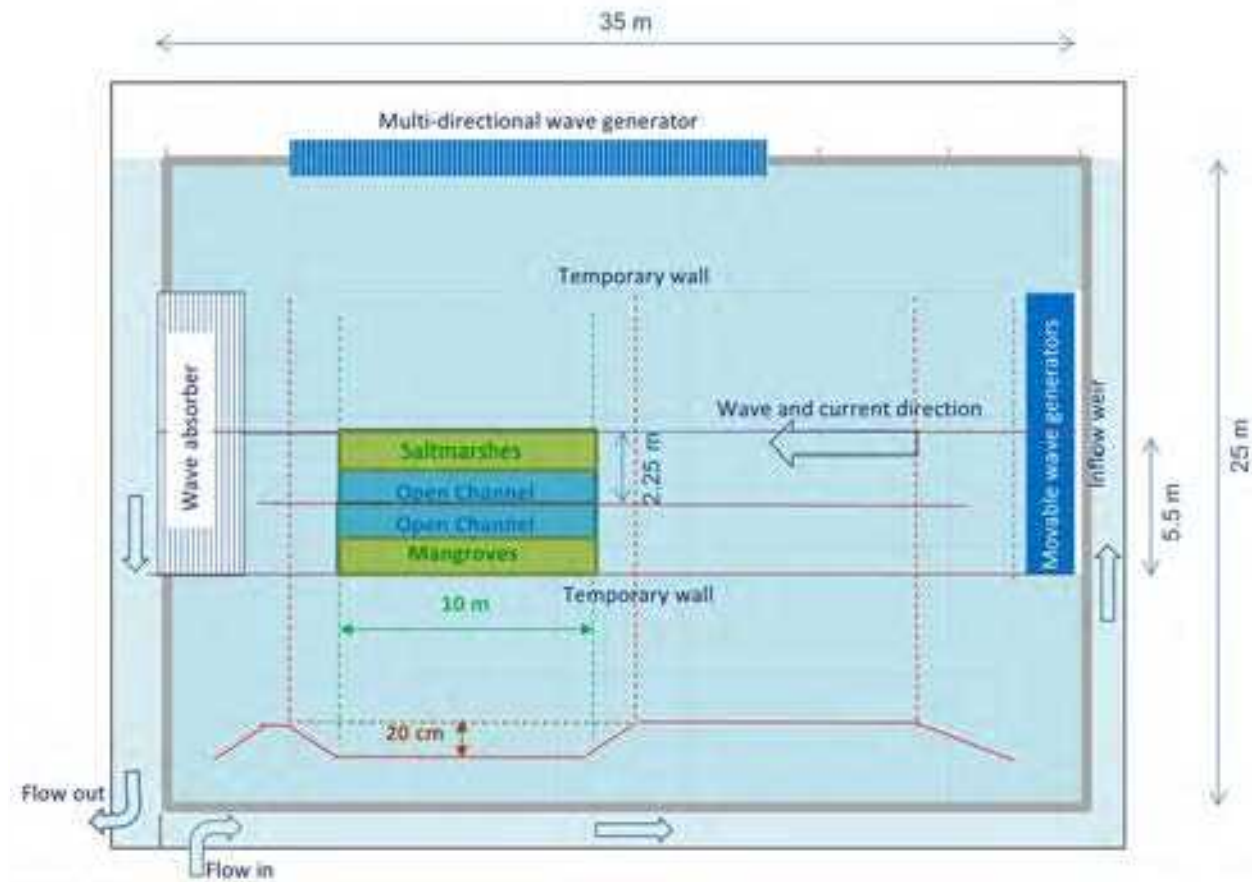


• **Conclusions**

Experimental set-up

- Tests were carried out in the wave tank at the Denmark Hydraulics Institute (DHI) in Denmark:

- Maximum discharge: 1 m³/s
- Water depth: 0.30 m
- Velocity: 0.30 m/s
- Test section width: 5.5 m
- Two channels: 2.75 m
- Vegetation fields: 1.25 m
- Open channels: 1.5 m



- Vegetation mimics:
 - Field 10 m long x 1.25 m wide → 12.5 m²
 - Saltmarshes: plastic tubes
 - 420 stems/m² → 5250 stems
 - Simplified geometry: flexible cylinders
 - Diameter: 0.005 m
 - Length: 0.30 m
 - E = 14 MPa
 - Mangroves: wood cylinders
 - 84 stems/m² → 1050 stems
 - Simplified geometry: rigid cylinders
 - Diameter: 0.03 m
 - Length: 1 m
 - Rigid

Experimental set-up



Experimental set-up

- Hydrodynamic conditions:
 - Water depth: 0.30 m
 - Unidirectional current: 0.30 m/s

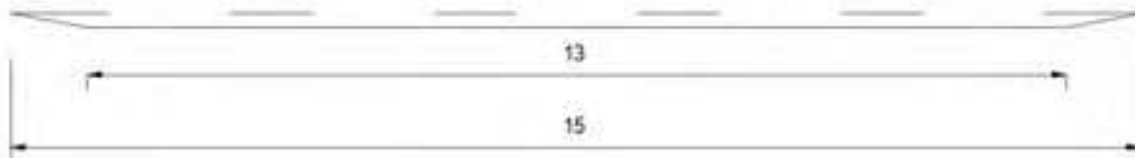


Experimental set-up

- Sediment area:
 - 0.20 m of depth
 - Smooth slopes 1:5
 - Total volume: 15.4 m³
- Sediment:
 - Nominal diameter equal to 0.18 mm
 - Availability/characteristics/movement initiation based on Van Rijn 1989 and Soulsby 1997 formulations

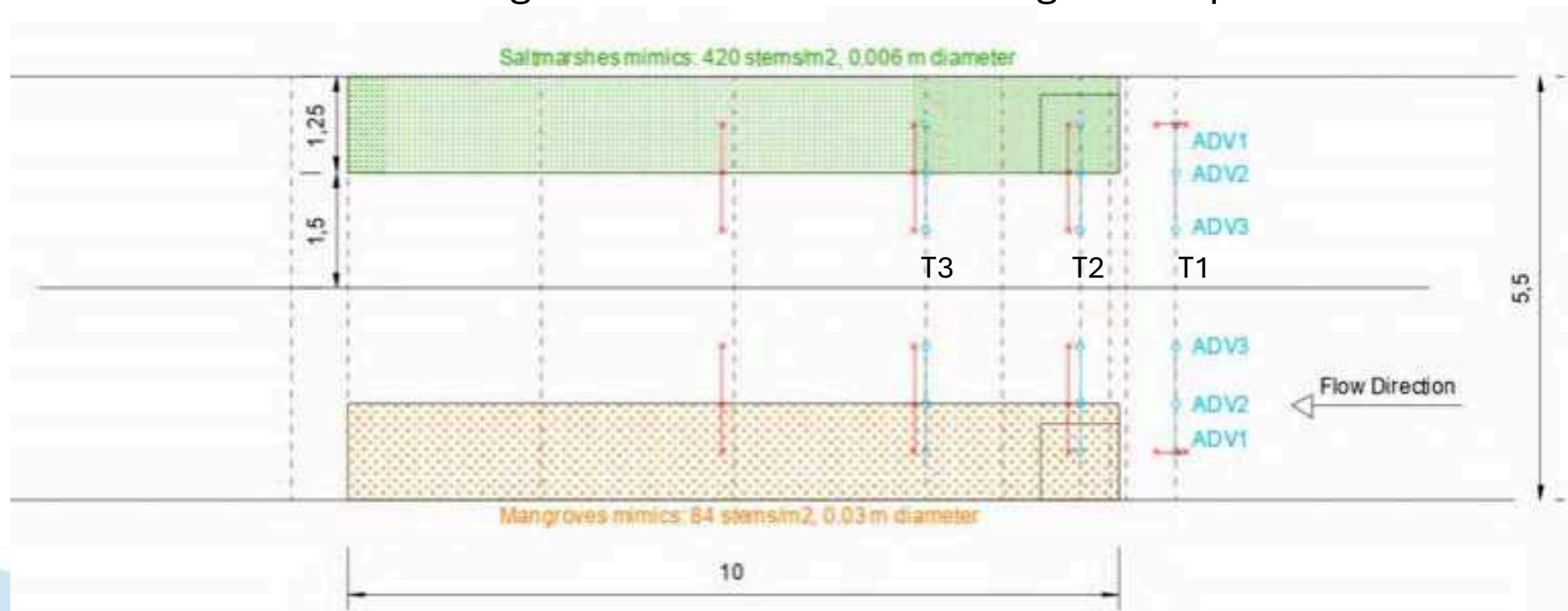


Sand Pit: 1:5 slopes, 20 cm deep, 5.5 m wide

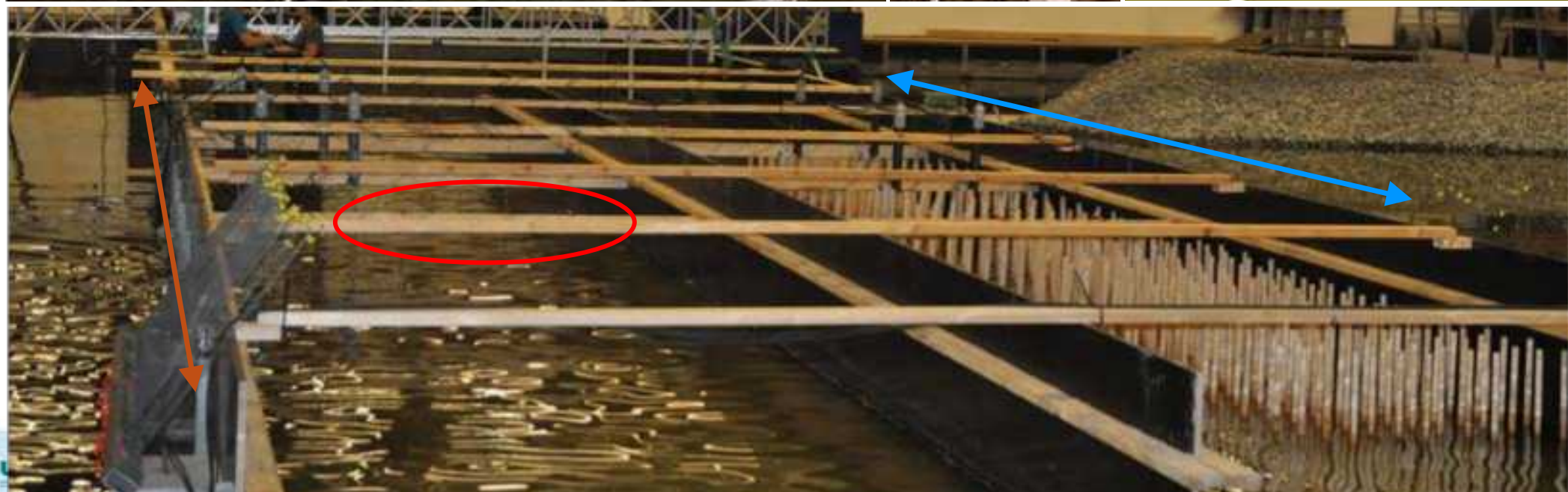


Experimental set-up

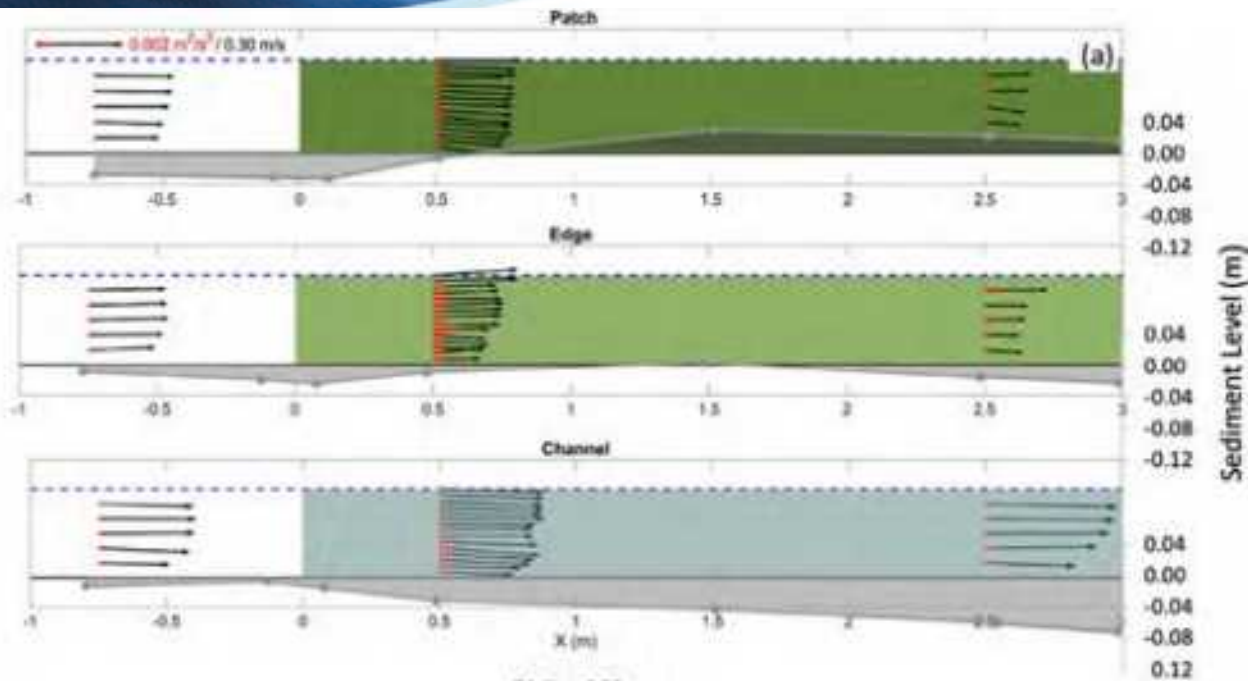
- 24 free surface sensors at 4 longitudinal positions
- 6 ADVs: profiles at 3 lateral positions and 3 longitudinal ones
- Sediment elevation using 60 sediment bars at 10 longitudinal positions



Experimental set-up

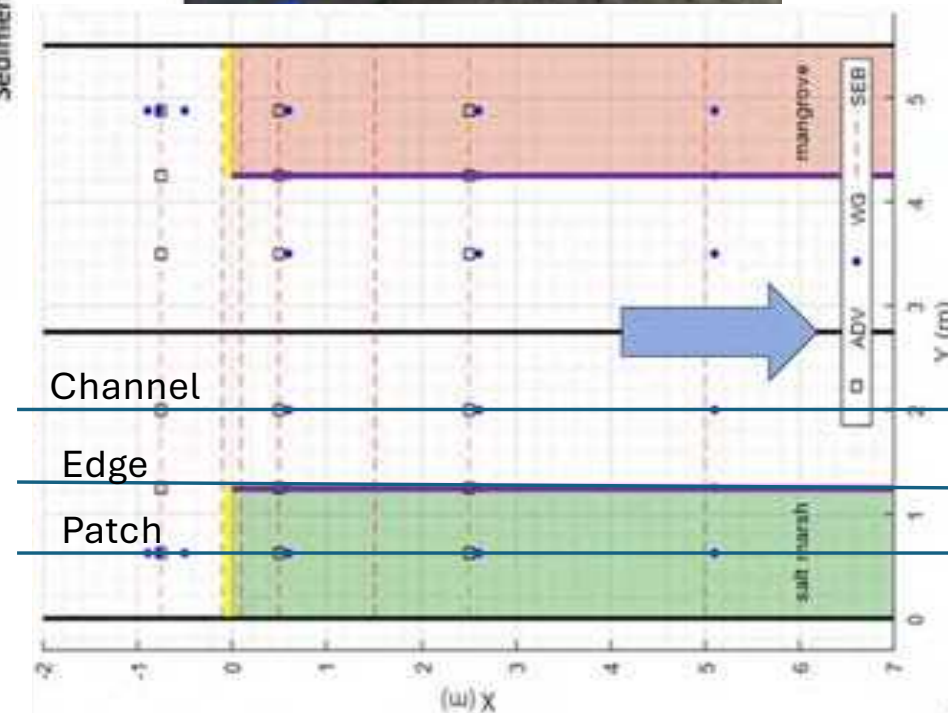


Results

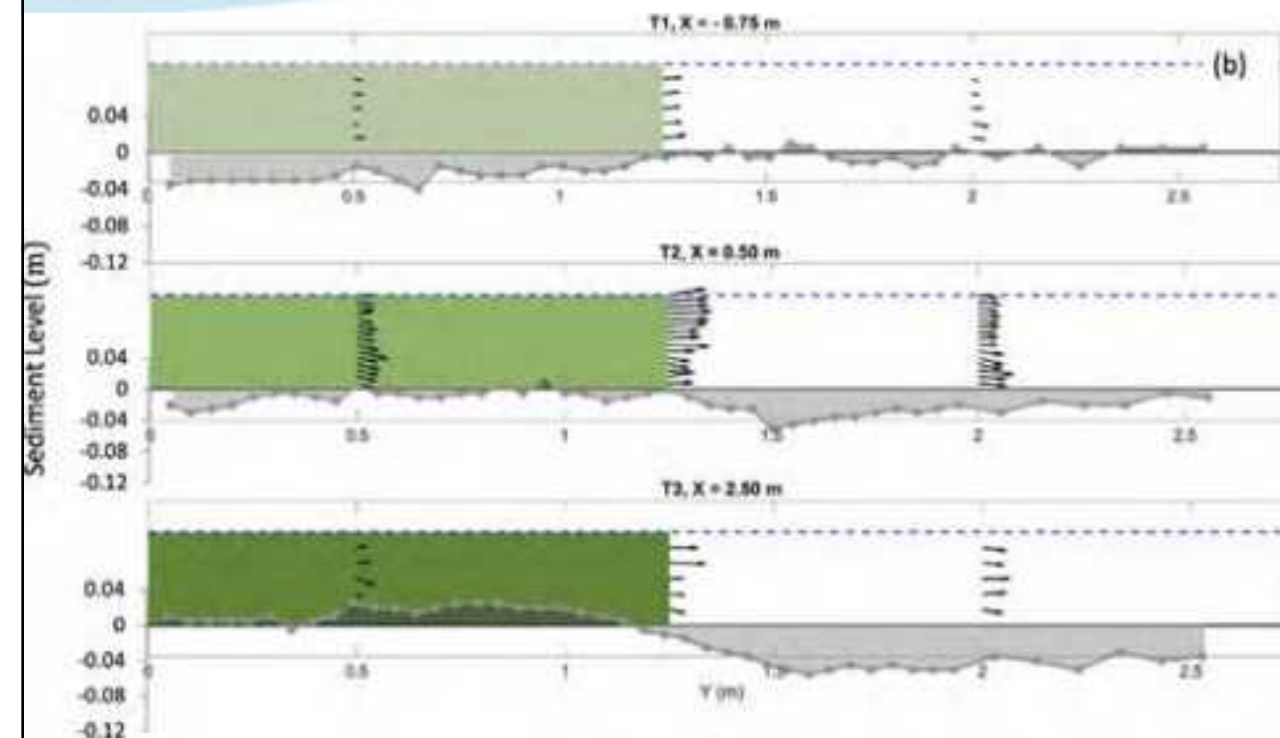


Longitudinal sections (inside the patch $Y = 0.625 \text{ m}$, dark green, at the lateral edge $Y = 1.25 \text{ m}$, light green, and at the channel $Y = 2.00 \text{ m}$, blue). Velocity profiles obtained using X and Z components.

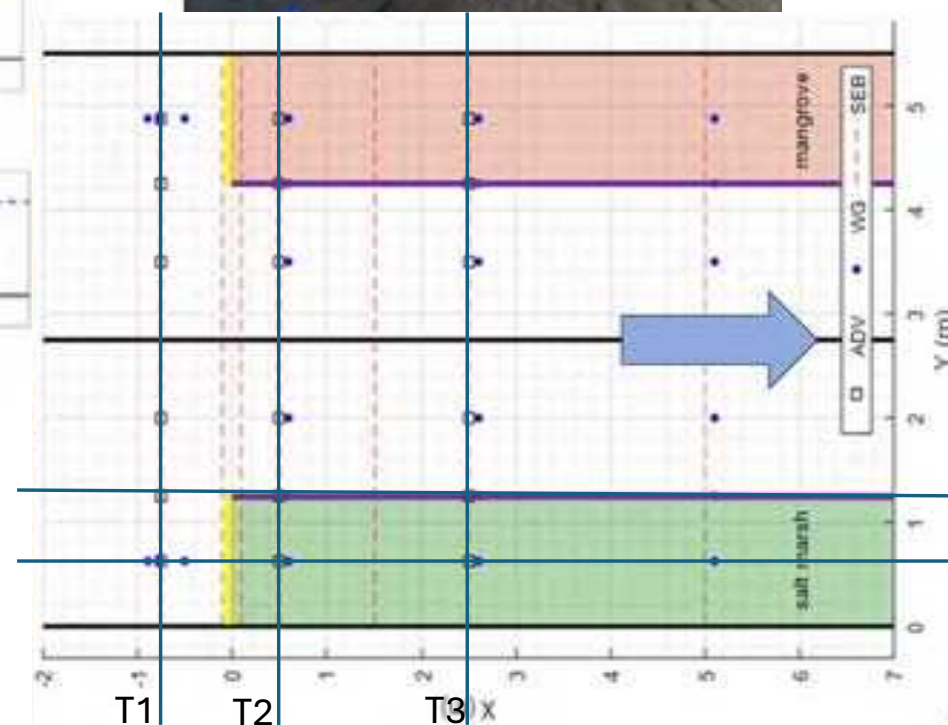
- Flow velocity (black arrows)
- TKE magnitude (red lines)
- Sediment elevation (gray lines)

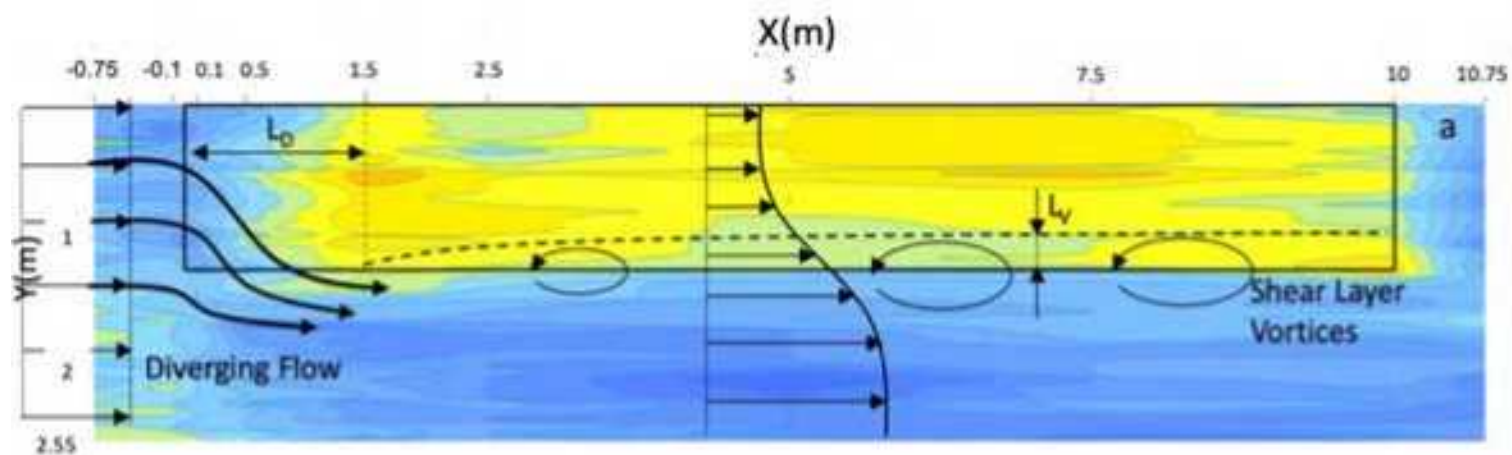


Results

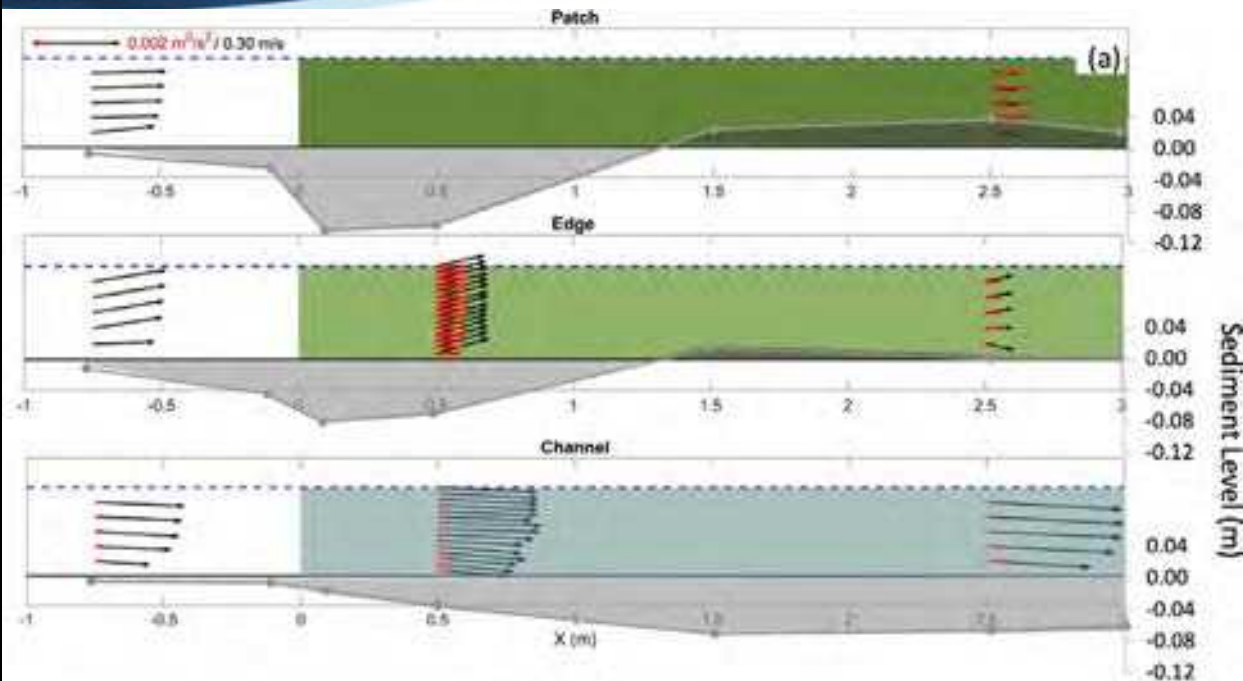


Cross sections (at T1 X = -0.75 m, T2 X = 0.50 m, and T3 X = 2.50 m). Velocity profiles obtained using Y and Z components.



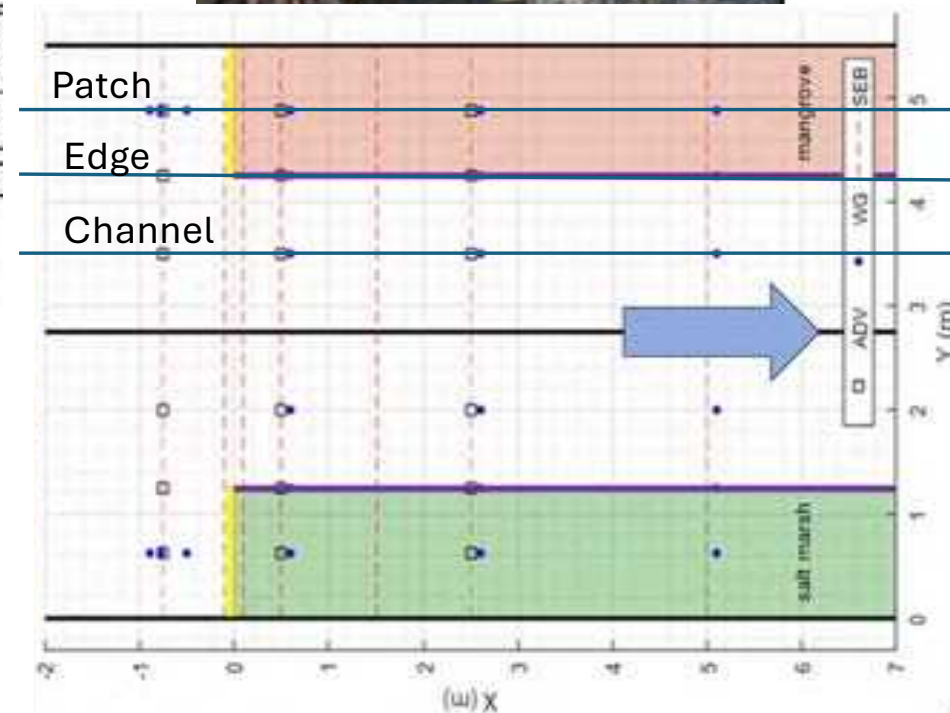


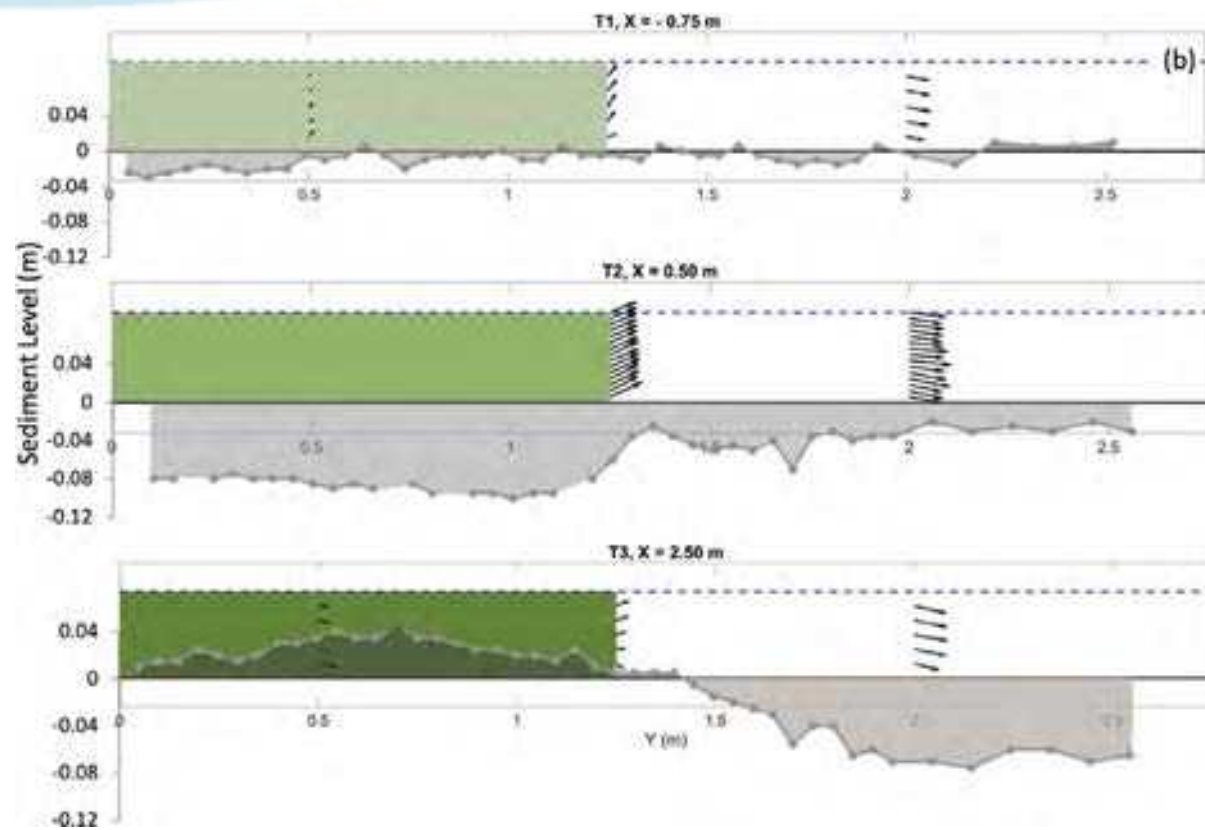
Results



Longitudinal sections (inside the patch $Y = 0.625$ m, dark green, at the lateral edge $Y = 1.25$ m, light green, and at the channel $Y = 2.00$ m, blue). Velocity profiles obtained using X and Z components.

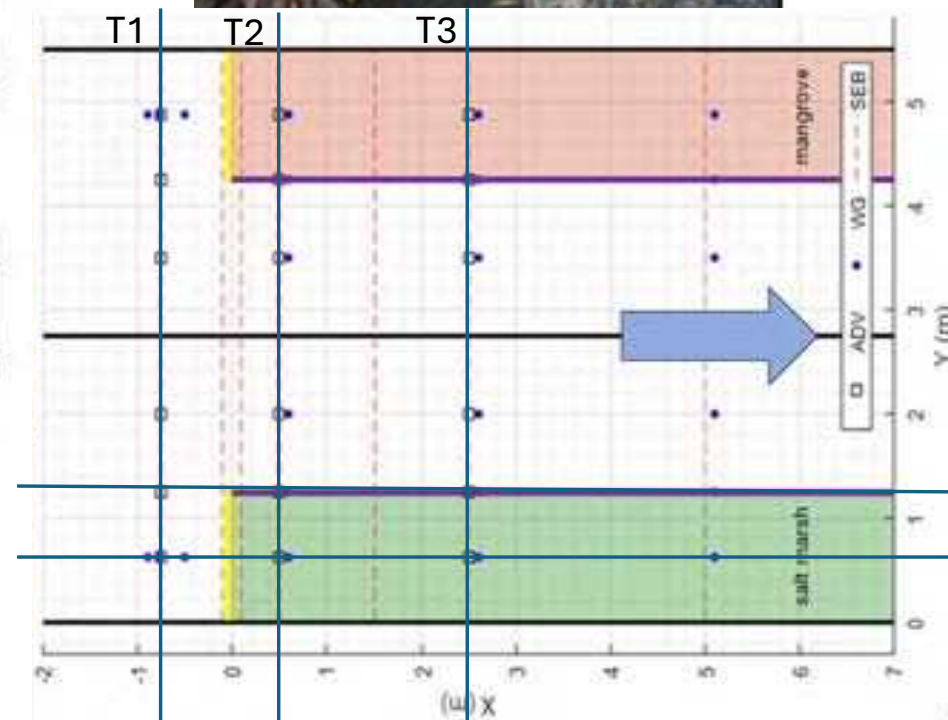
- Flow velocity (black arrows)
- TKE magnitude (red lines)
- Sediment elevation (gray lines)



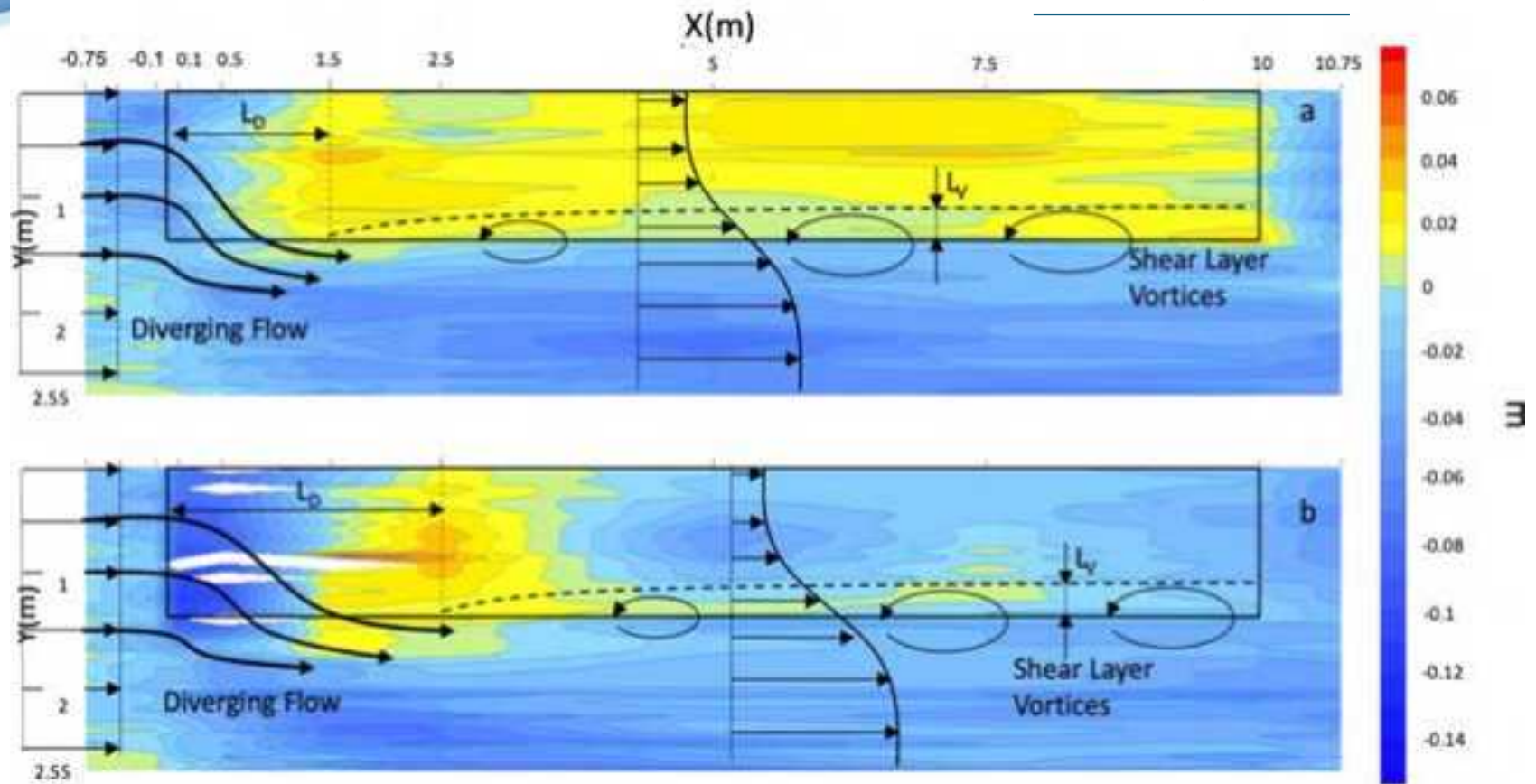


Cross sections (at T1 $X = -0.75$ m, T2 $X = 0.50$ m, and T3 $X = 2.50$ m). Velocity profiles obtained using Y and Z components.

Results

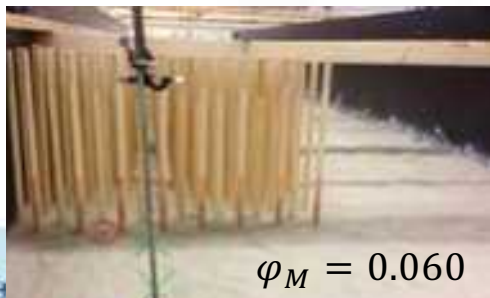
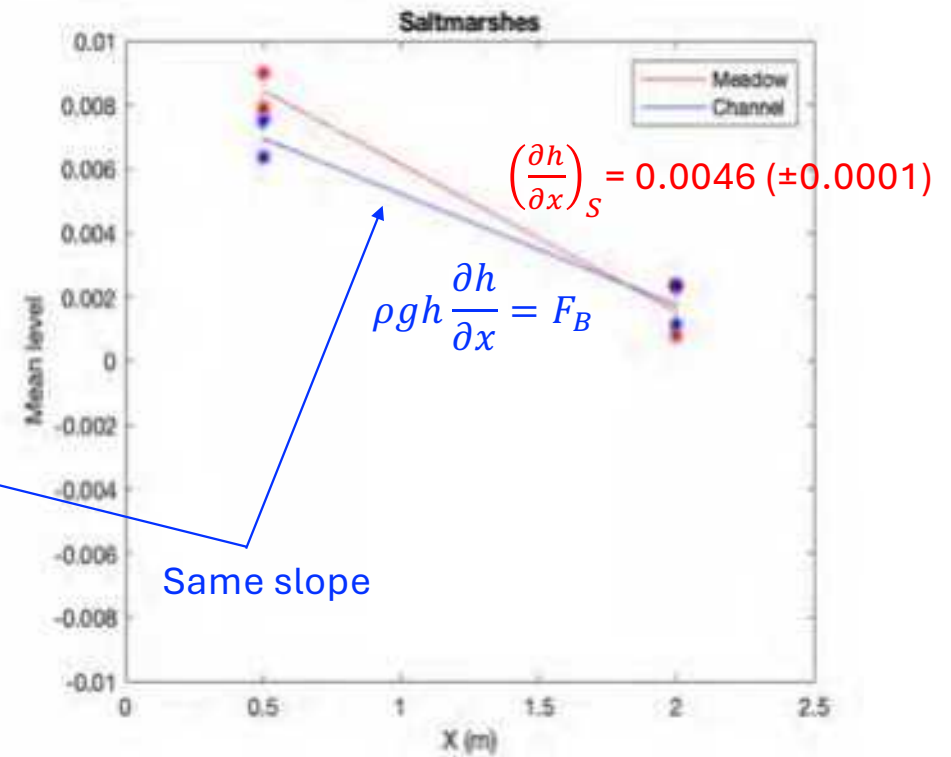
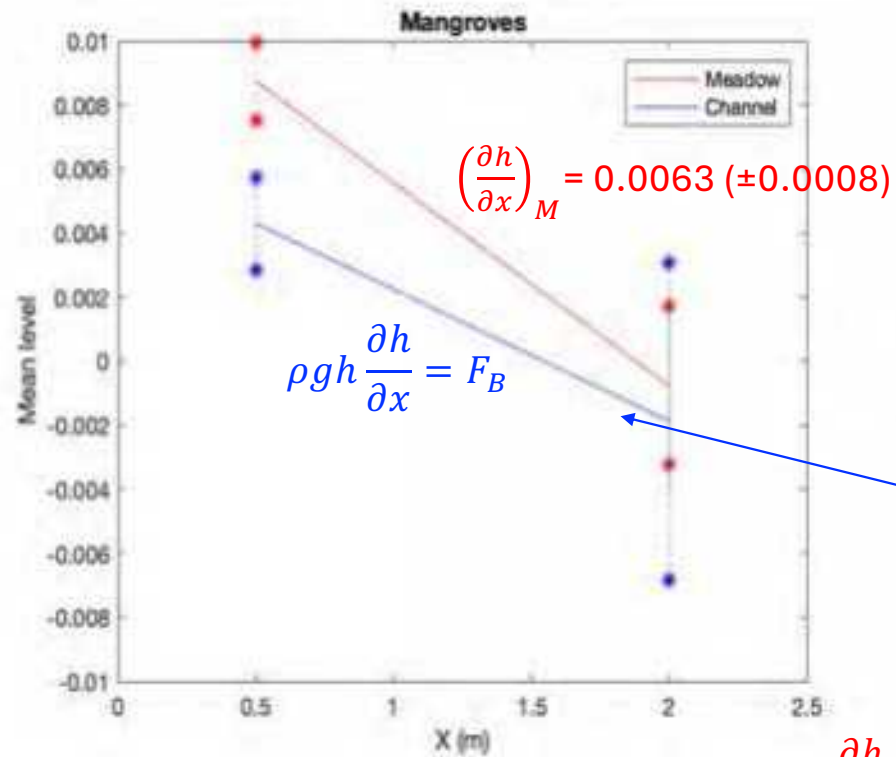


Results



Diverging region, L_D :

Downstream of L_D the flow field evolves into a flow field where the velocity within the vegetation is smaller than the velocity in the open channel. $L_D = 1.5$ m for saltmarshes and $L_D = 2.5$ for mangroves.



$$\rho g h \frac{\partial h}{\partial x} = F_D + F_B$$

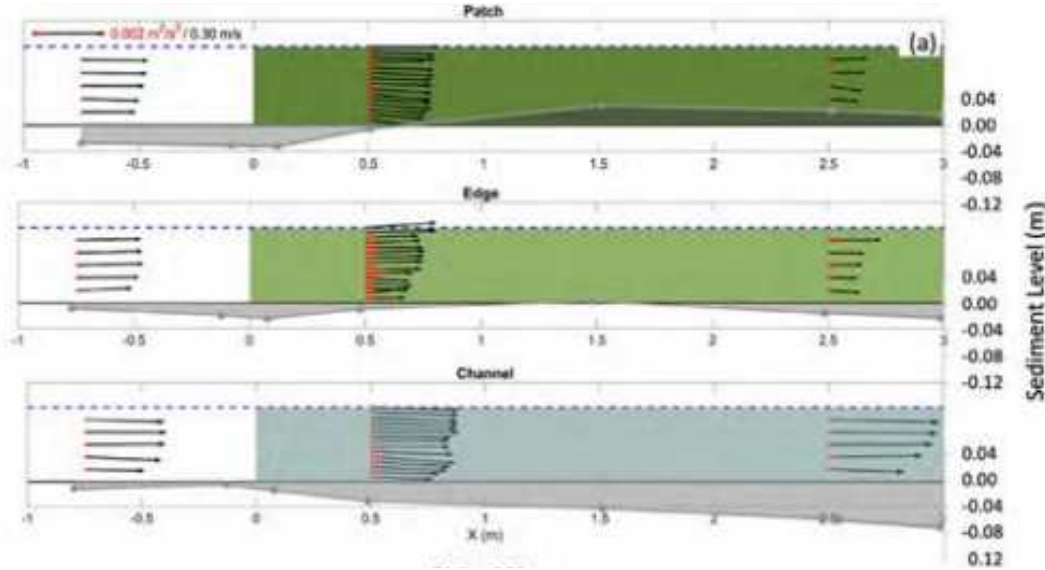
$$\left(\frac{\partial h}{\partial x}\right)_M > \left(\frac{\partial h}{\partial x}\right)_S$$

$$(F_D)_M > (F_D)_S$$

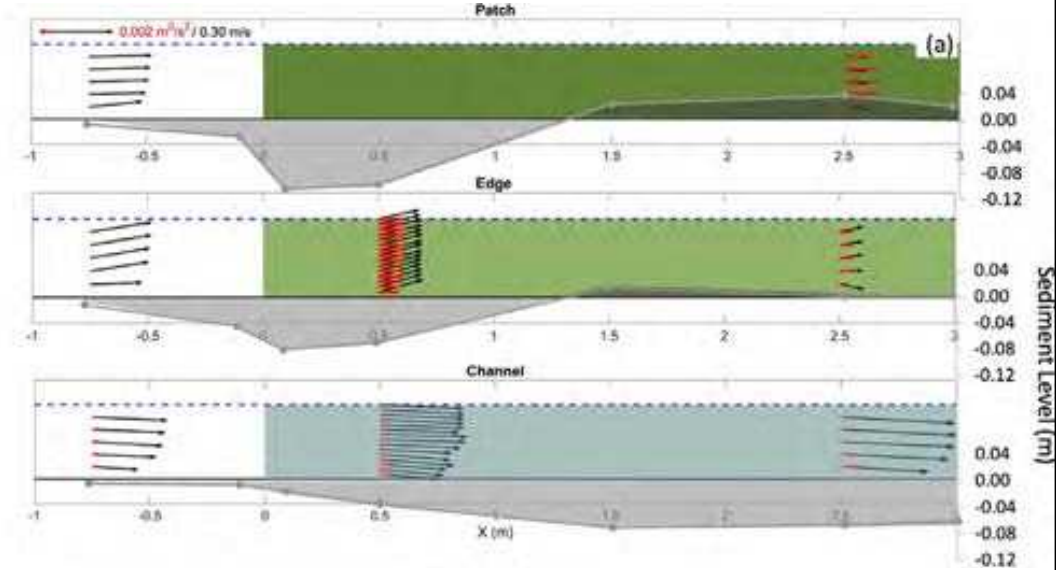


Results

$$\varphi_S = 0.012$$



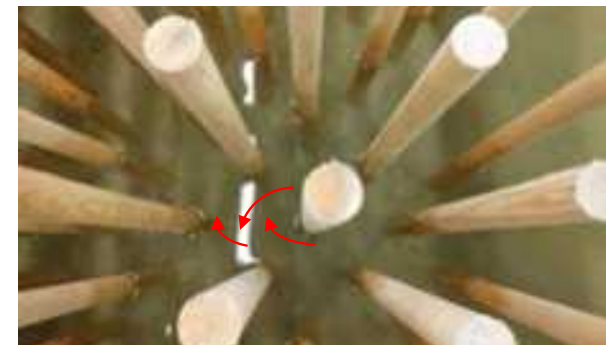
$$\varphi_M = 0.060$$

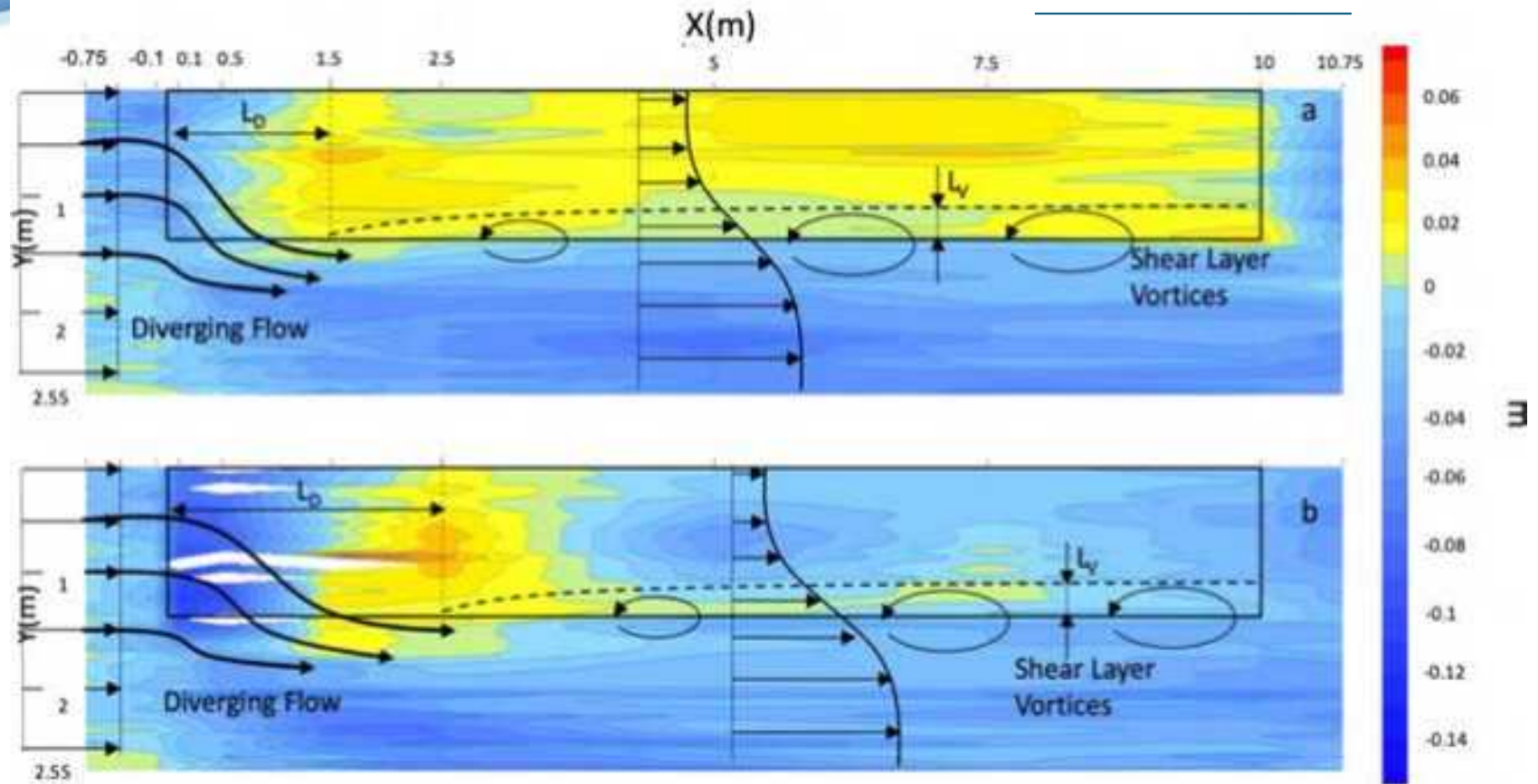


$$\frac{\sqrt{TKE}}{U} = 1.1 \left[C_D \frac{\varphi}{(1-\varphi)\pi/2} \right]^{1/3}$$

Saltmarsh $TKE = 0.001 \text{ m}^2/\text{s}^2$

Mangrove $TKE = 0.006 \text{ m}^2/\text{s}^2$



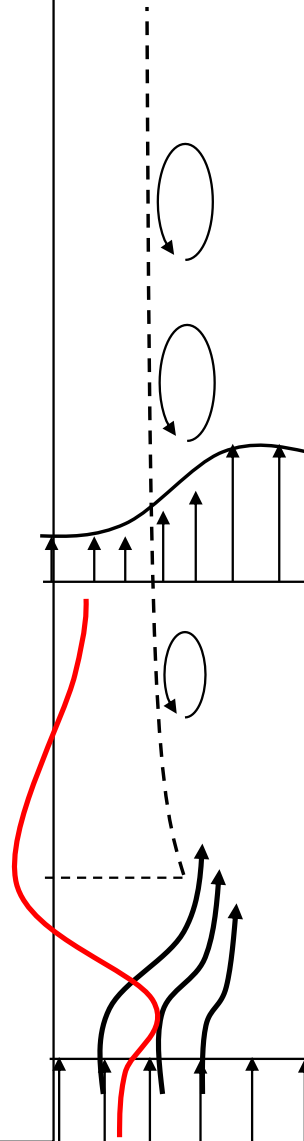
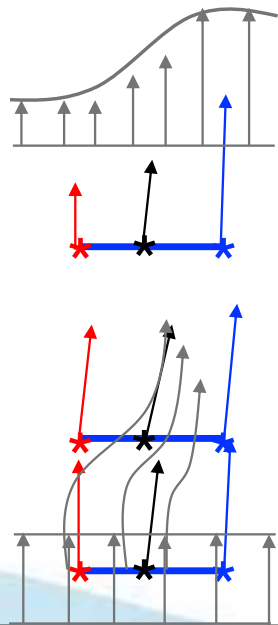


Length-scale of vortex penetration, L_v :

A shear layer forms at the interface between the patch and the lateral channel, where shear layer vortices develop. Since both patches present the same frontal area per volume, L_v is expected to be similar for both cases, being slightly bigger for the rigid vegetation due to its larger C_D value. Taking $C_D = 1$: $L_v = 0.5(C_D a)^{-1} \approx 0.2 \text{ m}$

Results

400 sticks/m²
6 - 8 mm diameter



Bouma et al. (2005)



- **Motivation**



- **HyWedges**

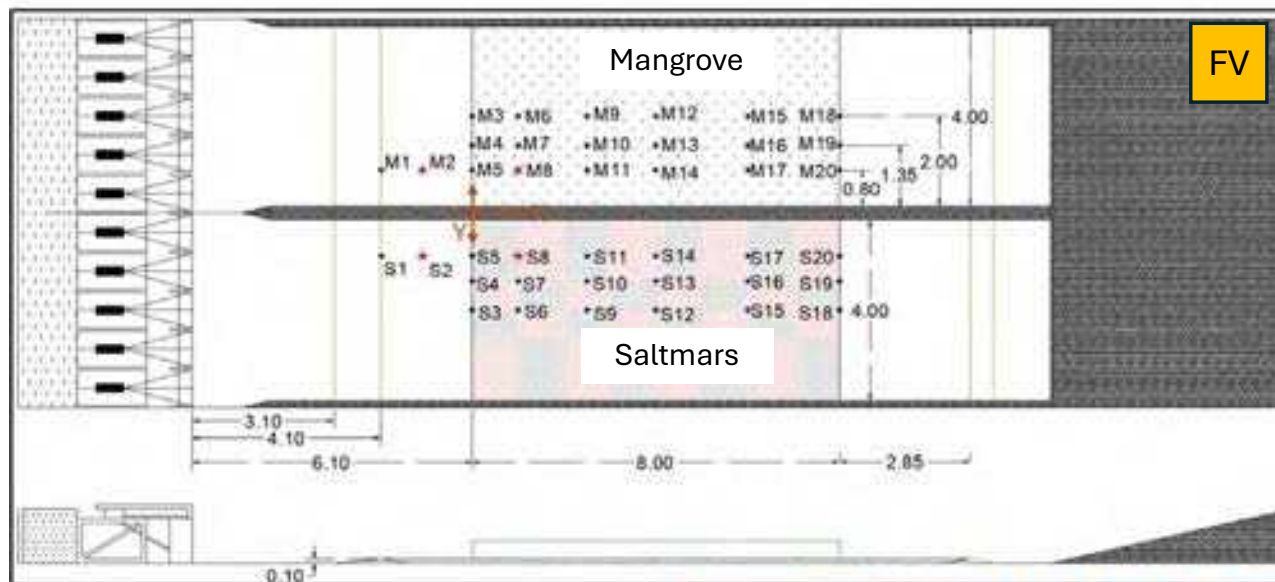


- **SHACC**



- **Conclusions**

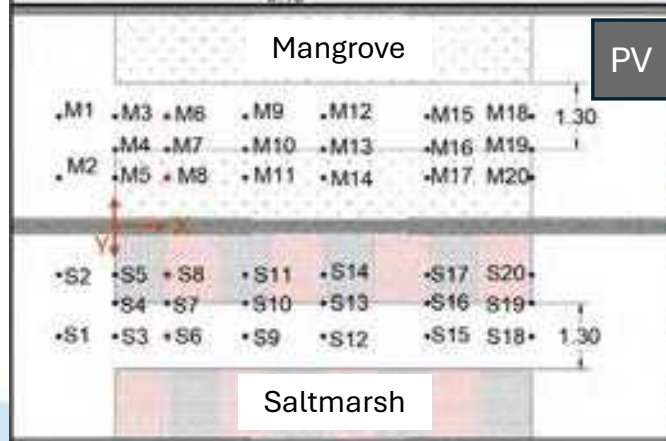
Experimental set-up



FV



FV



PV



PV

Saltmarsh

Experimental set-up

Saltmarsh characteristics

$$b_v = 0.6 \text{ cm}$$

$$h_v = 40 \text{ cm}$$

$$N = 312.5 \text{ stems}/\text{m}^2$$

$$\Delta X = \Delta Y = 0.04 \text{ m}$$

Maza et al. (2016), Norris et al. (2019)



Mangroves characteristics

$$b_v = 3 \text{ cm}$$

$$h_v = 40 \text{ cm}$$

$$N = 12.5 \text{ stems}/\text{m}^2$$

$$\Delta X = \Delta Y = 0.2 \text{ m}$$

Schulze et al. (2019), Vuik et al. (2018);
Zhu et al. (2020)

Sediment

$$d_{50} = 0,168 \text{ mm}$$

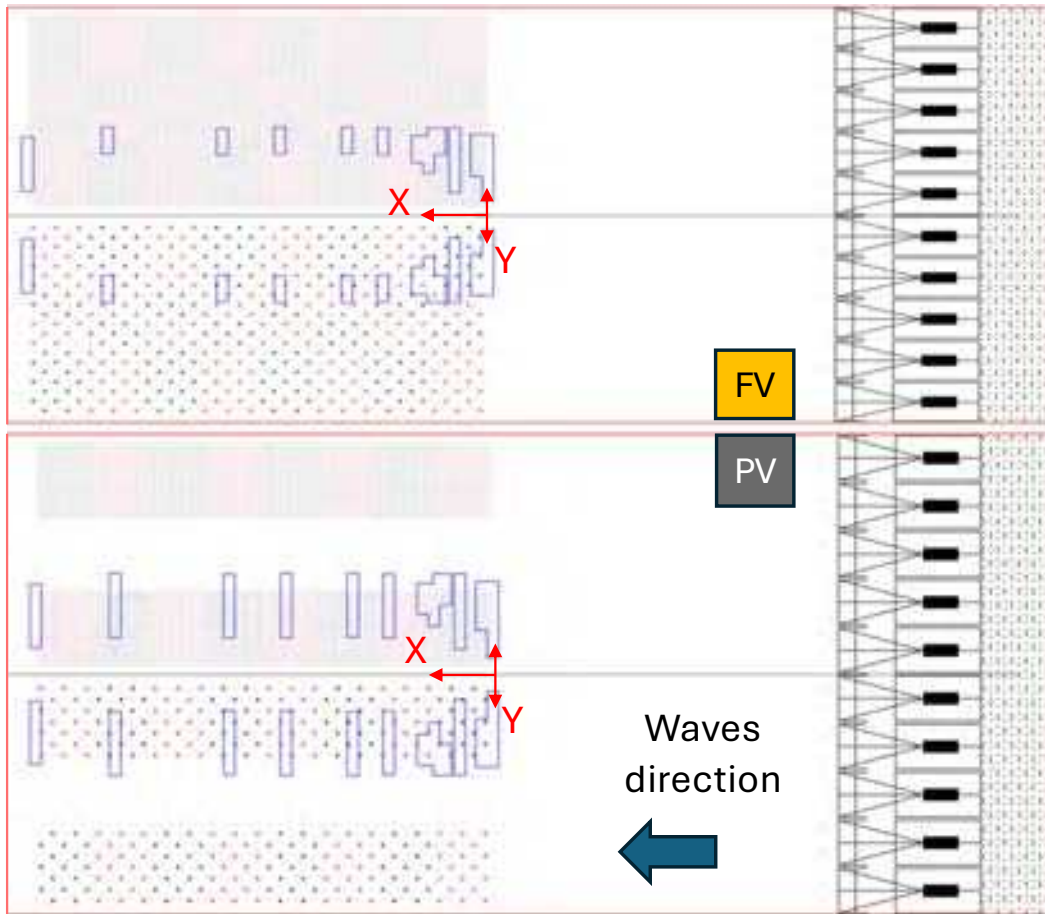
(Horstman et al., 2014; Hu et al., 2021)

Regular waves

Test	h (m)	H (m)	T (s)	L (m)	H/h	H/L
C13	0.4	0.1	1.5	2.61	0.25	0.04
C24	0.4	0.1	2.5	4.74	0.25	0.02
C35	0.6	0.2	1.5	2.99	0.33	0.07
C46	0.2	0.1	1.5	1.97	0.50	0.05
C57	0.2	0.1	2.5	3.43	0.50	0.03
C68	0.4	0.2	1.5	2.61	0.50	0.08
C79	0.6	0.3	1.5	2.99	0.50	0.10



Experimental set-up



Laser scanner

- Minimum resolution: 0.4 mm
- Full Vegetation: 20 areas $\approx 20 \times 40$ cm
- Partial Vegetation: 25 areas $\approx 20 \times 40$ cm



Mangroves initial bed elevation

Y (m)

FV

Z (m)

Waves



Y (m)

PV

Z (m)

X (m)

Saltmarsh initial bed elevation

Y (m)

FV

Z (m)

Waves



Y (m)

PV

Z (m)

X (m)



Mangroves – bed elevation evolution

PV

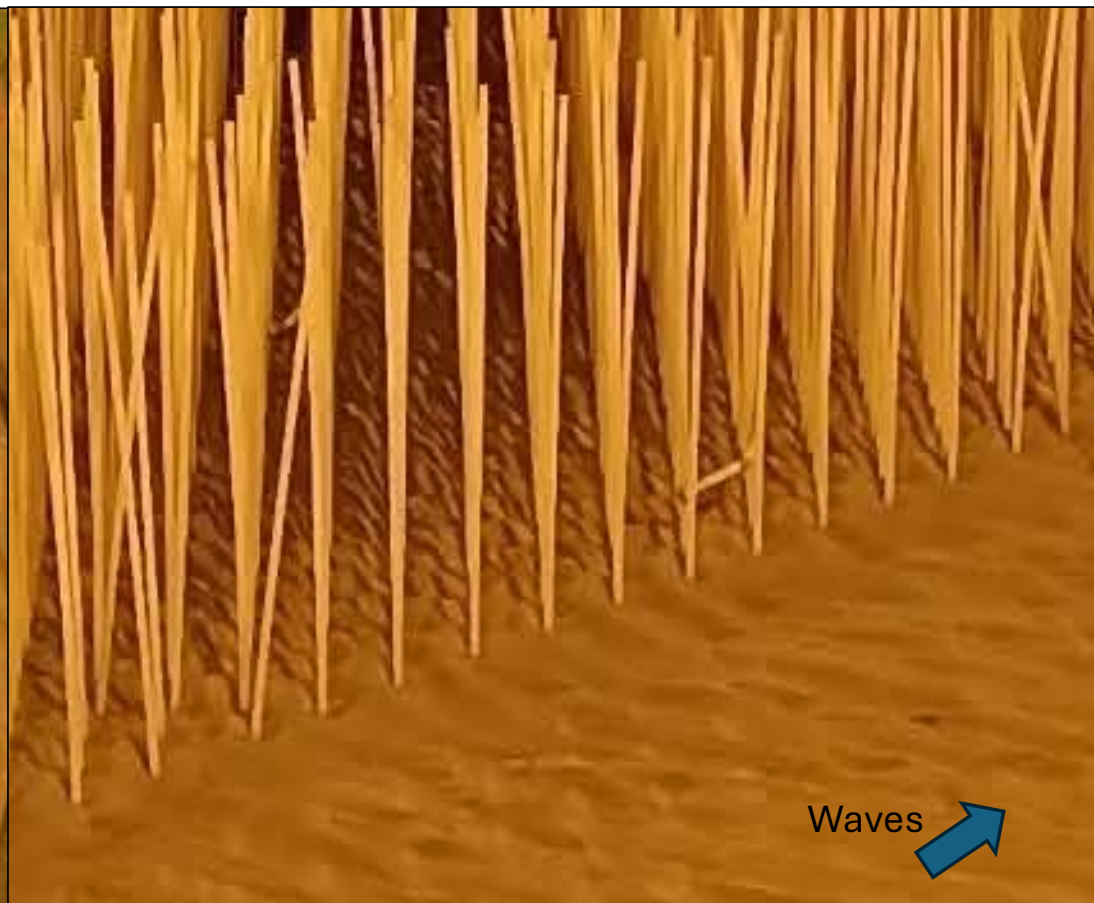
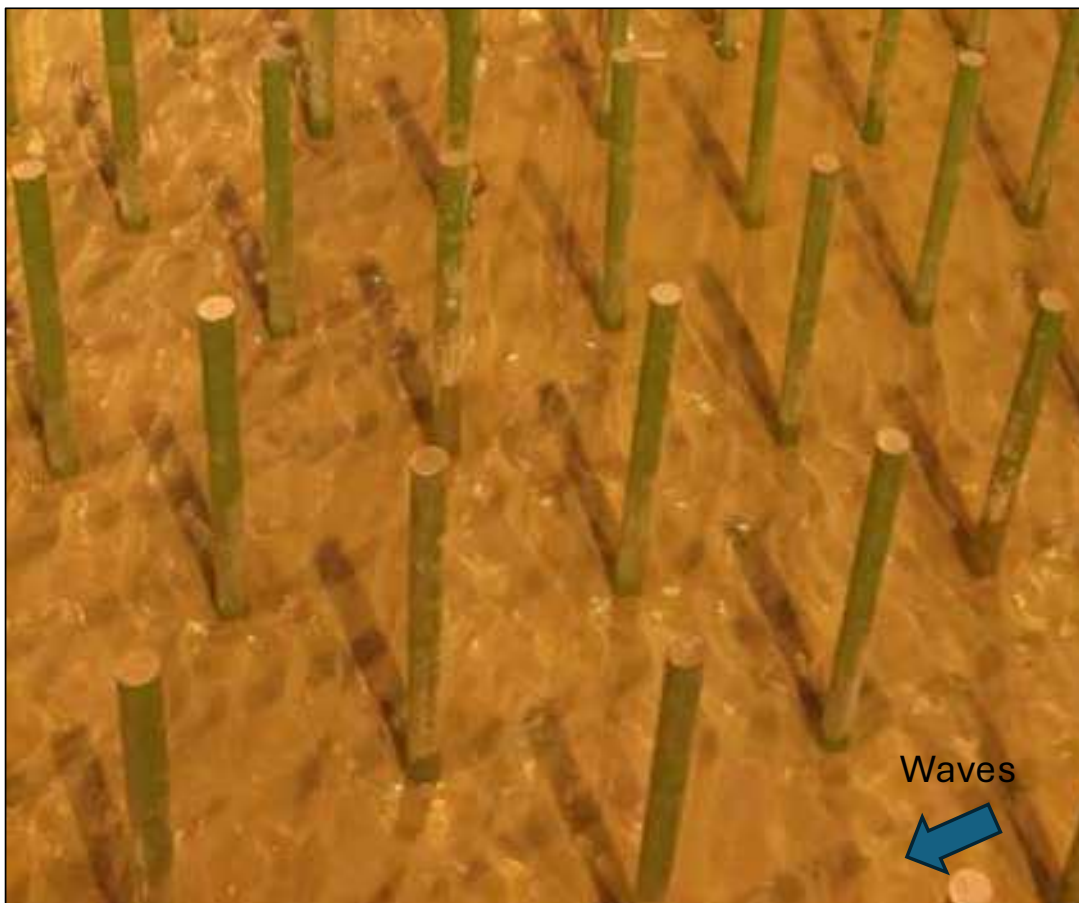
Test	h (m)	H (m)	T (s)
C57	0.2	0.1	2.5
C68	0.4	0.2	1.5
C79	0.6	0.3	1.5

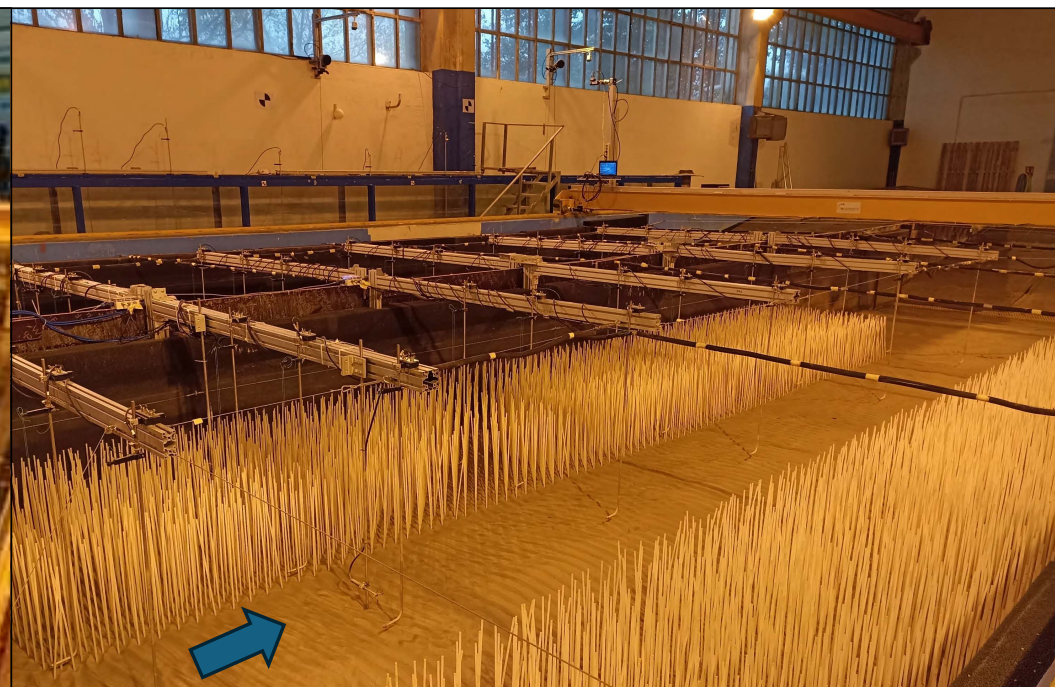
No significant erosion/accretion patterns

Saltmarshes – bed elevation evolution

Test	h (m)	H (m)	T (s)
C57	0.2	0.1	2.5
C68	0.4	0.2	1.5
C79	0.6	0.3	1.5

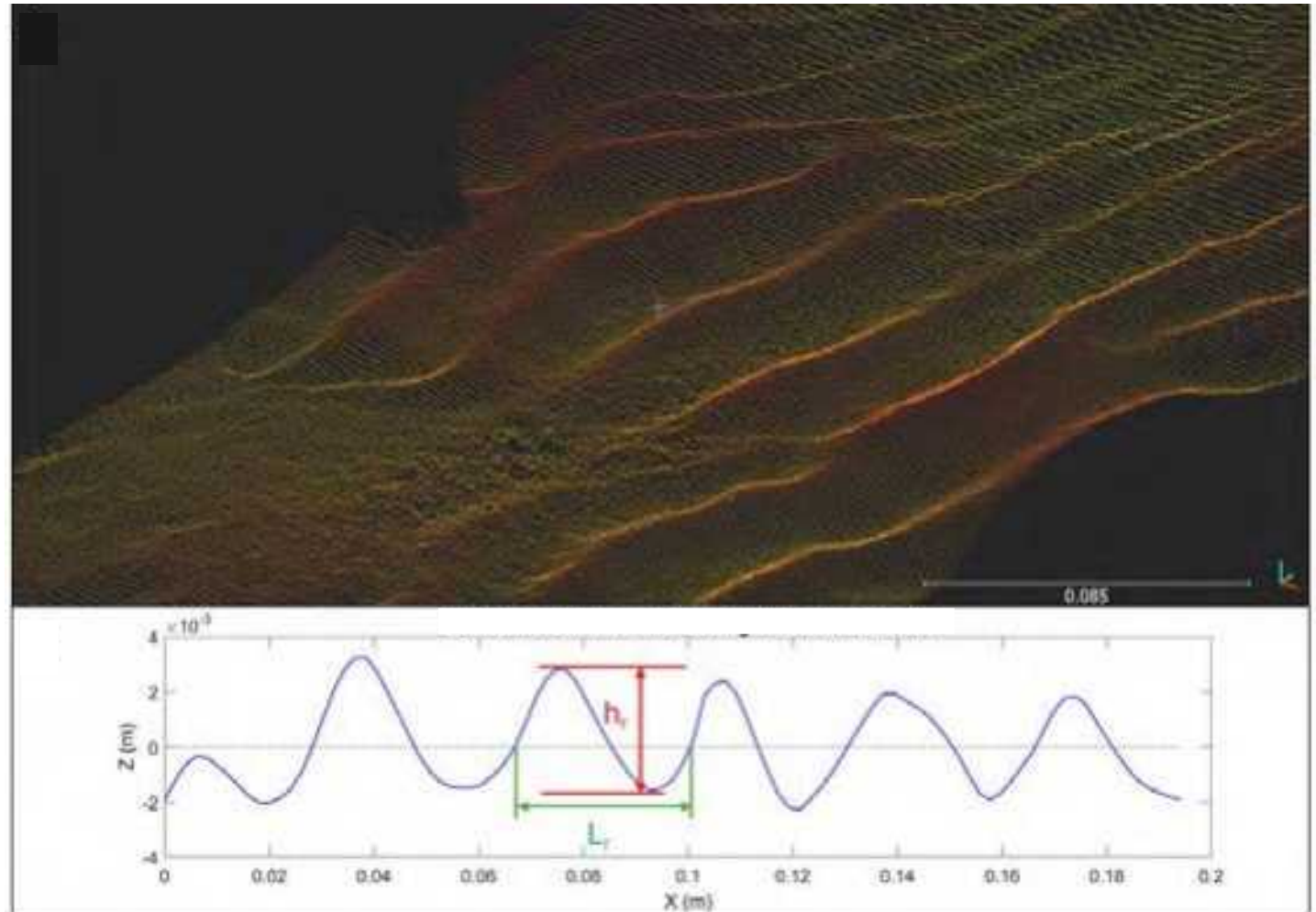
No significant erosion/accretion patterns

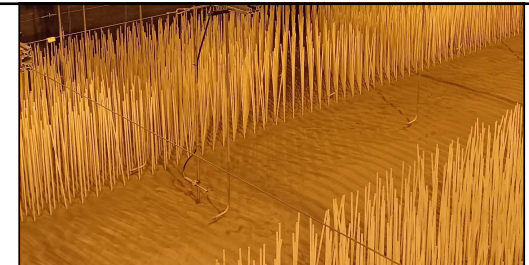




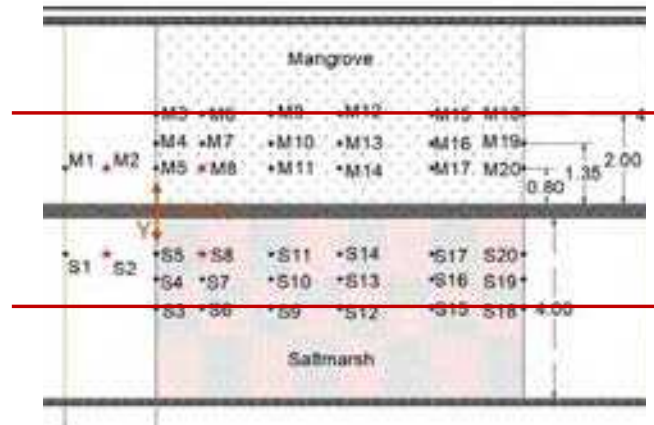
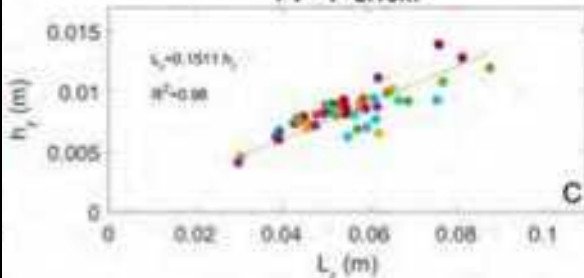
Ripples characterization

- h_r : ripples height
- L_r : ripples length
- $X \approx 0, 0.48, 1.7, 2.33, 3.5, 4.5, 6.5$ y 8 m
- Measured at the center of the channel ($Y \approx 2.15$ m) and within the vegetation fields ($Y \approx 0.95$ m)

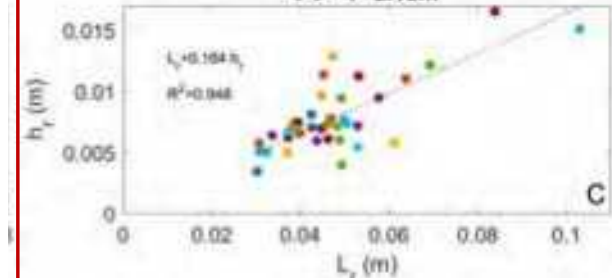




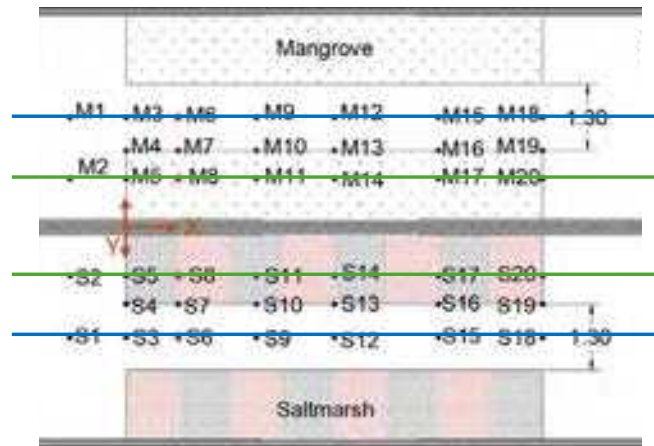
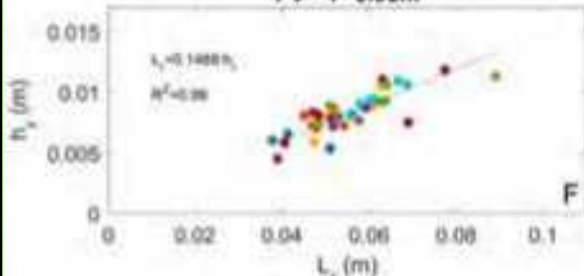
FV - Y=2.15m



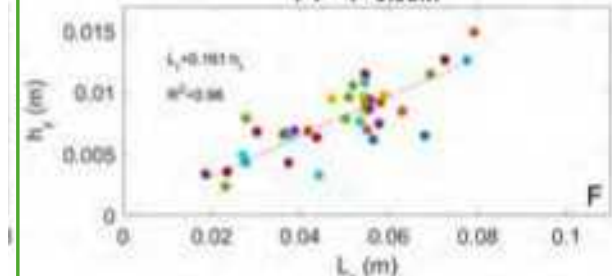
FV - Y=2.15m



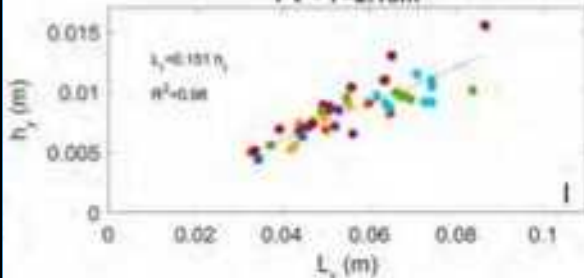
PV - Y=0.95m



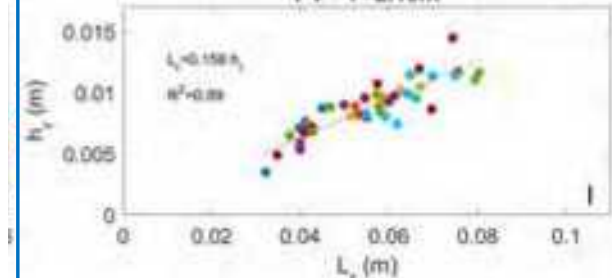
PV - Y=0.95m



PV - Y=2.15m

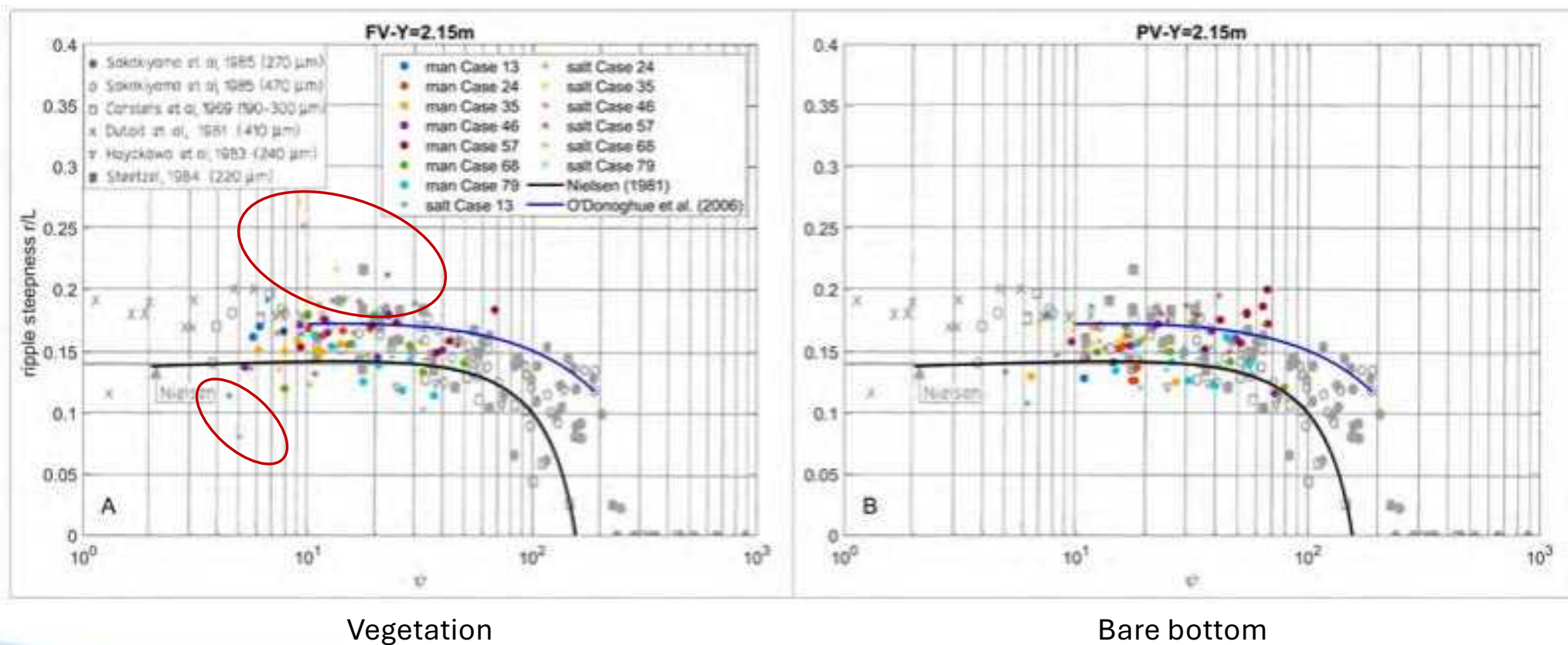


PV - Y=2.15m



Ripples steepness

Measured bedforms geometry in the laboratory is compared to van Rijn (1993)



Ripples steepness

Can we estimate their geometry within vegetation fields?

Vegetation type	Formula	RMSE within vegetation	RMSE at the channel
Saltmarsh	Nielsen (1981)	0.047	0.026
	O'Donoghue et al. (2006)	0.039	0.023
	Nelson et al. (2013)	0.063	0.043
Mangrove	Nielsen (1981)	0.023	0.026
	O'Donoghue et al. (2006)	0.023	0.027
	Nelson et al. (2013)	0.041	0.037

Nielsen (1981)

$$\frac{h_r}{L_r} = \frac{0.275 - 0.022 \psi^{0.5}}{2.2 - 0.345 \psi^{0.34}}$$

O' Donoghue et al. (2006)

$$\frac{h_r}{L_r} = \frac{0.275 - 0.022 \psi^{0.42}}{1.97 - 0.44 \psi^{0.21}}$$

Nelson et al. (2013)

$$\frac{L_r}{A_{w,b}} = \left\{ 0.72 + 2.0 \times 10^{-3} \frac{A_{w,b}}{d_{50}} \left[1 - \exp \left(- \left(1.57 \times 10^{-4} \frac{A_{w,b}}{d_{50}} \right)^{1.15} \right) \right] \right\}^{-1}$$

ψ : mobility parameter

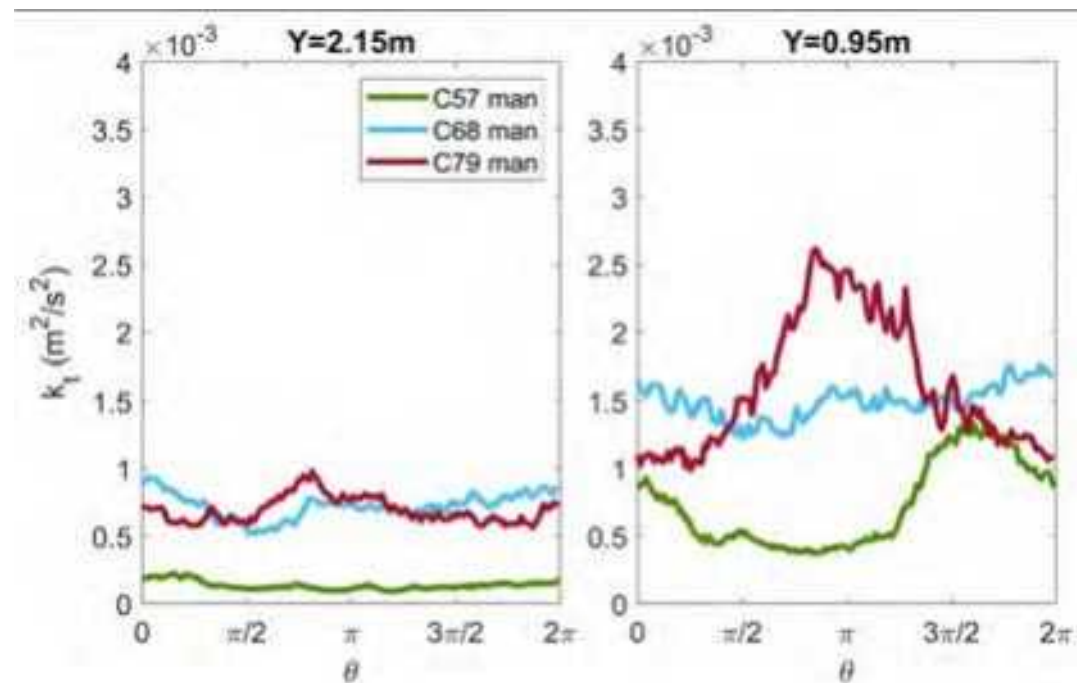
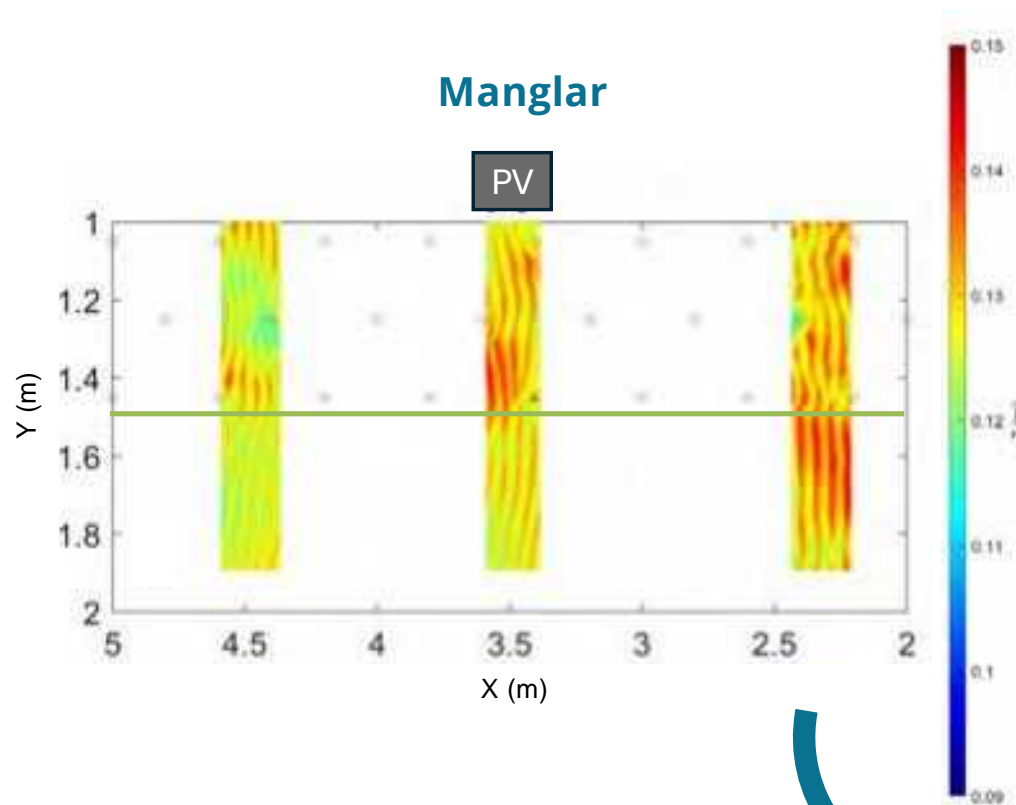
$$\frac{h_r}{L_r} = 0.120 L_r^{-0.056}$$

$A_{w,b}$: orbital excursion at the bottom

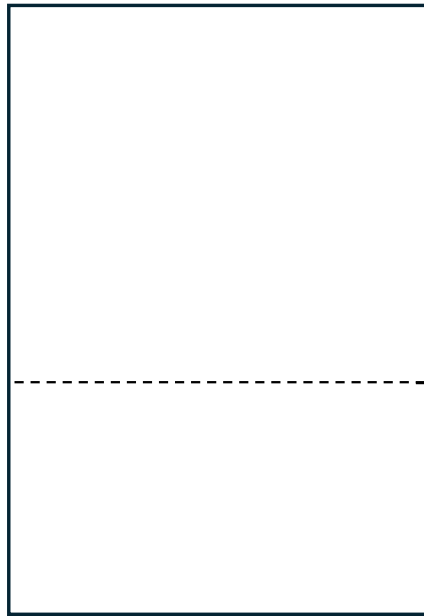
Ripples pattern

Manglar

PV

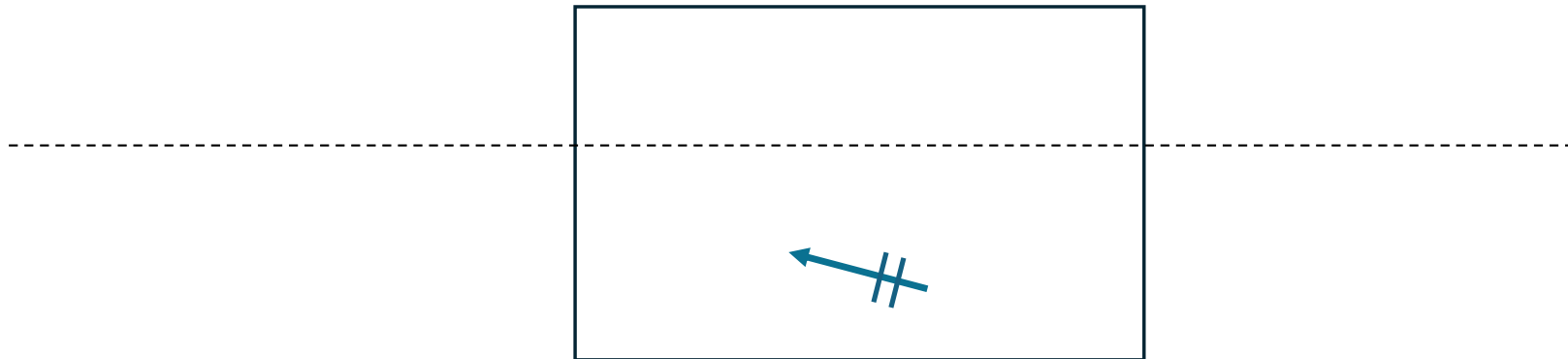


Ripples and wave energy dissipation



Ripples and wave energy dissipation

Ripples orientation



Ripples orientation





- **Motivation**



- **HyWedges**



- **SHACC**

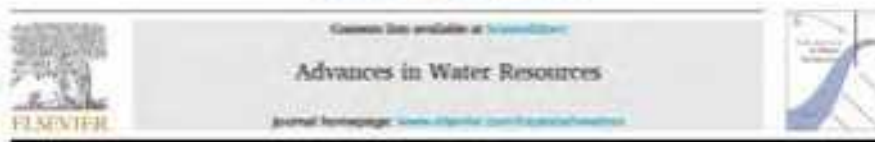


- **Conclusions**

- The flow and sediment transport patterns observed under **currents** show the expected divergence region, which is influenced by the vegetation field properties.
- Vegetation fields allow trapping sediment and creating soil while preventing erosion but **edge effects** that may result in local ecosystem loss must be considered.
- Under the tested **wave conditions** significant erosion and accretion areas were not observed.
- **Ripples** size within the vegetation area in the mangrove mimics can be estimated using existing formulations. That is not the case for saltmarshes mimics. For both the pattern is not regular due to the turbulence produced by the stems and the orientation of the ripples is affected by the transformation processes produced by the vegetation in the waves.
- More studies are still needed to well characterized flow-sediment-ecosystem interactions.



Advances in Water Resources 104 (2022) 106027



Living on the edge: How traits of ecosystem engineers drive bio-physical interactions at coastal wetland edges

Gillies LG^{a,*}, M Maza^b, J Garcia-Maribon^b, JL Laca^b, T Szoski^c, M Arjemi Cierco^c, M Pind^d, AM Folkard^e, T Bulke^a

Acknowledgments

Thank you for your attention!



mazame@unican.es

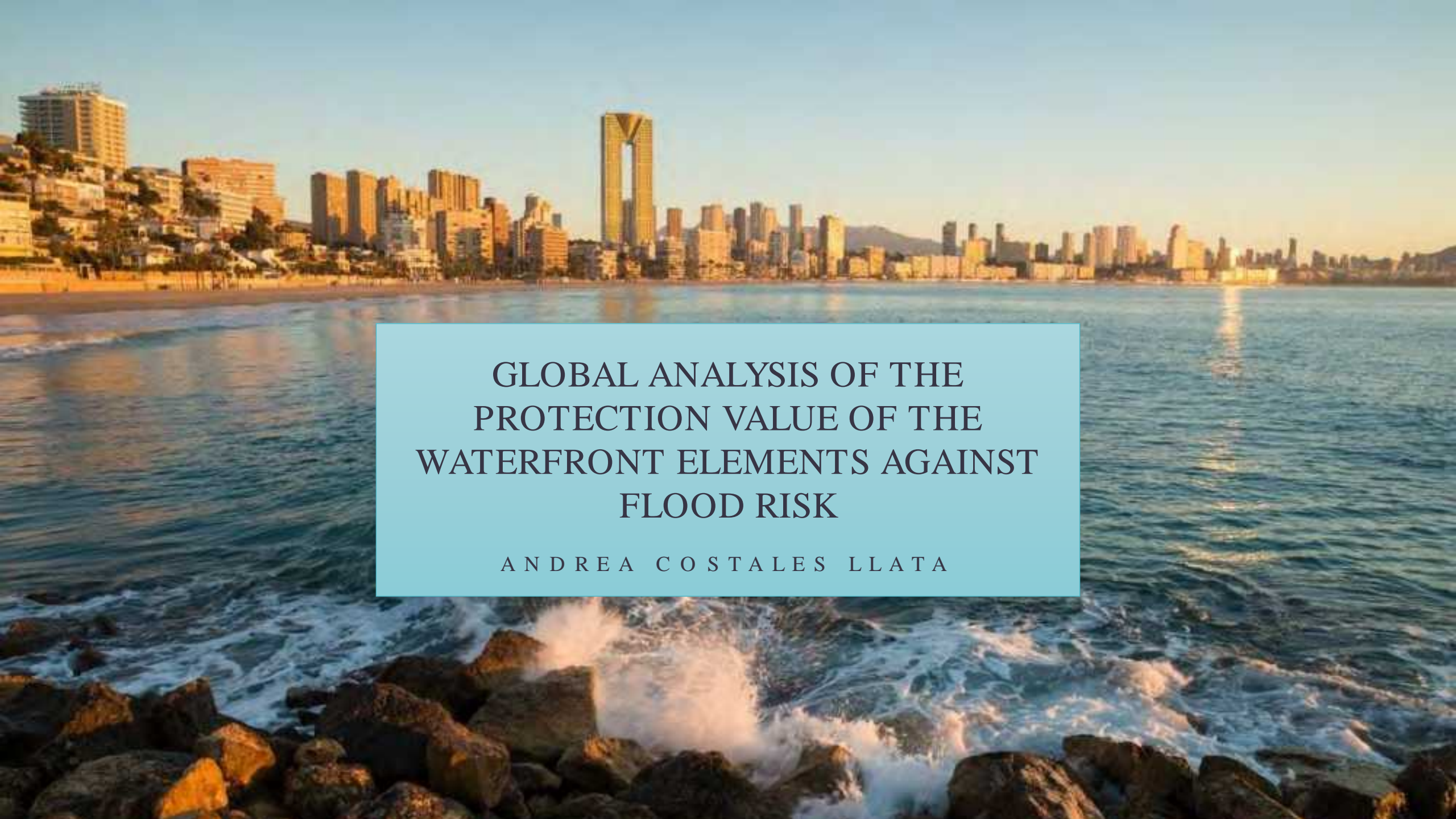


@MariaE_Maza



Maria Maza

Interactive session with FIHAC PhD students by Andrea Costales, Lucas de Freitas and Arnau García (IHCantabria)

The background image shows a coastal city skyline at sunset. The sky is a clear, pale blue, and the sun is low on the horizon, casting a warm, golden light over the scene. The city skyline is composed of numerous buildings of varying heights, with a prominent, tall, rectangular building featuring a large, dark, rectangular cutout in its center. The buildings are reflected in the calm water of the bay. In the foreground, dark, jagged rocks are visible, with white, frothy waves crashing against them, creating a dynamic contrast with the calm water in the background.

GLOBAL ANALYSIS OF THE PROTECTION VALUE OF THE WATERFRONT ELEMENTS AGAINST FLOOD RISK

ANDREA COSTALES LLATA

Author: Andrea Costales Llata

Supervisors: Íñigo J. Losada Rodríguez
Alexandra Toimil Silva

PhD programme: Coastal Engineering,
Hydrobiology and Management of
Aquatic Systems

1. BACKGROUND AND OBJETIVES

2. THE CASE OF BENIDORM

3. METHODOLOGY

3.1. LONG TERM MODELLING

3.2. SHORT TERM MODELLING

3.3. FLOOD MODELLING

3.4. ECONOMIC ASSESSMENT

4. NEXT STEPS

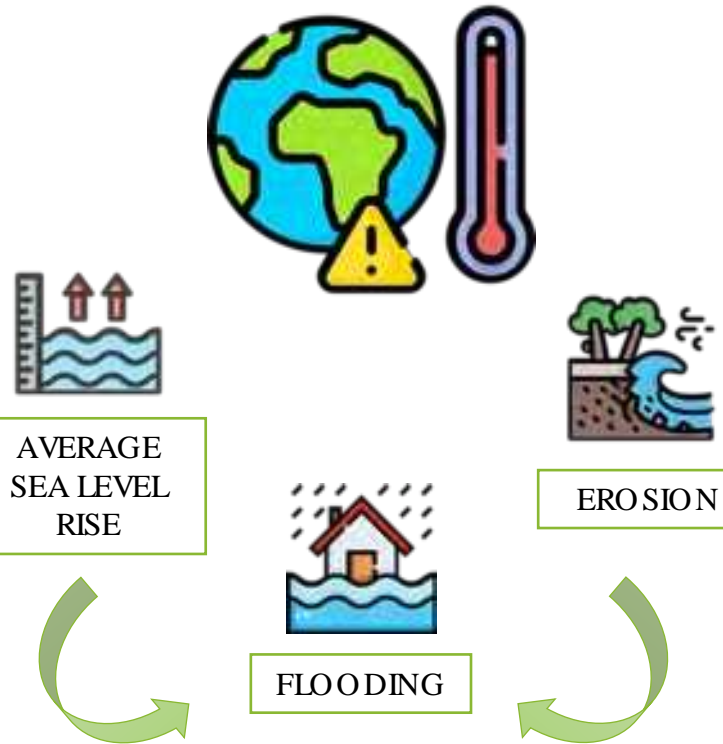
4.1. ADAPTATION AND CLIMATE CHANGE

4.2. APPLICATION AT REGIONAL SCALE

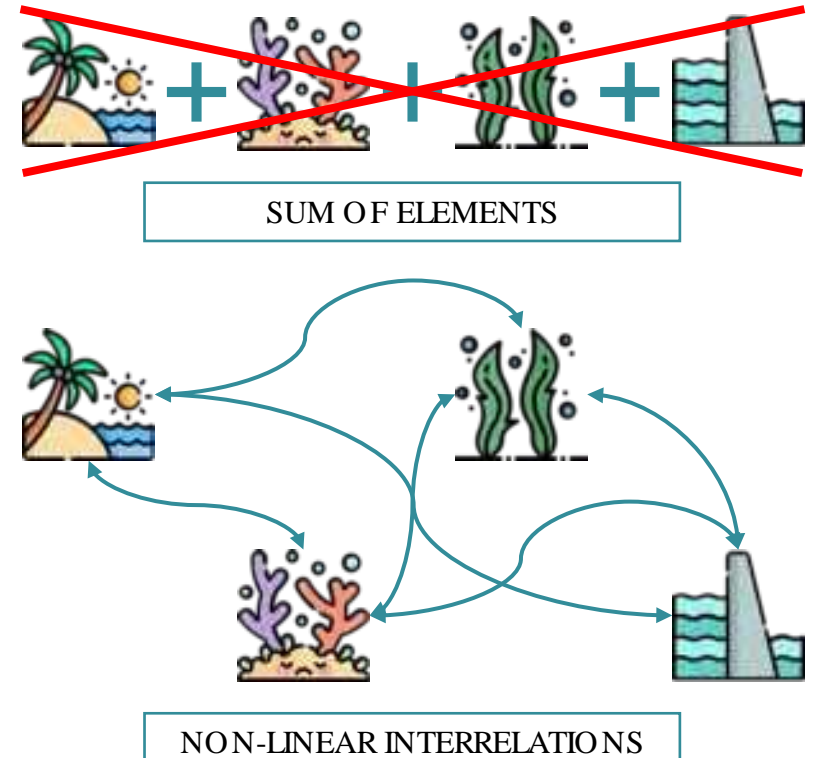
5. REFERENCES

BACKGROUND AND OBJECTIVES

COASTAL RISK ASSOCIATED WITH CLIMATE CHANGE



WATERFRONT PROTECTION SERVICE



MAIN GOAL

Development of a methodology to economically assess the protection against flooding (and implicitly erosion) offered by the different elements of the waterfront both in isolation and as a whole by identifying the non-linearities derivate from their combination

OBJETIVES

IMPROVING THE FLOOD
MODELLING



APPLICATION AT LOCAL
SCALE



IMPROVING THE ANALYSIS OF
ASSOCIATED RISK



APPLICATION AT REGIONAL
SCALE



IMPROVING THE ECONOMIC
QUANTIFICATION



ADAPTATION AND CLIMATE
CHANGE



THE CASE OF BENIDORM



HR TOPOBATHYMETRY

- MDT02-ETRS-HU30 (IGN, 2016).
- Ecocartografía de Alicante (MITECO, 2006-2007).
- EMODnet (2020).



WAVE DATA

- GOW2 ERA 5 (IHData).
- GOS (IHData).
- GOT (IHData).



WATERFRONT ELEMENTS

SEAGRASS

Posidonia oceanica

Cymodocea nodosa

Caulerpa racemosa

Height (m)
Diameter (m)

Ondiviela et al. (2014)

Klein et al., 2008

Density (p/m²)

Instituto de Ecología
Litoral

Drag coefficient

Infantes et al. (2012)



BEACHES

Poniente

Levante



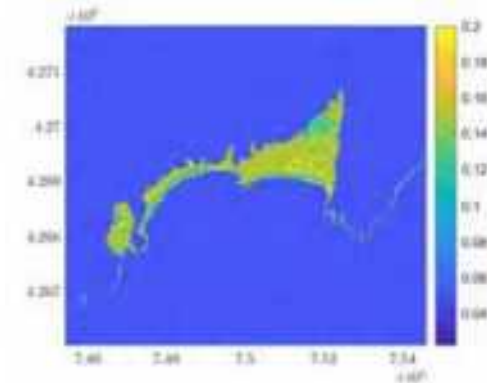
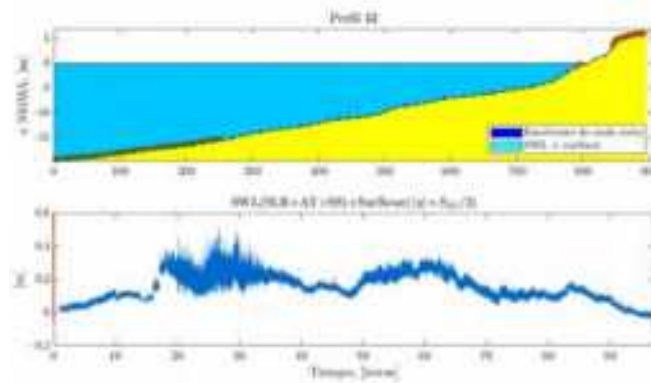
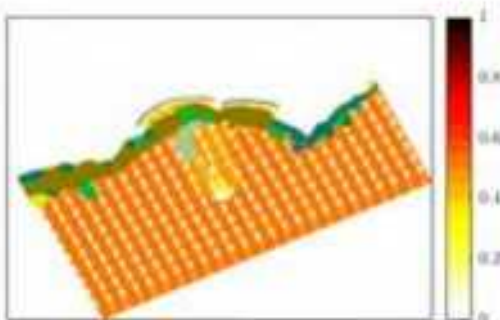
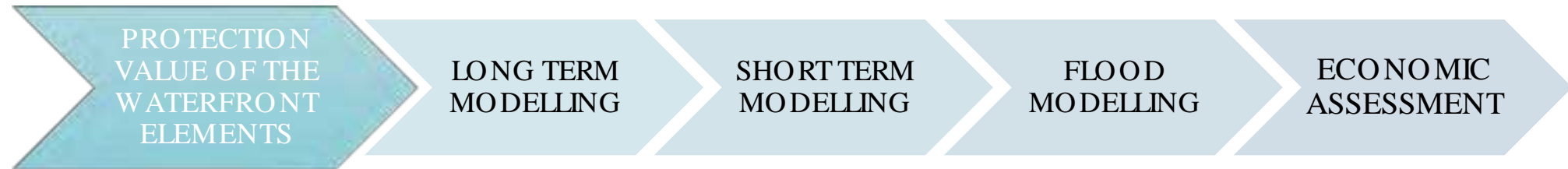
STRUCTURES

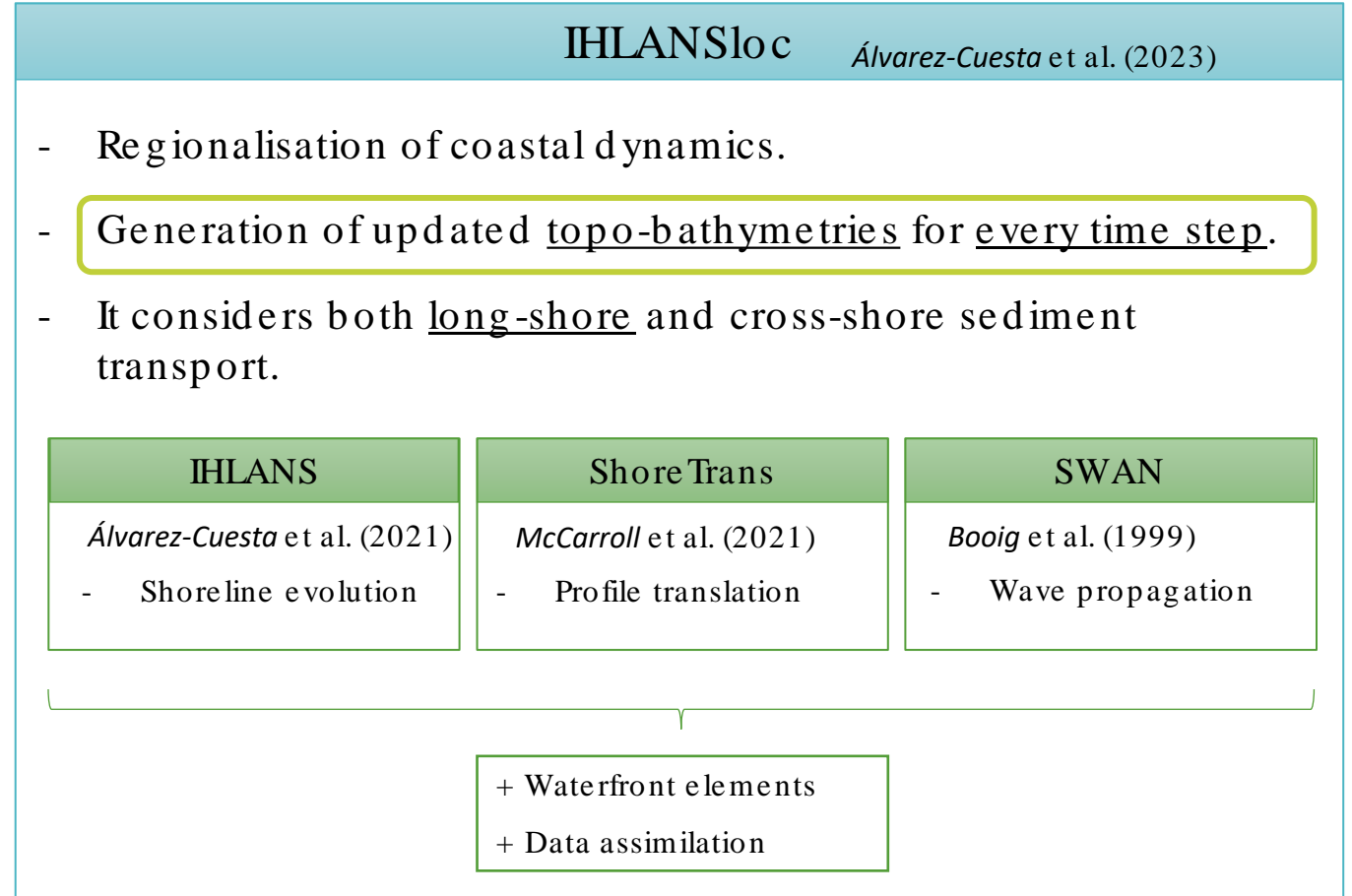
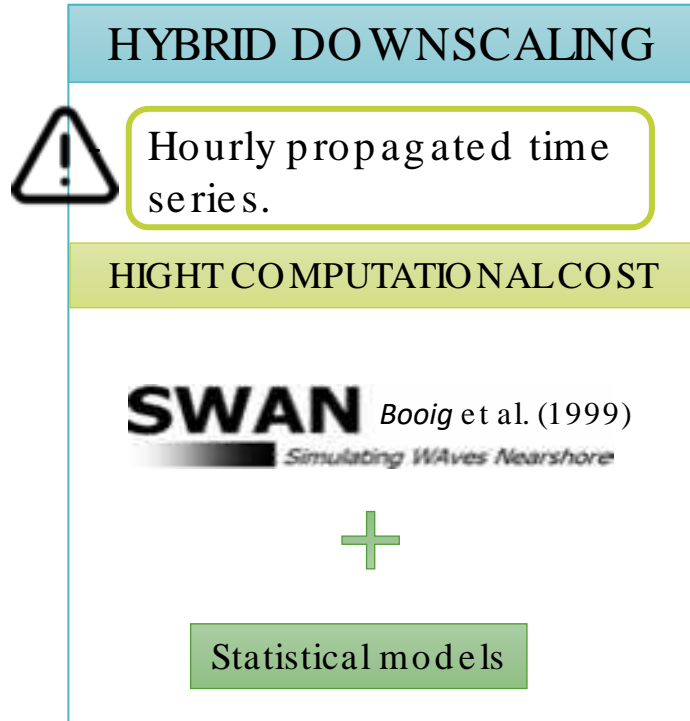
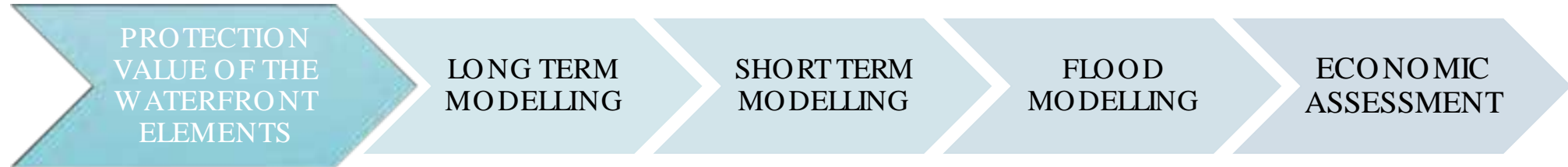
Promenade

Breakwater



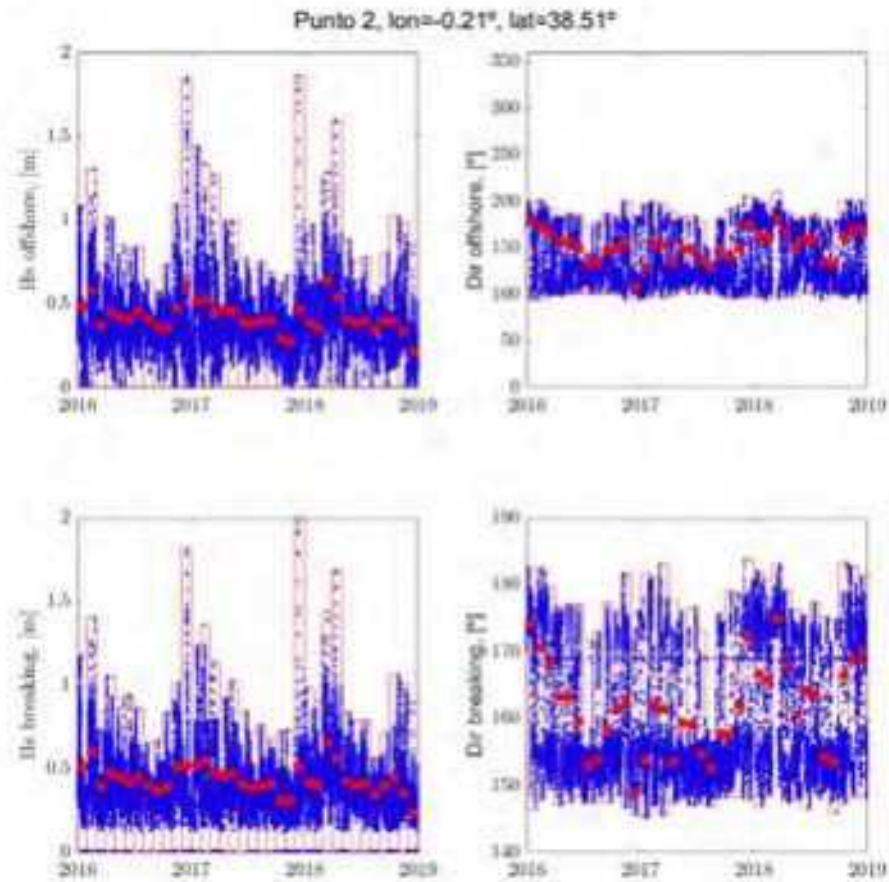
METHODOLOGY



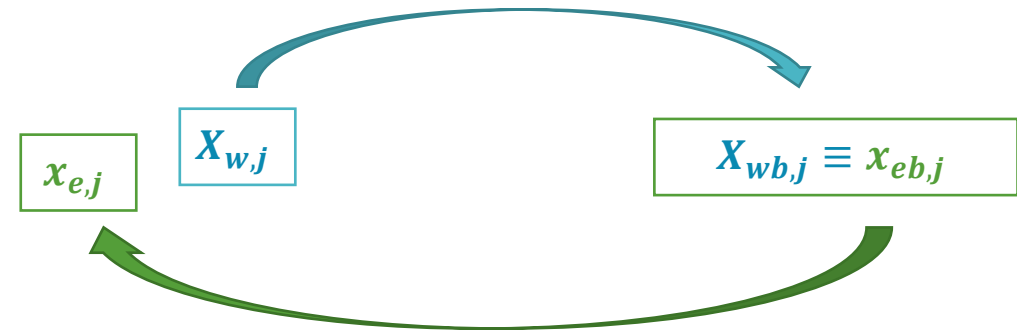


Input Reduction

Scipione et al. (2024)



PROPAGATION UP TO THE BREAKING POINT



BACK-PROPAGATION OF THE REDUCED SERIES

X_w

x_e

Same longshore sediment transport.

Assumption

Shore line evolution induced only by the
longshore sediment transport.

Cross-shore sediment transport is neglected.

DATA ASSIMILATION

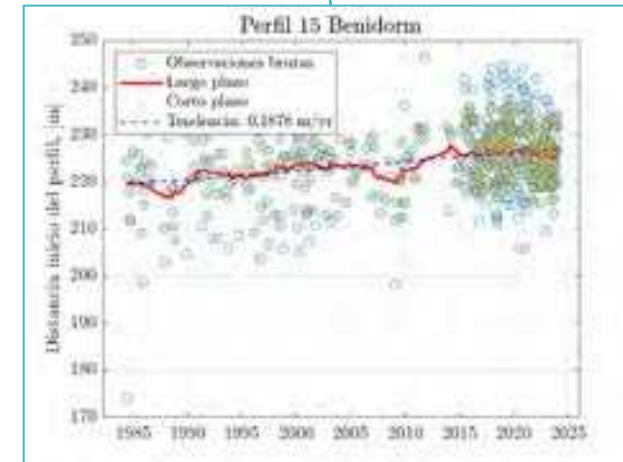


CoastSat

Vos et al. (2019)



It allows us to introduce sand
nourishments

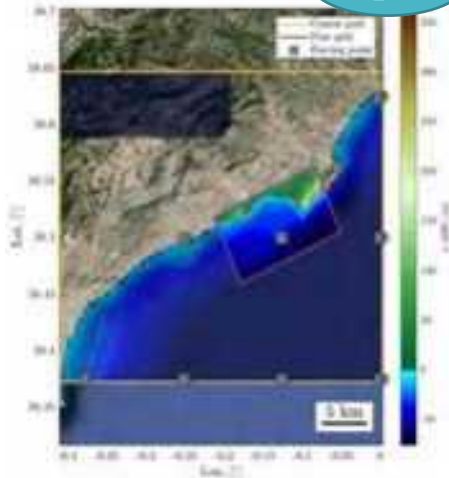


DOWNSCALING HÍBRIDO



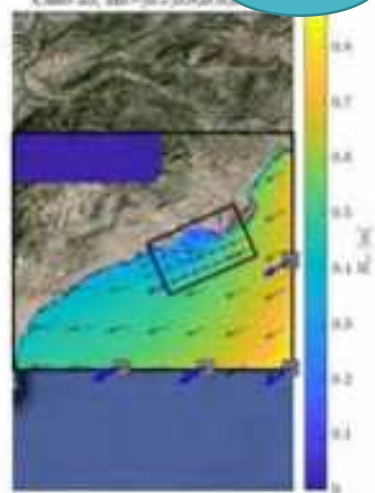
IHLANSloc

Input



HR topobathymetry
Wave data

Output



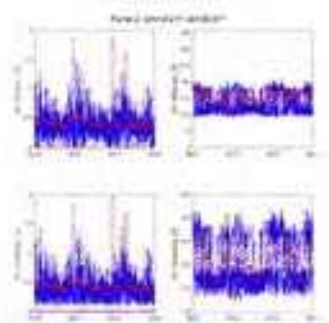
Hourly propagated
time series

372525 time steps

Monthly
propagated time
series

510 time steps

Running time:
From 8:42 to 15:28



Input

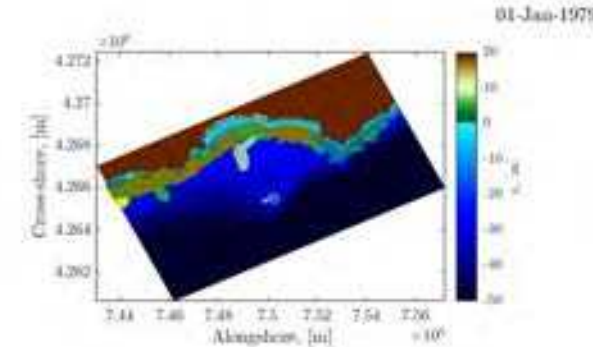
HR topobathymetry
Propagated series
Data assimilation
Waterfront elements

Output

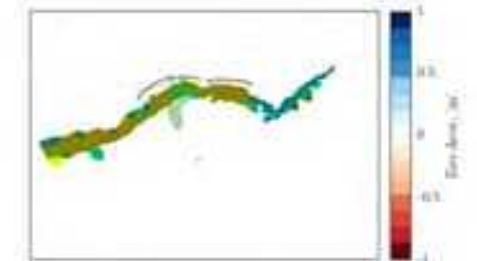
HR topobathymetry for
every time step



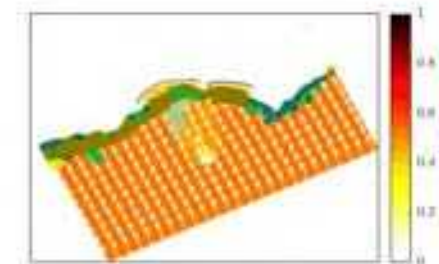
Monthly HR topobathymetries generated in
a very short space of time.



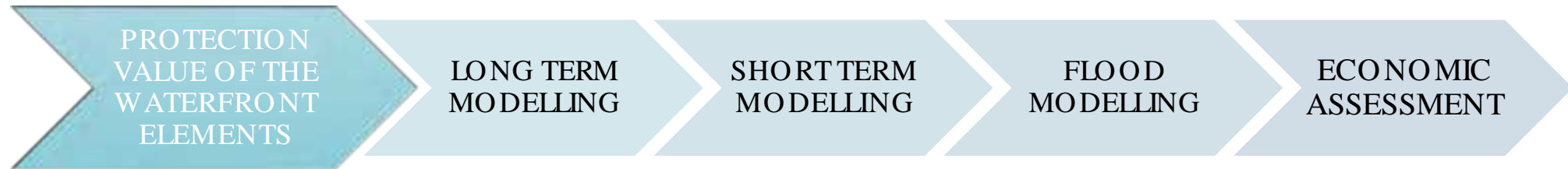
Propagated dynamics



Erosion/Acretion



Shore line/Break



XBeach

Roelvink et al. (2009)

Surfbeat mode (instationary)

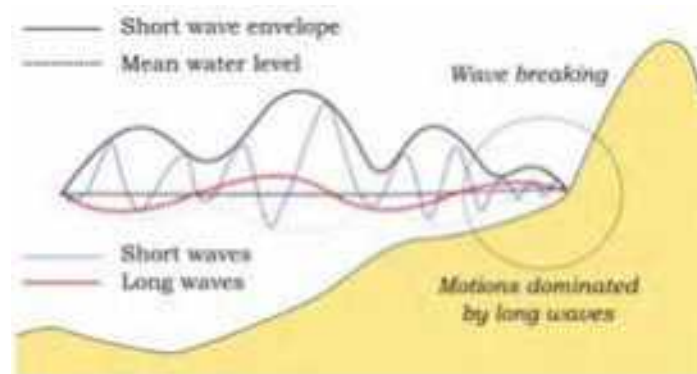
Hydrodynamics



Morphodynamics

- Waves
- Currents
- Sediment transport
- Seabed changes

- Resolves the short-wave envelope of the wave group and the associated long-wave envelope.
- In 1D cross-shore mode it solves the transversal sediment transport.
- This mode doesn't allow capturing fine details of sediment transport on very small scales (grain by grain). This is done by Non-hydrostatic mode.



Principle sketch of the relevant wave profile
(XBeach manual)



Allows us to introduce different types of elements in the model.



Structure

Promenade



Non-erodible layer

struct = 1

Assumption

Non-erodible layers are infinitely deep.

Input

- File with the same format as bathymetry with the width (m) of the erodible layer [0-10].



Seagrass

Posidonia oceanica

Cymodecea nodosa



Vegetation module

vegetation = 1

Assumption

Mendez and Losada (2004);
Suzuki et al.,(2012)

Vertically uniform vegetation.

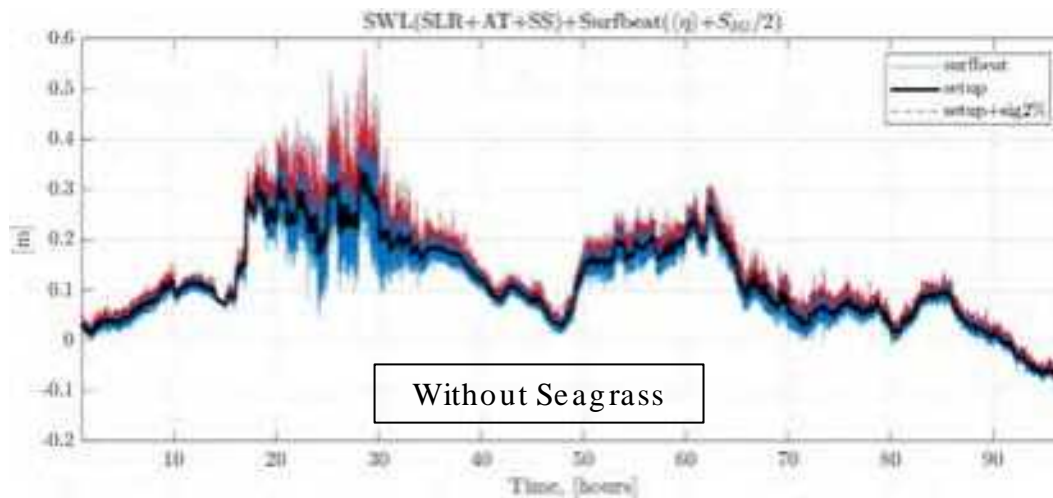
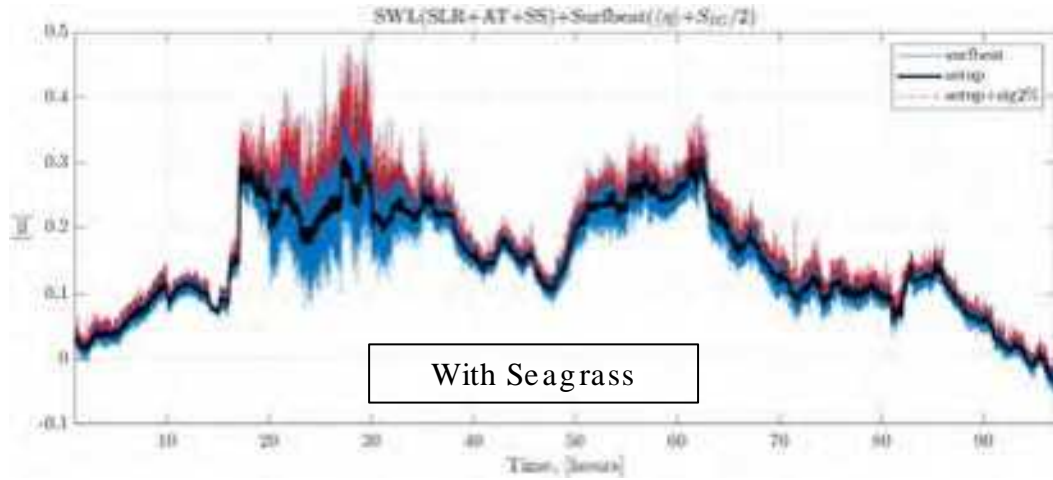
$$D_{veg} = \frac{1}{2\sqrt{\pi}} \rho \bar{C}_D N \left(\frac{kg}{2\sigma} \right)^3 \frac{(\sinh^3 k\alpha h - \sinh^3 k\alpha_{veg} h) + 3(\sinh k\alpha h - \sinh k\alpha_{veg} h)}{3k \cosh^3 kh} H_{sea}^3$$

Van Rooijen et al. (2015)

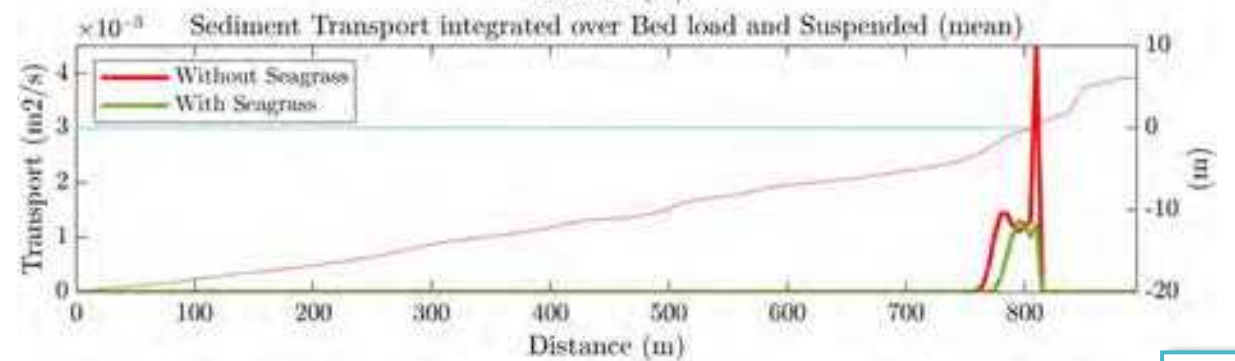
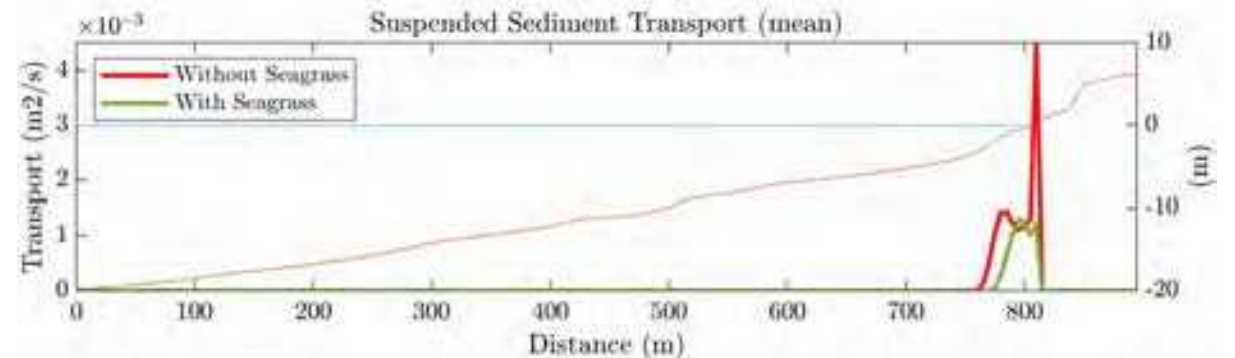
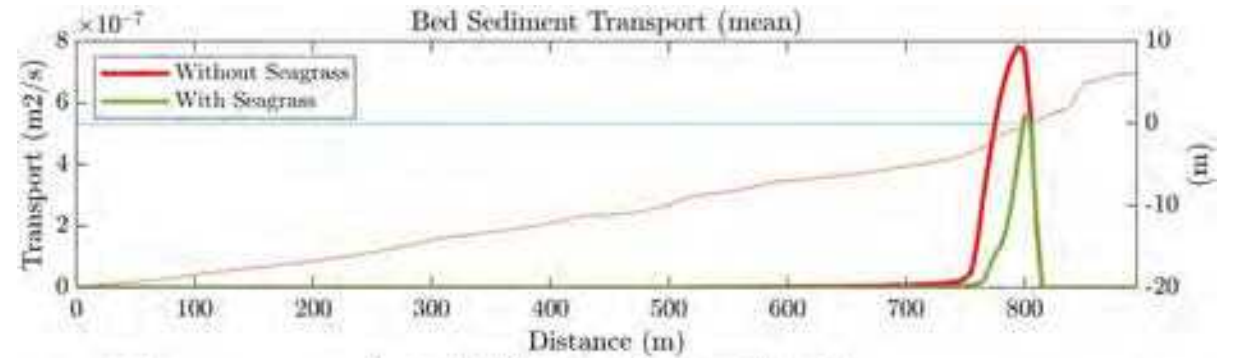
Input

- File with the same format as bathymetry with the location.
- ah: height (m).
- Cd: drag coefficient (-).
- bv: stem diameter (m).
- N: density (shoots/m2).

Hydrodynamics



Morphodynamics



Input

HR long-term topobathymetry
(storm month, IHLANSloc)

Wave data

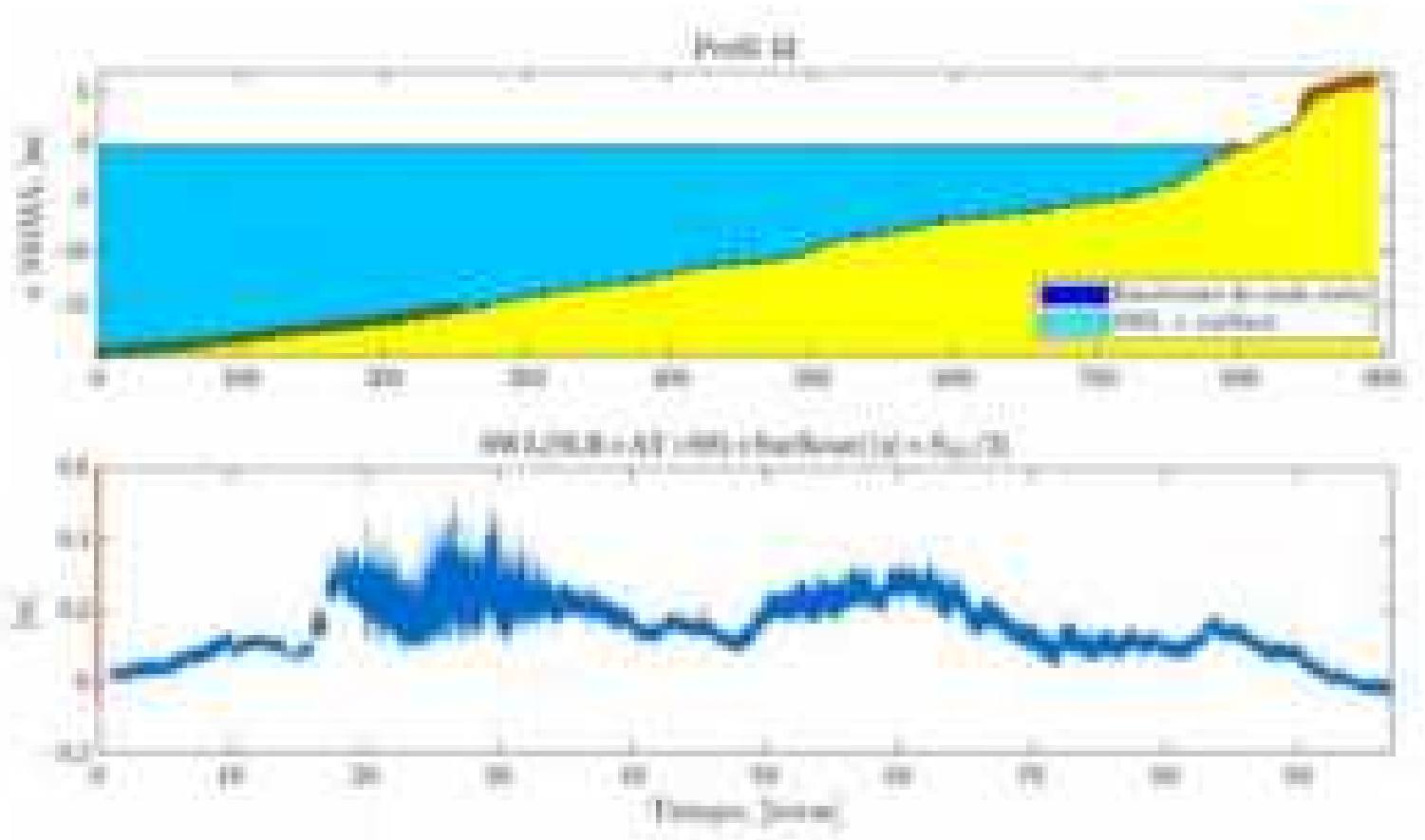
Waterfront elements

Output

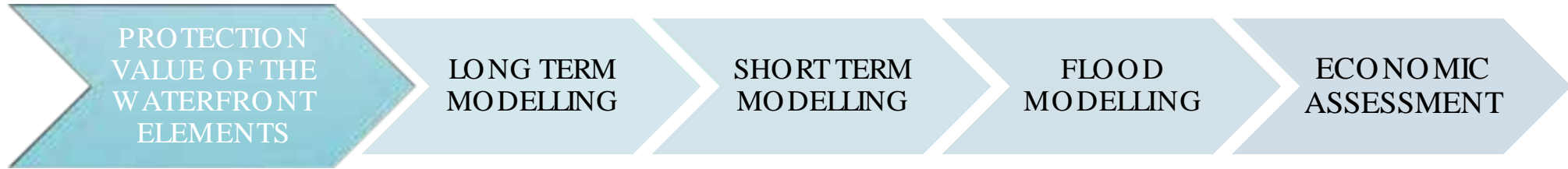
HR topobathymetry (post storm)

Set-up series

IG wave series



- Seagrass meadows have a clear effect on morphology (sediment transport and seabed changes).
- Reduced effect on hydrodynamics (reduction of the IG waves).



SFINCS

Leijnse et al. (2021)

Reduced complexity model designed to rapidly
modelling compound flooding

FORCINGS

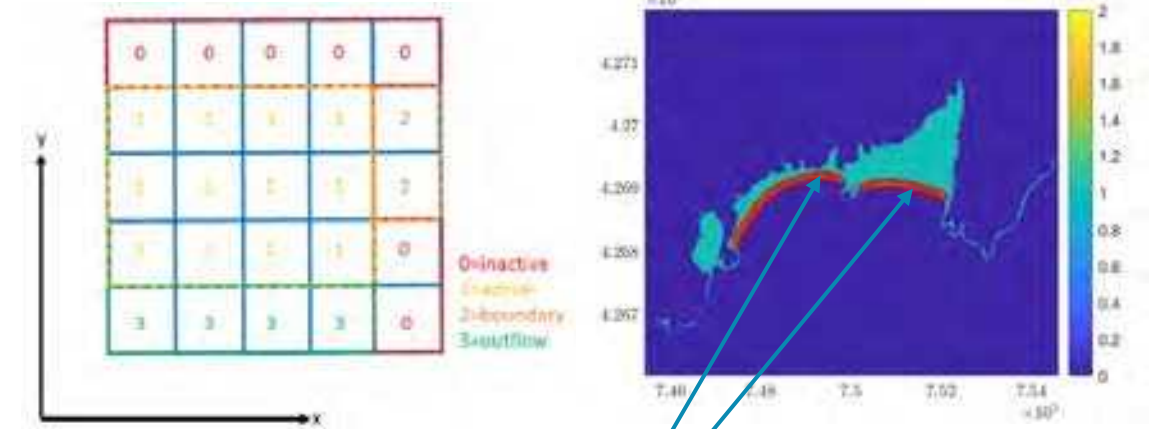
Fluvial

Tide

Rainfall

Waves

Wind



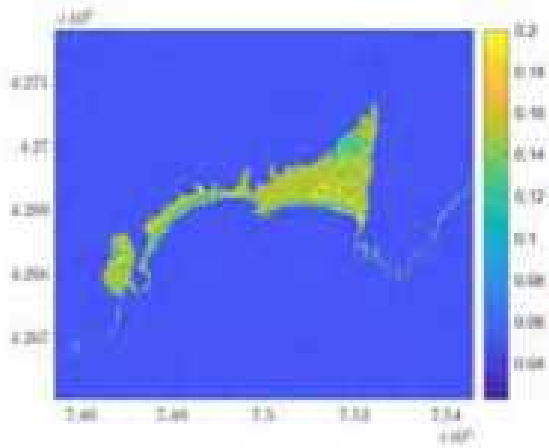
Example of the different mask values on a grid
(SFINCS manual)

- Generally winds, tides and waves are forced at -2.
- In this case, we will force after maximum dissipation.

Input

HR topobathymetry
(post storm, XBeach)

Manning roughness map



Slowly varying water level

at + ss + set up
(XBeach) + ref



Quickly varying water level

Infragravity wave (XBeach)

- Unseparated incident and reflected component.
- Random phase .



- The incident component of the IG wave series has been separated.
- The same phase (randomly chosen) has been applied.

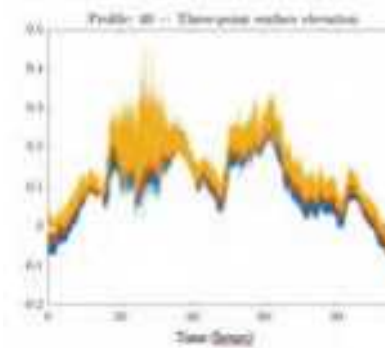


- Create the flood map for Gloria event.
- Maybe add the rainfall component?



Deltares Wave Toolbox

de Ridder et al. (2023)

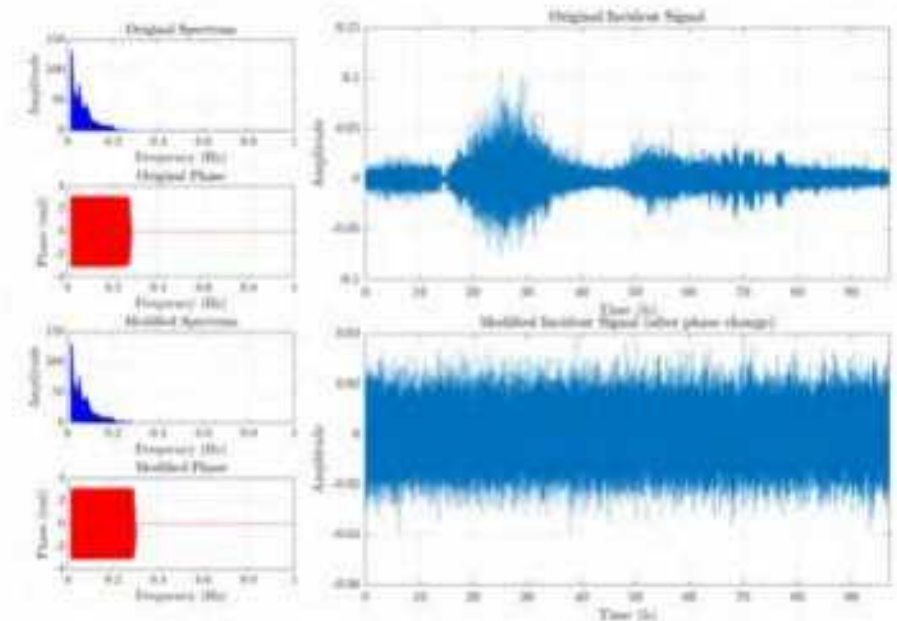


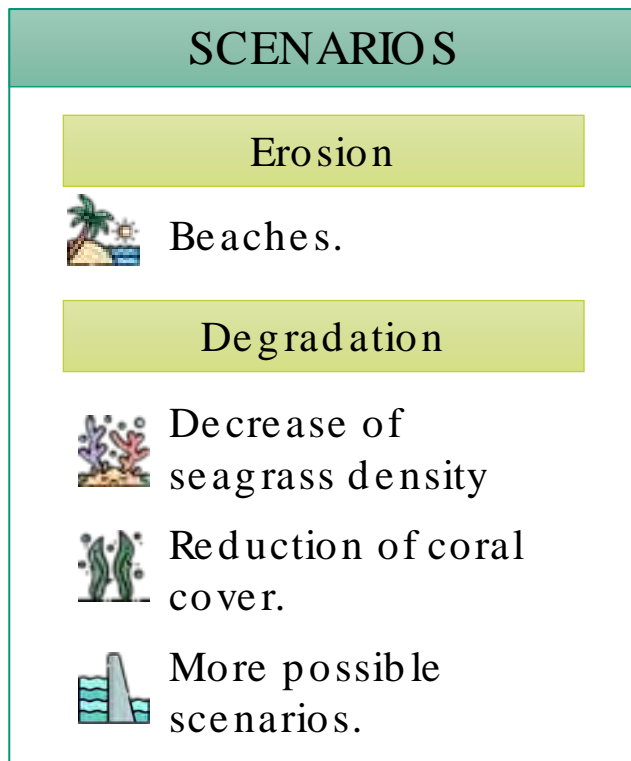
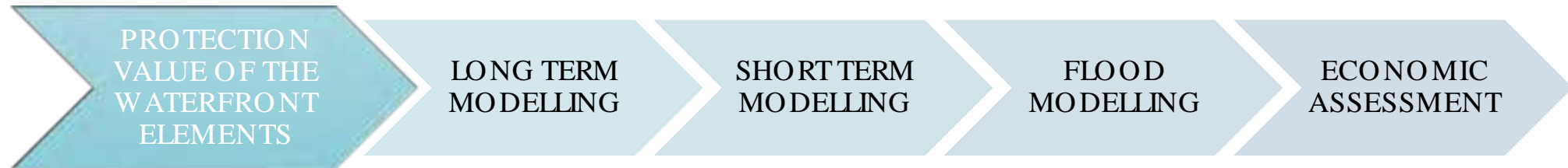
2 signals

Goda and Suzuki (1976)

3 signals

Mansard and Funke (1980)





NEXT STEPS

ADAPTATION AND CLIMATE CHANGE

Simulation of climate change scenarios

SSP1 - 2.6

SSP2 - 4.5

SSP5 - 8.5



Implementation of adaptation actions through
dynamics pathways



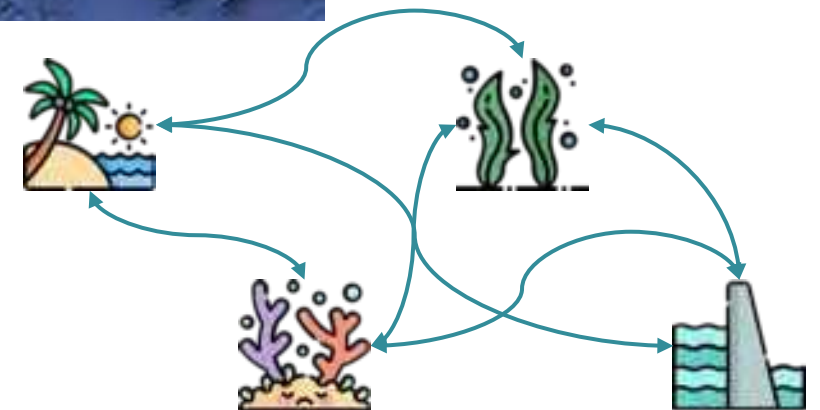
Cost-Benefit analysis of dynamic pathways

APPLICATION AT REGIONAL SCALE



O'ahu, Hawaii (USA)

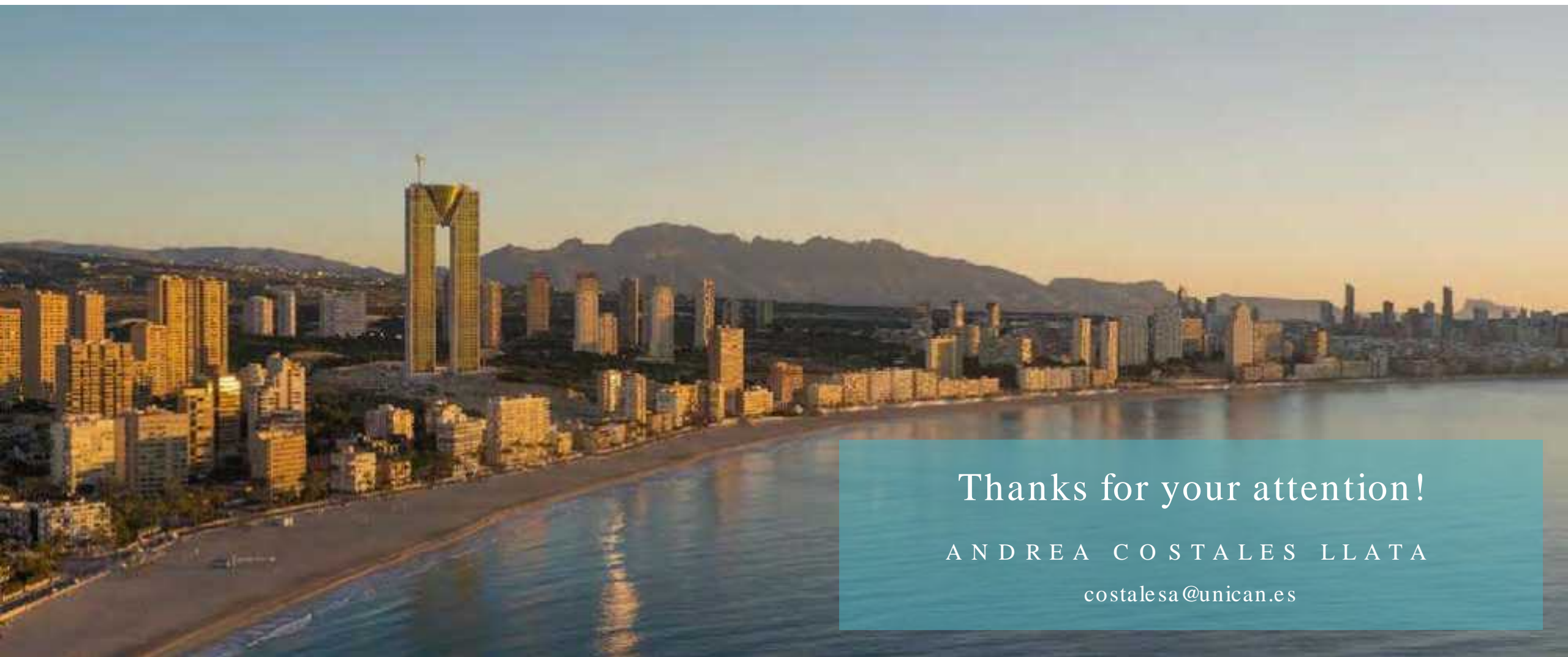
- Different levels of development of beaches.
- Coral reefs.
- Seagrass.



REFERENCES

- Álvarez-Cuesta, Moisés & Losada, I.J. & Toimil, Alexandra. (2023). A nearshore evolution model for sandy coasts: IH-LANSloc. *Environmental Modelling & Software*. 169. 105827. 10.1016/j.envsoft.2023.105827.
- Álvarez-Cuesta, Moisés & Toimil, Alexandra & Losada, I.J.. (2021). Modelling long-term shoreline evolution in highly anthropized coastal areas. Part 1: Model description and validation. *Coastal Engineering*. 169. 103960. 10.1016/j.coastaleng.2021.103960.
- Booij, N., Ris, R. C. & Holthuijsen, L. H. A third-generation wave model for coastal regions 1. Model description and validation. *J. Geophys. Res.: Oceans*, 104, 7649–7666 (1999).
- de Ridder, Menno & Kramer, Jan & den Bieman, Joost & Wenneker, Ivo. (2023). Validation and practical application of nonlinear wave decomposition methods for irregular waves. *Coastal Engineering*. 183. 104311. 10.1016/j.coastaleng.2023.104311.
- Goda, Y, Suzuki, Y, 1977. Estimation of incident and reflected waves in random wave experiments. In: *Coastal Engineering 1976*. pp. 828–845. <http://dx.doi.org/10.9753/icce.v15.47>.
- Infantes, Eduardo & Orfila, Alejandro & Simarro, Gonzalo & Terrados, Jorge & Luhar, Mitul & Nepf, Heidi. (2012). Effect of a seagrass (*Posidonia oceanica*) meadow on wave propagation. *Marine Ecology Progress Series*. 456. 63-72. 10.3354/meps09754.
- Klein, Judith & Verlaque, Marc. (2008). The *Caulerpa racemosa* invasion: A critical review. *Marine pollution bulletin*. 56. 205-25. 10.1016/j.marpolbul.2007.09.043.
- Leijnse, Tim & Ormond, Maarten & Nederhoff, Kees & van Dongeren, Ap. (2021). Modeling compound flooding in coastal systems using a computationally efficient reduced-physics solver: Including fluvial, pluvial, tidal, wind- and wave-driven processes. *Coastal Engineering*. 163. 103796. 10.1016/j.coastaleng.2020.103796.
- Mansard, E.P.D., Funke, E.R., 1980. The measurement of incident and reflected spectra using a least squares method. In: *Coastal Engineering 1980*. pp. 154–172. <http://dx.doi.org/10.9753/icce.v17.8>.

- McCarroll, Robert & Masselink, Gerhard & Valiente, Nieves & Scott, Tim & Wiggins, Mark & Kirby, Josie & Davidson, Mark. (2021). A rules-based shoreface translation and sediment budgeting tool for estimating coastal change: ShoreTrans. *Marine Geology*. 435. 106466. 10.1016/j.margeo.2021.106466.
- Mendez, Fernando & Losada, I.J.. (2004). An empirical model to estimate the propagation of random breaking and nonbreaking waves over vegetation fields. *Coastal Engineering*. 51. 103-118. 10.1016/j.coastaleng.2003.11.003.
- Ondiviela, Bárbara & Losada, I.J. & Lara, Javier & Maza, Maria & Galván, Cristina & Bouma, Tjeerd & van Belzen, Jim. (2013). The role of seagrasses in coastal protection in a changing climate. *Coastal Engineering*. 87. 10.1016/j.coastaleng.2013.11.005.
- Roelvink, Dano J.A. & Reniers, Ad & van Dongeren, Ap & Thiel de Vries, Jaap & McCall, Robert & Lescinski, Jamie. (2009). Modelling storm impacts on beaches, dunes and barrier islands. *Coastal Engineering*. 56. 1133-1152. 10.1016/j.coastaleng.2009.08.006.
- Scipione, Francesca & de girolamo, Paolo & Castellino, Myrta & Pasquali, Davide & Celli, Daniele & Di Risio, Marcello. (2024). Reduced wave time series for long-term morphodynamic applications. *Coastal Engineering*. 189. 104453. 10.1016/j.coastaleng.2024.104453.
- Suzuki, Tomohiro & Zijlema, Marcel & Burger, Bastiaan & Meijer, Martijn & Narayan, Siddharth. (2012). Wave dissipation by vegetation with layer schematization in SWAN. *Coastal Engineering*. 59. 64-71. 10.1016/j.coastaleng.2011.07.006.
- van Rooijen, Arnold & Thiel de Vries, Jaap & McCall, Robert & van Dongeren, Ap & Roelvink, Dano J.A. & Reniers, Ad. (2015). Modeling of wave attenuation by vegetation with XBeach.
- Vos, Kilian & Splinter, Kristen & Harley, Mitchell & Simmons, Joshua & Turner, Ian. (2019). CoastSat: A Google Earth Engine-enabled Python toolkit to extract shorelines from publicly available satellite imagery. *Environmental Modelling & Software*. 122. 104528. 10.1016/j.envsoft.2019.104528.



Thanks for your attention!

ANDREA COSTALES LLATA

costalesa@unican.es



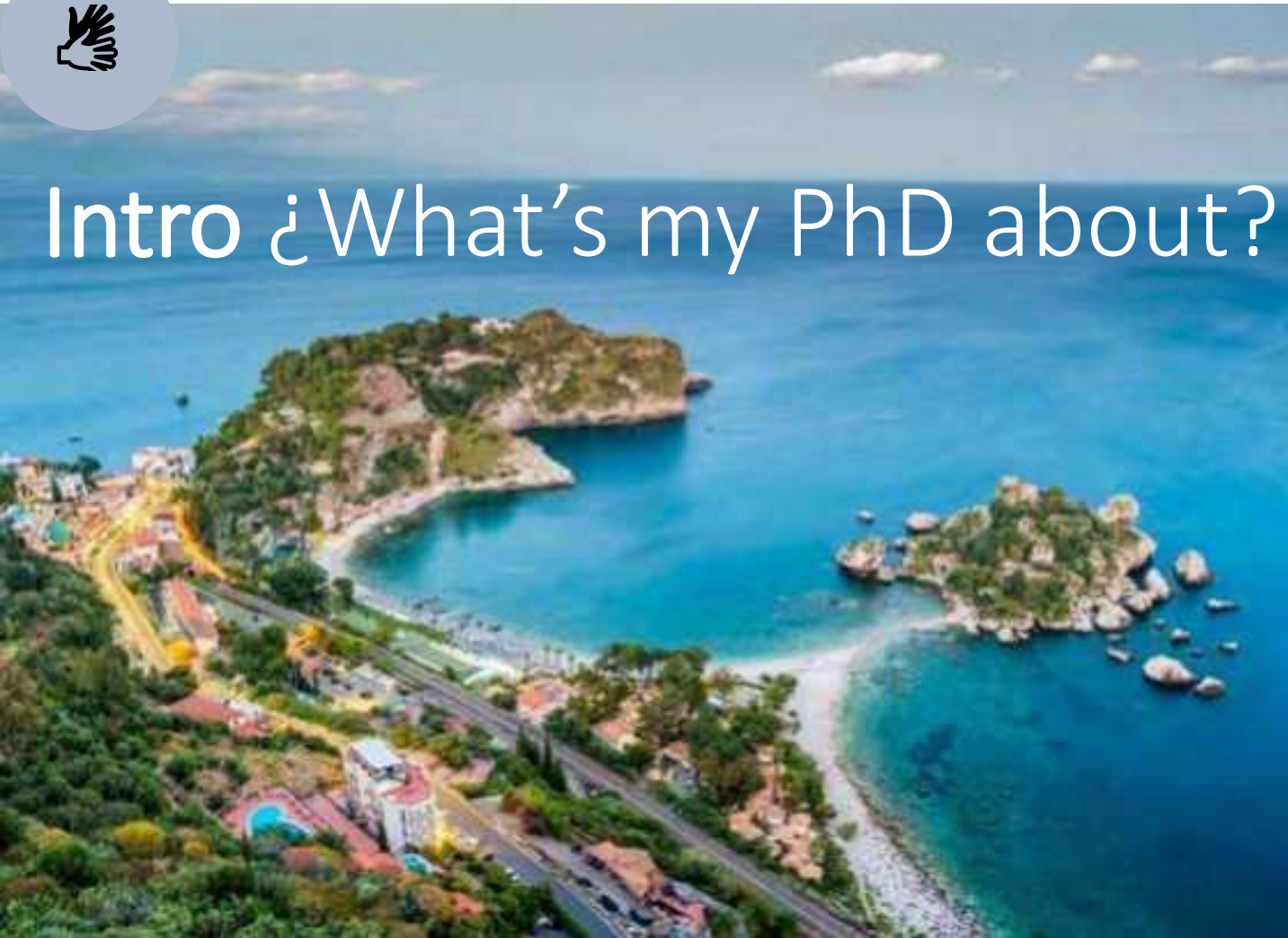
Brief talk about some beaches and machine learning

Arnau Garcia Tort





Intro ¿What's my PhD about?



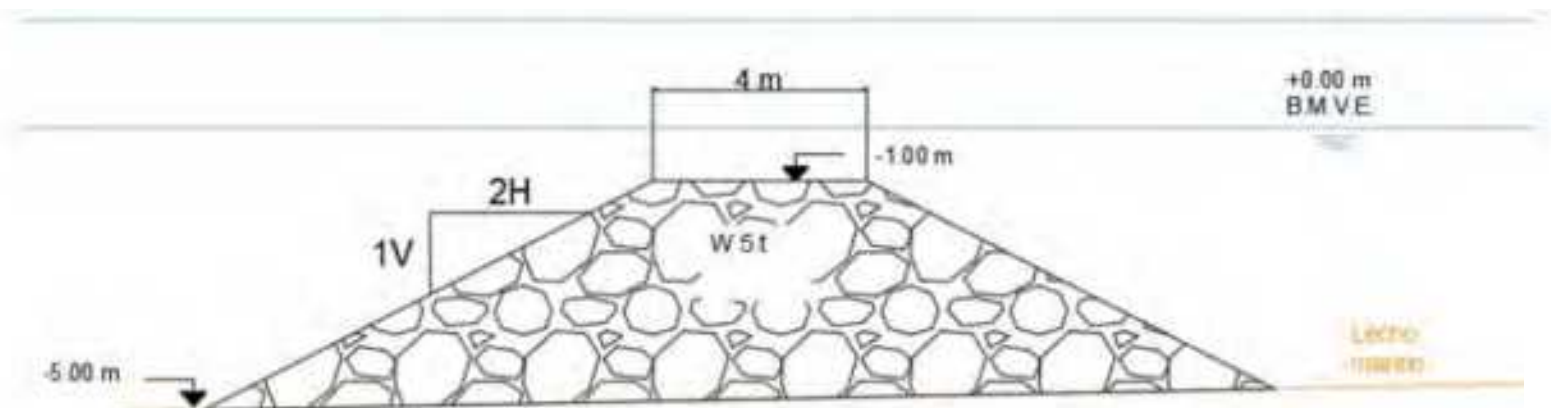


Morphology of equilibrium beaches protected by submerged detached structures

PhD Student: **Arnau Garcia Tort**

Tutor: **Dra. Erica Pellón**

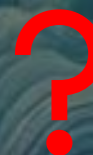
Director: **Dr. Ernesto Mauricio González**



SAFE EMERGENT ZONE



DANGER SUBMERGED ZONE





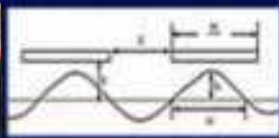
METHODS & WORKPLAN



T1. Review literature

T2. Apply/use ML techniques

2.1 Aplicación y caracterización de la forma en planta en playas en situación de equilibrio estático y dinámico

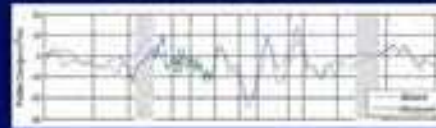


2.2 Evaluación y análisis de los diferentes algoritmos y técnicas de ML utilizados



T3. Numerical modelling in ST

3.1 Simulación numérica de los procesos hidrodinámicos (XBeach)

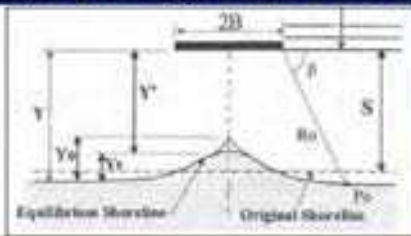
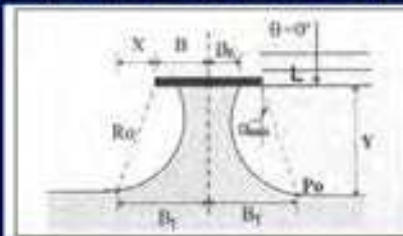


3.2 Análisis de sensibilidad de las variables implicadas tanto en la respuesta hidrodinámica como morfológica



T4. Planform Empirical Mod. in LT

4. Desarrollo de nuevo modelo de forma en planta de equilibrio aplicable a playas protegidas por DSS.



T5. Validate the model

Gruth data Lab experiments

Methodologic plan for the model applicability

Useable
UNCY Ranges
 BIASS

Apply it to pilot sites



T6. Present and share all the amounted knowledge

Can ML algorithms help us to reduce the uncertainty in these detached beaches?



First paper: Classification



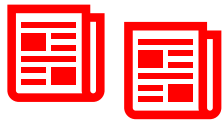
Second paper: Regression



Inputs



The idea here is to benchmark some previous empirical models versus our ML results to see if helps to improve



Params
geomorphological

Params
hydrodynamical

Parameters considered





The > 370 beaches of our DATABASE were grouped by:

Their level of submergence :

Estructuras emergidas (ED)



Estructuras low-crested (LC)



Estructuras sumergidas (SD)



Their formation origin process :

Human-made Breakwaters (BW)



Natural emerged (Island)



Natural submerged (Reef)



The size of their response :

Mega (XL)

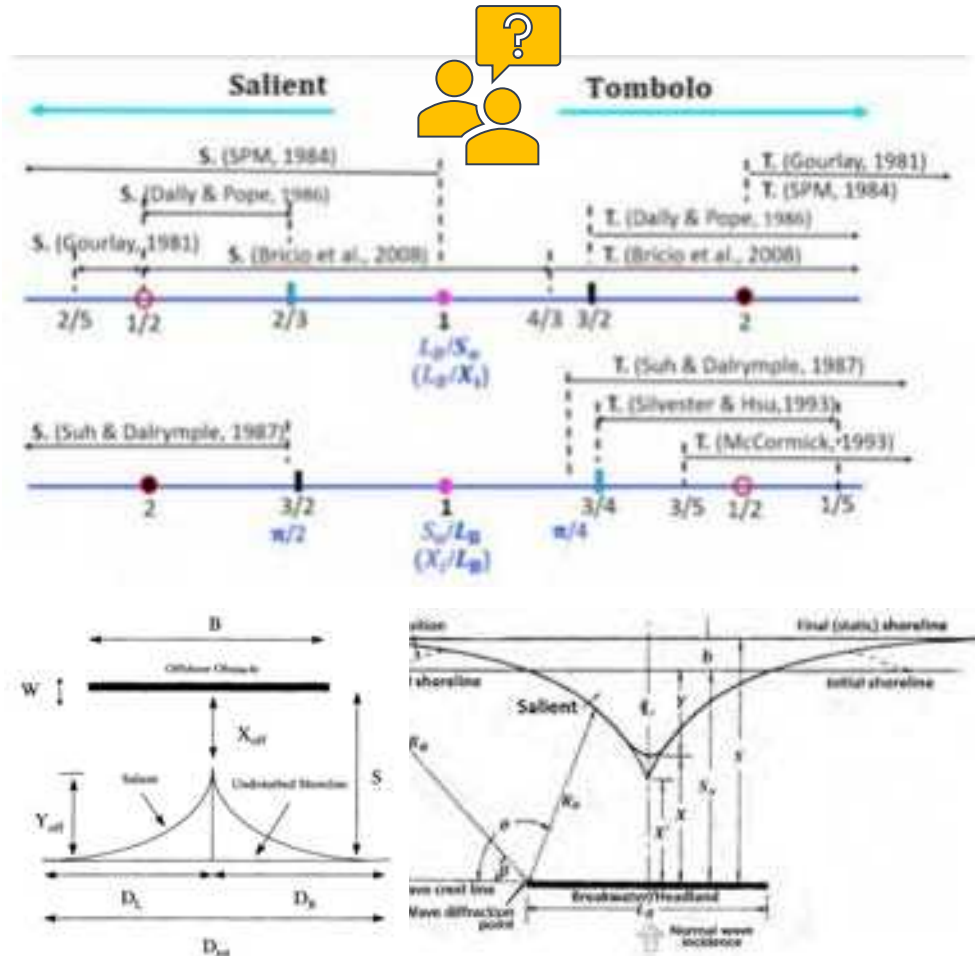
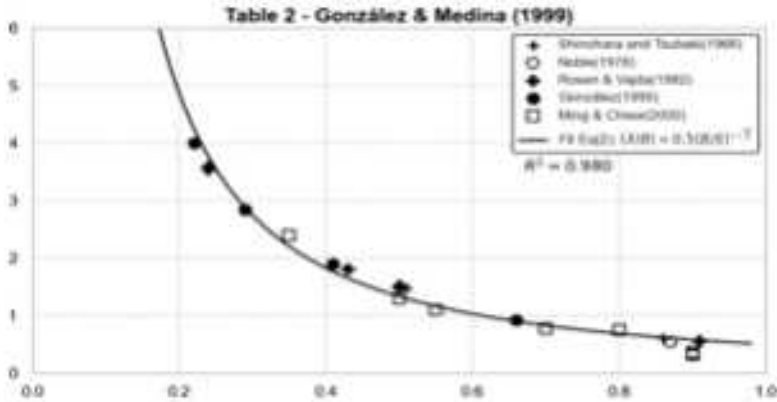
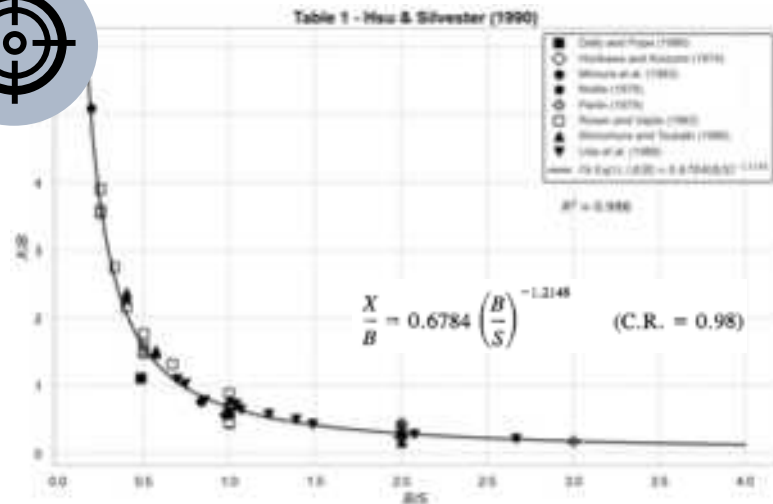
Large (L)

Medium (M)

Small (S)

Y > 1000 m

Y < 100 m



Previous literature equations, fits and knowledge ...

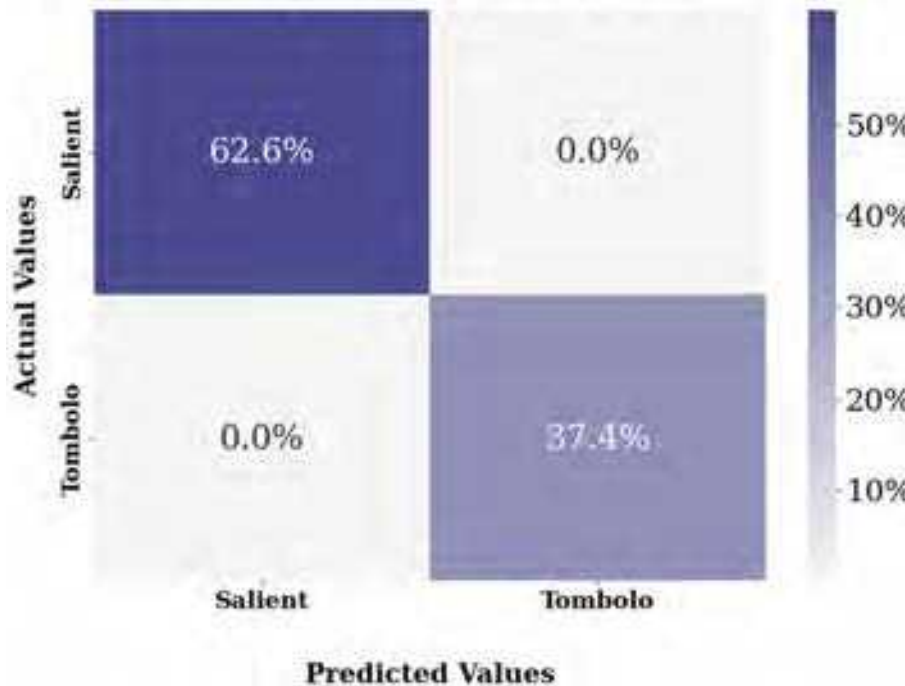


¿What about the ML results?
¿They are better than previous models?

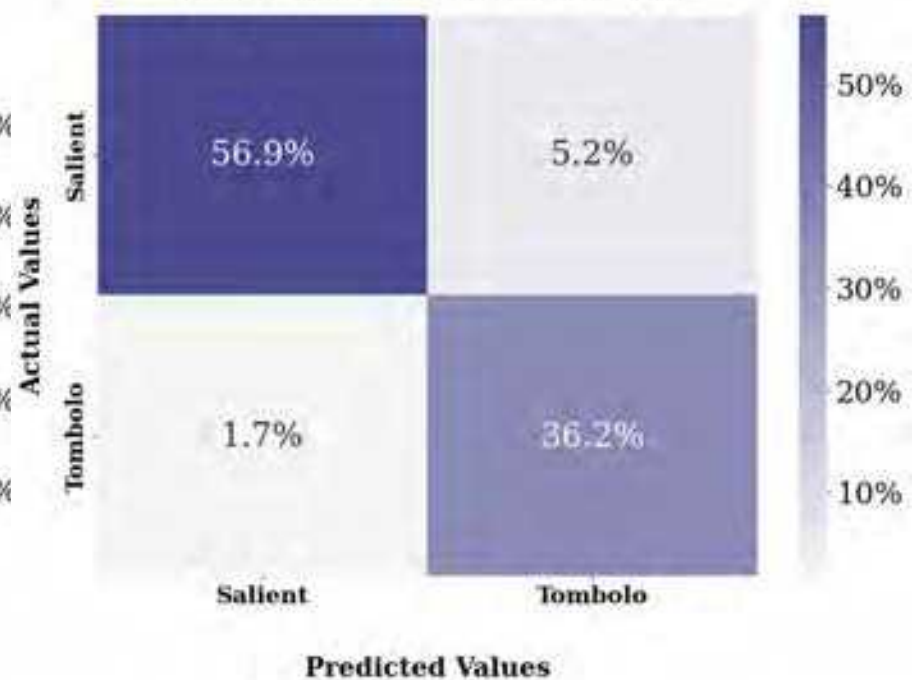


The model must predict from the given inputs if it is more likely to form T or S

Train Set Confusion Matrix (N=214)



Test Set Confusion Matrix (N=116)



From all predicted events the model only misclassify eight!

What can we extract from the misclassified events?



¿How many beaches misclassified?

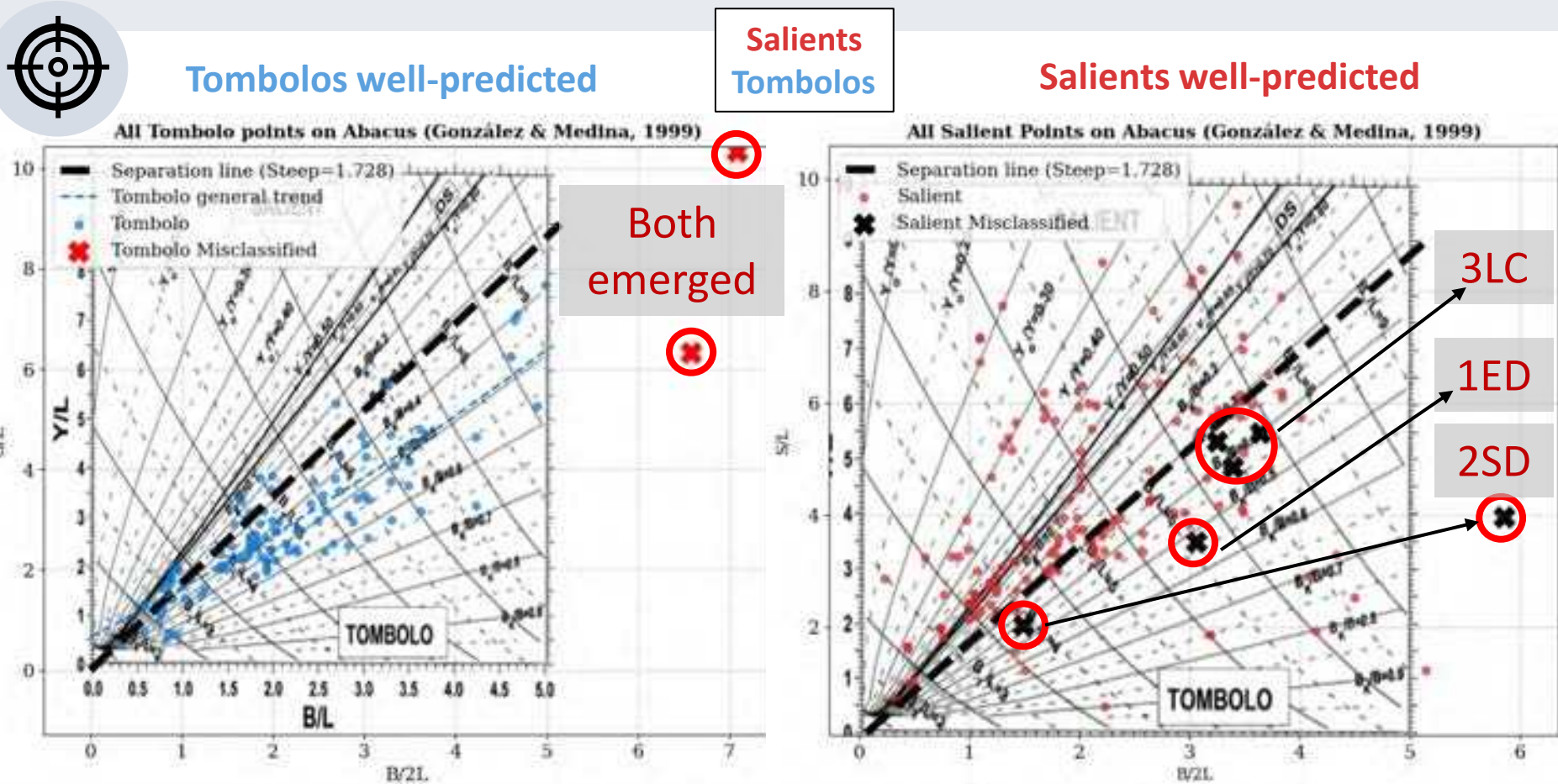
Only 8 data misclassified! < (2,45%)
2 Tombolo y 6 Salients



¿Are they logical errors?



What can we extract from the misclassified events?

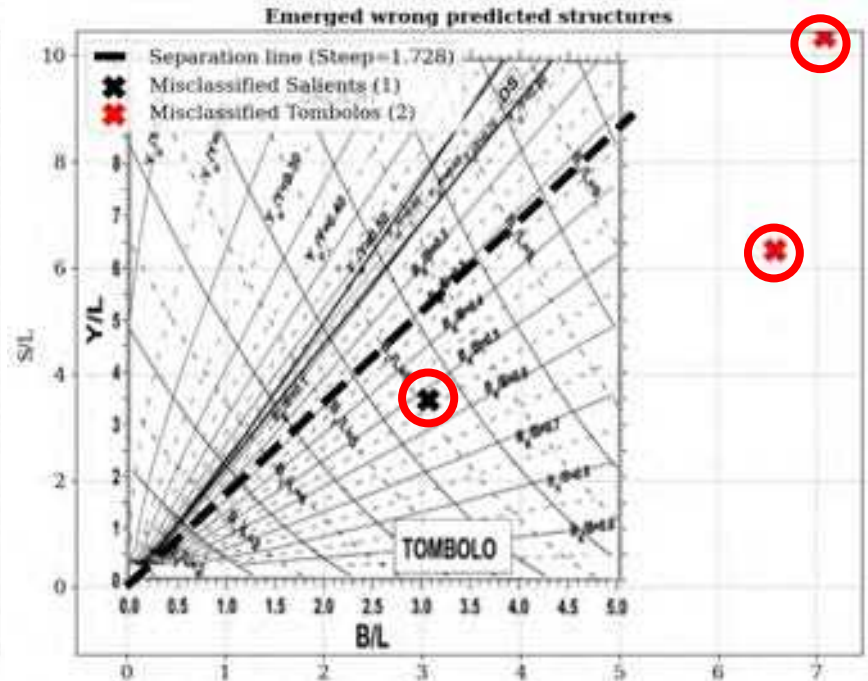
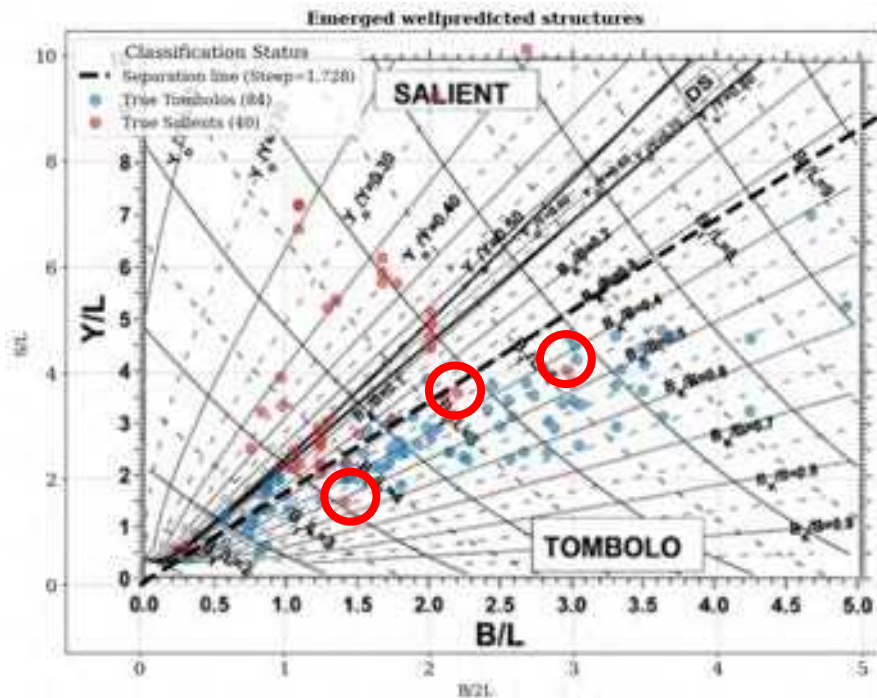


The major part of the events are correctly classified and the missed ones are logic and consistent, always the same

What can we extract from the results?

From 127 Emerged structures
2 tombolos and only 1 salient misclassified

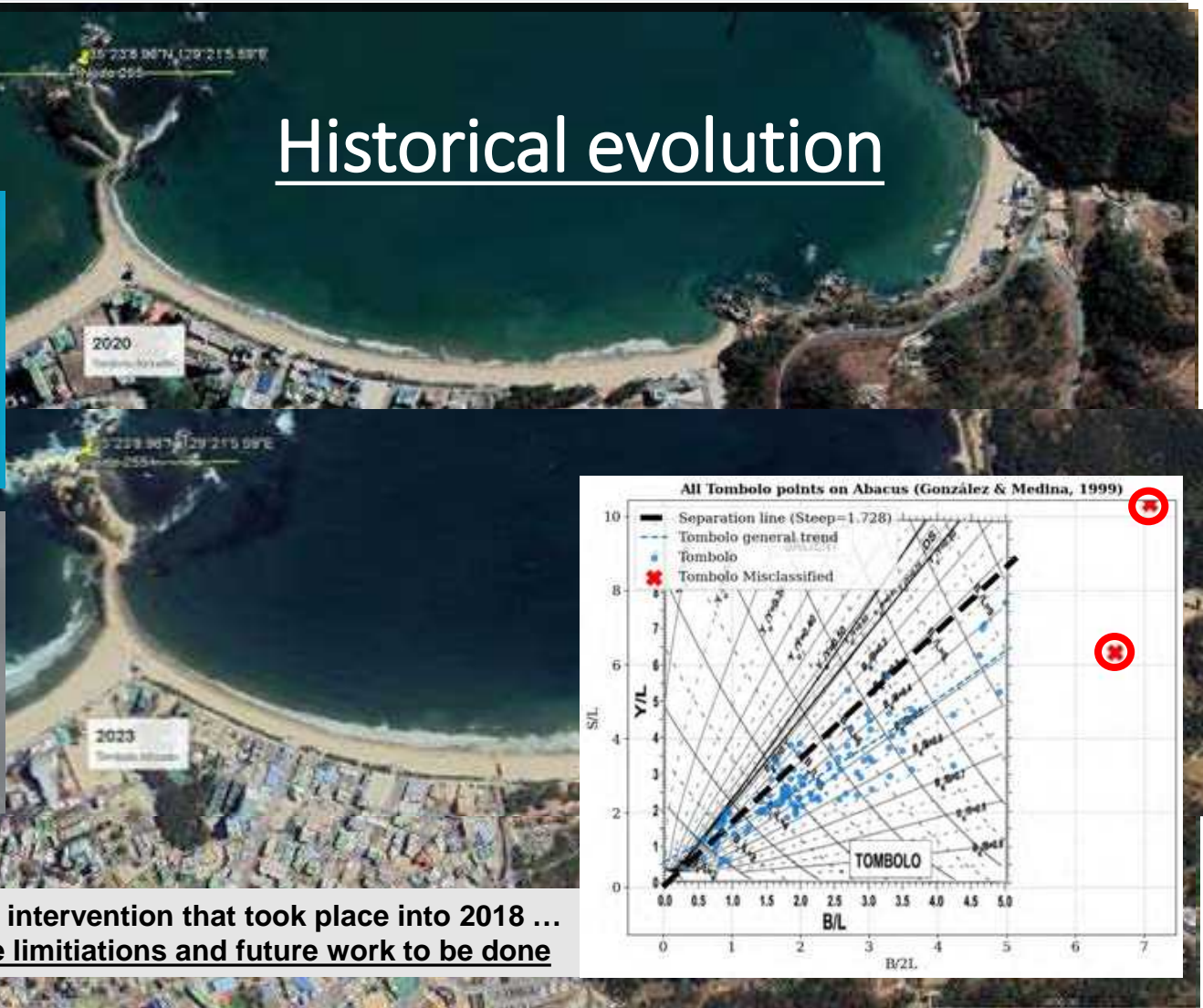
Salients
Tombolos



The model was able to correctly classify some complex events that exceeds the previous literature ranges & limits capabilities

Some inherent problems ...

Historical evolution



The model can't know the human intervention that took place into 2018 ...
As you can see there is still some limitations and future work to be done



Same inputs and training methodology



Before: Classification problem



Now: Regression problem



The target here is to predict the cross-shore extension that the Tombolo/Salient will have

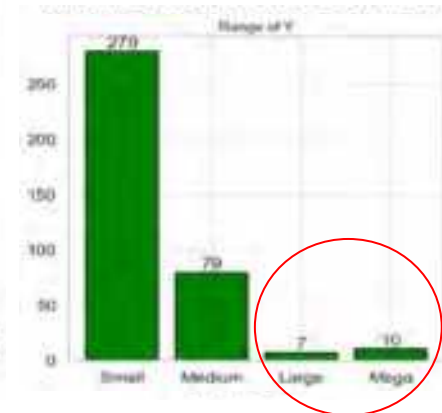
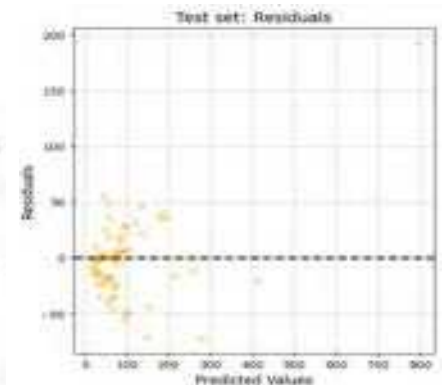
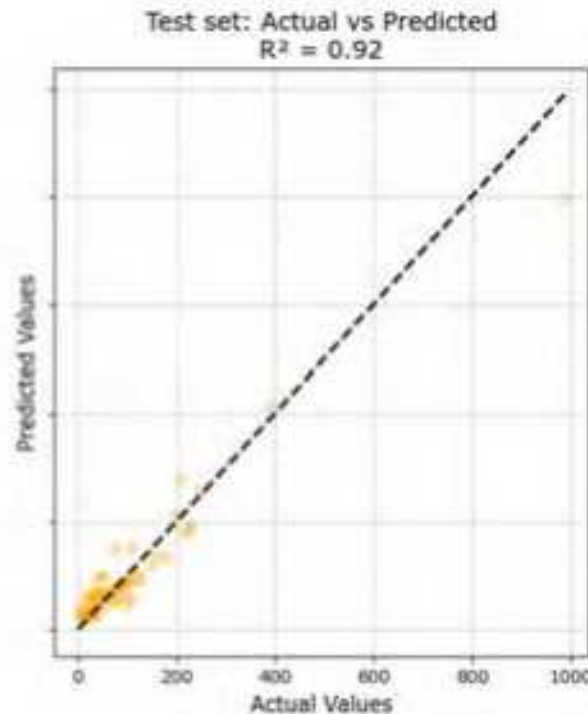
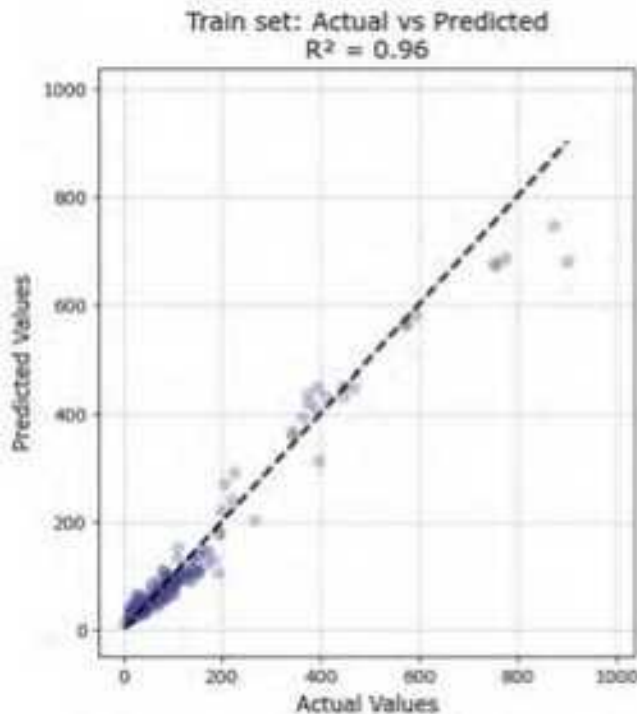
What can we extract from the misclassified events?



Given to data distribution, the model struggles with large Y values

ML models to predict: Y (m) →

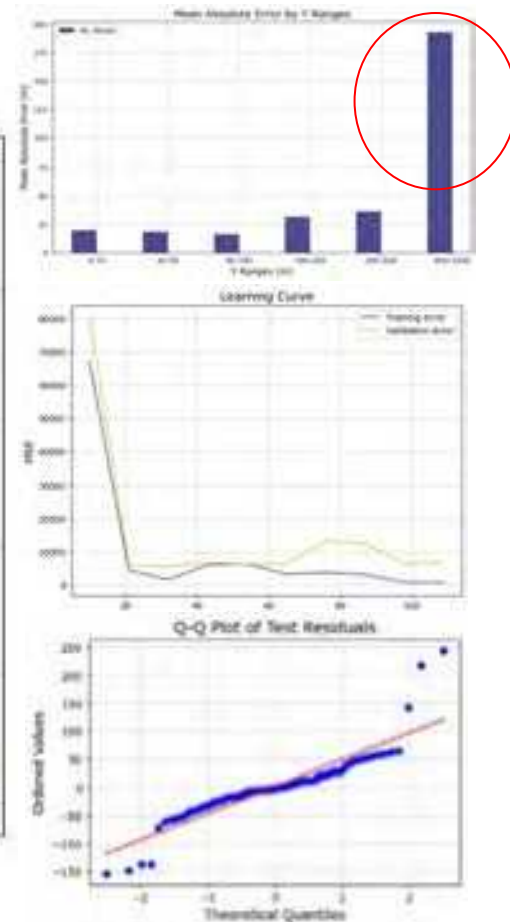
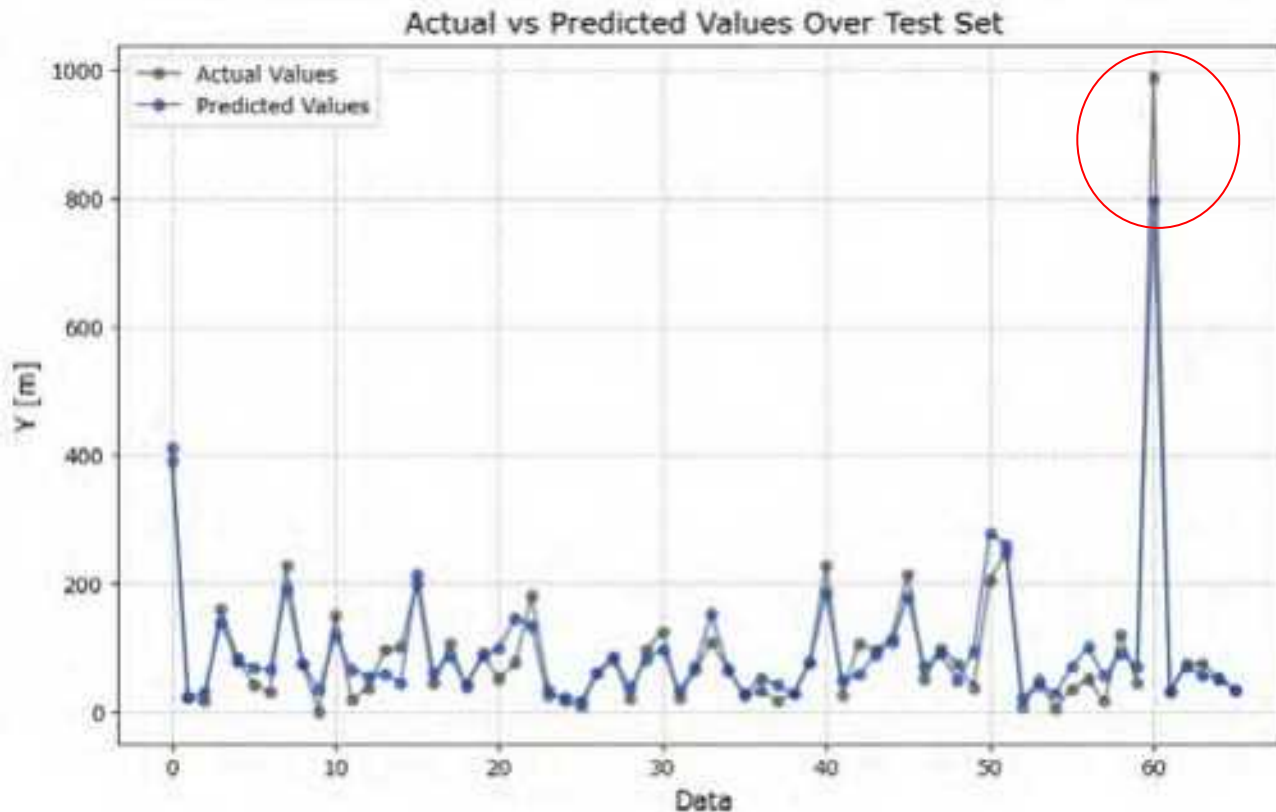
Small data well-predicted but model has **bigger errors** on larger salient events



What can we extract from the misclassified events?



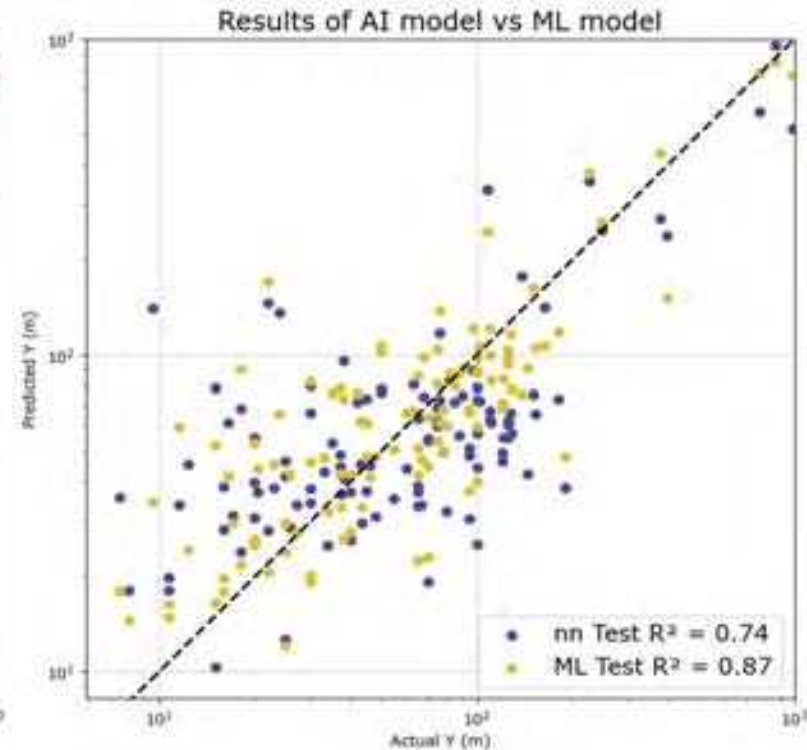
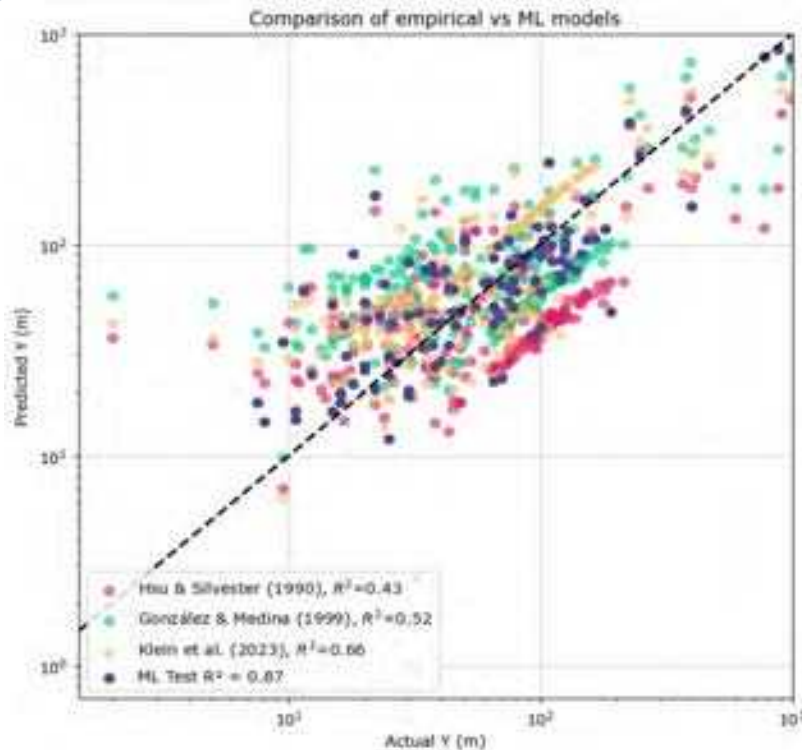
Given to data distribution, the model struggles with the large Y values



What can we extract from the benchmarks?



3. Benchmarking vs other previous models



ML beats some empirical models but still need some refinements to overcome all the limitations

What are the ML strengths or potential benefits?



Generality and suitability

Is more general, can be globally applied and it's not restricted to a limited set of data and conditions

Training and Model Optimization

ML procedure it's simple and effective, allowing interpretability and explainable learning

Robust and powerful

**Potential host and manage large amounts of data
→ Scalability (The more data, the better)**

¿How would you classify if you were a ML model?



¿3 Tombolos? ¿3 Salients? ¿Both?



¿How would you handle this intermittent events?

References

For deeper understanding

- [1] A. Lamberti, R. Archetti, M. Kramer, D. Paphitis, C. Mosso, and M. Di Risio, 'European experience of low crested structures for coastal management', *Coastal Engineering*, vol. 52, no. 10, pp. 841–866, Nov. 2005, <https://doi.org/10.1016/j.coastaleng.2005.09.010>.
- [2] M. A. Chasten, J. D. Rosati, J. W. McCormick, and R. E. Randall, 'Engineering Design Guidance for Detached Breakwaters as Shoreline Stabilization Structures', US Army Corps of Engineers, Dec. 1993.
- [3] V. Negro, J. J. Diez Gonzalez, L. Bricio Garberí, and J. S. López Gutiérrez, 'Coastal erosion. Geometric detached breakwaters indicators for preventing the shoreline erosion. Fringe session', Proceedings of the Coasts, Marine Structures and Breakwaters 2009.
- [4] L. C. Van Rijn., 'Coastal erosion and control', *Ocean & Coastal Management*, vol. 54, no. 12, pp. 867–887, Dec. 2011, <https://doi.org/10.1016/j.ocecoaman.2011.05.004>.
- [5] R. Ranasinghe and I. Turner, 'Shoreline response to submerged structures: A review', *Coastal Engineering*, vol. 53, pp. 65–79, Jan. 2006, <https://doi.org/10.1016/j.coastaleng.2005.08.003>.
- [6] R. Macêdo, V.A.V. Manso, and A.E.F Klein, 'The geometric relationships of salients and tombolos along a mesotidal tropical coast', *Geomorphology*, <https://doi.org/10.1016/j.geomorph.2022.108311>.
- [7] A. H. da F. Klein, L. B. Filho, and D. H. Schumacher, 'Short-Term Beach Rotation Processes in Distinct Headland Bay Beach Systems', *Journal of Coastal Research*, vol. 18, no. 3, pp. 442–458, 2002.

Insights into long-term shoreline modelling and my Phd

Lucas de Freitas Pereira

Supervisors:

Mauricio González and Camilo Jaramillo



Introduction

Atafona, la comunidad costera brasileña en riesgo por la erosión

El nivel del agua en la región podría elevarse otros 10 cm hasta 2050

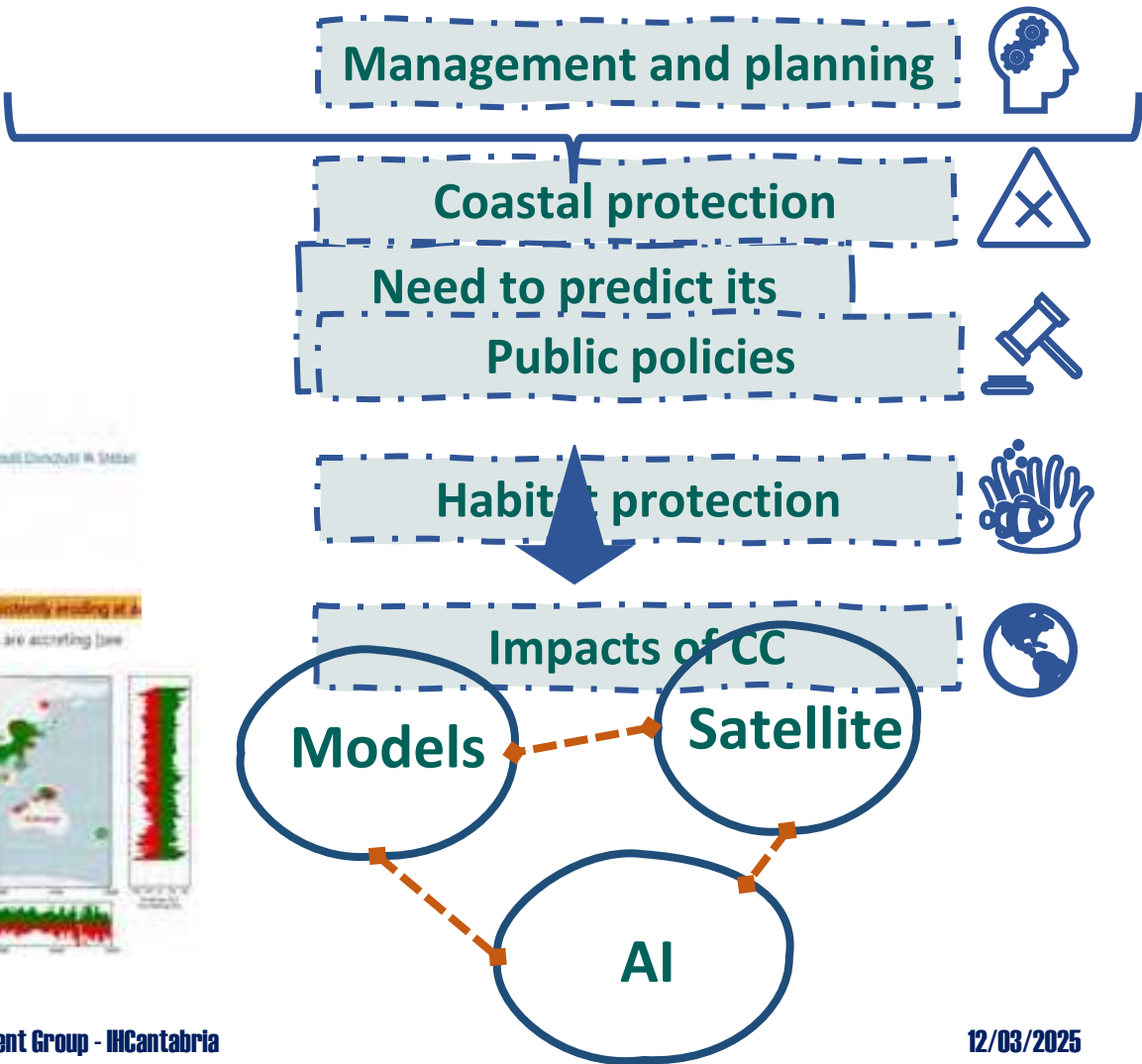


La erosión en Atafona, una comunidad costera de Brasil.

Las playas de Italia desaparecen debido a la erosión costera

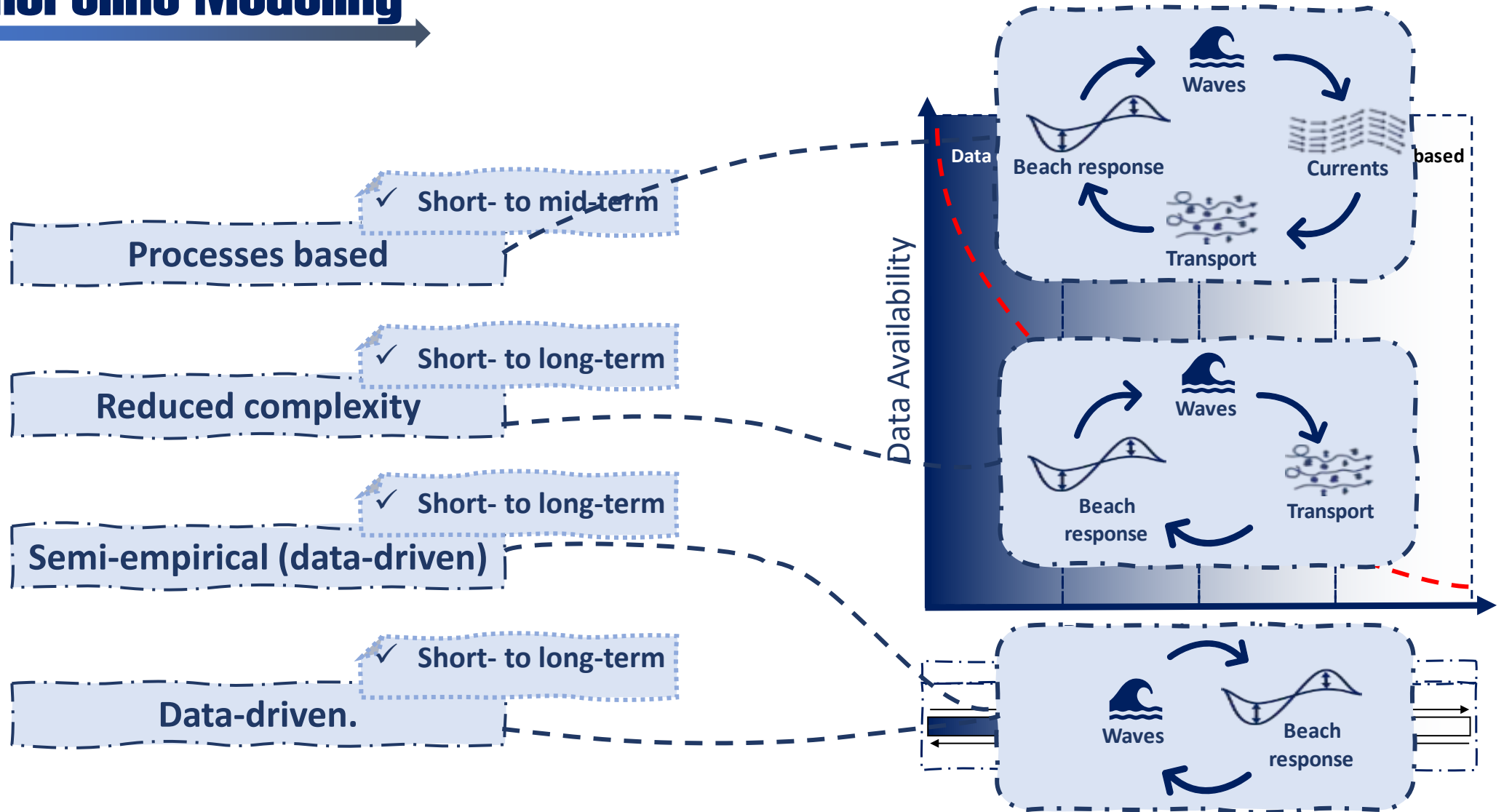


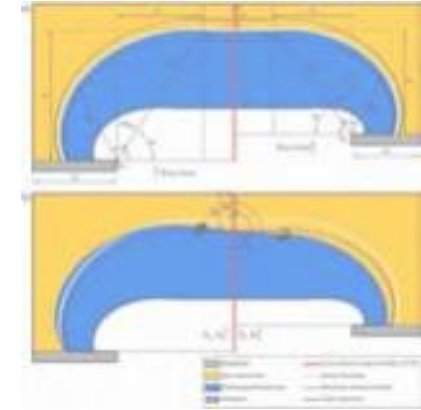
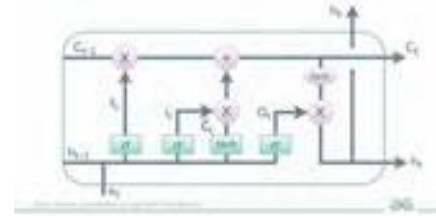
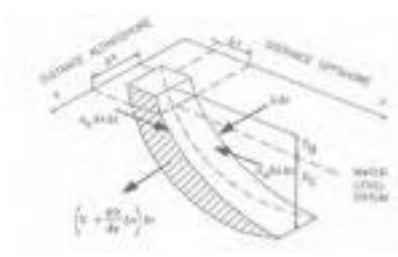
Una muestra de cómo la actividad humana afecta al entorno (AFP)





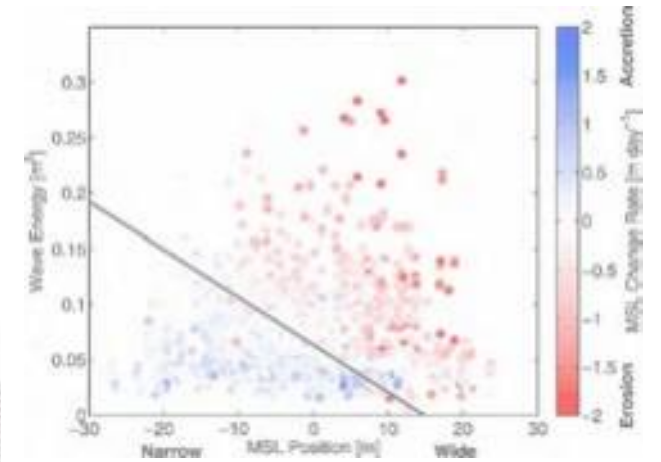
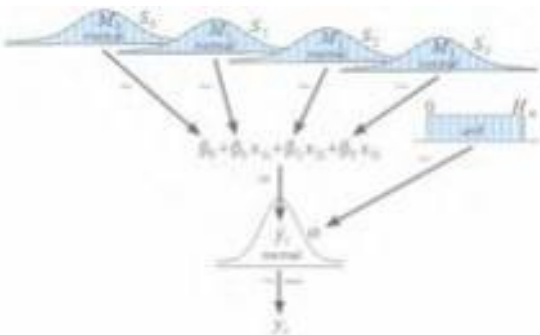
Shoreline Modeling





For long-term forecasts, which models are best?

$$\frac{\partial y_s}{\partial t} = -\frac{1}{(h_s + h_b)} \left(\frac{\partial Q_L}{\partial x} - q \right) + q_{FS}$$





ShoreShop (2019)

scientific reports

Explore content ▾ About the journal ▾ Publish with us ▾

nature > scientific reports > articles > article

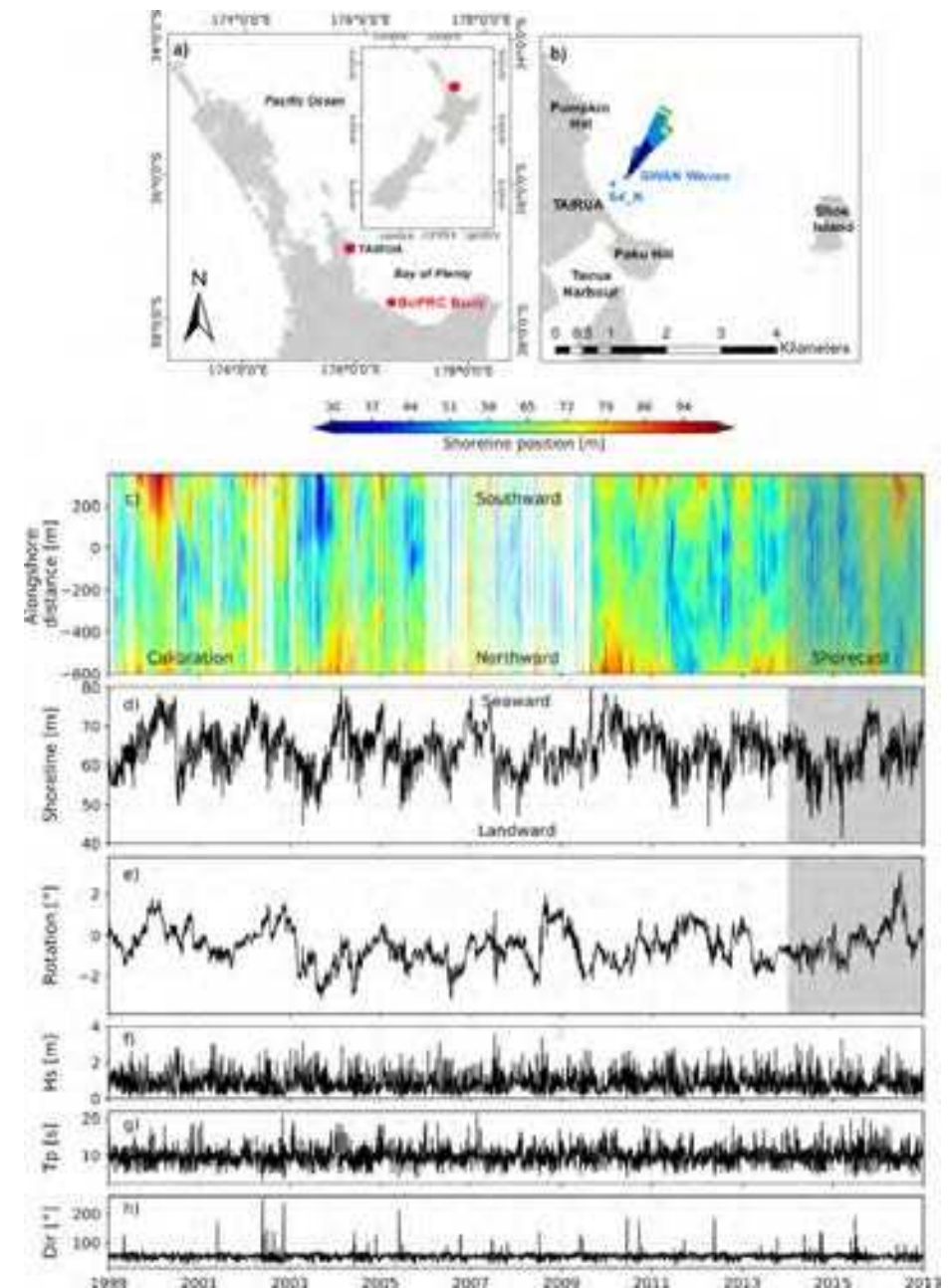
Article | [Open access](#) | Published: 07 February 2020

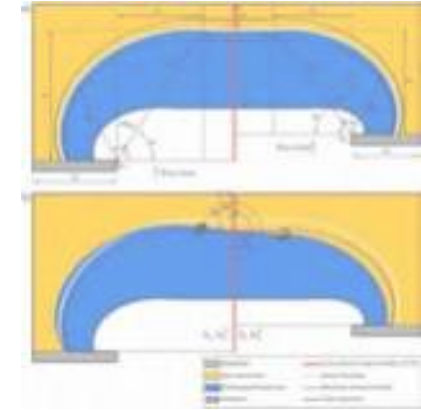
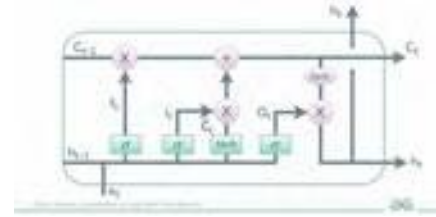
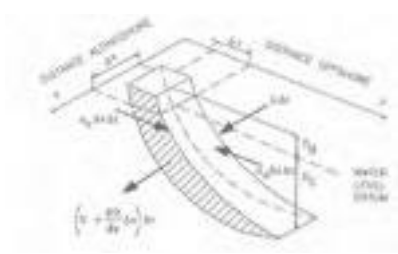
Blind testing of shoreline evolution models

Jennifer Montabon , Giovanni Cossu, Jose A. A. Antillón, Tomas Bruzau, Karin R. Bryan, Laura Capigai, Bruno Castañe, Mark A. Davidson, Evan B. Goldstein, Raimundo Maceta, Deborah Idier, Bonnie C. Ludka, Sina Masoud Ansari, Fernando J. Méndez, A. Brad Murray, Nathaniel G. Plant, Katherine M. Rutliff, Arthur Rubinetti, Ana Rueda, Nadia Sémichat, Joshua A. Simmons, Kristen O. Solinger, Scott Stephens, Ian Townsend, Sean Vitousek  & Kiban Viss  [Show fewer authors](#)

Scientific Reports 10, Article number: 2137 (2020) | [Cite this article](#)

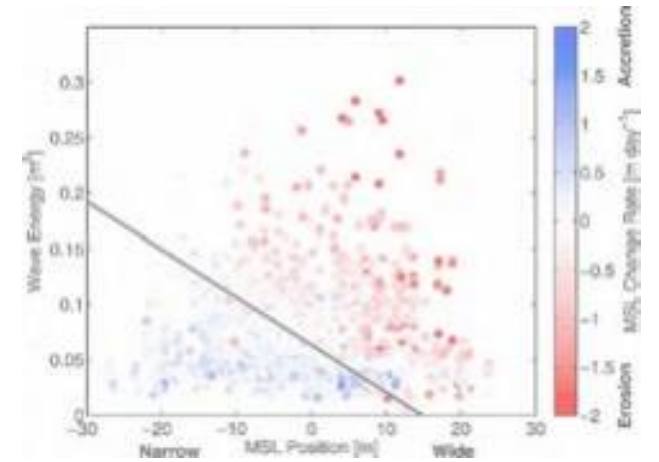
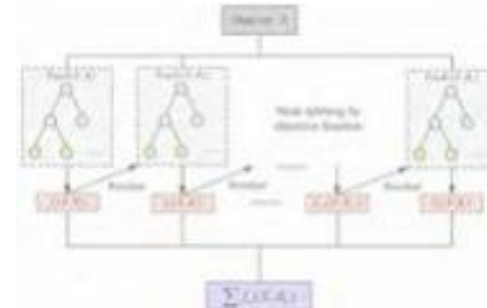
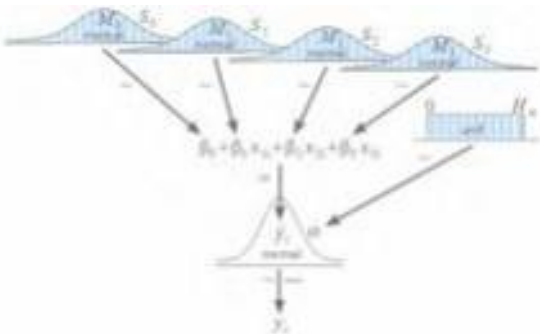
8599 Accesses | 105 Citations | 33 Altmetric | [Metrics](#)





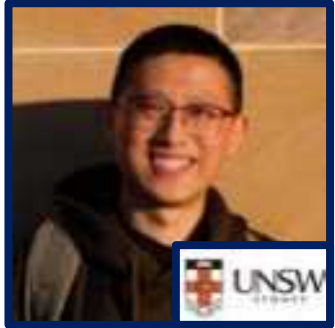
5 years latter...

$$\frac{\partial y_s}{\partial t} = -\frac{1}{(h_s + h_b)} \left(\frac{\partial Q_L}{\partial x} - q \right) + q_{FS}$$



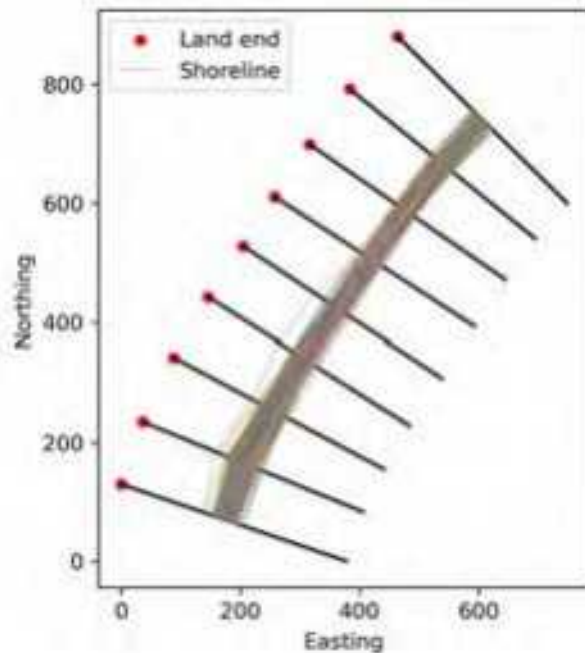


ShoreShop 2.0 (2024)



Yongjing
Mao

BEACH X:



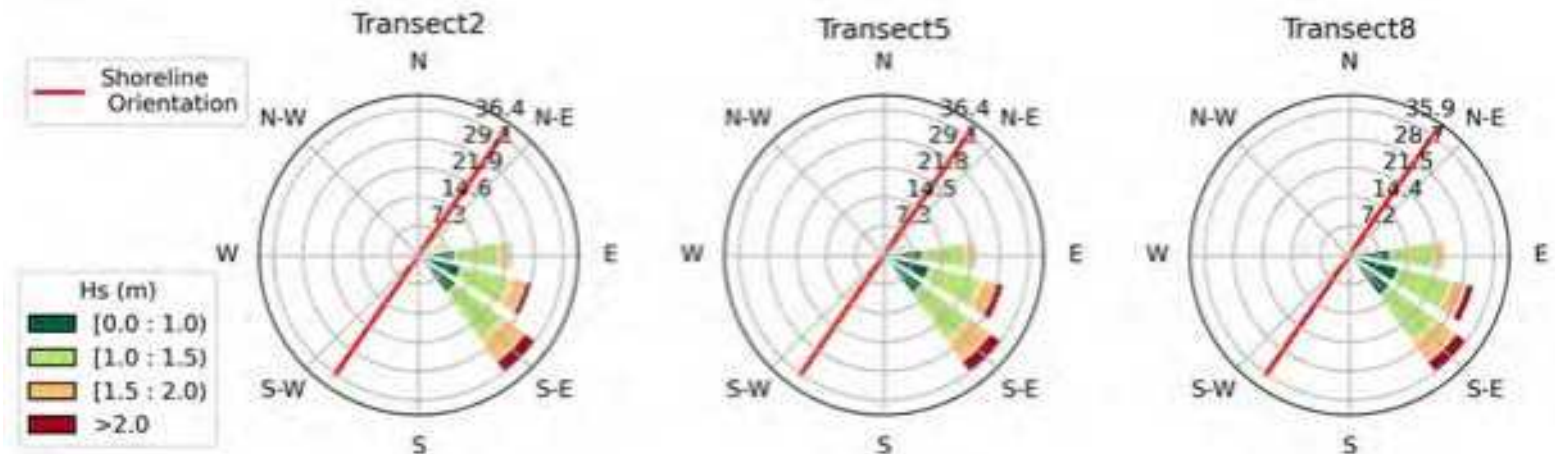
ShoreShop 2.0: Advancements in Shoreline Change Prediction Models

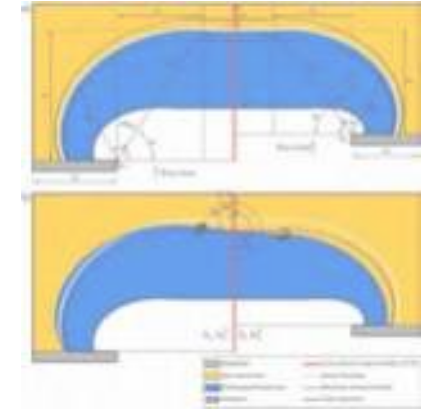
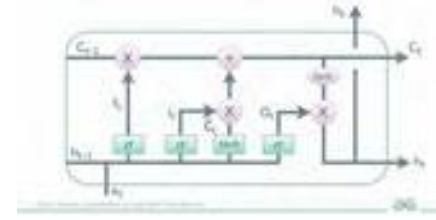
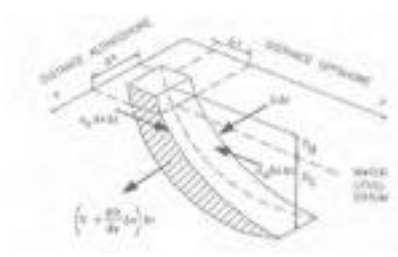
This repository is a testbed for shoreline modelling algorithms. It contains all benchmark datasets, input files, codes, and results.

Tasks

Given 20 years shoreline position data in the 1999-2018 period, along with the shoreline position in 1951-05-01 as well as wave and sea level data spanning from 1940 to 2100, participants are tasked with:

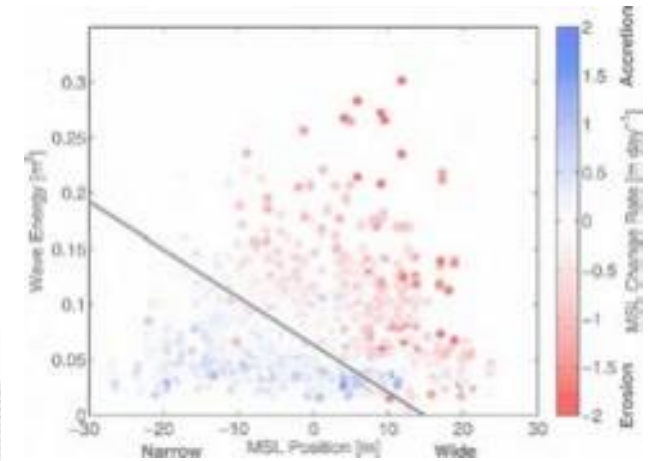
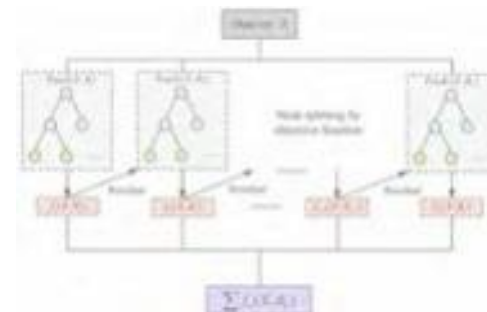
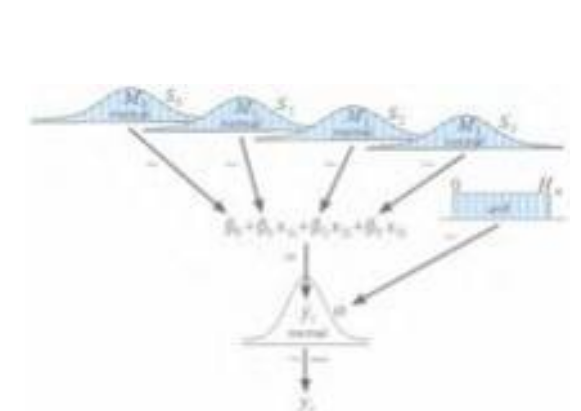
- **Task1.Short-term prediction:** Predict the shoreline position between 2019-01-01 and 2023-12-31 with daily timestep.
- **Task2.Medium-term prediction:** Predict the shoreline position between 1951-05-01 and 1998-12-31 with daily timestep.
- **Task3.Long-term prediction:** Predict the shoreline position between 2019-01-01 and 2100-12-31 with daily timestep (no evaluation).

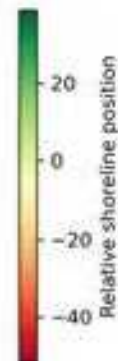
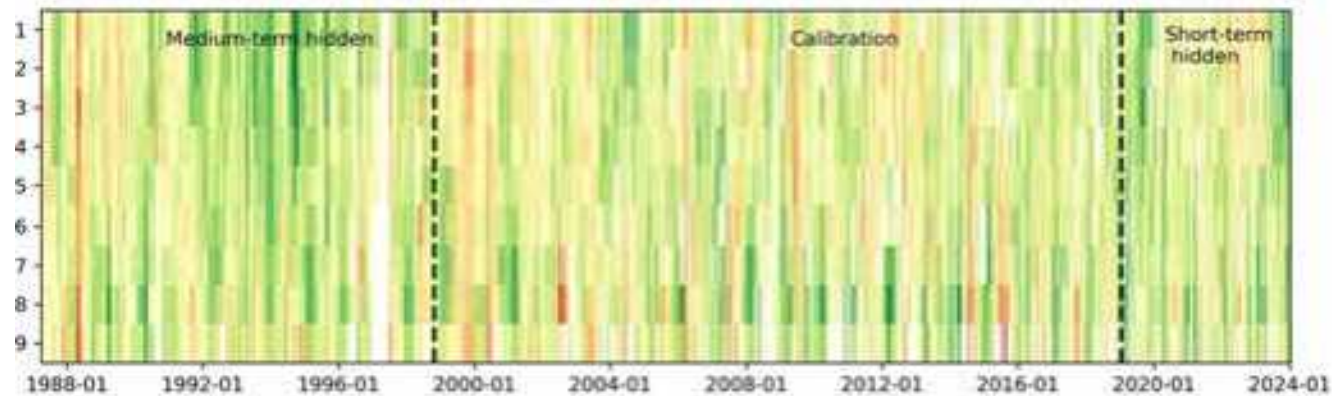
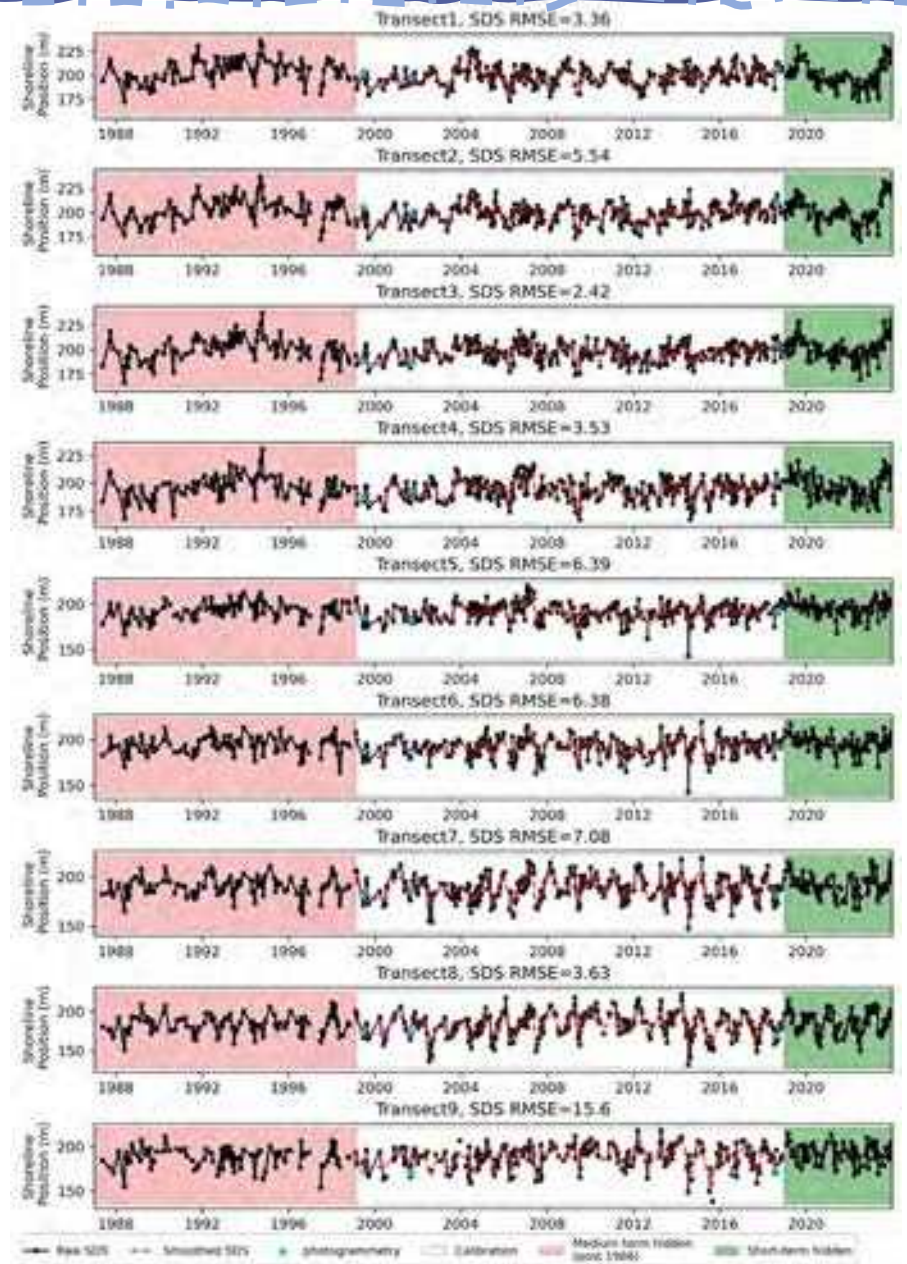
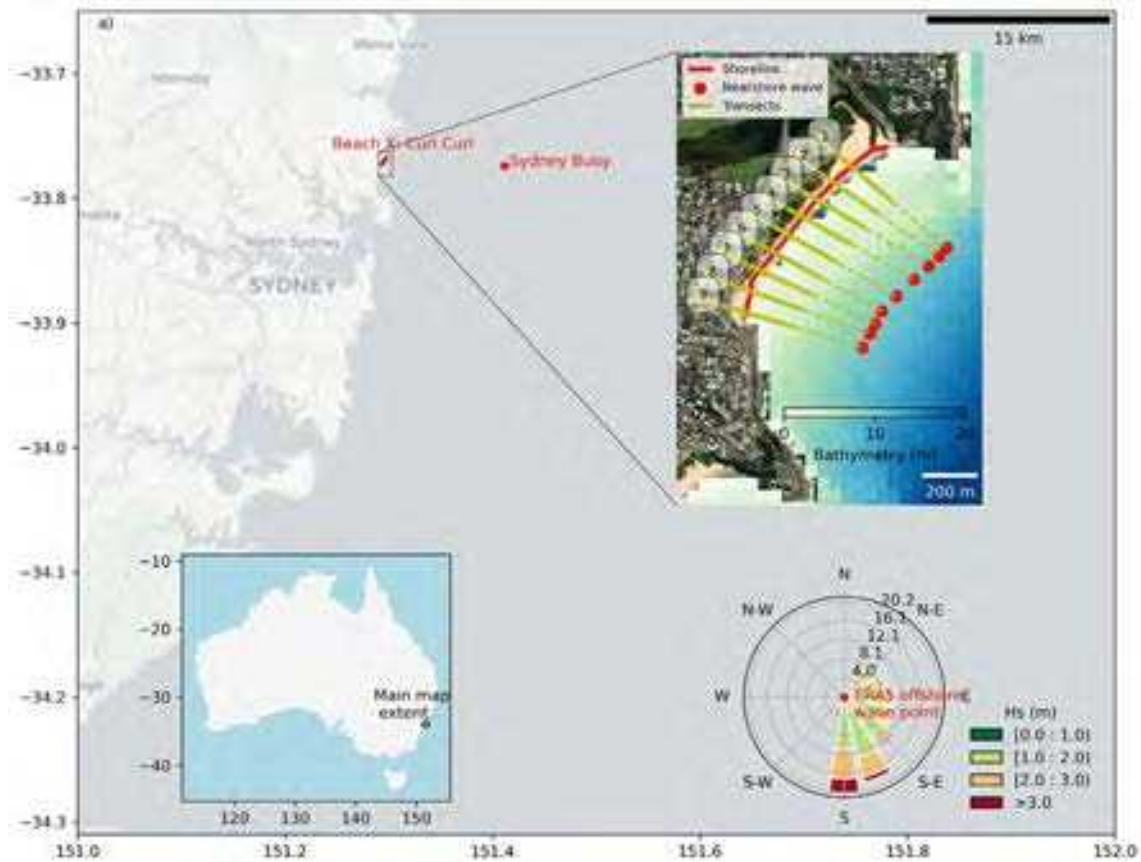


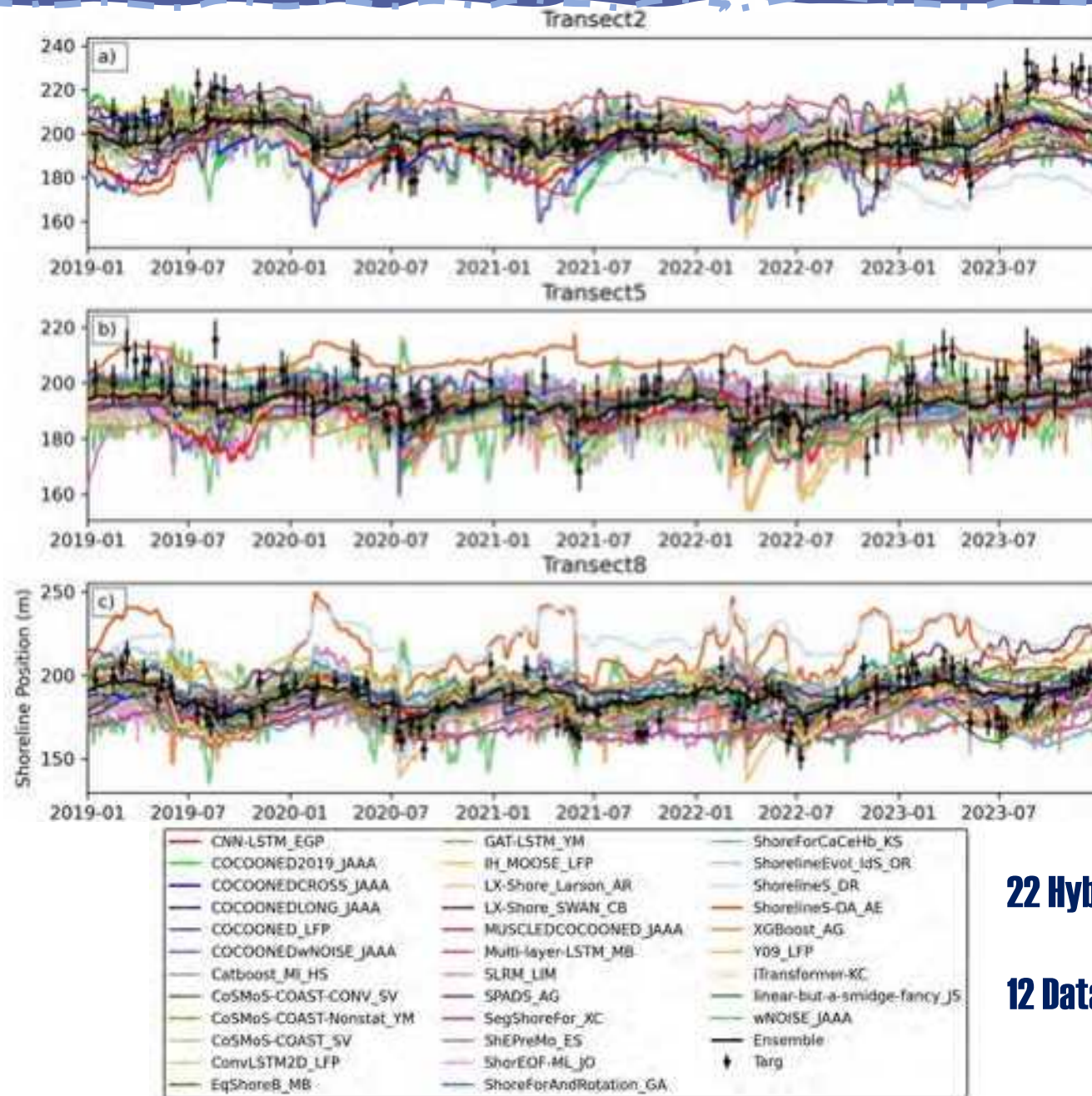


Can AI beat traditional models?

$$\frac{\partial y_s}{\partial t} = -\frac{1}{(h_s + h_b)} \left(\frac{\partial Q_L}{\partial x} - q \right) + q_{FS}$$

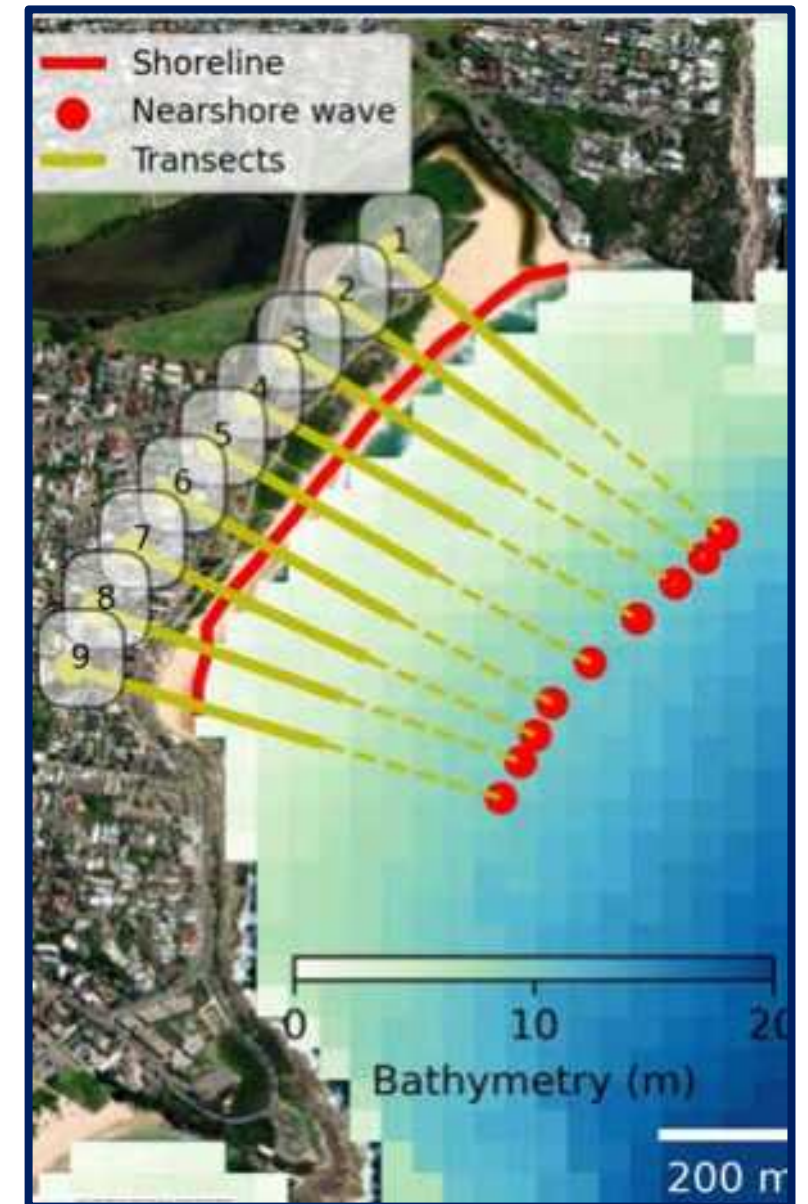




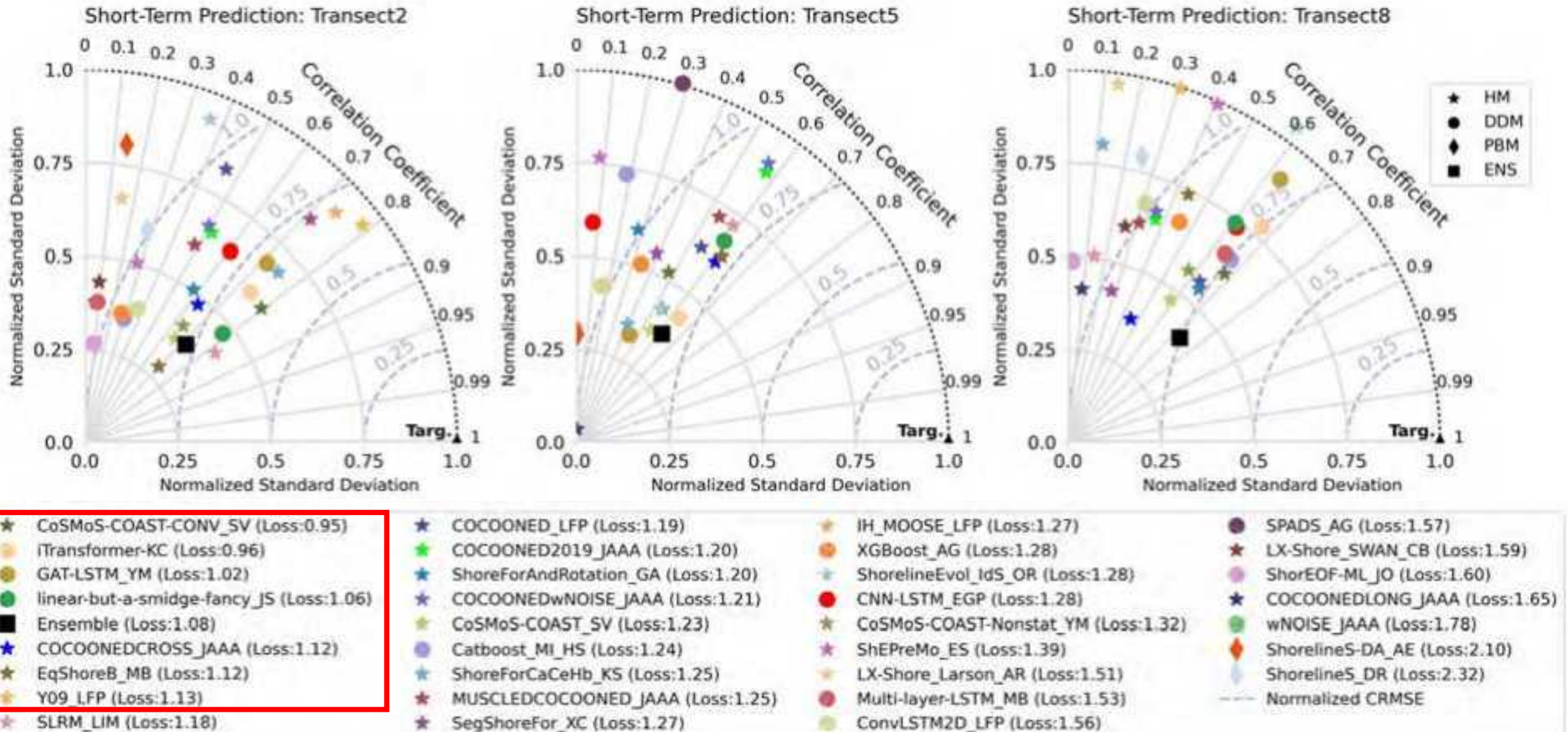


22 Hybrid

12 Data driven



$$L_i = \sqrt{(0 - RMSE_{norm})^2 + (1 - Corr)^2 + (1 - STD_{norm})^2}$$





Best models



CoSMoS-COAST-CONV

1 convolution + 5 params



iTransformer

$> 10^6$ params



GAT-LSTM

$> 10^6$ params



Bayesian Autoregression

$> 10^2$ params



Miller and Dean

3 params

Smoothed
data

Hybrid models

DNN
(attention based)

DD models

7 of the 10 best models were not AI models



What do we know so far?

There is no better model yet...

There are better modelers

Apparently, ensembles perform great...

But not for extreme events

Hybrid models are fast and stable...

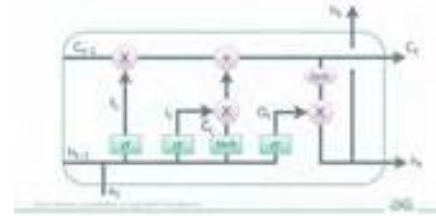
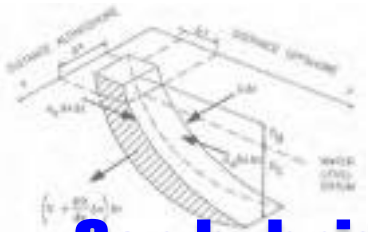
No “but” for this one

AI is coming with heavy guns...

But you are what you eat

SDS are the present, and future...

But the error is big



Can hybrid models be better explored?

How we can improve the extreme events?

Where is my shoreline modelling research going?



$$\frac{\partial y_s}{\partial t} = -\frac{1}{(h_s + h_b)} \left(\frac{\partial Q_L}{\partial x} - q \right) + q_{FS}$$

What is between 10^6 and 10^{10} parameters?



How do we deal with SDS errors?



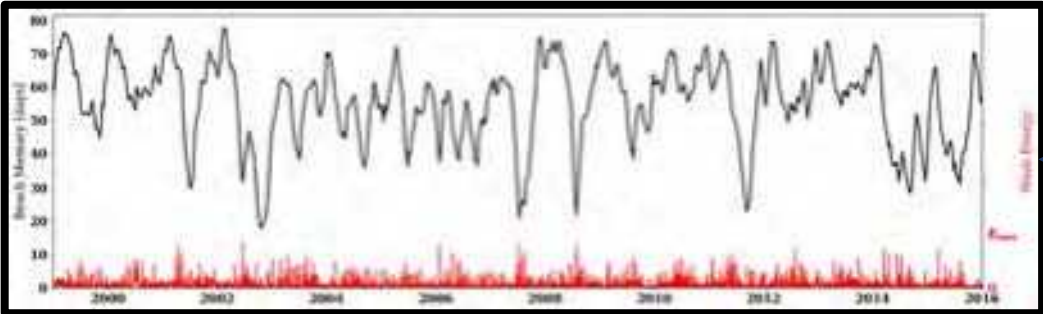
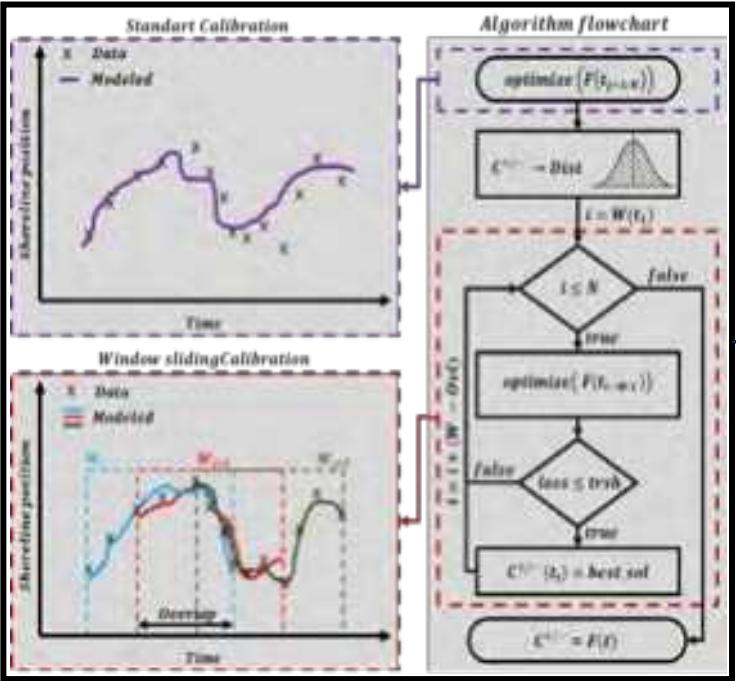
Can hybrid models be better explored?

What is between 10^6 and 10^0 parameters?

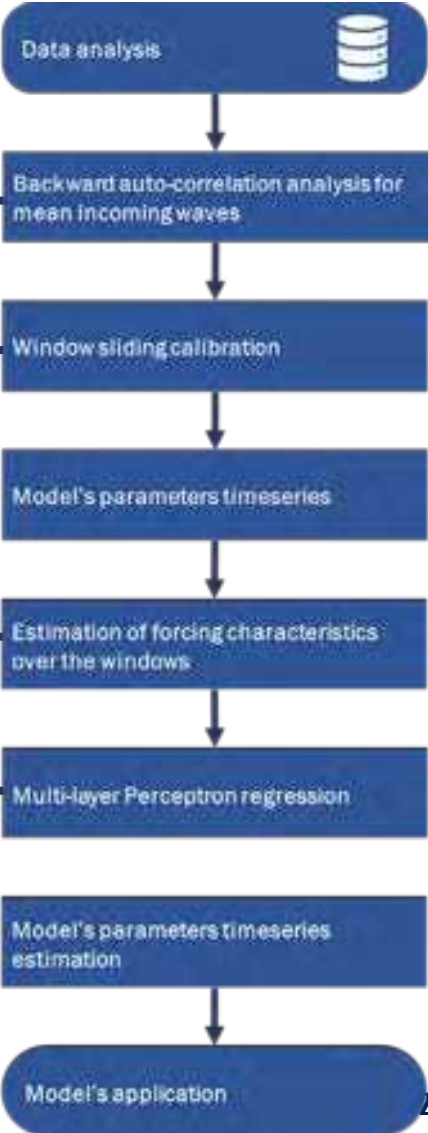
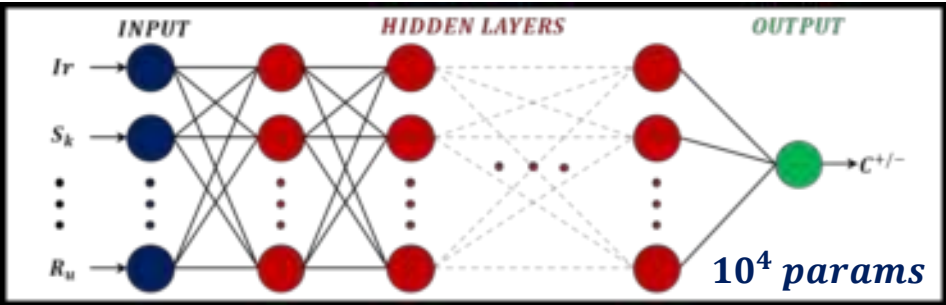
How we can improve the extreme events?

How do we deal with SDS errors?

Increase their complexity



Irribarren number (I_r)	Wave swewness (S_k)
Wave power (P)	Number of storms (N_s)
Mean angle (θ_m)	Mean sea level (MSL)
Dean's parameter (Ω)	Wave energy (E)
Wave energy std. (σ_E)	Runup (R_u)

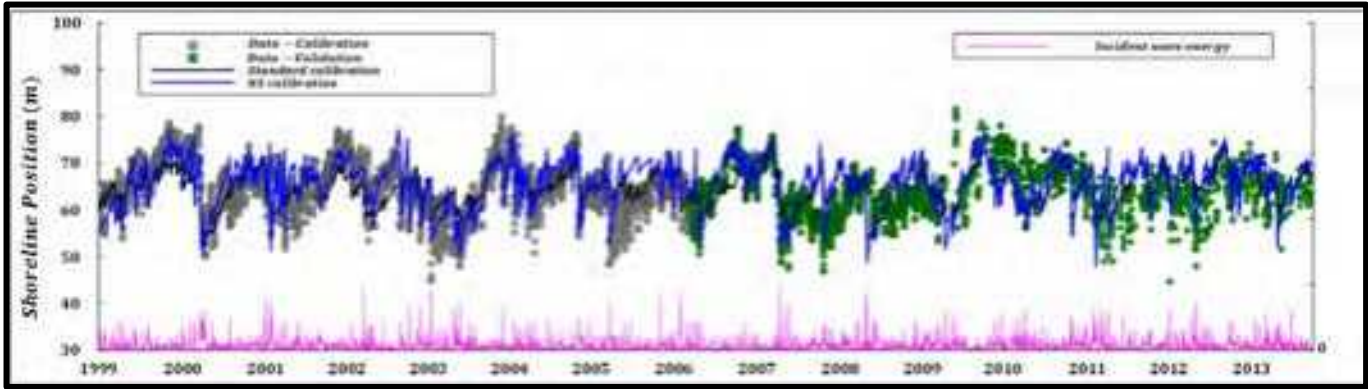
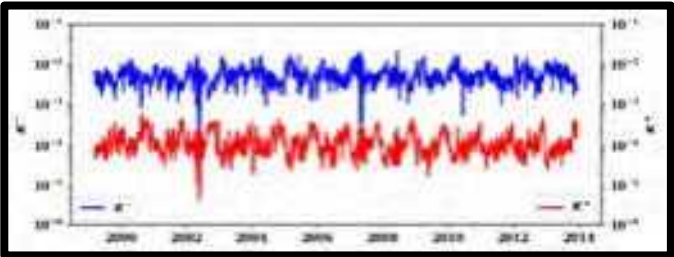


Can hybrid models be better explored?

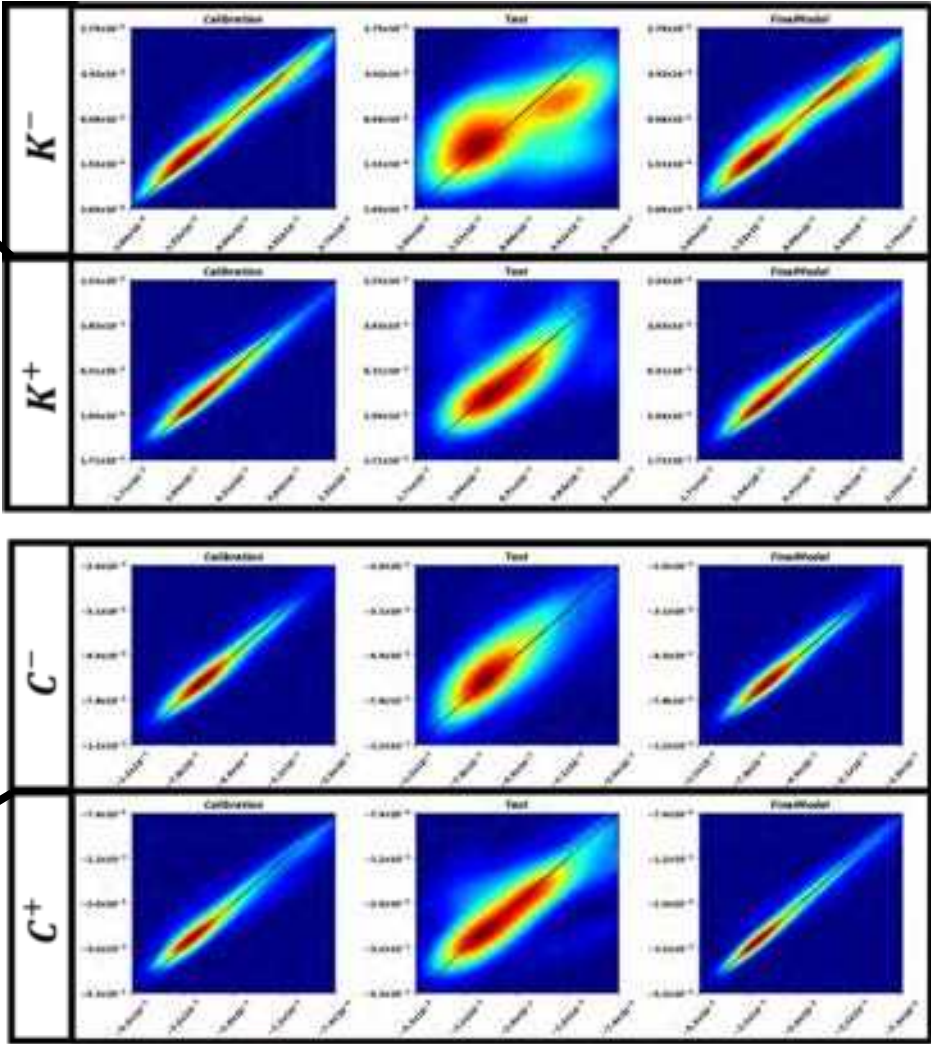
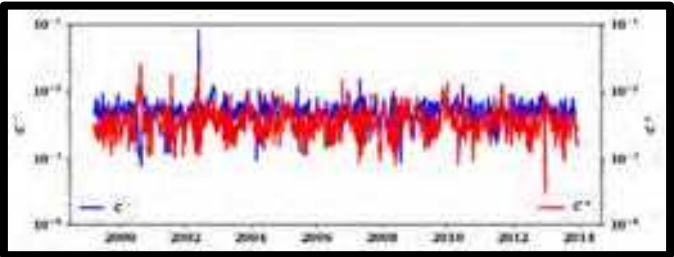
What is between 10^6 and 10^0 parameters?

How we can improve the extreme events?

How do we deal with SDS errors?



Period	Metric	Standard Calibration	Proposed Methodology
Calibration	λ_M	0.38	0.58
	RMSE	4.58 m	4.38 m
Validation	λ_M	0.30	0.40
	RMSE	5.25 m	5.03 m



Can hybrid models be better explored?

What is between 10^6 and 10^0 parameters?

How we can improve the extreme events?

How do we deal with SDS errors?



COASTAL DYNAMICS 2025

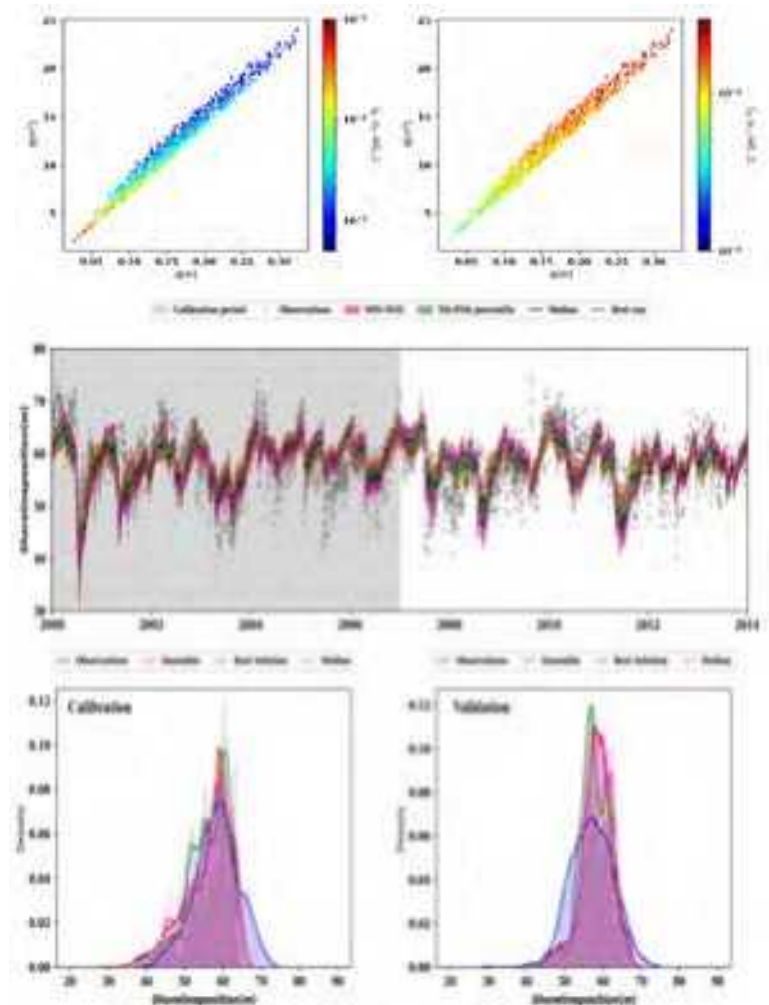
7-11 April, Aveiro, Portugal

PROBABILISTIC FORECASTING OF SHORELINE EVOLUTION: A CASE STUDY USING GENETIC ALGORITHMS

Lucas de Freitas¹, Camilo Jaramillo¹, José A. A. Antolinez², Mauricio González¹, Raúl Medina¹

¹ IHCantabria – Instituto de Hidráulica Ambiental de la Universidad de Cantabria, Santander, Spain.

² Hydraulic Engineering Department, Delft University of Technology, Delft, The Netherlands. lucas.defreitas@unican.es

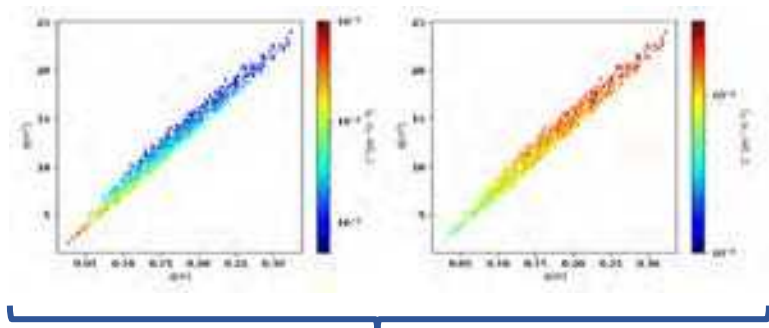


Can hybrid models be better explored?

What is between 10^6 and 10^0 parameters?

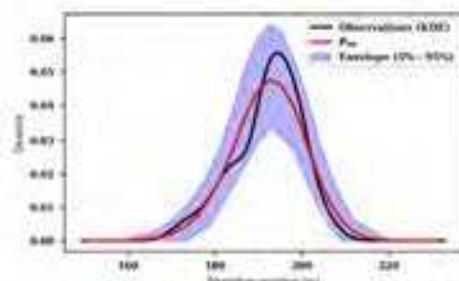
How we can improve the extreme events?

How do we deal with SDS errors?

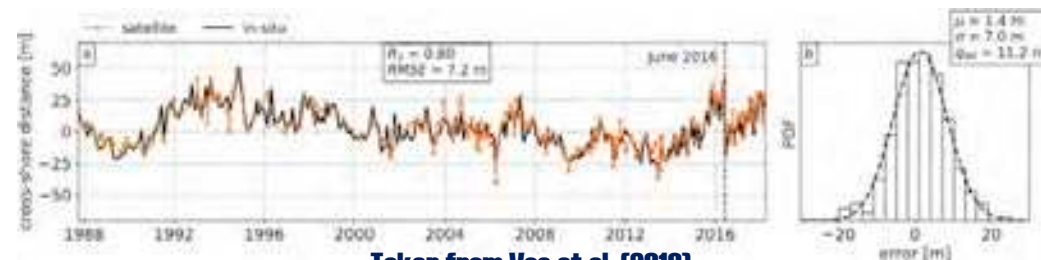


Multivariate prior

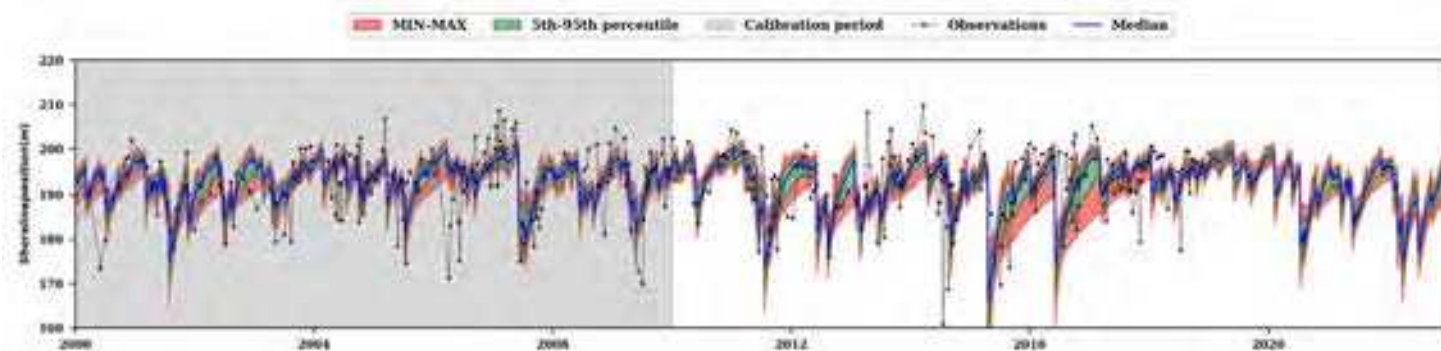
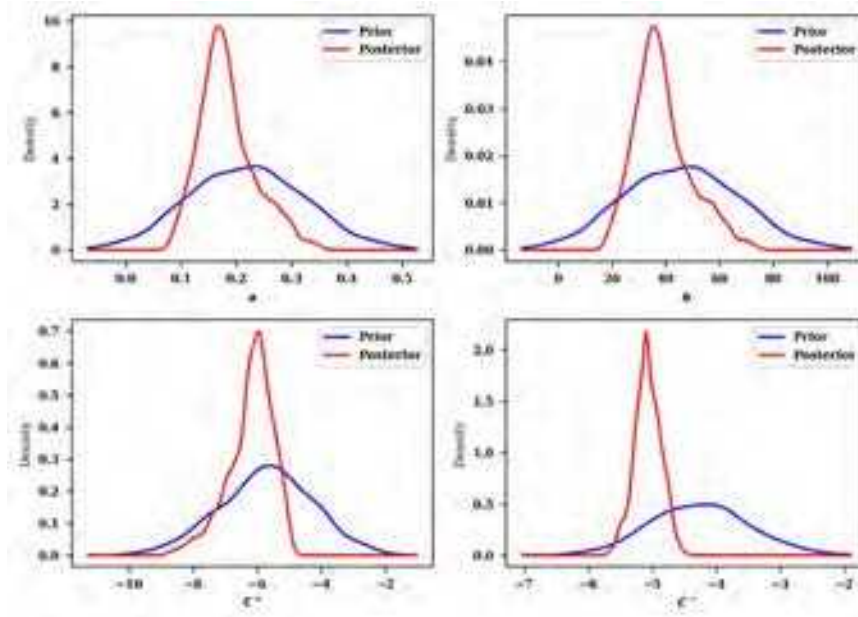
$$+ \mathcal{N}(\epsilon_{obs})$$



Bayesian inference



Taken from Vos et al. (2019).

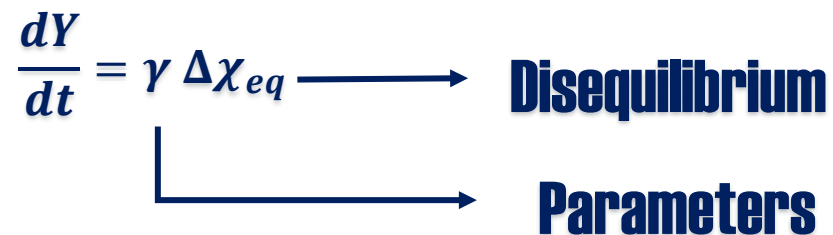


Can hybrid models be better explored?

What is between 10^6 and 10^0 parameters?

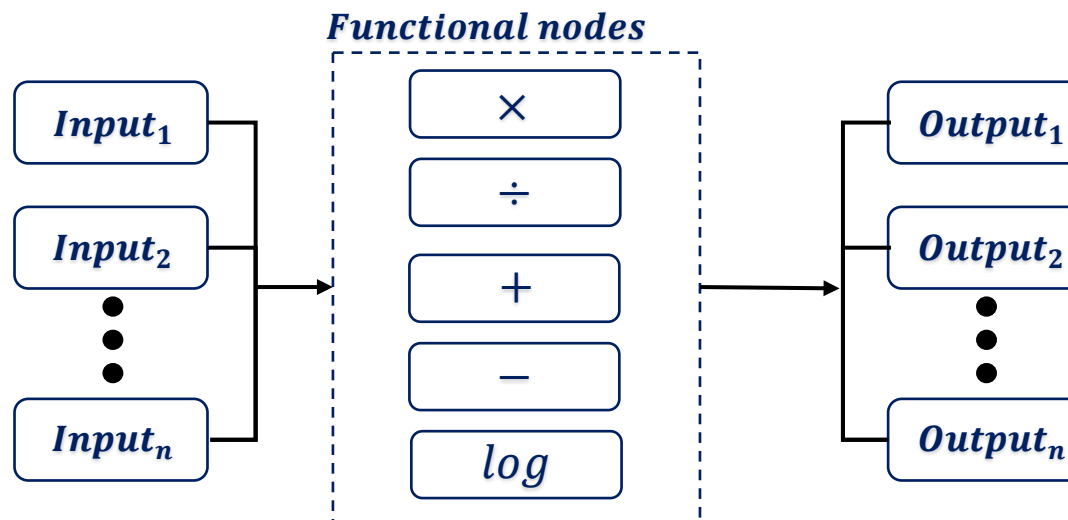
How we can improve the extreme events?

How do we deal with SDS errors?



$$\forall \gamma \rightarrow \gamma = \theta + \epsilon(t, \text{forcing})$$

Cartesian Genetic Programming



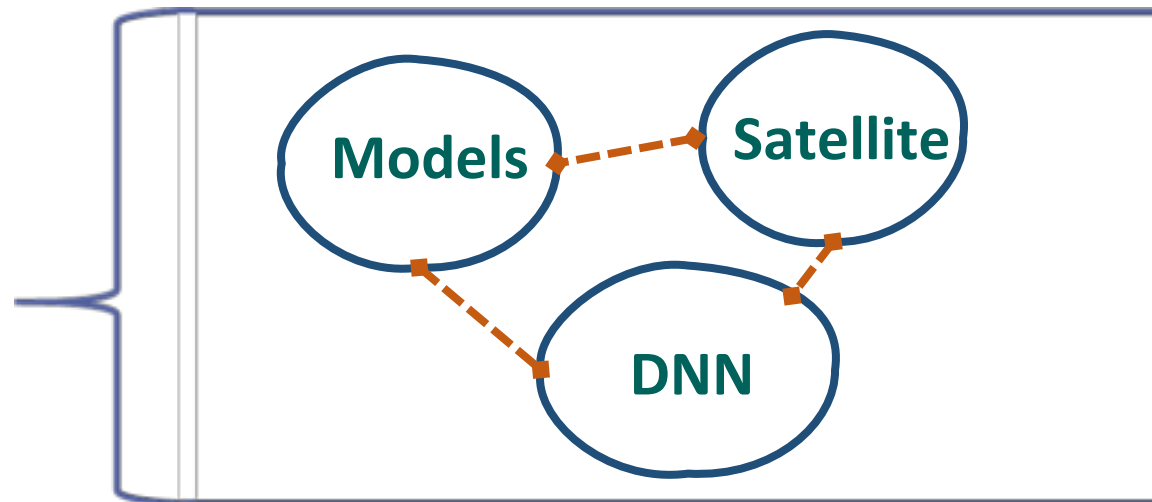
- Use EBSEM stability
- Add uncertainty to the ensemble
- Scalability (LS+CS)
- Increase complexity
- Improve extreme events prediction quality



Key takeaways



The present and the future



Our main challenges



Where my thesis is going

- Hybridizing traditional models
- Statistical shoreline modeling
- Improving predictions
- Developing models aided by DNNs (ongoing)

DC Presentations

Morphodynamic Analysis of the upper confined and unconfined beach profiles during Episodic events

06/ 11/ 2024

SEDIMARE Workshop
Santander, Spain

Buckle Subbiah Elavazhagan

SEDIMARE – DC 05
IH-Cantabria, Universidad de
Cantabria

Javier López Lara

Professor, Universidad de
Cantabria

María Emilia Maza Fernández

Ass. Professor, Universidad de
Cantabria

Understanding on numerical simulations using bichromatic conditions from large scale experiment

New Experiments to be considered for the numerical study

Model development for vegetation case

01

INTRODUCTION

02

BACKGROUND IH2VOF-SED

03

IMPLEMENTING LABORATORY CASE

04

RESULTS

05

SUMMARY

06

LABORATORY EXPERIMENTS CONSIDERED

07

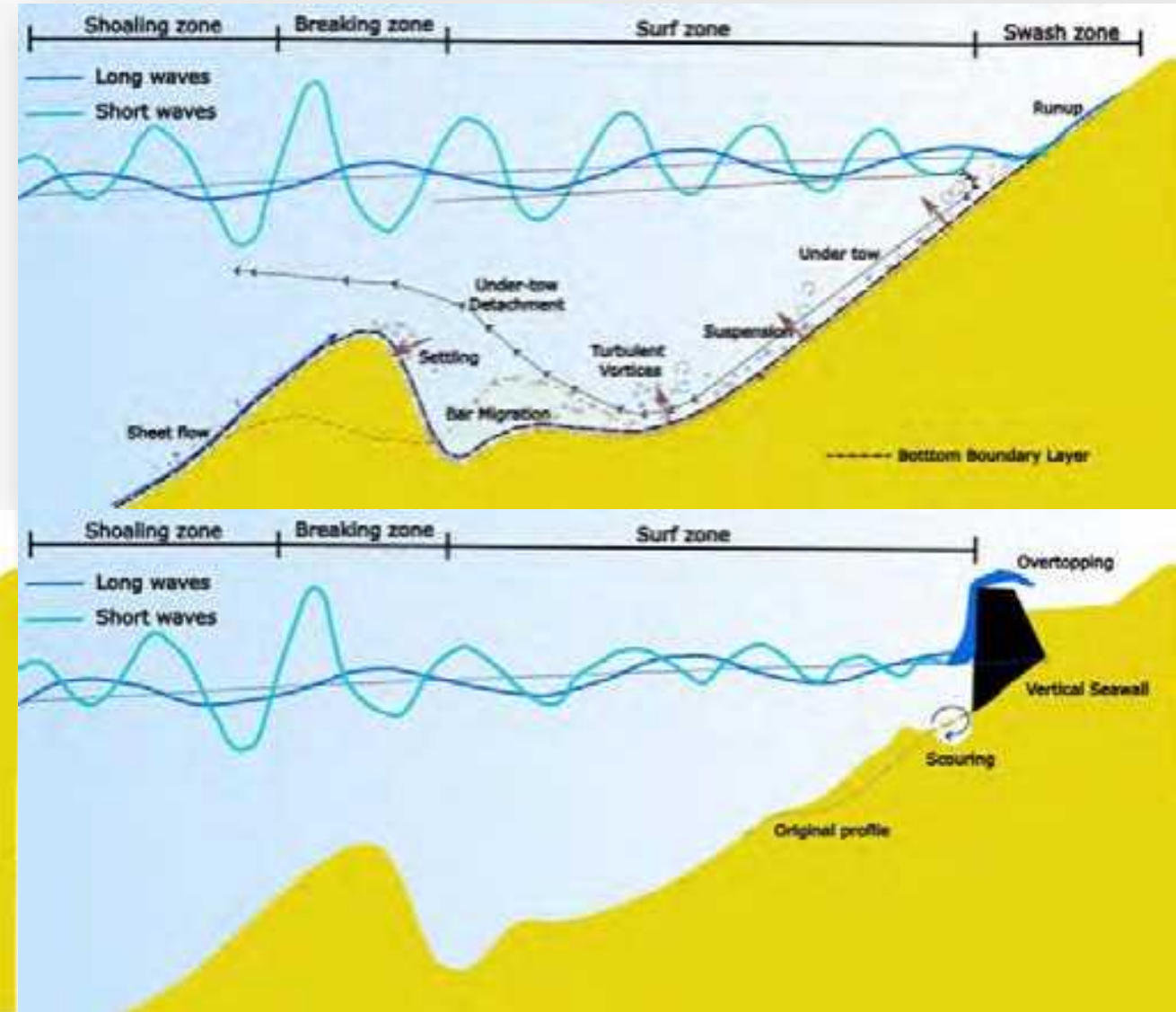
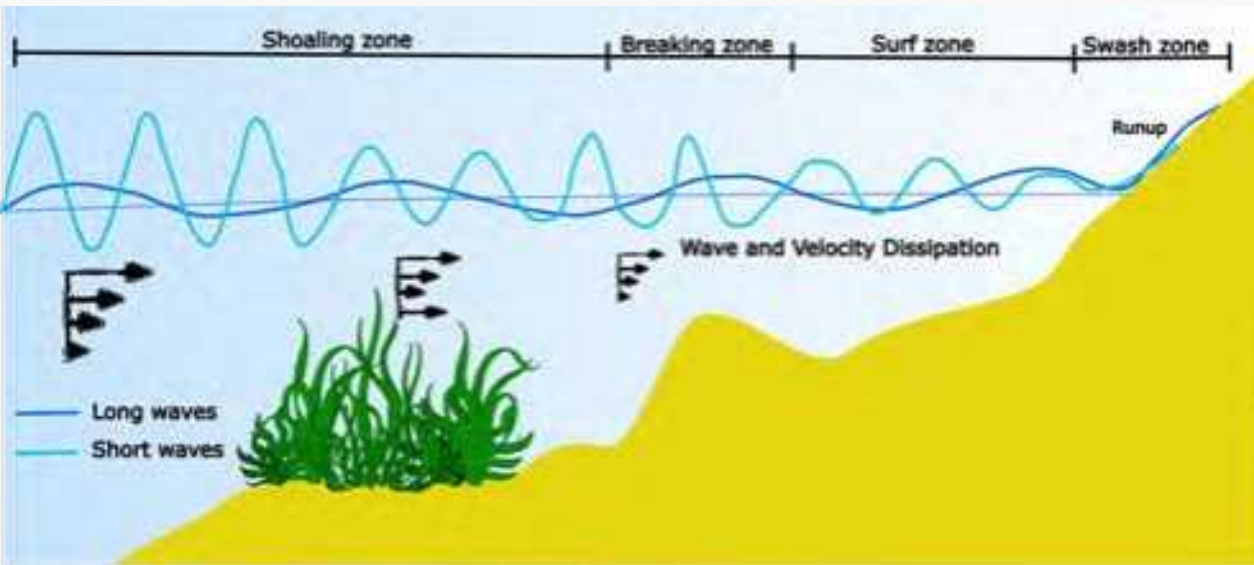
IMPLEMENTING VEGETATION SCHEME

08

WHAT'S NEXT

I INTRODUCTION

Applying IH2VOF –SED model to model different morphodynamic processes and the governing hydrodynamics on different beach configurations and sustainable protection measures



II Background IH2VOF- SED

2DV RANS based solver

Turbulence is accounted using a $k-\varepsilon$ closure model

Finite difference computational approach in a structured orthogonal mesh

Free surface reconstruction using Volume of Fluid technique

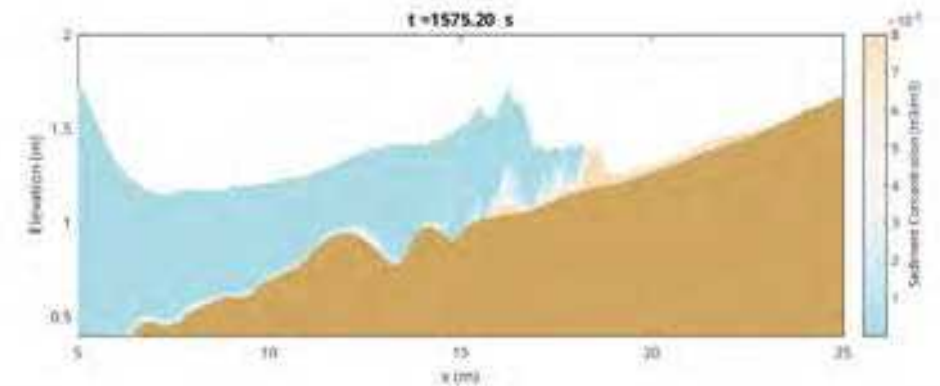
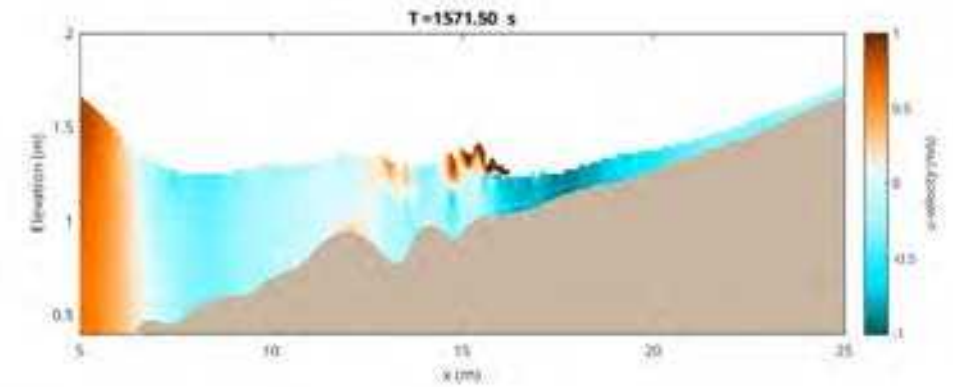
Incorporation of solid boundary using partial cell treatment

Two step projection method is used as numerical solving procedure

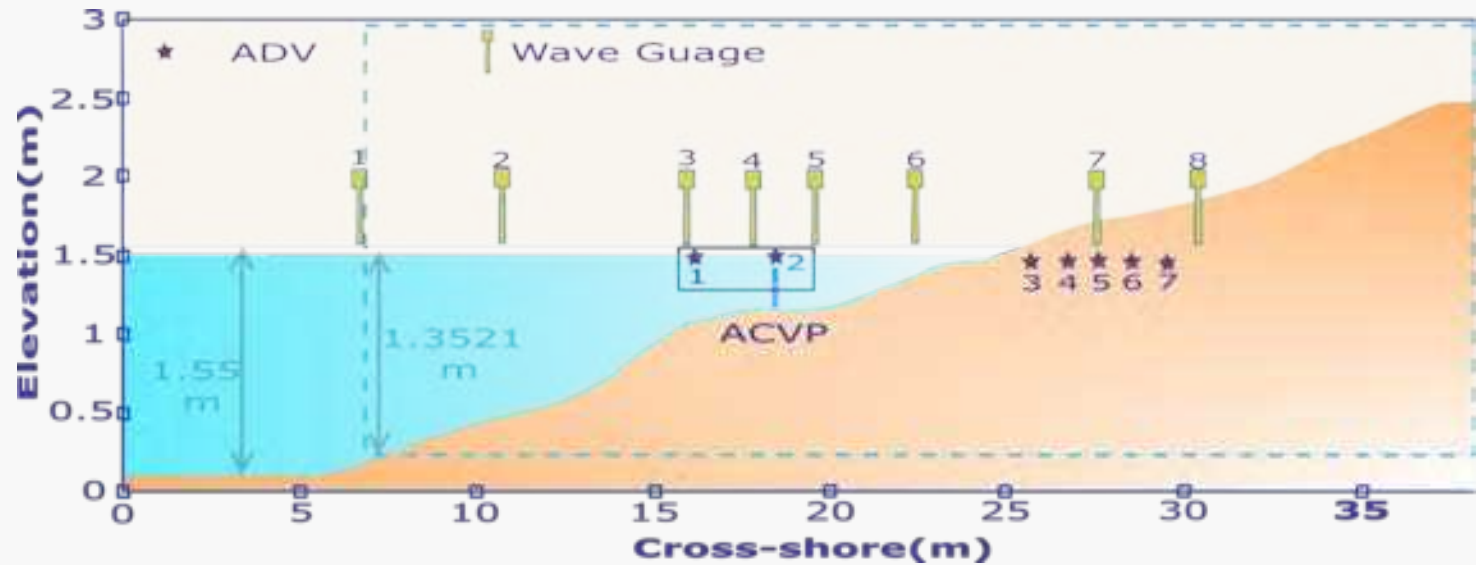
Empirical formula by Roulond 2004 is used for Bed load Estimation

Advective Diffusive equation is solved for Suspended load Estimation

Two point friction velocity estimation is used



III Implementing Laboratory case



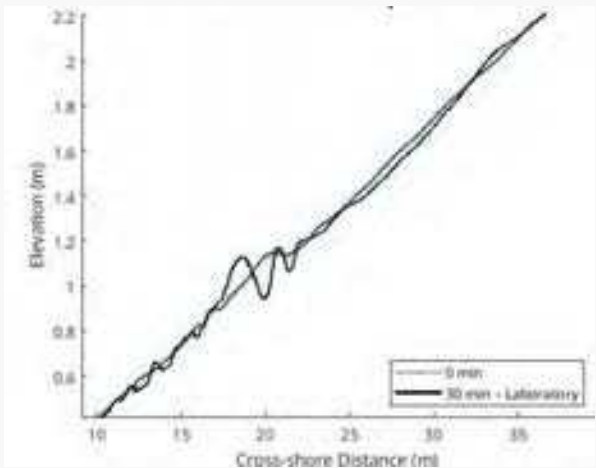
Near-Bed Sediment Transport during offshore bar migration in large-scale experiments . Florian Grossman et.al 2022

Erosive case using Bi-chromatic Waves

H1(m)	H2(m)	F1(Hz)	F2 (Hz)
0.245	0.245	0.3041	0.23657

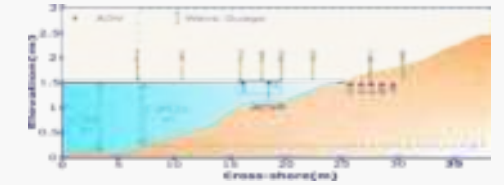
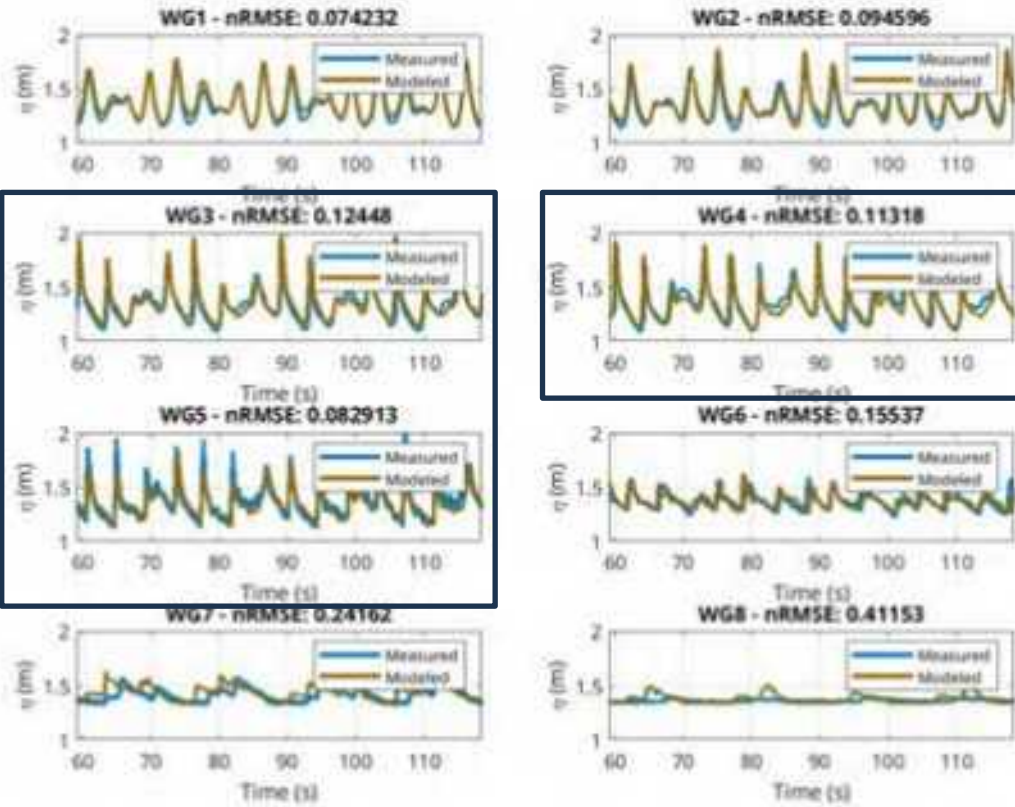
Initial and final beach states

Bar formation

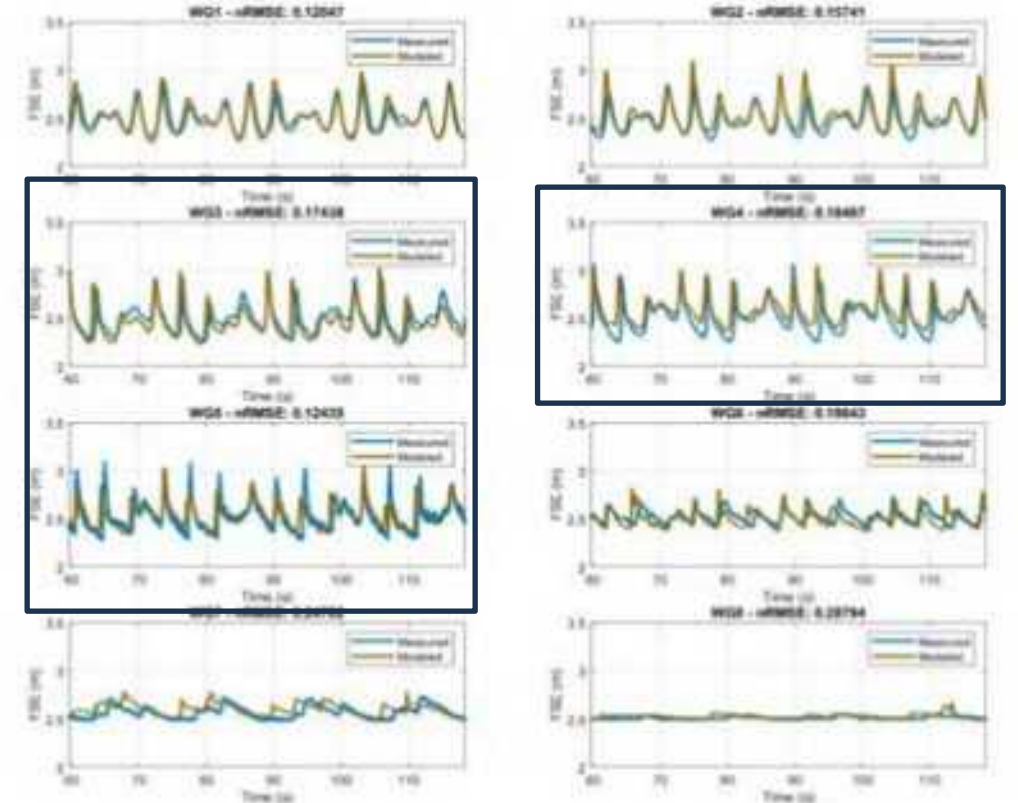


IV Results - Free Surface Elevation (First 4 wave groups)

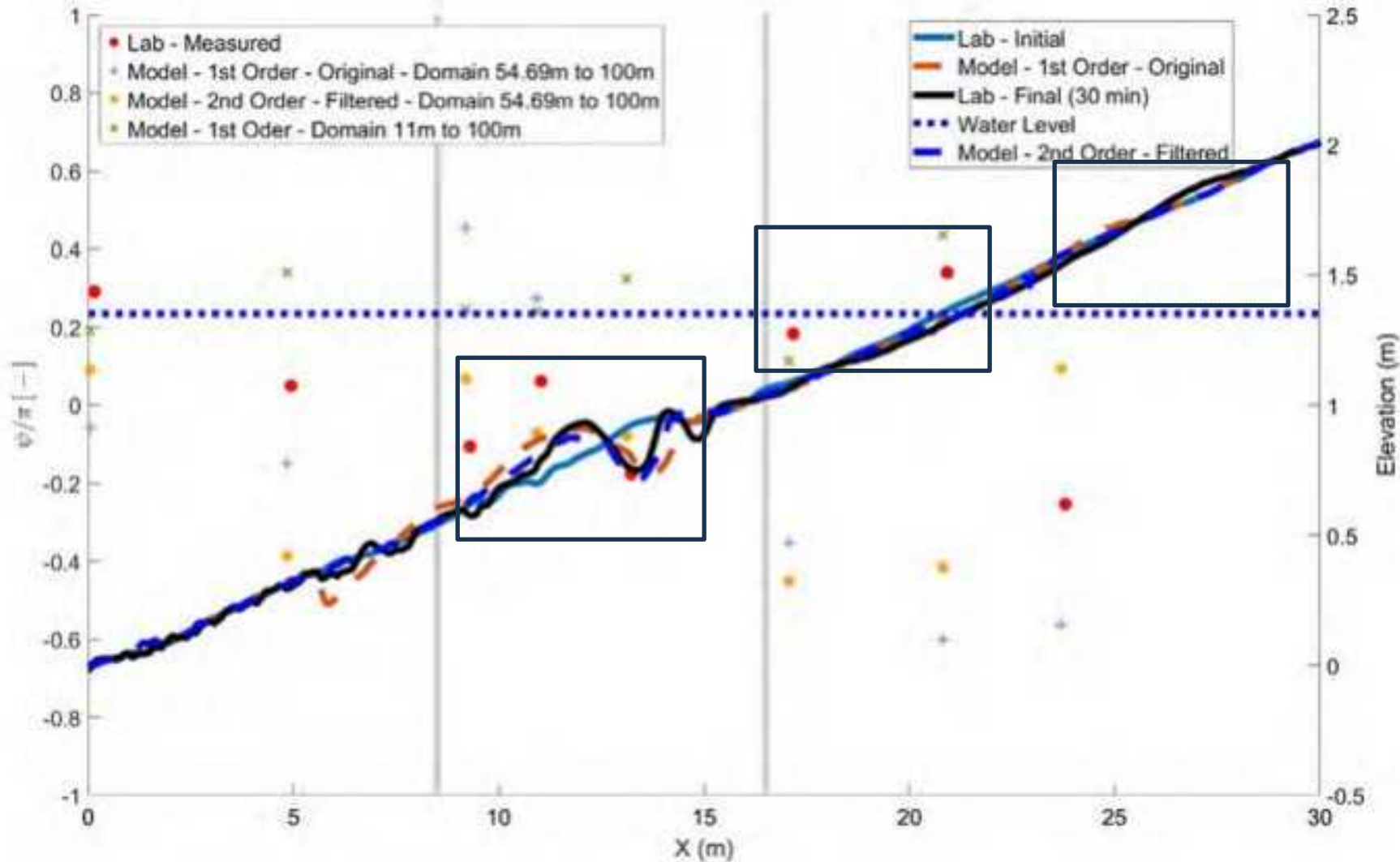
Origin 54 m from the wave maker



Origin 11 m from the wave maker



IV RESULTS- Phase Difference between long wave and short wave components and beach profile evolution



- Deviations in phase difference between long and short wave components of model and laboratory is significant
- Closer representation in breaking zone resulted in better bar formation when driven with theoretical 2nd order waves replacing existing components
- Overwash in the inshore is underestimated.

IV Results- Phase Difference between long wave and short wave components and beach profile evolution

J.W.M. Kranenborg et.al, 2024

Effects of free surface modelling and wave-breaking turbulence on depth-resolved modelling of sediment transport in the swash zone, Coastal Engineering.

The closest study using similar wave conditions.

The model is run using a fixed bed and only for 3 minutes with no bed evolution.

Wave maker signals are available in this case

Jose M Alsina et.al, 2016

Sediment transport and beach profile evolution induced by bi-chromatic wave groups with different group periods.

During shoaling process broad banded wave conditions tend to dissipate more and energy transformation into long wave components

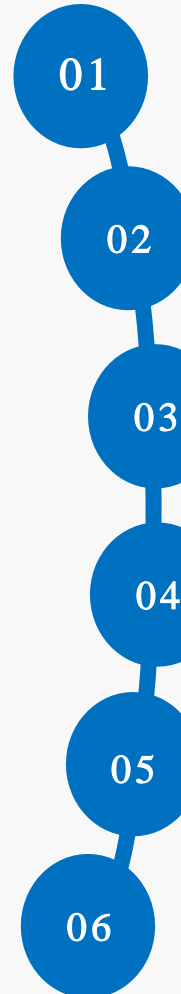
It is observed ingoing free long wave is 27% of energy of the primary wave group

Baldock TE et.al, 2010

Sediment transport and beach morphodynamics induced by free long waves, bound long waves and wave groups.

Wave conditions with free long waves tend to increase offshore transport in the surf zone and onshore transport in the swash zone, but with bound longwave offshore transport is predominant in surf and swash zone.

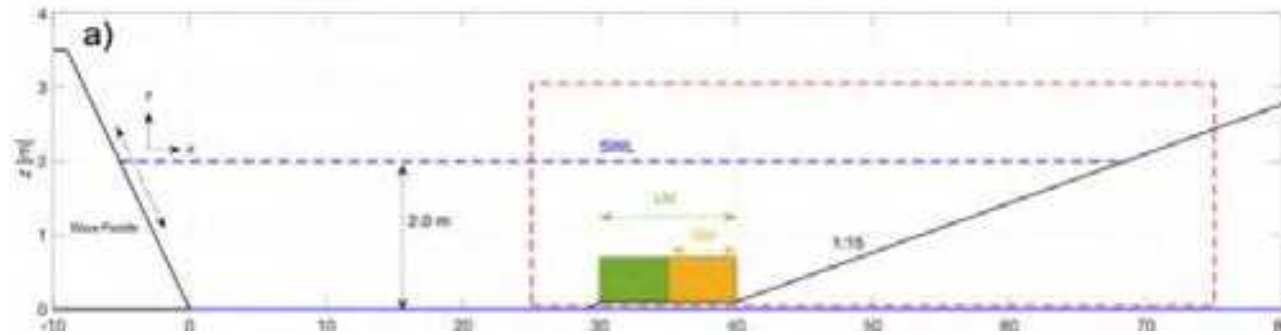
V Summary

- 
- 01 Phase difference between long wave and short wave components are different for laboratory and for numerical simulations
 - 02 Using different wave gauge data and changing the domain length accordingly introduces different longwave components into model
 - 03 Lack of Wave maker signal information is a deficiency for replicating the entire length of the flume
 - 04 Breaking point decides the breaker bar formation
 - 05 Longwave not exactly replicated reduces overwash deposition
 - 06 Subsequent experiments are planned considering this impact

VI Morphodynamic evolution due to the presence of seagrass meadow

1. Development of Numerical scheme to incorporate the impact of *Posidonia Oceania*
2. Validation against CIEM Flume experiments which used a surrogate vegetation model
3. Evaluate the morphodynamic response due to the presence of the seagrass meadow

Validation case



Physical model setup - Astudillo et al., 2022; Astudillo-Gutierrez et al., 2024)

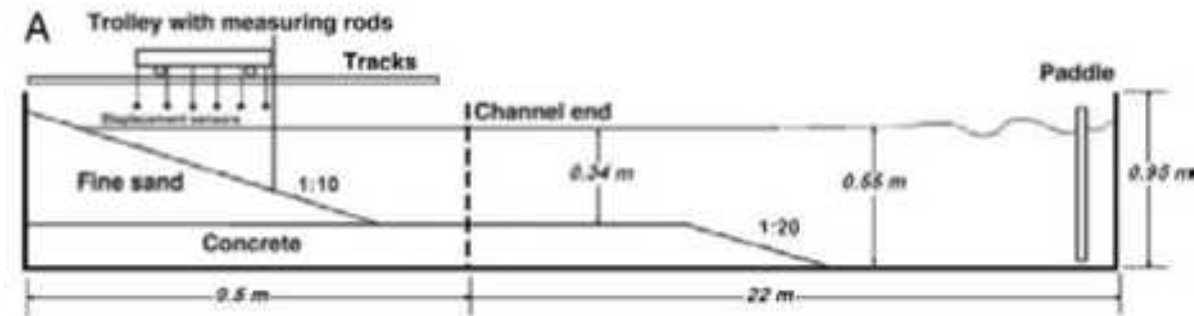
Key expected outputs

1. Functional numerical model incorporating submerged vegetation
2. Role of submerged meadow of different lengths in attenuating waves and velocities
3. Impact of vegetation in breaker bar dynamics

VI Sediment transport and beach morpho dynamics induced by free long waves, bound long waves and wave groups

1. Validation against medium scale experiments of Baldock et.al 2010
2. Experiments highlighted response of a beach profile to different wave conditions
3. Experiments include free long waves and bound long waves

Validation case



Physical model setup – Baldock et.al 2010

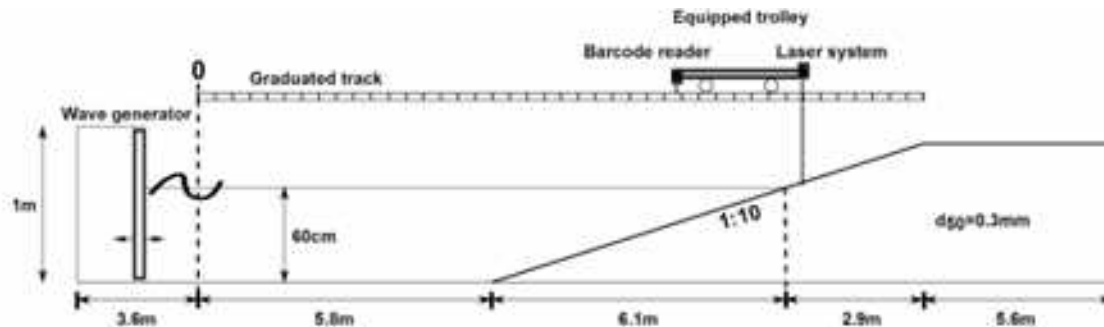
Key expected outputs

1. Role of free long waves and bound long waves in morphodynamic response of a beach profile

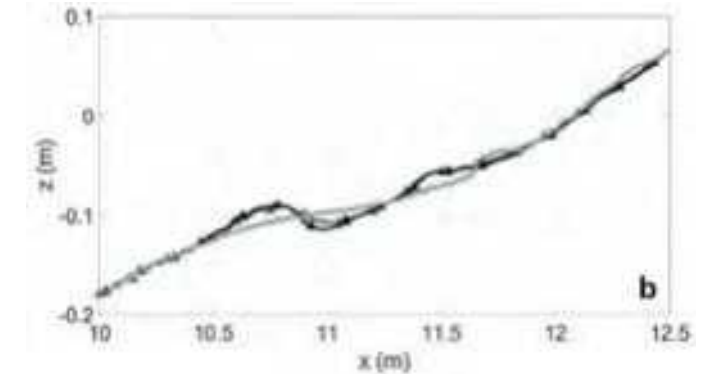
VI Study on dynamic equilibrium of a Beach profile

1. Validation against medium scale experiments of Baldock et.al 2017
2. Experiments about static and dynamic equilibrium of a beach profile
3. Erosive and accretive wave conditions are used cyclically

Validation case



Physical model setup – Baldock et.al 2017



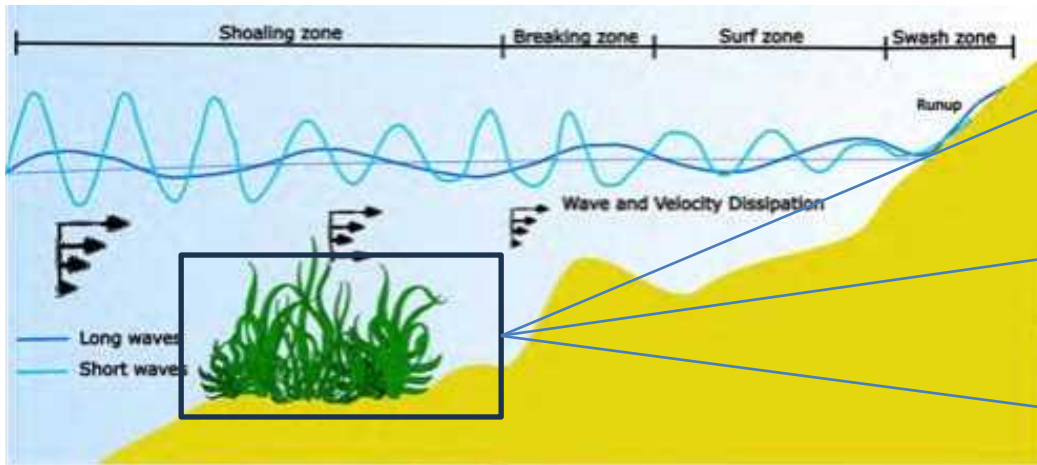
An example dynamic equilibrium state achieved in the experiments– Baldock et. Al 2017

Key expected outputs

1. Long term morphological responses of beach profile to reach a state of equilibrium
2. Cyclical wave conditions and dynamic equilibrium

VII Vegetation Implementation in the IH2VOF-SED model

1. Existing implementation by Maria Maza et.al 2013 will be modified and implemented within the IH2VOF-SED model
2. Existing implementation have provision for only implementing vegetation in defined rectangular shape horizontally
3. Provision will be made to include vegetation as complex orientations and geometries



Plan motion is solved by Morrison equation

Additional Drag force term in the governing RANS equation

Additional terms in k-Epsilon model

$$\bar{F}_{Dj} = \frac{1}{2} \cdot C_D \cdot \alpha \cdot N \cdot \bar{u}_{rel,j} \cdot |\bar{u}_{rel,j}|$$

Drag force consideration in RANS equation

$$\frac{\partial u_i}{\partial t} + \bar{u}_j \frac{\partial u_i}{\partial x_j} = -\frac{1}{\rho} \frac{\partial p}{\partial x_i} + g_i + \frac{1}{\rho} \frac{\partial \tau_{ij}}{\partial x_j} - \frac{\partial (\overline{u'_i u'_j})}{\partial x_j} - \bar{F}_{Dj}$$

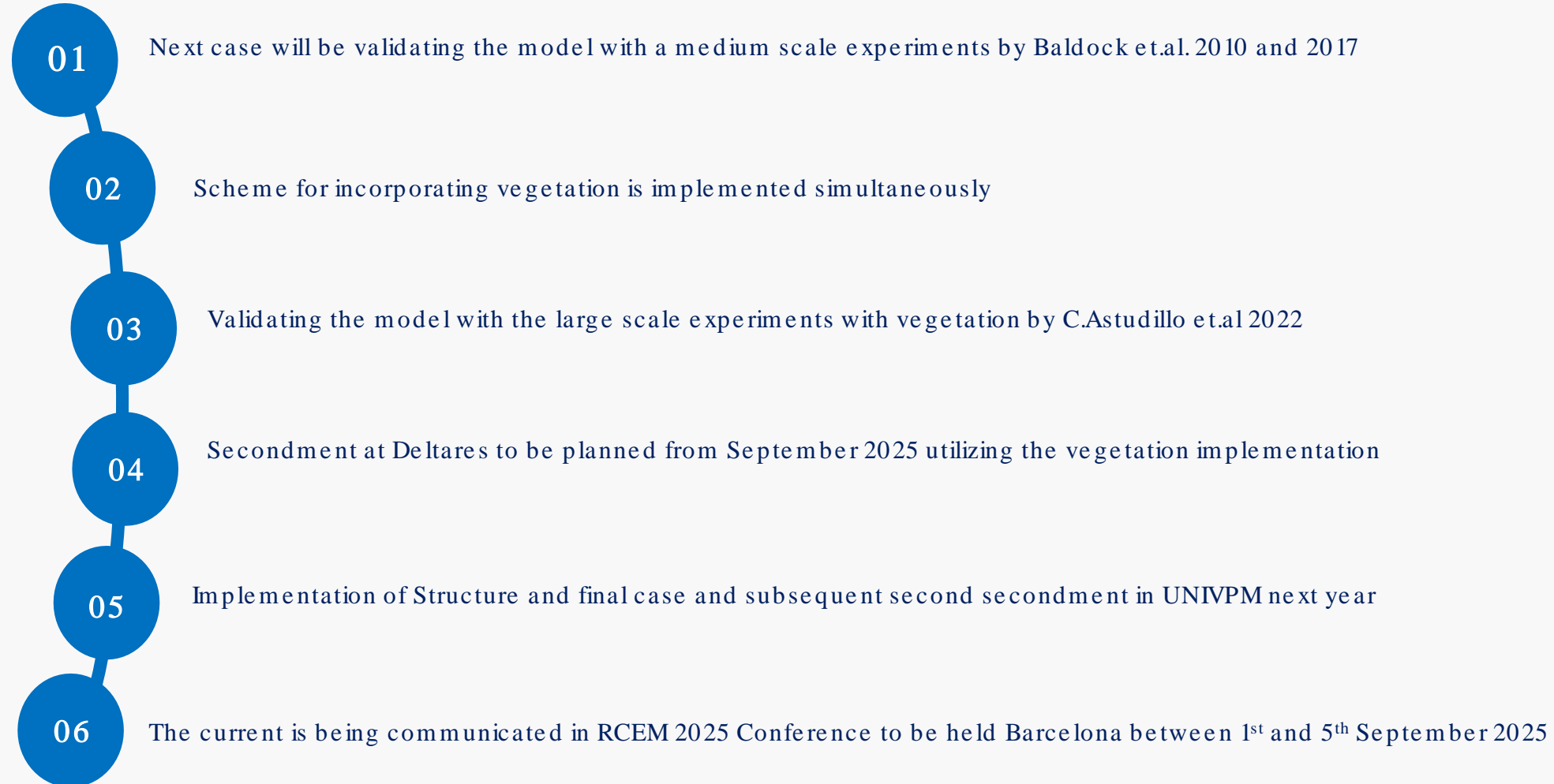
$$\begin{aligned} &+ \underbrace{\rho C_{kp} C_D \alpha N \sqrt{\bar{u}_{rel,j} \bar{u}_{rel,j}} k}_{\epsilon_k} \\ &+ \underbrace{\rho C_{\epsilon p} C_D \alpha N \sqrt{\bar{u}_{rel,j} \bar{u}_{rel,j}} \epsilon}_{\epsilon_{\epsilon}} \end{aligned}$$

Dispersive stresses consideration in K-ε model

$$\begin{aligned} m_0 \frac{\partial^2 \xi_i}{\partial t^2} + C \frac{\partial \xi_i}{\partial t} + \left(EI \frac{\partial^4 \xi_i}{\partial z^4} \right) = \\ - \frac{1}{2} \cdot \rho \cdot C_D \cdot \alpha \cdot \left(\bar{u} - \frac{\partial \xi_i}{\partial t} \right) \cdot \left| \bar{u} - \frac{\partial \xi_i}{\partial t} \right| + (\rho_s - \rho) g \cdot V_p \frac{\partial \xi_i}{\partial z} + \rho \cdot V_p \cdot \frac{\partial \bar{u}}{\partial t} + \rho \cdot C_m \cdot V_p \cdot \left(\frac{\partial \bar{u}}{\partial t} - \frac{\partial^2 \xi_i}{\partial t^2} \right) \end{aligned}$$

Morrison equation for plant motion

VIII What's Next





Thank you !

References

1. Astudillo, C., Gracia, V., Cáceres, I., Sierra, J. P., & Sánchez-Arcilla, A. (2022). Beach profile changes induced by surrogate *Posidonia Oceanica*: Laboratory experiments. *Coastal Engineering*, 175. <https://doi.org/10.1016/j.coastaleng.2022.104144>
2. Astudillo-Gutierrez, C., Gracia, V., Cáceres, I., Sierra, J. P., & Sánchez-Arcilla, A. (2024). Influence of seagrass meadow length on beach morphodynamics: An experimental study. *Science of the Total Environment*, 921. <https://doi.org/10.1016/j.scitotenv.2024.170888>
3. García-Maribona, J., Lara, J. L., Maza, M., & Losada, I. J. (2021). An efficient RANS numerical model for cross-shore beach processes under erosive conditions. *Coastal Engineering*, 170. <https://doi.org/10.1016/j.coastaleng.2021.103975>
4. García-Maribona, J., Lara, J. L., Maza, M., & Losada, I. J. (2022). Analysis of the mechanics of breaker bar generation in cross-shore beach profiles based on numerical modelling. *Coastal Engineering*, 177. <https://doi.org/10.1016/j.coastaleng.2022.104172>
5. Grossmann, F., Hurther, D., Sánchez-Arcilla, A., & Alsina, J. M. (2023). Influence of the Initial Beach Profile on the Sediment Transport Processes During Post-Storm Onshore Bar Migration. *Journal of Geophysical Research: Oceans*, 128(4). <https://doi.org/10.1029/2022JC019299>
6. Lara, J. L., Losada, I. J., & Guanche, R. (2008). Wave interaction with low-mound breakwaters using a RANS model. *Ocean Engineering*, 35(13), 1388–1400. <https://doi.org/10.1016/j.oceaneng.2008.05.006>
7. Lara, J. L., Ruju, A., & Losada, I. J. (2011). Reynolds averaged Navier-Stokes modelling of long waves induced by a transient wave group on a beach. *Proceedings of the Royal Society A: Mathematical, Physical and Engineering Sciences*, 467(2129), 1215–1242. <https://doi.org/10.1098/rspa.2010.0331>
8. Maza, M., Lara, J. L., & Losada, I. J. (2013). A coupled model of submerged vegetation under oscillatory flow using Navier-Stokes equations. *Coastal Engineering*, 80, 16–34. <https://doi.org/10.1016/j.coastaleng.2013.04.009>
9. Roulund, A., Sumer, B. M., Fredsøe, J., & Michelsen, J. (2005). Numerical and experimental investigation of flow and scour around a circular pile. *Journal of Fluid Mechanics*, 534, 351–401. <https://doi.org/10.1017/S0022112005004507>
10. Streicher, M. ; Kortenhaus, A. ; Altomare, C. ; Gruwez, V. ; Hofland, B. ; Chen, X. ; Marinov, K. ; Scheres, B. ; Schüttrumpf, H. ; Hirt, M., Cappiotti, L., Esposito, A., Saponieri, A., Valentini, N., Tripepi, G., Pasqualini, D., Di Risio, M., Aristodemio, F., Damiani, L., & Kaste, . . (2017). (Wave Loads on Walls) Large-Scale Experiments in the Delta Flume.

Initiation of motion for sand-mud bed types

Jowi Miranda

SEDIMARE

 jowi.miranda@deltares.nl
p.s.miranda@utwente.nl

 psmiranda

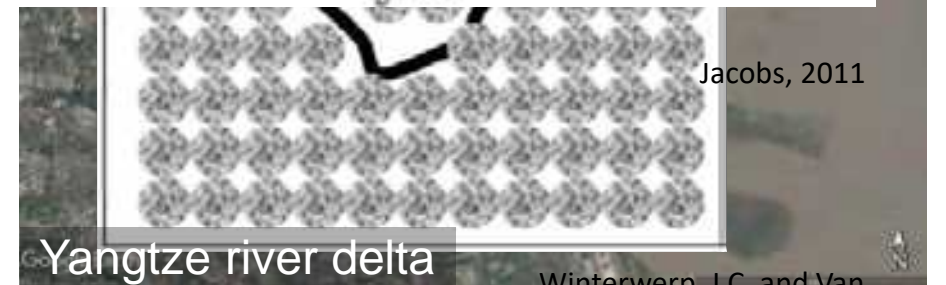
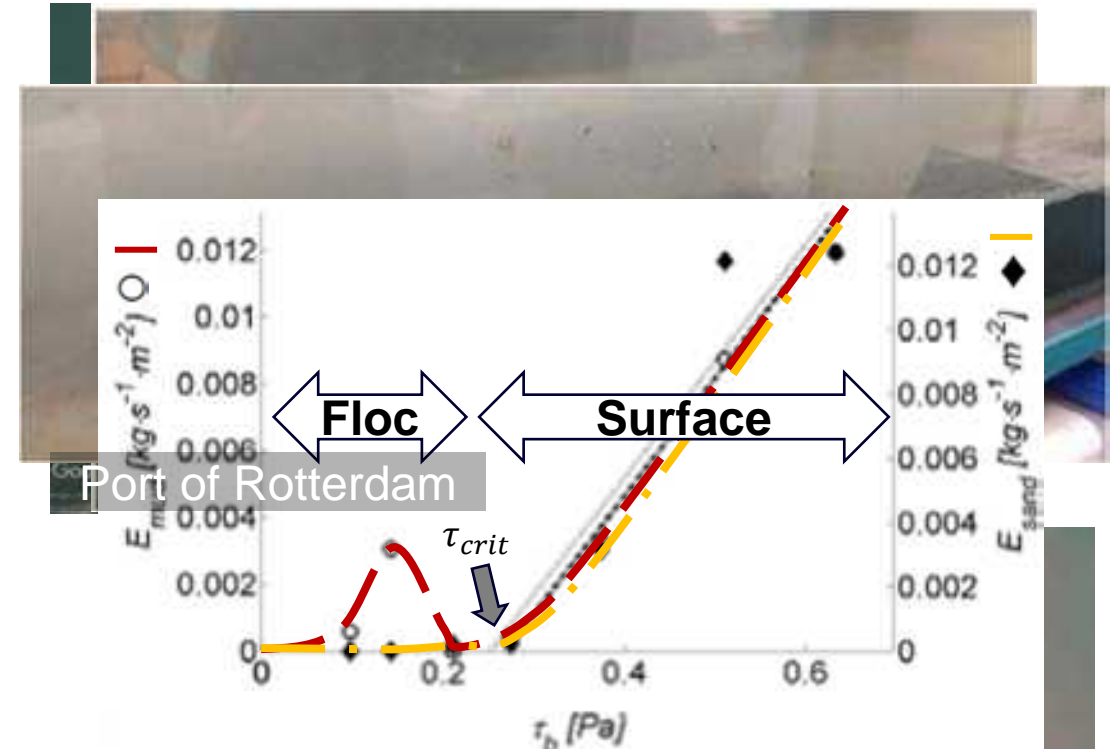
Outline

- **Sand-mud erosion and initiation of motion**
 - Study objectives
- **Data and framework selection**
- **Compiled dataset**
- **Bed type classification**
- **Conclusions**

Sand-mud erosion

- Sand erosion
- Mud erosion
 - Floc erosion
 - Surface erosion
 - Mass erosion
- Estimating sand-mud erosion requires a definition for initiation of motion for both sand and mud
 - E [$\text{kg}/(\text{m}^2\text{s})$] vs τ_b (Pa)
 - Definition of τ_{crit}
- **Determining τ_{crit}** during erosion experiments remains **subjective**

van Rijn, 2020



Jacobs, 2011

Winterwerp, J.C. and Van Kesteren, W.G.M. 2004

Sand-mud erosion

- Current estimation methods for initiation of motion are a function of bulk geotechnical parameters:
 - Bulk or dry density, ρ_{bulk} or ρ_{dry}
 - Median grain size diameter, D_{50}
 - Mass fraction of mud or silt, P_{mud} or P_{silt}

Mitchener & Torfs, 1996

$$\tau_{cr} = 0.015(\rho_b - 1000)^{0.73}$$

Van Rijn, 2007

$$\tau_{cr} = \begin{cases} (1 + P_{clay})^3 \tau_{cr,0} & : d \geq 62\mu m \\ \left(\frac{c_{gel}}{c_{gel,s}}\right) \left(\frac{d_{sand}}{d_{50}}\right)^\gamma \tau_{cr,0} & : d < 62\mu m \end{cases}$$

Wu et al., 2018

$$\tau_{cr} = \begin{cases} 1.25 P_{mud} (\tau_{cr,0} - \tau_{cr,mud}) + \tau_{cr,mud} & P_{mud} < 5\% \\ \tau_{cr,L} + (\tau_{cr,0} - \tau_{cr,L}) \exp \left[-\alpha \left(\frac{P_{sand}}{P_{mud}} \right)^\beta \right] & 0 < P_{mud} < 100\% \\ 10.29 r^{1.7} & \text{Pure mud} \end{cases}$$

Yao et al., 2022

$$\tau_{cr} = \begin{cases} \tau_{cr,0} & : P_{silt} \leq 35\% \\ (1 + \beta_{ss}) \tau_{cr,0} & : P_{silt} > 35\% \end{cases}$$

Study objectives

1. To combine results of sand-mud erosion experiments that used **wide variations in clay-silt ratios**.
2. To examine a framework that highlights the **contribution of each sediment fraction (i.e. sand, silt, clay)** in the initiation of motion process.

Data selection

- Sediment sizes and cohesive properties
- Reported geotechnical parameters
- Flow type
- Calculation of bed shear stress
- Determination of critical bed shear stress

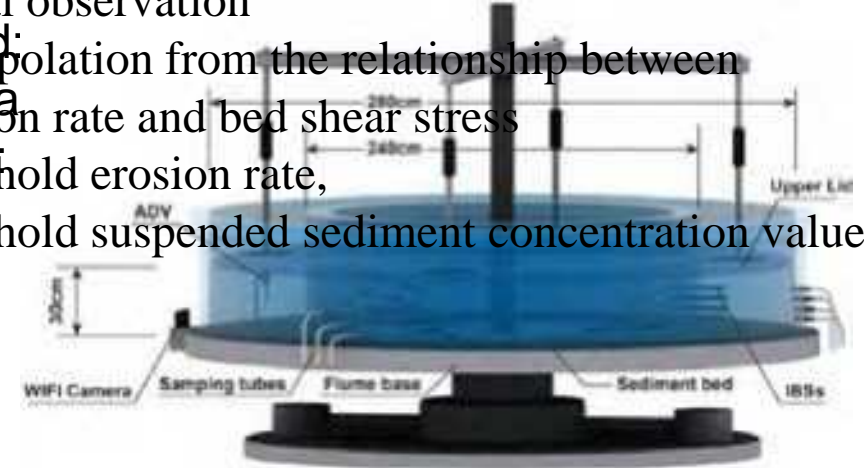


Calculating bed shear stress, τ_b :

- from law of the wall velocity profiles
- from the measured near-bed turbulence

Calculating critical bed shear stress, τ_{crit} :

- visual observation
- Sand: extrapolation from the relationship between erosion rate and bed shear stress
- Silt: a threshold erosion rate,
- Clay: threshold suspended sediment concentration value

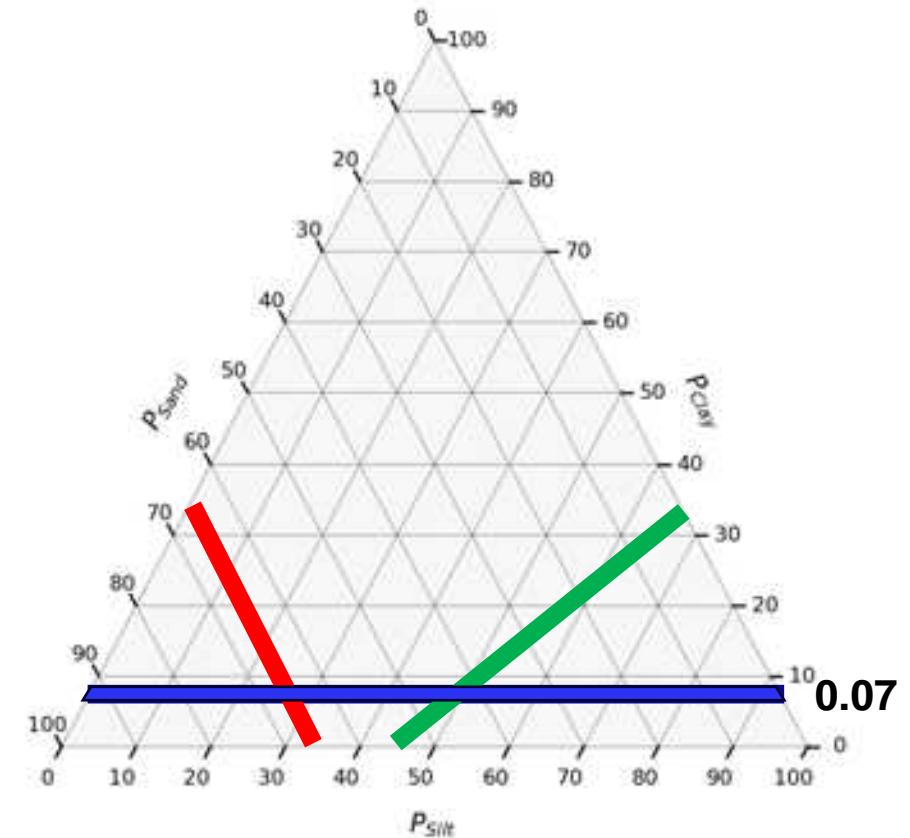


Yao, et al., 2022

Annular flume

Framework selection

- Van Leiden bed types (Van Ledden et al., 2003)
 - Based on mass fraction of clay
 - Literature suggests a lower limit of 5-10%
 - Framework characteristic
 1. Cohesion
 2. Network structure



Mass fractions:

$$1 = P_{sand} + P_{silt} + P_{clay} = P_{sand} + P_{mud}$$

Volume fractions:

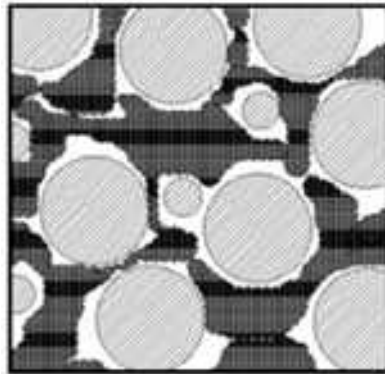
$$1 = \phi_{sand} + \phi_{silt} + \phi_{clay} + \phi_{water}$$

Framework selection

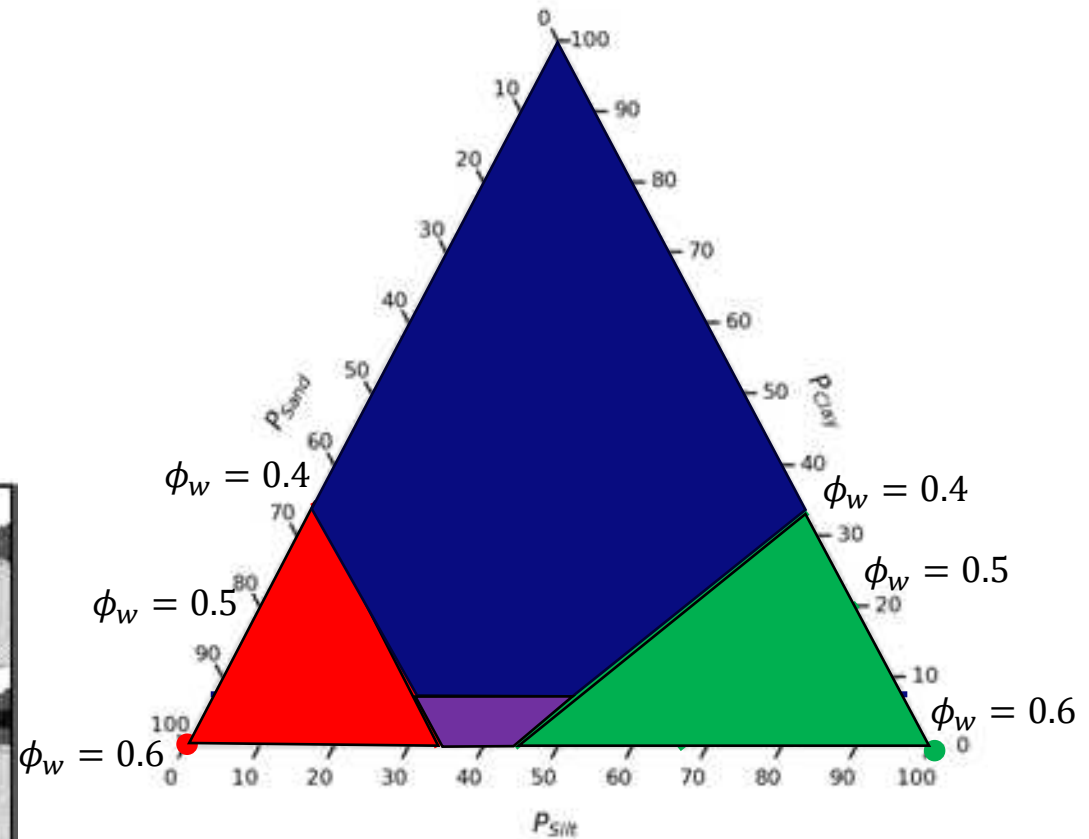
- Network structure
 - Interaction of sediment particles and volume fraction of water, ϕ_{water} .
 - Sand-dominated network structure:

$$\phi_{sand} \geq 40\%$$
 - Silt-dominated network structure:

$$\frac{\phi_{silt}}{(1 - \phi_{sand})} \geq 40\%$$
 - Other network structures:
 1. Clay-water matrix
 2. Mixed structures



Jacobs, 2011



Mass fractions:

$$1 = P_{sand} + P_{silt} + P_{clay} = P_{sand} + P_{mud}$$

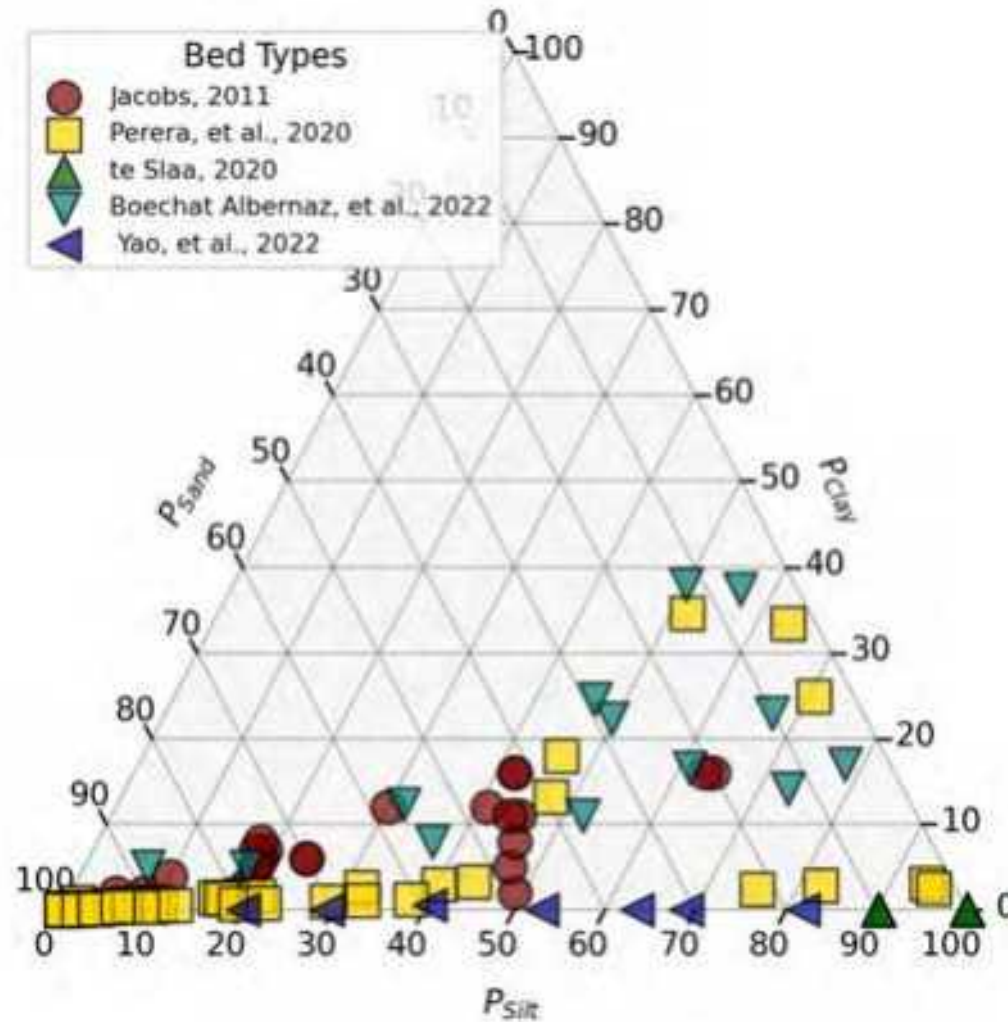
Volume fractions:

$$1 = \phi_{sand} + \phi_{silt} + \phi_{clay} + \phi_{water}$$

Framework selection

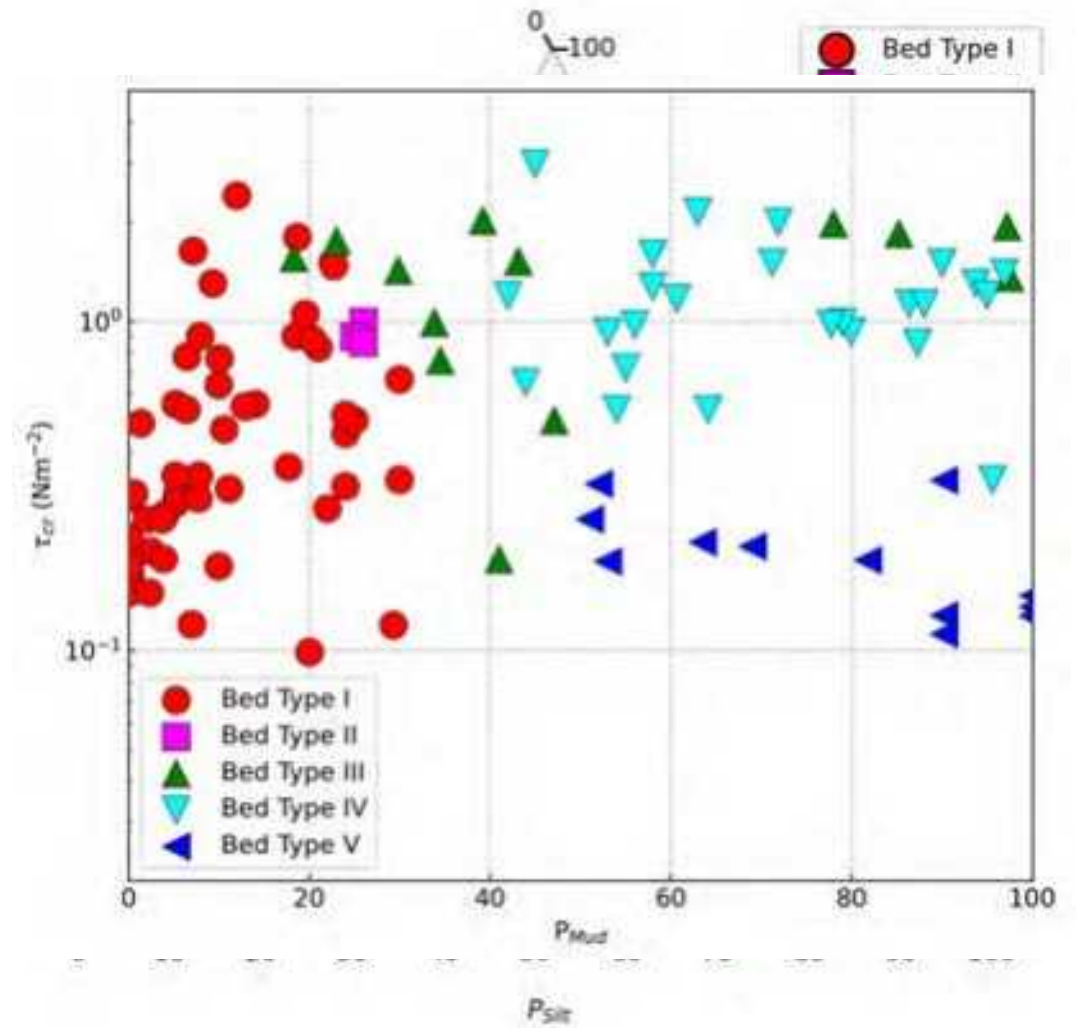
Van Ledden bed types		Cohesion	
		Non-cohesive ($P_{clay} < 7\%$)	Cohesive ($P_{clay} \geq 7\%$)
Network Structure	Sand $\phi_{sand} \geq 40 - 50\%$	Type 1: Sand-dominated, non-cohesive sediment bed I. Sand-dominated non-cohesive	Type 2: Sand-dominated, cohesive sediment bed II. Sand-dominated cohesive
	Silt $\frac{\phi_{silt}}{(1 - \phi_{sand})} \geq 40 - 50\%$	Type 5: III. Mixed structure Silt-dominated, clay-water matrix, cohesive sediment bed V. Silt-dominated non-cohesive	Type 6: IV. Mixed structure Silt-dominated, cohesive sediment bed VI. Silt-dominated cohesive
	Clay ϕ_{sand} AND $\frac{\phi_{silt}}{(1 - \phi_{sand})} < 40 - 50\%$	Type 3: Mixed structure, non-cohesive sediment bed	Type 4: Clay-water matrix, cohesive sediment bed

Compiled dataset



Bed type classification

- Classified dataset:
 - Sand-dominated, non-cohesive (I): **54**
 - Sand-dominated, cohesive (II): **3**
 - Mixed-structure, non-cohesive (III): **13**
 - Clay-water matrix, cohesive (IV): **25**
 - Silt-dominated, non-cohesive (V): **12**
 - Silt-dominated, cohesive (VI): **0**
- Behavior per bed type:
 - Median grain size, d_{50}
 - Mass fraction of mud, P_{mud}



Conclusions

- Built dataset with large spectrum of **sand-silt-clay combinations** and other **bulk geotechnical parameters**
- Classification into bed types
 - **Reduced complexity** within each bed from a physical basis
 - Bed types help **focus** research **on dominant parameters** in initiation of motion process

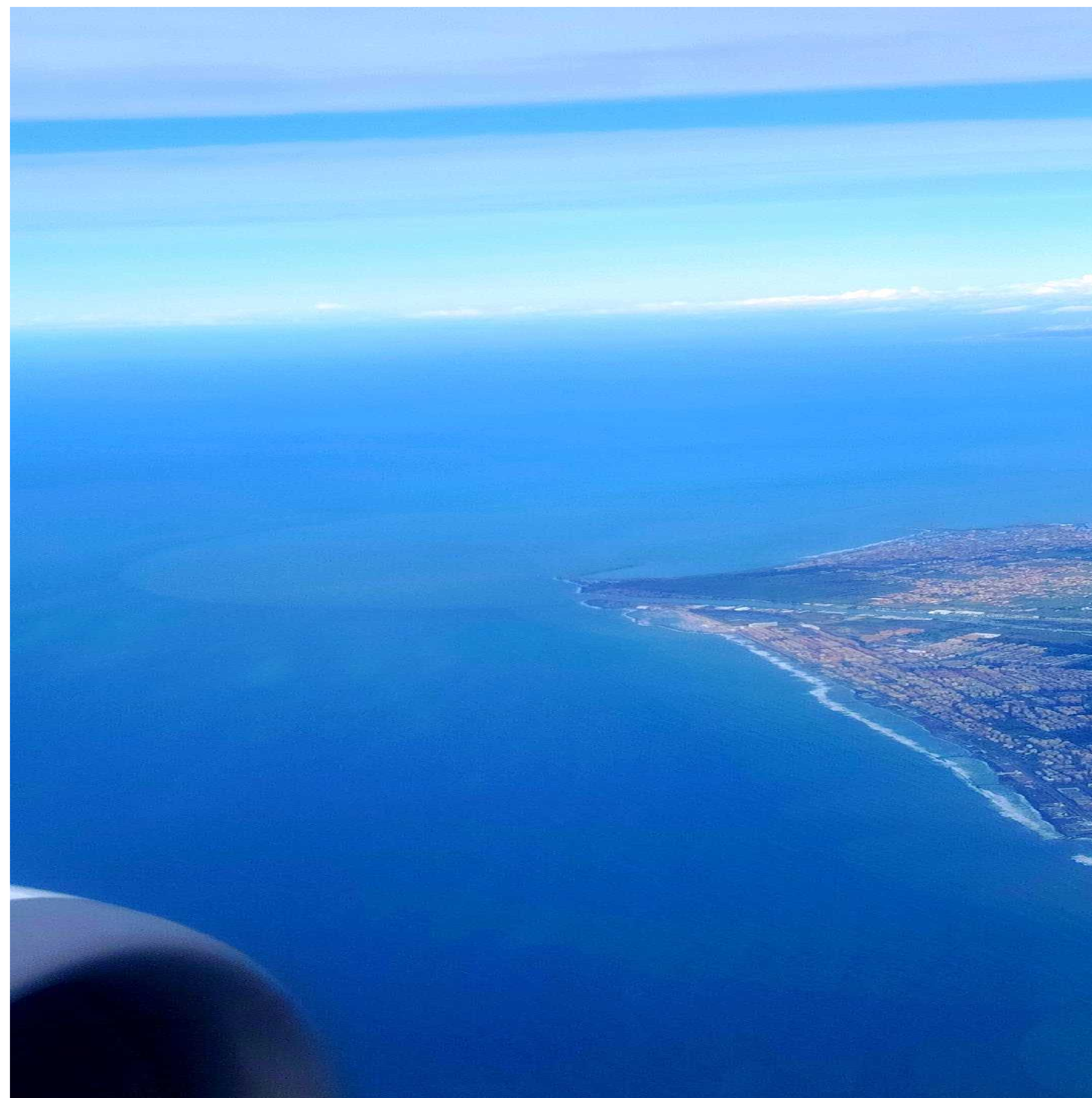
Initiation of motion for sand-mud bed types

Jowi Miranda

SEDIMARE

 jowi.miranda@deltares.nl
p.s.miranda@utwente.nl

 psmiranda

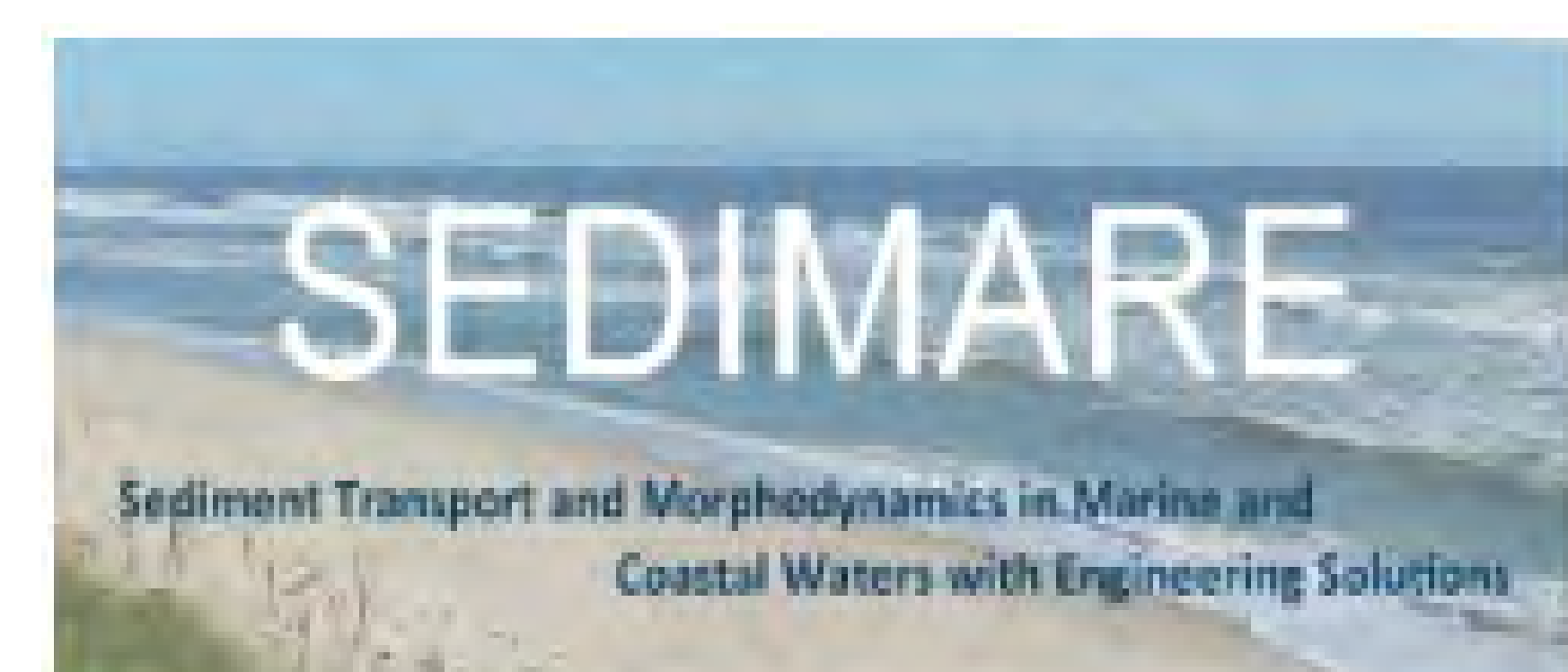


Nasim Soori

Supervisors:

Prof. Maurizio Brocchini – UNIVPM
Prof. Athanassios Dimas – UPATRAS
Prof. Matteo Postacchini – UNIVPM

DC 4: Mixing and transport in the coastal area



This project has received funding from the European Union's (EU) Horizon Europe Framework Programme (HORIZON) under Grant Agreement No 101072443 as a MSCA Doctoral Network (HORIZON-MSCA-0001-EN-01)



11 Mar., 2025, IHCantabria- Spain

1. Governing Equations

Calculate the position of each particle (x_p , y_p) over time using a discrete time-stepping approach based on velocity components

$$x_{p,n} = x_{p,n-1} + u_{p,n-1} \Delta t$$

$$y_{p,n} = y_{p,n-1} + v_{p,n-1} \Delta t$$

- ✓ u_p and v_p are velocity components at the particle's location,
- ✓ Δt is the time step.

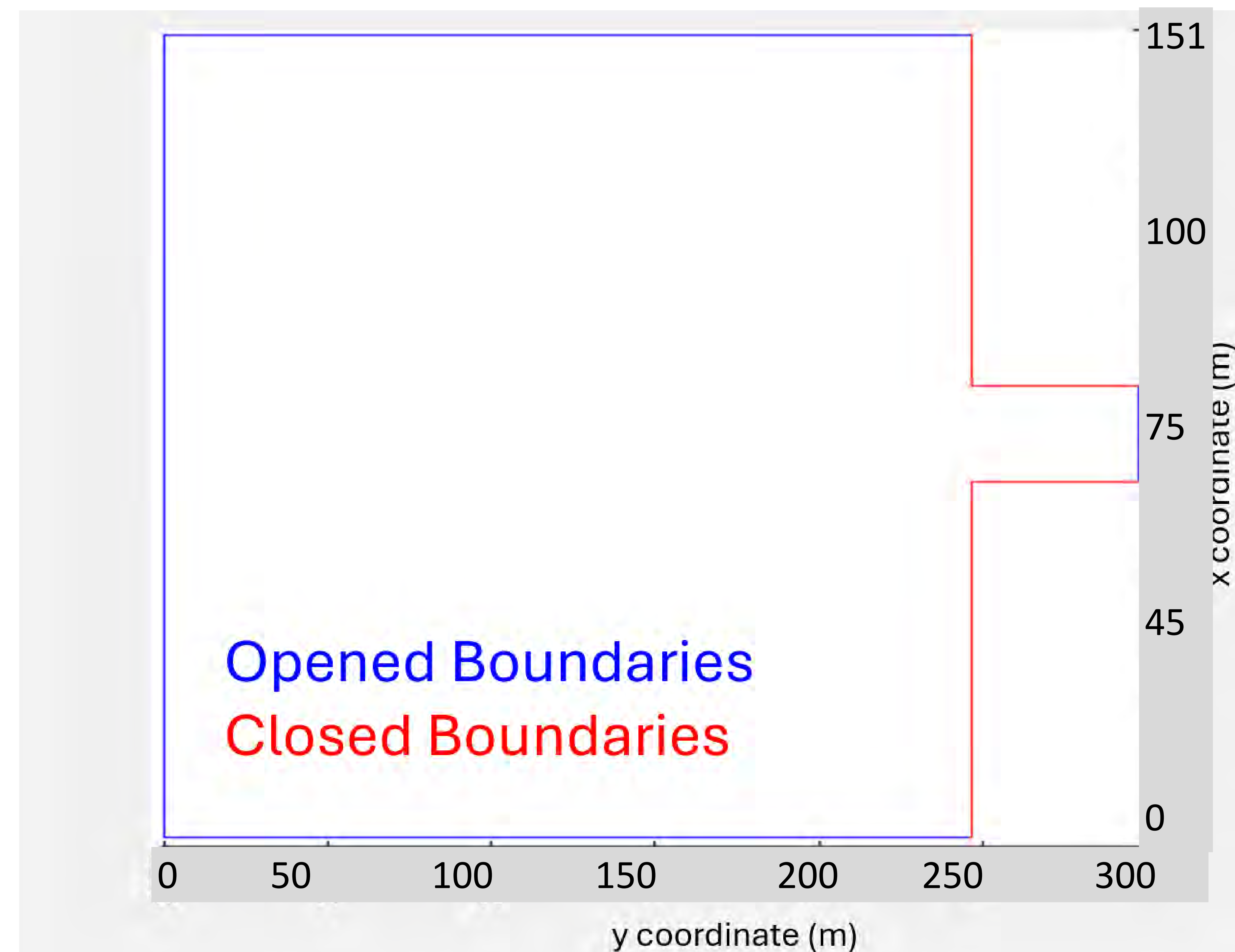
This method follows the **Lagrangian approach**, meaning we track individual particles as they move with the flow.

2. Boundary Conditions

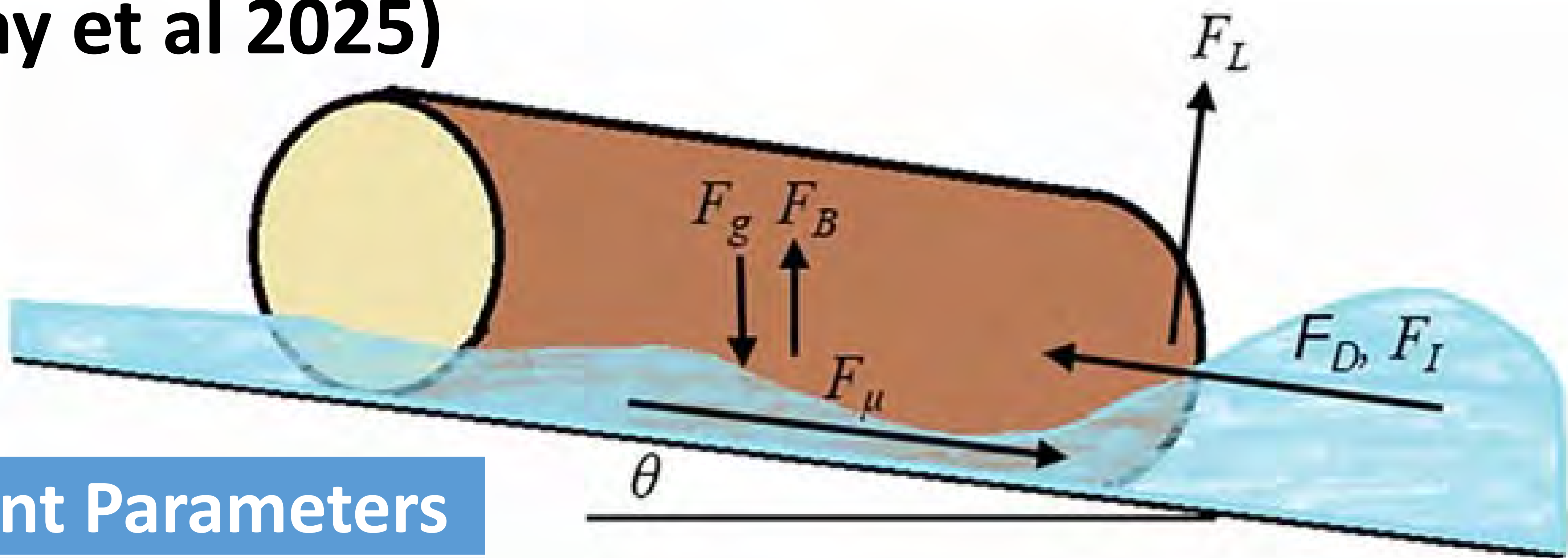
To ensure realistic movement:

- Inside the estuary:
- Outside the estuary:

If a particle hits the shoreline (y_p outside bounds), it reflects back within valid limits.



Forces acting on woods (Murphy et al 2025)



$$F_H = F_D + F_I$$

Forces	Formula	Dependent Parameters
Drag	$F_D = \frac{1}{2} \rho C_D D_p L_p U U \cos \alpha$	ρ_f, D_p, L_p, U
Inertia	$F_I = \frac{\pi}{4} \rho C_M D_p^2 L_p \frac{\partial U}{\partial t} \cos \alpha$	ρ_f, D_p, L_p, U
Lift	$F_L = \frac{1}{2} \rho C_L D_p L_p U U \cos \alpha$	ρ_f, D_p, L_p, U

CD=drag coefficient;
CM=inertia coefficient;
U=local velocity (including the wave induced current);
α=angle between the local velocity vector and the long axis of the driftwood.
CL=lift coefficient

The displacement of each particle:

$$\frac{dX_p}{dt} = Adv + Disp$$

$$✓ Adv = U_p \qquad U_p = U(x, y, z, t)$$

$$✓ Disp = \frac{R}{\Delta t} \sqrt{2K\Delta t}$$

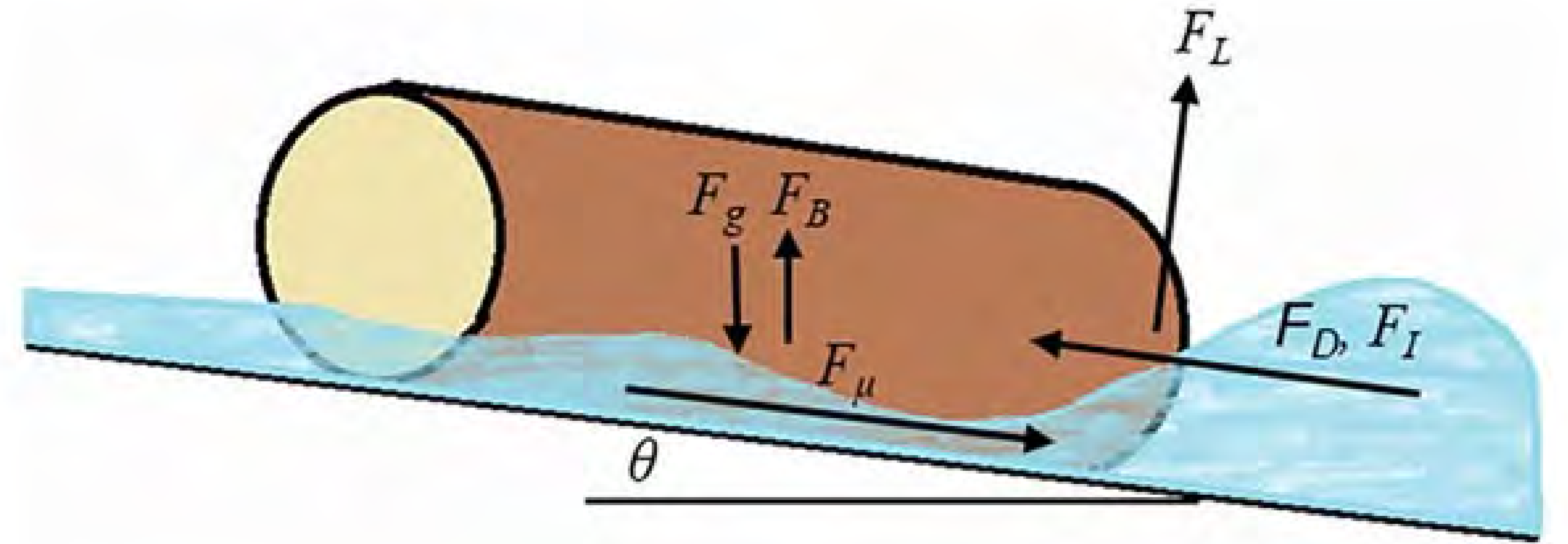
- U_p* : The deterministic component is based on the Eulerian flow field (fluid velocity),
- R* : Random number from a normal distribution,
- K* : Eddy diffusivity or dispersion coefficient from the hydrodynamic model,
- Δt* : Time step

■ In WOODRIFTSIM, *U_p* is calculated as:

$$u_p = u(x_p, y_p, t) , v_p = v(x_p, y_p, t) , w_p = 0$$

- ✓ *u* and *v* are the fluid velocity components interpolated from the hydrodynamic model at the particle location.
- ✓ *w_p*=0 because driftwood is assumed buoyant and remains at the water surface.

- ✓ F_μ acts in the opposing direction to the resultant destabilizing force parallel to the bed, which is **the sum of the inline (drag and inertia) forces** and the net buoyancy/gravitational component parallel to the bed: $(F_D + F_I + (F_g - F_B)\sin\theta)$.



Forces	Formula
Friction	$F_\mu = \mu F_N$ $F_N = (F_g - F_B) \cos \theta - F_L$
Lift	$F_L = \frac{1}{2} \rho C_L D_p L_p U U \cos \alpha$
Buoyancy	$F_B = \rho g A_s L_p$

θ = bed slope in the direction of in-line forces acting on the driftwood,
 μ = a coefficient of (static or dynamic) friction.

- The **stabilizing frictional force** mobilized at the sloping bed is **the product of the normal force at the wood–bed interface, F_N** .

□ Condition:

- ✓ If $|F_\mu| \geq |F_D + F_I + (F_g - F_B)\sin\theta|$, the driftwood is beached and stationary; all associated particles retain their positions at the next time step.
- ✓ If $|F_\mu| < |F_D + F_I + (F_g - F_B)\sin\theta|$ and $|F_D + F_I| > |(F_g - F_B)\sin\theta|$, contact with the bed does not result in beaching, wave-driven hydrodynamics, control driftwood motion, and particles are advected and dispersed.
- ✓ If $|F_\mu| < |F_D + F_I + (F_g - F_B)\sin\theta|$ and $|F_D + F_I| \leq |(F_g - F_B)\sin\theta|$, the beached driftwood motion is controlled by gravity (i.e., sliding or rolling), and particles are translated at a velocity determined by the resultant net force and Newton's second law :

$$U_p = \frac{|(F_g - F_B)\sin\theta| \pm |F_D + F_I| - |F_\mu|}{\rho_D \frac{\pi D_p^2}{4} L_p}$$

- The particle displacement over one time-step is:

$$x_{p,n} = x_{p,n-1} + u_{p,n-1}\Delta t$$

$$y_{p,n} = y_{p,n-1} + v_{p,n-1}\Delta t$$

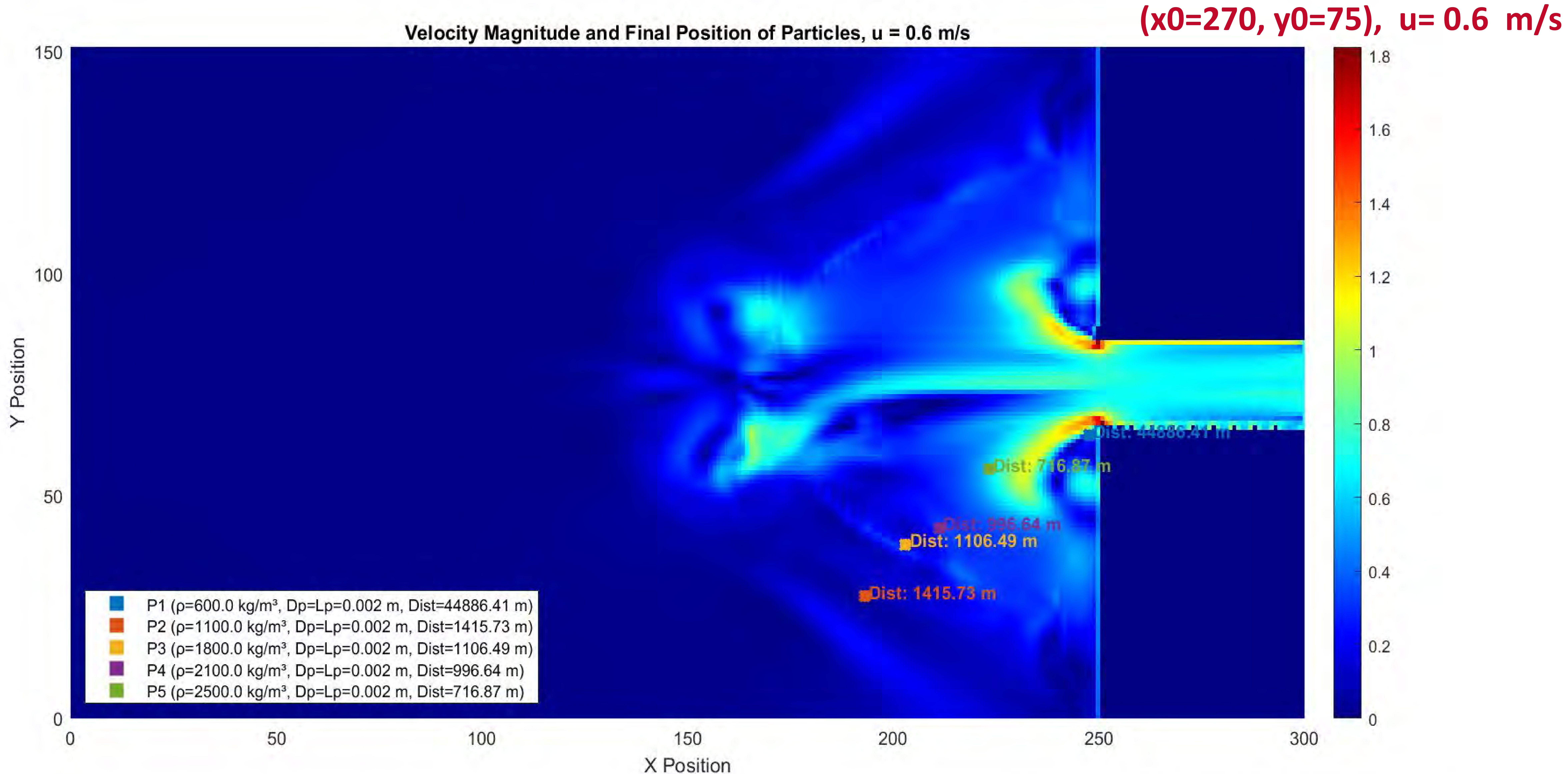
$$z_{p,n} = z_{p,n-1} + w_{p,n-1}\Delta t$$

Number of particles = 5

density (kg/m^3) $\rho_{\text{(wood)}}$ = [600, 1100, 1800, 2100, 2500];

diameter (m), D_p = [0.002, 0.002, 0.002, 0.002, 0.002];

length (m), L_p = [0.002, 0.002, 0.002, 0.002, 0.002];



Total Distance Traveled by Each Particle (Sorted: Most to Least):

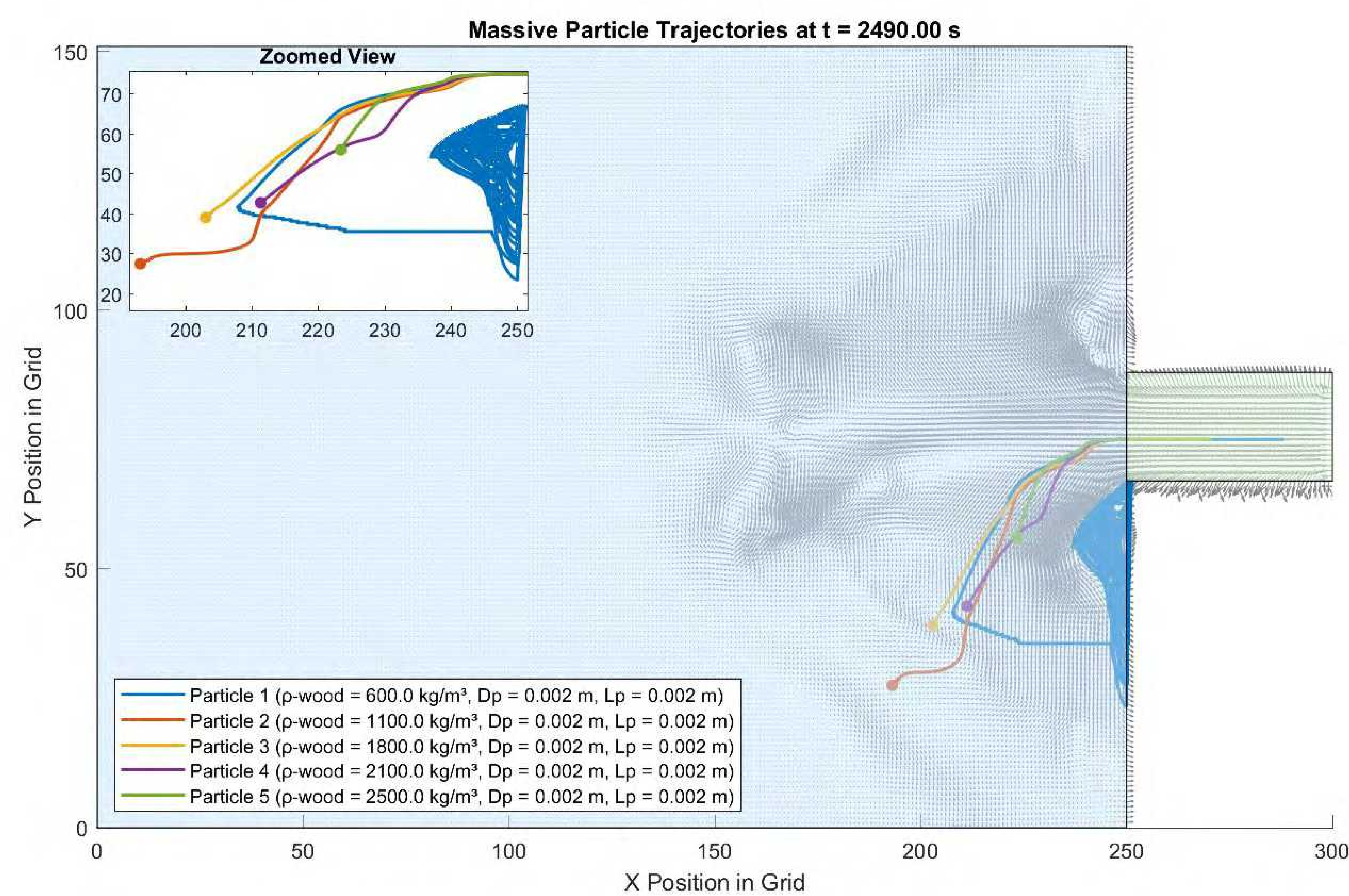
Particle 1 ($\rho_{\text{(wood)}} = 600.0 \text{ kg/m}^3$, $D_p = L_p = 0.002 \text{ m}$): 44886.41 m

Particle 2 ($\rho_{\text{(wood)}} = 1100.0 \text{ kg/m}^3$, $D_p = L_p = 0.002 \text{ m}$): 1415.73 m

Particle 3 ($\rho_{\text{(wood)}} = 1800.0 \text{ kg/m}^3$, $D_p = L_p = 0.002 \text{ m}$): 1106.49 m

Particle 4 ($\rho_{\text{(wood)}} = 2100.0 \text{ kg/m}^3$, $D_p = L_p = 0.002 \text{ m}$): 996.64 m

Particle 5 ($\rho_{\text{(wood)}} = 2500.0 \text{ kg/m}^3$, $D_p = L_p = 0.002 \text{ m}$): 716.87 m

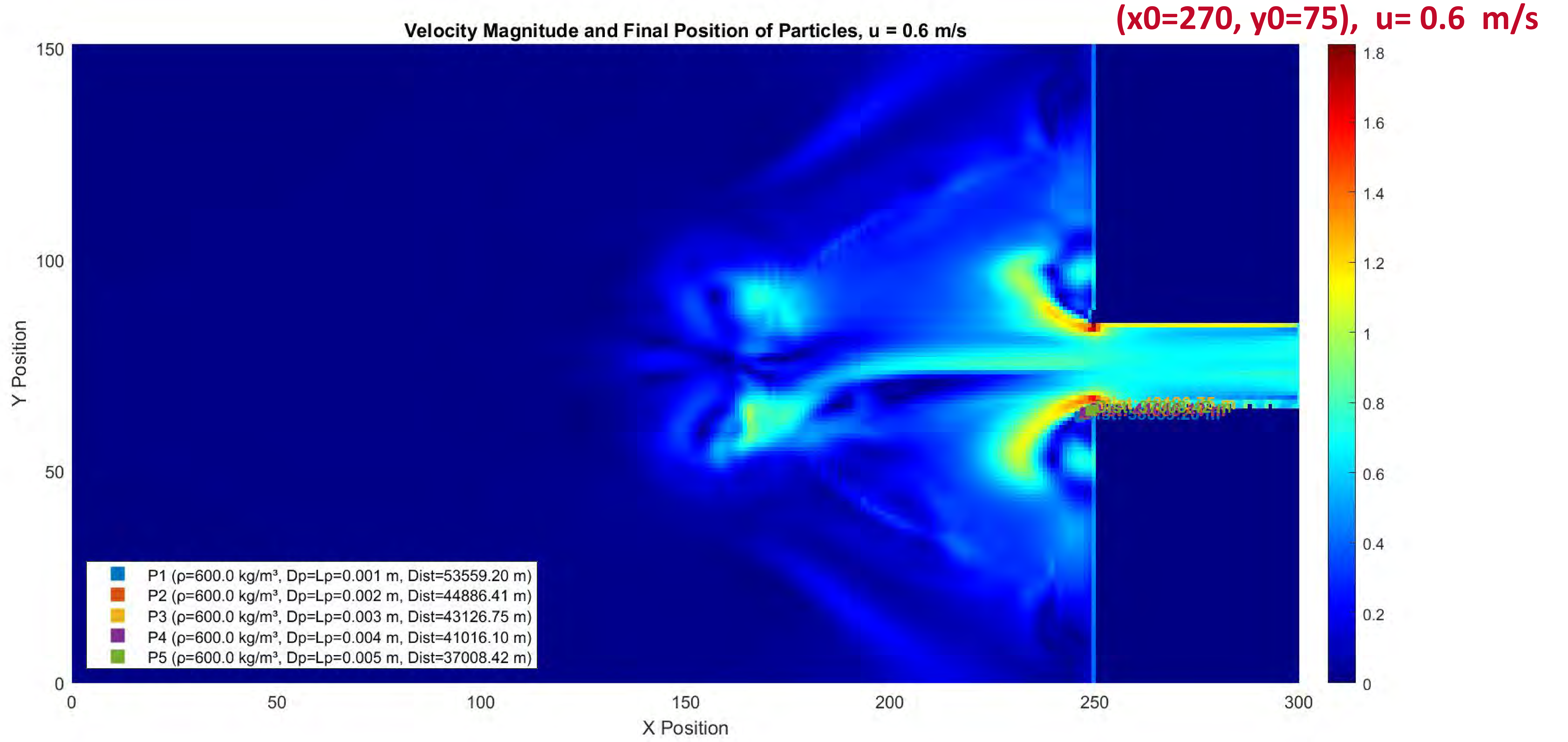


Number of particles = 5

density (kg/m^3) $\rho_{\text{(wood)}} = [600, 600, 600, 600, 600]$; less than water density

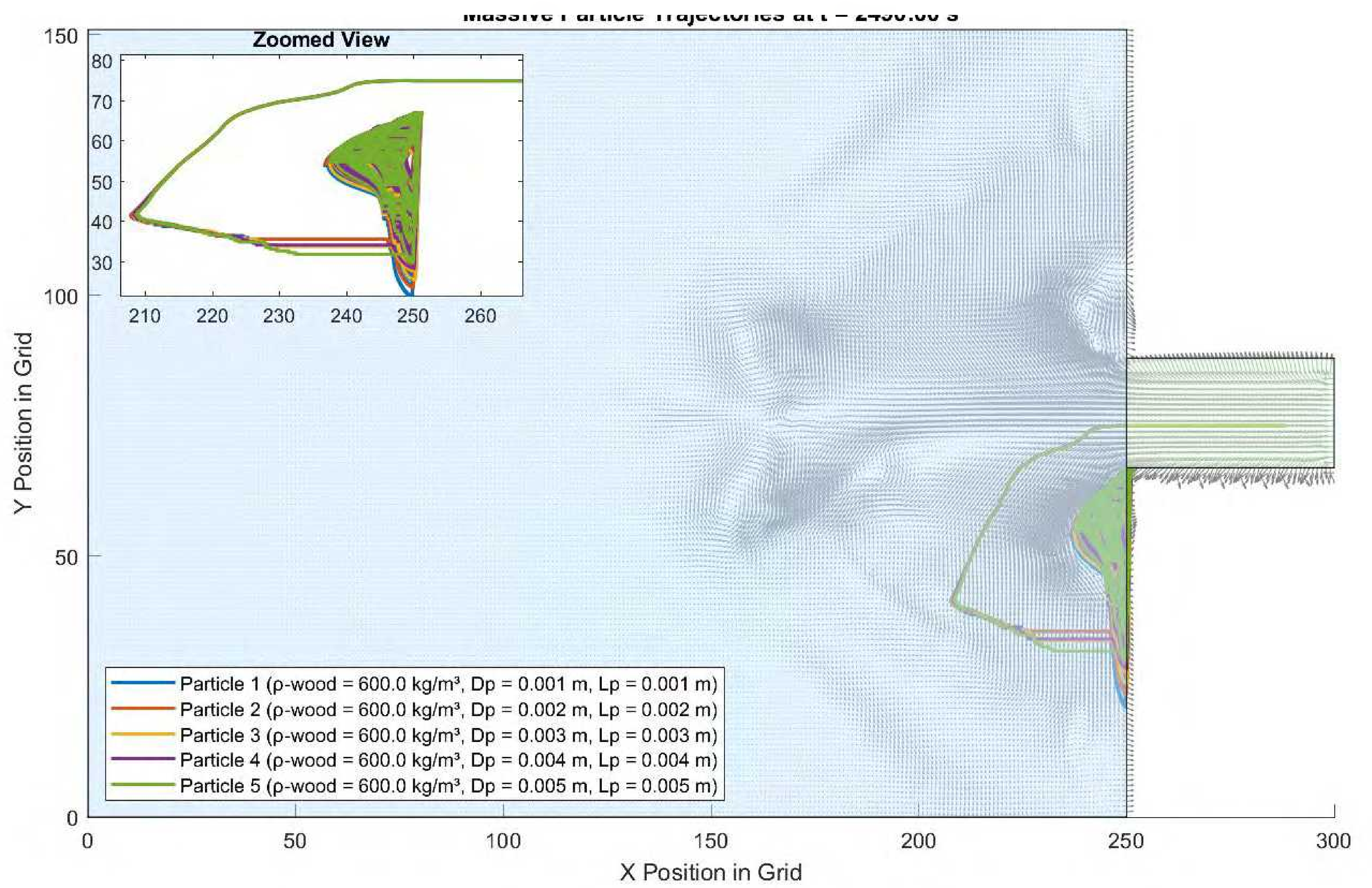
diameter (m), $D_p = [0.001, 0.002, 0.003, 0.004, 0.005]$;

length (m), $L_p = [0.001, 0.002, 0.003, 0.004, 0.005]$;



Total Distance Traveled by Each Particle (Sorted: Most to Least):

- Particle 1** ($\rho_{\text{(wood)}} = 600.0 \text{ kg/m}^3$, $D_p = L_p = 0.001 \text{ m}$): 53559.20 m
- Particle 2** ($\rho_{\text{(wood)}} = 600.0 \text{ kg/m}^3$, $D_p = L_p = 0.002 \text{ m}$): 44886.41 m
- Particle 3** ($\rho_{\text{(wood)}} = 600.0 \text{ kg/m}^3$, $D_p = L_p = 0.003 \text{ m}$): 43126.75 m
- Particle 4** ($\rho_{\text{(wood)}} = 600.0 \text{ kg/m}^3$, $D_p = L_p = 0.004 \text{ m}$): 41016.10 m
- Particle 5** ($\rho_{\text{(wood)}} = 600.0 \text{ kg/m}^3$, $D_p = L_p = 0.005 \text{ m}$): 37008.42 m



Number of particles = 5

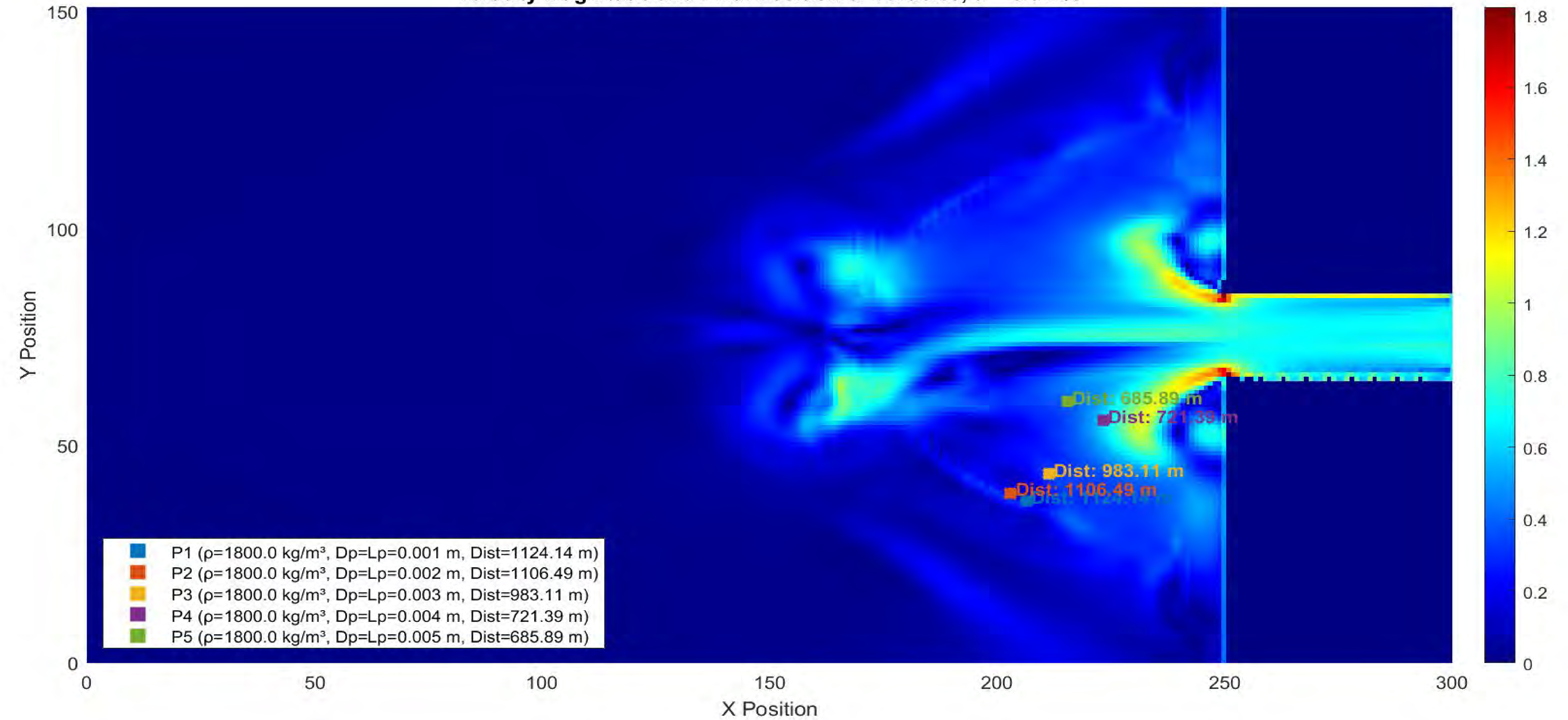
density (kg/m^3) $\rho_{\text{(wood)}} = [1800, 1800, 1800, 1800, 1800]$; more than water density

diameter (m), $D_p = [0.001, 0.002, 0.003, 0.004, 0.005]$;

length (m), $L_p = [0.001, 0.002, 0.003, 0.004, 0.005]$;

(x0=270, y0=75), u= 0.6 m/s

Velocity Magnitude and Final Position of Particles, u = 0.6 m/s



Total Distance Traveled by Each Particle (Sorted: Most to Least):

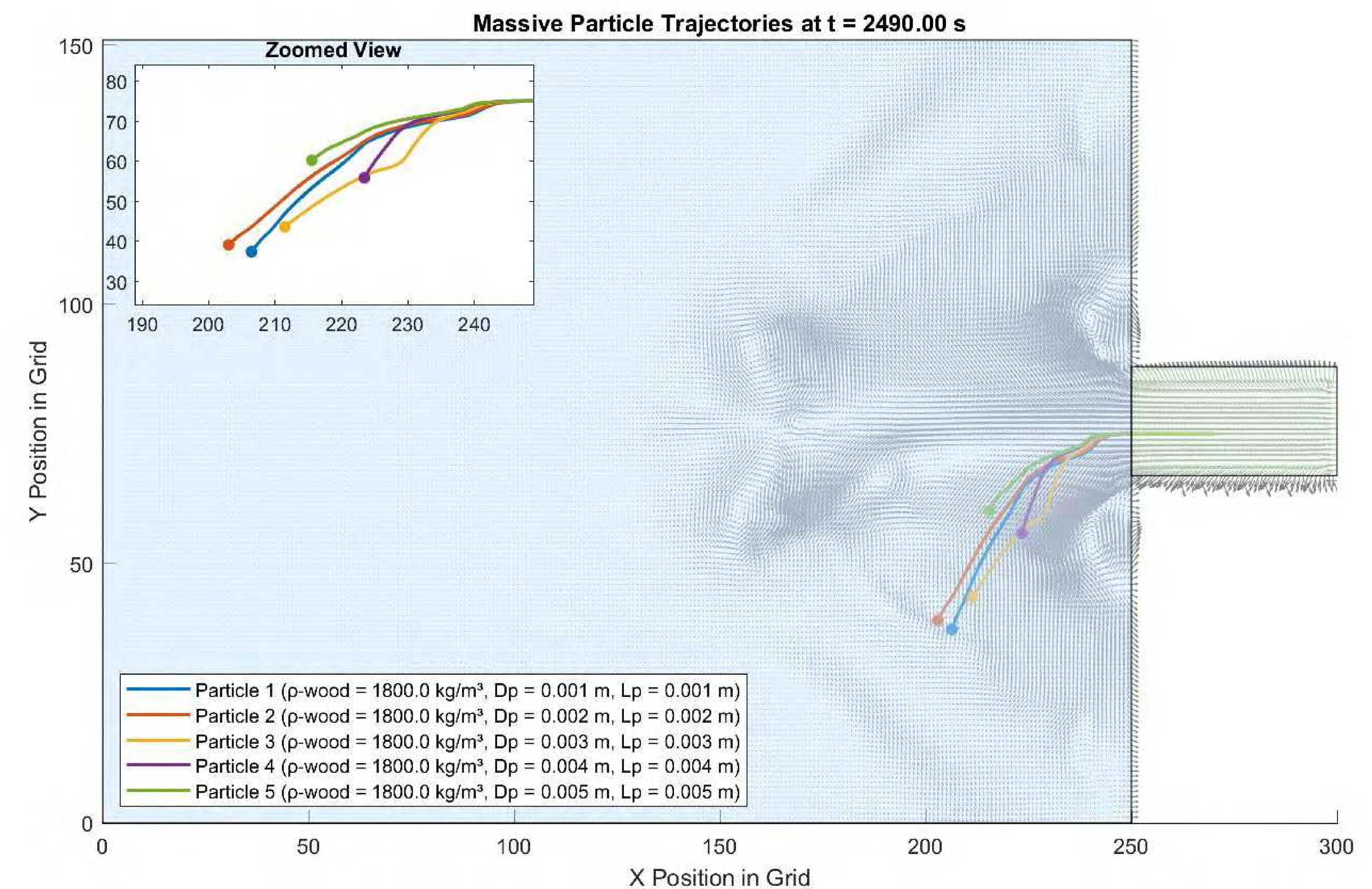
Particle 1 ($\rho_{\text{(wood)}} = 1800.0 \text{ kg/m}^3$, $D_p = L_p = 0.001 \text{ m}$): 1124.14 m

Particle 2 ($\rho_{\text{(wood)}} = 1800.0 \text{ kg/m}^3$, $D_p = L_p = 0.002 \text{ m}$): 1106.49 m

Particle 3 ($\rho_{\text{(wood)}} = 1800.0 \text{ kg/m}^3$, $D_p = L_p = 0.003 \text{ m}$): 983.11 m

Particle 4 ($\rho_{\text{(wood)}} = 1800.0 \text{ kg/m}^3$, $D_p = L_p = 0.004 \text{ m}$): 721.39 m

Particle 5 ($\rho_{\text{(wood)}} = 1800.0 \text{ kg/m}^3$, $D_p = L_p = 0.005 \text{ m}$): 685.89 m



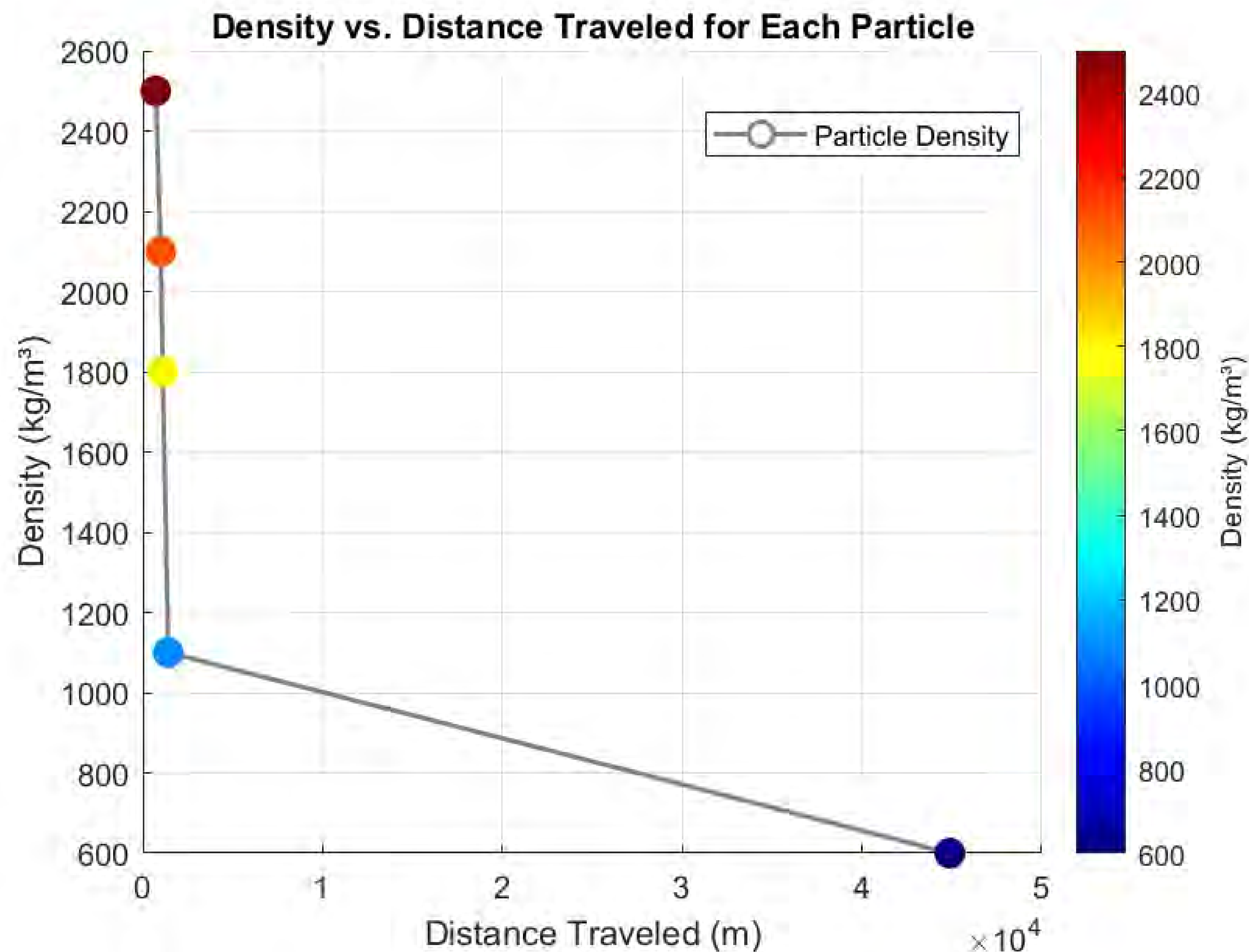
□ Effect of Changing Particle Density

- **Higher Density Particles:**

- o Experience stronger gravitational pull, leading to faster settling.
- o Have lower buoyancy forces, making them sink faster.
- o Travel shorter distances before settling at the bottom.

- **Lower Density Particles:**

- o Remain suspended longer due to higher buoyancy.
- o Travel farther as they are carried by currents before settling.
- o Are more influenced by turbulent flow and diffusion.



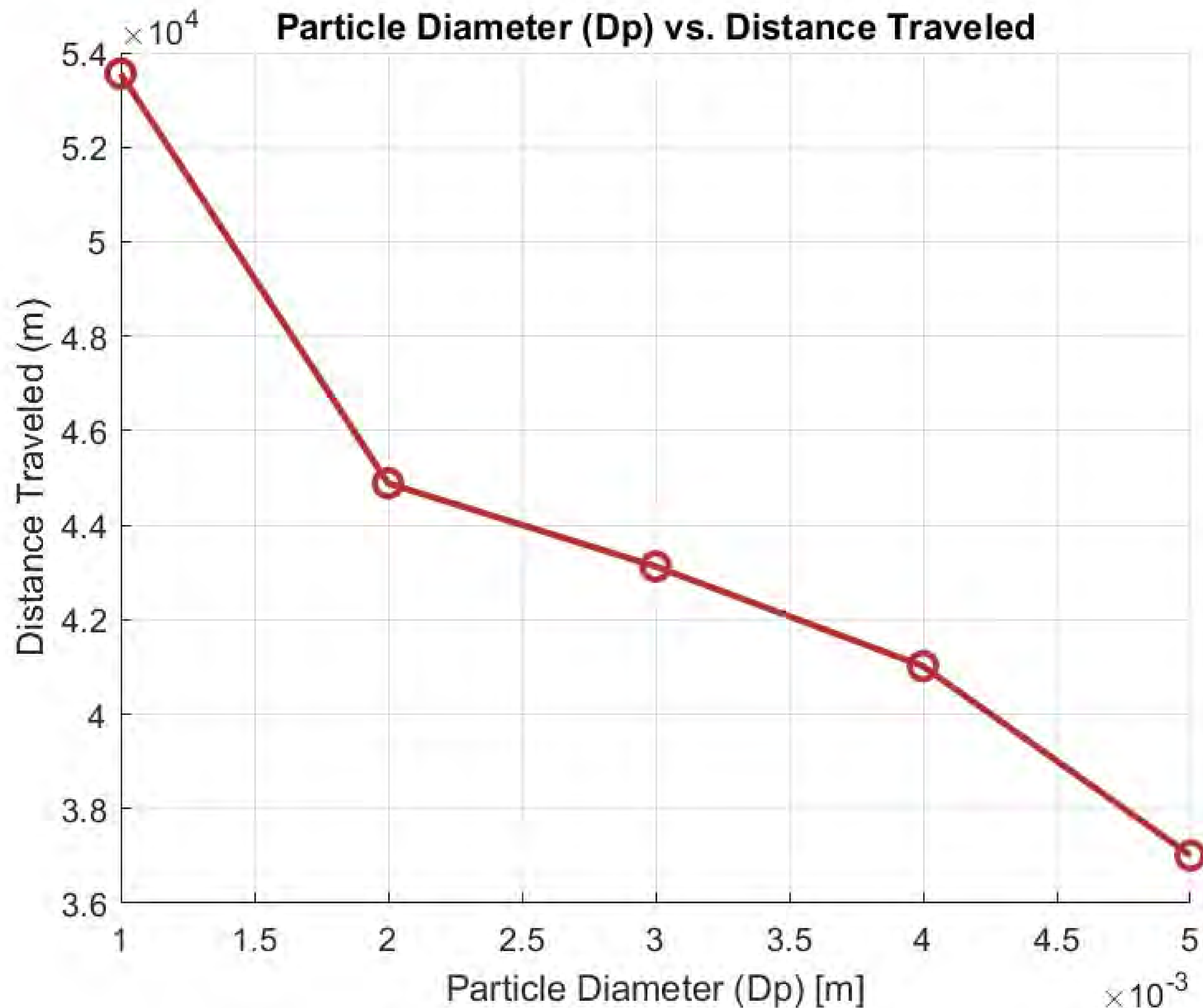
□ Effect of Changing Particle Diameter

- **Larger Particles:**

- o Have greater mass and higher settling velocity, sinking quickly.
- o Experience stronger drag, limiting their horizontal transport.
- o Settle closer to the source.

- **Smaller Particles:**

- o Are more affected by drag and turbulence, staying in suspension longer.
- o Travel farther before settling.
- o Are more likely to be carried by estuarine flows.



❖ Summary

❖ Impact on Distance Traveled

The combination of **density** and **diameter** determines whether a particle moves short distances (settling quickly) or long distances (remaining in suspension).

- ✓ **High-Density, Large Particles → Short Distance**
- ✓ **Low-Density, Small Particles → Long Distance**

By varying **density** and **diameter**, we can predict how different particles will move in water environments.

- ✓ This understanding is essential for sediment transport modeling, environmental protection, and predicting pollutant dispersion.

□ Next Steps

Validation step is crucial to ensure that the script can be used confidently for practical applications in coastal engineering and environmental analysis.

- Apply this model to a real case study, comparing the model's predicted trajectories with observed or simulated particles paths,
- Assess the accuracy of the approach and refine the model parameters as needed.
- Consider the effect of wave on travelled distance of particles.

- **Reference:** Murphy, E., Cornett, A., Nistor, I., & Pilechi, A. (2025). Development and Experimental Validation of a Lagrangian Particle-Tracking Model to Simulate Wave-Driven Transport of Coastal Driftwood. *Journal of Waterway, Port, Coastal, and Ocean Engineering*, 151(3), 04025003.
- olabarrieta, m., geyer, w.r., & kumar, n. (2014). the role of morphology and wave-current interaction at tidal inlets: an idealized modeling analysis, *journal of geophysical research: oceans*. 119(12), 8818–8837.



Thank you
for your attention!

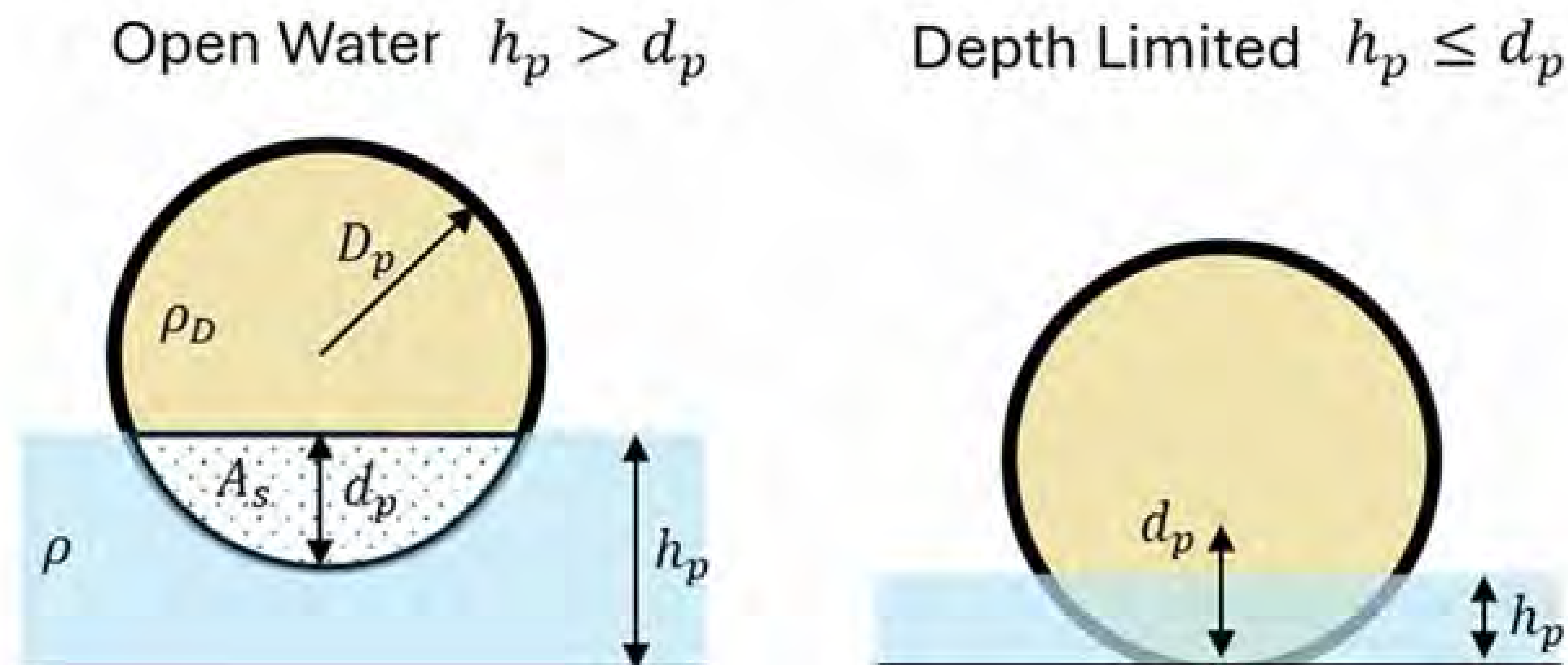


Fig. 4. Schematic showing: (a) calculation of submerged area, theoretical open-water draft; and (b) criteria for assessing contact with the bed.

$$\frac{A_s}{\pi D_p^2/4} = \frac{\rho_D}{\rho}$$

$$A_s = \frac{D_p^2}{4} \cos^{-1} \left(1 - \frac{2d_p}{D_p} \right) - \left(\frac{D_p}{2} - d_p \right) \sqrt{\frac{D_p^2}{4} - \left(\frac{D_p}{2} - d_p \right)^2}$$

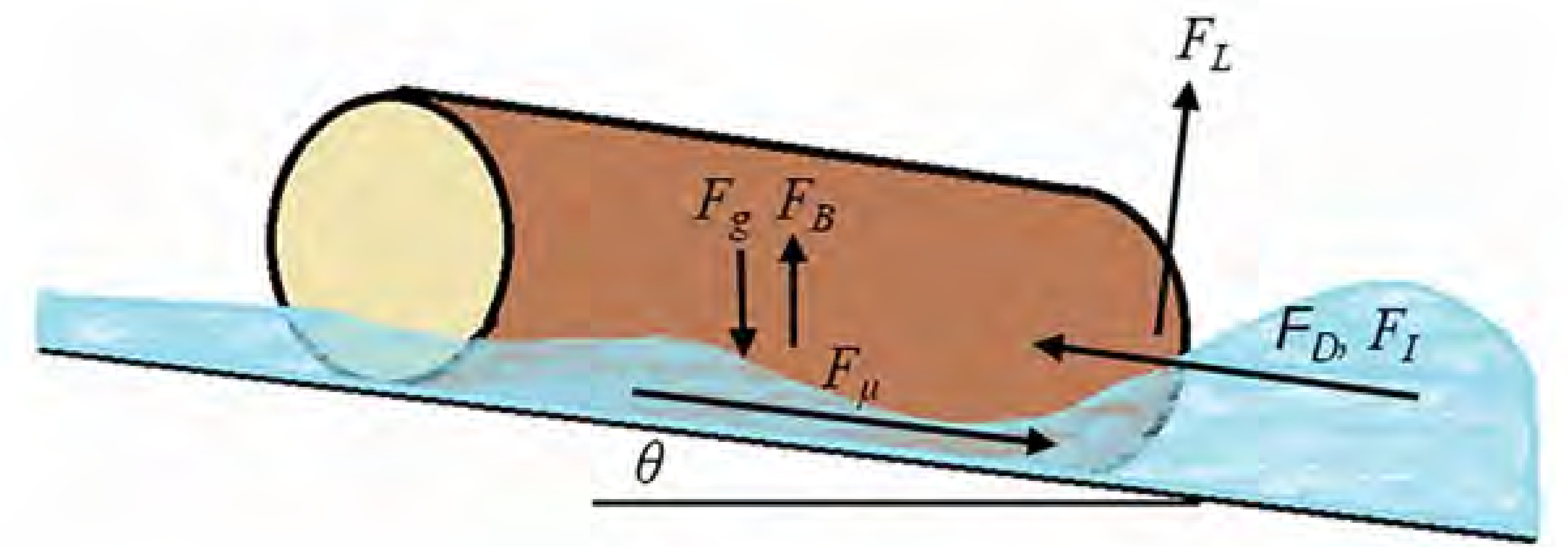


Fig. 3. Forces acting on a piece of driftwood in contact with a sloping beach and exposed to waves.

Setting the submerged cross-sectional area, A_s , equal to the area of a circular segment in the force balance then yields [Fig. 4(a)].

- Force balance in a system involving a submerged circular segment:
 - ✓ The equation is derived based on the assumption that *the submerged cross-sectional area (A_s)* is equal to the area of a circular segment.
 - ✓ The force balance likely considers buoyancy forces acting on the submerged portion of the circle.
 - ✓ The goal is to determine d_p , the depth of submergence.

Multi-model approach to scour in dynamic areas

Nishchay Tiwari
HR Wallingford, UK

Supervisors and Advisors:
Michiel A.F. Knaapen
Sina Haeri
Richard Whitehouse

SEDIMARE 3rd Training School at Santander 11-13 March 2025

Marie Curie Grant Agreement Number: 101072443



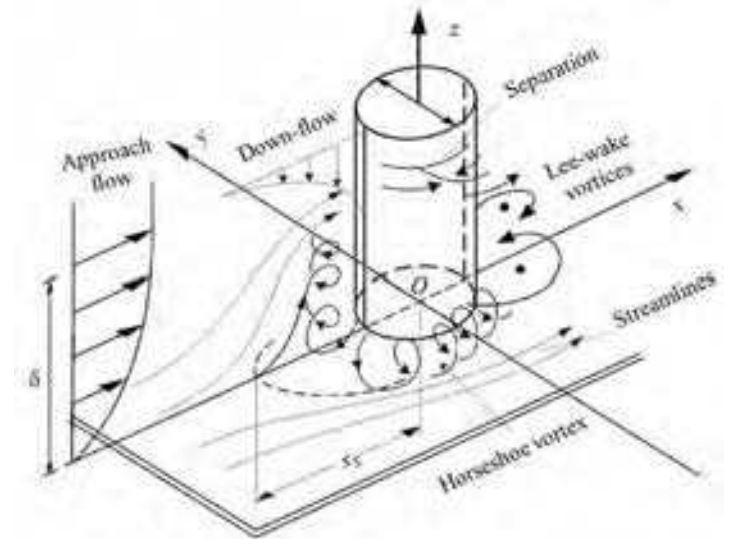
Contents

- Scour Phenomenon
- CASE 1: sedFoam with OpenFOAM v2012
 - Methodology
 - Main Features
 - Results
- CASE 2: sedInterFoam with OpenFOAM v2012
 - Methodology
 - Preliminary Results
- Conclusion
- Future Work
- Dissemination

Scour Phenomenon

Hydrodynamic Forces

- *Flow Acceleration* :
 - Structures disrupt flow, creating high-velocity zones and turbulence.
 - Flow accelerates around the structures, increasing bed shear stress.
- *Vortex Formation* :
 - Horseshoe vortices at the base of structures erode sediment.
 - Wake vortices downstream deepen scour holes.



Sediment Transport Dynamics

- *Erosion* : High shear stress lifts sediment particles into suspension.
- *Deposition* : Sediment settles in low-energy zones (e.g., downstream of structures).

sedFoam: Methodology

Inputs

Experimental Data

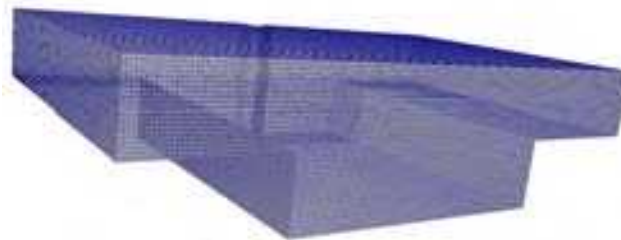
- Obtaining the transport properties of sand and water phase used in Flumes experiment.
- Use the geometrical dimensions of cofferdam models.
- Using the input flow velocity



Solver

Two-phase Eulerian RANS OpenFOAM

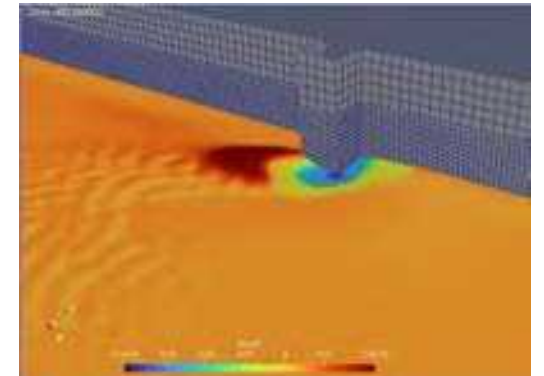
- Creating 3D domain
- Using sedFoam :
 - Granular Rheology properties (mul)
 - Interfacial properties (drag model)
 - Transport properties
 - Modified Two-phase RAS equations



Outputs

Scour Depth

- Estimation of volume fraction of water and sand to predict the bed formation.
- Comparison with experiments



Main Features

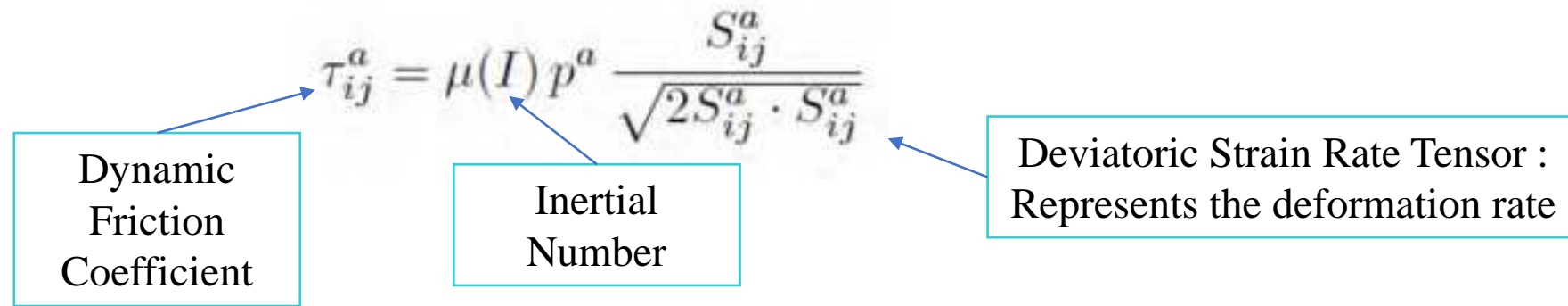
Closure Models for Stress Tensors

- **Turbulence Models**

- SedFoam uses different turbulence closures for fluid flow, such as $k-\epsilon$, $\mathbf{k}-\boldsymbol{\omega}$, and a simple mixing length model, to capture the effects of turbulent eddies on sediment transport.

- **Granular Stress Models**

- SedFoam implements granular stress models to simulate dense granular flows. The kinetic theory of granular flows and the $\mu(I)$ -rheology (derived from the Jop et al., 2006 model) are commonly used.
- In dense flows, the granular stress is influenced by **particle-particle collisions** and **inter-particle friction**, represented by the effective viscosity, which is a function of the shear rate and pressure.
- Unlike the kinetic theory of granular flows (which works well for dilute conditions), the $\mu(I)$ rheology is phenomenological and based on dimensional analysis, focusing on frictional contacts.

$$\tau_{ij}^a = \mu(I) p^a \frac{S_{ij}^a}{\sqrt{2S_{ij}^a \cdot S_{ij}^a}}$$


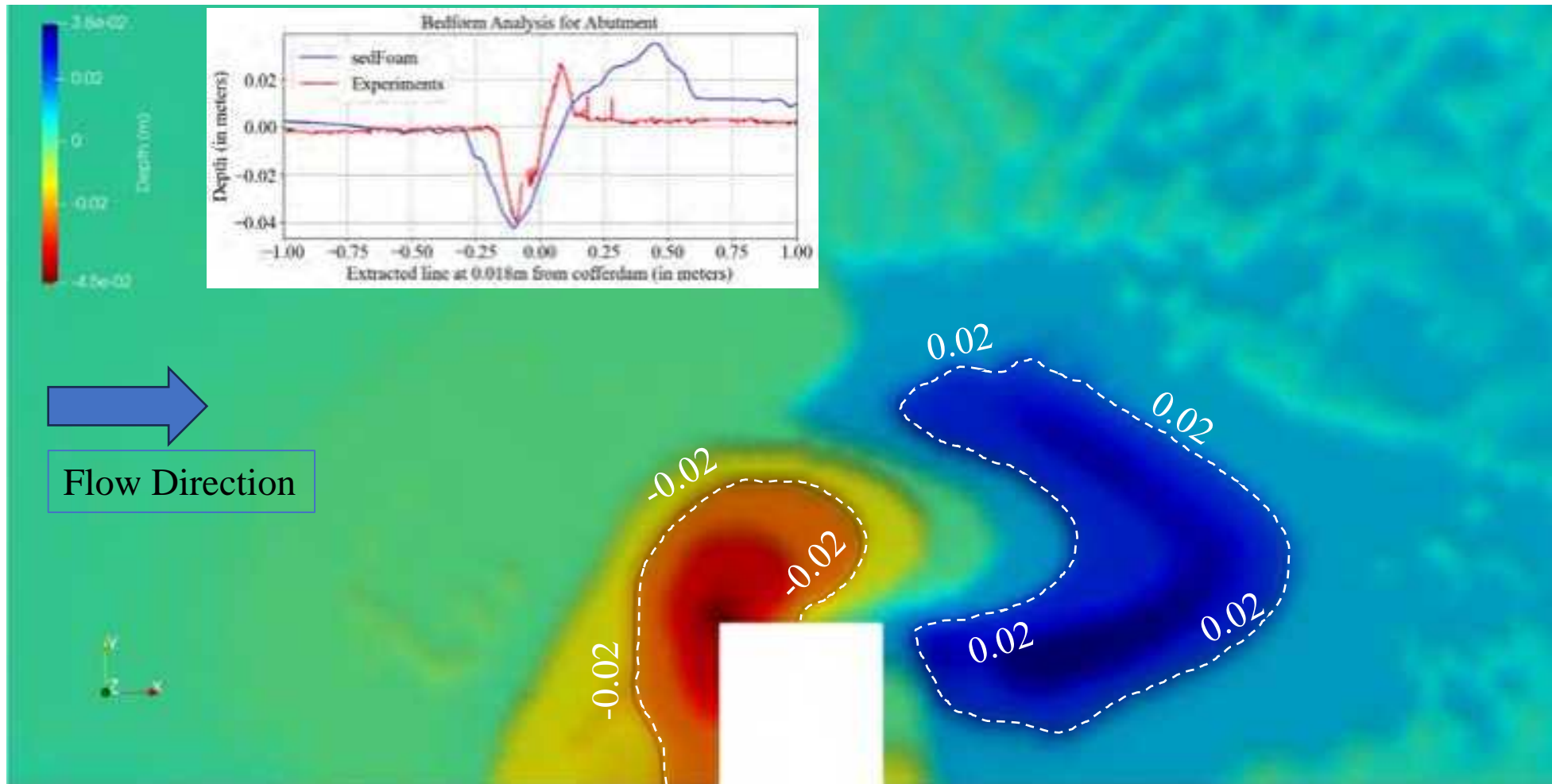
Dynamic Friction Coefficient

Inertial Number

Deviatoric Strain Rate Tensor : Represents the deformation rate

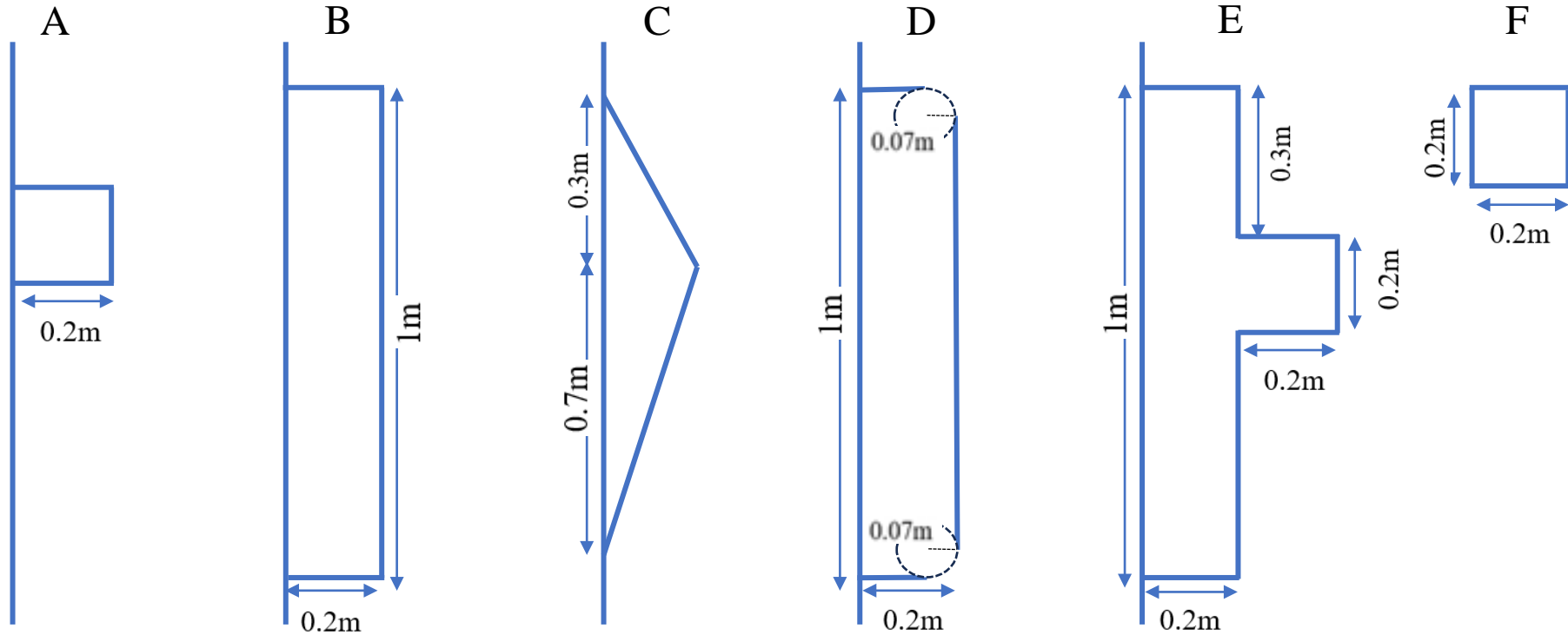
Results

Sand bed after 1hr, $U = 0.244$ m/s



Results

Different cofferdam geometries

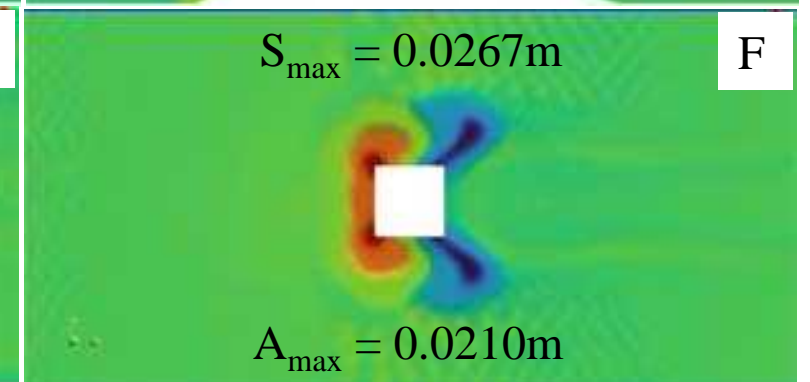
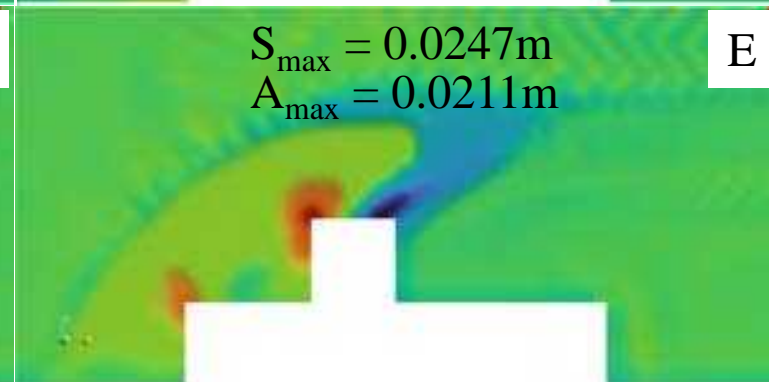
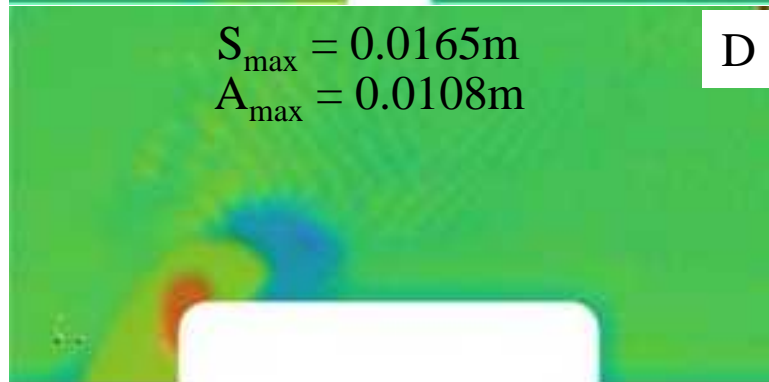
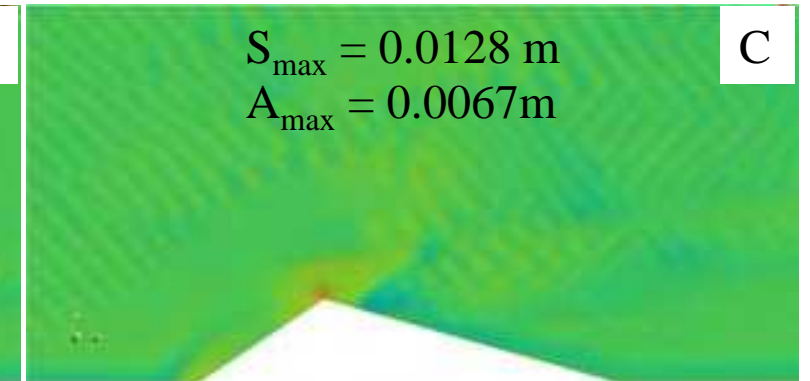
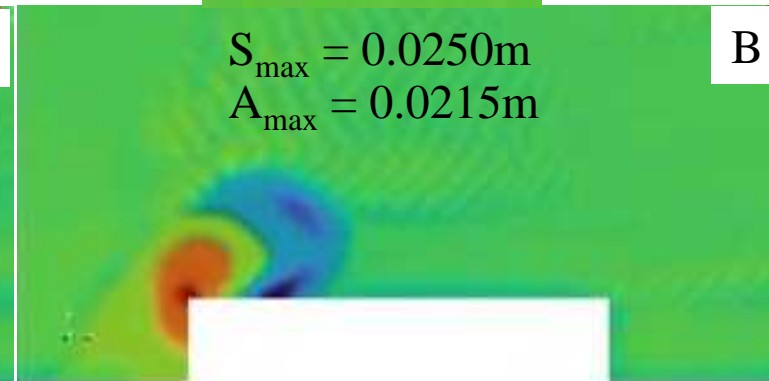
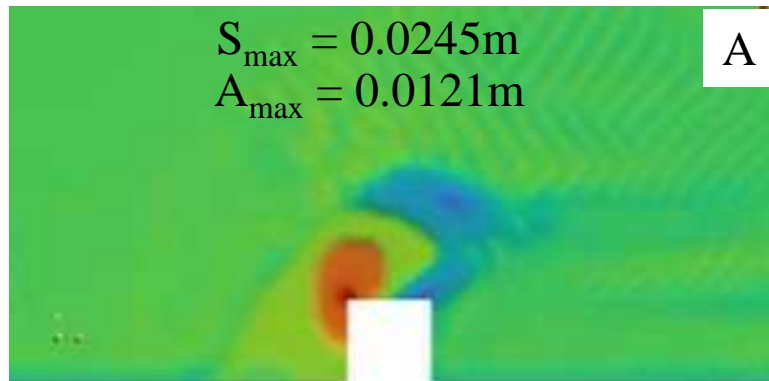


Max Scour and Max Accretion

After 900 seconds, $U = 0.17\text{m/s}$

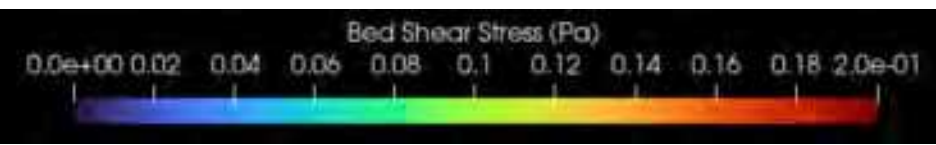
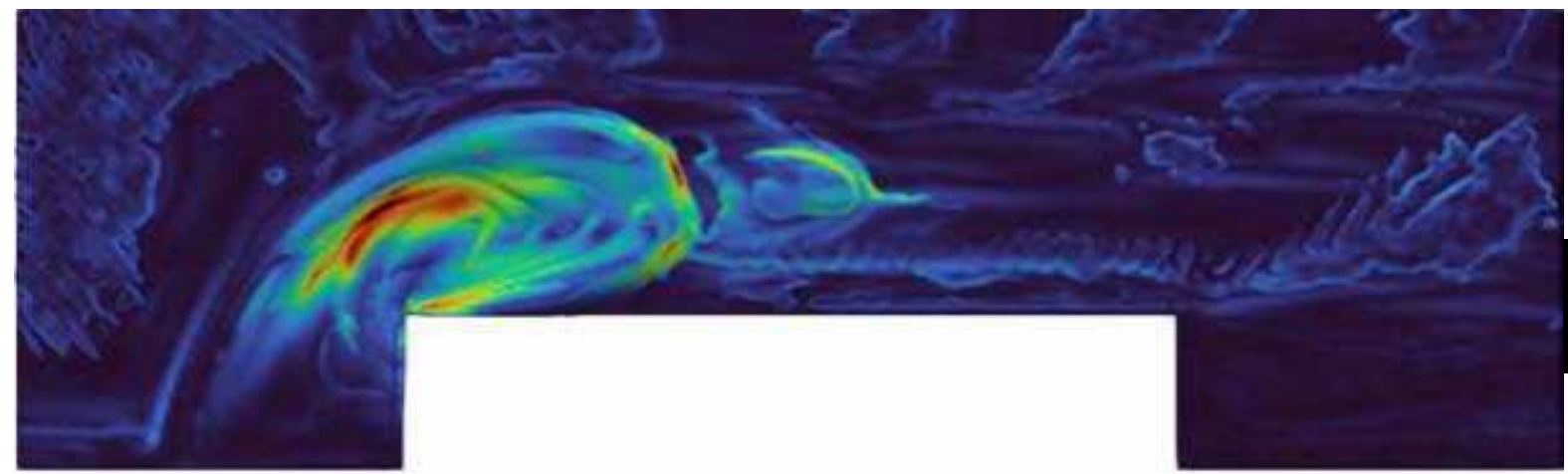
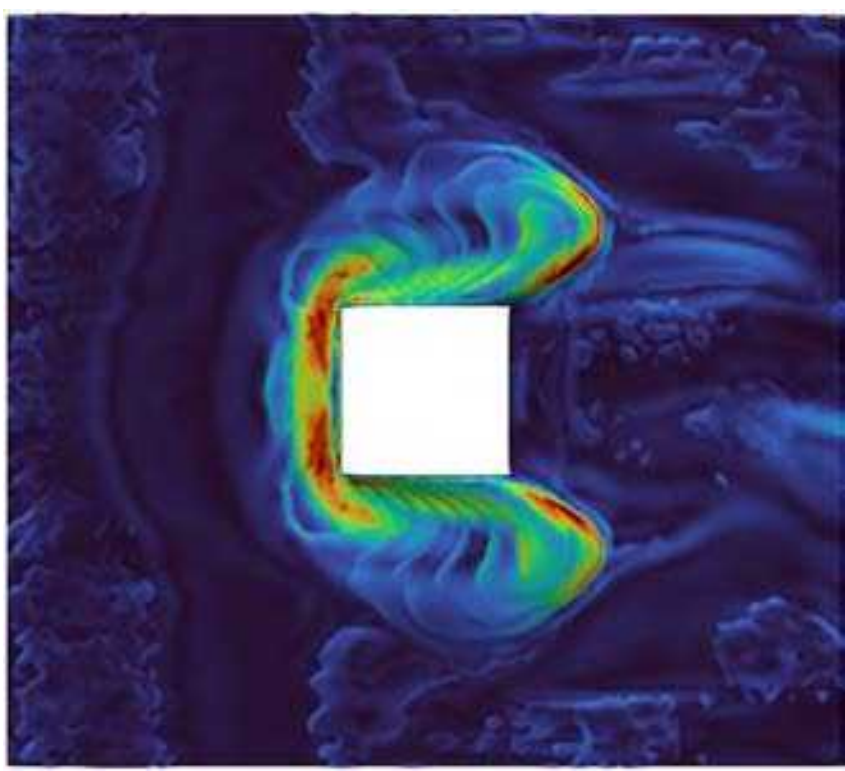
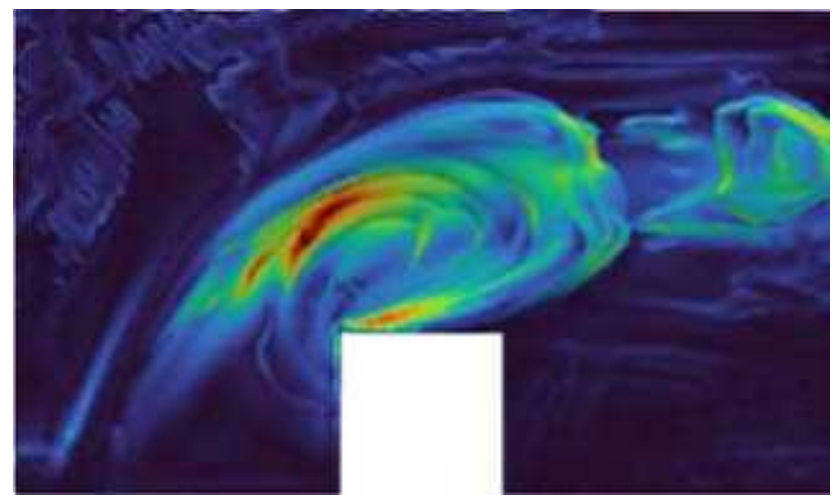


Time: 900.000000

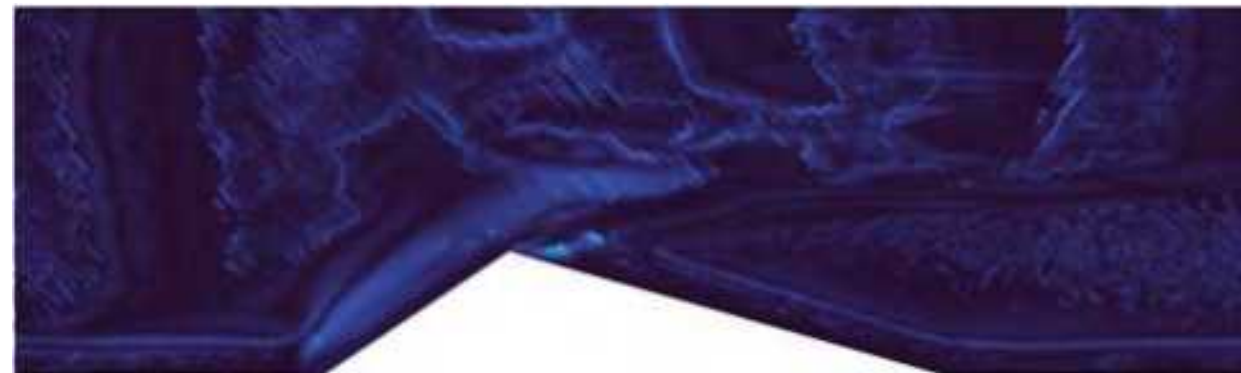
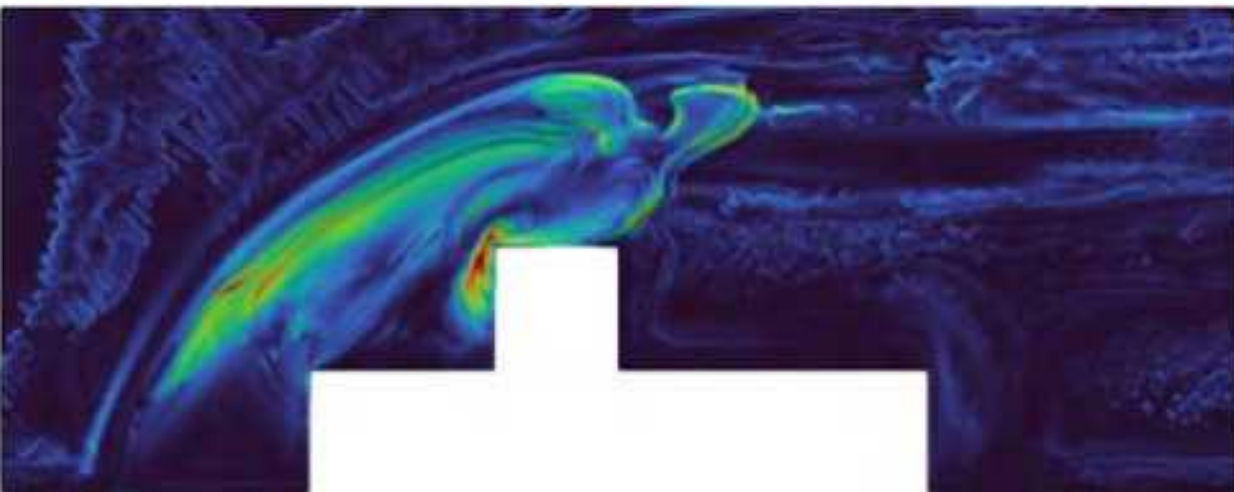
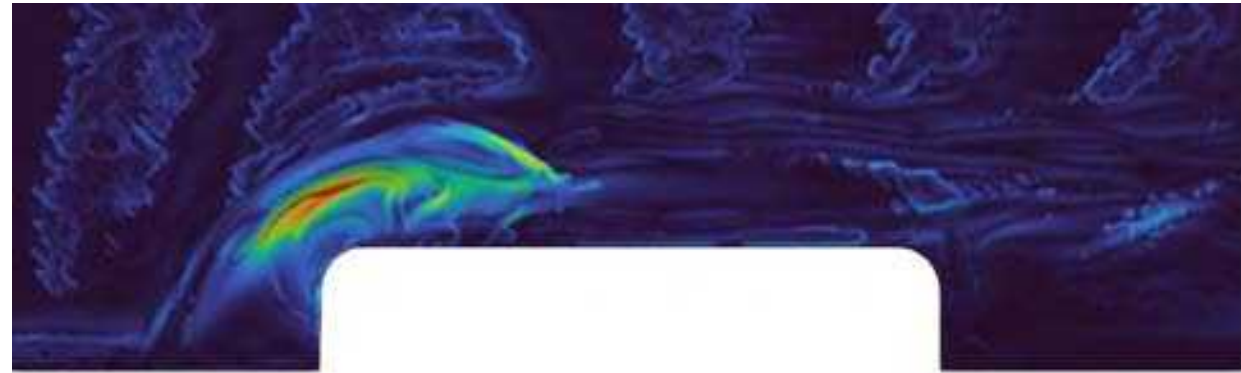
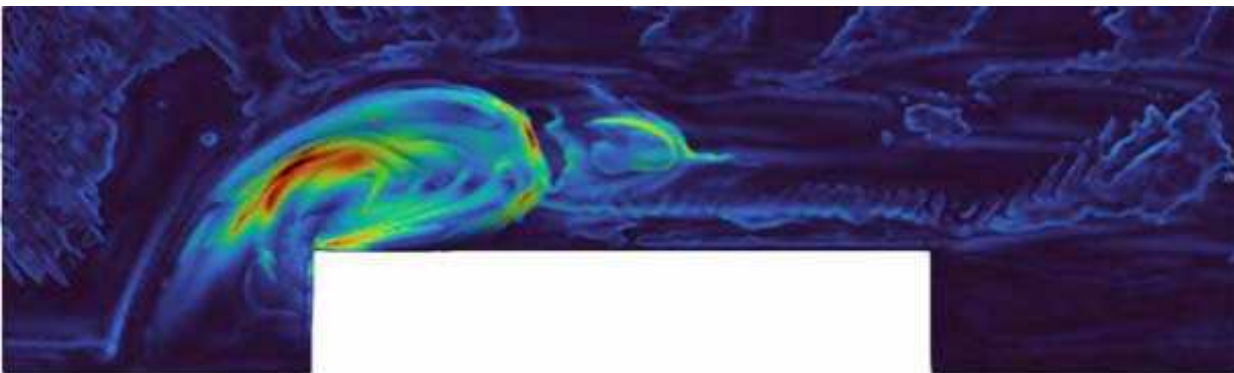


Bed Shear Stress

After 450 seconds, $U = 0.17 \text{ m/s}$



After 450 seconds, $U = 0.17$ m/s



sedInterFoam: Methodology

Inputs

Experimental Data

- Obtaining the transport properties of sand and water phase used in Flumes experiment.
- Use the geometrical dimensions of monopile models.
- Using the 3 input flow velocities



Solver

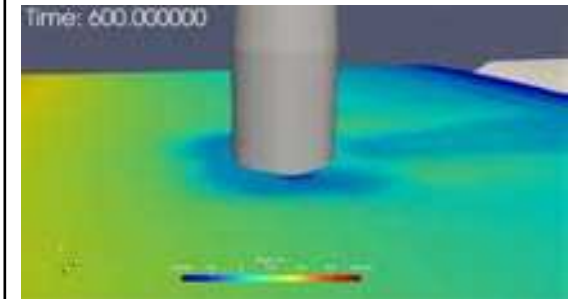
Three-phase Eulerian RANS OpenFOAM

- Creating 3D domain
- Using sedInterFoam :
 - VOF for water-air interface
 - Granular Rheology properties (muI)
 - Interfacial properties (drag model)
 - Transport properties
 - Modified Two-phase RAS equations

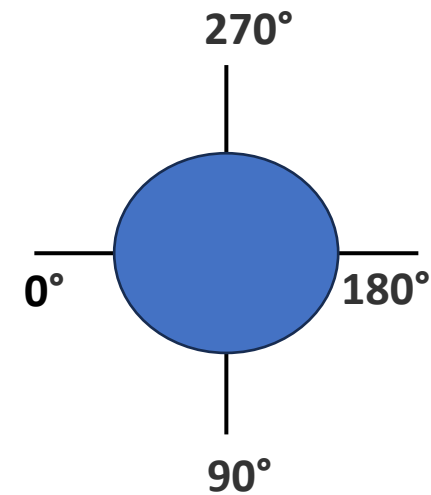
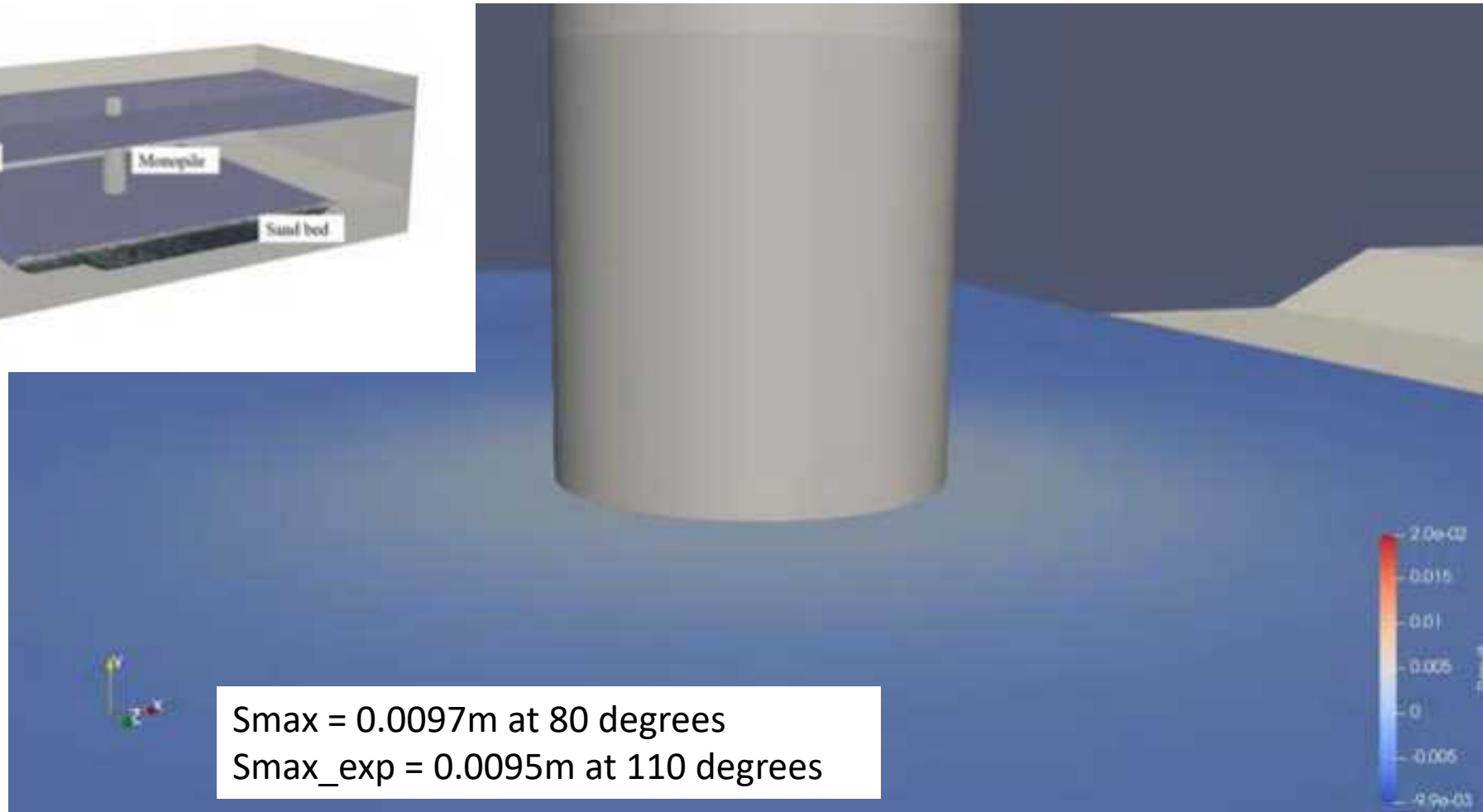
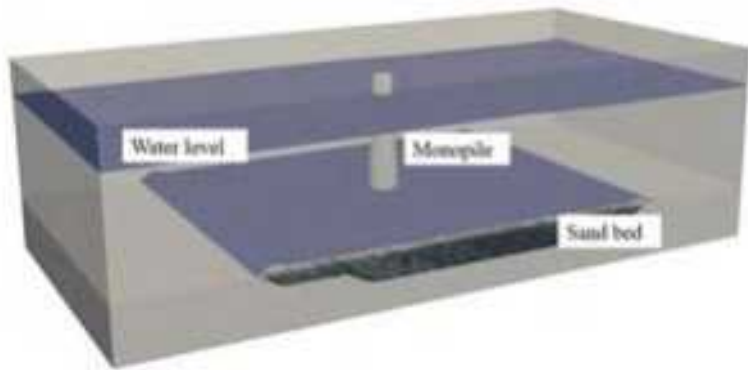
Outputs

Scour Depth

- Estimation of volume fraction of water and sand to predict the bed formation.
- Comparison with experiments



Preliminary Results (Current only)



Conclusions

- **sedFoam Validation :**
 - Successfully captured scour patterns around cofferdams.
 - Demonstrated the role of turbulence models ($k-\omega$) and granular rheology ($\mu(I)$ -model) in simulating bed evolution.
- **sedInterFoam Preliminary Results :**
 - Initial validation for monopile scour under currents showed close agreement with experiments.
 - Highlighted the importance of VOF for air-water interface tracking in three-phase flows.

Future Work

- **Vortex Dynamics and Flow Structures :**
 - Use Q-criterion and λ_2 -method to analyse vortex evolution and its impact on sediment mobilization, enhancing understanding of scour mechanics.
- **Wave-Current Interaction Modeling :**
 - Expand Case 2 (monopile scour) to include combined wave-current interactions using waves2Foam for wave generation.
 - Investigate turbulence-sediment coupling under cyclic wave loading to refine predictions of vortex shedding and horseshoe vortex dynamics.
- **Field-Scale Applications :**
 - Scale simulations to real-world scenarios by integrating bathymetric and hydrodynamic field data.
 - Validate against field measurements to assess model robustness in complex environments.

Dissemination

- **Conference Presentations and Proceedings**

- *Upcoming*: Paper presentation at Coastal Dynamics 2025, Aveiro, Portugal. Tiwari, N., Knaapen, M., Haeri, S., & Whitehouse, R. (2025, April 7–11). Numerical modelling for scour near cofferdams using Eulerian two-phase flow model.

- **Outreach Activities**

- *Completed*: Presentation at ARC conference at The Open University in Milton Keynes, UK (2024, 27–28 Nov)

Thank You

The project has received funding from Horizon Europe Marie Skłodowska-Curie Actions, Grant Agreement no. **101072443 - SEDIMARE**. Experimental data is taken from the Fast Flow Facility at Froude Modelling Hall, HR Wallingford Ltd.





UNIVERSITÀ
POLITECNICA
DELLE MARCHE



DIPARTIMENTO
INGEGNERIA
CIVILE EDILE
ARCHITETTURA
18|22 23|27 ECCELLENZA



SEDIMARE DC MEETING

11.03.2025-13.03.2025

Santander, Spain

Nearshore Wave Processes by Remote Sensing

Name	Muhammed Said Parlak (#2)
Supervisors	Maurizio Brocchini Nicholas Dodd Matteo Postacchini

Processing SGS Data

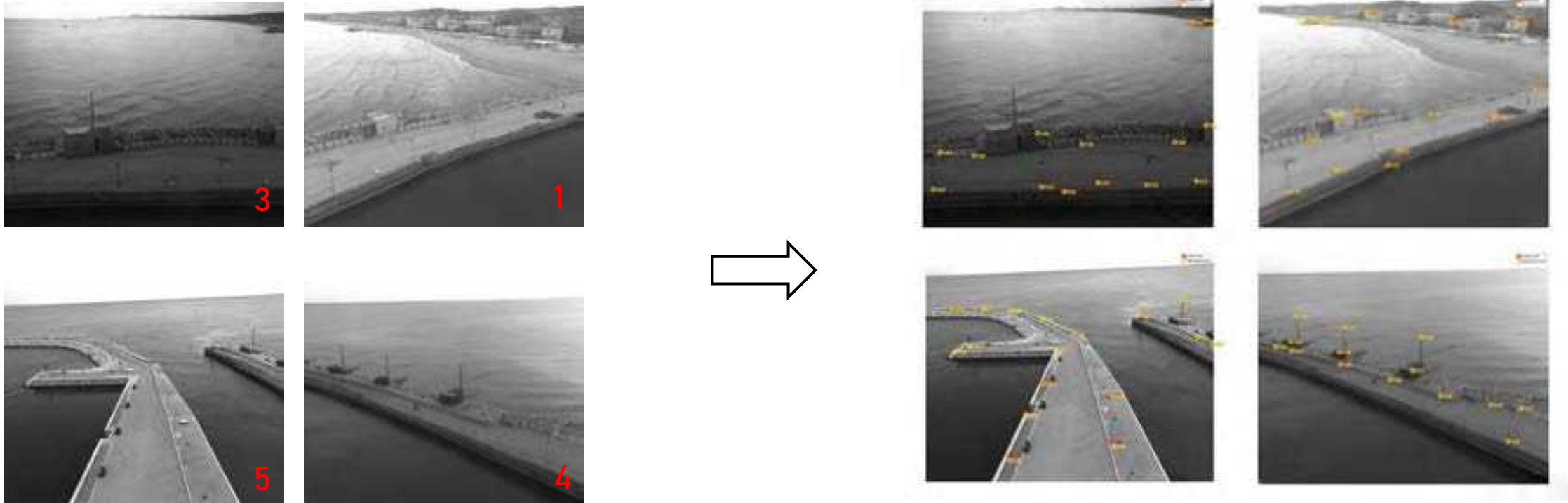
→ SGS (Sena Gallica Speculator) is a fixed multi-camera monitoring system.

- 10 mins recording for each 60 mins.
- 5 cameras, 2 Hz sampling rate.



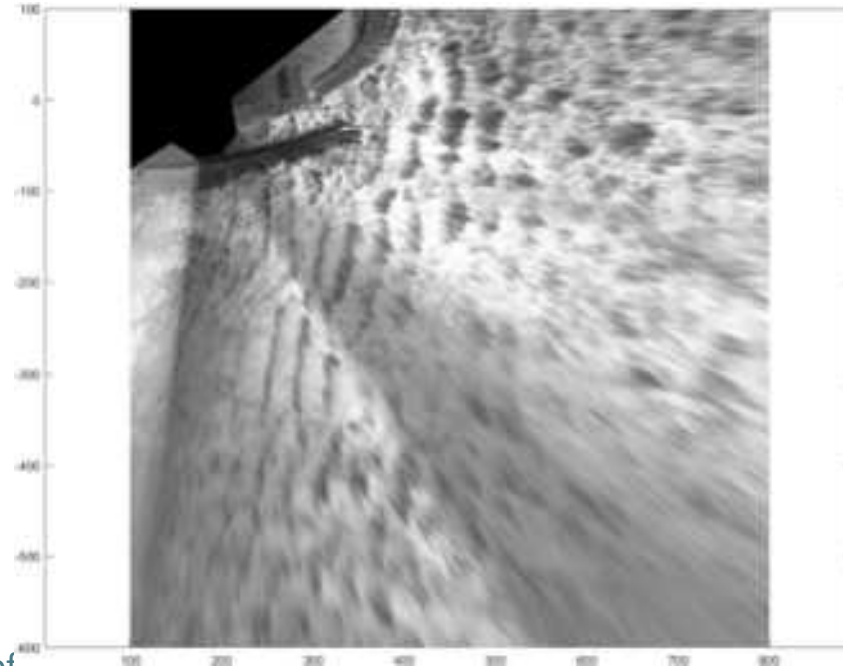
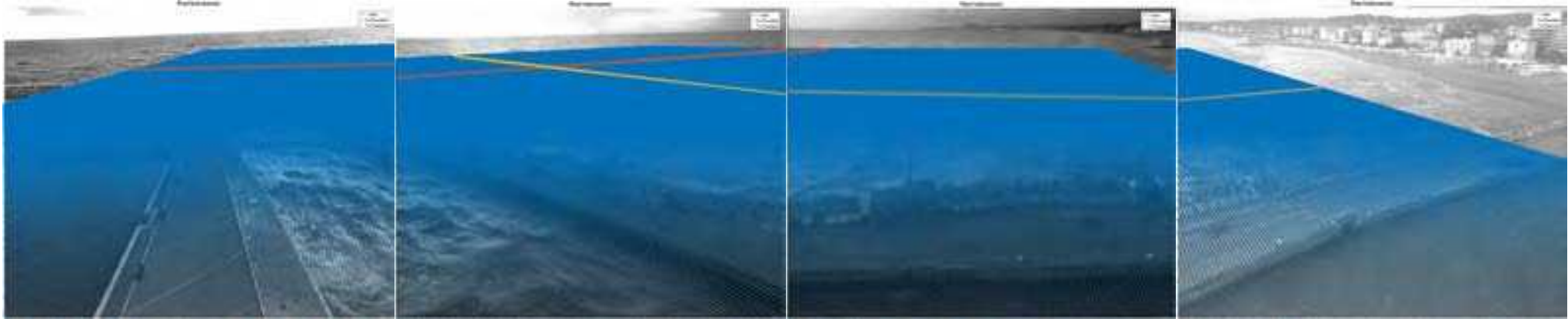
Processing SGS Data

- SGS (Sena Gallica Speculator) is a fixed multi-camera monitoring system.
- Images need to be orthorectified for geometric consistency.
 - Quantitative Coastal Imaging Toolbox is utilized to complete the procedure*.



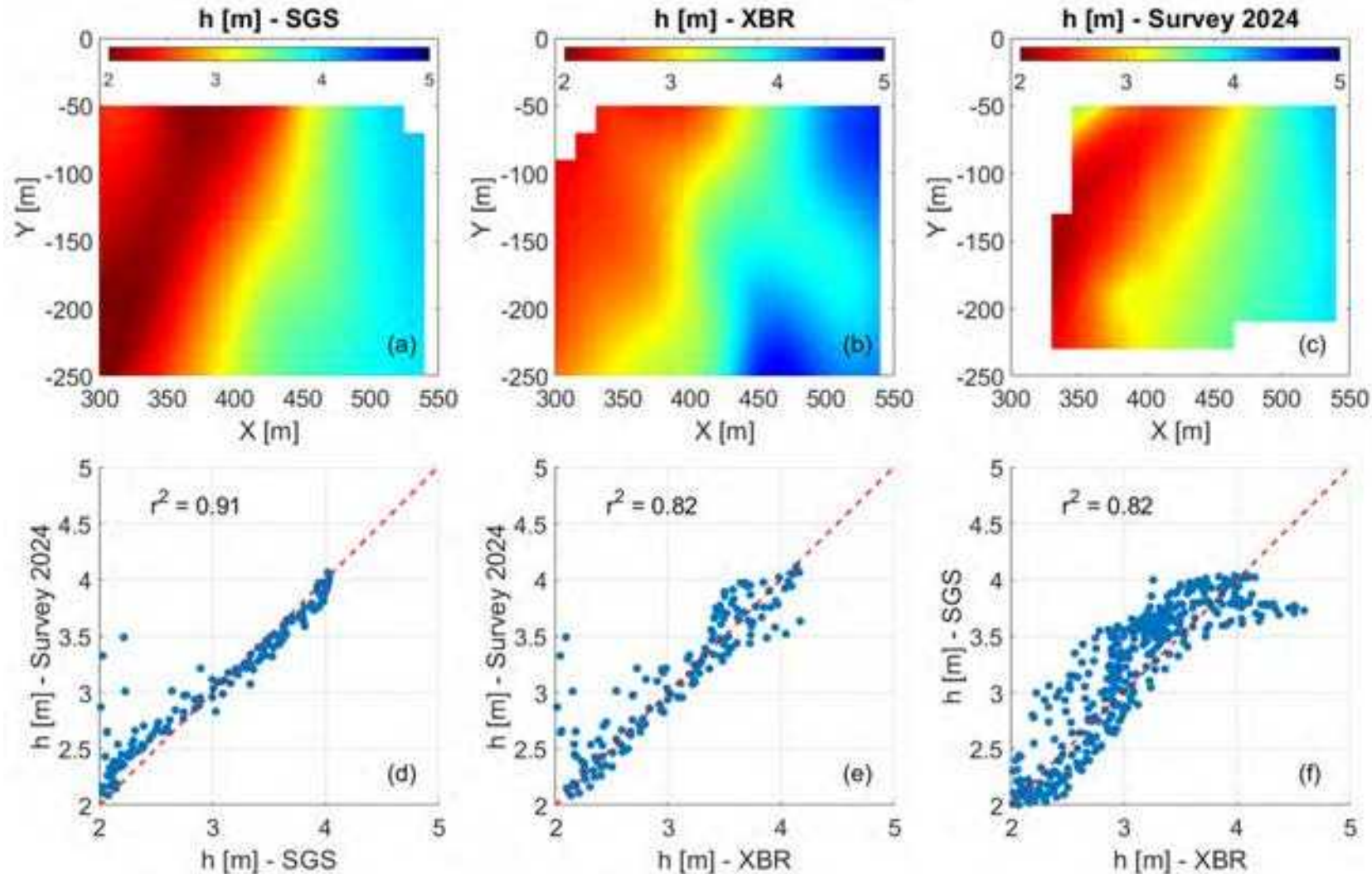
Processing SGS Data

- SGS (Sena Gallica Speculator) is a fixed multi-camera monitoring system.
- Grids and stacks are extracted from the processed images.

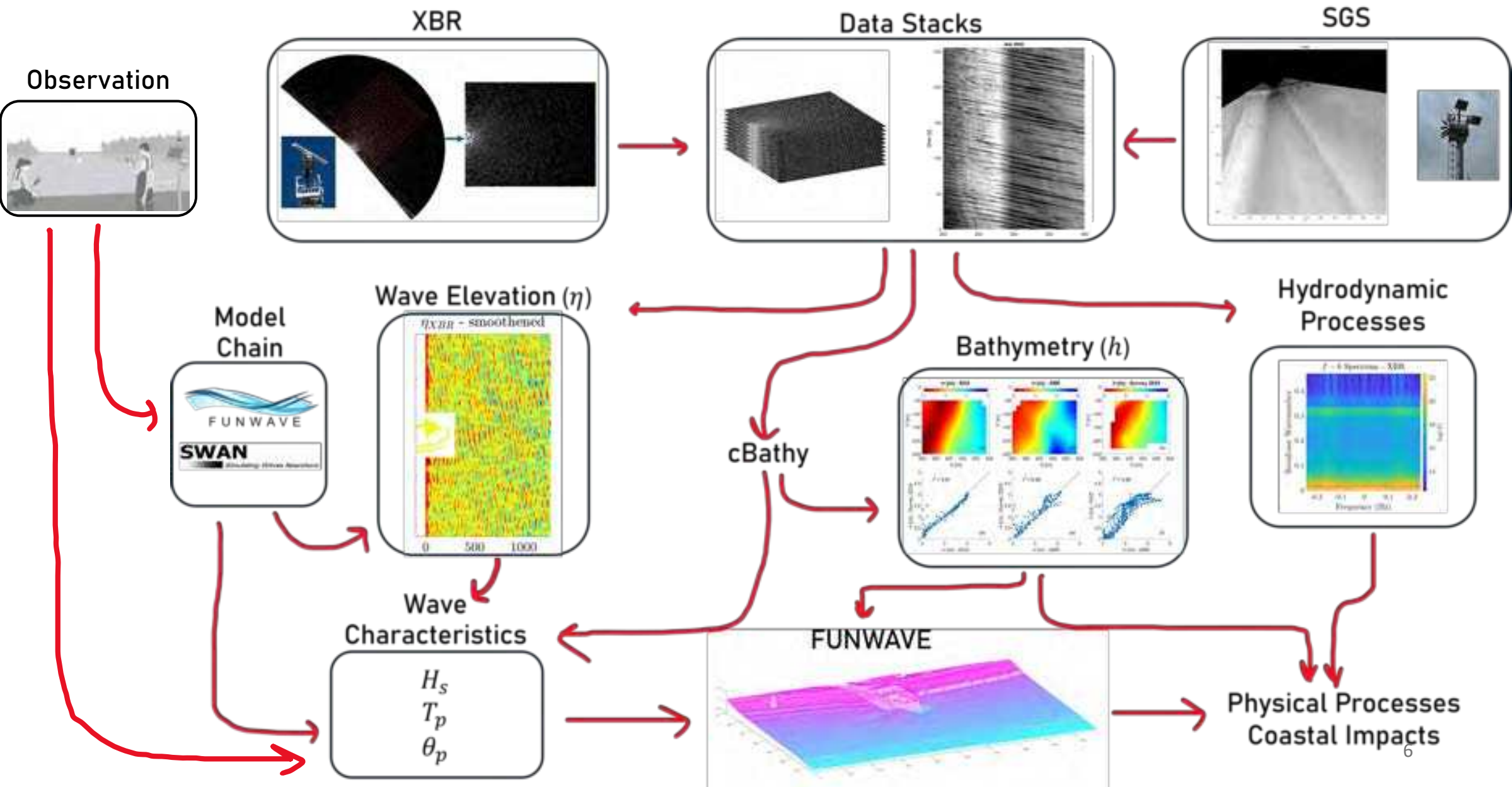


Processing SGS Data

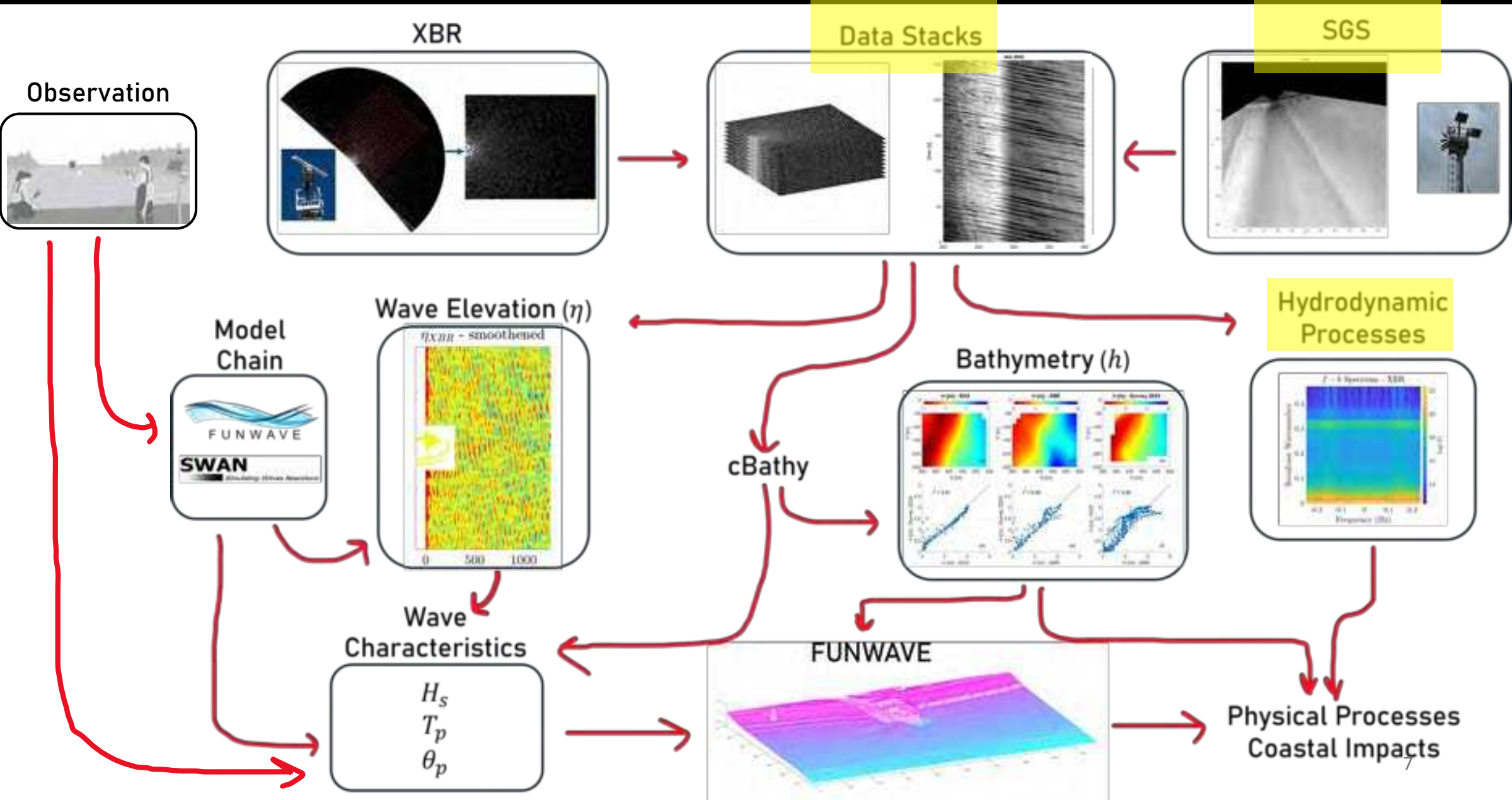
- SGS (Sena Gallica Speculator) is a fixed multi-camera monitoring system.
- Quality assessment is done by comparing bathymetry result to field observation and results from X-Band RADAR (XBR).



Framework for Nearshore Dynamics

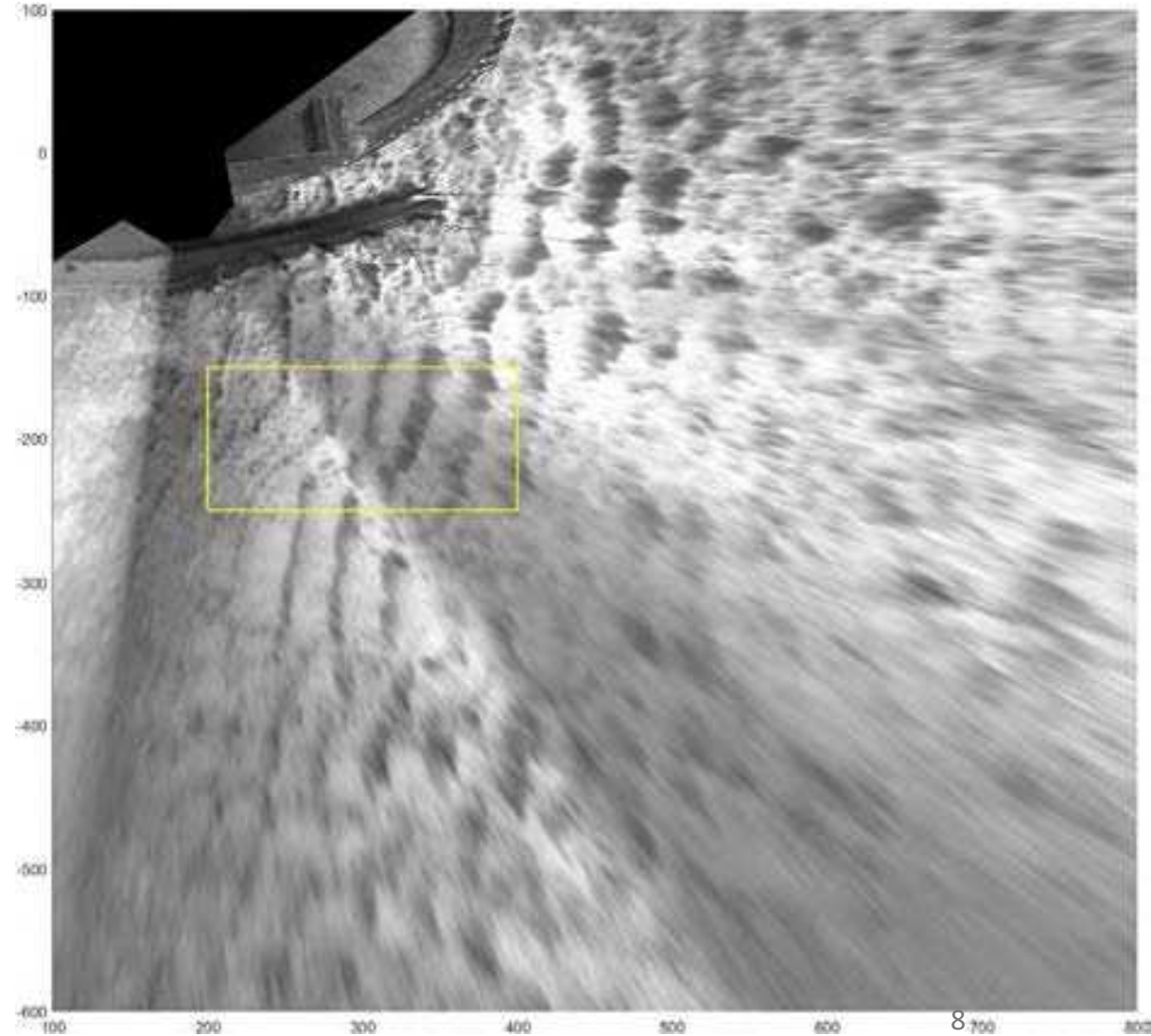


Framework for Nearshore Dynamics



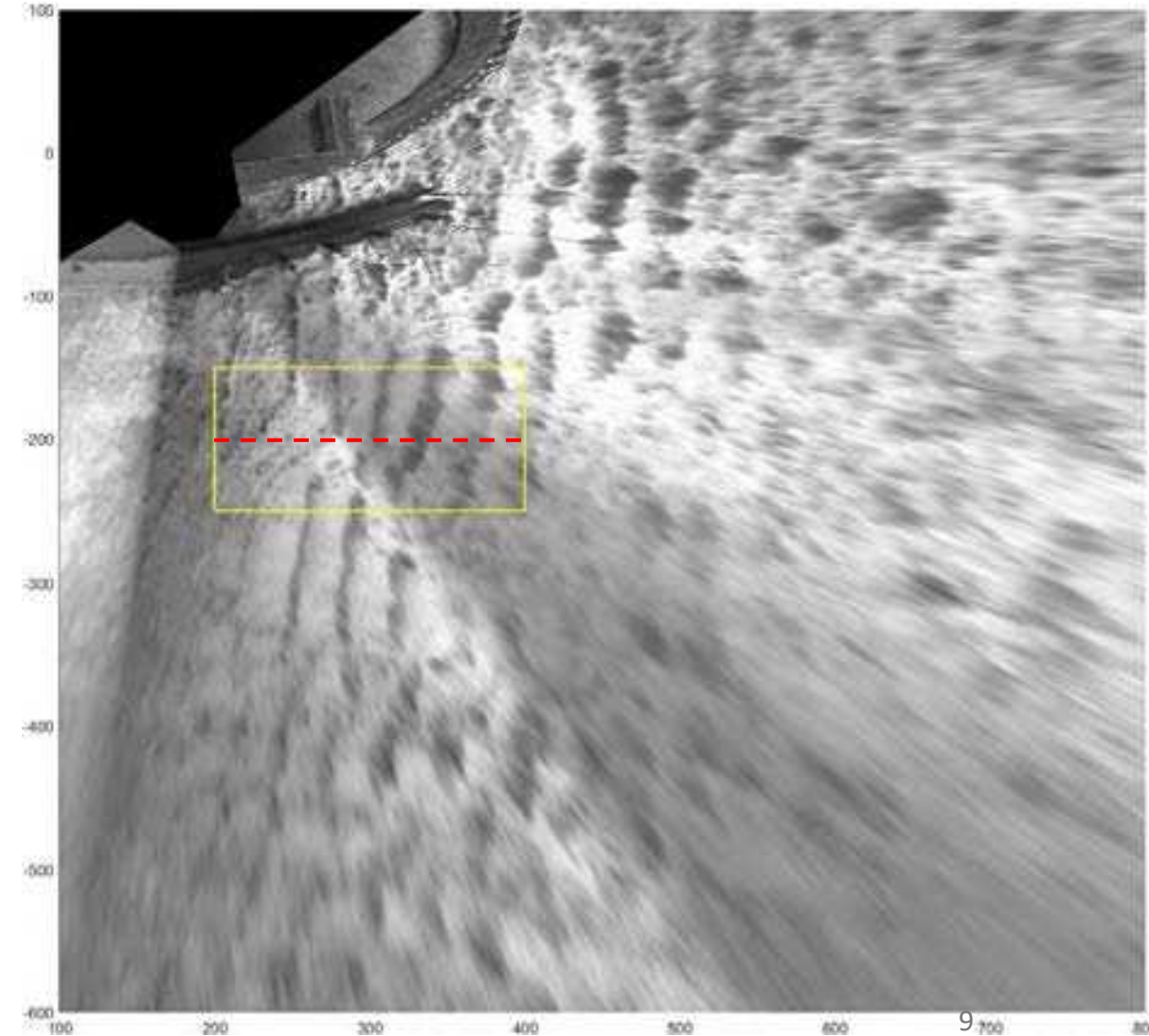
Processing SGS Data

- Image processing with SGS data to extract information
- Small patch is chosen.



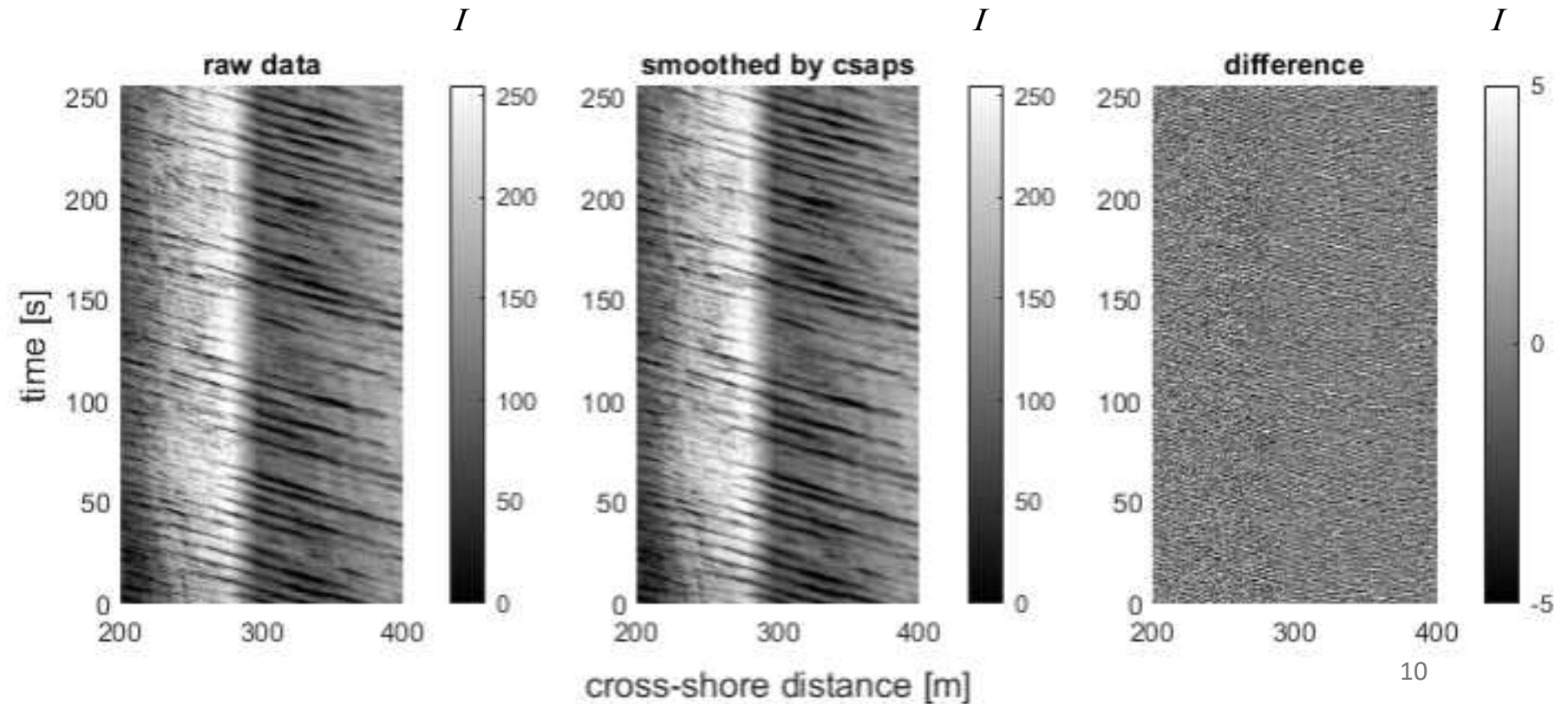
Processing SGS Data

- Image processing with SGS data to extract information
- Small patch is chosen.
 - Time-stacked image is created(---).



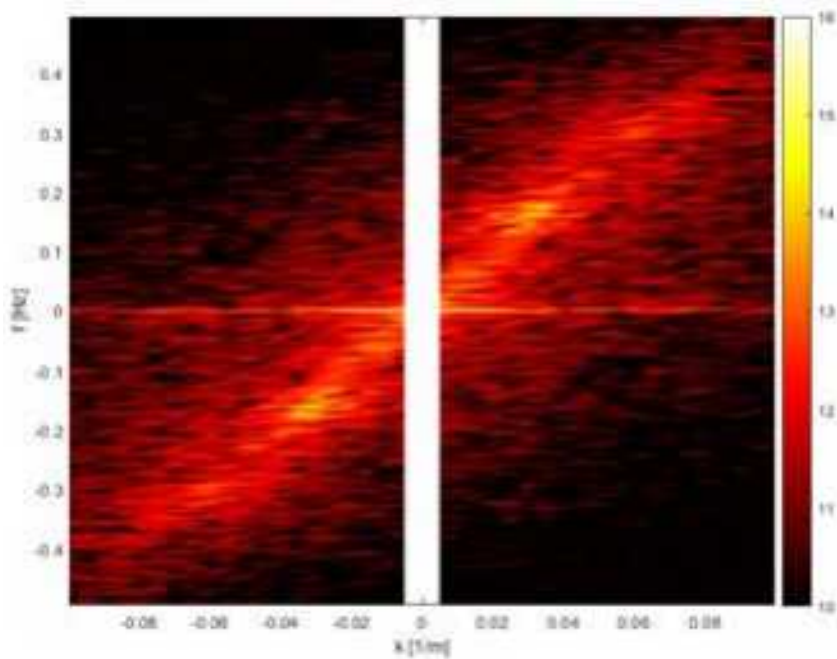
Processing SGS Data

- Image processing with SGS data to extract information
- Data is smoothed to eliminate noise (cubic smoothing spline, csaps).



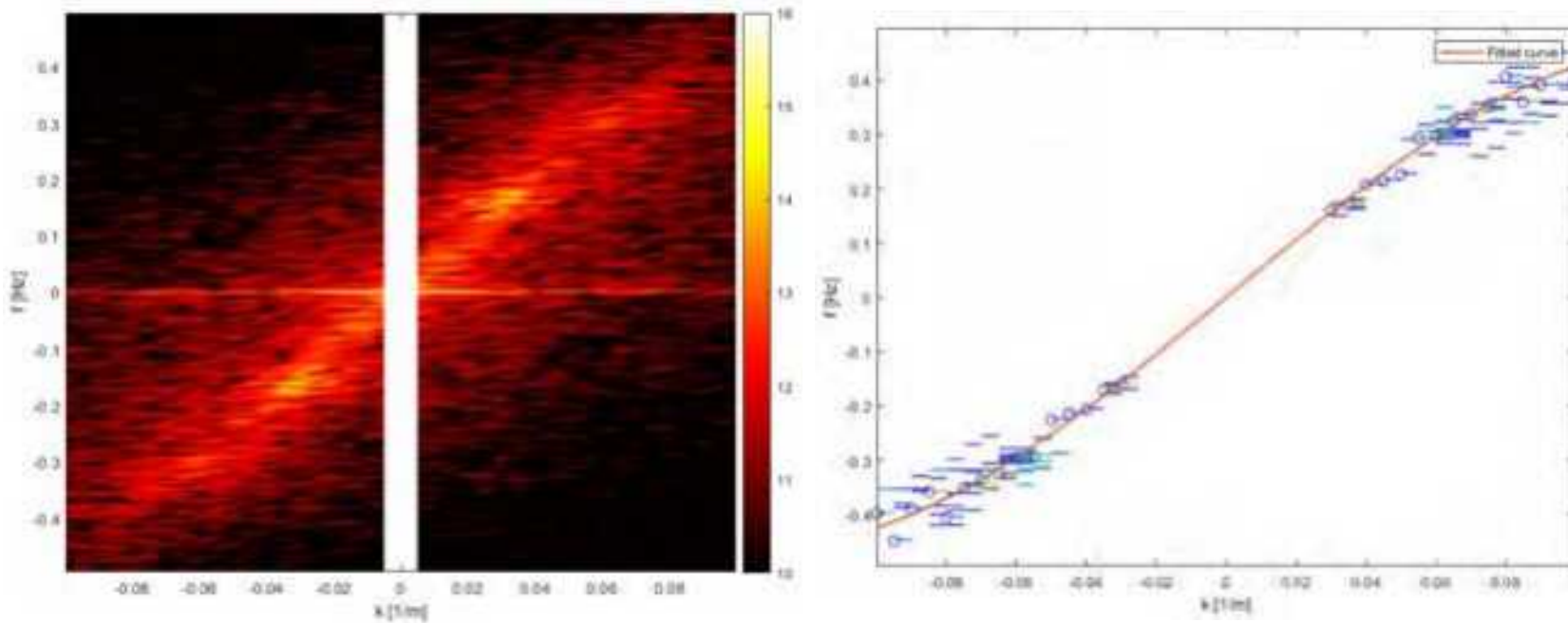
Processing SGS Data

- Image processing with SGS data to extract information
- Data is smoothed to eliminate noise (cubic smoothing spline, csaps).
 - f - k spectrum is obtained by FFT



Processing SGS Data

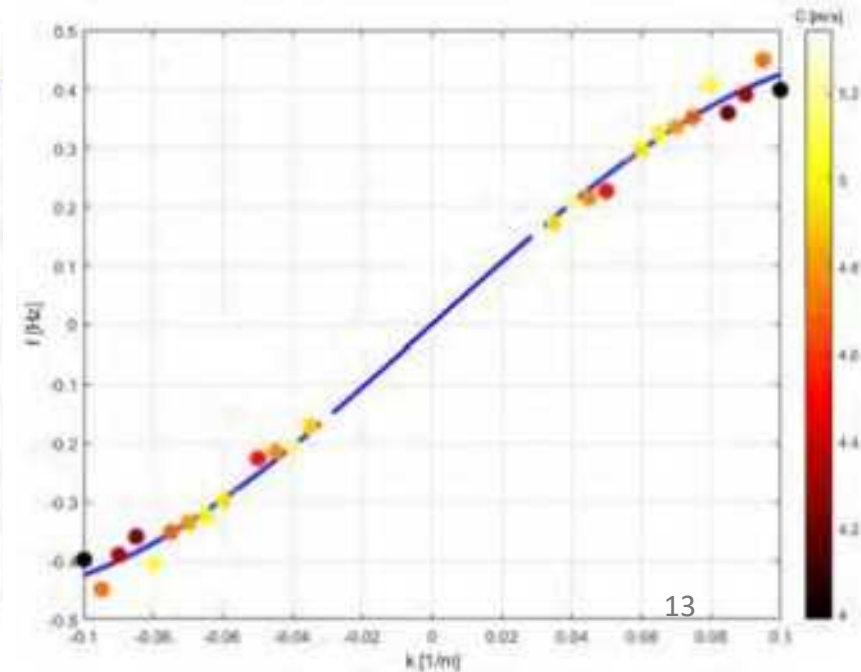
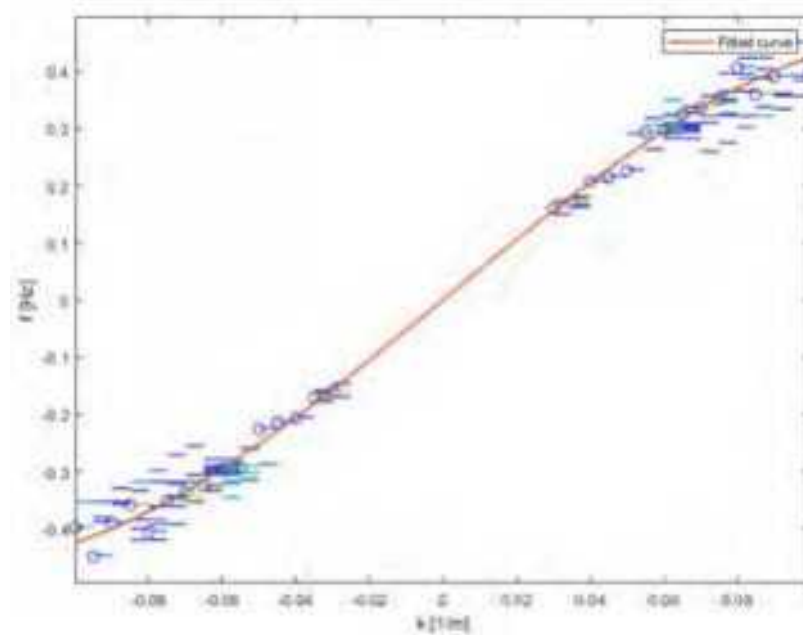
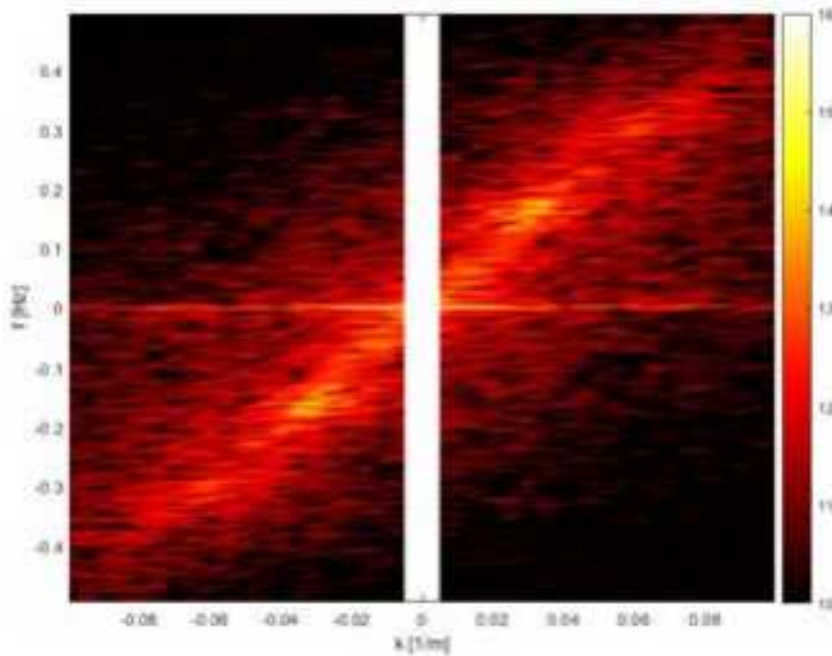
- Image processing with SGS data to extract information
- Data is smoothed to eliminate noise (cubic smoothing spline, csaps).
 - f - k spectrum is obtained by FFT
 - Maxima locations are extracted and fitted with 3rd order polynomial.



Processing SGS Data

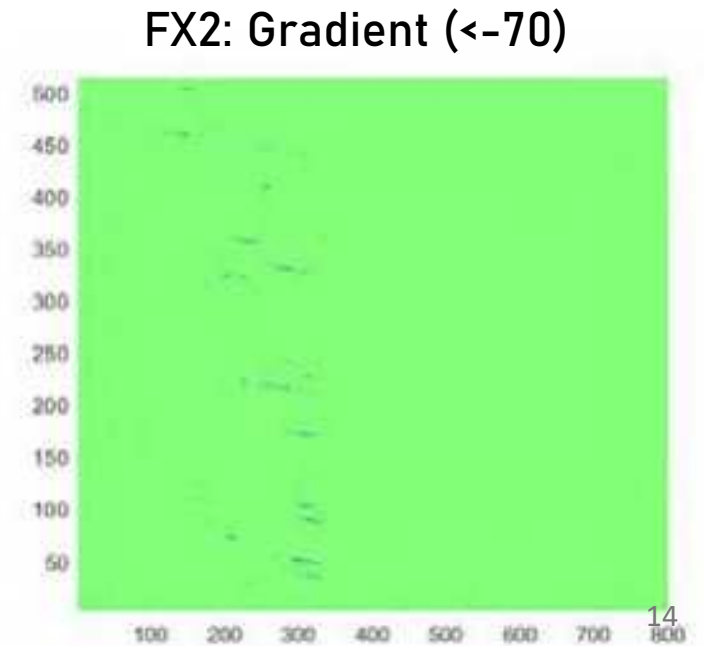
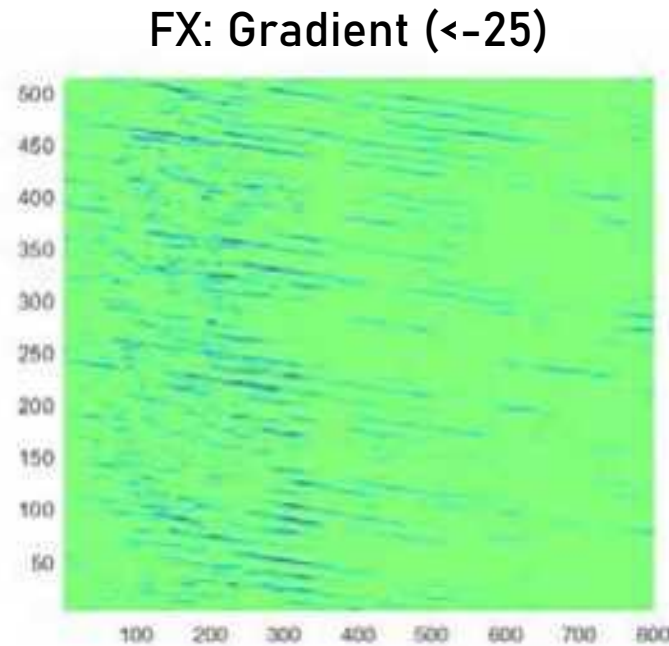
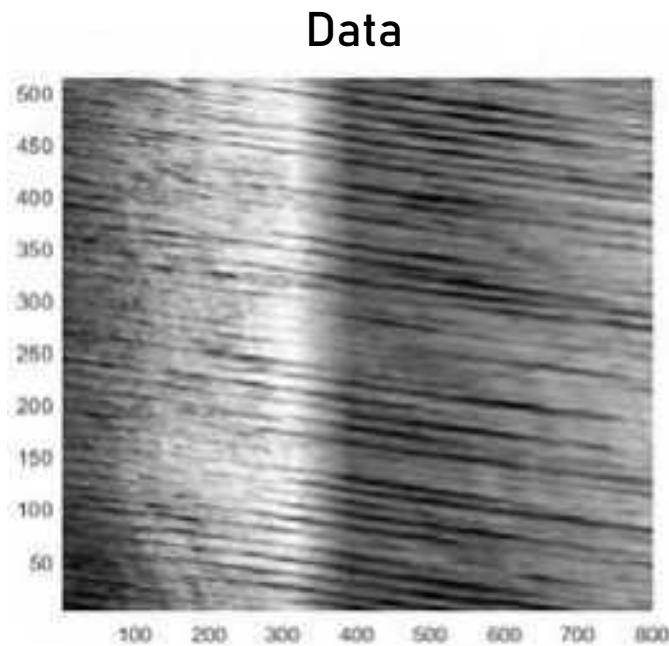
→ Image processing with SGS data to extract information

- Data is smoothed to eliminate noise (cubic smoothing spline, csaps).
- f - k spectrum is obtained by FFT
- Maxima locations are extracted and fitted with 3rd order polynomial.
- Celerity is calculated by $C = \omega/k$



Celerity by Wave Crest Tracking

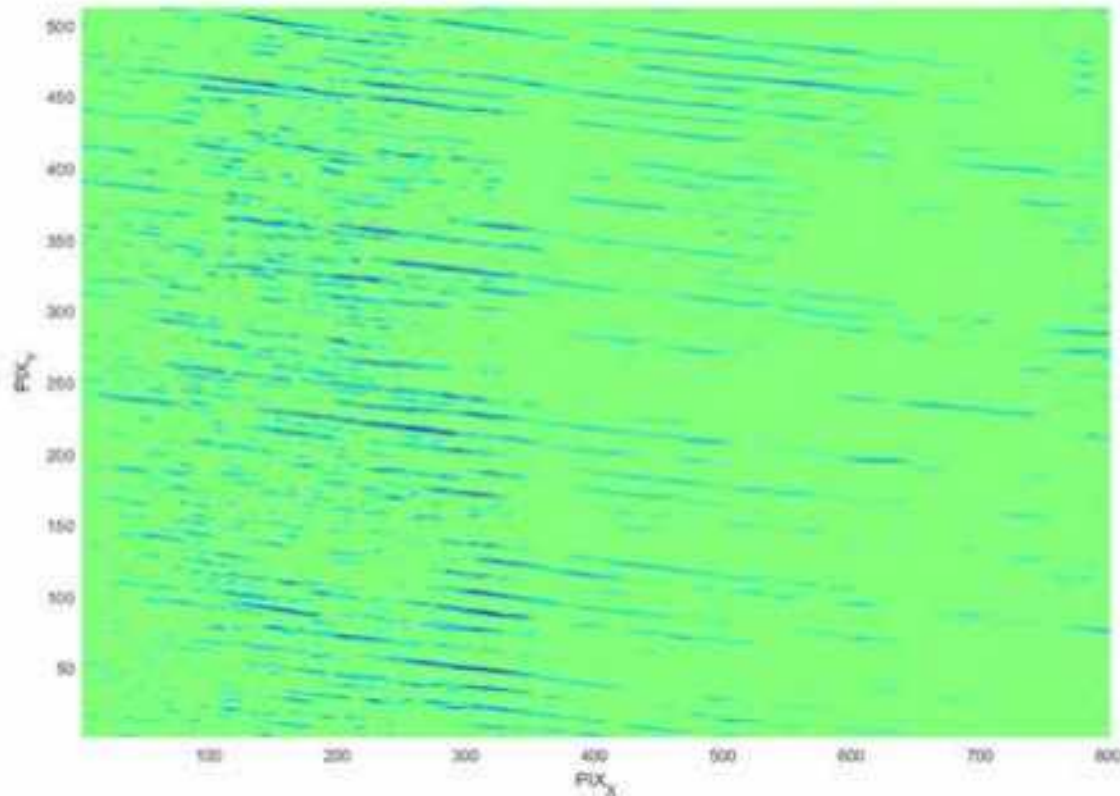
- Development of a tracking algorithm
- Two gradient matrices based on different thresholds.
 - FX2: Identification of dominant gradients.
 - FX: Collection of sample points.



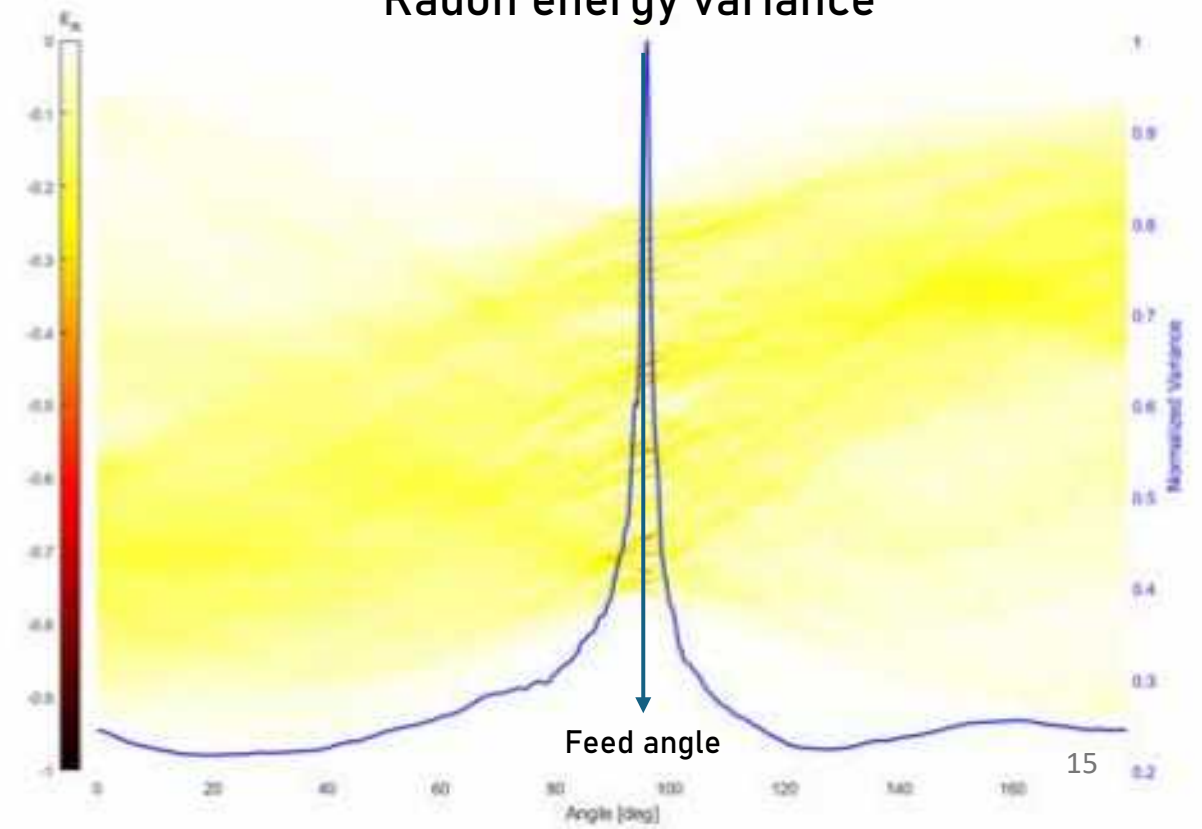
Celerity by Wave Crest Tracking

- Development of a tracking algorithm
- Two gradient matrices based on different thresholds.
 - FX2: Identification of dominant gradients.
 - FX: Collection of sample points.
 - Radon transformation to determine feed angle.

FX: Gradient (≤ -25)

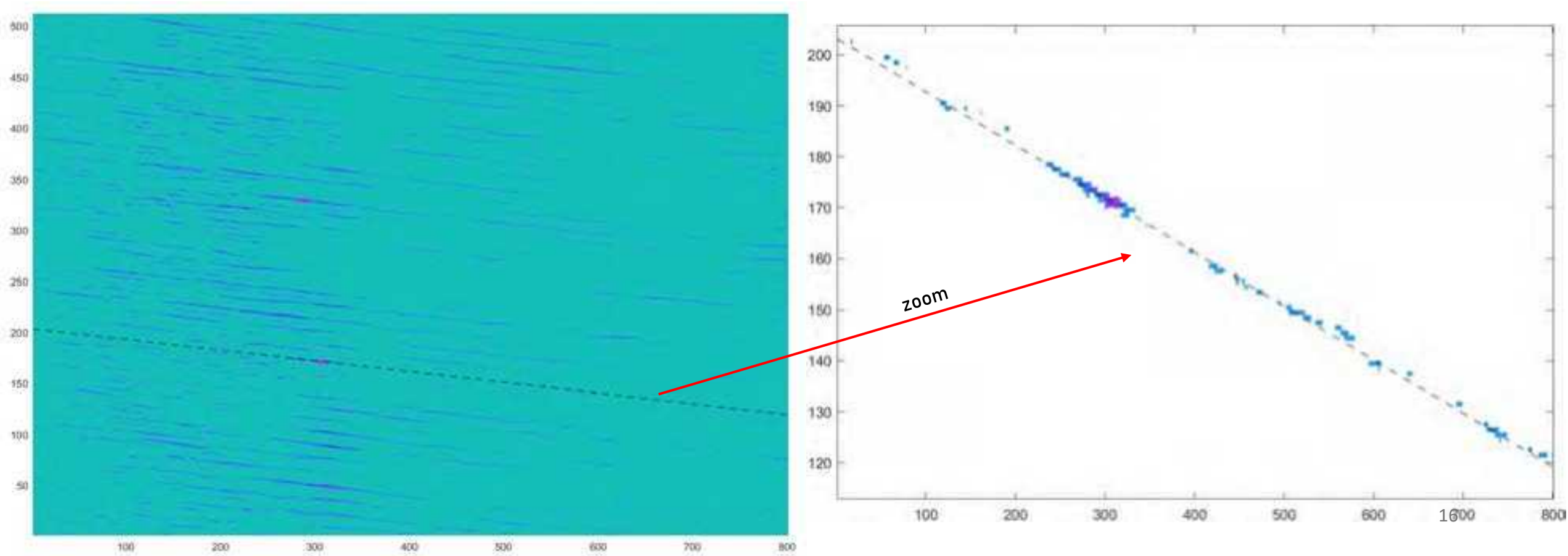


Radon energy variance



Celerity by Wave Crest Tracking

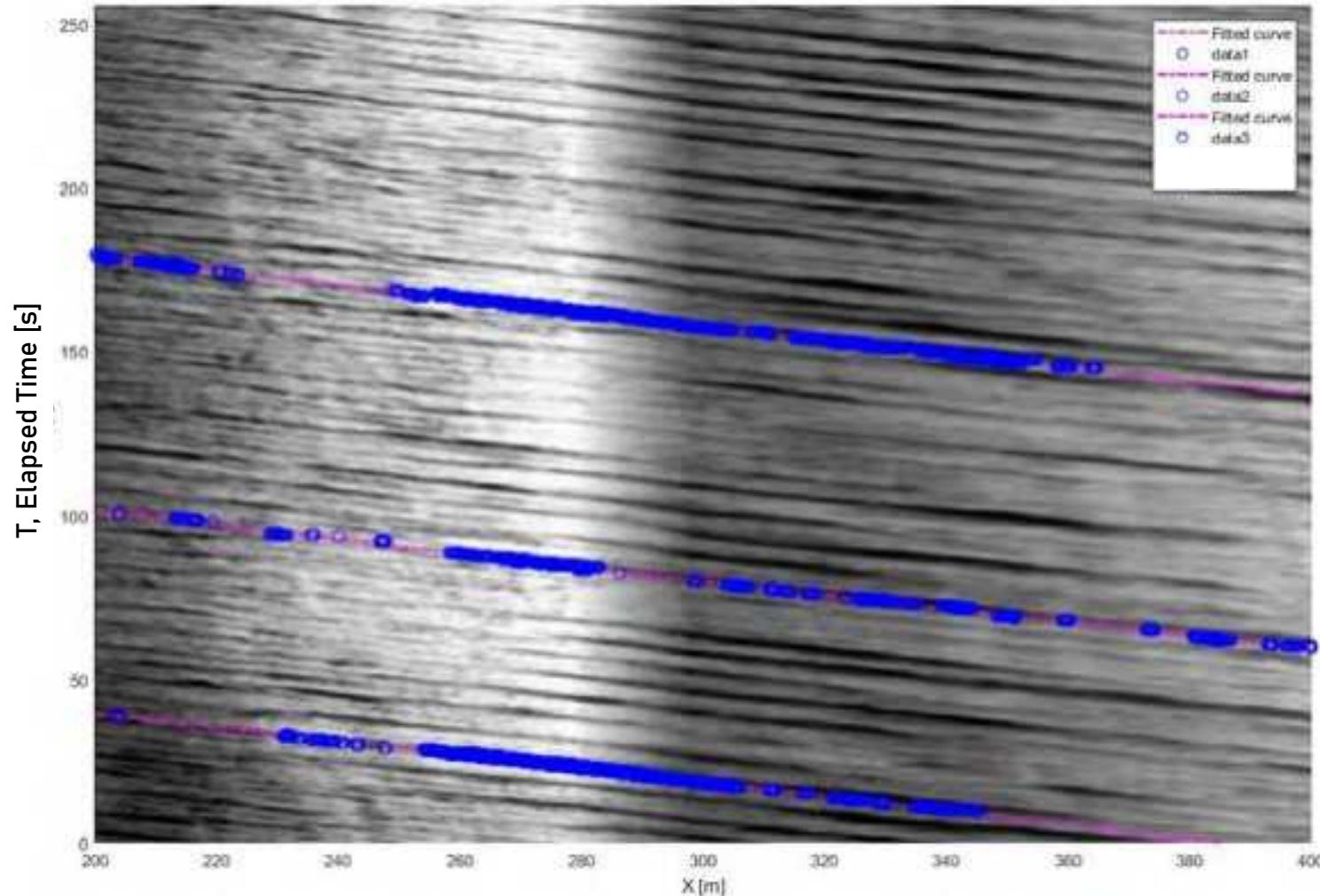
- Development of a tracking algorithm
- Approximation line constructed based on feed angle.



Celerity by Wave Crest Tracking

→ Development of a tracking algorithm

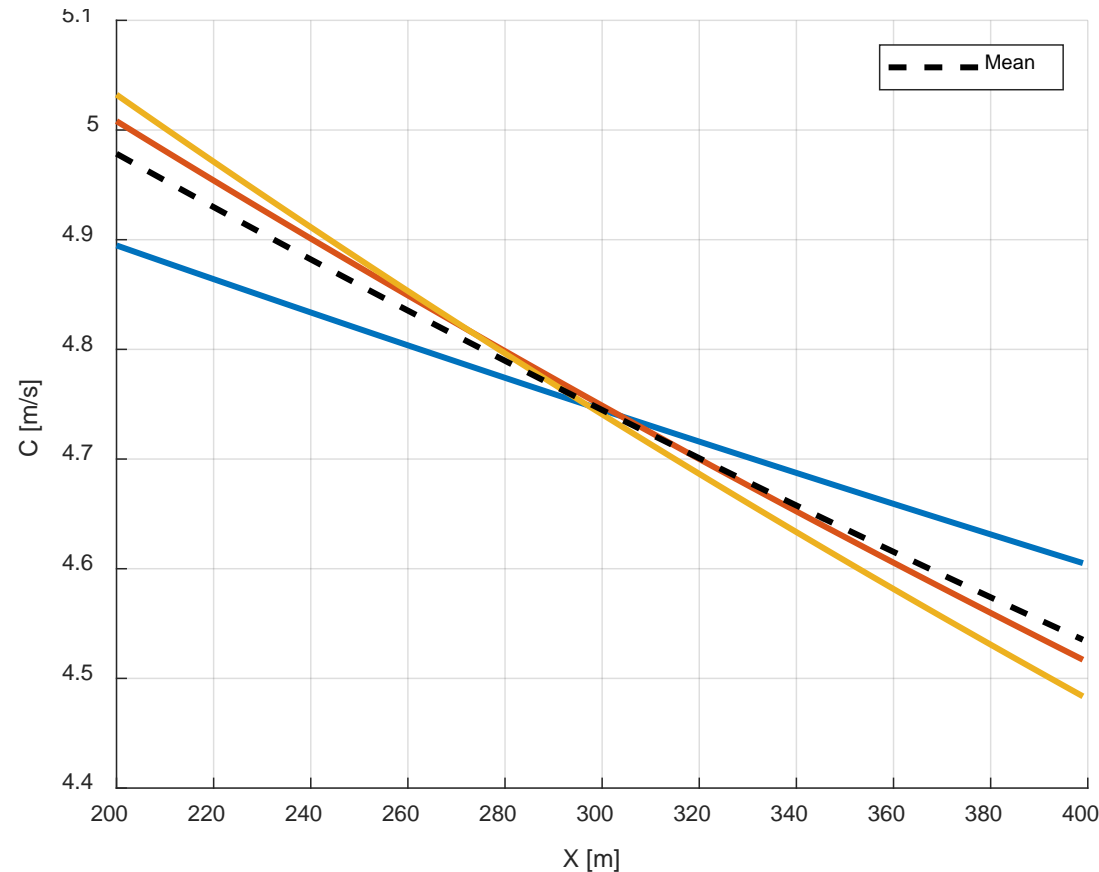
- Approximation line constructed based on feed angle.
- Fitted 2nd order polynomials for $X[m]$, $T[s]$ relation (displacement, velocity, acceleration).



Celerity by Wave Crest Tracking

→ Development of a tracking algorithm

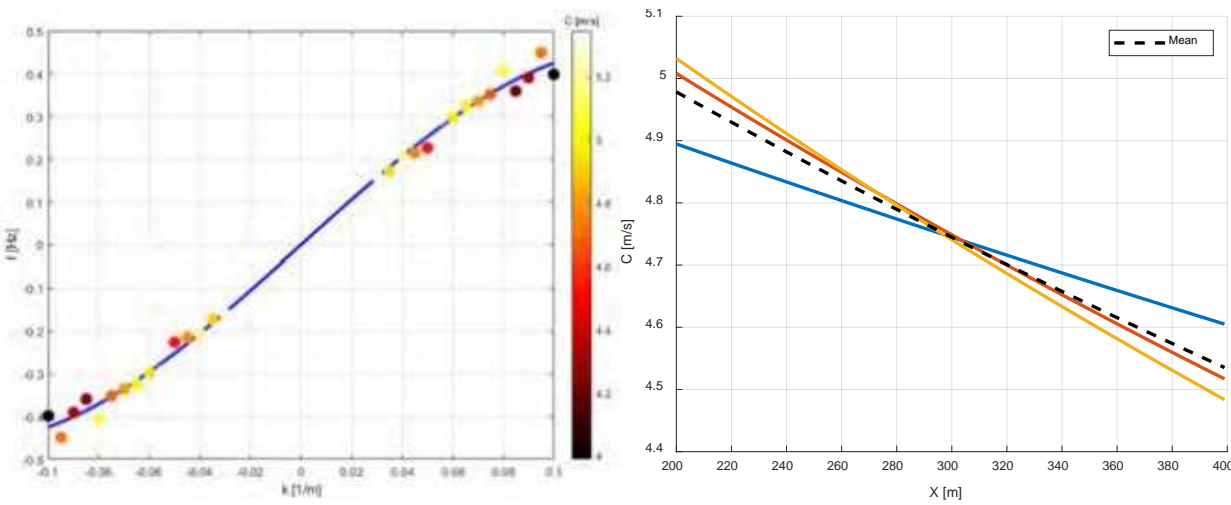
- Approximation line constructed based on feed angle.
- Fitted 2nd order polynomials for $X[m]$, $T[s]$ (elapsed time) relation (displacement, celerity, acceleration).



What is Next?

- Coupling information between methodologies.
- Flow field estimation by wave-current interaction.

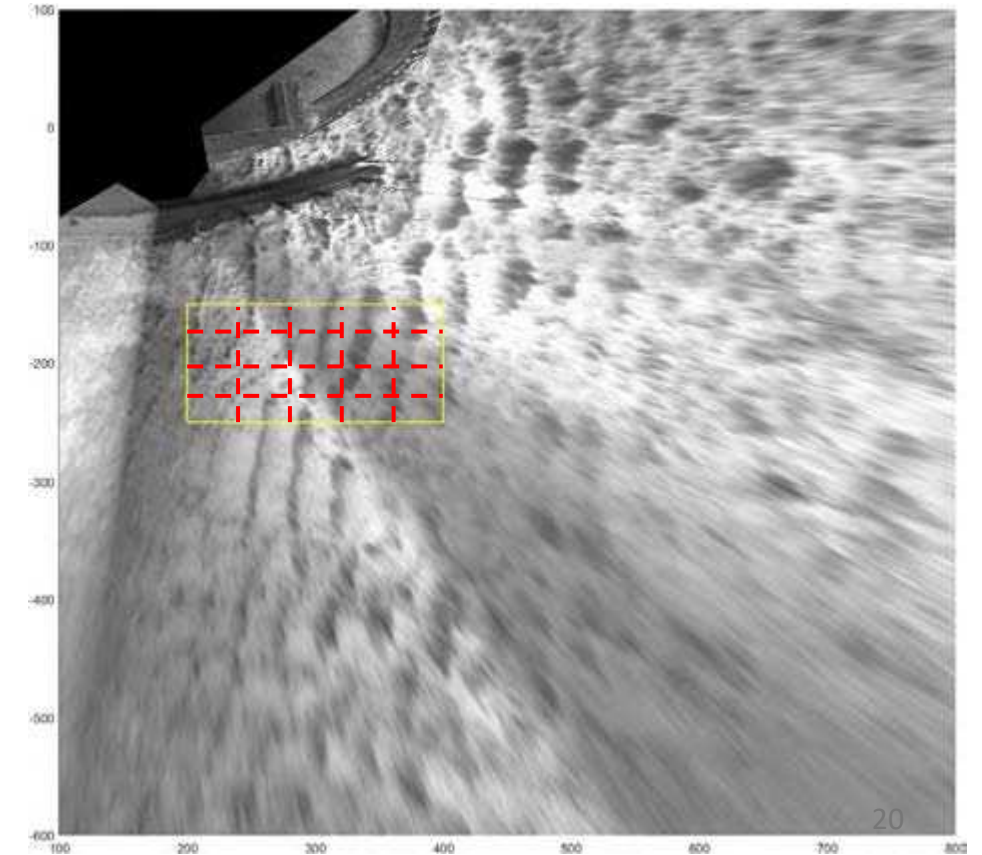
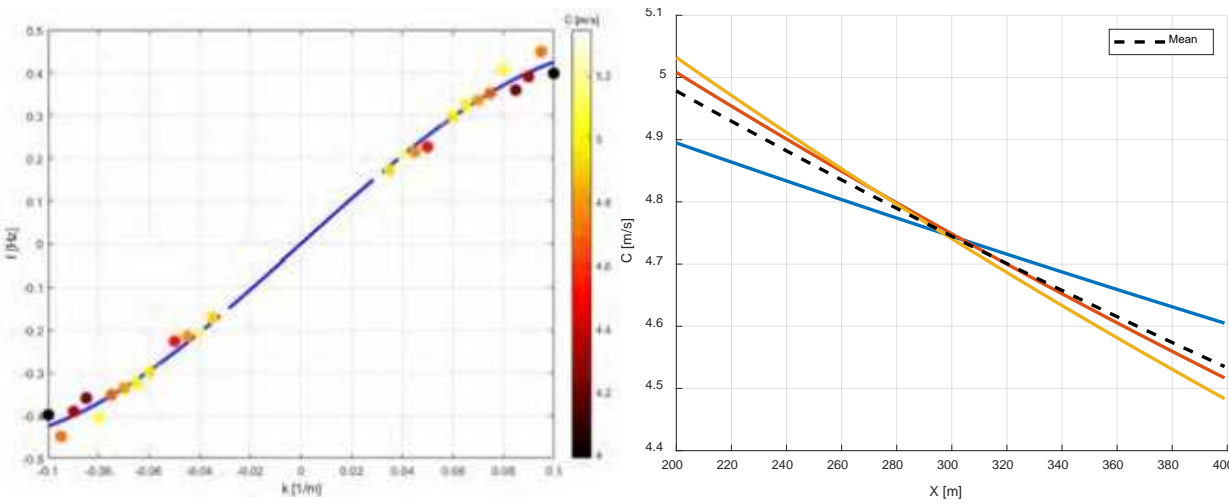
$$\sigma = \omega - \vec{k} \vec{U} \rightarrow \text{Doppler shift}$$



What is Next?

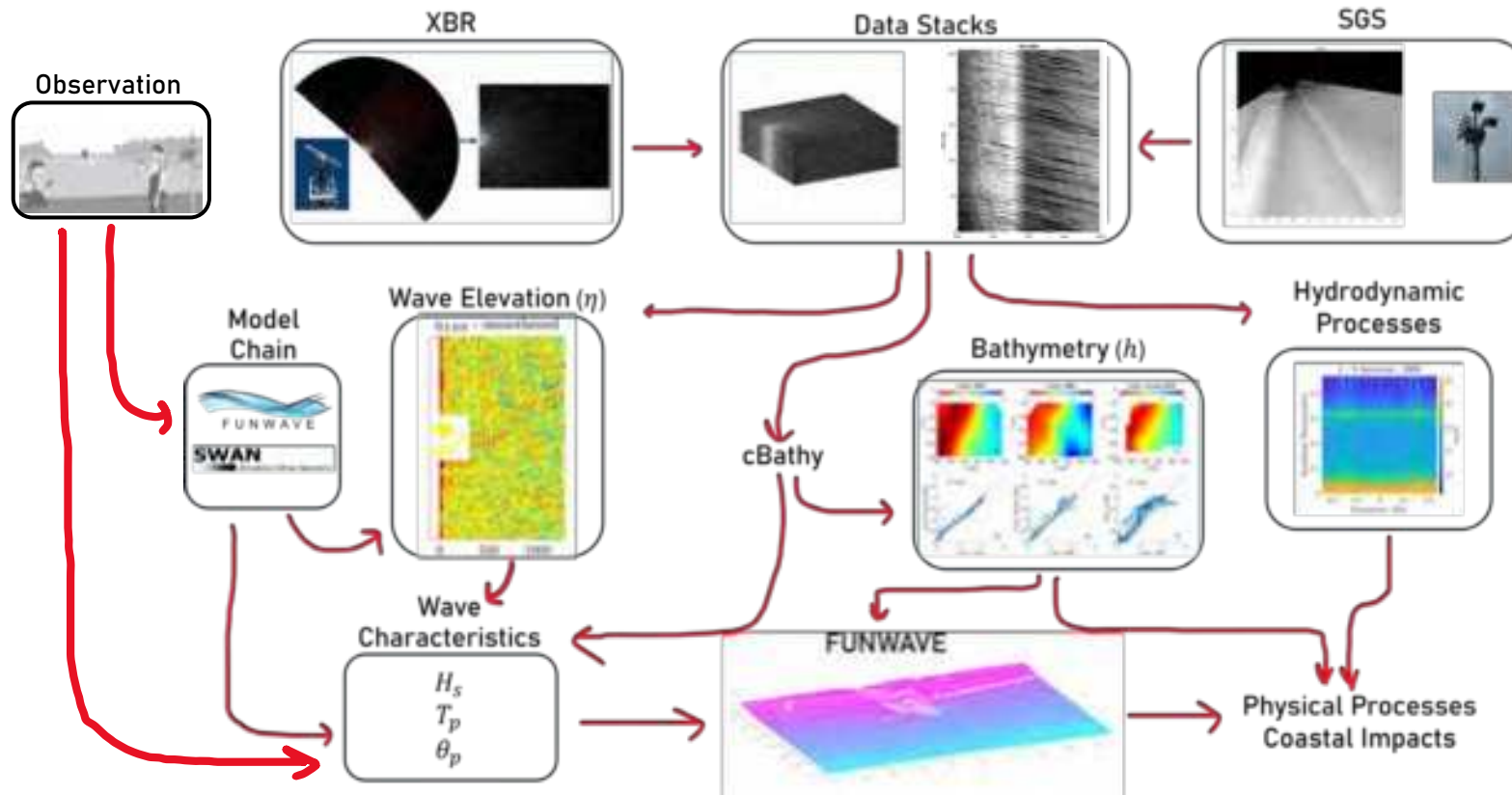
- Coupling information between methodologies.
- Flow field estimation by wave-current interaction.
- Increasing sampling to work on 2D evolution of characteristics from offshore to nearshore.

$$\sigma = \omega - \vec{k} \vec{U} \rightarrow \text{Doppler shift}$$



What is Next?

- Coupling information between methodologies.
- Flow field estimation by wave-current interaction.
- Increasing sampling to work on 2D evolution of characteristics from offshore to nearshore.
- Investigation on incorporation and combination of Artificial Intelligence (AI) to enhance performance



SEDIMARE DC MEETING

11.03.2025-13.03.2025

Santander, Spain

Nearshore Wave Processes by Remote Sensing

Muhammed Said Parlak

m.s.parlak@univpm.it

<https://sedimare.eu>

Acknowledgement: This project has received funding from the European Union's (EU) Horizon Europe Framework Programme (HORIZON) under Grant Agreement No 101072443 as a MSCA Doctoral Network (HORIZON-MSCA-2021-DN-01) of

SEDIMARE PROJECT_DC #3

Santander Meeting

TRANSPORT AND WAVE RIPPLES DEVELOPMENT OF SAND-SILT MIXTURES

PhD Candidate: Nguyen, Thi To Van (Van)

Promotor: P.C. Roos (Pieter)

Co-promotor: J.J. van der Werf (Jebbe)

Date: 2025 March 12th



Contents

1. Introduction
2. Transport and bedform development of sand-silt mixtures: the main experiments
3. Conclusion

1. Introduction

In nature, especially in coastal and fluvial systems, most of sediments are mixes of sand and fines (clay and silt).

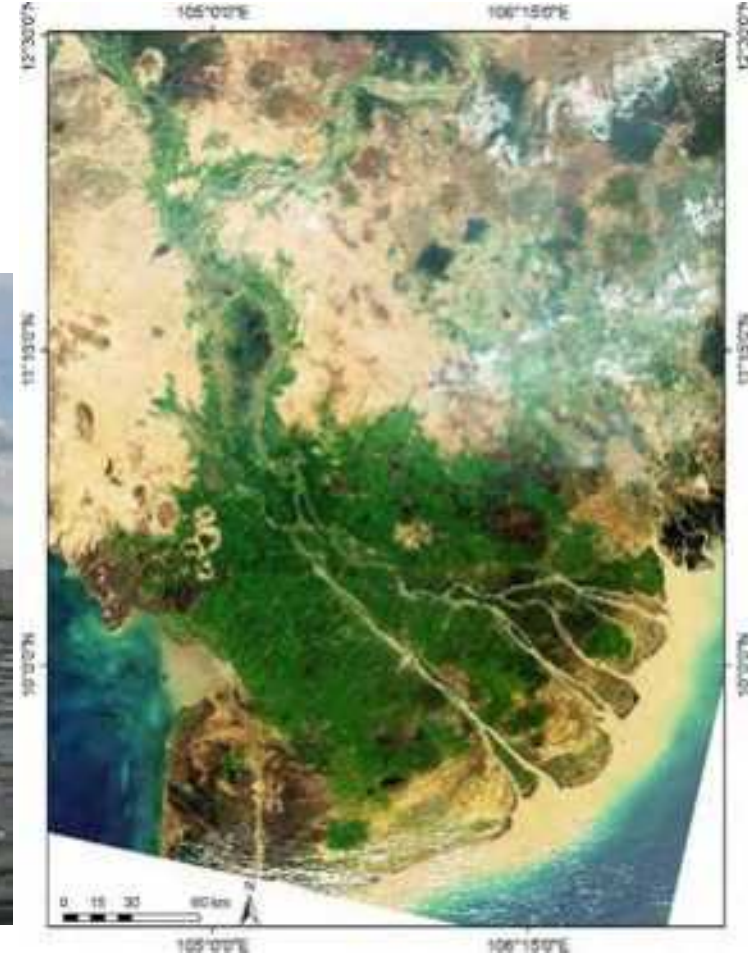
Recently, there have been more studies focusing on the transport of sand-mud mixtures. However, most of these studies treated clay and silt collectively as mud (*Mitchener and Torfs, 1996; Van Ledden, 2003; Jacobs, 2011; Winterwerp et al., 2012; Colina Alonso et al., 2023*).



Silty sediments in Mekong Delta, Vietnam
[Photo by [MangLub project](#)]

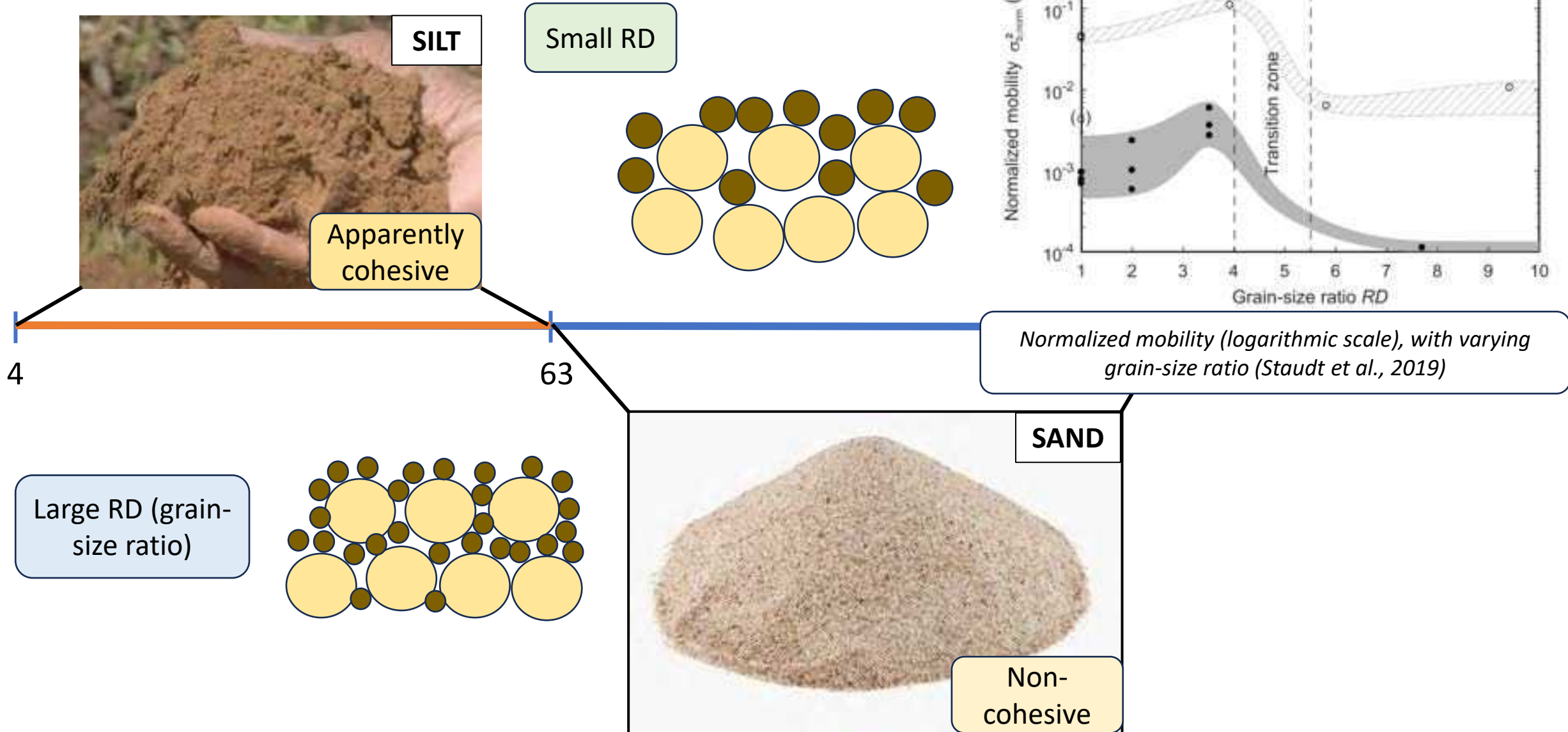


Mudflat, Wadden Sea, Netherlands.

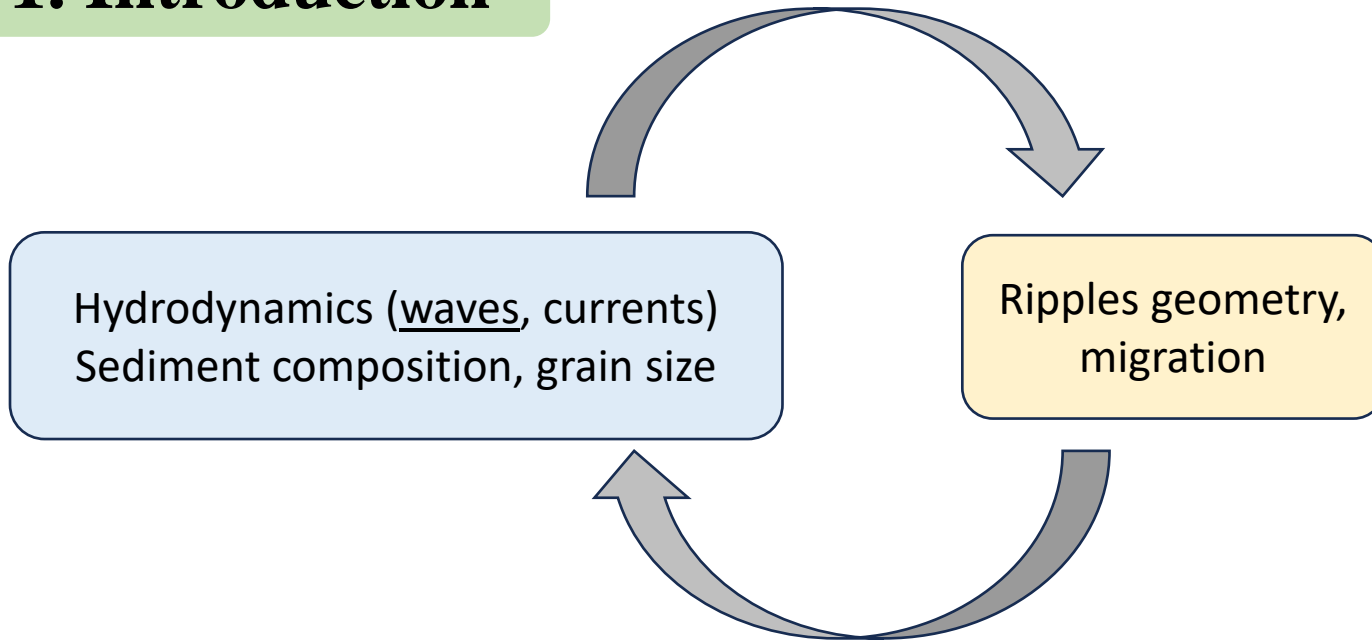


Satellite images of the Mekong Delta taken by Envisat

1. Introduction



1. Introduction

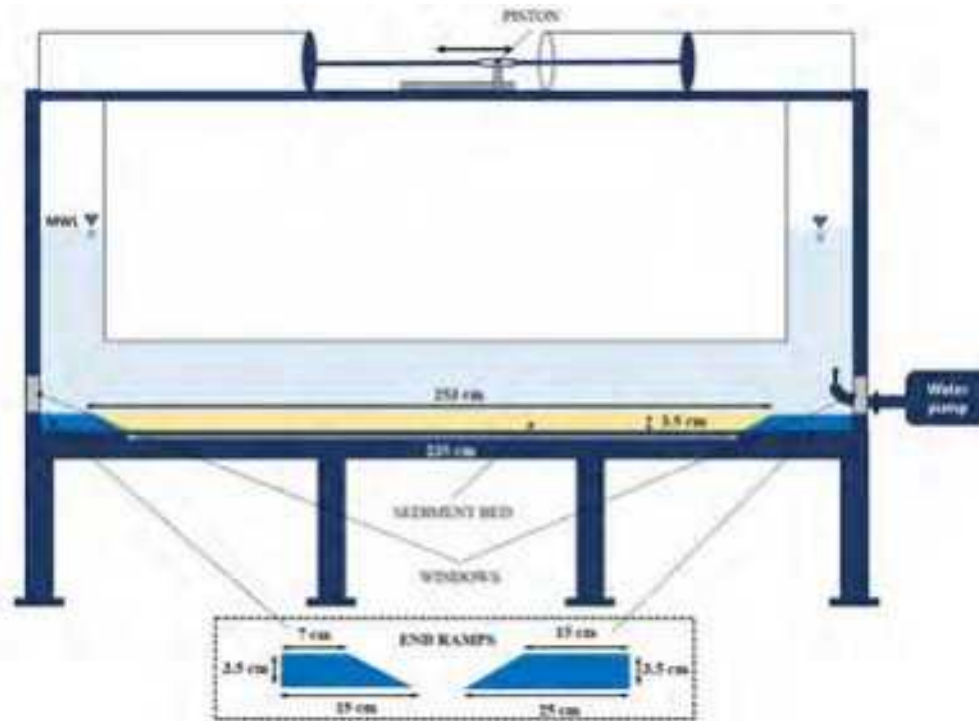


F Bed 8: 2D-3D ripples, 7·2% mud



Field examples of 2D–3D ripples (percentages denote subsurface mudcontents, the scale bar is 200 mm long (Baas et al., 2019)

2. Sand-silt experiments



Previous preparatory experiment in the Mini tunnel

Observations

Experiences

Pure-sand (after 550 cycles)

SaCs40 (after 550 cycles)

SaMs20 (after 650 cycles)

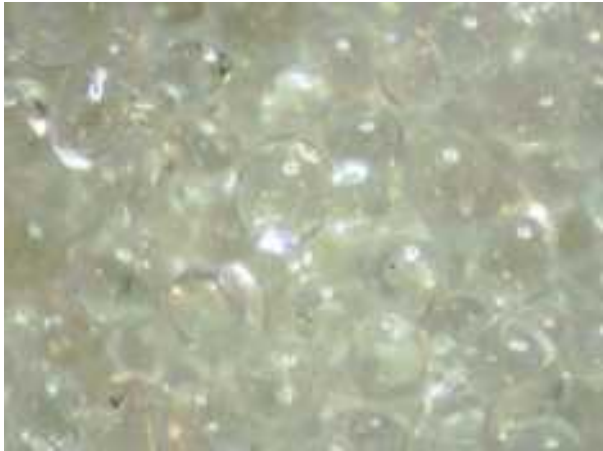
RQ1: What is the effect of silt (e.g., silt contents, grain-size ratio, compaction of the bed) on **the initial motion** of sand-silt mixtures?

RQ2: What is the effect of silt on the **transport processes** of sand-silt mixtures?

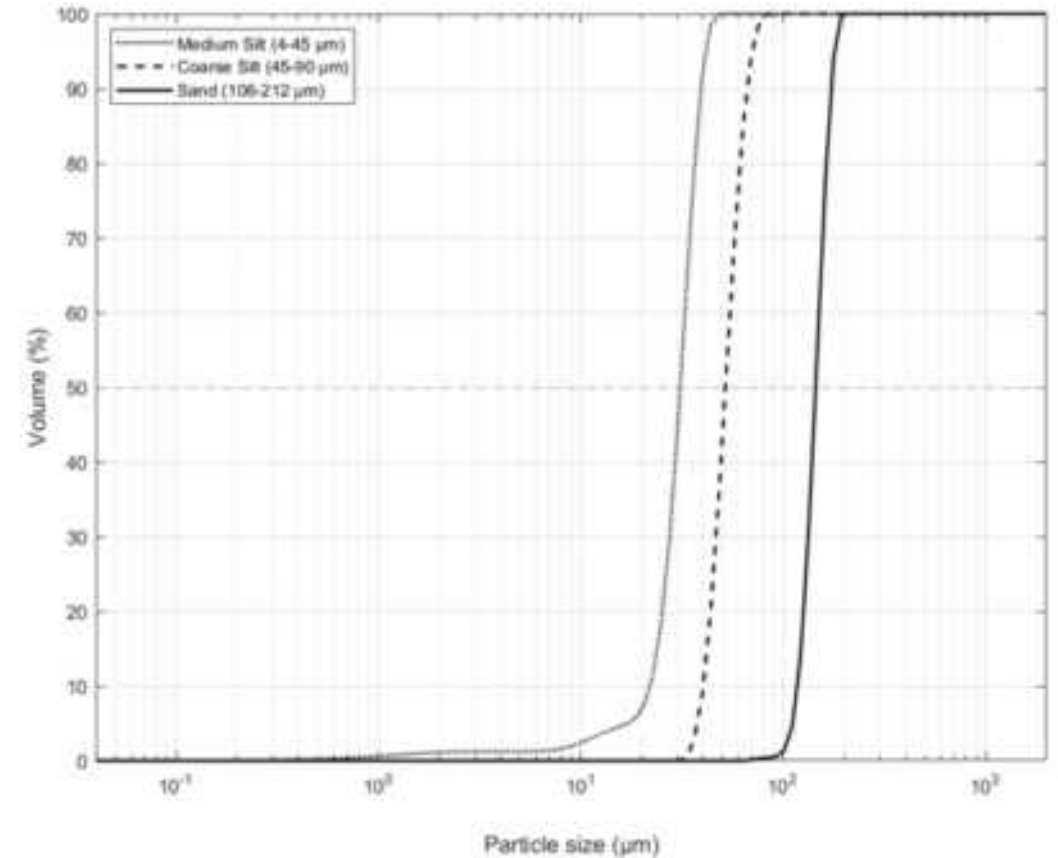
RQ3: What are the effects of silt and sand-silt interactions on the **development and geometry of bedforms**?

2. Sand-silt experiments

Sediment fractions	D ₁₀ (μm)	D ₁₆ (μm)	D ₅₀ (μm)	D ₈₄ (μm)	D ₉₀ (μm)	σ _g (-)
Medium silt	21.90	24.12	30.95	37.62	39.27	1.25
Coarse silt	40.17	42.30	51.76	62.90	66.54	1.22
Sand	117.03	123.09	144.34	167.49	173.15	1.17



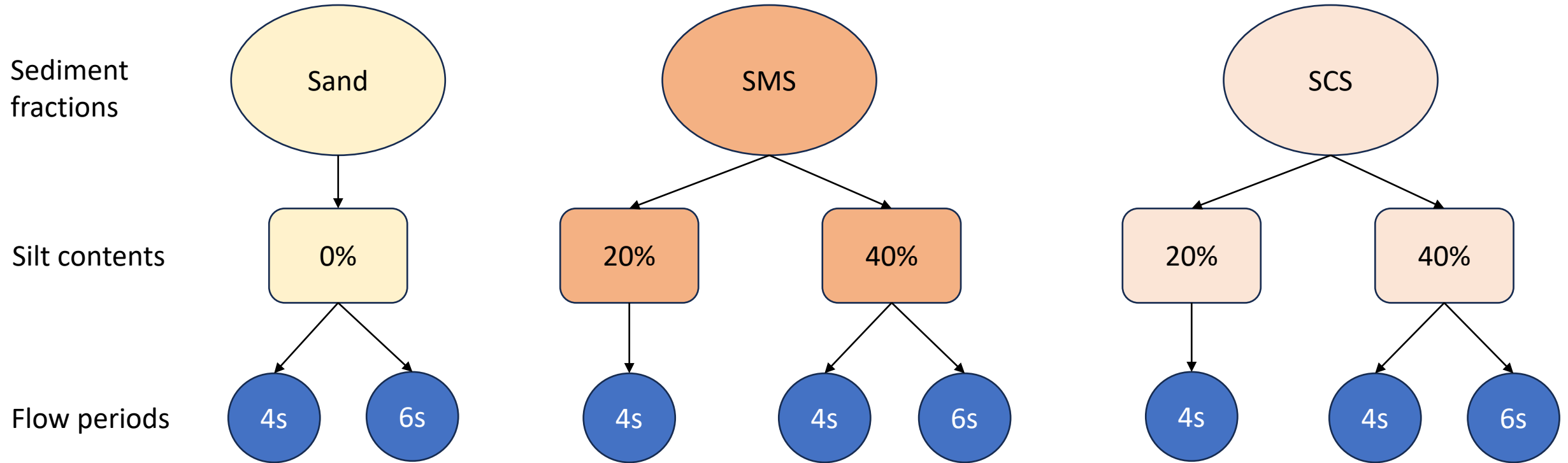
Glass Bead is a chemically inert soda lime glass that is round in shape, well-sort in distribution and has main composition is silica ($\rho_s = 2500 \text{ kg/m}^3$).



Particle-size distributions of glass beads using a laser diffraction particle size analyzer (Beckman Coulter LS13320)

2. Sand-silt experiments

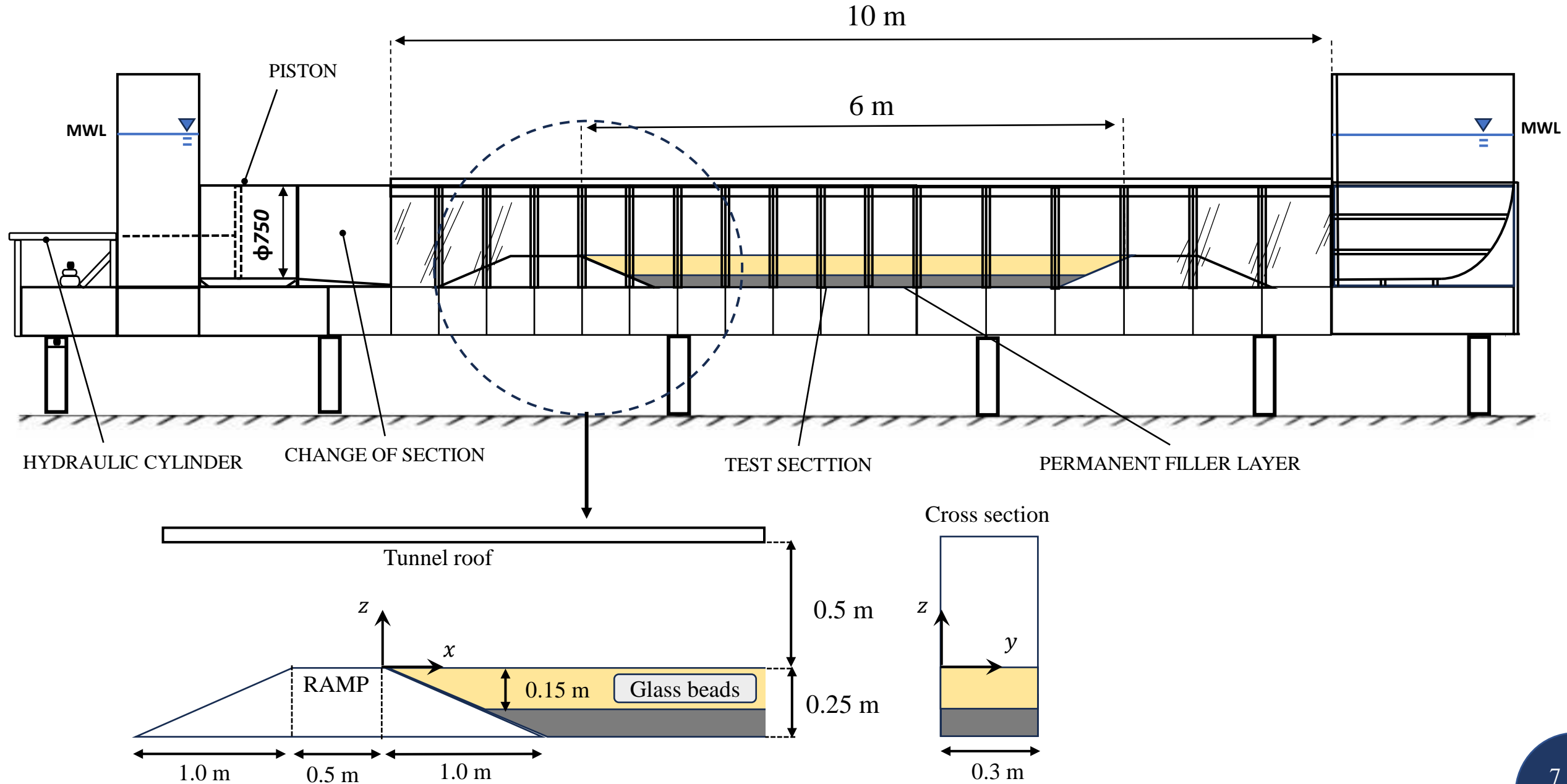
Experimental conditions



Flow velocities

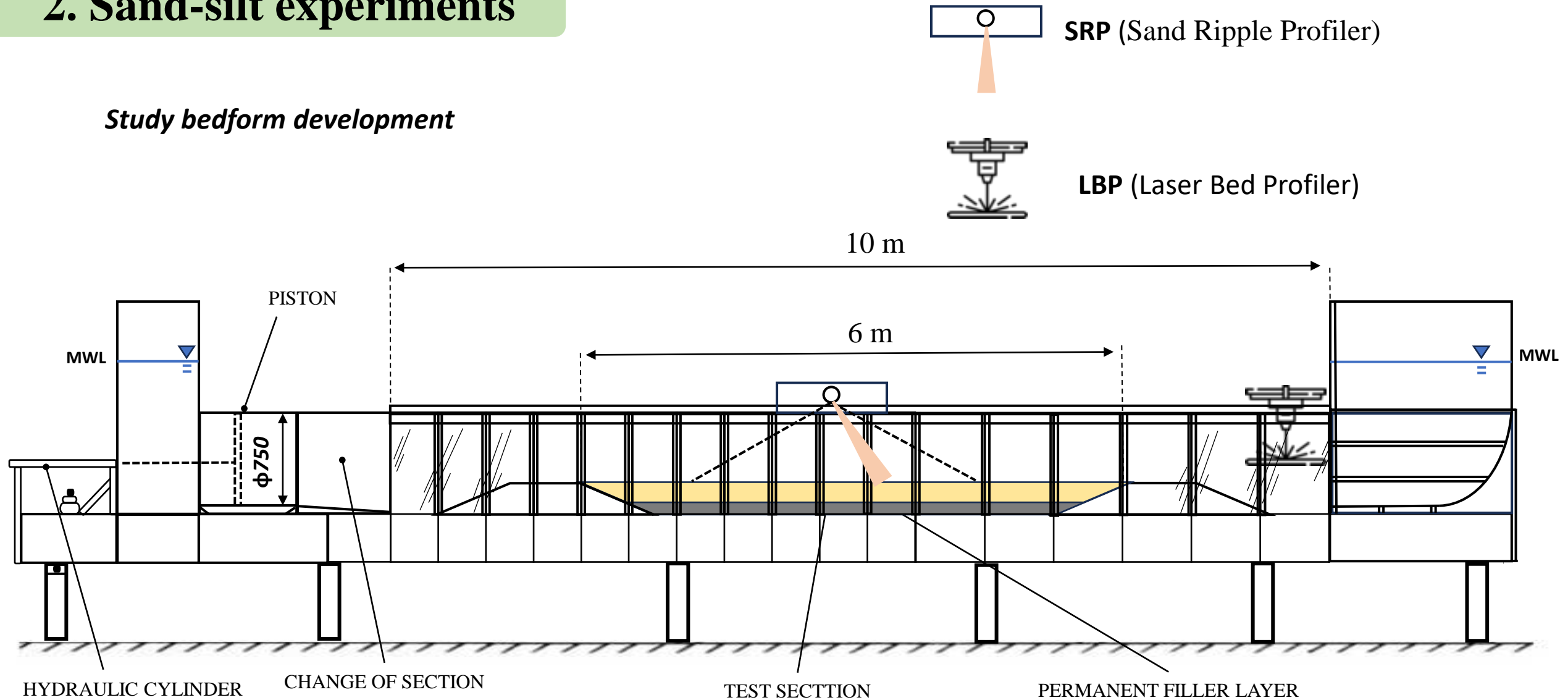
All will be tested with three velocities conditions: 0.2, 0.3 and 0.4 m/s.
=> In total, there will be 24 tests excluding some repetitions.

2. Sand-silt experiments



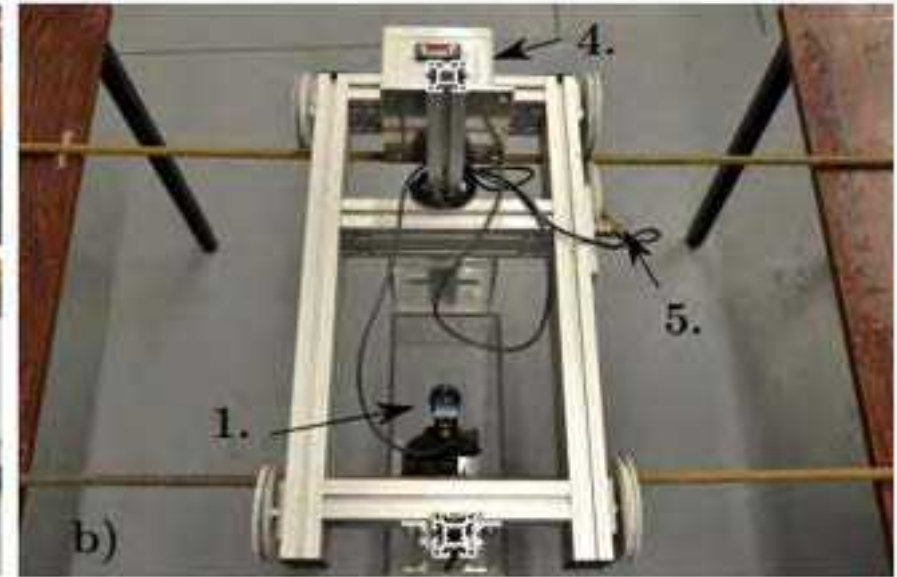
2. Sand-silt experiments

Study bedform development



2. Sand-silt experiments

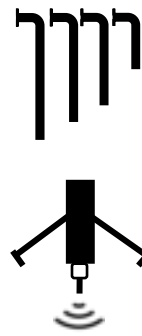
(a) In-house built Laser Bed Profiler; (b) top view of the LBP (Boscia, 2021)



(c) Sand Ripple Profiler head probe; (d) SRP tunnel mounting (pictures taken from Boscia (2021))

2. Sand-silt experiments

Detailed measurements of velocity and SSC after the bed reaches its equilibrium state

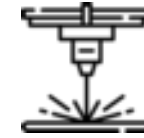


TSS (Transverse Suction System)

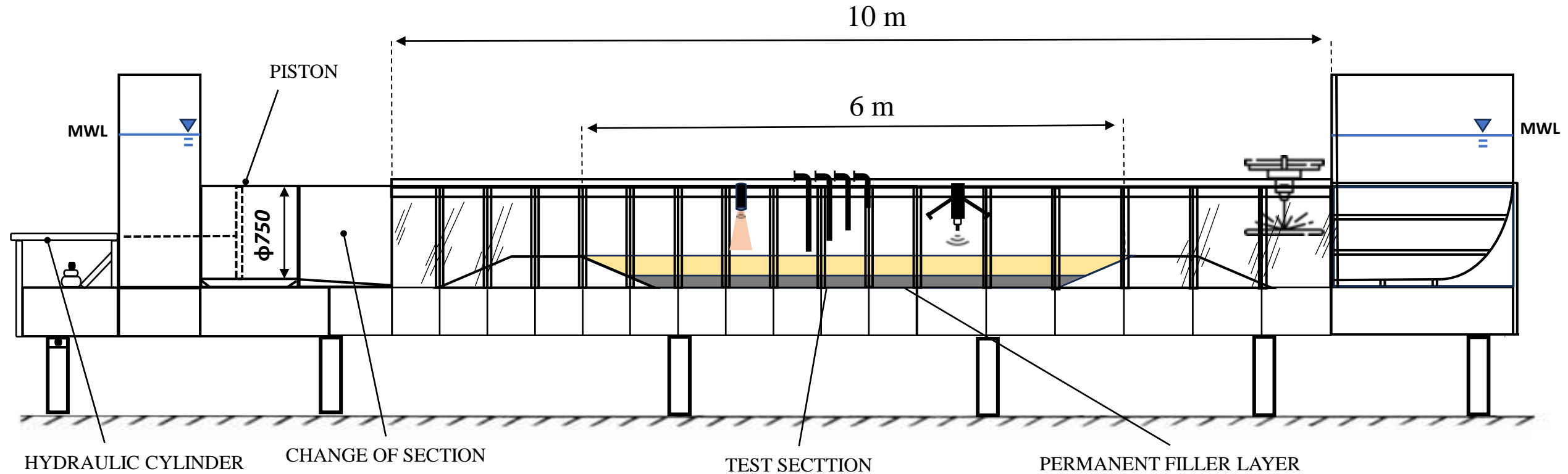
Ubertone (commercial ACVP – Acoustic Concentration and Velocity Profiler)



ABS (Acoustic Backscatter System)



Laser system



2. Sand-silt experiments

(a) TSS nozzles in position in the tunnel.
(b) Peristaltic pump (Boscia, 2021)



(a)



(b)



UB-Lab 2C main components (Boscia, 2021)

2. Sand-silt experiments

Experiment phase	Instruments	Output	Research question
Phase 1	Ubertone, ABS, TSS, camera	SSC and velocity profiles, videos.	RQ1: Initiation motions
Phase 2	SRP, LBP	Time-varying, pre- and post experiment bed levels	RQ3: Development and geometry of bedforms
Phase 3	Ubertone, ABS, TSS, LBP	SSC and velocity profiles, sand mass from traps in two ends	RQ2: Transport processes

3. Conclusion

- There is still a lack of knowledge about the effect of silt on transport and ripple characteristics in sand-silt mixtures.
- There are very few experimental studies on the development of ripples in sand-silt mixed beds.

We are now working on the main experiment and expect to finish it by July 2025.

An aerial photograph of a beach during sunset or sunrise. The water on the left shows complex, wavy sand patterns created by the receding tide. The sun is a bright, glowing orb in the upper center, casting a shimmering reflection across the water's surface. The sand on the right is a smooth, light-colored expanse.

**THANK YOU FOR YOUR
ATTENTION**



Formulating guidelines for the design of breach experiments

Siyuan Wang

s.wang-4@utwente.nl

Supervised by:

Dr. Ir. P.C. Roos (UT)

Dr. J. J. Warmink (UT)

Prof. Dr. S. Soares-Frazão (UCLouvain)

Dr. N. D. Volp (Nelen & Schuurmans)

12 March 2025



Ebrahimi et al. (2024)



This project has received funding from the European Union's (EU) Horizon Europe Framework Programme (HORIZON) under Grant Agreement No 101072443 as a MSCA Doctoral Network (HORIZON-MSCA-2021-DN-01).

Overview

1. Problem investigation
2. Research objective and steps
3. Methodology
4. Planning



Ebrahimi et al. (2024)



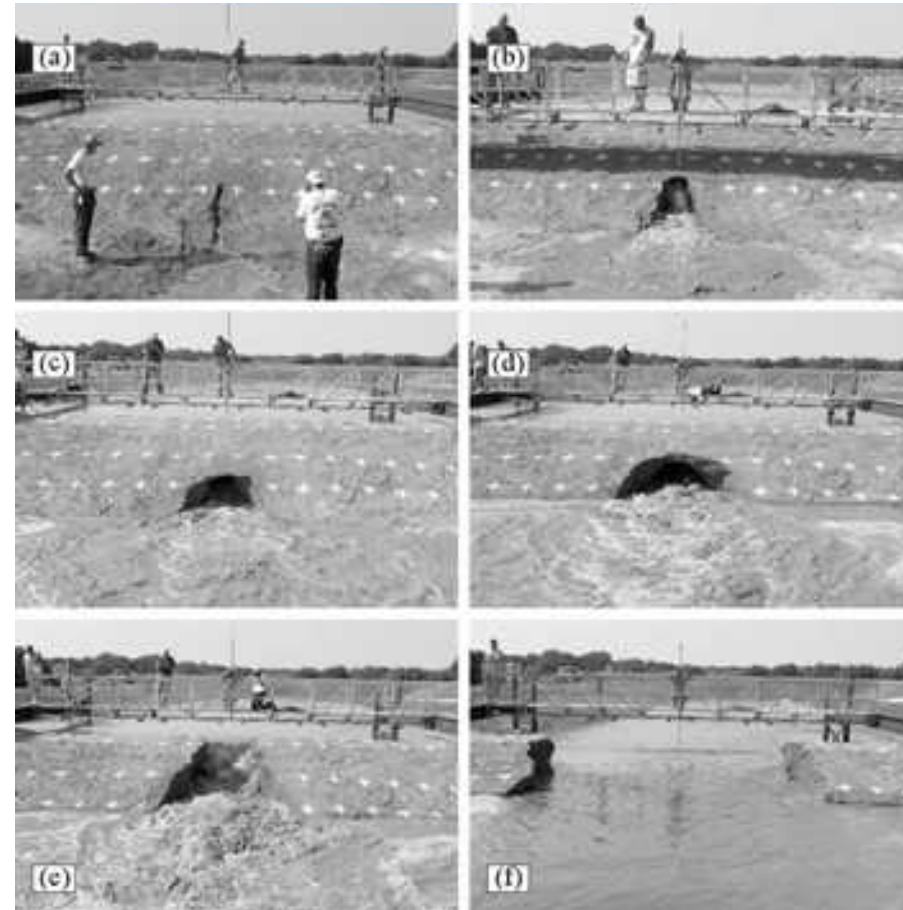
Dam breaching



Main causes: overtopping and piping



Hanson et al. (2005)

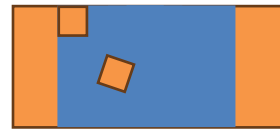


Hanson et al. (2010)

Overtopping dam breaching



Side view



Downstream view



(a) 9:10 July 31, 2018



(b) 9:30 July 31, 2018



(c) 9:40 July 31, 2018



(d) 10:00 July 31, 2018



(e) 10:15 July 31, 2018



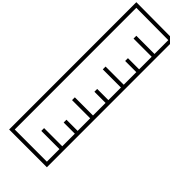
(f) 10:50 July 31, 2018

dam breach process of Sheyuegou Dam in China

Overtopping dam breaching experiments

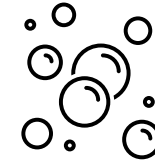
Scale

- Small scale < 1m
- Medium scale 1m – 3m
- Large scale > 3m



Cohesion

- Non-cohesive
- Cohesive
- Wide grain size distribution



Hydraulic forcing

- Constant inflow
- Constant upstream water level



Measurements

- Photogrammetry
- Laser-sheet
- Ultrasonic gauges
- ...



Problem statement

Key challenges

- Lack of parameterization
- Differences in experiment setups
- Lack of systematic criteria
- Challenge of measuring the key variables

Consequences

- Hindered model calibration and validation
- Reduced comparability of results
- Difficult in deriving reliable and generalized conclusions

Problem

Absence of systematic guidelines for overtopping dam breaching experiments to repeat the same experiment



Main goal:

Develop **systematic guidelines** for overtopping dam breaching **experiments** to standardize experimental **setup procedures** and provide clear **decision criteria**, ensuring experiments provide reliable, comparable, and sufficient data for **numerical model** calibration and validation.

Design step 1: What are the current practices and methodologies used in dam breaching experiments?

Design step 2: How can dam breaching experiments be systematically designed to better support numerical modelling?

Design step 3: Do the guidelines clearly explain how to design dam breaching experiments and provide parameters for modelling?

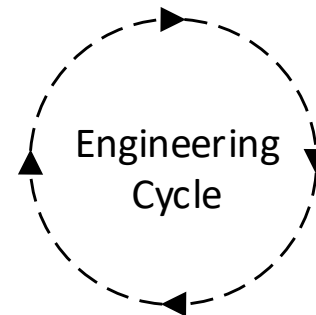


**D1/D5 Problem Investigation /
Implementation Evaluation**

- Stakeholders? Goals?
- Mechanisms? Effects?
- Lack of contribution to goals?

D4 Treatment Implementation

- Utilize in practice!

**D2 Treatment Design**

- Specify requirements!
- Requirements contribute to goals?
- Available treatments?
- Design new ones!

D3 Design Validation

- Effects of treatment in this context?
- Effects satisfy requirements?
- Trade-offs?
- Sensitivity for different contexts?

Design step 1: What are the current practices and methodologies used in dam breaching



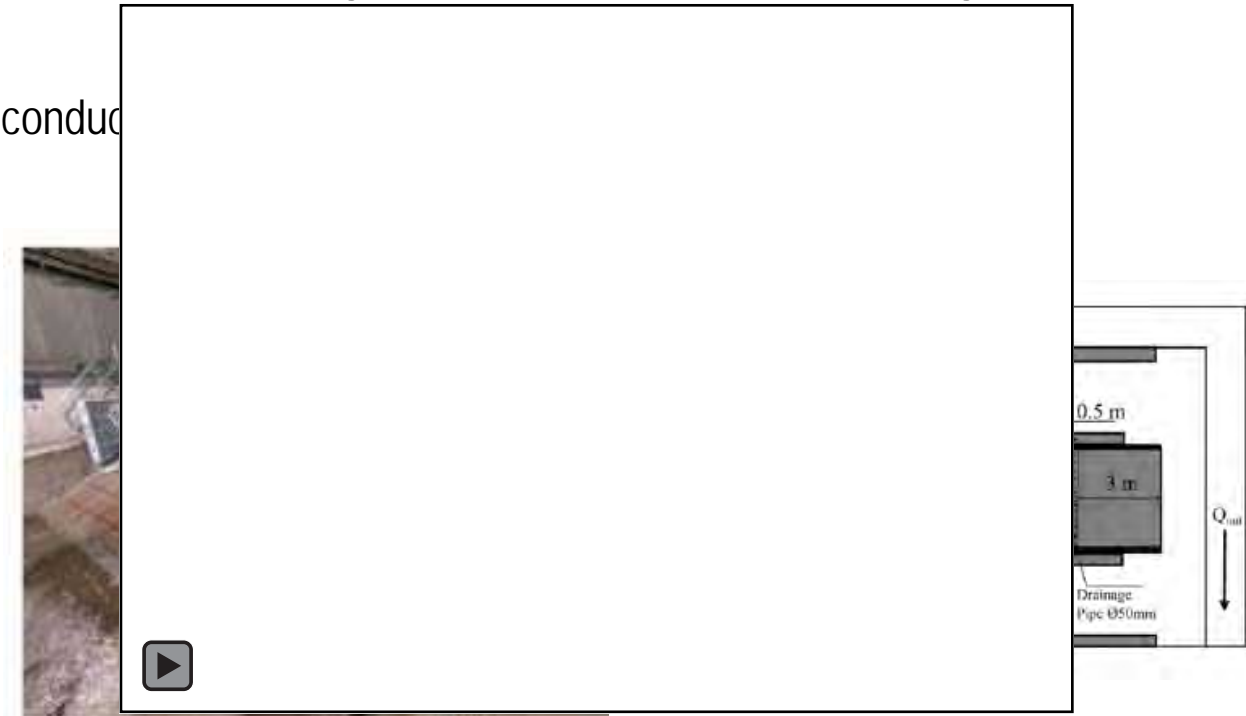
Small scale

Non-cohesive

Constant inflow

Laser-sheet, Current meter and Water level gauges

Delpierre et al. (2024)



Medium scale

Non-cohesive

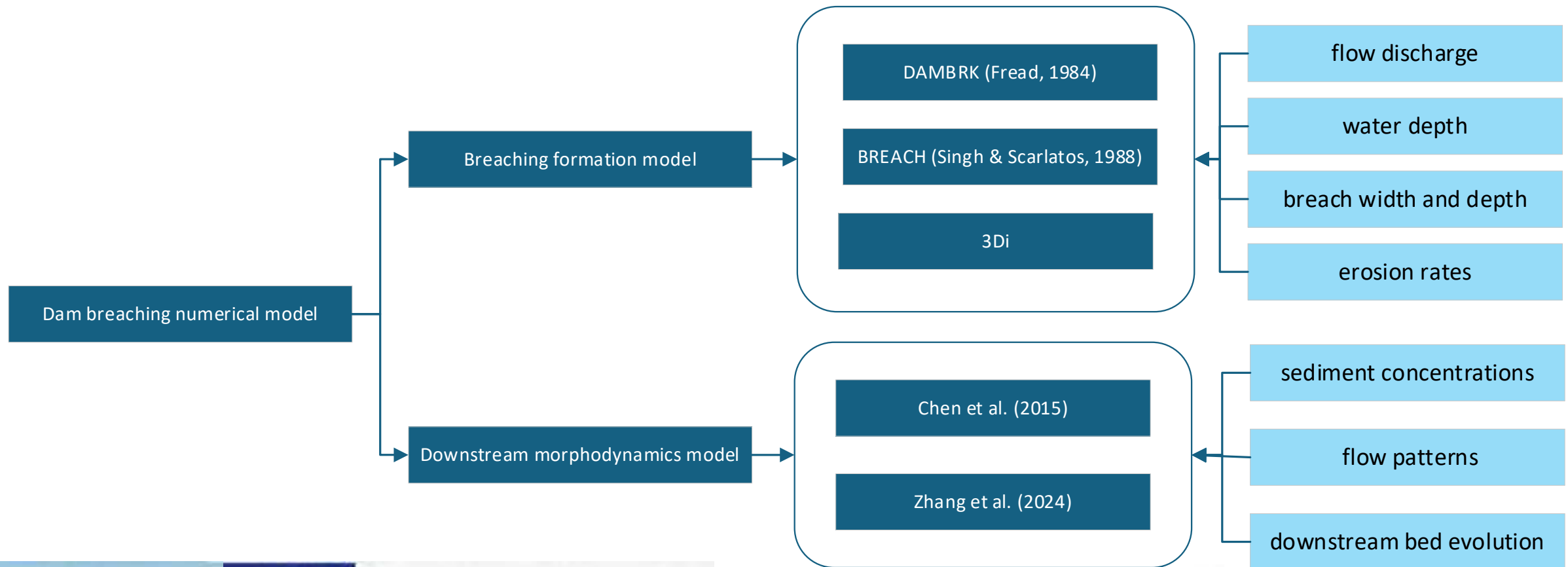
Constant water level or constant inflow

Photogrammetry, Pore pressure, Hydrostatic and Ultrasonic gauges

Ebrahimi et al. (2024)

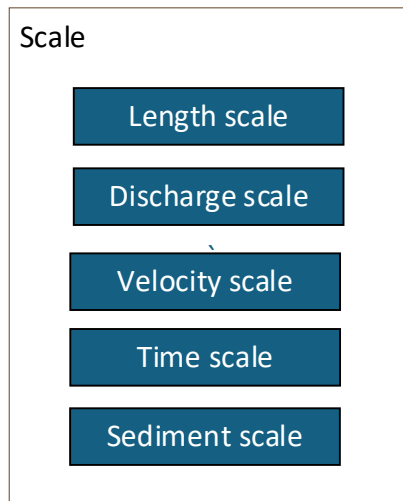
Design step 1: What are the current practices and methodologies used in dam breaching experiments?

b. What **parameters** are required to meet the needs of different types of **numerical modelling**?



Design step 2: How can dam breaching experiments be systematically designed to better support numerical modelling?

a. How can **experimental dimensions** be defined, and how can data from different scales be normalized?



Dynamic similarity: Froude similarity

$$Fr = \frac{V}{\sqrt{gL}}$$

$$\lambda_L = \frac{L_{model}}{L_{prototype}}$$

$$\lambda_V = \lambda_L^{0.5}$$

$$\lambda_t = \lambda_L^{0.5}$$

$$\lambda_Q = \lambda_L^{2.5}$$

Design step 2: How can dam breaching experiments be systematically designed to better support numerical modelling?

- b. How can **measurement settings** and techniques be effectively selected?
- c. What **procedural steps** are necessary to ensure experimental setups are consistent, reliable, and reproducible?

Procedural steps

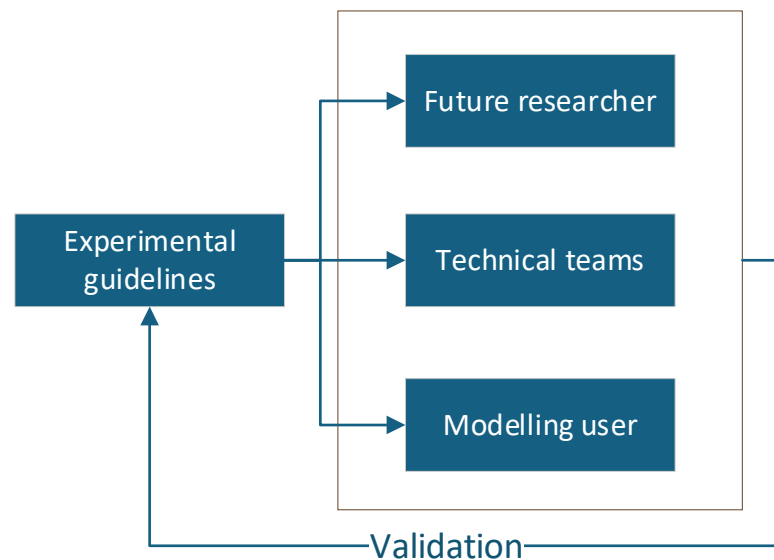
Construction dams

Calibrating
measurements

Controlling
hydraulic forces

Design step 3: Do the guidelines clearly explain how to design dam breaching experiments and provide parameters for modelling?

- a. How effectively does the **guidelines** provide a systematic approach to **designing** dam breaching **experiments** with comparable results across different scales?
- b. To what extent do the experimental results provide sufficient **parameters** for calibration and validation of **numerical models**?



- Reliability
- Repeatability
- Scalability
- Feasibility

D	Task	2025												2026			
		2	3	4	5	6	7	8	9	10	11	12	1	2	3	4	
1a	Current experiments review																
1b	Numerical modelling review																
2a	Dimension define																
2b	Measurements setting																
2c	Procedural setup																
3a	Validation through experiments																
3b	Ensure sufficient results availability																
	Experiment participate and test																
	Writing																
	Defence																



Formulating guidelines for the design of breach experiments

Siyuan Wang
s.wang-4@utwente.nl

Supervised by:

Dr. Ir. P.C. Roos (UT)

Dr. J. J. Warmink (UT)

Prof. Dr. S. Soares-Frazão (UCLouvain)

Dr. N. D. Volp (Nelen & Schuurmans)

12 March 2025



Ebrahimi et al. (2024)



This project has received funding from the European Union's (EU) Horizon Europe Framework Programme (HORIZON) under Grant Agreement No 101072443 as a MSCA Doctoral Network (HORIZON-MSCA-2021-DN-01).

Santander Workshop

Characterization of stratification and near-bed dense layers in high-density sediment-laden flow

D.C 9- Eloah Rosas

Promoter

Benoît Spinewine

Sandra Soares



This project has received funding from the European Union's (EU) Horizon Europe Framework Programme (HORIZON) under Grant Agreement No 101072443 as a MSCA Doctoral Network (HORIZON-MSCA-2021-DN-01).



UCLouvain



Sediment transport shapes coastlines, sustains ecosystems, and challenges engineering—understanding its dynamics is key to predicting and managing our changing environment.



High-Density Sediment Laden Flow

Sediment-laden flow is characterized by unsteady, highly dense sediment concentrations and vertical stratification.

High-density sediment-laden flows is common in natural systems like rivers, deltas and coastal environments, and it can be initiated by natural or anthropogenic factors in the marine environment, such as:

**Tsunamis, Earthquakes, Storms waves,
Submarine Landslides, Dredging.**



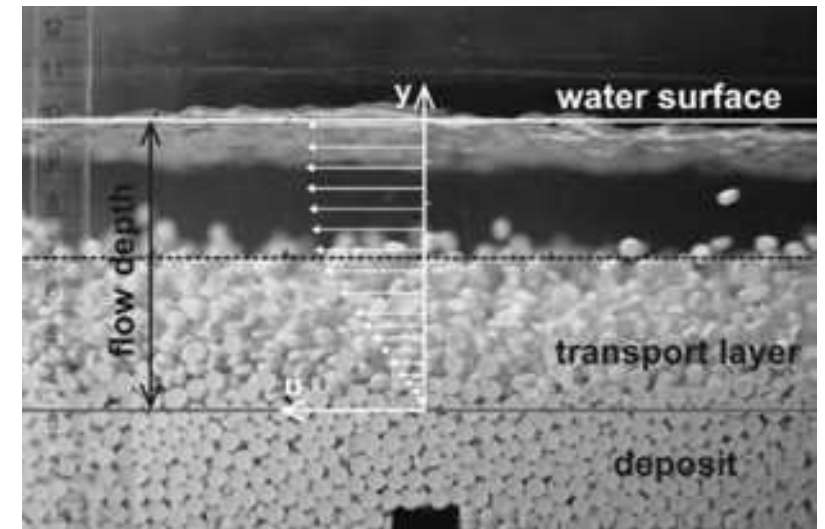
High Density Sediment Laden



Debris Flow



Turbidity Flow



Sheet Flow

Threats of High-Density Sediment Laden



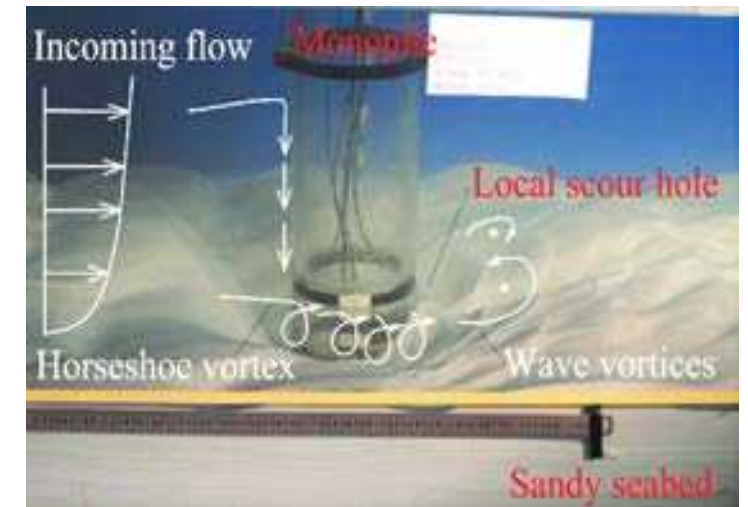
Damage Power Cables and Pipelines

Turbidity currents
debris flows
submarine landslides



Shoreline Retreat or Dune Instability

Storm induced sheet flow



Gao, F., & Qi, W. (2022).

Local Scour hole around Infrastructures

Waves-induced flow

Sheet Flow: High-Density Sediment Flow

Sheet flow occurs when intense shear stress mobilizes a dense, near-bed sediment layer, creating a high-concentration transport regime.

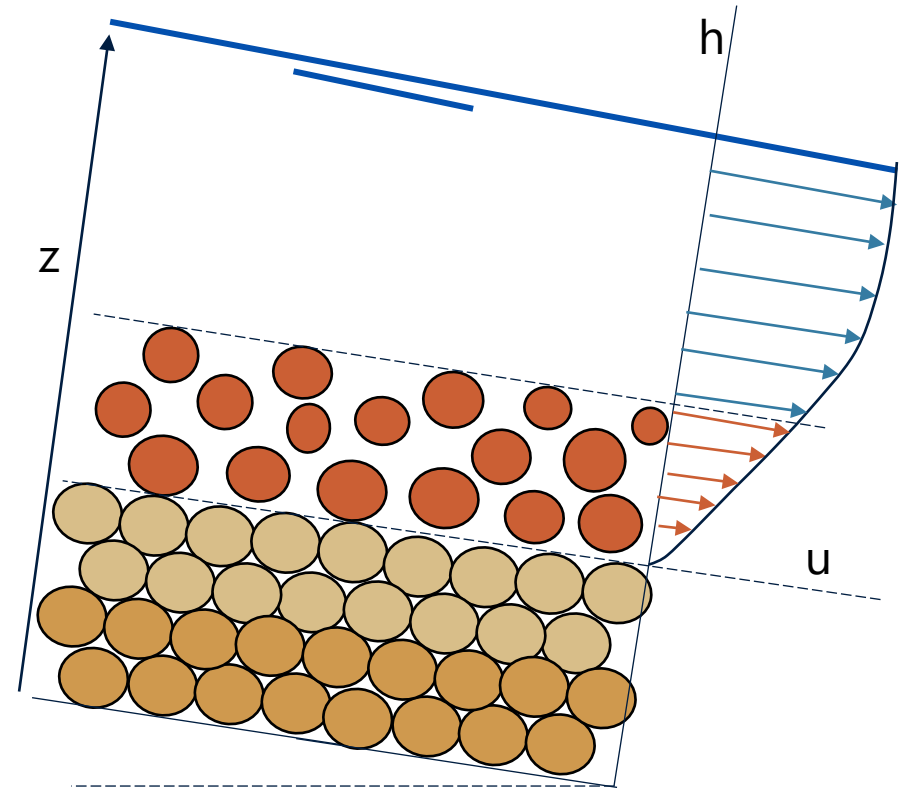
1. Vertical Density Structure

- Composed of two layers:
 - A **dense, mobile sediment layer** near the bed.
 - An **upper clearer water layer** free of sediment

2. Velocity Profile

- **Near-bed velocity is close to zero**, increasing with height.
- **Logarithmic velocity distribution** in the water layer.
- **More linear velocity profile** within the transport layer.

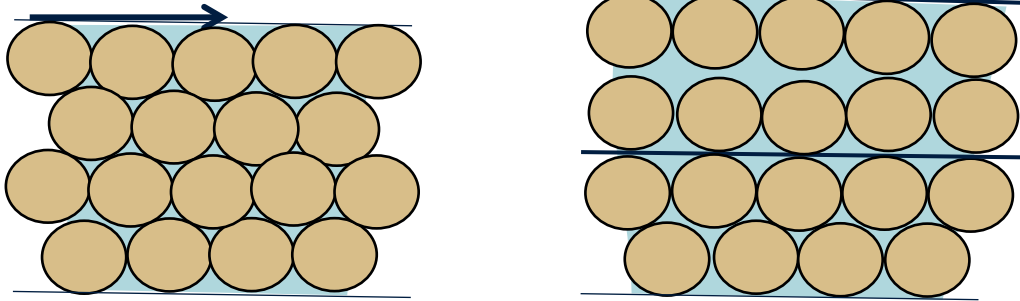
3. Dilatancy & Particle Mobility



Process Governing Vertical layer Granular Dilatancy

Dilatancy refers to the increase in volume or expansion of the sediment matrix when the sediment undergoes shear deformation.

Inflow of water



Key Factors Affecting Flow Dynamics:

1. Pore Pressure Relaxation Effect

When sediment is sheared, pore pressure can fluctuate. Relaxation of pore pressure may reduce resistance between particles, facilitating flow in the sediment bed.

2. Suspension

As the sediment undergoes shear deformation, fine particles may become suspended in the flow

3. Vertical Mass and Momentum Exchange

The exchange of mass and momentum between the sediment bed and the overlying fluid layer impacts the velocity profile of the flow.

Turbidity Flow: Gravity-Driven Sediment Transport

Turbidity currents are sustained by a **density contrast** between sediment-laden water and the surrounding fluid, allowing them to propagate under gravity.

1. Density Stratification

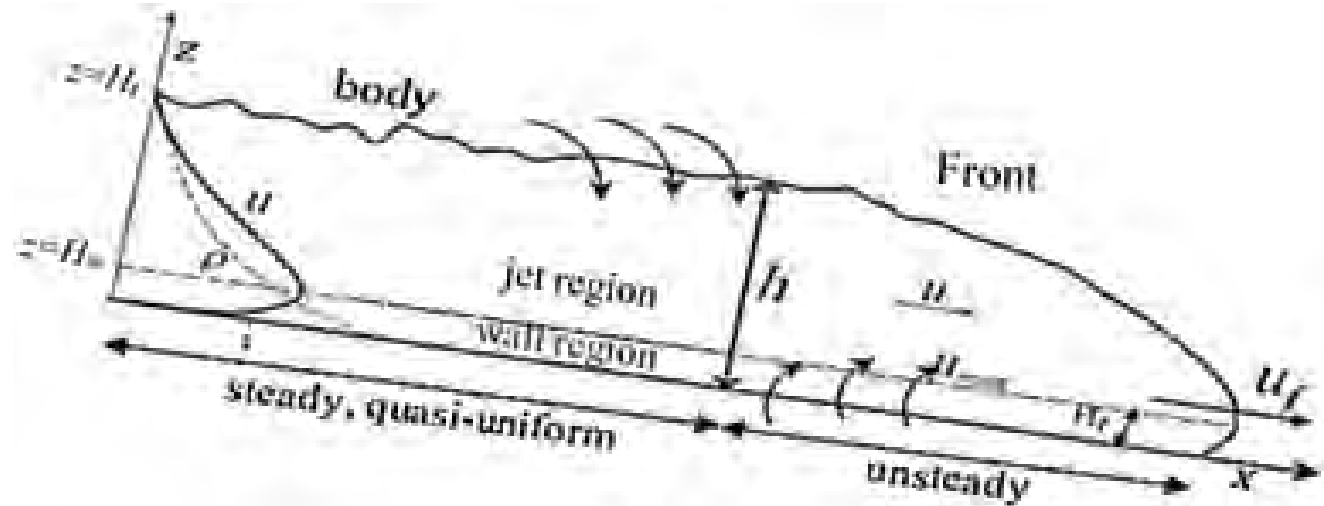
- The leading edge of the flow has a **high sediment concentration**, creating a sharp density contrast with ambient water.
- Suspended particles generate a **vertical density gradient**, influencing flow stability and mixing.

2. Velocity Profile

- The flow follows a **layered velocity structure**.
- Maximum velocity occurs at an intermediate depth**, rather than at the bed or surface.

3. Entrainment of Water and Particles

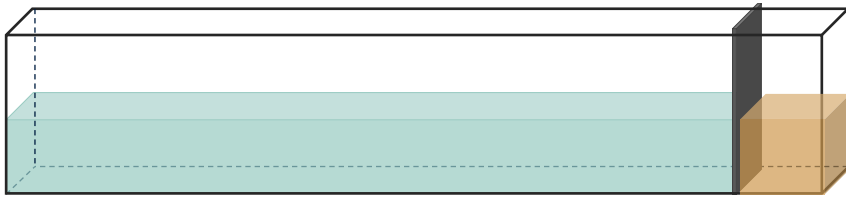
- The current **entrains ambient water**, altering its density and momentum.
- Sediment resuspension and settling** continuously adjust the flow's composition and behavior.



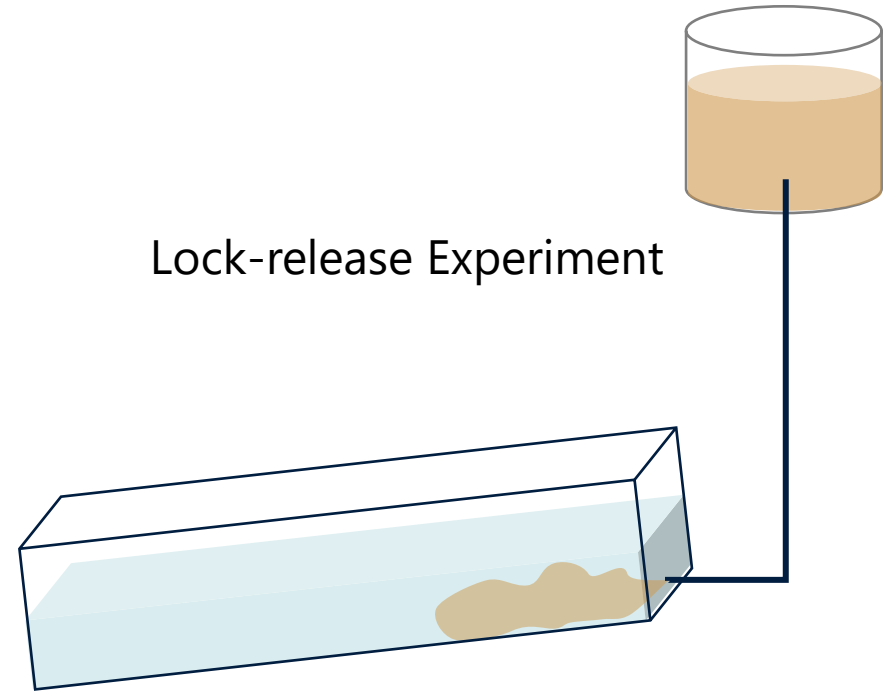
Methods to study High-density Sediment Flow

Laboratory experiments

Lock-exchange Experiment



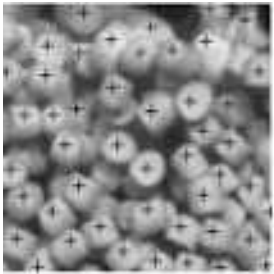
Lock-release Experiment



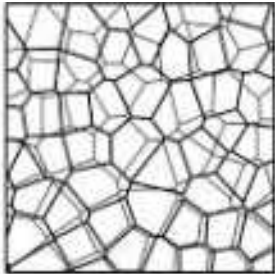
Methods to study High-density Sediment Flow

Laboratory experiments

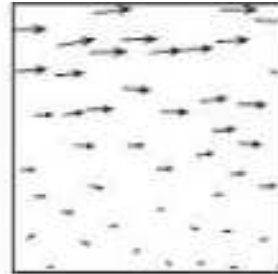
Voronoi Pattern-based For Particle Tracking



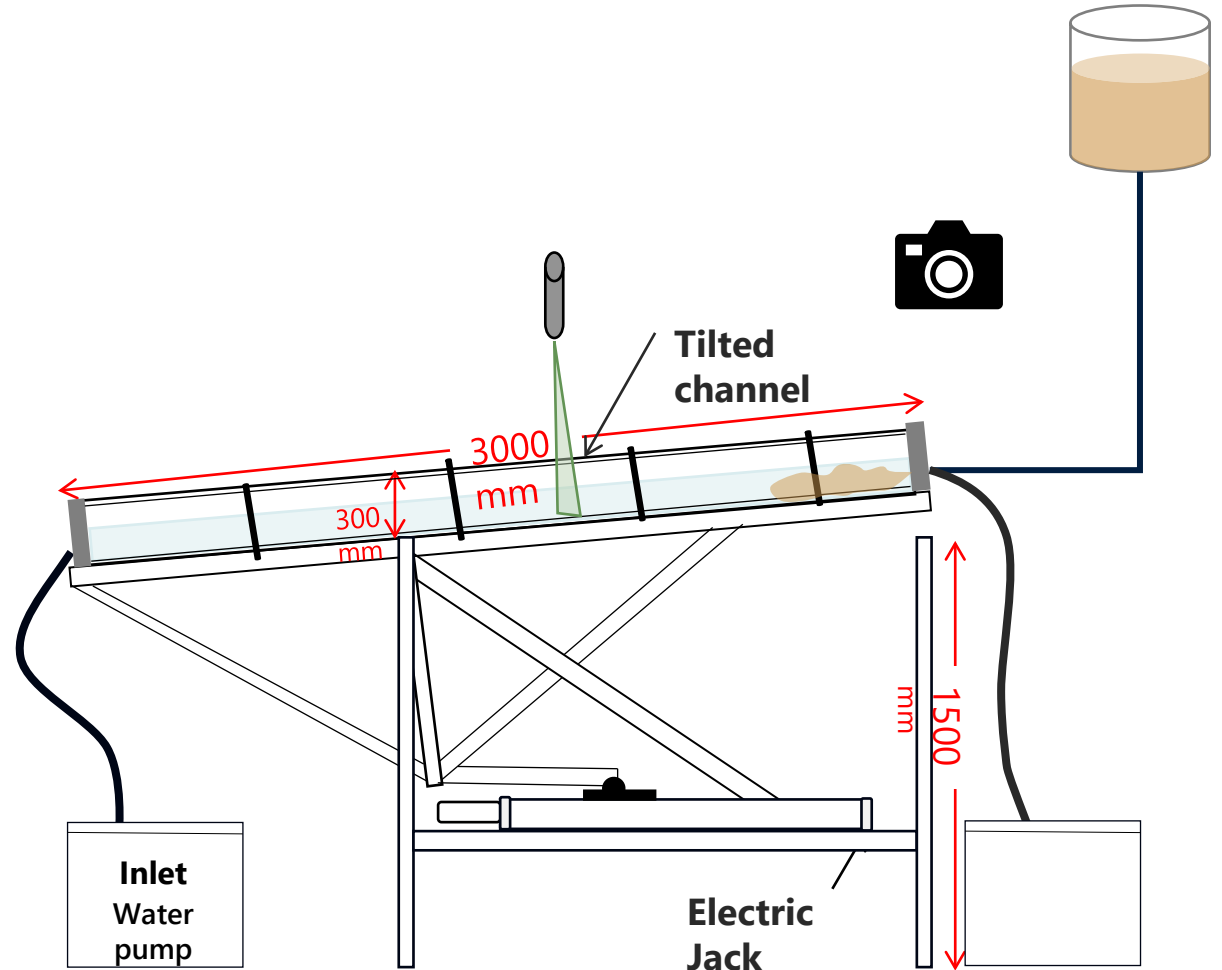
(a)



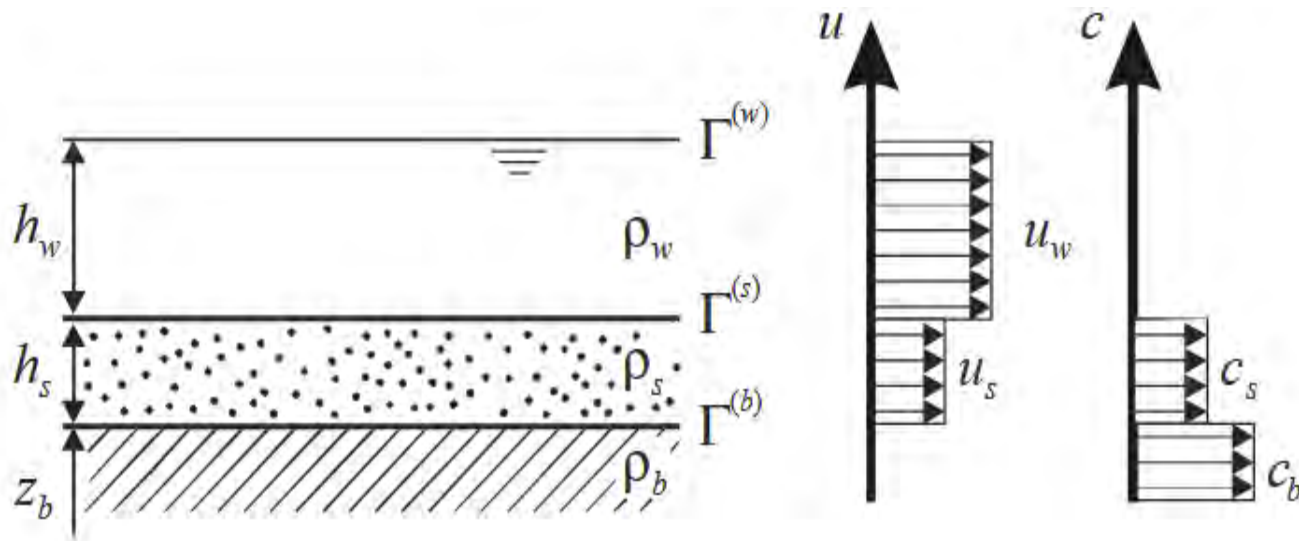
(b)



(c)



Modelling the Sediment Transport



Two-layer Shallow water Model

$$\left. \begin{aligned} \frac{\partial h_w}{\partial t} + \frac{\partial(h_w u_w)}{\partial x} &= 0 \\ \frac{\partial h_s}{\partial t} + \frac{\partial(h_s u_s)}{\partial x} &= 0 \end{aligned} \right\} \text{Mass Conservation}$$

$$\frac{\partial(h_w u_w)}{\partial x} + \frac{\partial}{\partial x} \left(h_w u_w^2 + \frac{g h_w^2}{2} \right) + g h_w \frac{\partial(z^{(b)} + h_s)}{\partial x} = 0$$

$$\frac{\partial(h_s u_s)}{\partial x} + \frac{\partial}{\partial x} \left(h_s u_s^2 + \frac{g h_s^2}{2} \right) + g h_s \left(\frac{\partial z^{(b)}}{\partial x} + \frac{\rho_w}{\rho_s} \frac{\partial h_w}{\partial x} \right) = 0$$

Momentum conservation

Governing Equations

Vertical exchange of the Mass and Momentum

Dilatancy – Erosion and Deposition Rate

Evolution of the bed

$$\frac{\partial z_b}{\partial t} = -e^b$$

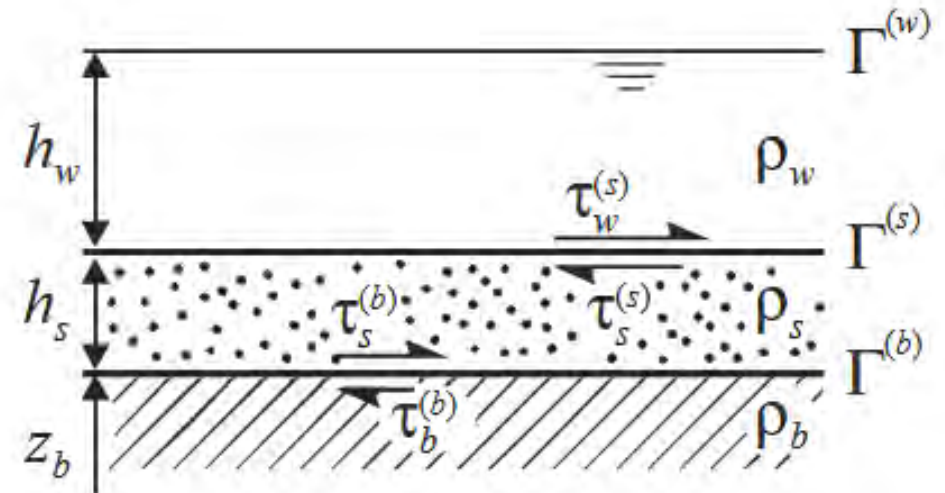
$$e^{(b)} = \frac{1}{\rho_b u_s} \left(\tau_s^{(b)} - \tau_b^{(b)} \right)$$

$e^{(b)} > 0$ **EROSION**

$e^{(b)} < 0$ **DEPOSITION**

Sediment Transport Layer

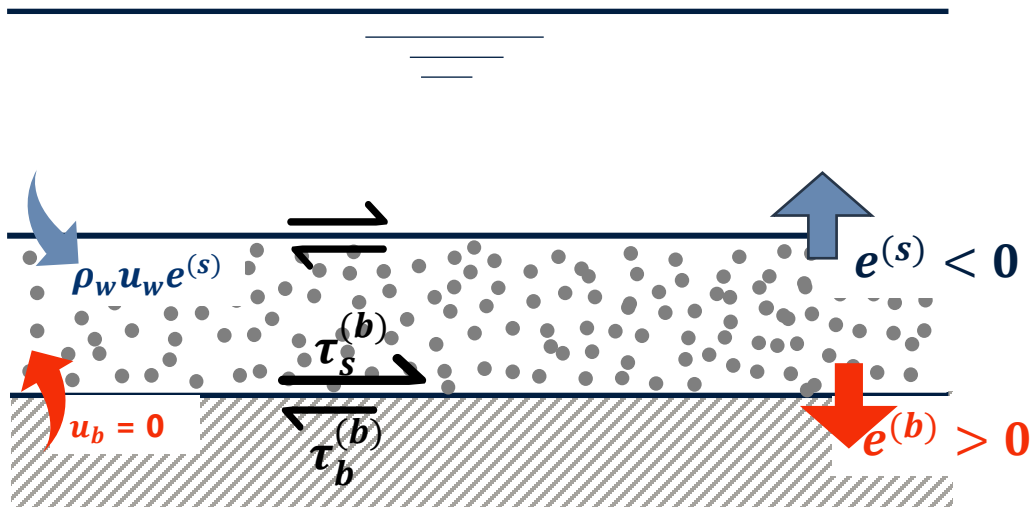
$$e^{(s)} = -\frac{\rho_b - \rho_s}{\rho_s - \rho_w} e^{(b)}$$



Governing Equations

Vertical exchange of the Mass and Momentum

Erosion



$$\tau_s^{(b)} \geq \tau_b^{(b)}$$

$$\frac{\partial h_w}{\partial t} = e^{(s)}$$

$$\frac{\partial h_s}{\partial t} = e^{(b)} - e^{(s)}$$

$$\frac{\partial z^{(b)}}{\partial t} = -e^{(b)}$$

Mass
Transfer

$$\frac{\partial (h_w u_w)}{\partial t} = u_w e^{(s)} - \frac{\tau_w^{(s)}}{\rho_w}$$

Momentum
Transfer

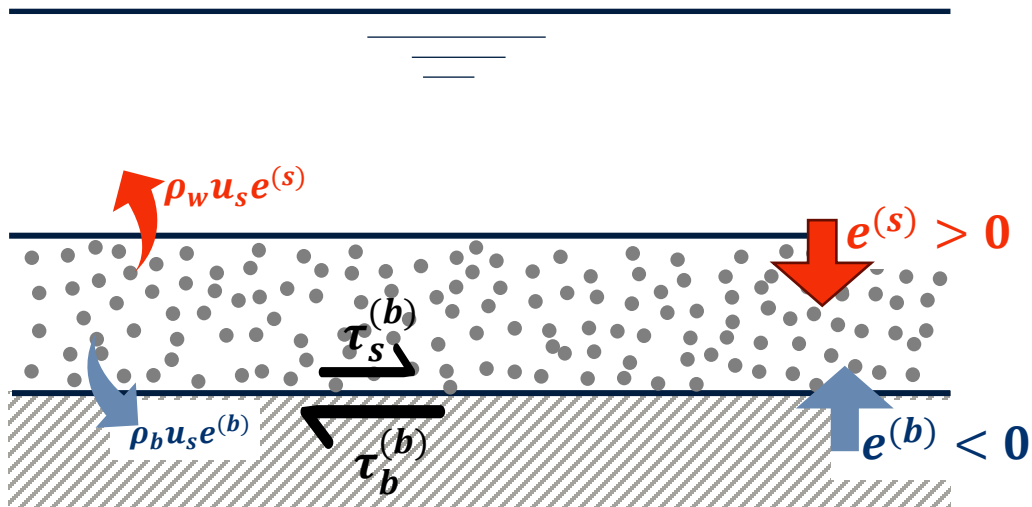
$$\frac{\partial (h_s u_s)}{\partial t} = -\frac{\rho_w}{\rho_s} u_w e^{(s)} + \frac{\tau_w^{(s)}}{\rho_s} - \frac{\tau_b^{(b)}}{\rho_s} + 0$$

Governing Equations

Mass and Momentum Transfer

Deposition

$$\tau_s^{(b)} < \tau_b^{(b)}$$

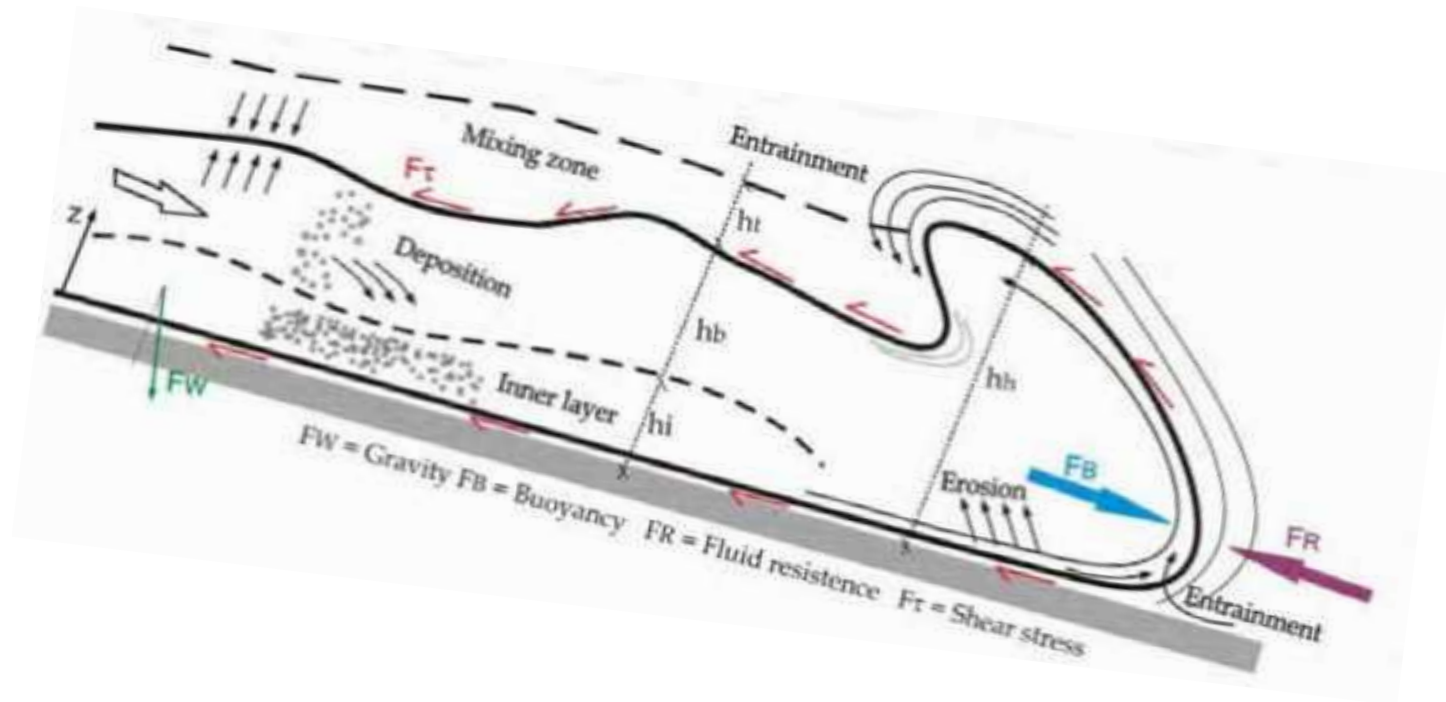


$$\frac{\partial(h_w u_w)}{\partial t} = u_s e^{(s)} - \frac{\tau_s^{(s)}}{\rho_w}$$

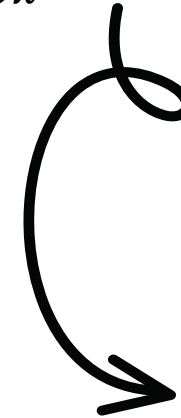
$$\frac{\partial(h_s u_s)}{\partial t} = -\frac{\rho_w}{\rho_s} u_s e^{(s)} + \frac{\tau_s^{(s)}}{\rho_s} - \frac{\tau_s^{(b)}}{\rho_s} + \frac{\rho_b}{\rho_s} u_s e^{(b)}$$

Governing Equations

Entrainment



$$\frac{\partial h}{\partial t} + \frac{\partial U h}{\partial x} = e_w U$$

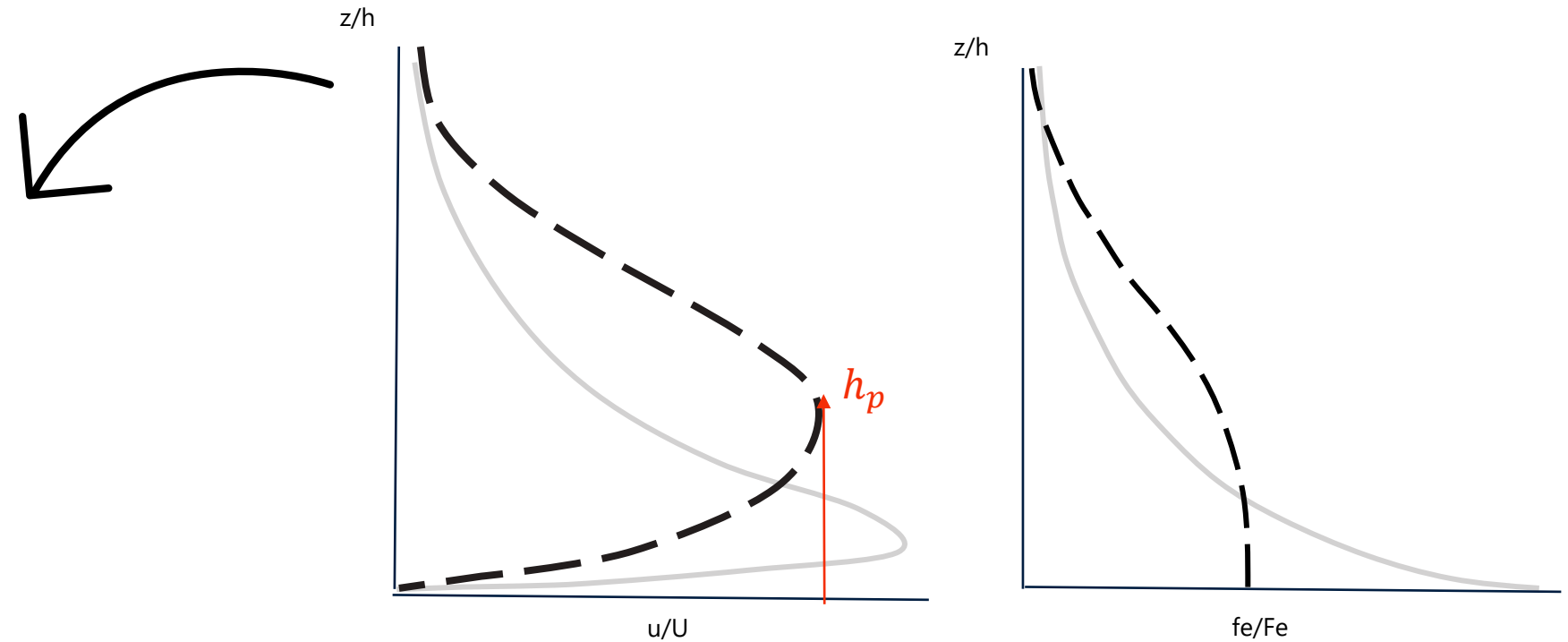


$$e_w = \frac{0.075}{\sqrt{1 + 718(1/F_d^{4.8})}}$$

Parker et al. 1987

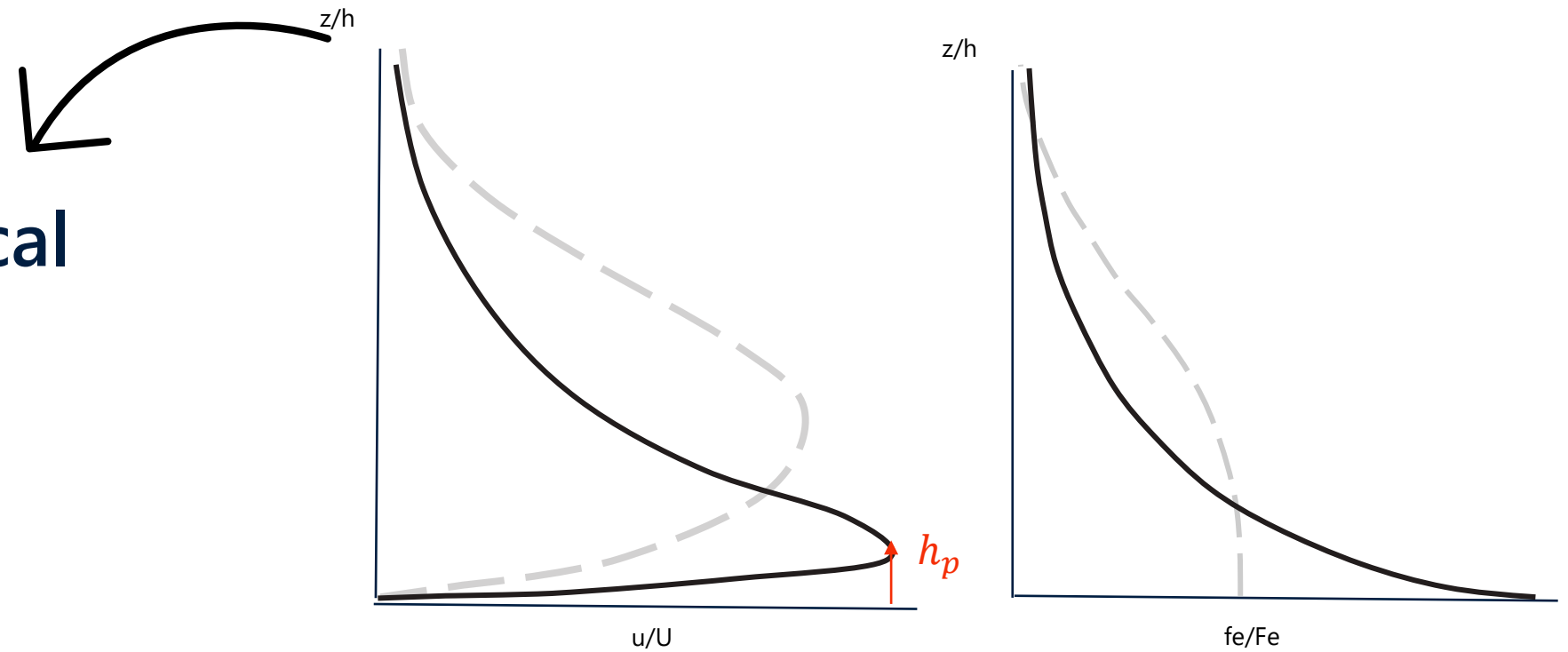
Vertical dynamics – Velocity and concentration profile

Subcritical

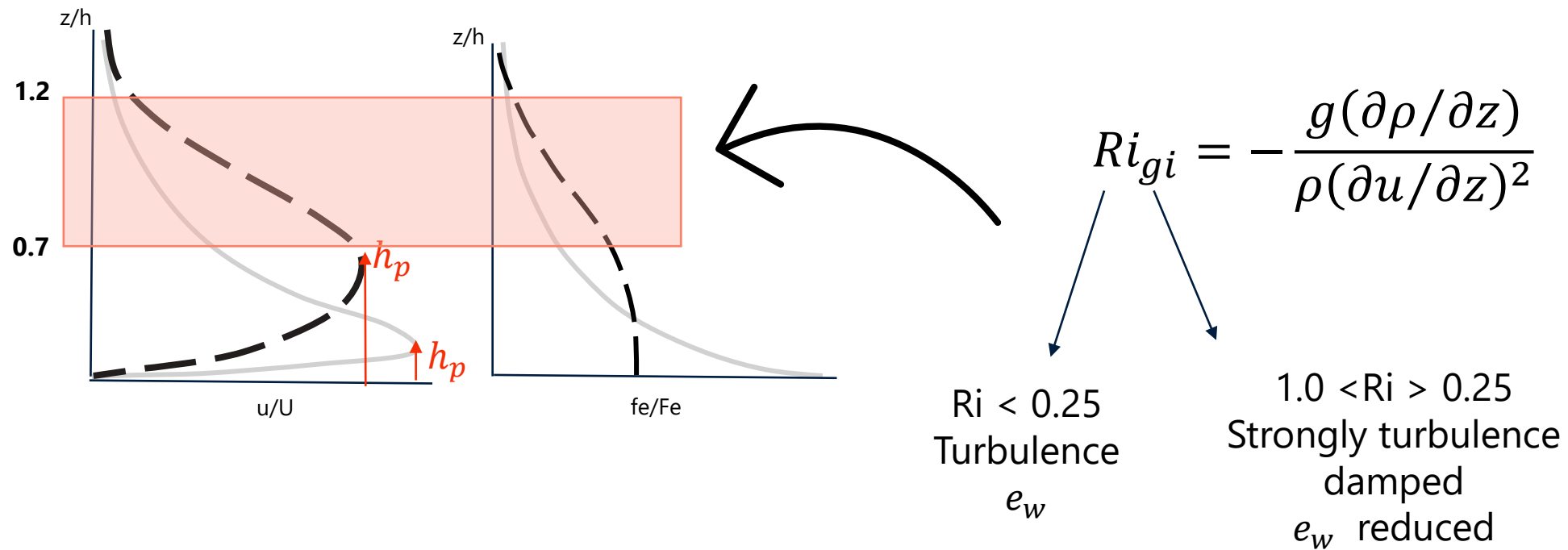


Vertical dynamics – Velocity and concentration profile

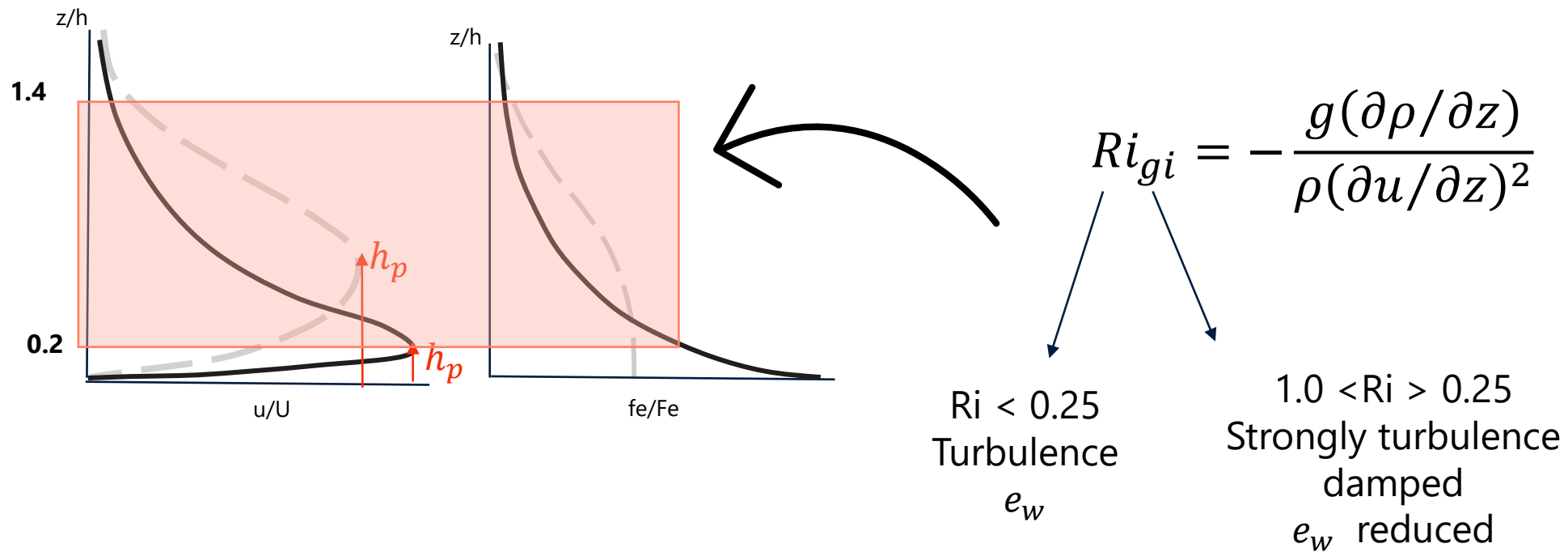
Supercritical



Vertical dynamics – Water Entrainment



Vertical dynamics – Water Entrainment



Next Steps & Ongoing Work

1. Experimental Setup & Data Collection

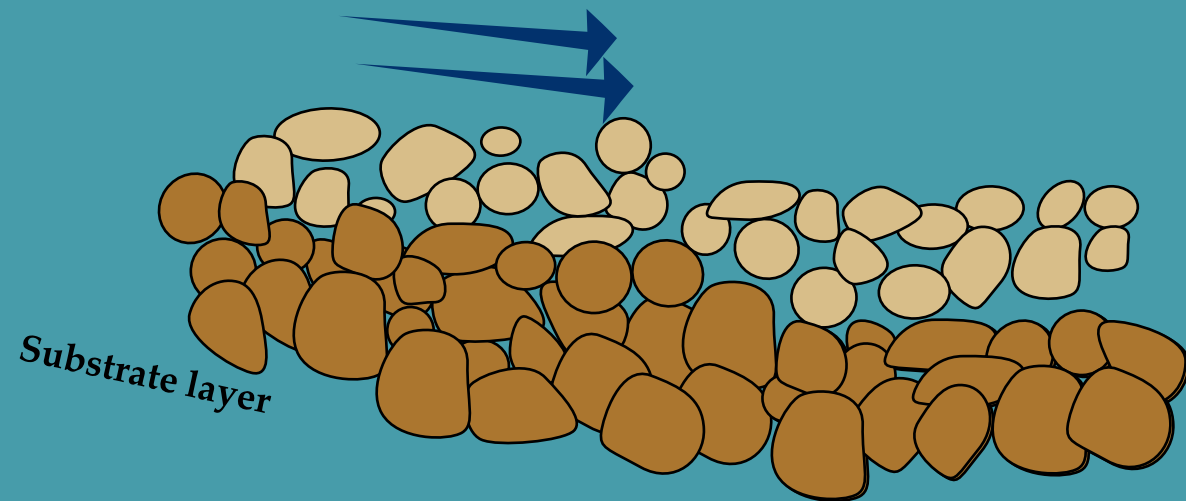
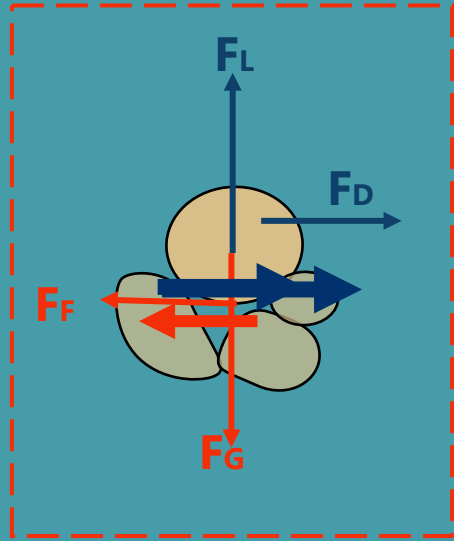
- Finalizing modifications to the flume system.
- Preparing initial high-density sediment-laden flow experiments for data collection.

2. Numerical Modelling

- Testing and familiarizing with the two-layer shallow water model
- Implementing the entrainment process based on literature and initial parameter assumptions



Sediment Transport



Overtopping Breakwater For Energy Conversion (OBREC)

Saeed Osouli

Supervisors:

Prof. Matteo Postacchini – UNIVPM

DR. Ivan Sabbioni – MAC

Prof. Maurizio Brocchini – UNIVPM

SEDIMARE

3rd Network Training School: Advanced Integrated Coastal Zone Monitoring and Management

IHCantabria/Santander

11-13 March 2025

Selecting Waves

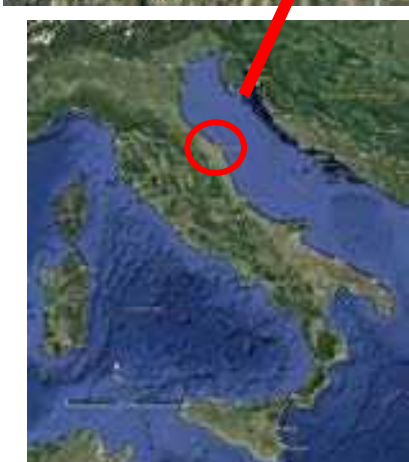
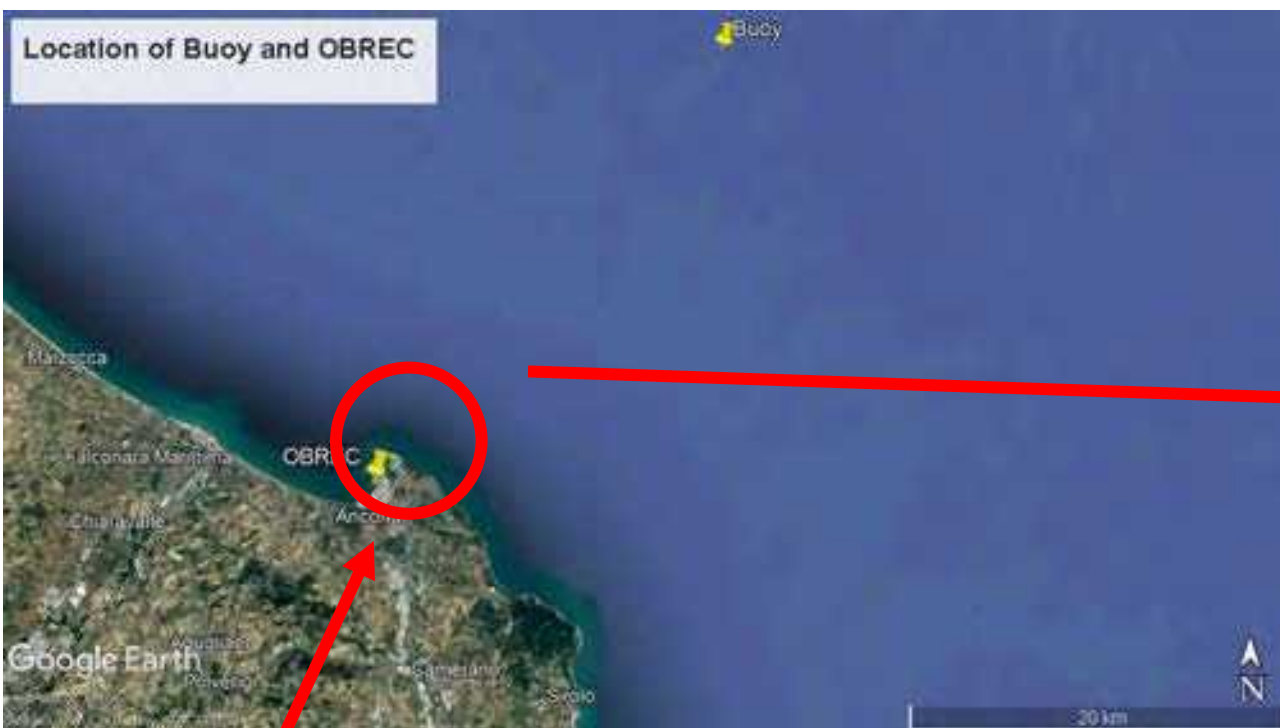
- Mean Waves and Joint PDF waves based on buoy were selected.

Transforming Waves

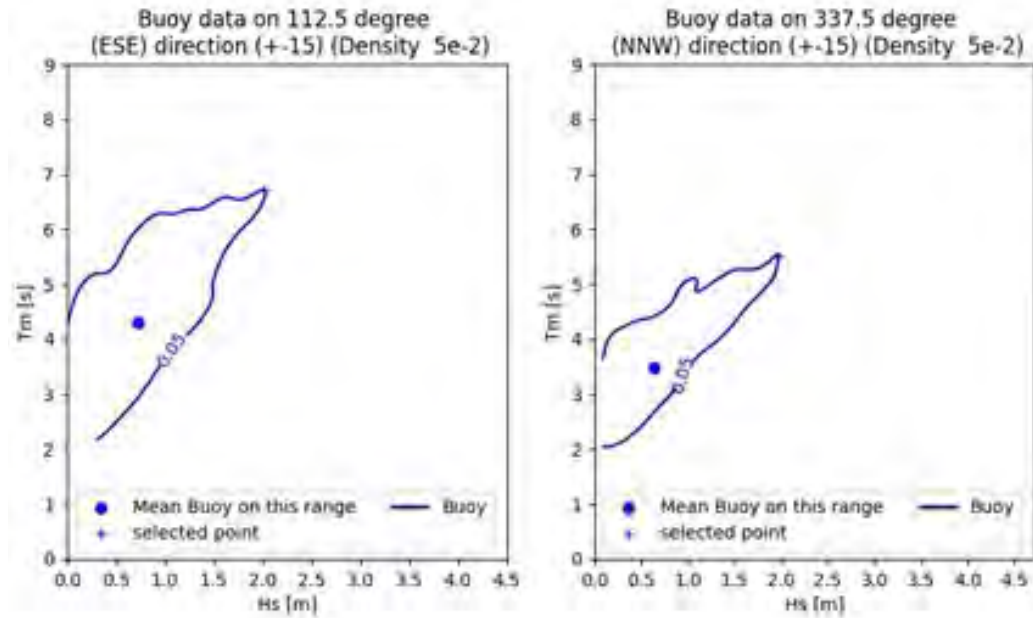
- Analytical approach (Goda) from offshore to near shore.
- Wave resolving model inside the port.

Designing the Device and Construction

- Designing Ramp, Turbine and construct them.
- Monitor the functioning.



Inclination due to the boundary.



Applying Goda

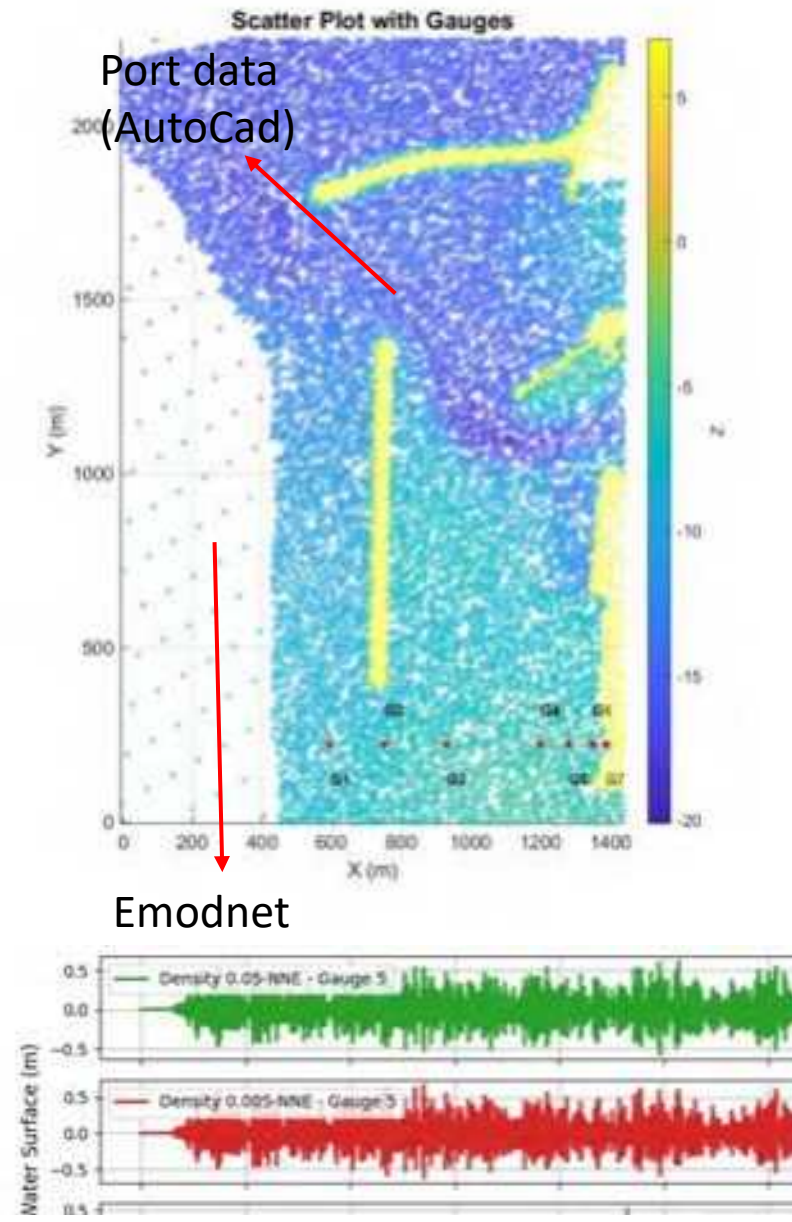
		NNE	NNW
Mean	Hs (m)	0.90	0.59
	Tp (s)	5.13	4.12
	Tm (s)	4.35	3.49
	ap,h1 [°]	56.00	35.00
Density 0.05	Hs (m)	2.53	1.67
	Tp (s)	7.81	6.51
	Tm (s)	6.62	5.52
	ap,h1 [°]	35.00	27.00
Density 0.005	Hs (m)	2.74	2.68
	Tp (s)	7.87	7.62
	Tm (s)	6.67	6.46
	ap,h1 [°]	35.00	23.00

Wave characteristics at nearshore after applying Goda.

FLOW-3D

FUNWAVE

- Bathymetry
- Simulation
- Outputs



- Eurotop
- Effect of wave steepness and front slope

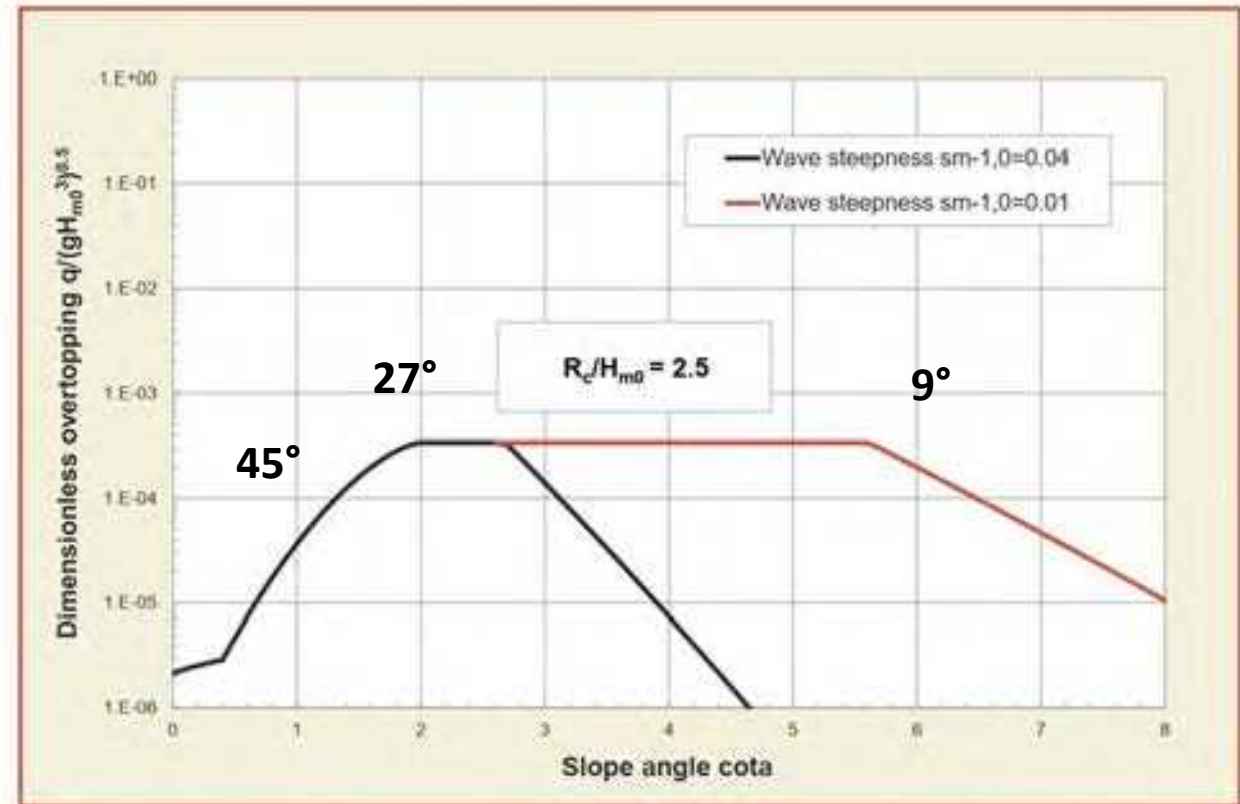
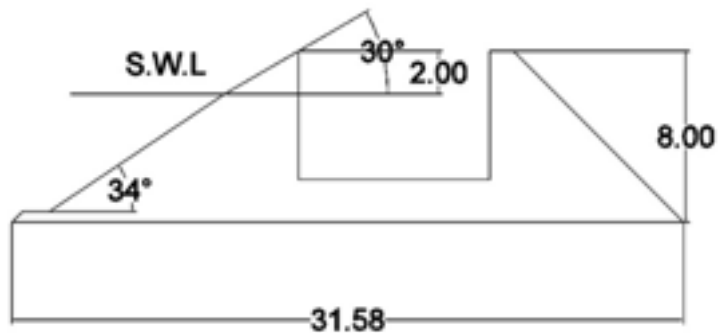
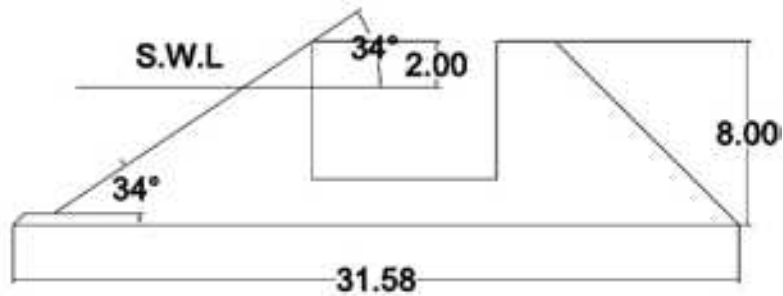


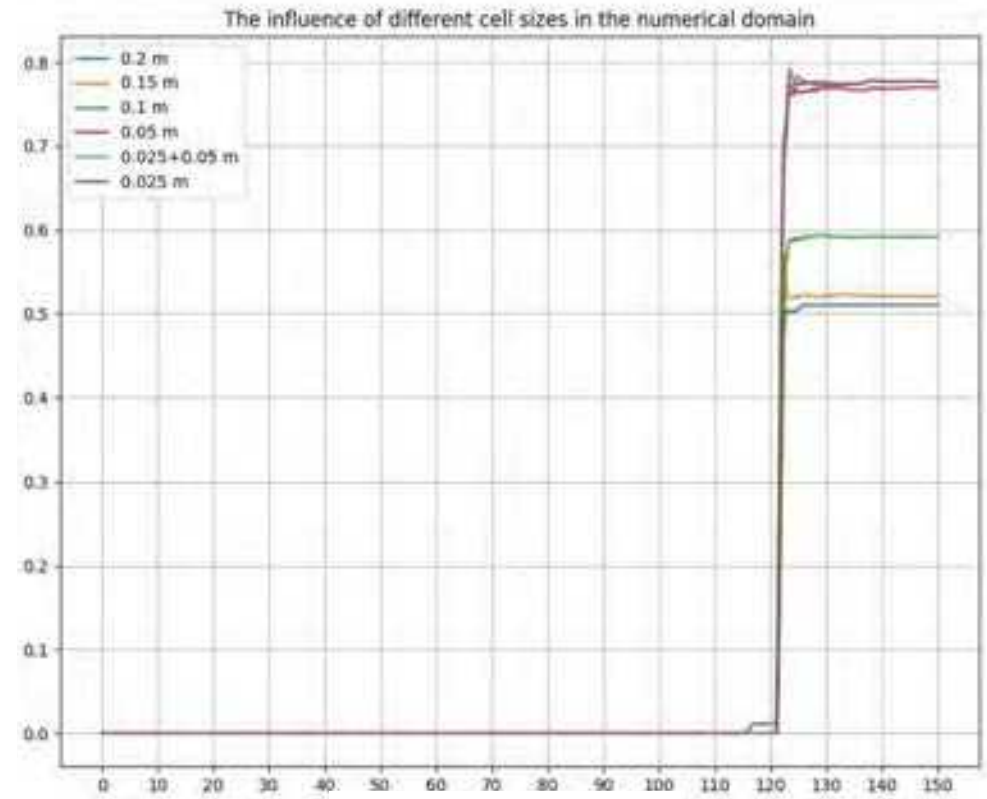
Figure 4.4: Comparison of wave overtopping as function of slope angle

There is a clear trend in Figure 4.4. Steep slopes around 1:2 to 1:3 give the largest overtopping, but for gentler slopes with much longer waves large overtopping is still observed, due to the fact that waves are still surging (non-breaking). Vertical structures with $\cot \alpha = 0$, but without an influencing foreshore, give quite low overtopping and this increases only slightly for battered walls, say up to $\cot \alpha = 0.5$. With

Sensitivity analysis

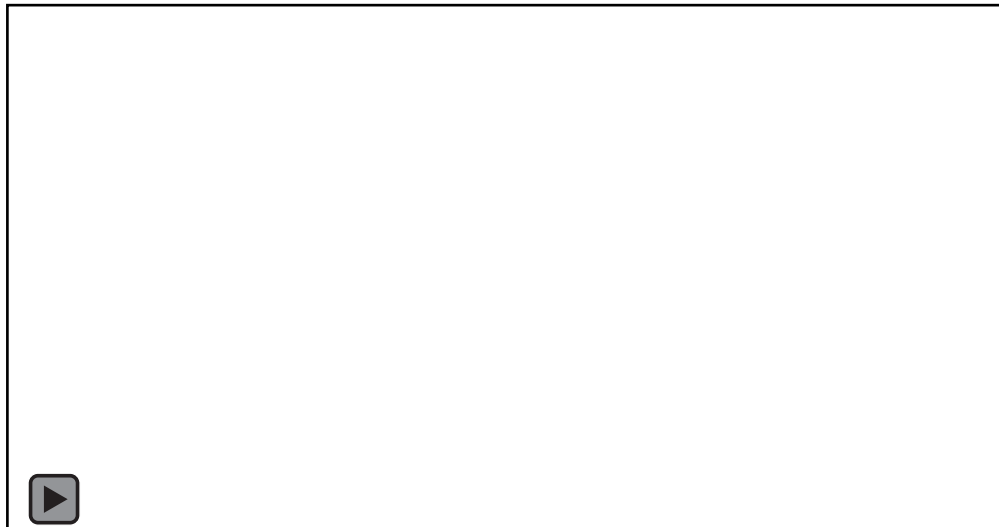
- Domain size: 72*1*10 m, cell size in y direction is 1m (one cell)
- Simulation Time: 150 seconds

Water volume (m³)



Time (s)

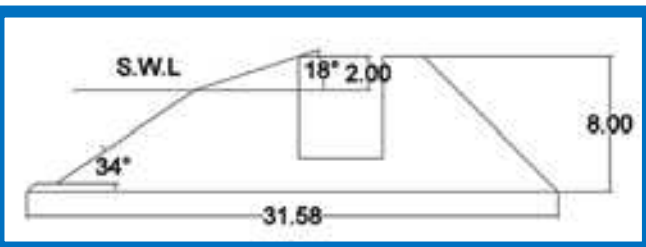
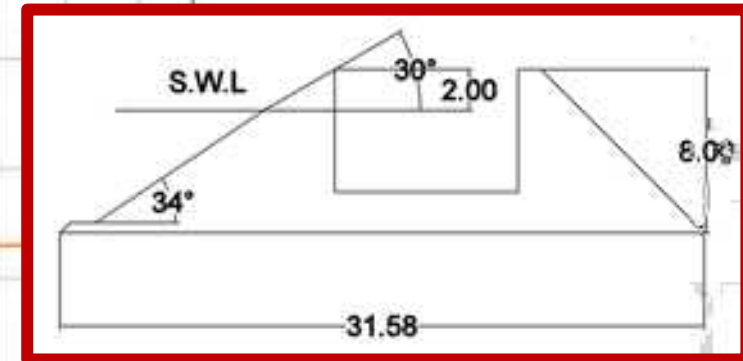
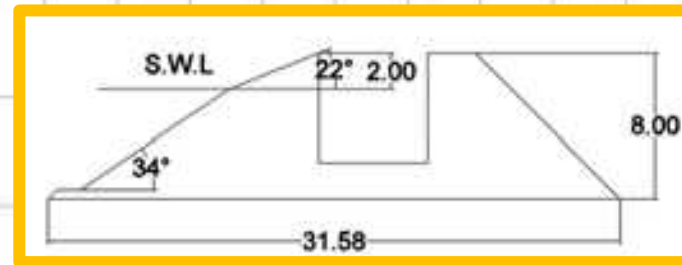
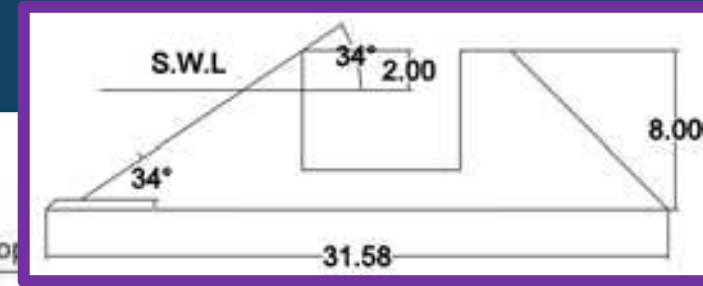
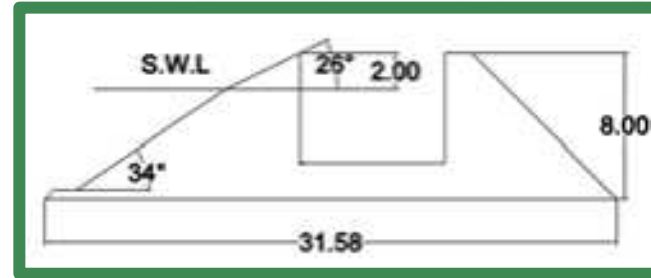
Cell size in x and z	0.2 m	0.15 m	0.1 m	0.05 m	0.05 +0.025	0.025 m
Total number of cells	18000	32160	72000	288000	793200	1152000
Time duration	3 minutes	5 minutes	9 minutes	50 minutes	~3 hours	~7 hours
Water volume (m ³)	0.51	0.57	0.59	0.77	0.79	0.78
Hardware	Processor: Intel(R) Core(TM) i9-14900KF 3.20 GHz (8 cores), RAM: 128GB					



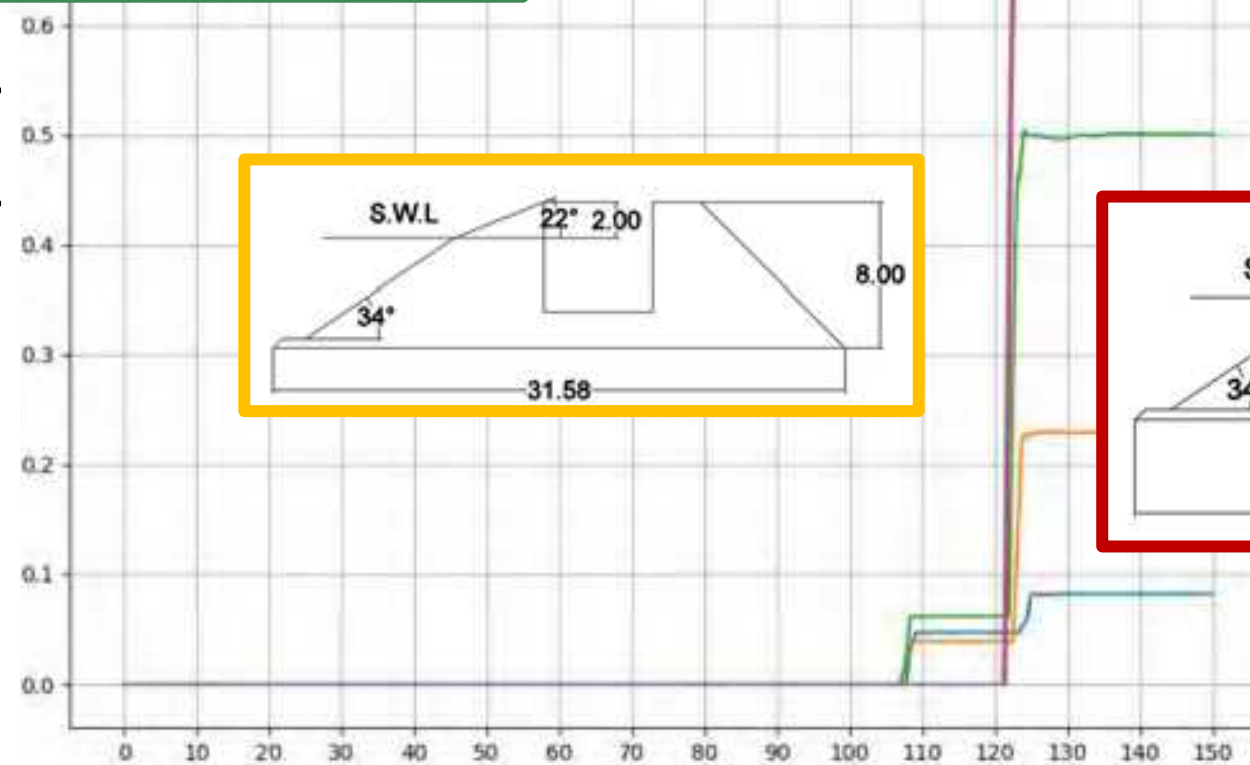
Wave characteristics

NNE scenario

- $H_s = 0.81\text{m}$
- $T_p = 7.02\text{ s}$
- $h_{\text{toe}} = 6\text{ m}$
- Freeboard = 2 m



Water volume (m^3)



Slope (°)	Discharge (m^3)
34	0.77
30	0.79
26	0.5
22	0.23
18	0.08

Time (s)



FLOW-3D- Results for NNW Waves



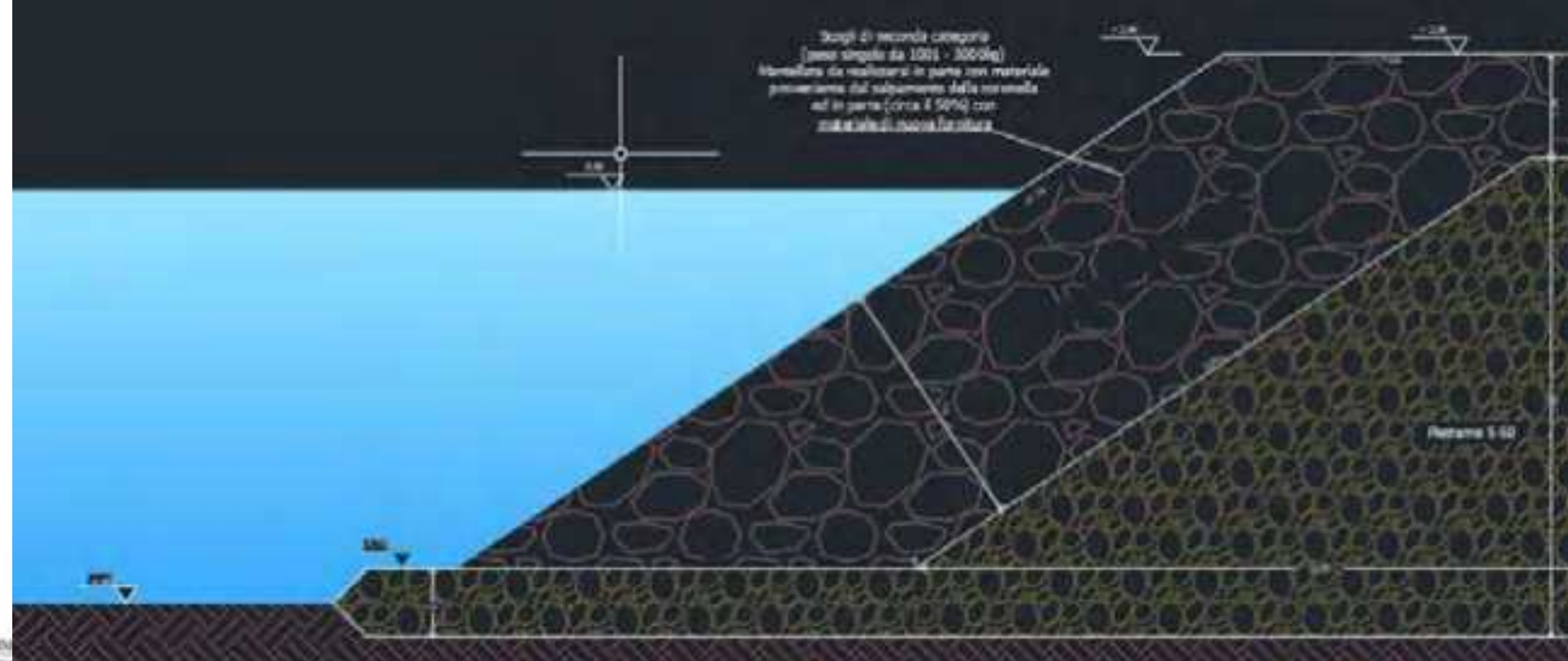
MENTUCCIA
INGEGNERIA E CONSULTING



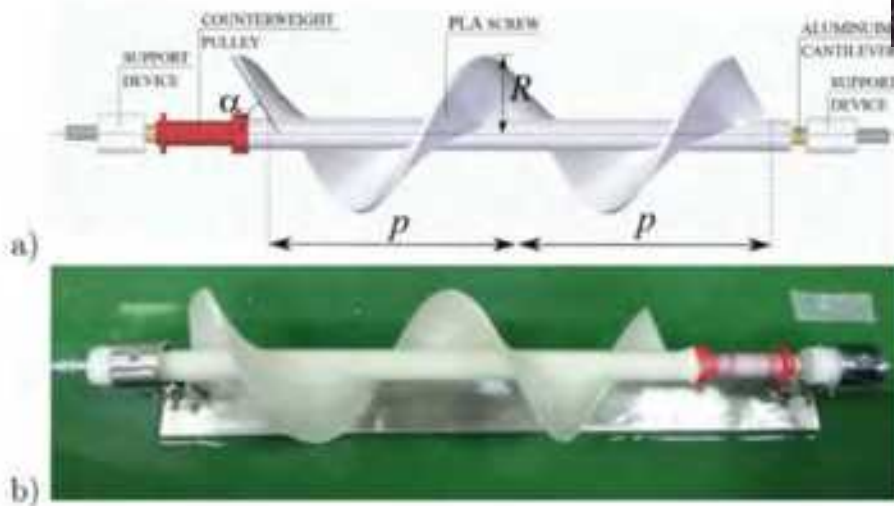
Location



- Cross-section of actual breakwater



G. Zitti et al. / Renewable Energy 146 (2020) 867–879



Hydrokinetic Archimedes turbine Zitti et al. (2020)

Efficiency evaluation of a ductless Archimedes turbine: Laboratory experiments and numerical simulations (Zitti et al.) 2020

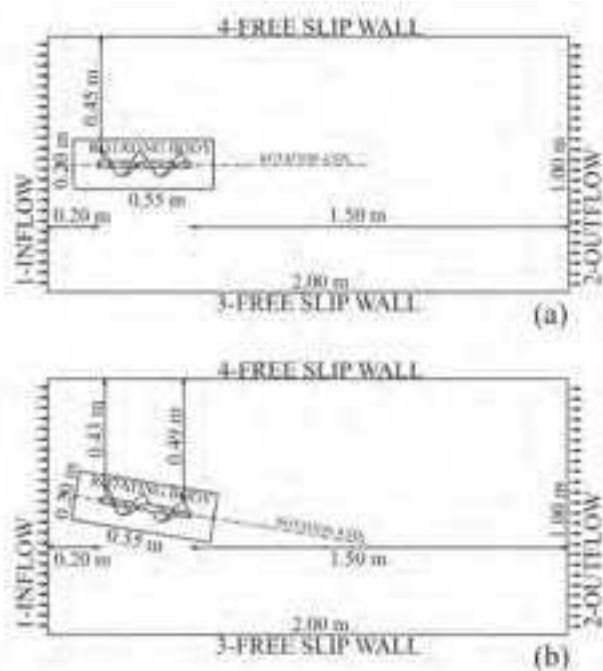
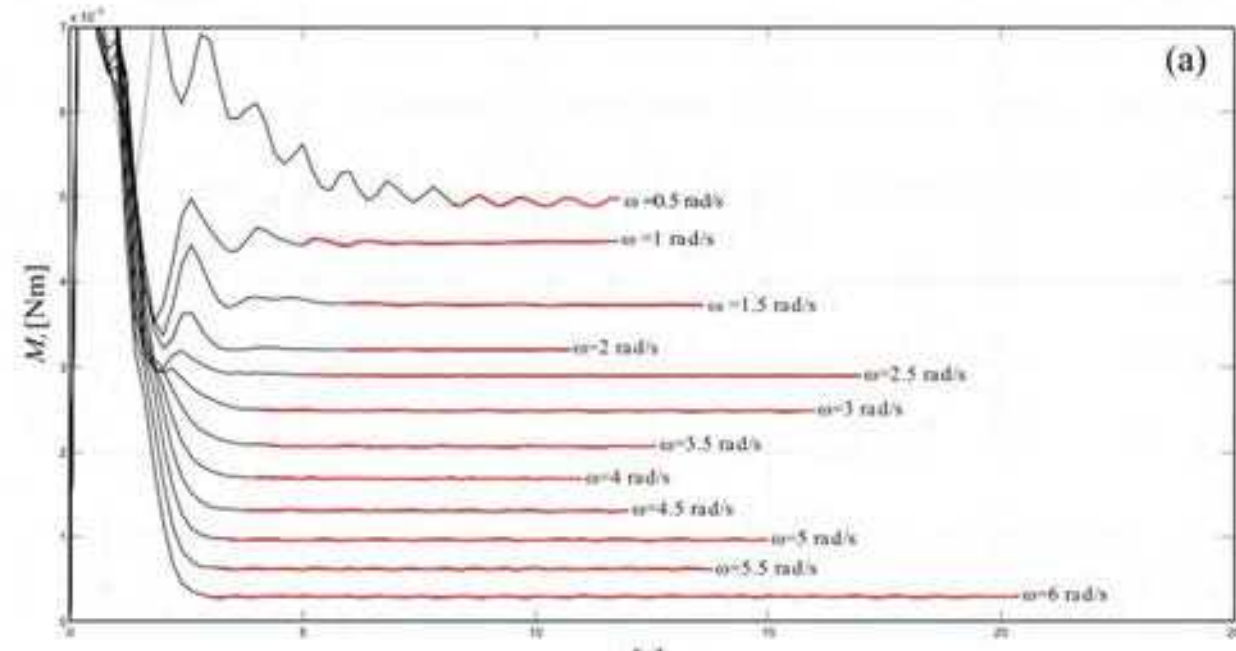
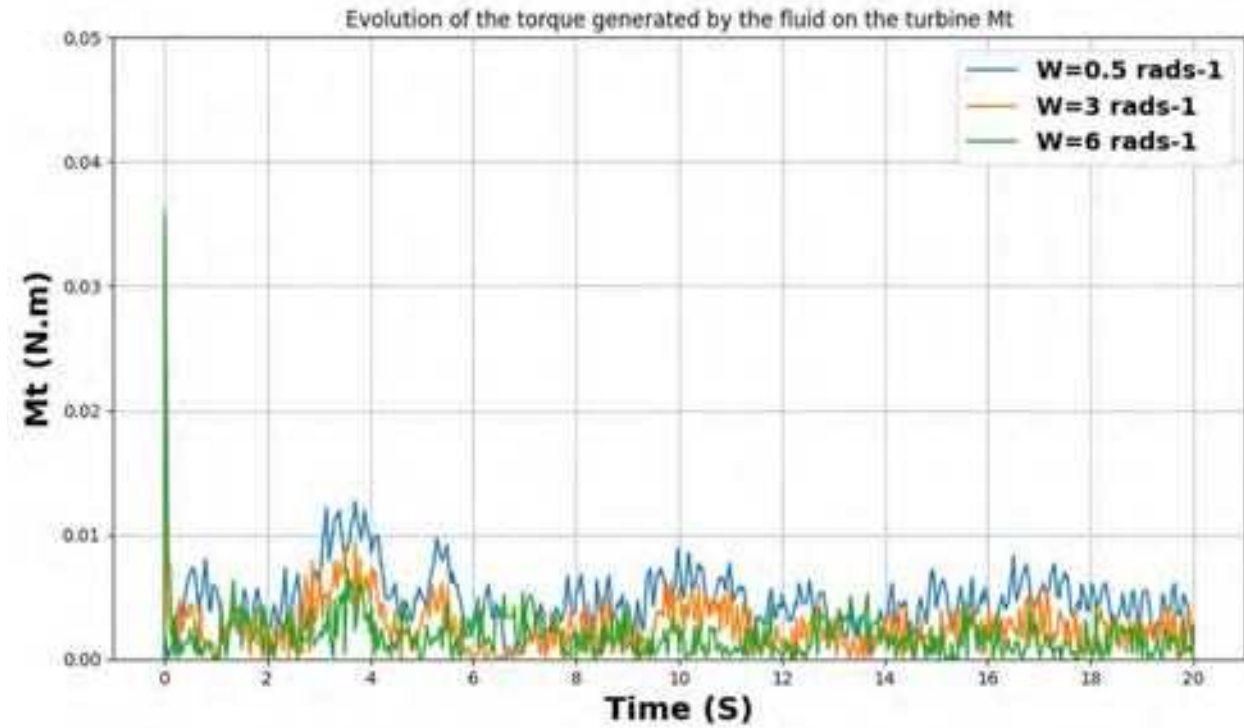


Fig. 5. Sketch of the horizontal plane of the geometry of the domains used in the numerical simulations. a) aligned turbine ($\theta = 0^\circ$); b) inclined turbine ($\theta = 10^\circ$).





(Zitti et al.) 2020



Modeling and experimental results of an Archimedes screw turbine (Rohmer et al (2016))

Analytical Model for Water Inflow of an Archimedes Screw Used in Hydropower Generation (Dirk M. Nuernbergk1 and Chris Rorres 2013)

- pitch ratio= λ , $P \tan(\theta) / 2ORn$
- radius ratio = ρ , IR/OR

$$1.36 \text{ m}^3 / 1\text{m} \xrightarrow{\text{2 m width of ramp and divided by 150}} Q = 0.018 \text{ m}^3 / \text{s}$$

- $OR = \left(\frac{0.018 \times \tan 10}{10.362 \times 0.06} \right)^{3/7} = 0.104 \text{ m}$
- $P = \frac{2\pi \times 0.104 \times 0.21}{\tan 10} = 0.778 \text{ m}$
- $IR = \rho \times OR = 0.053 \text{ m}$

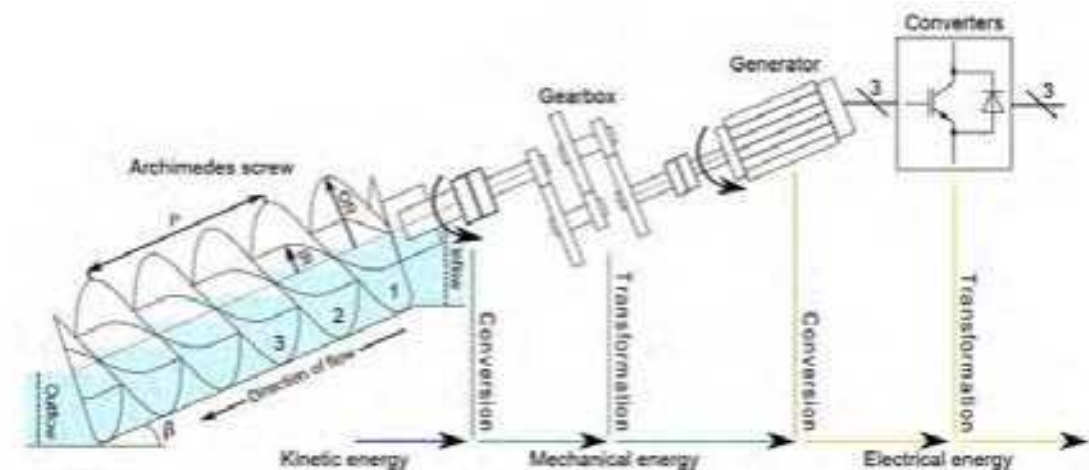
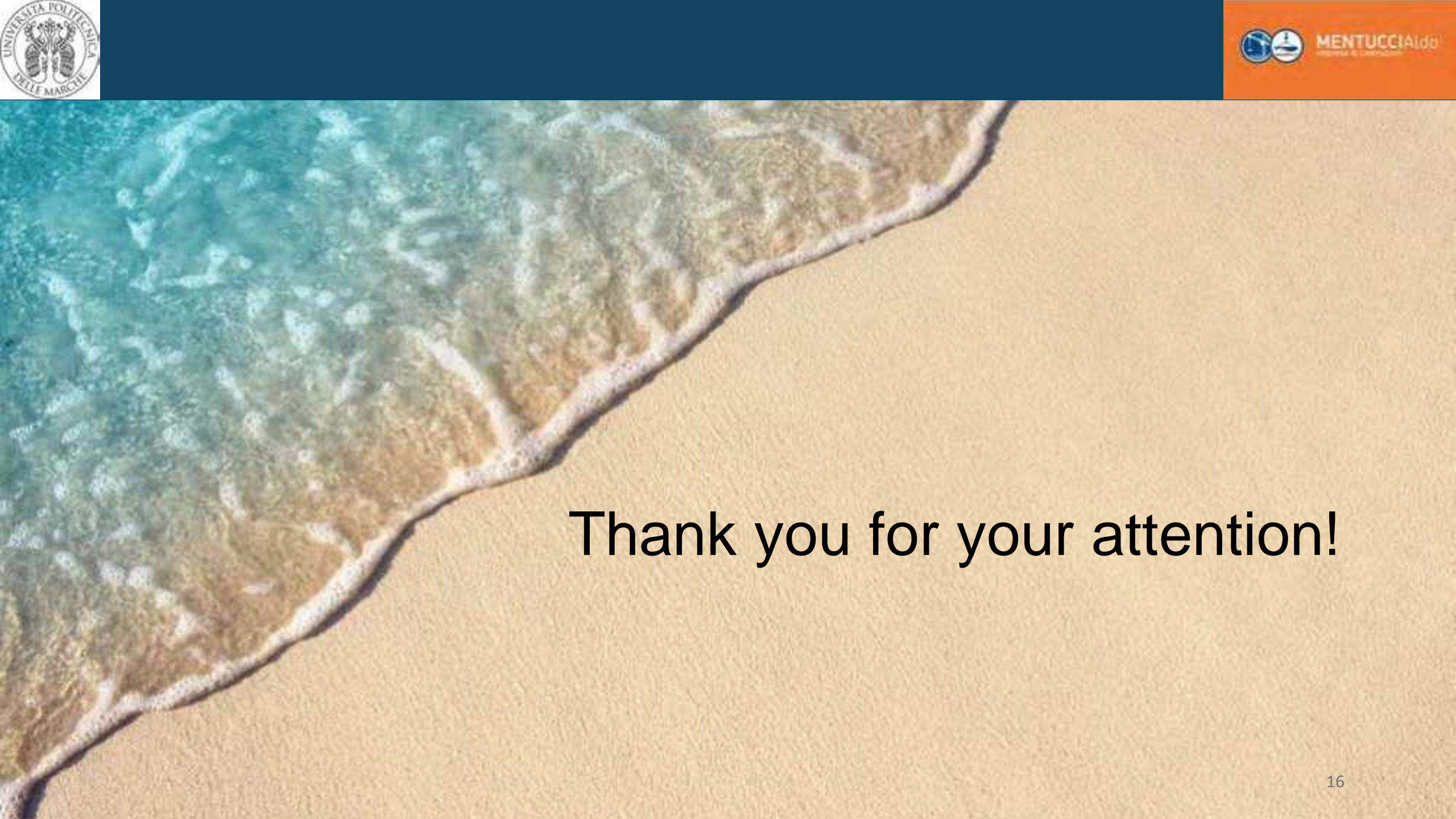


Fig. 1. General principle of an Archimedes screw plant.

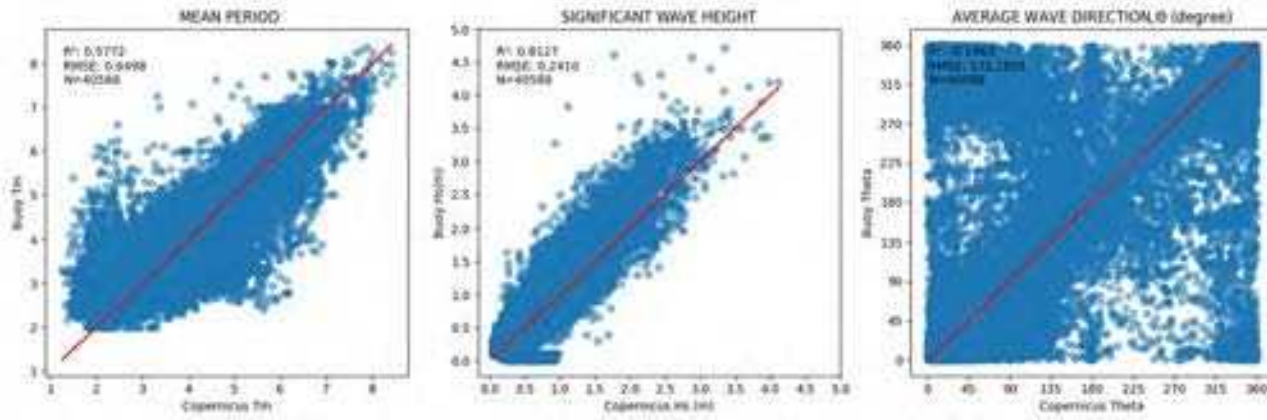
- Selecting waves based on 3 scenarios based on Buoy data.
- Transferring waves into Shallow water using Goda.
- Using FUNWAVE-TVD as the shallow water solver.
- FLOW-3D is used to simulate wave and structure interaction as a CFD tool.
- Archimedes Hydrokinetic turbine will be analyzed as a part of the conveying system.
- The device will be built in the port of Ancona and the performance will be monitored.

FUTURE WORK:

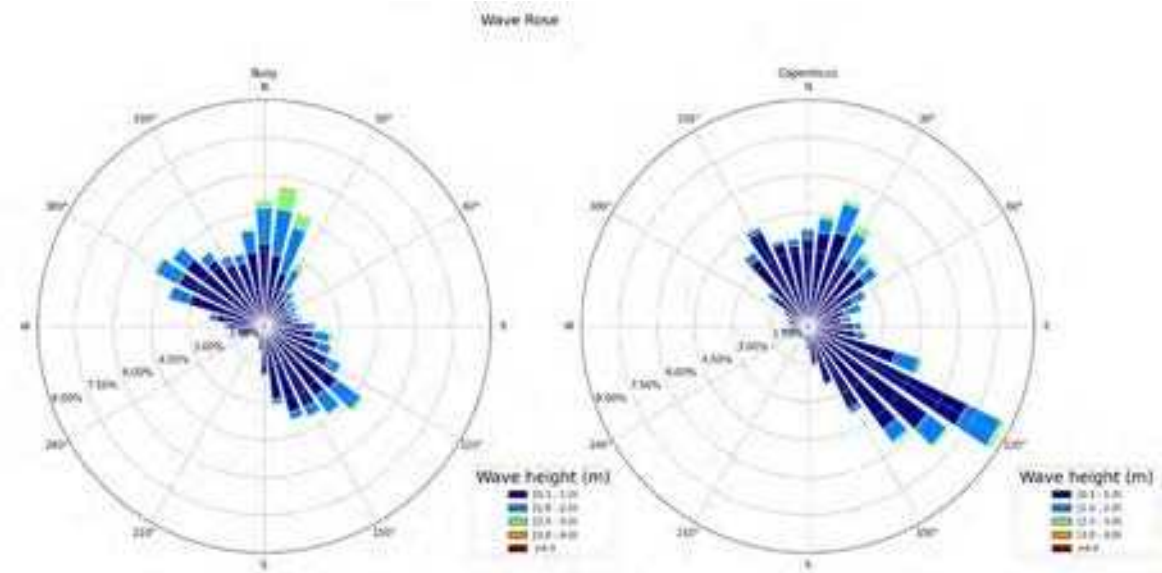
planned construction of ramp and reservoir, design of turbine.

The background of the slide is a photograph of a beach. In the foreground, there is a wide expanse of golden sand. To the left, the ocean waves are breaking, creating white foam and a mix of blue and green water. The horizon line is visible in the distance.

Thank you for your attention!



Comparison of wave parameters from buoy and Copernicus.



Wave Roses.

Condition															Condition														
dx (m)	dy (m)	simulation time (s)	Total number of Grids	Stability Condition	Smoothing (n)	Smoothing (Command)	obstacle height (m)	depth of WK and offshore platform	Froude number	CFL and min depth	Wall or Periodic boundary	VISCOSITY_BREAKING	dx (m)	dy (m)	simulation time (s)	Total number of Grids	Stability Condition	Smoothing (n)	Smoothing (Command)	obstacle height (m)	depth of WK and offshore platform	Froude number	CFL and min depth	Wall or Periodic boundary	VISCOSITY_BREAKING				
1	2	2	1000	806,314	stable	7	smoothdata2/sgolay/movmean	7	8 - monochromatic	no	1	0.5/0.01	P.B	no	9	2	2	936	806,314	instable (it happens around 480 s)	7	smoothdata2/sgolay/movmean	5	12 - monochromatic	no	1	0.5/0.01	P.B	no
2	2	2	1,000	806,314	stable	7	smoothdata2/sgolay/movmean	7	12 - monochromatic	no	1	0.5/0.01	P.B	no	10	1.5	1.5	399	1,432,629	instable (it happens around 150 s)	7	smoothdata2/sgolay/movmean	7	12 - monochromatic	no	1	0.5/0.01	P.B	no
3	2	2	1,000	806,314	stable	7	smoothdata2/sgolay/movmean	7	16 - monochromatic	no	1	0.5/0.01	P.B	no	11	1.5	1.5	185	1,432,629	instable (it happens around 122 s)	7	smoothdata2/sgolay/movmean	7	16 - monochromatic	no	1	0.5/0.01	P.B	no
4	2	2	1000	806,314	stable but a instability sign could be seen in the domain around 810 s	7	smoothdata2/sgolay/movmean	7	12 - monochromatic	no	1	0.5/0.1	P.B	no	12	1.5	1.5	151	1,432,629	instable (it happens around 120 s)	7	smoothdata2/sgolay/movmean	7	16 - monochromatic	no	3	0.5/0.01	P.B	no
5	2	2	4292	806,314	stable	7	smoothdata2/sgolay/movmean	7	12 - monochromatic	no	1	0.5/0.01	P.B	yes/Cbrk1 = 0.45 Cbrk2 = 0.35	13	2	2	7870	806,314	instable (it happens around 930 s)	7	smoothdata2/sgolay/movmean	7	12 - monochromatic	no	1	0.5/0.01	Wall boundary	no
6	2	2	7870	374,468	stable	7	smoothdata2/sgolay/movmean	7	12 - monochromatic	no	1	0.5/0.01	P.B	no-small domain	14	3	3	7870	358,771	stable	7	smoothdata2/sgolay/movmean	7	12 - monochromatic	no	1	0.5/0.01	P.B	no
7	2	2	467	806,314	instable (it happens around 330 s)	5	smoothdata2/sgolay/movmean	5	12 - monochromatic	no	1	0.5/0.01	P.B	no	15	5	5	7870	129,312	stable	7	smoothdata2/sgolay/movmean	7	12 - monochromatic	no	1	0.5/0.01	P.B	no
8	2	2	734	806,314	instable (it happens around 180 s)	5	smoothdata2/sgolay/movmean	7	12 - monochromatic	no	1	0.5/0.01	P.B	no	16	2	2	7870	806,314	stable	7	smoothdata2/sgolay/movmean	7	12 - monochromatic	yes	1	0.5/0.01	P.B	no
														17	2	2	7870	806,314	stable	7	smoothdata2/sgolay/movmean	7	16 - monochromatic	Yes	1	0.5/0.01	P.B	no	

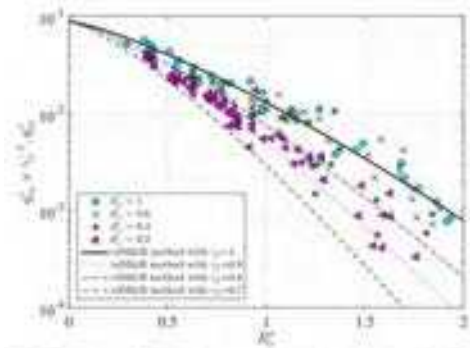
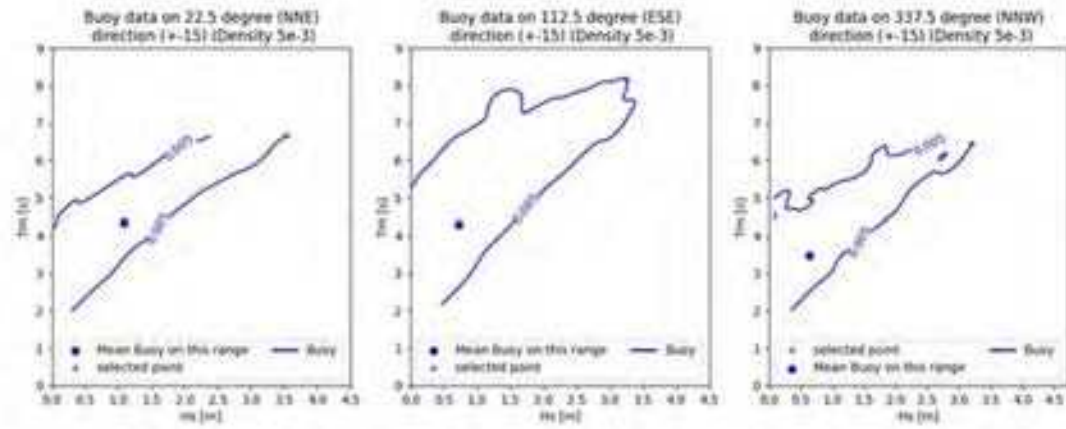


Fig. 9. Comparison of the average wave overtopping rates measured for all configurations tested in the present test and those estimated by the prediction method of van der Meer and Balch (2013) adopting four different values of β_1 . The experimental data were corrected using the coefficient β_2 .

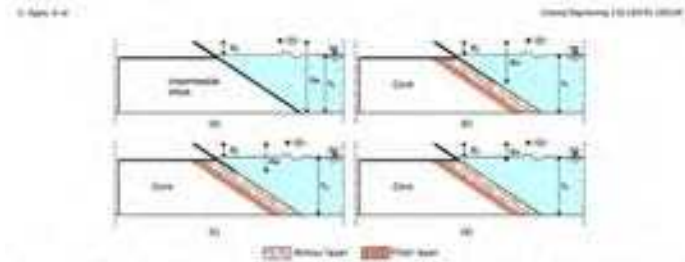


Fig. 10. Different configurations analyzed in the present experimental campaign: (a) $\beta_1 = 0.275 \text{ m}^2/\text{s}^2$, $\beta_2 = 1.0 \text{ m}^2/\text{s}^2$, $\beta_3 = 0.00 \text{ m}^2/\text{s}^2$, $\beta_4 = 0.00 \text{ m}^2/\text{s}^2$; (b) $\beta_1 = 0.275 \text{ m}^2/\text{s}^2$, $\beta_2 = 0.00 \text{ m}^2/\text{s}^2$, $\beta_3 = 0.00 \text{ m}^2/\text{s}^2$, $\beta_4 = 0.00 \text{ m}^2/\text{s}^2$; (c) $\beta_1 = 0.275 \text{ m}^2/\text{s}^2$, $\beta_2 = 0.00 \text{ m}^2/\text{s}^2$, $\beta_3 = 0.00 \text{ m}^2/\text{s}^2$, $\beta_4 = 0.00 \text{ m}^2/\text{s}^2$; (d) $\beta_1 = 0.275 \text{ m}^2/\text{s}^2$, $\beta_2 = 0.00 \text{ m}^2/\text{s}^2$, $\beta_3 = 0.00 \text{ m}^2/\text{s}^2$, $\beta_4 = 0.00 \text{ m}^2/\text{s}^2$.



With the previous coefficients, it is possible to determine the optimal outer radius OR of the Archimedes screw with the following equation [10,14,15]:

$$OR = \left(\frac{Q \cdot \tan(\beta)}{K_1 \cdot (\lambda P)} \right)^{3/7} \quad (1)$$

where K_1 is a constant between 10.362 and 11.606. According to Rorres and Nuernbergk, the thread pitch P and the inner radius IR can be calculated by equation (2) [10,14,15]:

$$P = \frac{2\pi \cdot OR \cdot \lambda}{\tan(\beta)} \quad IR = \rho \cdot OR \quad (2)$$

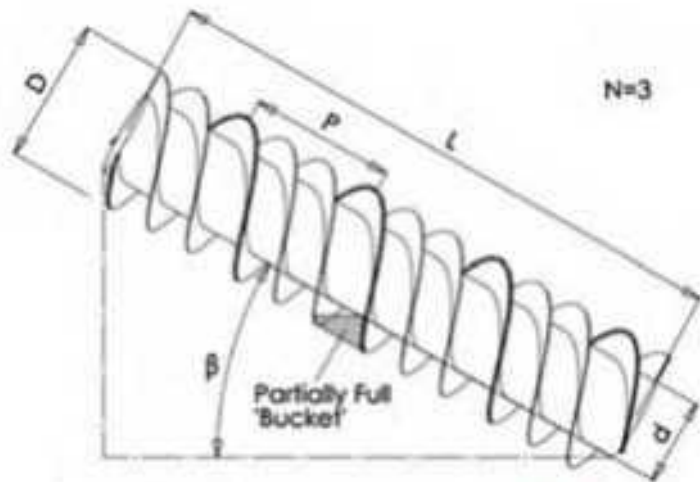


Fig. 4. Geometry of Archimedes Screw [41].

118

J. Rorres et al. / Renewable Energy 94 (2016) 106–146

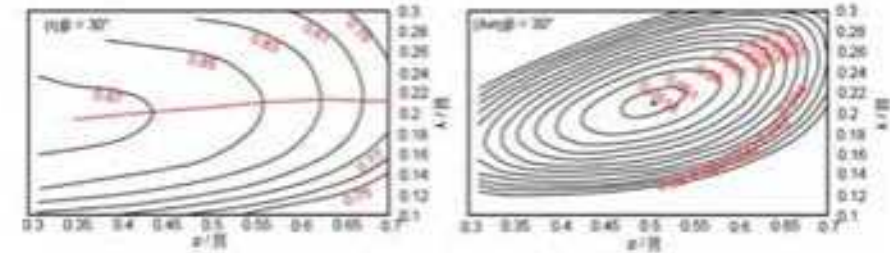


Fig. 2. Mechanical efficiency and optimal geometric parameters for a three-flighted Archimedes screw ($N = 3$) with an inclination β of 30° as a function of the pitch λ and radius r ratio [10,14,15].

Table 2

Performance ratios for optimisation.

Name	Ratio/relationship
Diameter ratio	$\delta = d/D$
<u>Pitch</u> ratio	$Pr = P/D$
Length ratio	$Lr = L/D$

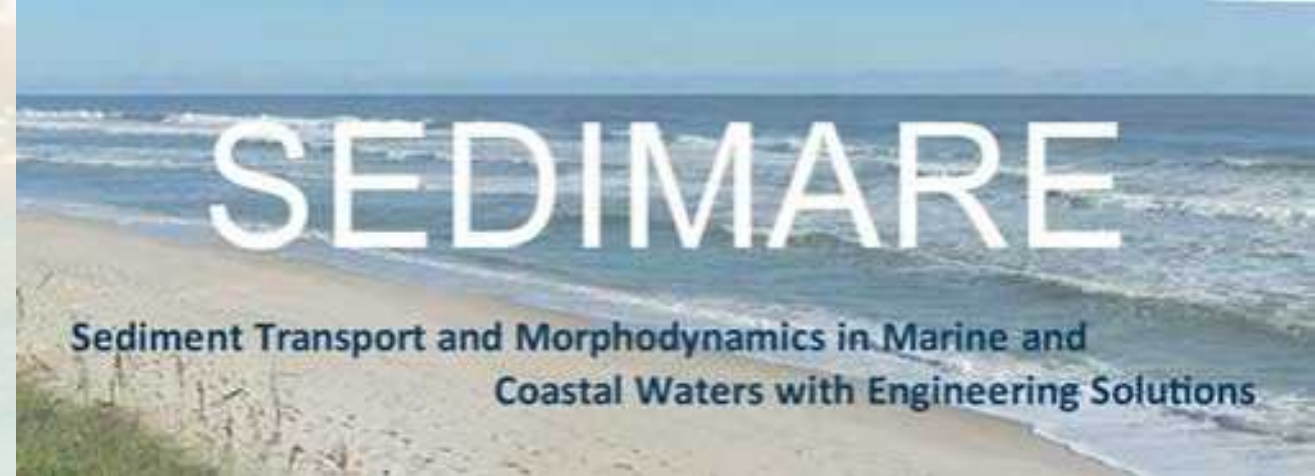
Table 1

Geometric Identities for Archimedes screw.

Symbol	Name	Internal (I)/External (E)
D	Outer diameter	E
d	Inner diameter	I
P	<u>Pitch</u>	I
L	Length of screw	E
θ	Angle of inclination	E
N	Number of flights	I
G	Thickness of spiral profile	I
n	Rotational speed	E
Q	Flow rate	E
H	Head	E
ω	Rotation rate	E



Laboratory of Hydraulic Engineering
Department of Civil Engineering
University of Patras



Large-eddy simulations of turbulent oscillatory flow and sediment transport induced by waves

Ioannis Gerasimos Tsipas

Supervisor: Athanassios A. Dimas, Professor

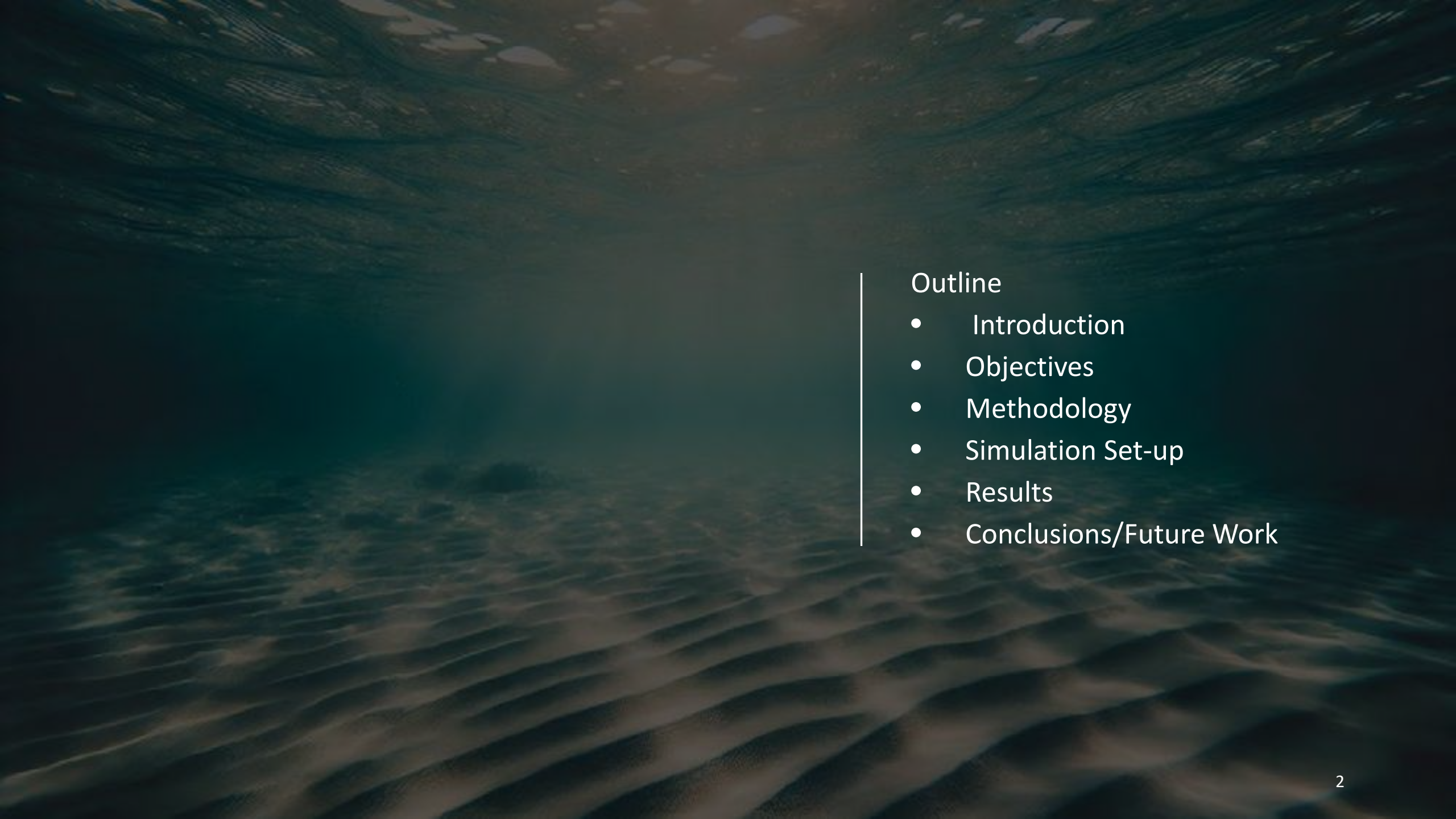


**Funded by
the European
Union**



This project has received funding
from the European Union's
Horizon Europe research and
innovation programme under the
Marie Skłodowska-Curie grant
agreement No 101072443.





Outline

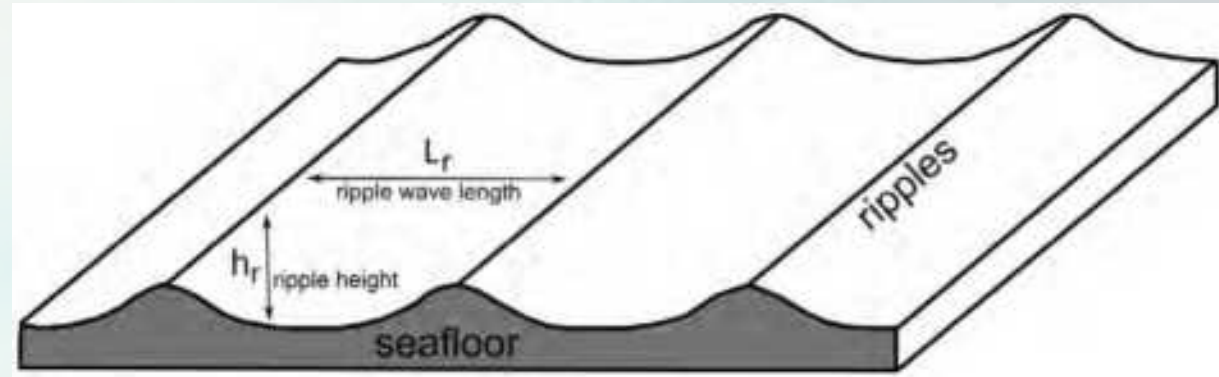
- Introduction
- Objectives
- Methodology
- Simulation Set-up
- Results
- Conclusions/Future Work

- Surface waves induce oscillatory flow at seabed
- Generation of bed forms (ripples, dunes, bars)
- Significant impact on wave propagation and sediment transport by increasing bed roughness and promoting sediment suspension due to vortex shedding

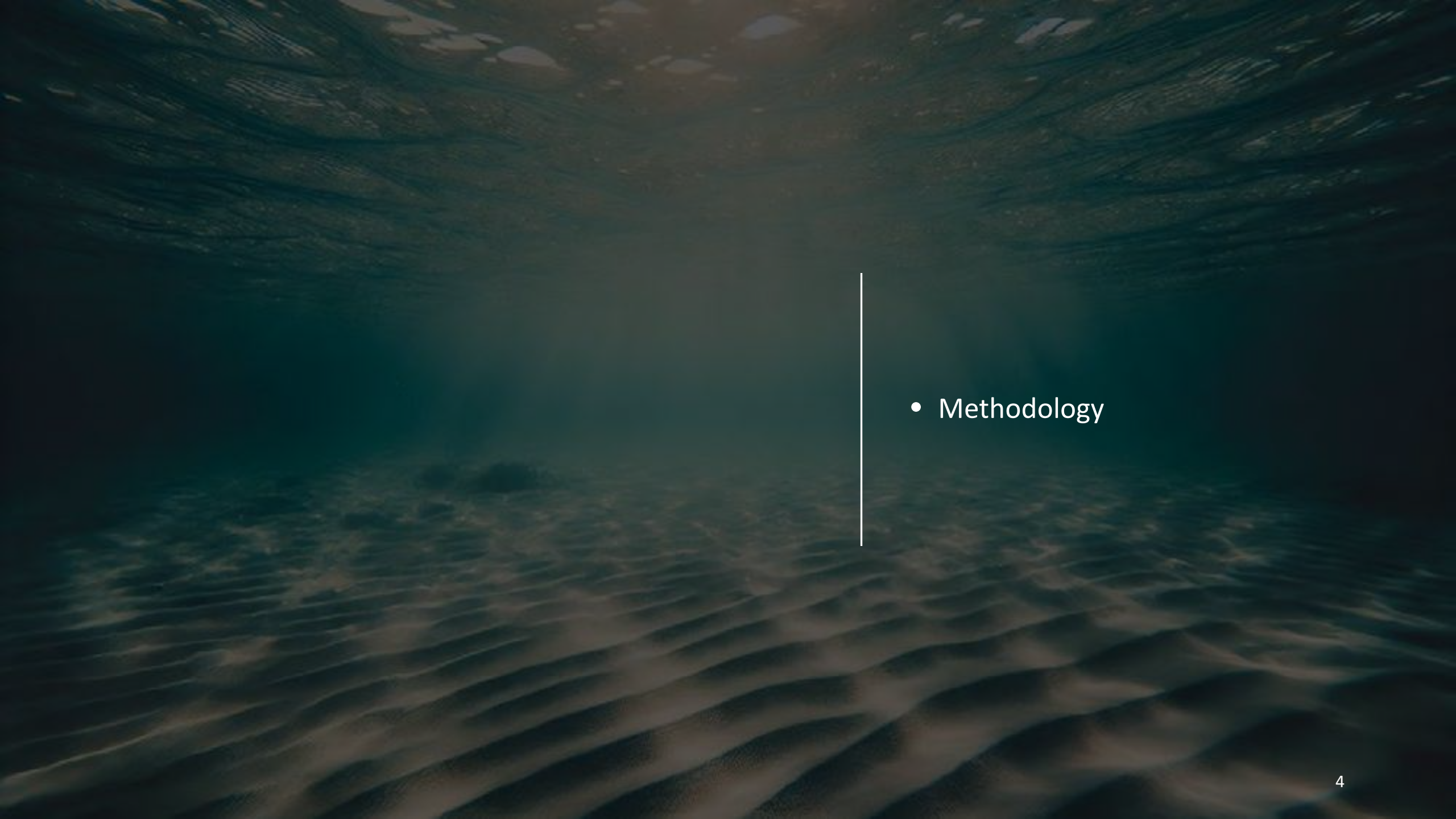
The dynamics of turbulent oscillatory flow and sediment transport over sandy beds is critical for understanding various environmental and engineering processes, such as coastal erosion, sedimentation patterns, and habitat formation.

Objectives

- Development of large-eddy simulation (LES) software to model turbulent oscillatory flow and mixed-grain sediment transport induced by waves.



https://www.vhv.rs/viewpic/hbJbwRw_transparent-water-ripples-png-ripple-of-water-diagram/

- 
- Methodology

Flow Equations (non-dimensional)

Continuity *equation*:

$$\frac{\partial u_i}{\partial x_i} = 0$$

Navier-Stokes equations:

$$\frac{\partial u_i}{\partial t} + \frac{\partial}{\partial x_j} (u_i u_j) = -\frac{\partial p}{\partial x_i} - \frac{\partial \tau_{ij}}{\partial x_j} + \frac{1}{\text{Re}} \frac{\partial^2 u_i}{\partial x_j \partial x_j} + f_i$$

$$\text{Re} = \frac{U_0 a_0}{\nu}$$

u_i is the resolved velocity field according to LES .

Dynamic pressure:

$$p = P_o + P \quad \text{where } P_o \text{ is the externally imposed pressure field.}$$



$$u_o(t) = U_o (\cos(\omega t) + B \cos(2\omega t))$$

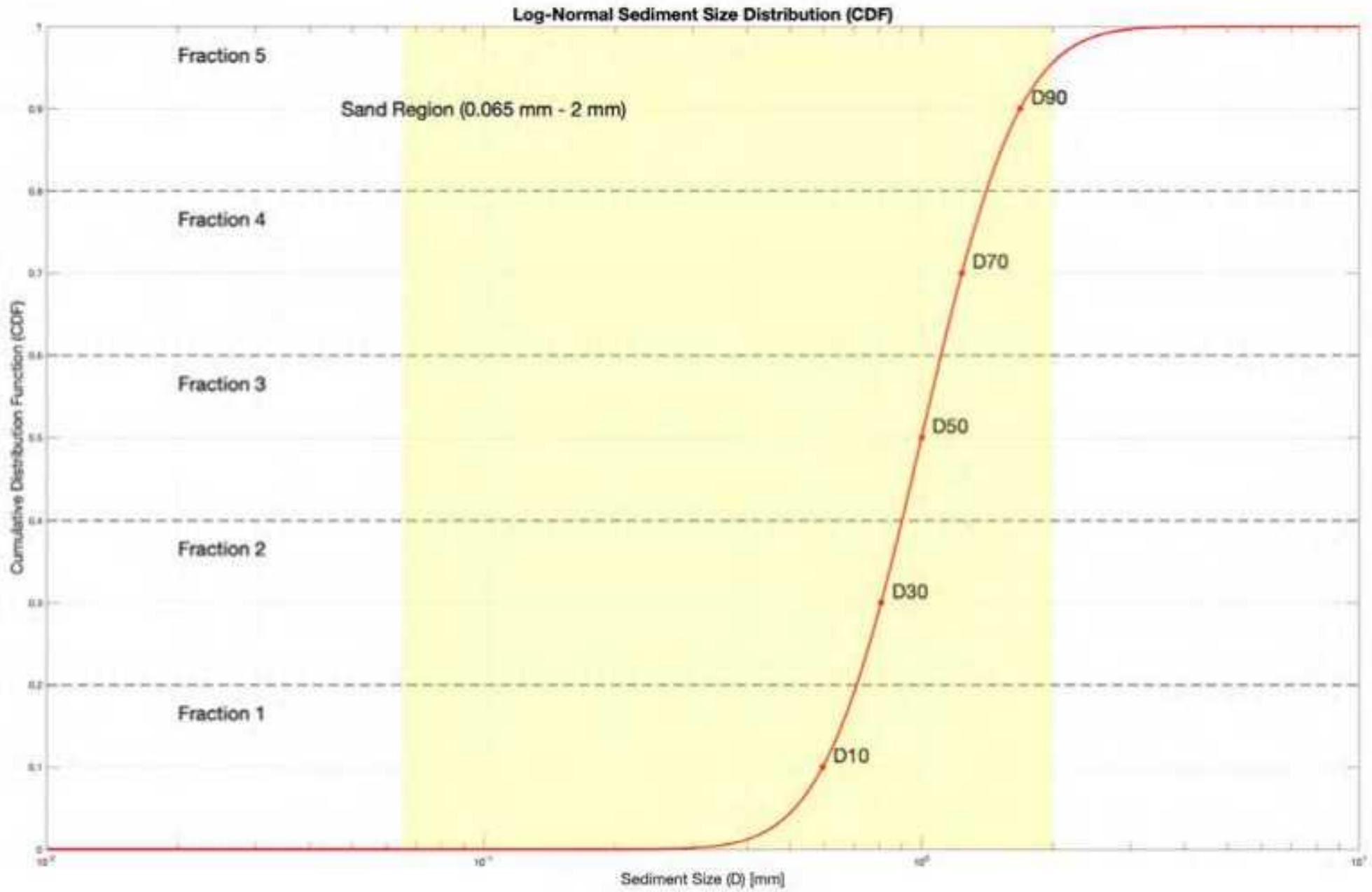
Subgrid-scale (SGS) stresses (Smagorinsky 1963) :

$$\tau_{ij} = -2D_{wall} \nu_{sgs} S_{ij} = -2D_{wall} (C_s \Delta)^2 |S| S_{ij}$$

$$S_{i,j} = \frac{1}{2} \left(\frac{\partial u_i}{\partial x_j} + \frac{\partial u_j}{\partial x_i} \right)$$

$$|S| = (2S_{ij}S_{ij})^{1/2}$$

$$\Delta = (\Delta x_1 \Delta x_2 \Delta x_3)^{1/3}$$



Sediment Transport Equations

Type equation here. Bed load transport rate (Engelund and Fredsøe, 1976):

$$\frac{q_{b(nd)}}{\sqrt{(S-1)gDg_{(nd)}^3}} = \begin{cases} \operatorname{sgn}(\theta) \frac{5\pi}{3} \left[1 + \left(\frac{\pi}{6} \frac{\mu_d}{|\theta_{(nd)}| - \theta_{c(nd)}} \right)^4 \right]^{-\frac{1}{4}} \left(\sqrt{|\theta_{(nd)}|} - 0.7 \sqrt{|\theta_{c(nd)}|} \right), & (\theta_{(nd)} > \theta_{c(nd)}) \\ 0, & (\theta_{(nd)} < \theta_{c(nd)}) \end{cases}$$

Shields number : $\theta = \frac{\tau_b}{\rho_w(S-1)gDg_{(nd)}^3}$

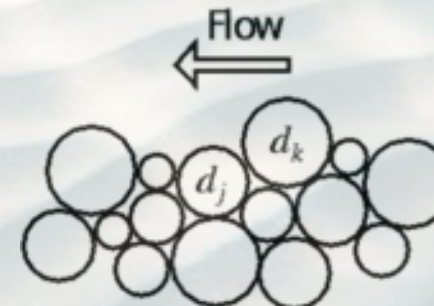
Critical Shields number: $\theta_c(D_{g(nd)}, S)$ $\xrightarrow{\text{Hide/Exposure factor}} \theta_{c(nd)} \left(\frac{p_{ek}}{p_{hk}} \right)^m$

Grain diameters: $D_{g(nd)}$

Sediment specific gravity: S

Dynamic friction coefficient: $\mu_d \approx 0.5\mu_s$

Hidden & Exposed probabilities of particles d_k



$$p_{hk} = \sum_{j=1}^N \left(p_{bj} \frac{d_j}{d_k + d_j} \right)$$

$$p_{ek} = \sum_{j=1}^N \left(p_{bj} \frac{d_k}{d_k + d_j} \right)$$

Advection-diffusion equation for the suspended sediment concentration:

$$\frac{\partial c_{(nd)}}{\partial t} + u_j \frac{\partial c_{(nd)}}{\partial x_j} - w_{s(nd)} \frac{\partial c_{(nd)}}{\partial x_3} = \frac{1}{\sigma Re} \frac{\partial^2 c_{(nd)}}{\partial x_j \partial x_j} - \frac{\partial \chi_j}{\partial x_i} + f_c$$

where $w_{s(nd)}$ is the sediment fall velocity (Hallermeier 1981) for each grain fraction:

$$\frac{w_{s(nd)} D g_{(nd)}}{\nu} = \begin{cases} D_{*(nd)}^3 / 18 & D_{*(nd)}^3 < 39 \\ D_{*(nd)}^{2.1} / 6 & \text{for } 39 < D_{*(nd)}^3 < 10^4 \\ 1.05 D_{*(nd)}^{1.5} & 10^4 < D_{*(nd)}^3 \leq 3 \cdot 10^6 \end{cases} \quad . \text{where. } D_{*(nd)} = D g_{(nd)} \left(\frac{(S-1)g}{\nu^2} \right)^{1/3}$$

σ is the Schmidt number, χ_j is the SGS turbulent term (Zedler and Street 2001): $\chi_j = \frac{v_{sgs}}{\sigma_t} \frac{\partial c_{(nd)}}{\partial x_j}$

and σ_t is the turbulent Schmidt number.

Suspended load transport rate: $q_{s1,2(nd)} = \int_{x_{3bed}}^{x_{3top}} u_{1,2} c_{(nd)} dx_3$

Bed Evolution modeling

Exner Equation: The bed elevation evolution follows the Exner Equation in two dimensions and expresses the coupling between the evolution of bed morphology and the sediment transport fluxes.

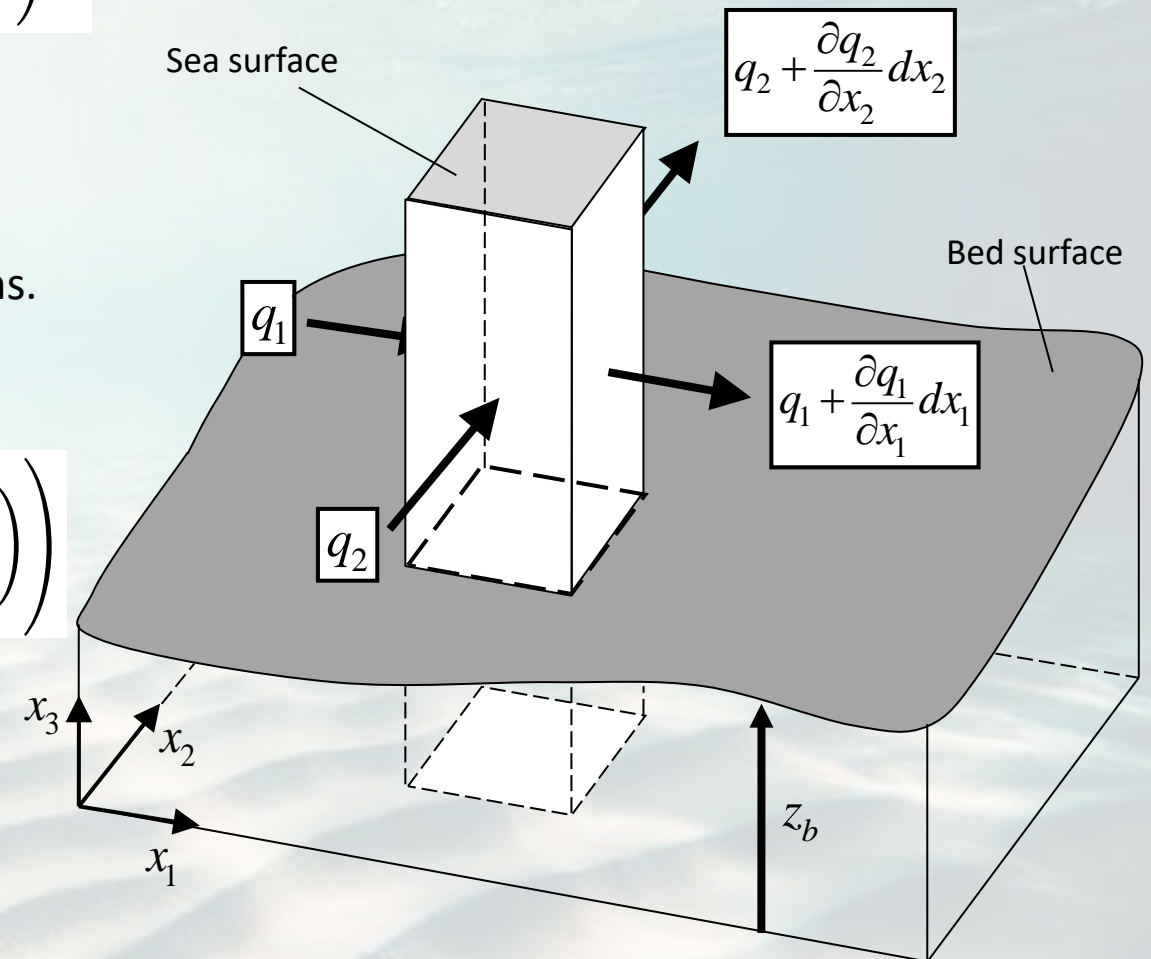
$$\frac{\partial z_b}{\partial t} + \frac{1}{1-n} \frac{\partial}{\partial t} \left(\int_{x_3 \geq z_b}^h c_{(nd)} dx_3 \right) = - \frac{1}{1-n} \left(\frac{\partial q_{1(nd)}}{\partial x_1} + \frac{\partial q_{2(nd)}}{\partial x_2} \right)$$

z_b is the bed level

n is the bed sediment porosity

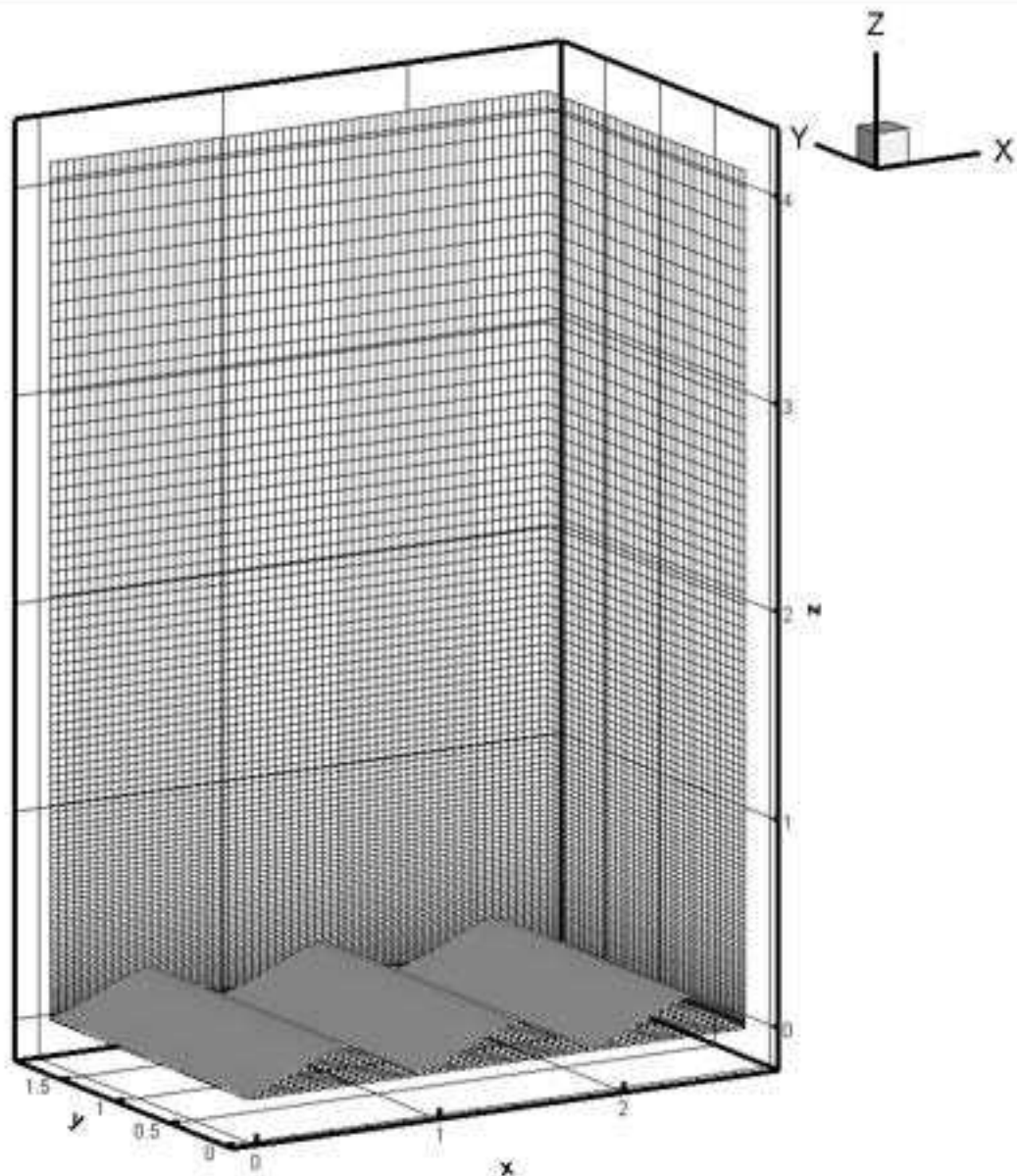
$q_{1,2} = (q_b + q_s)_{1,2}$ is the total sediment flux in the horizontal directions.

$$\frac{\partial z_b}{\partial t} = - \frac{1}{1-n} \sum_{nd=1}^N \left(\frac{\partial}{\partial t} \left(\int_{x_3 \geq z_b}^h c_{(nd)} dx_3 \right) + \left(\frac{\partial q_{1(nd)}}{\partial x_1} + \frac{\partial q_{2(nd)}}{\partial x_2} \right) \right)$$



Simulation Set-up

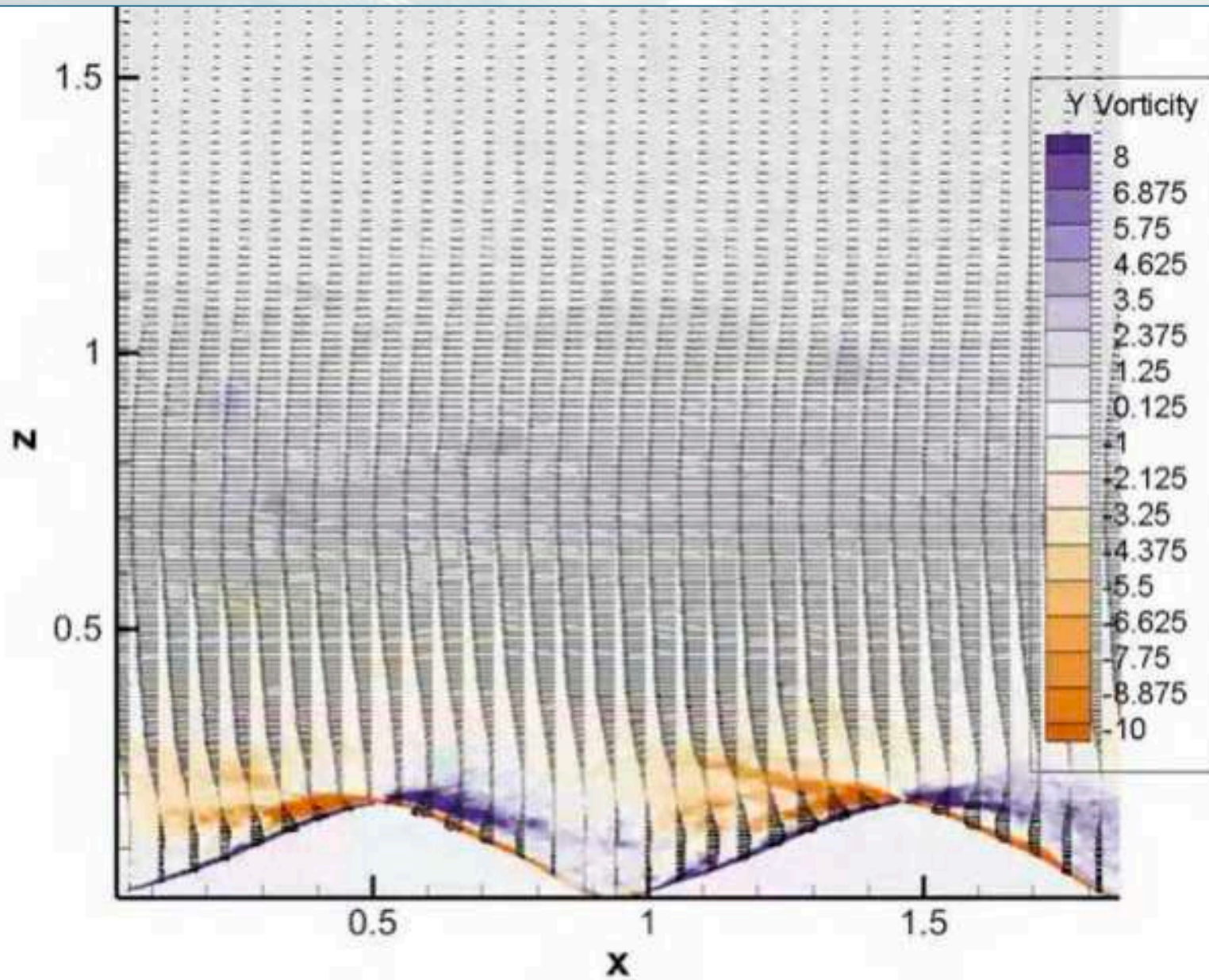
Van Der Werf et al.(2007) , experiment Mr5b63



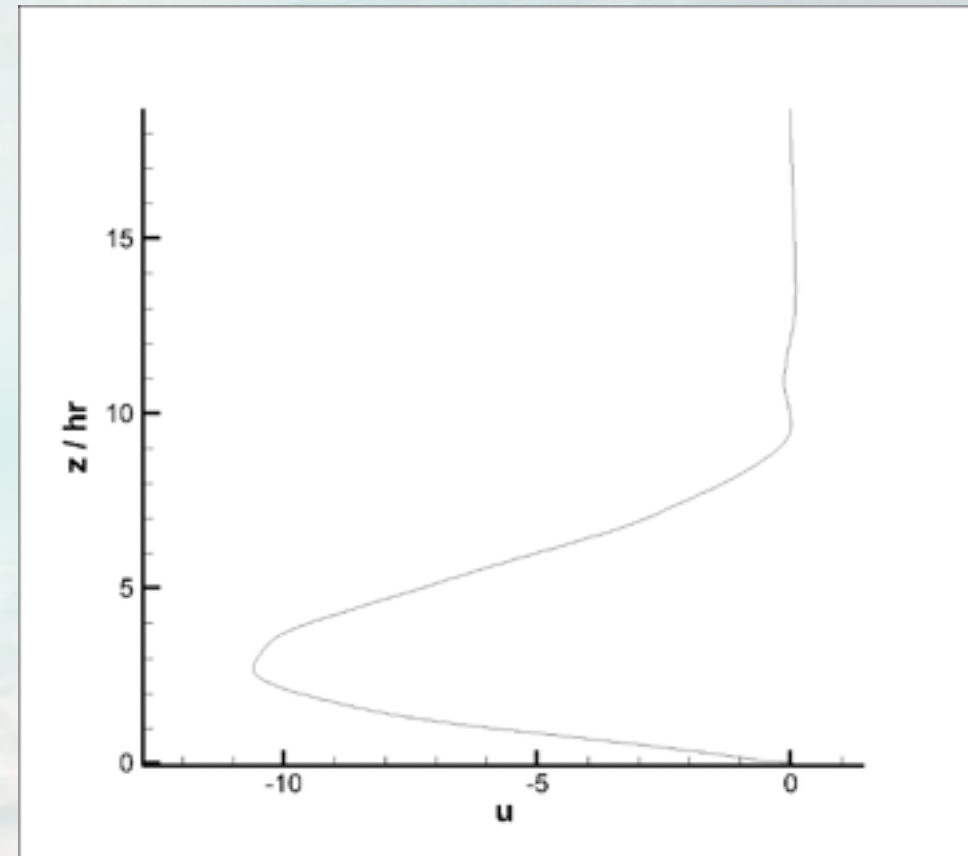
$Re = 23000$
 $L_r = 0.9425$
 $h_r = 0.18$
 $\Delta x = 0.00368\text{ m}$
 $\Delta y = 0.00368\text{ m}$
 $\Delta z = 0.001 \rightarrow 0.04853\text{ m}$
Grid = $513 \times 33 \times 650 =$
11.003.850 cells

$D_g(m)$	Ψ	a_0/D_g
0.00025	104.4	2100
0.00035	74.5	1500
0.00044	59.3	1193
0.00053	49.2	990
0.00066	39.5	¹⁰ 795

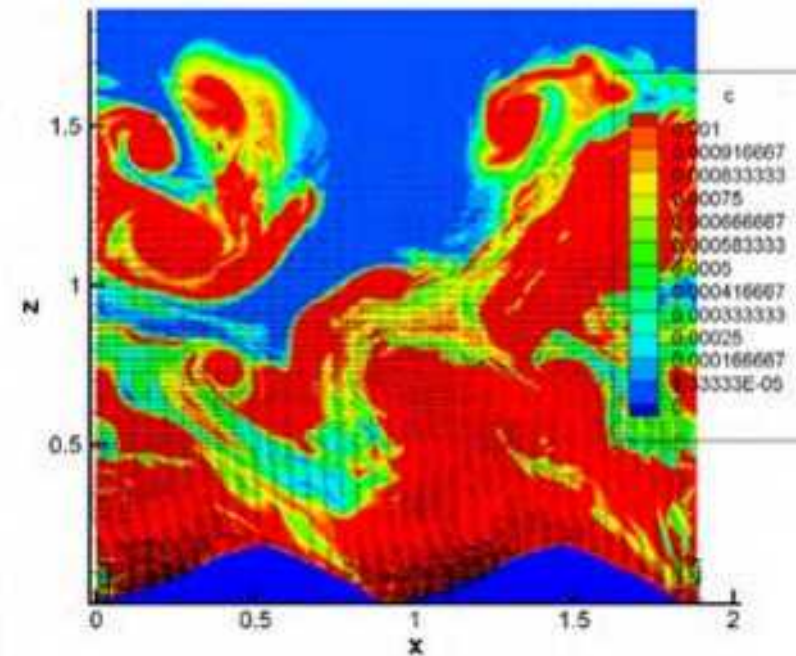
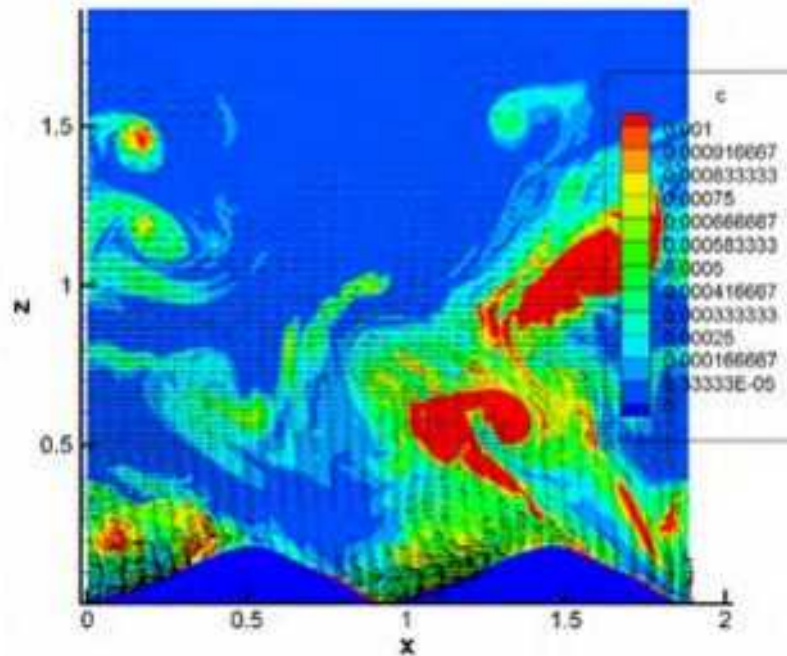
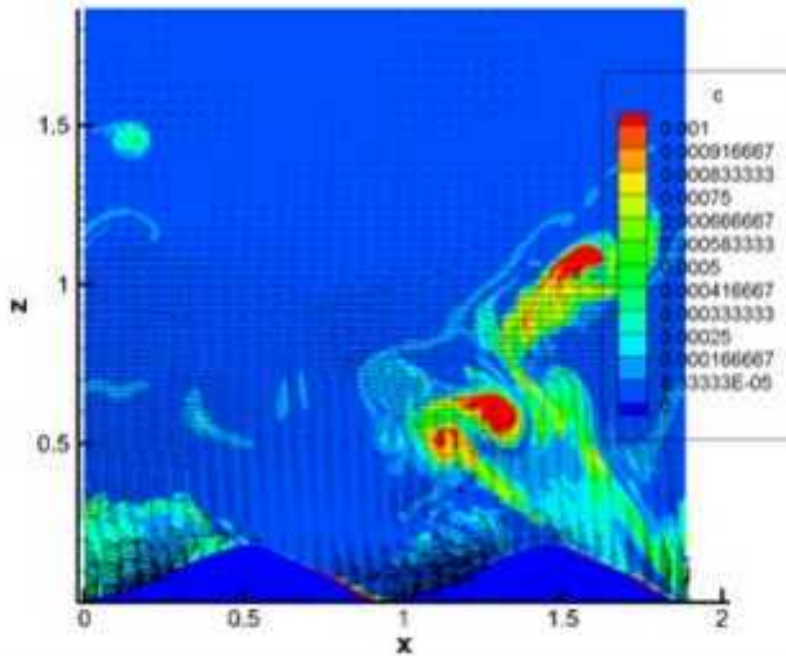
The period- and spanwise-averaged velocity field (vectors) and Y vorticity field



Profile of the mean streamwise velocity, u



Instantaneous snapshots of the distribution of the suspended sediment on the 1T of the 12th Period

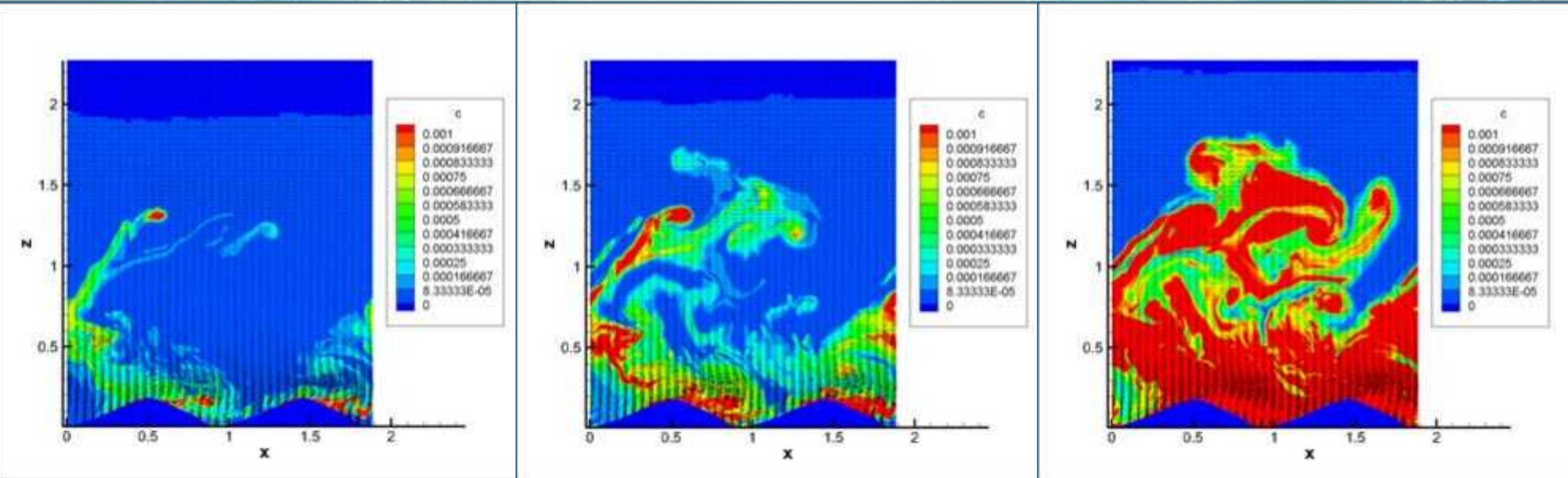


(a) 0.66mm dimension size fraction

(b) 0.44mm dimension size fraction

(c) 0.25mm dimension size fraction

Instantaneous snapshots of the distribution of the suspended sediment on the T/4 12th Period

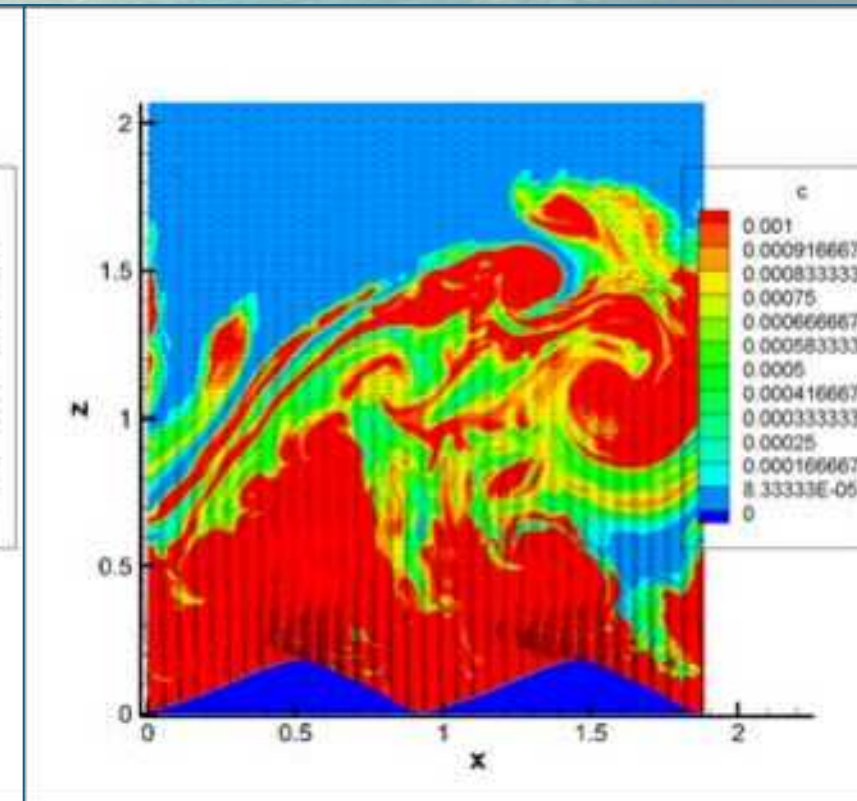
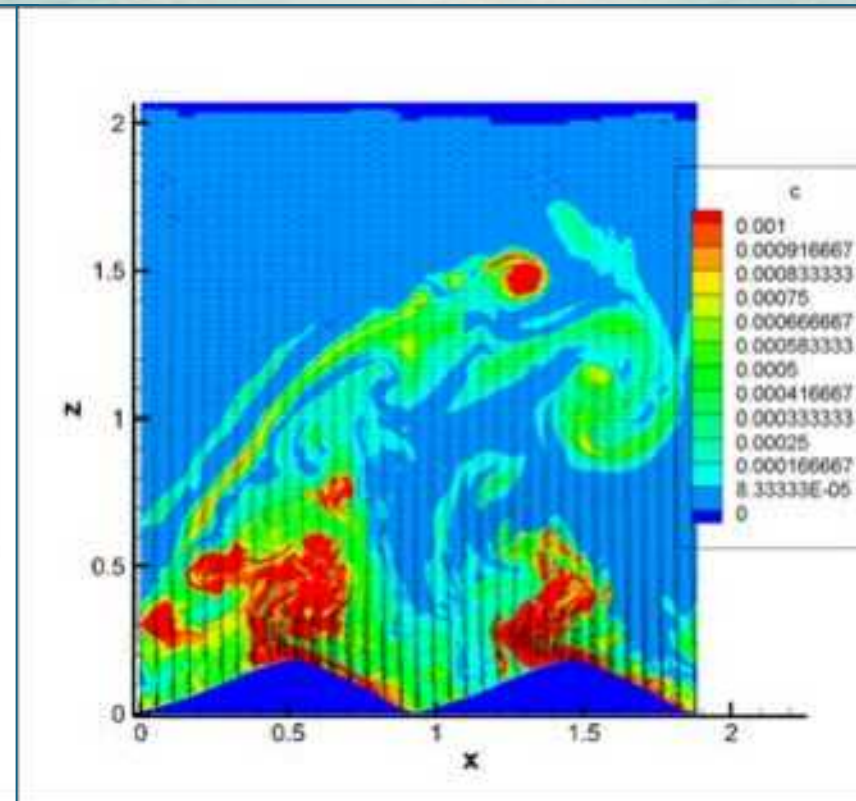
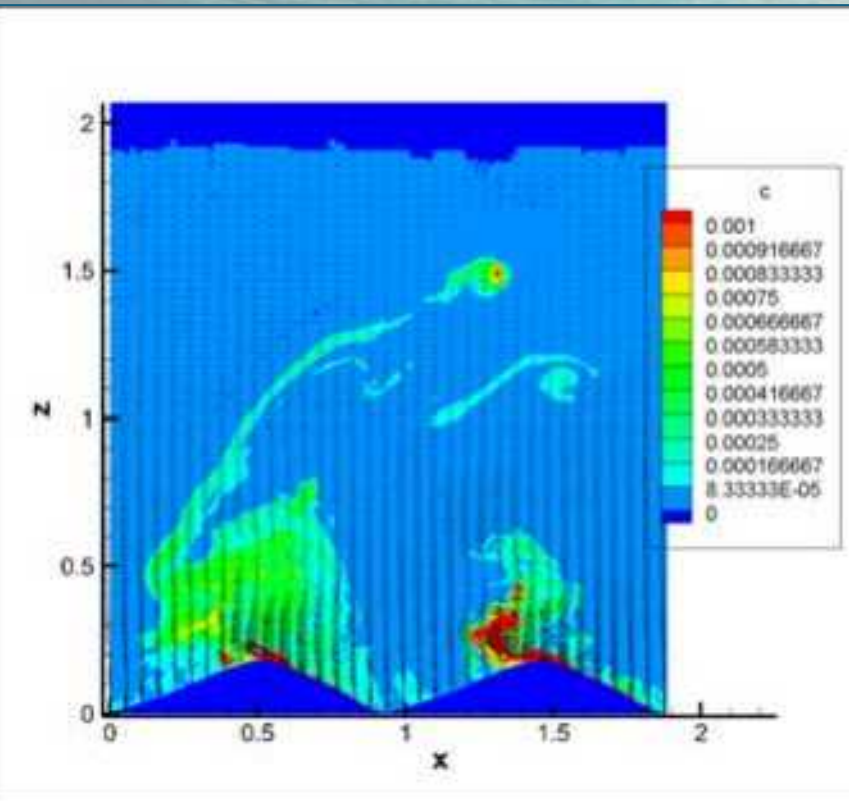


(a) 0.66mm dimension size fraction

(b) 0.44mm dimension size fraction

(c) 0.25mm dimension size fraction

Instantaneous snapshots of the distribution of the suspended sediment on the T/2 12th Period

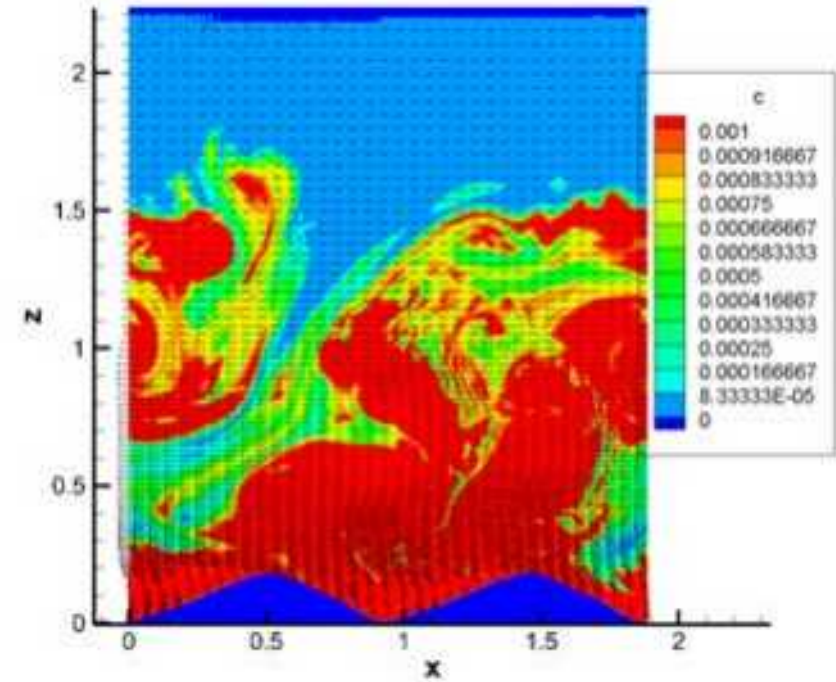
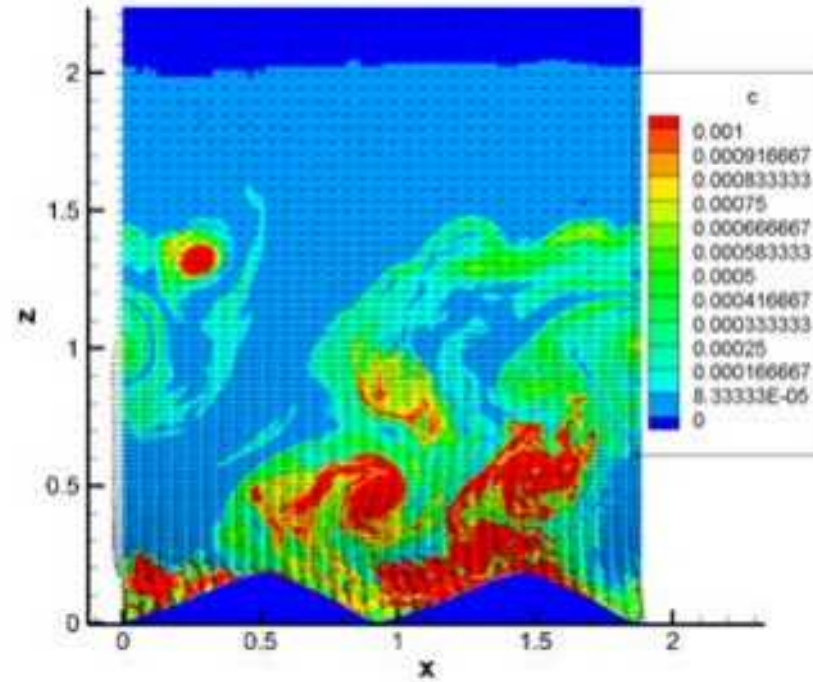
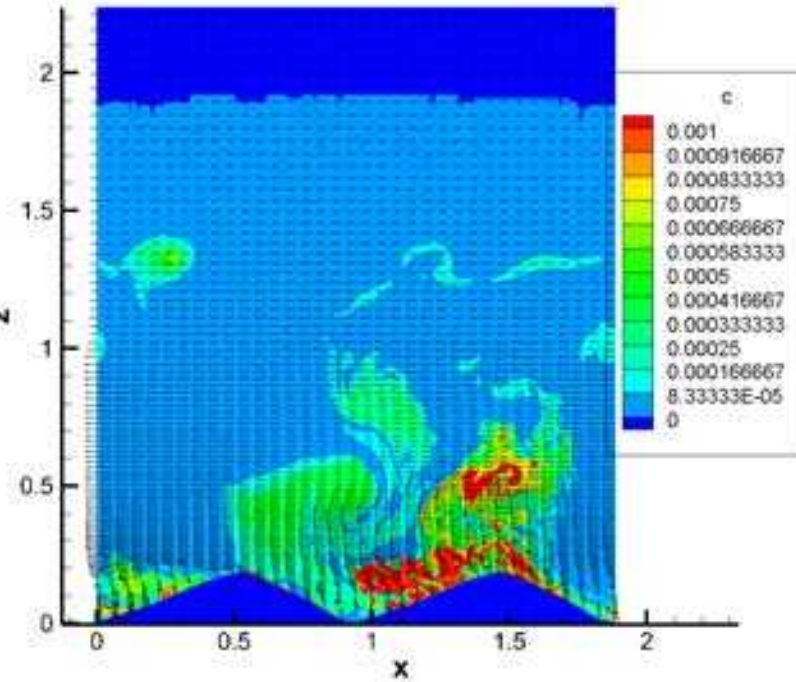


(a) 0.66mm dimension size fraction

(b) 0.44mm dimension size fraction

(c) 0.25mm dimension size fraction

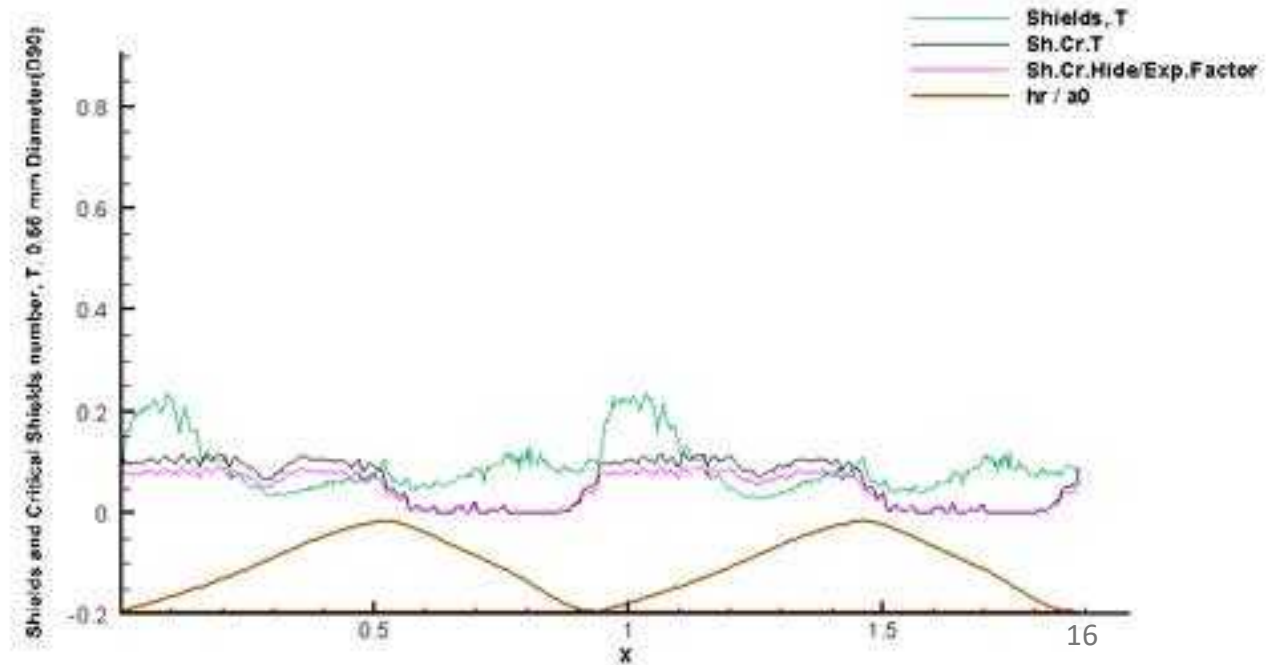
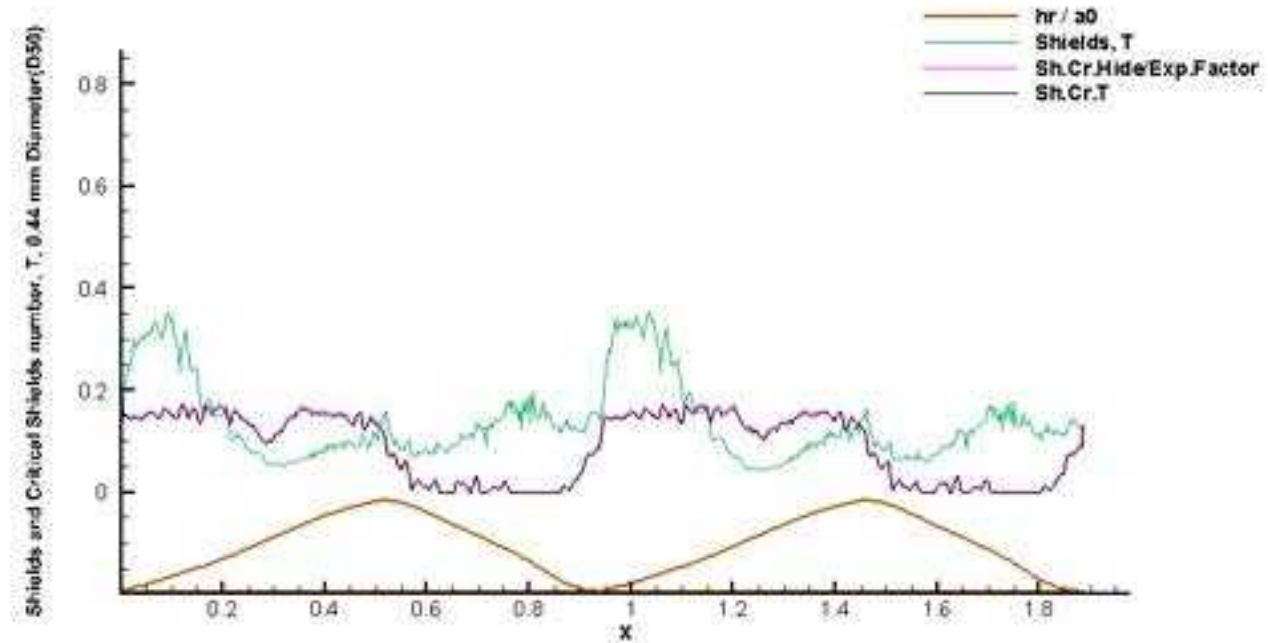
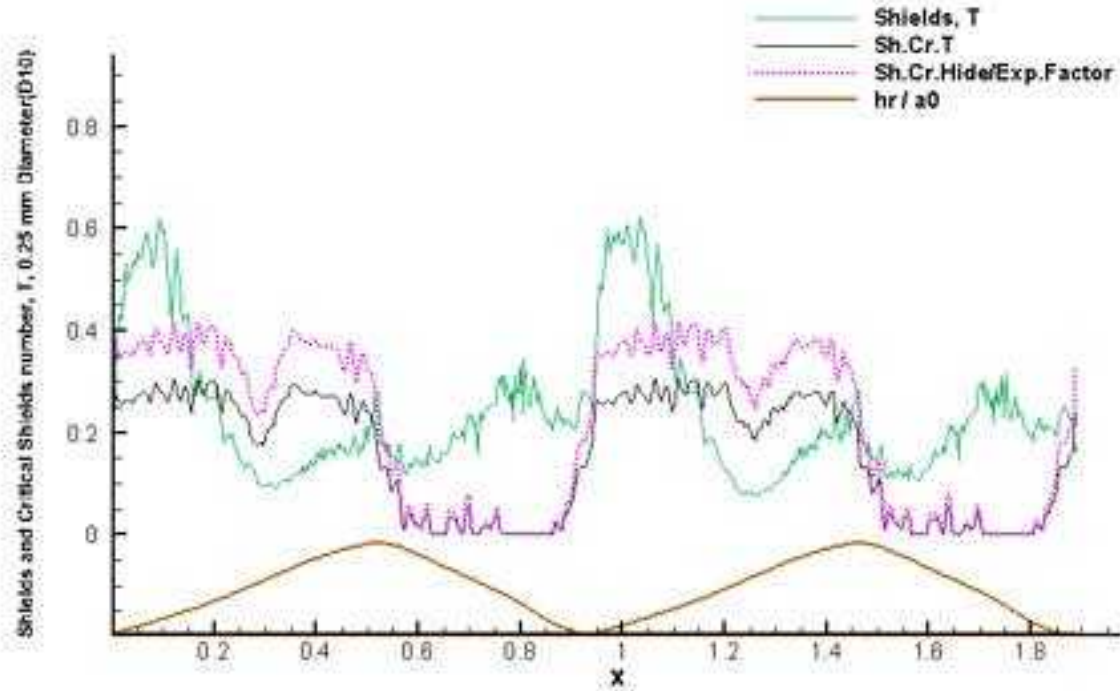
Instantaneous snapshots of the distribution of the suspended sediment on the 3T/4 12th Period



(a) 0.66mm dimension size fraction

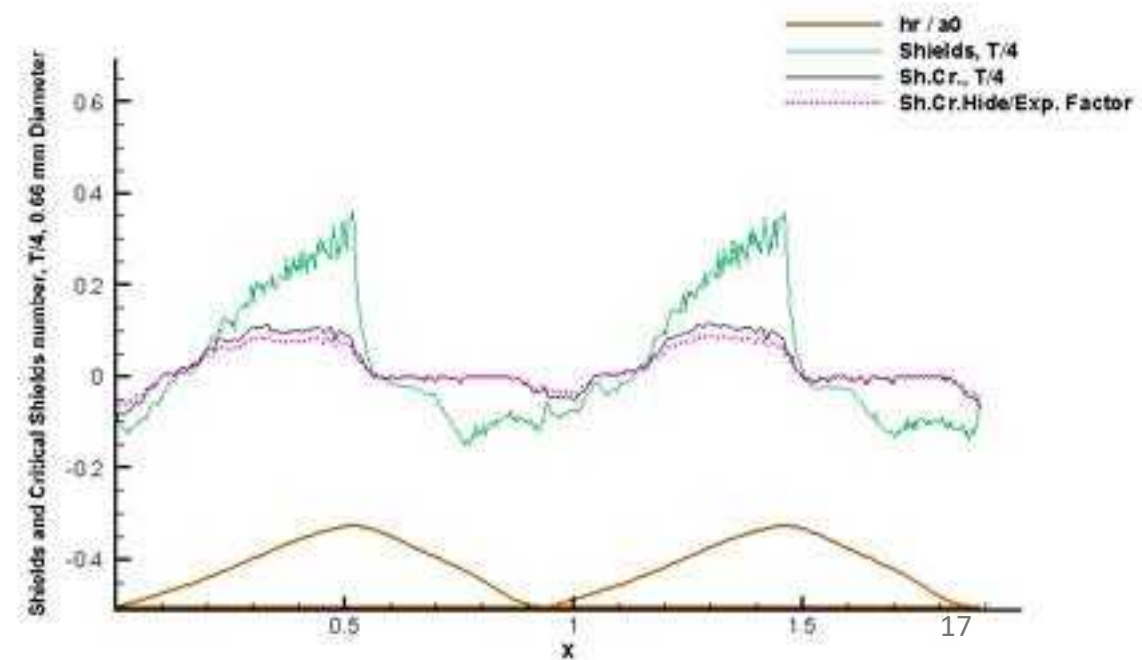
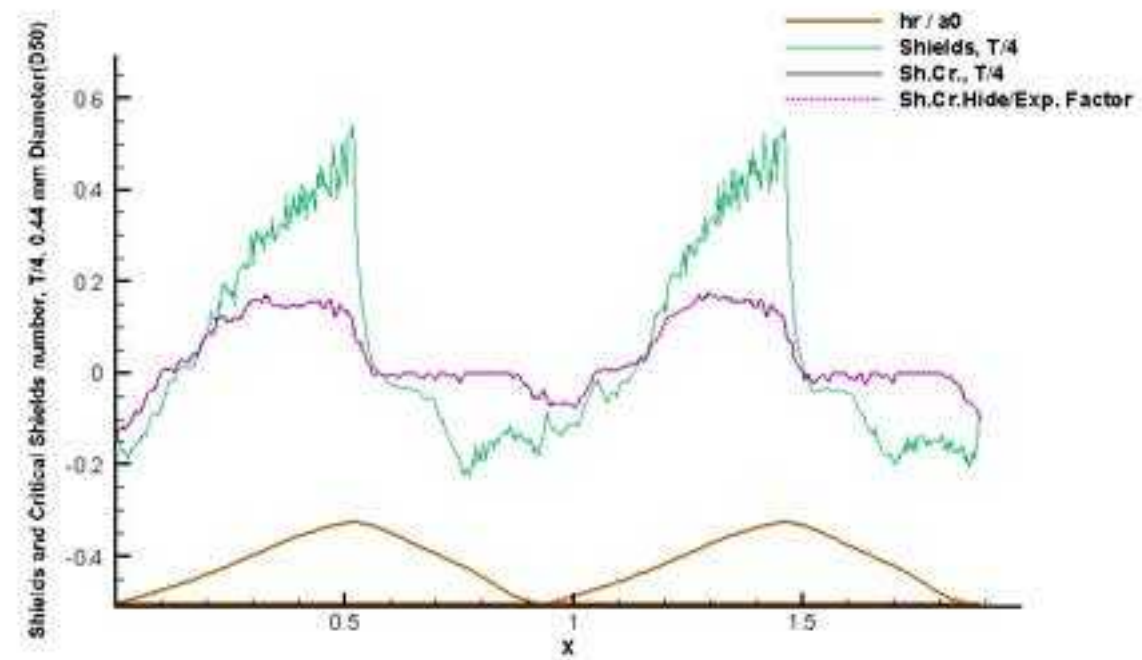
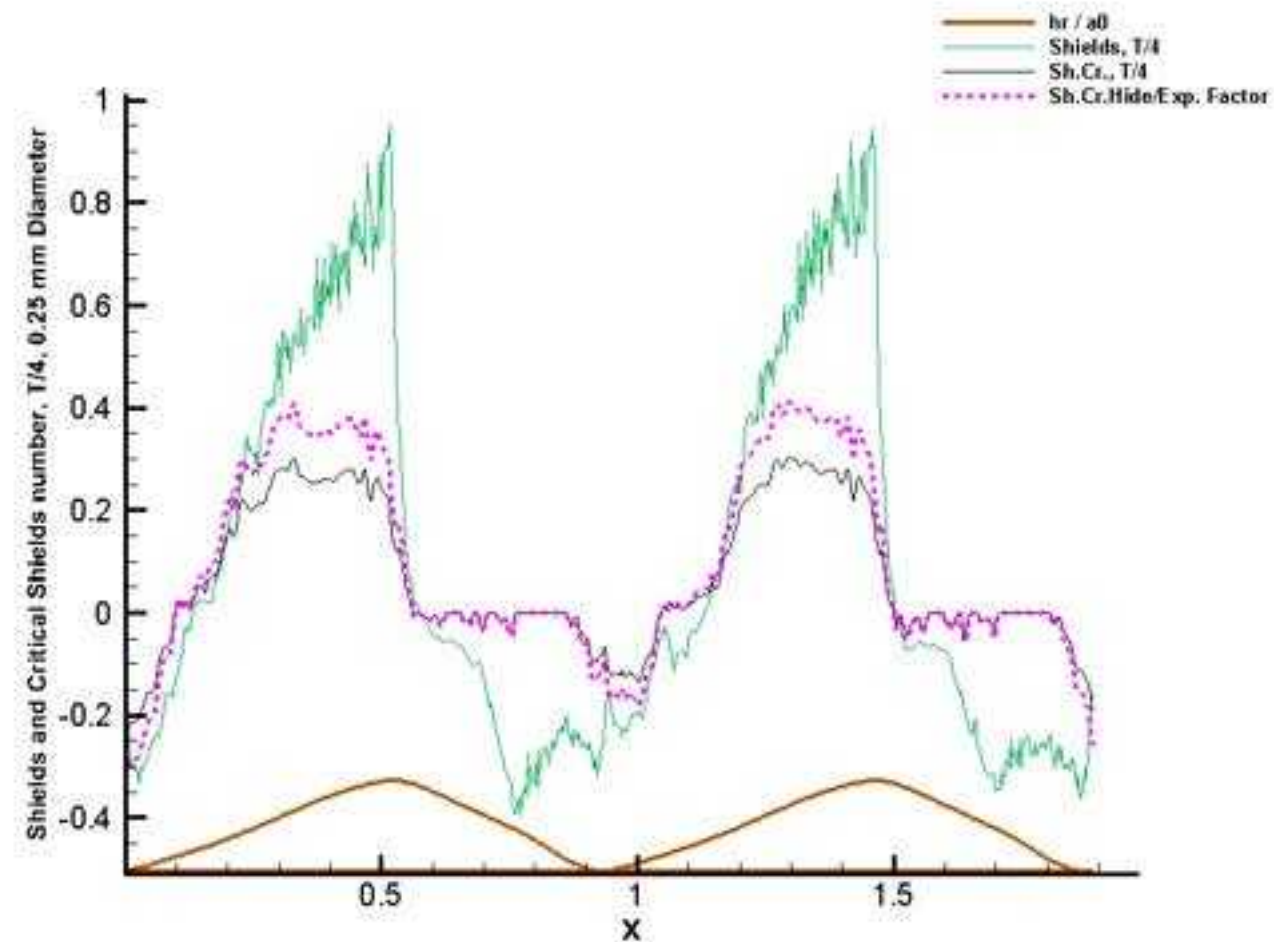
(b) 0.44mm dimension size fraction.

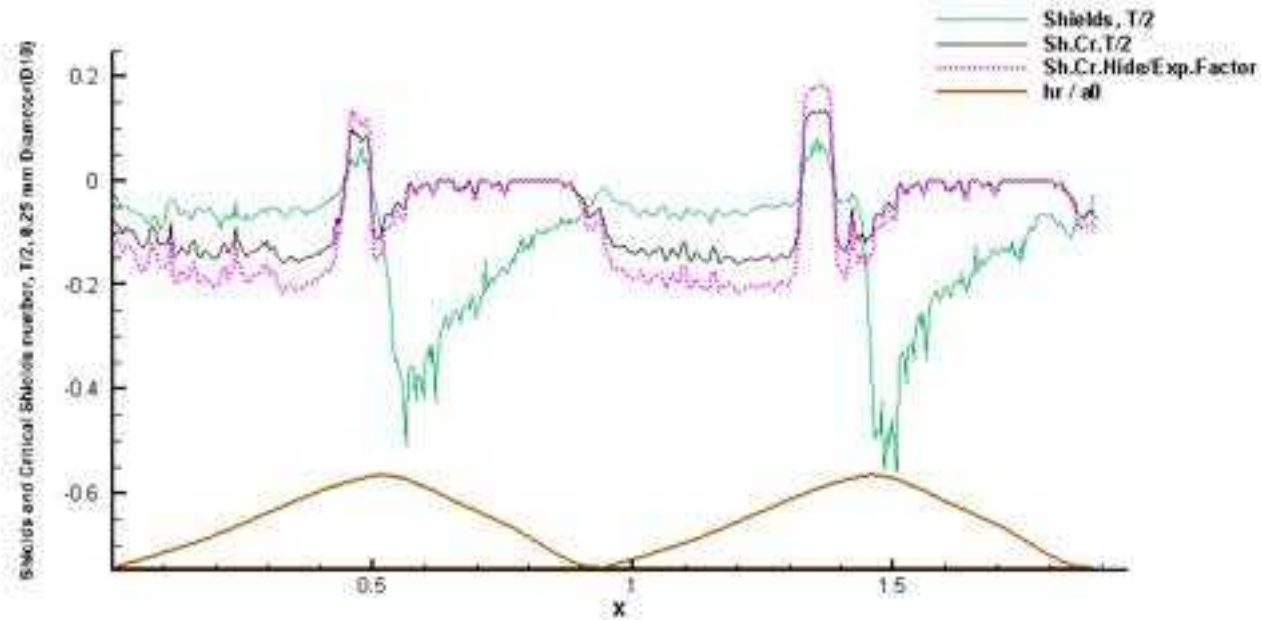
(c) 0.25mm dimension size fraction



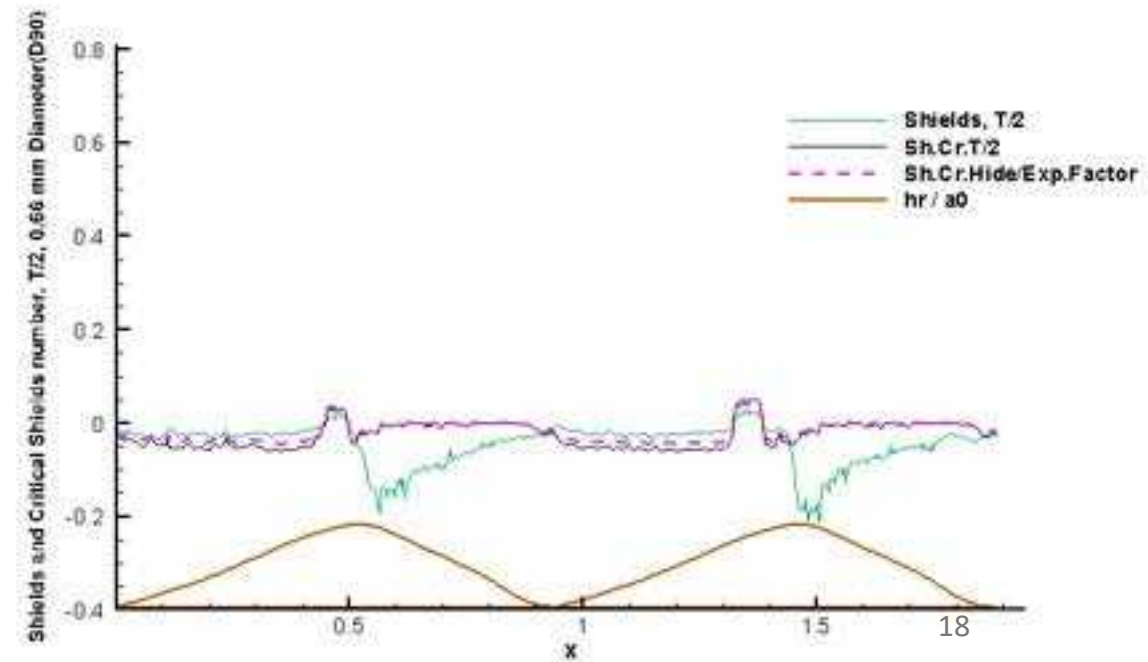
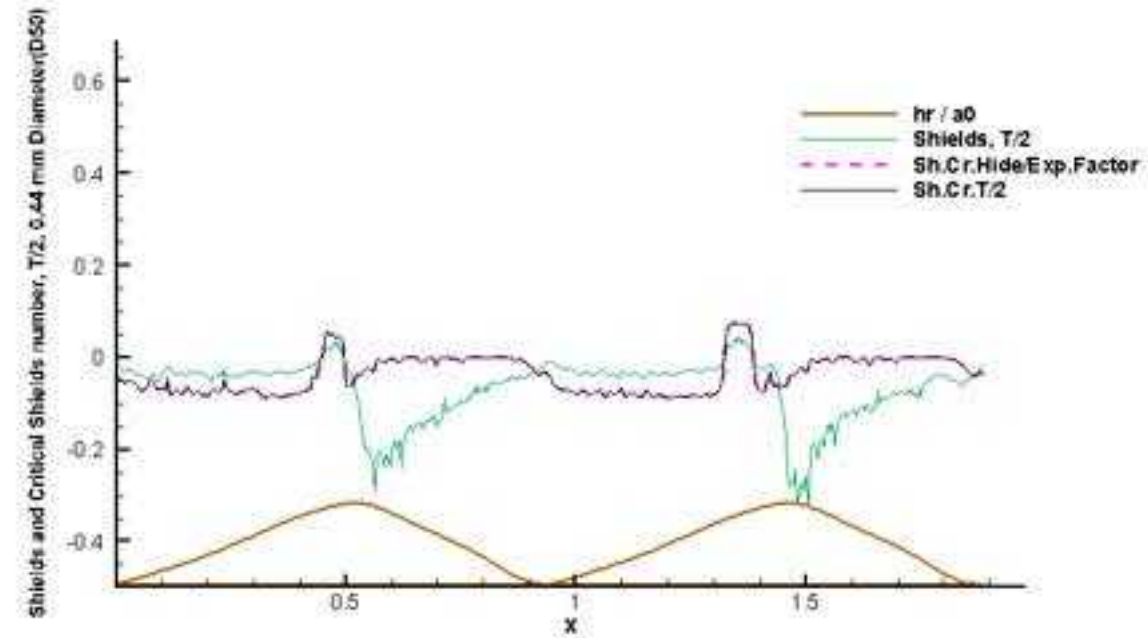
Profiles of Phase and Spanwise average Shields number & comparison between critical Shields number with and without the hide/exposure factor for the smallest, the median and the biggest fraction of sediment in 1T of 13 periods.

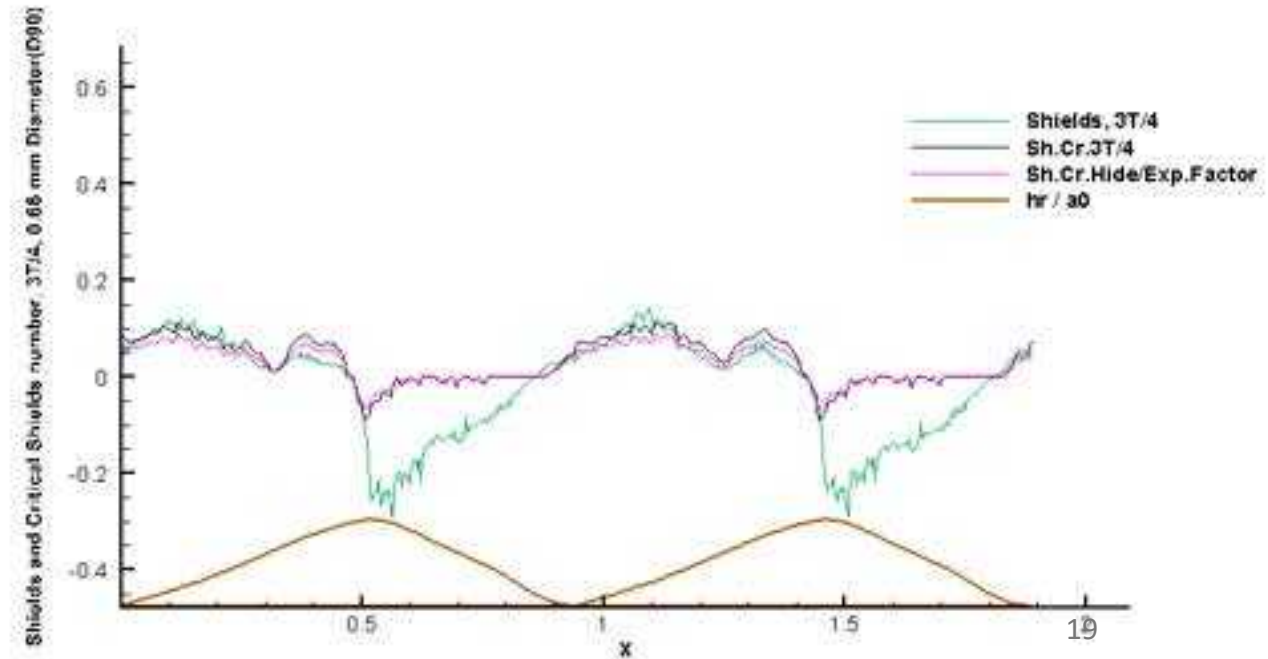
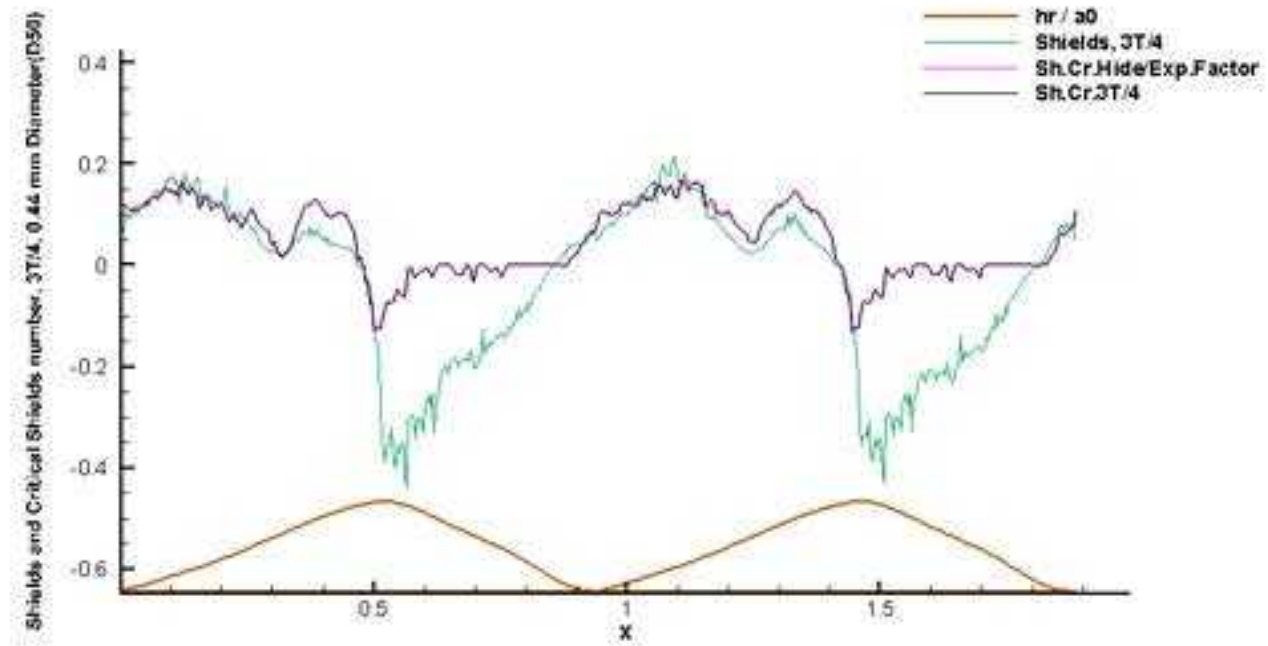
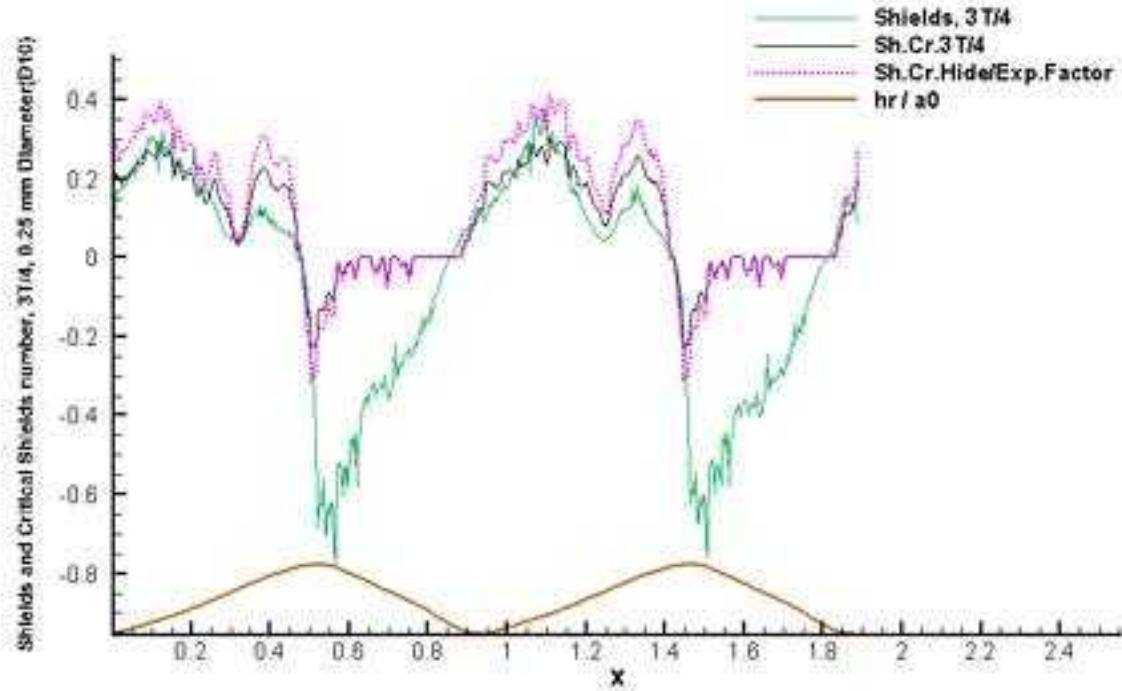
Profiles of Phase and Spanwise average Shields number & comparison between the critical Shields number with and without the hide/exposure factor for the smallest, the median and the biggest fraction of sediment in T/4 of 13 periods.





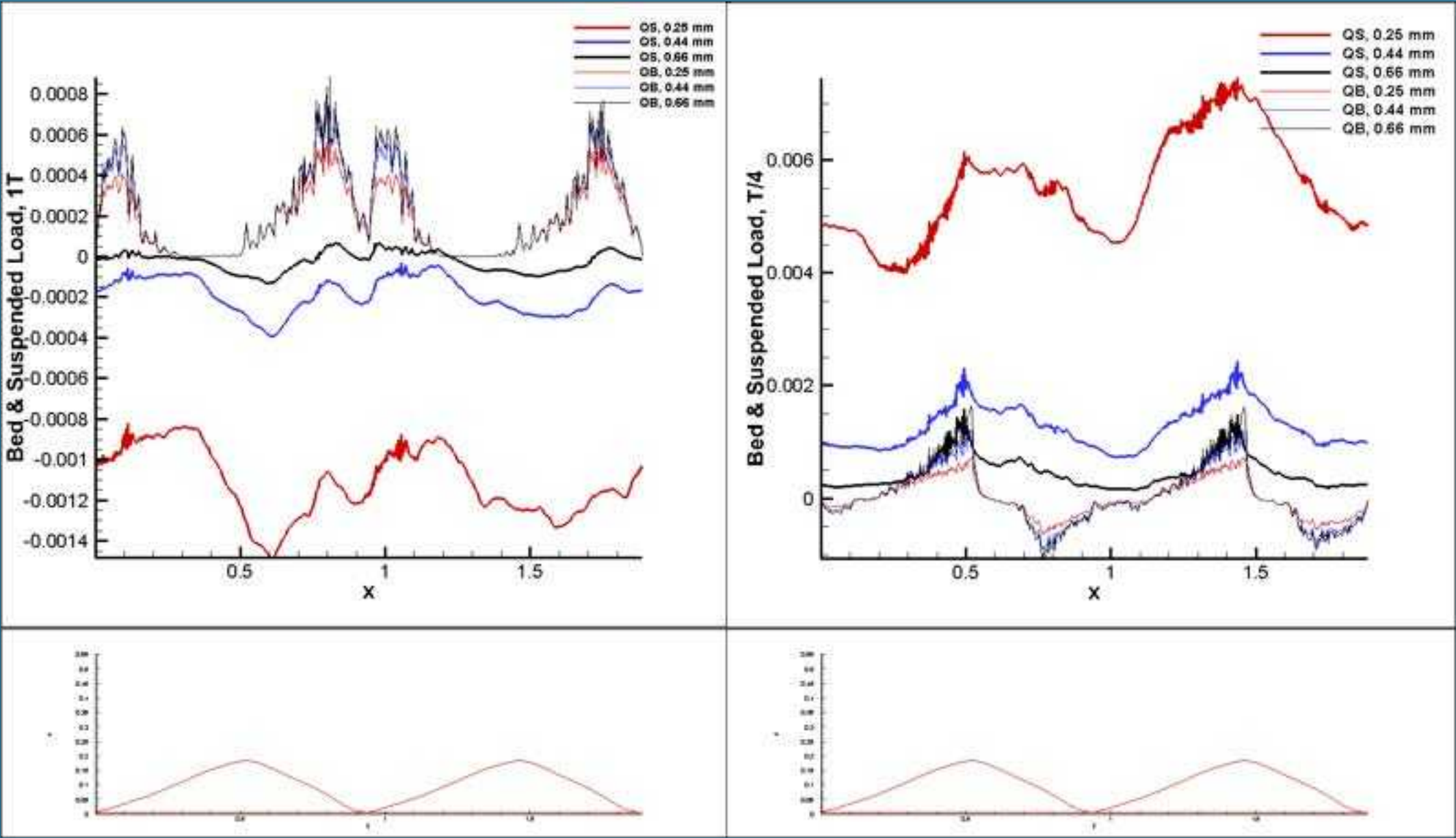
Profiles of the Phase and Spanwise average Shields number and comparison between the critical Shields number with and without the hide/exposure factor for the smallest, the median and the biggest fraction of sediment in T/2 of 13 periods.



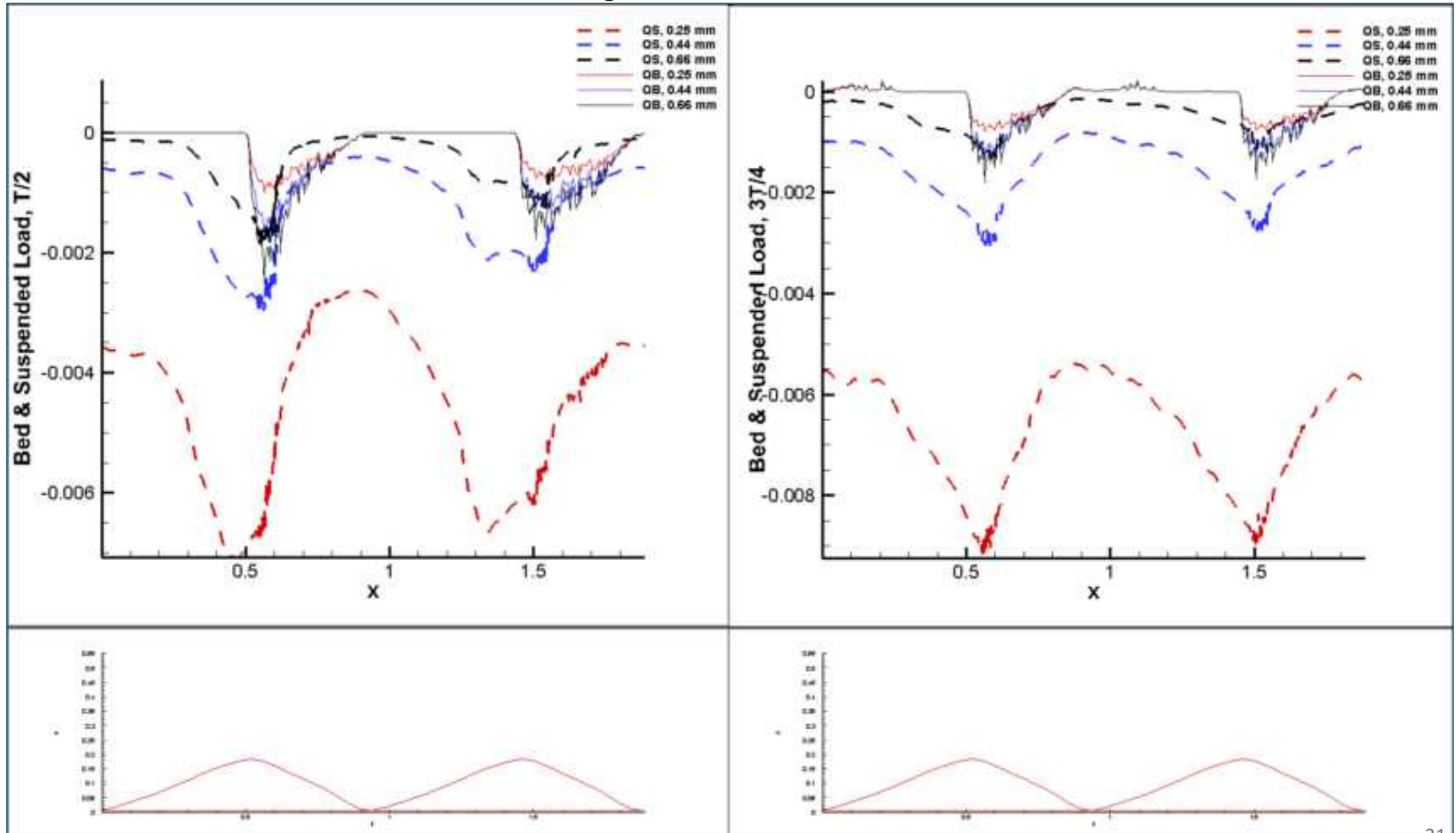


Profiles of the Phase and Spanwise average Shields number & comparison between the critical Shields number with and without the hide/exposure factor for the smallest, the median and the biggest fraction of sediment in 3T/4 of 13 periods.

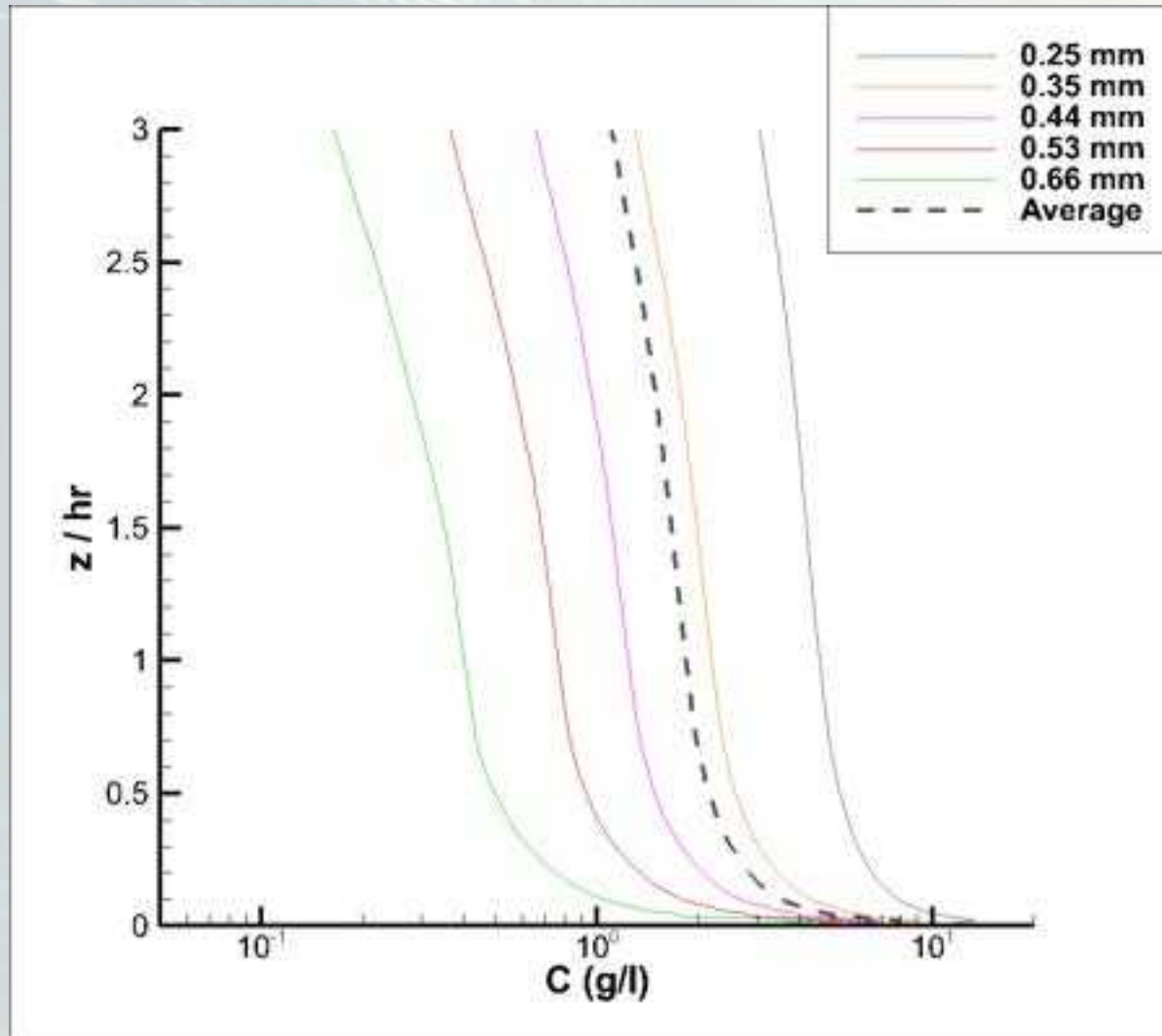
Period and spanwise averaged Bed(qb) and Suspended(qs) Load for 1T and T/4 of 13 periods for the smallest, median and largest sediment fraction.



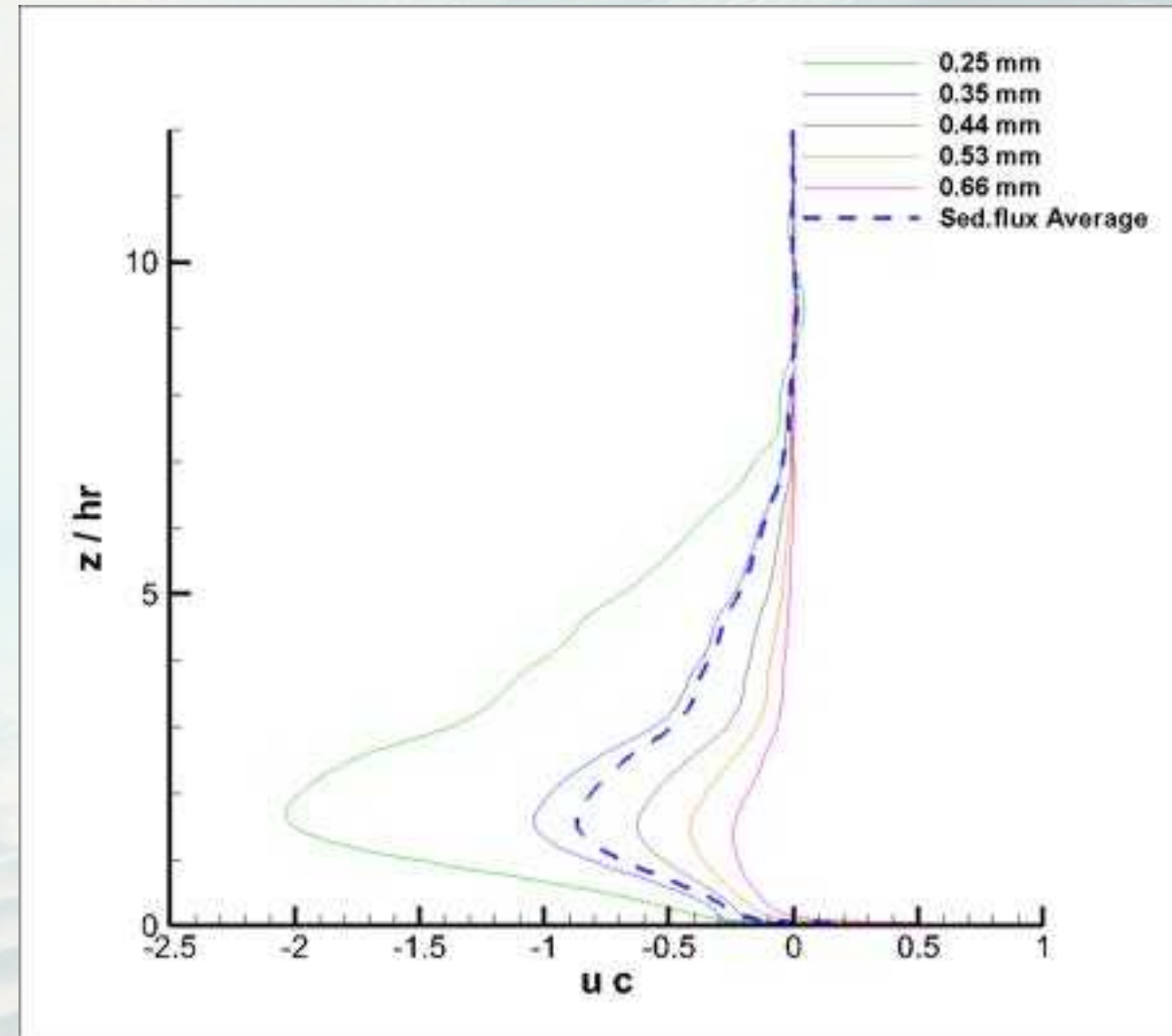
Period and spanwise averaged Bed(qb) and Suspended(qs) Load for T/2 and 3T/4 of 13 periods for the smallest, median and largest sediment fraction.



Profiles of the mean suspended sediment concentration of each sediment size fraction up to $3 h_r$



Profiles of the mean suspended sediment flux, uc , for all the sediment size fractions and the average of the sediment fluxes of the fractions.



Conclusions

In this Configuration :

- Shields Critical with Hide & Exposure factor is larger than normal Shields Critical for the fractions with diameter size smaller than D_{50} , it is smaller for the ones with diameter size larger than D_{50} , they are almost equal to each other for D_{50} .
- The fractions with diameters larger than D_{50} contribute more to the bed load.
- Suspended Load : Diameter Size Decreases -> Suspended Load Increases
- Concentration : Diameter Size Decreases -> Concentration Increases





University of
Nottingham
UK | CHINA | MALAYSIA



UK Research
and Innovation



SEDIMARE 2023-2027
Sediment Transport and Morphodynamics in Marine and
Coastal Waters with Engineering Solutions

**3rd Network Training School:
Advanced Integrated Coastal Zone Monitoring and Management
IH Cantabria, Spain
Santander, 11 – 13 March 2025**

Numerical investigations of bottom boundary layer hydrodynamics under a dam-break-driven swash event

Doctoral Candidate: Quan NGUYEN

Supervising Scientists: Nicholas DODD and Riccardo BRIGANTI



Overview of the project



Overview of the project

The swash zone

- Difficulty in adequately represent the wave boundary layer in the swash zones.
- Difficulty in directly measure the bed shear stress within the bottom boundary layer (BBL)
- An existing BBL sub-model for a **fixed bed** in the swash zone

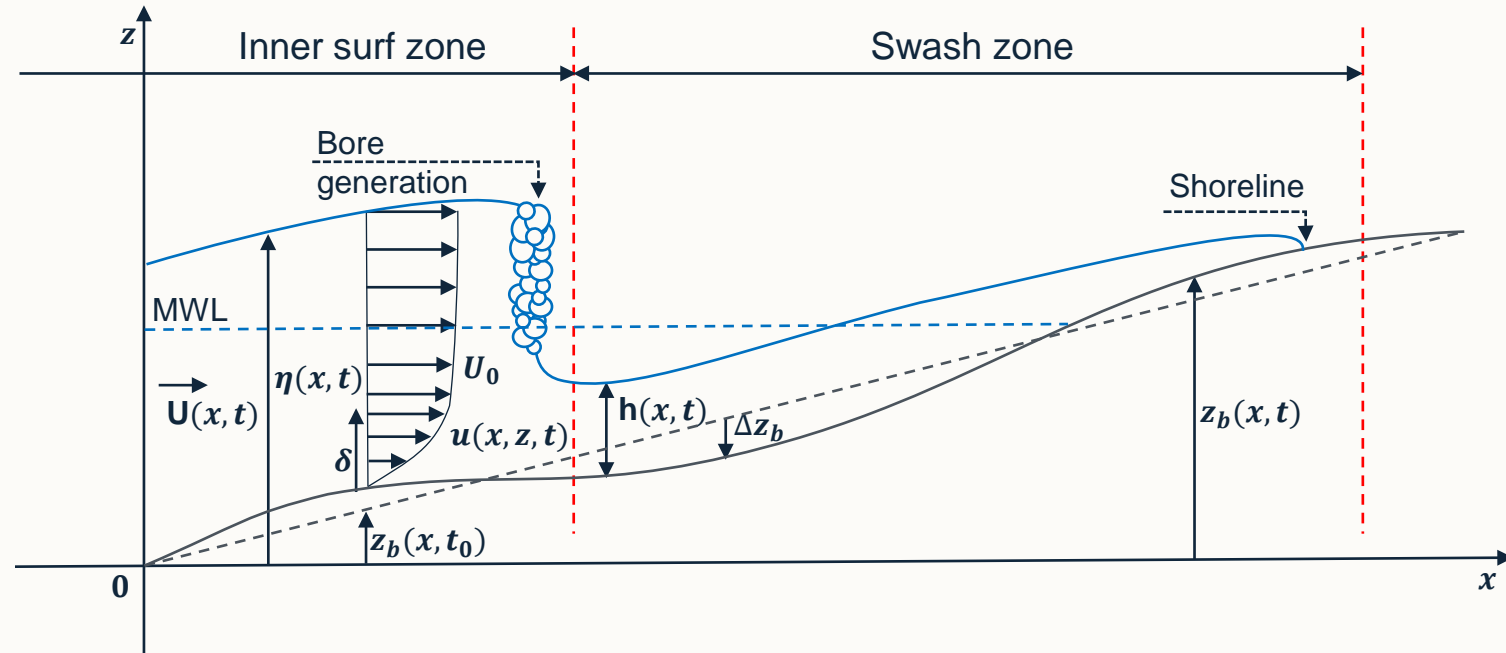


Figure 1. Schematic of general swash geometry.

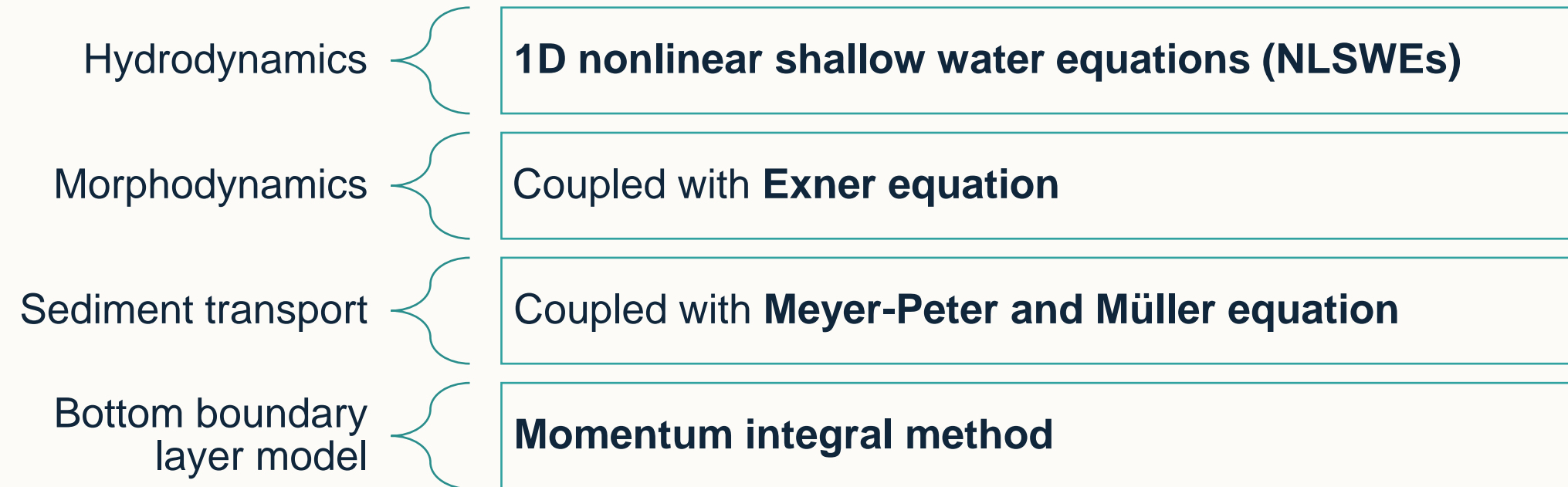
- To develop an **improved** boundary layer description (sub-model) for a **mobile bed** that is suitable for incorporation into a Nonlinear Shallow Water Wave Equation (NLSWE) morphodynamic solver.



Research methodology

Numerical model

❖ Depth-averaged, phase-resolving, fully-coupled model





Research methodology

Numerical model calibration and validation

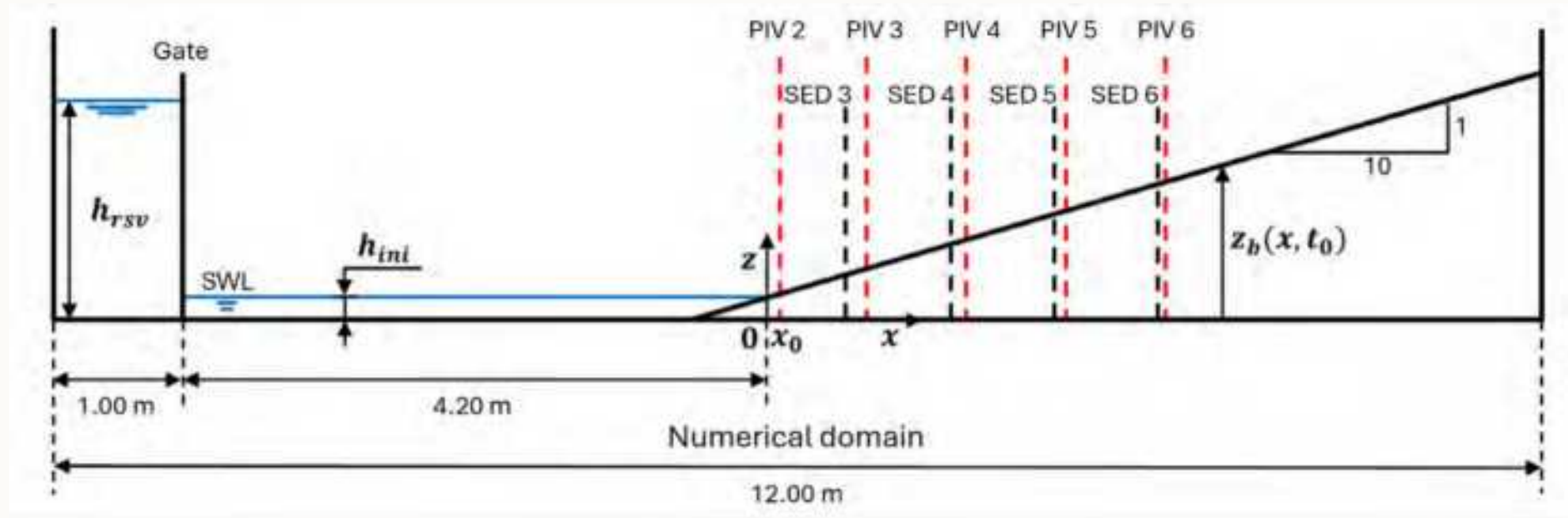


Figure 2. Schematic of the numerical setup based on the Aberdeen Swash facility.

Laboratory-based datasets

- Experimental study of bore-driven swash hydrodynamics on impermeable rough slopes (Kikkert et al., 2012).
- Intra-swash hydrodynamics and sediment flux for dam-break swash on coarse-grained beaches (O'Donoghue et al., 2016).

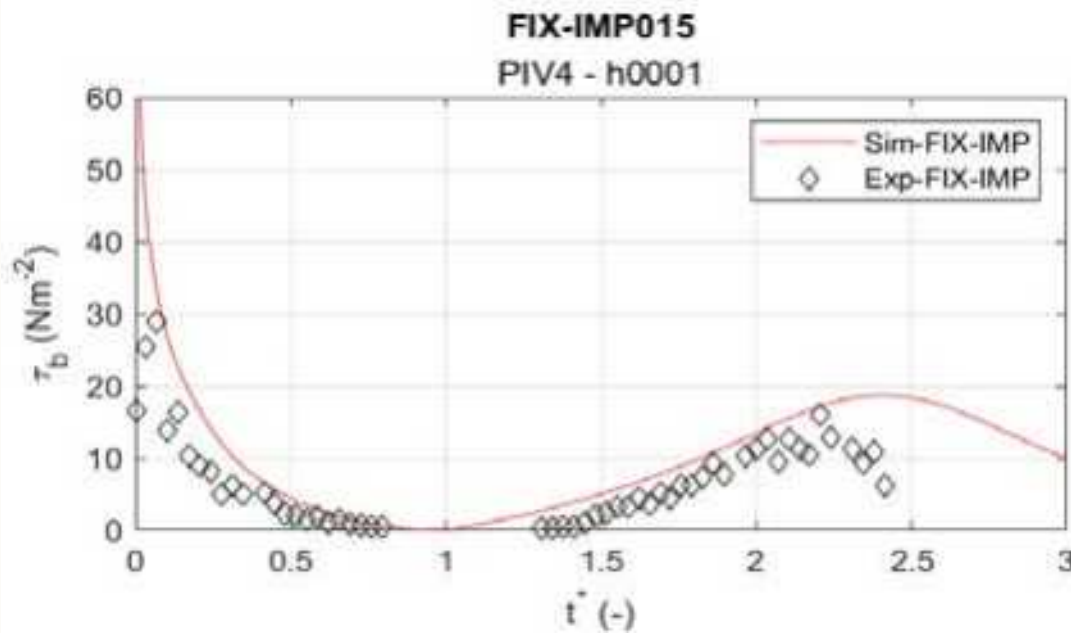
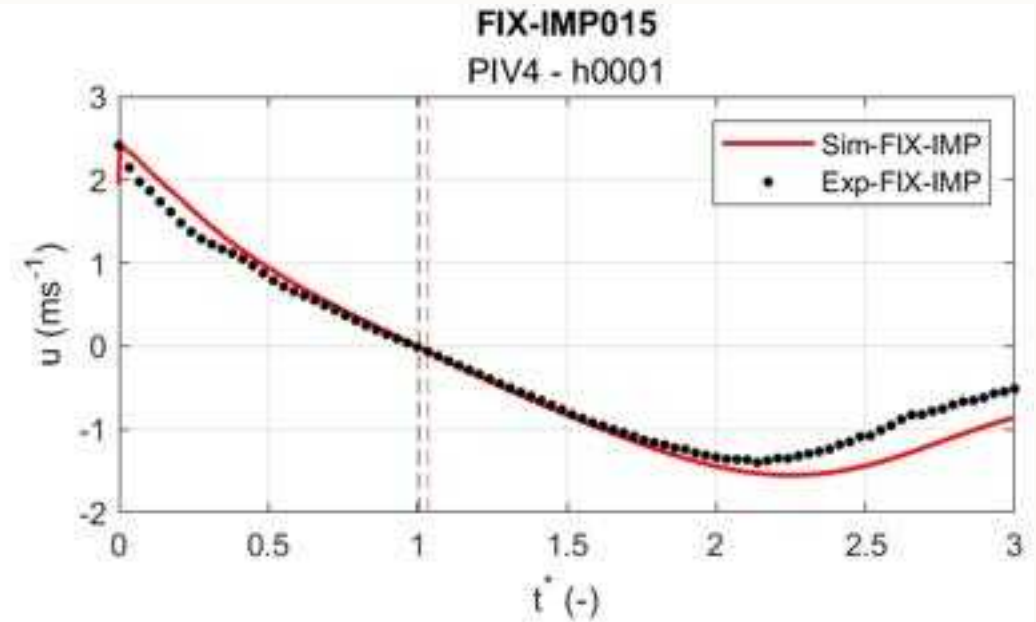
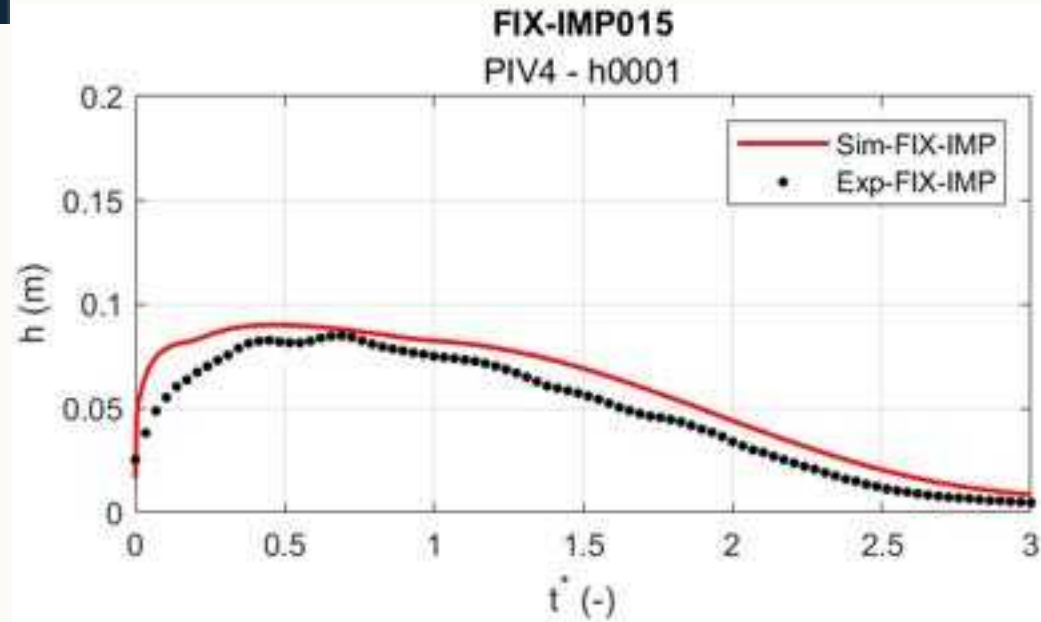


Previous results

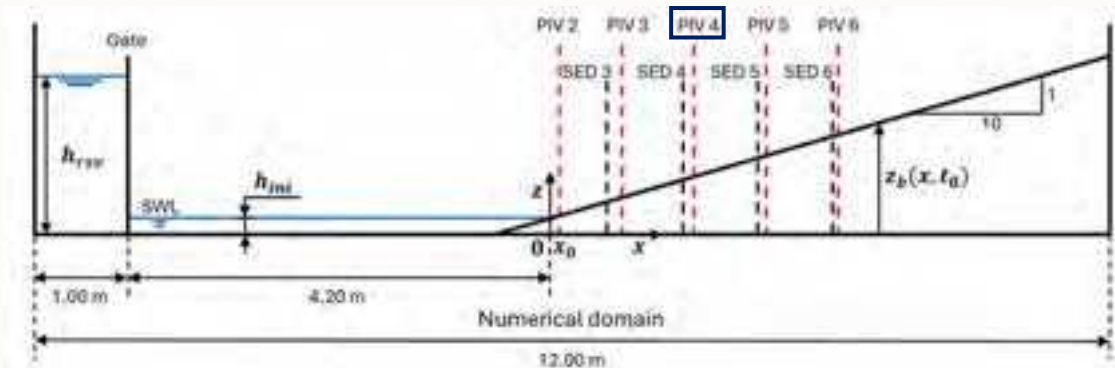
Simulation of single swash events on impermeable fixed beds



Water depth - Depth-averaged velocity – Bed shear stress



$$t^* = \frac{t - t_{bore\ arrival}}{t_{flow\ reversal} - t_{bore\ arrival}}$$





Model advancements and Limitations

- The model accurately predicts the depth-averaged horizontal velocity in the run-up phase
 - X **Overestimation of boundary layer thickness and underestimation of velocity profile**
- The modelled bed shear stress is well predicted when compared with the log-law-derived shear stress
 - X **Uncertainties in bed shear stress modelling**
- Numerical results of the flow variables for the validation tests are close to the experimental results
 - X **Overestimation of Flow Variables**



On-going work and research results

The calculation of w-component of the velocity



Comparing with 2DV RANS (VOF) equation solver

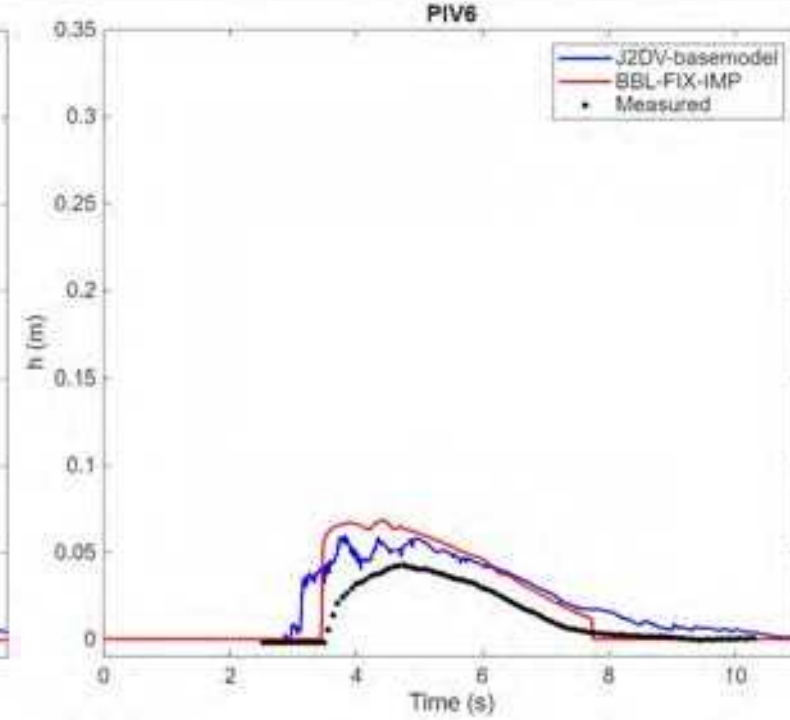
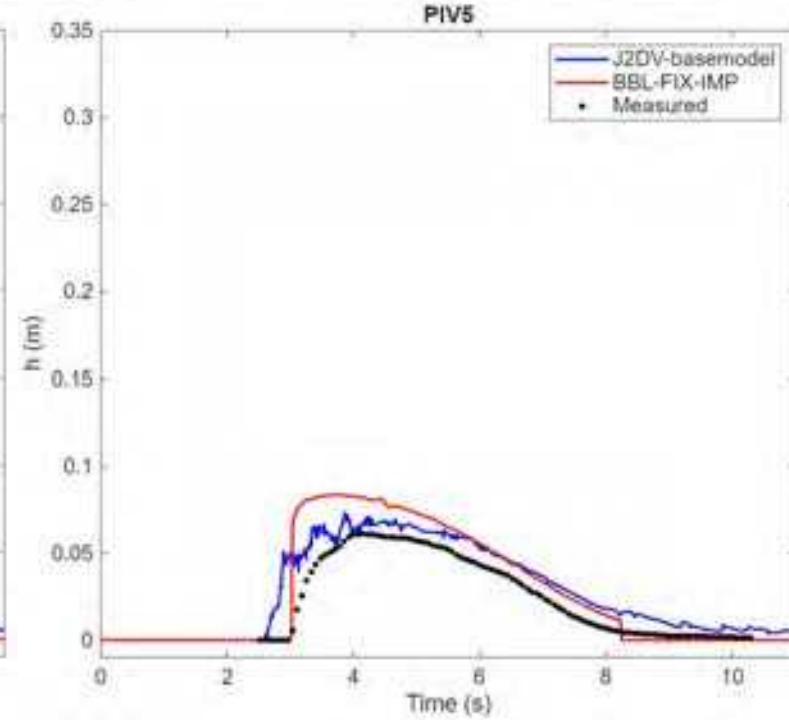
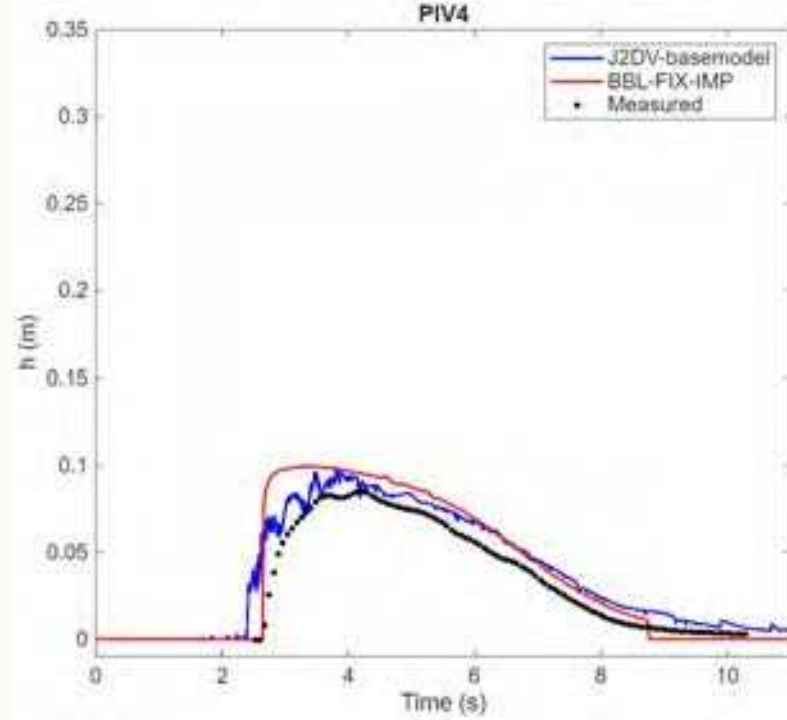
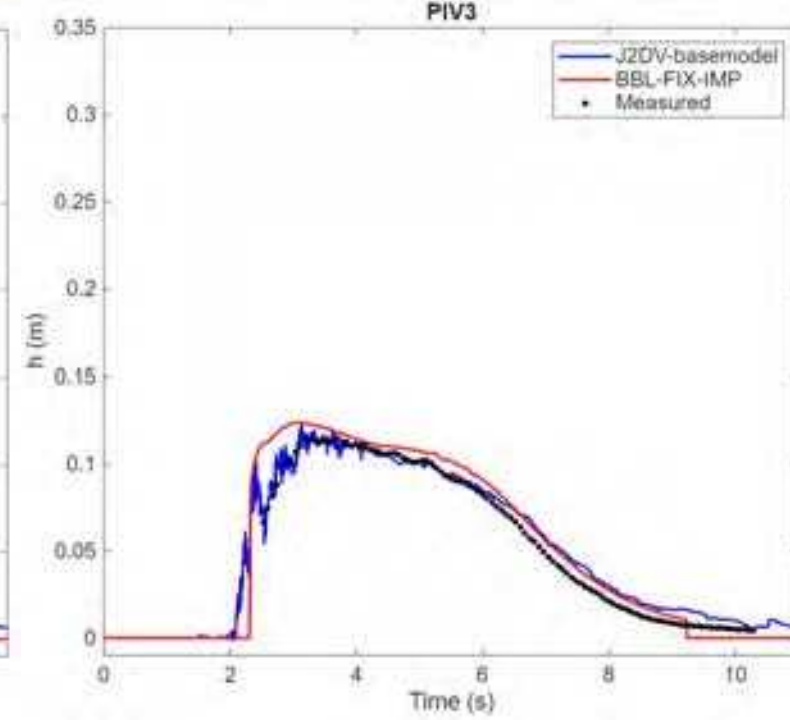
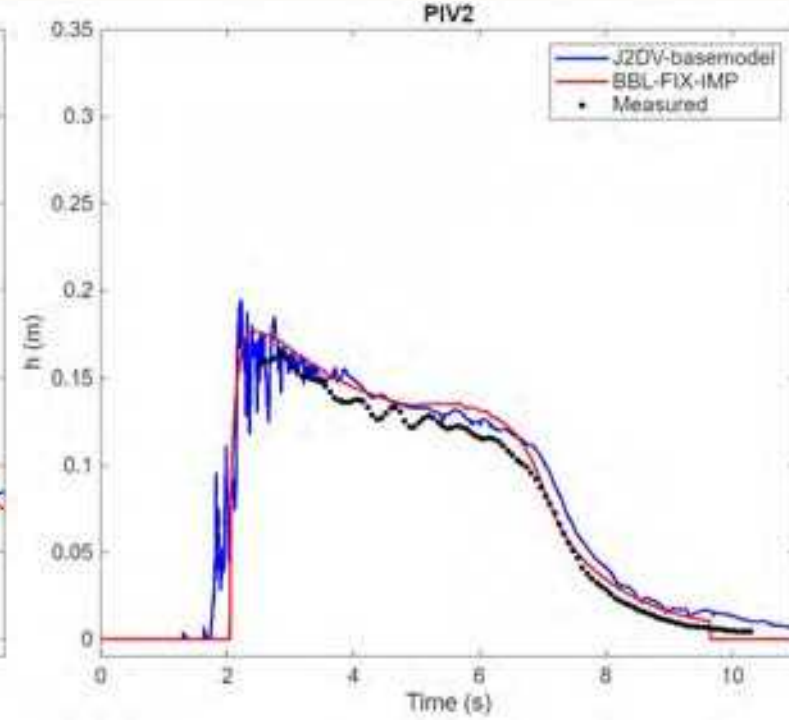
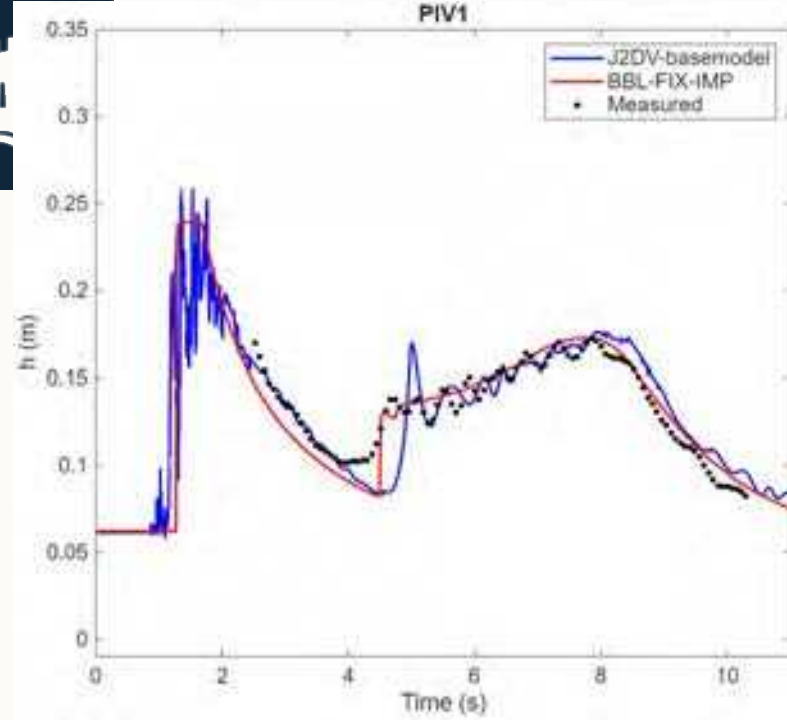
Compared against corresponding simulation data for the same event, generated from a 2DV RANS (VOF) equation solver (Kranenborg et al., 2022).

- Water depth
- Depth-averaged velocity
- Velocity profile



Comparing with 2DV RANS (VOF) equation solver

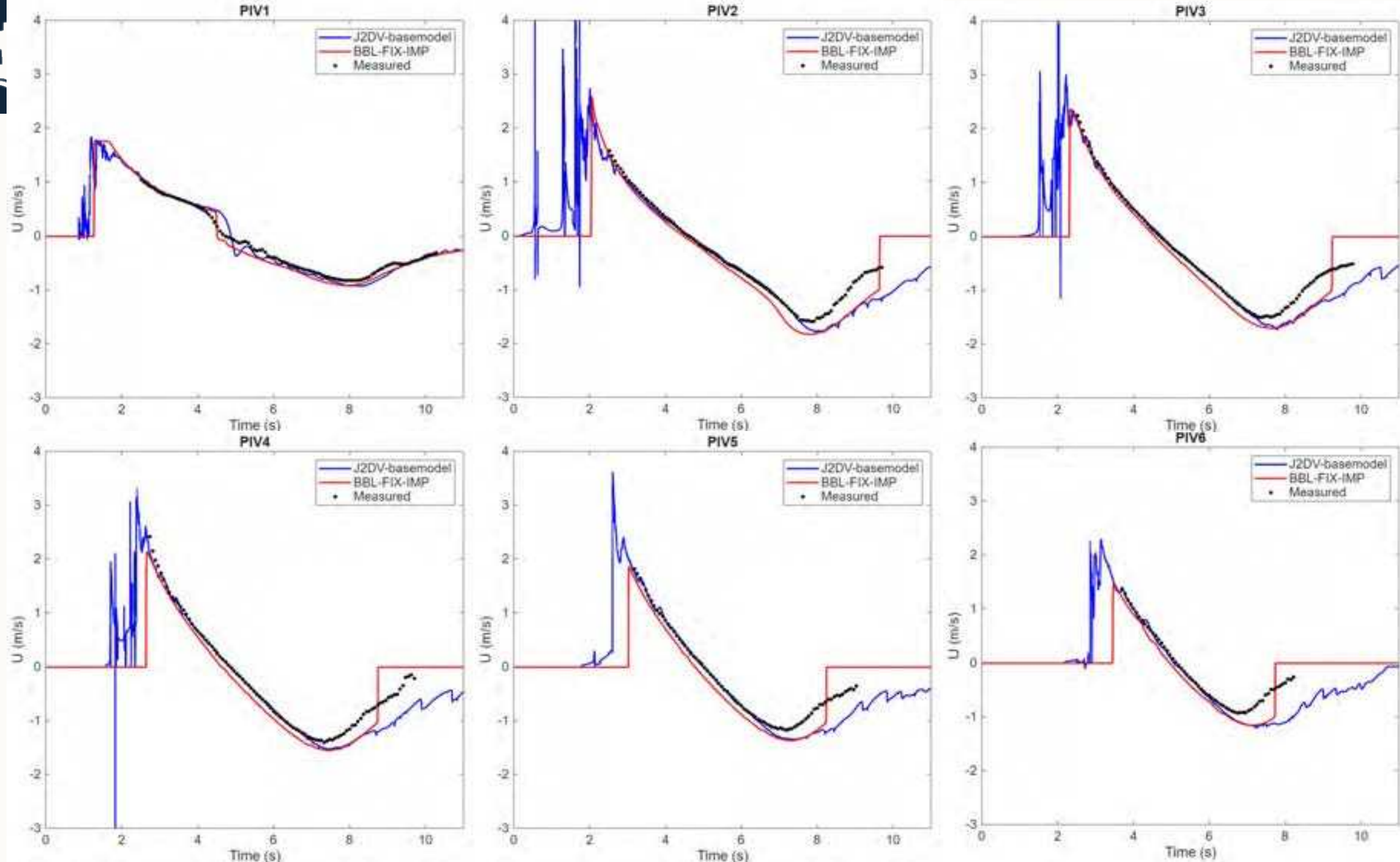
- Water depth





Comparing with 2DV RANS (VOF) equation solver

- Depth-averaged velocity





Re-construct of vertical velocity

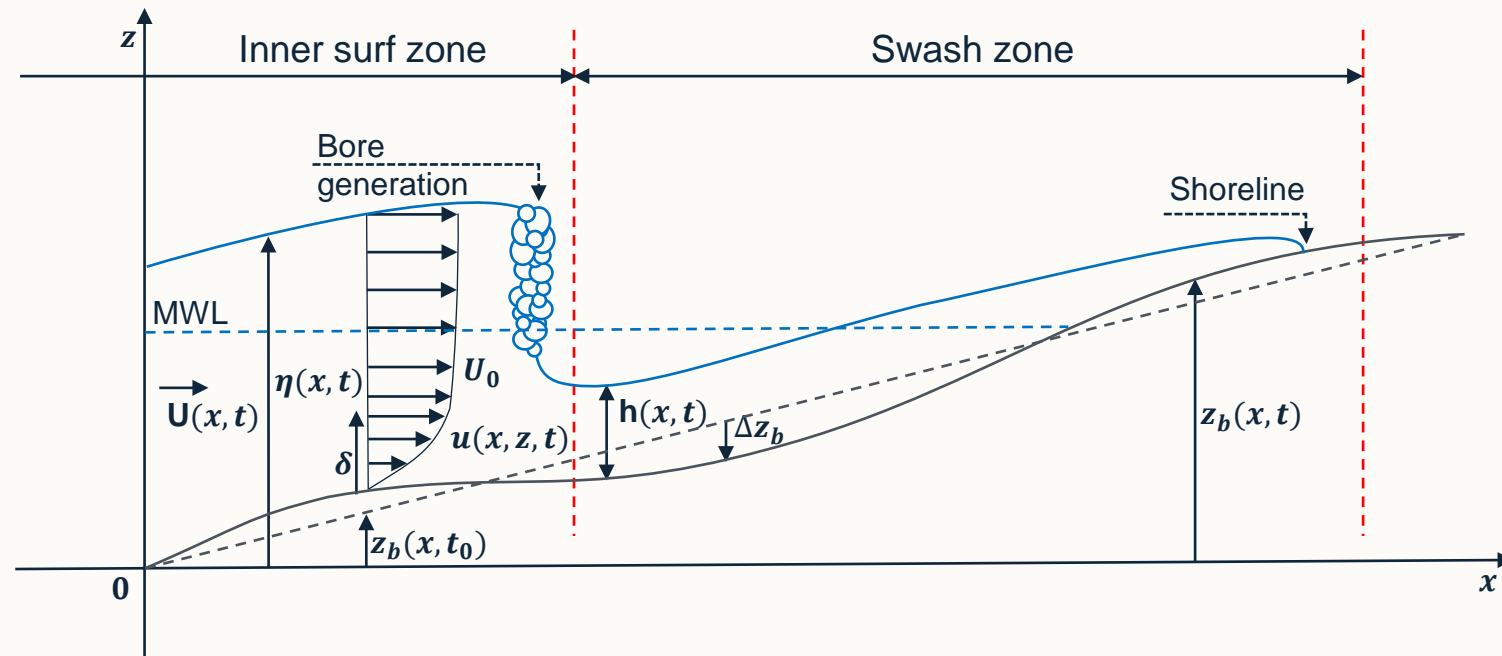
- In the bottom boundary layer, $u(x, z, t)$ increases with z , starting from zero at $z = z_0$ reaching a maximum at the top of the boundary layer, i.e., $z = z_0 + \delta(x, t)$.

z_0 is the bed roughness length, which is defined as the height at which the velocity is assumed to be zero.

- The horizontal velocity at the top of the boundary layer is called the free stream velocity, denoted as U_0 .
- Inside the BBL, $u(x, z, t)$ can be approximated using the logarithmic law:

$$u(x, z, t) = \frac{U_f}{\kappa} \ln \left(\frac{z}{z_0} \right)$$

U_f is the friction velocity, κ is von Karman's constant ($\kappa = 0.4$).



- Integrate the Continuity Equation

The 2D continuity equation is:

$$\frac{\partial u}{\partial x} + \frac{\partial w}{\partial z} = 0$$

Integrate the continuity equation from z_0 to z :

$$\int_{z_0}^z \frac{\partial w}{\partial z} dz = - \int_{z_0}^z \frac{\partial u}{\partial x} dz$$

$$w(x, z) - w(x, z_0) = - \int_{z_0}^z \frac{\partial u}{\partial x} dz$$

At the lower limit of the BBL ($z = z_0$), assuming an impermeable bed, the normal velocity is zero. Then, $w(x, z_0) = 0$ and the w -component of the velocity is expressed as:

$$w(x, z) = - \int_{z_0}^z \frac{\partial u}{\partial x} dz$$

In which, the horizontal velocity $u(x, z)$ is expressed as follows:

For z within the bottom boundary layer ($z_0 \leq z \leq z_0 + \delta(x)$), the logarithmic law is typically expressed as:

$$u(x, z) = \frac{u_*'(x)}{\kappa} \ln \left(\frac{z}{z_0} \right)$$

For z within the free-stream region ($z_0 + \delta(x) < z \leq h(x)$):

$$u(x, z) = U_0(x)$$

Leibniz Rule

$$\frac{\partial}{\partial x} \int_{z_0}^z u(x, z) dz = u(x, z) \frac{\partial z}{\partial x} - u(x, z_0) \frac{\partial z_0}{\partial x} + \int_{z_0}^z \frac{\partial u(x, z)}{\partial x} dz$$

$$\frac{\partial}{\partial x} \int_{z_0}^z u(x, z) dz = u(x, z) \frac{\partial z}{\partial x} + \int_{z_0}^z \frac{\partial u(x, z)}{\partial x} dz$$

$$- \int_{z_0}^z \frac{\partial u(x, z)}{\partial x} dz = u(x, z) \frac{\partial z}{\partial x} - \frac{\partial}{\partial x} \int_{z_0}^z u(x, z) dz$$

$$w(x, z) = u(x, z) \frac{\partial z}{\partial x} - \frac{\partial}{\partial x} \int_{z_0}^z u(x, z) dz$$

The term

$$\int_{z_0}^z u(x, z) dz$$

is expressed as:

$$\int_{z_0}^z u(x, z) dz = \int_{z_0}^z \frac{u_f(x, z)}{\kappa} \ln \left(\frac{z}{z_0} \right) dz$$

$$\int_{z_0}^z u(x, z) dz = \frac{u_f(x, z)}{\kappa} \int_{z_0}^z \ln \left(\frac{z}{z_0} \right) dz$$

$$\int_{z_0}^z u(x, z) dz = \frac{u_f(x, z)}{\kappa} \left[z \ln \left(\frac{z}{z_0} \right) - (z - z_0) \right]$$

Then:

$$\frac{\partial}{\partial x} \int_{z_0}^z u(x, z) dz = \frac{\partial}{\partial x} \left(\frac{u_f(x, z)}{\kappa} \left[z \ln \left(\frac{z}{z_0} \right) - (z - z_0) \right] \right)$$

$$\frac{\partial}{\partial x} \int_{z_0}^z u(x, z) dz = \left(\frac{1}{\kappa} \left[z \ln \left(\frac{z}{z_0} \right) - (z - z_0) \right] \right) \frac{\partial u_f(x, z)}{\partial x}$$

So, inside the BBL, the $w(x, z)$ is expressed as:

$$w(x, z) = \frac{u_f}{\kappa} \ln \left(\frac{z}{z_0} \right) \frac{1}{10} - \left(\frac{1}{\kappa} \left[z \ln \left(\frac{z}{z_0} \right) - (z - z_0) \right] \right) \frac{\partial u_f(x, z)}{\partial x}$$

In which, $\frac{\partial z}{\partial x}$ is the slope of the bed $\frac{\partial z}{\partial x} = \frac{1}{10}$.

Outside the BBL, the $w(x, z)$ is expressed as:

$$w(x, z) = w(x, z_0 + \delta) - \frac{dU_0}{dx} [z - (z_0 + \delta)]$$



Re-construct of vertical velocity

➤ Inside the bottom boundary layer:

$$w(x, z) = \frac{u_f}{\kappa} \ln \left(\frac{z}{z_0} \right) \frac{1}{10} - \left(\frac{1}{\kappa} \left[z \ln \left(\frac{z}{z_0} \right) - (z - z_0) \right] \right) \frac{\partial u_f(x, z)}{\partial x}$$

➤ Outside the bottom boundary layer:

$$w(x, z) = w(x, z_0 + \delta(x)) - \frac{\partial U_0(x)}{\partial x} [z - (z_0 + \delta(x))]$$

U_0 is free stream velocity;

U_f is the friction velocity;

δ is the bottom boundary layer thickness;

z_0 is the bed roughness length;

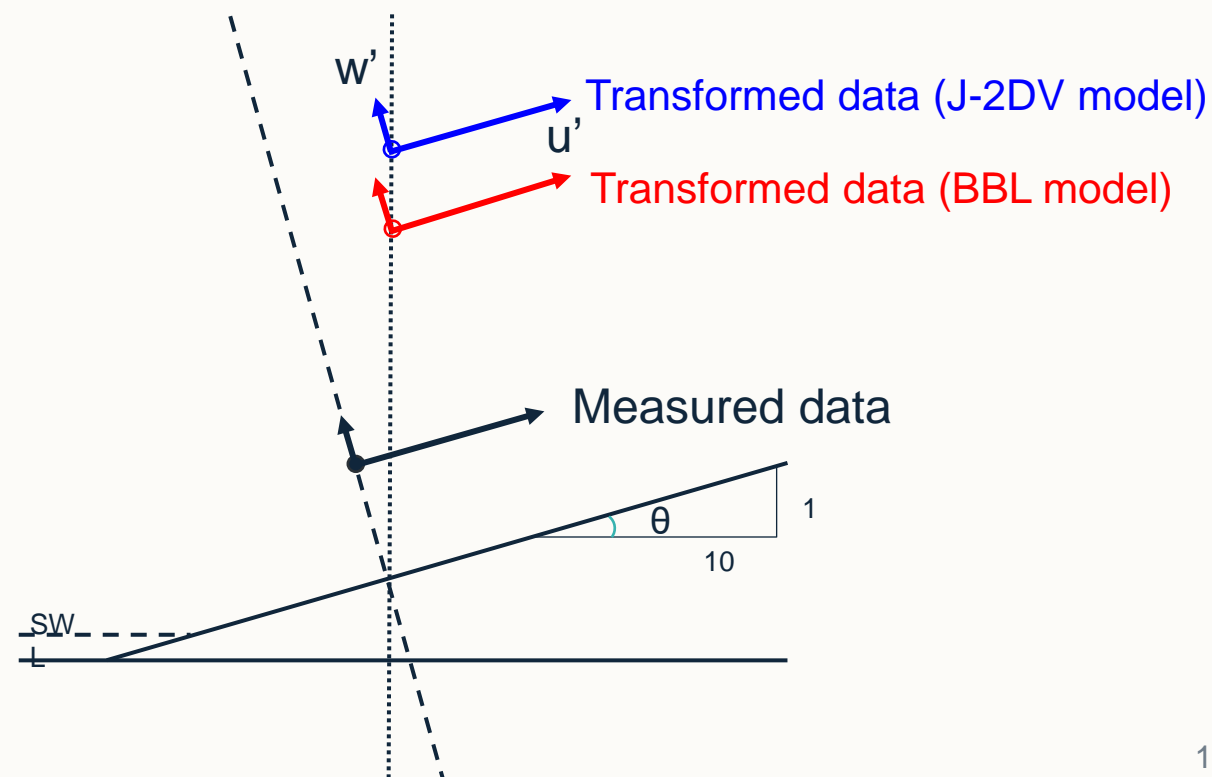
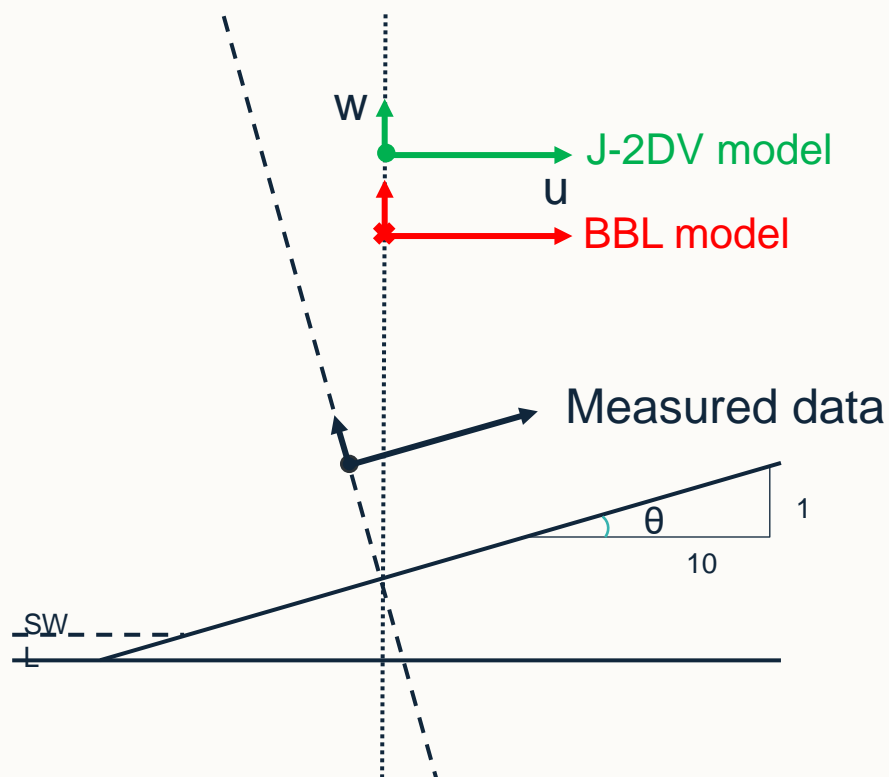
κ is von Karman's constant ($\kappa = 0.4$).



Comparing with 2DV RANS (VOF) equation solver

- Data pre-processing

$$\begin{bmatrix} u' \\ w' \end{bmatrix} = \begin{bmatrix} \cos(\theta) & \sin(\theta) \\ -\sin(\theta) & \cos(\theta) \end{bmatrix} \times \begin{bmatrix} u \\ w \end{bmatrix}$$

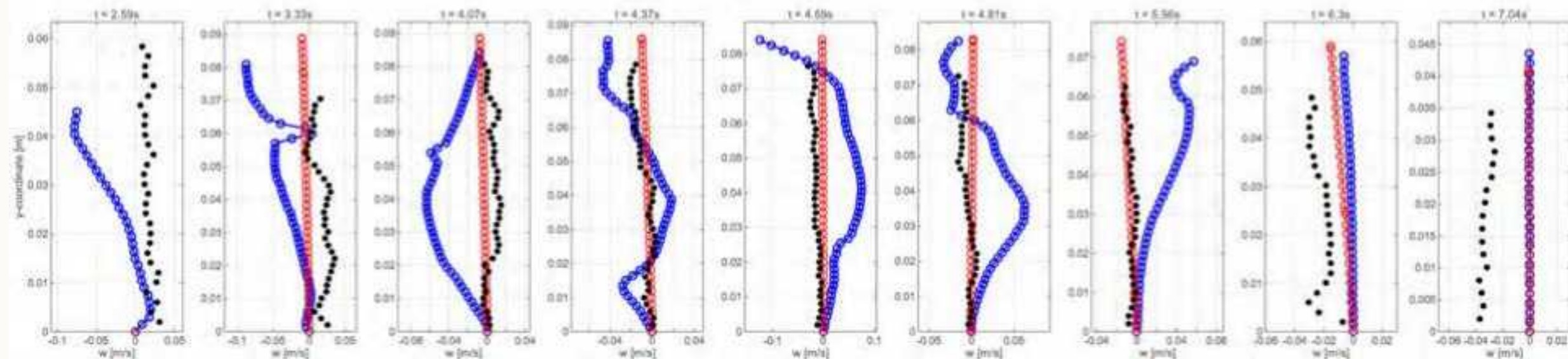
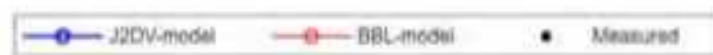
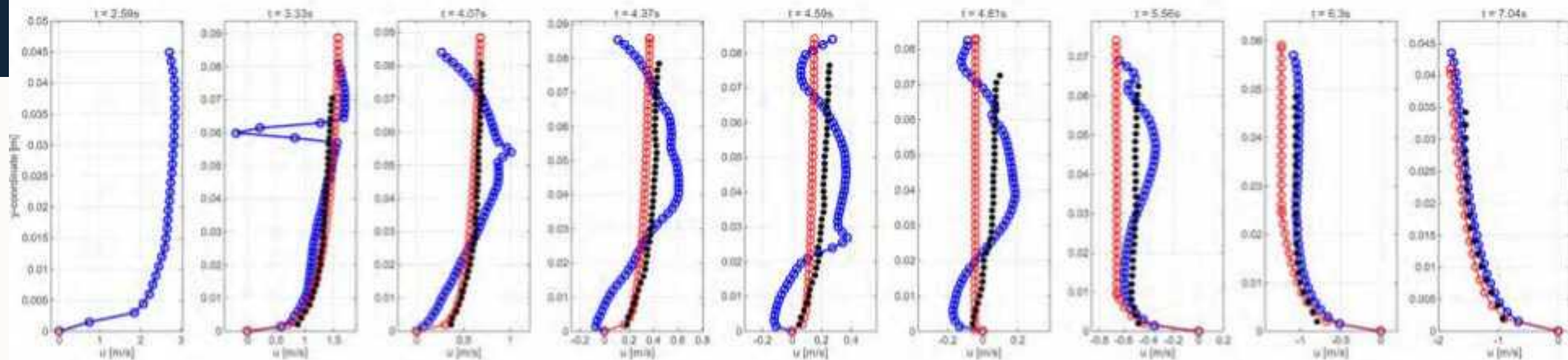




Comparing with 2DV RANS (VOF) equation solver

- Velocity profile

PIV4

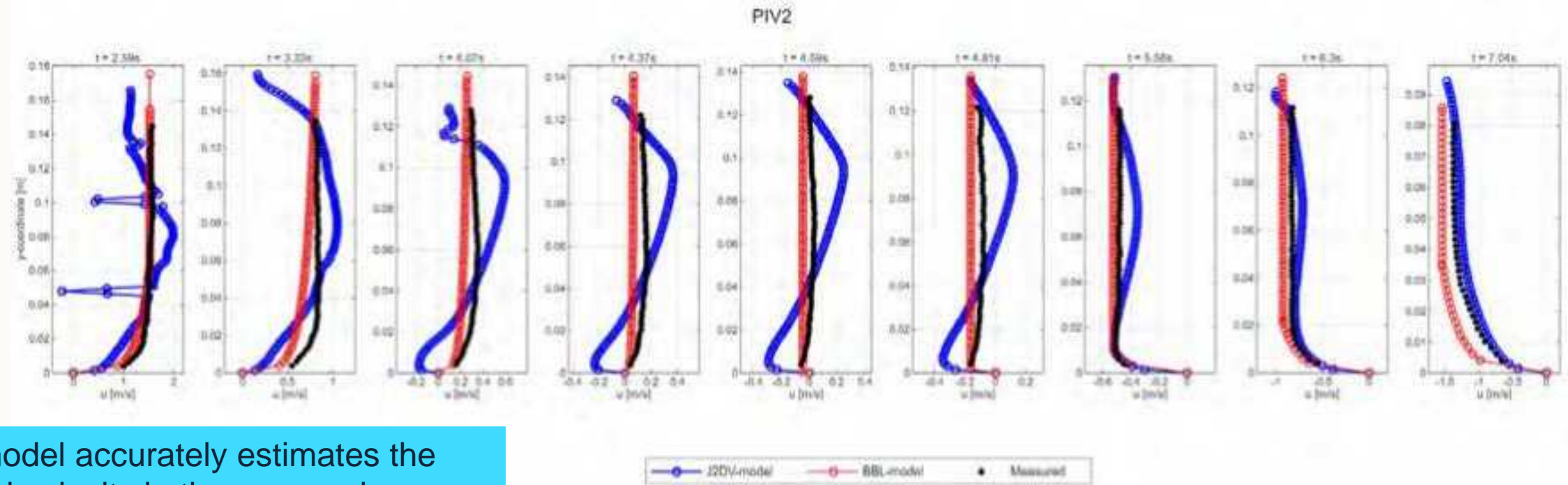




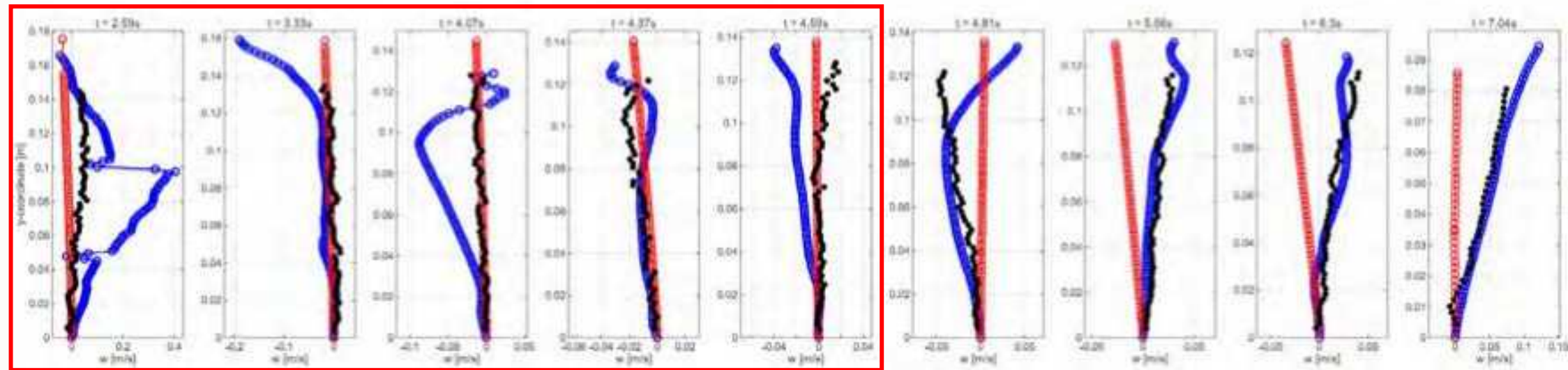
Conclusion



Model advancements

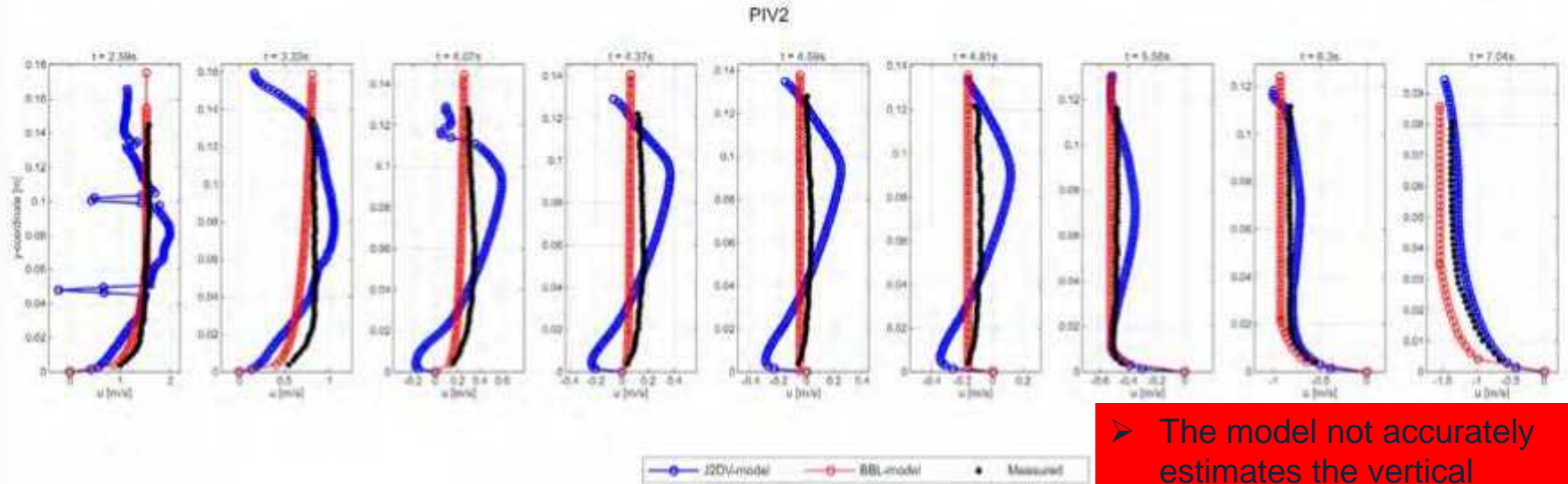


- The model accurately estimates the vertical velocity in the run-up phase

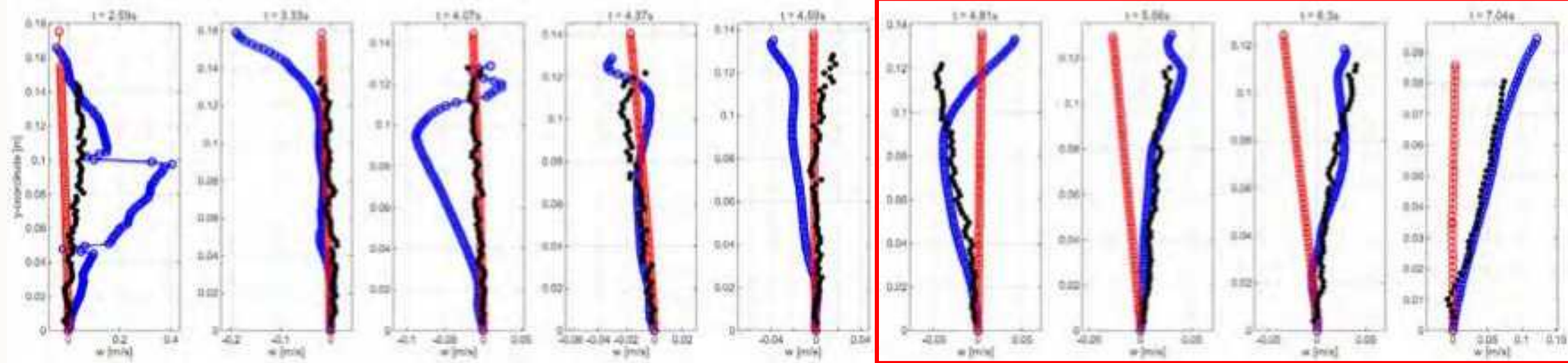




Model Limitations



➤ The model not accurately estimates the vertical velocity for the backwash







Future works

- Improving the simulation of the velocity profile, with a focus on the velocity profile at the **flow reversal**.
- Re-construct the vertical velocity for the **mobile** bed.



University of
Nottingham
UK | CHINA | MALAYSIA



UK Research
and Innovation



SEDIMARE 2023-2027

Sediment Transport and Morphodynamics in Marine and
Coastal Waters with Engineering Solutions

3rd Network Training School

IH Cantabria, Spain

Santander, 11 – 13 Mar 2025

Numerical investigations of bottom boundary layer hydrodynamics under a dam-break-driven swash event

^{1*}Quan T. Nguyen, ³Joost W.M. Kranenburg,

¹Nicholas Dodd, ¹Riccardo Briganti, ²Fangfang Zhu, ^{3,4}Jebbe J. van der Werf, ⁴Pieter C. Roos

*lead presenter

¹University of Nottingham, UK

²University of Nottingham Ningbo Campus, China

³Deltares, Delft, The Netherlands

⁴University of Twente, Enschede, The Netherlands

Mathematical modeling and numerical simulations of water-saturated granular materials with emphasis to sediment transport

Evangelos Petridis

UCLouvain

Institute of Mechanics, Materials and Civil Engineering



Funded by
the European
Union



This project has received funding
from the European Union's
Horizon Europe research and
innovation programme under the
Marie Skłodowska-Curie grant
agreement No 101017243.



Introduction

Payne and Straughan (1999) established continuous dependence in the Brinkman-Forchheimer equations with constant porosity . When the porosity is space dependent :

- Velocity is not divergence free.
- The term describing viscous shear stresses is not the Laplacian .
- We have normal viscous stresses (bulk viscosity ζ) .
- The shear viscosity μ enters the expression for the interfacial drag (Darcy coefficient a) .
- We are working in the weighted L^2 space with the porosity $\phi(\mathbf{x})$ being the weight .

$$\|\mathbf{u}\| = \left(\int_{\Omega} \phi |\mathbf{u}|^2 d\mathbf{x} \right)^{1/2}$$

Model

The Brinkman–Forchheimer equations for flow in porous media with variable porosity are

$$\phi \frac{\partial \mathbf{u}}{\partial t} + \phi \nabla p = \nabla \cdot (\phi \zeta (\nabla \cdot \mathbf{u}) \mathbf{I}) + \nabla \cdot (\phi \mu \mathbf{V}^d) - a^*(\phi) \mathbf{u} - b^*(\phi) |\mathbf{u}| \mathbf{u} + \phi \mathbf{f} \quad , \quad \zeta, \mu > 0$$

$$\nabla \cdot (\phi \mathbf{u}) = 0$$

$$\mathbf{V}^d(\mathbf{u}) = \frac{1}{2}(\nabla \mathbf{u} + (\nabla \mathbf{u})^T) - \frac{1}{3} \nabla \cdot \mathbf{u} \mathbf{I}$$

$$b^*(\phi) = b(1 - \phi) + d(1 - \phi)^2 \quad , \quad a^*(\phi) = a\mu(1 - \phi) \quad , \quad a, b, d > 0$$

$$0 < \phi_{\min} \leq \phi \leq \phi_{\max} < 1$$

where \mathbf{u} is the average fluid velocity in the porous medium, a is the Darcy coefficient, b is the Forchheimer coefficient, ζ is the bulk viscosity, μ is the shear viscosity, p is the pressure, \mathbf{f} is the gravity and ϕ is the variable porosity.

- Established continuous dependence of solutions on the parameters of the problem, namely, the Darcy and Forchheimer coefficients of interphasial drag and the shear and bulk viscosities of the fluid.
- The solution difference for different parameter values decays always with time.
- Derived lower and upper bounds for the kinetic energy of the fluid. The kinetic energy decays exponentially but faster than in pure-fluid domains because of the interphasial drag.

- Underwater landslides are often hard to observe but their consequences can be dramatic. At short term, the sudden fall of an important column of sand under its own weight disturbs the surrounding fluid and might initiate strong waves. At long term, it might change completely the shape of the river or ocean floor, thus changing the conditions of flow. This has an impact on the ecosystem and the management of river flooding
- Here, the granular column collapse is modelled using a 2-pressure, 2-velocity flow model for fluid-solid mixtures

Governing equations

$$\frac{\partial \phi_f}{\partial t} + \nabla \cdot (\phi_f u_f) = 0,$$
$$\rho_f \frac{\partial \phi_f u_f}{\partial t} + \rho_f \nabla \cdot (\phi_f u_f \otimes u_f) = \nabla \cdot \sigma_f - f + \rho_f \phi_f g$$

Interphasial momentum exchange

$$f = p_f \nabla \phi_s + \delta(u_f - u_s)$$

Stress tensor - Newtonian viscous stresses

$$\sigma_f = -p_f \phi_f I + \tau_f,$$

For simple isotropic fluids, τ_s is further decomposed as the sum of a diagonal and a deviatoric component,

$$\tau_f = \phi_f \zeta_f (\nabla \cdot u_f) I + 2\phi_f \mu_f D_f^d,$$

Governing equations

$$\frac{\partial \phi_s}{\partial t} + \nabla \cdot (\phi_s u_s) = 0,$$
$$\rho_s \frac{\partial \phi_s u_s}{\partial t} + \rho_s \nabla \cdot (\phi_s u_s \otimes u_s) = \nabla \cdot \sigma_s + f + \rho_s \phi_s g$$

Interphasial momentum exchange

$$f = p_f \nabla \phi_s + \delta(u_f - u_s)$$

Stress tensor - Non - Newtonian viscous stresses

$$\sigma_s = -\phi_s p_s I + C_s + \tau_s.$$

$$\sigma_s = -\phi_s p_s I + C_s + \tau_s .$$

$$C_s = \gamma_s \nabla \phi_s \otimes \nabla \phi_s ,$$

where the coefficient γ_s accounts for the spatial distribution of the grains

$$\tau_s = ((\zeta_s + \zeta_{s'}) \nabla \cdot u_s + \chi_1) \phi_s I + 2(\mu_s + \mu_{s'}) \phi_s D_s^d + \chi_2 \phi_s D_s \cdot D_s$$

where

$$\mu_s = \mu_f \left[\left(2.5 - \frac{2}{\phi_m} \right) + \left(5.2 - \frac{3}{\phi_m^2} \right) \phi_s + \frac{\phi_m^2}{\phi_s (\phi_m - \phi_s)^2} - \frac{1}{\phi_s} \right]$$

Solid phase - Stress tensor

In particular, all these parameters are nonlinear functions of the strain-rate tensor and read as follows,

$$\mu_{s'} = \frac{\mu_n}{\sqrt{2}} \frac{\det D_s}{(D_s : D_s)^{\frac{3}{2}}}, \quad \zeta_{s'} = \frac{\mu_n \sqrt{2}}{3} \frac{\det D_s}{(D_s : D_s)^{\frac{3}{2}}},$$
$$\chi_1 = -\sqrt{2} \mu_n \left(2 \sqrt{D_s^d : D_s^d} - \frac{3}{2} \frac{D_s^d : D_s^d}{\sqrt{D_s : D_s}} \right), \quad \chi_2 = -\frac{\sqrt{2} \mu_n}{\sqrt{D_s : D_s}},$$

Where

$$\mu_n = 0.75 \mu_f \frac{\phi_s}{(\phi_m - \phi_s)^2}.$$

Compaction equation

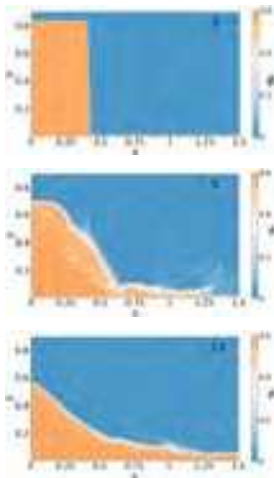
The above system of balance laws is closed with an evolution equation for the volume fraction ϕ_s . This equation is referred to as *compaction equation*

$$\frac{\partial \phi_s}{\partial t} + u_s \cdot \nabla \phi_s = Re \frac{\phi_s \phi_f}{\mu_c} (p_s - p_f - \beta_s + \nabla \cdot (\gamma_s \nabla \phi_s))$$

β_s is the configuration pressure which is a logarithmic function of ϕ_s and ϕ_{\max} . γ_s is related to the microstructure - power law function of ϕ_s .

Simulations

The algorithm to solve the aforementioned equations is based on a predictor-corrector time-integration scheme with a generalised projection method for the phasial pressures



Future work

We will work on a problem include the flow of currents over deformable dunes in a channel.

Detailed numerical simulations of shear-driven (Couette) of water-sand mixtures. (Emphasis on sediment mobilization and resuspension)

